Evaluation of GPR55 and GPR120 as novel therapeutic targets for the treatment of type 2 diabetes

A thesis presented for the degree of

Doctor of Philosophy

in the

School of Biomedical Sciences

Faculty of Life & Health Sciences

Andrew Gerard McCloskey, BSc (Hons).

May 2019

(I can confirm the word count for this thesis is less than 100,000 words)

Contents

Acknowledgments

Firstly, I would like to express my sincere gratitude to my PhD supervisor Prof. Aine McKillop for her invaluable advice, guidance and continued support throughout my studies. I would like to thank Prof. Peter Flatt for his scientific advice and insightful recommendations during my research.

I would like to thank all past and present members of the Diabetes Research Group for their support and friendship during my PhD. Thanks to Michael, Chris, Ryan, Shruti and Neil for being great friends and for making my time at Ulster University most enjoyable.

I would also like to thank all my family and friends, especially my parents and brothers for their never-ending support. Finally, special thanks to Kate for her help, enthusiasm and constant encouragement throughout my PhD.

Summary

G-protein coupled receptors (GPCRs) are expressed in the gut-brain-pancreatic axis and regulate energy metabolism through a range of cellular responses, including hormone release, cell proliferation, neurological signalling and immune responses. Novel therapies that maintain glucose homeostasis and enhance islet cell proliferation are required with research focusing on cannabinoid and free fatty acid receptors. This research study aims to evaluate the therapeutic potential of two GPCRs, namely GPR55 and GPR120.

BRIN-BD11 cells were used to assess the effects of endogenous and synthetic GPR55 and GPR120 agonists on insulin release, cell proliferation and cytotoxicity, followed by GPCR expression and intracellular signalling analysis. CRISPR/Cas9 gene editing was utilised to assess agonist specificity. Metabolic effects of GPCR agonist therapies *in-vivo* were explored in high fat fed (HFF) induced diabetic mice. GPR55 and GPR120 activation exhibited insulinotropic and proliferative effects on pancreatic BRIN-BD11 cells, with modulations in intracellular Ca^{2+} and MAPK signalling. Assessment of agonist specificity using knockout beta cell lines developed by CRISPR/Cas9 revealed that ALA (GPR120) and Abn-CBD (GPR55) were the most potent selective agonists. Expression and localisation of GPR55 and GPR120 were demonstrated in clonal beta cells and murine islets with areas of co-localisation observed with insulin. Orally administered GPR55/GPR120 agonists improved glucose tolerance and circulating insulin, GLP-1 and GIP in HFF mice, with further improvements in combination with DPP-IV inhibitor (Sitagliptin). Long term administration of ALA and Abn-CBD based therapies improved glycaemic control, bodyweight, insulin sensitivity and enhanced islet cell regeneration. Biochemical analysis revealed improvements towards circulating insulin, dyslipidaemia and CVD risk markers. Collectively, this study highlights GPR55 and GPR120 as novel therapeutic targets for the treatment of diabetes and obesity related diseases.

Abbreviations

2-AG	2-arachidonoylglycerol
Abn-CBD	Abnormal cannabidiol
ADA	American Diabetes Association
AEA	Anandamide
ALA	α-linolenic acid
AMC	7-amino-4-methylcoumarin
AOC	Area over the curve
AUC	Area under the curve
BSA	Bovine serum albumin
Ca^{2+}	Calcium
$CaCl_2.2H_2O$	Calcium chloride dihydrate
cAMP	Cyclic adenosine monophosphate
$CaSO_4$	Calcium sulphate
CB1	Type 1 cannabinoid receptor
CB2	Type 2 cannabinoid receptor
CBD	Cannabidiol
CBN	Cannabinol

CCK	Cholecystokinin
CRISPR	Clustered regularly interspaced short palindromic repeats
CNS	Central nervous system
Da	Dalton
DAG	Diacylglycerol
DAPI	4',6-diamidino-2-phenylindole
DEXA	Dual energy X-ray absorption
DHA	Docosahexaenoic acid
DKA	Diabetic ketoacidosis
DMSO	Dimethyl sulphoxide
DPP-IV	Dipeptidyl peptidase-IV
EASD	European Association for the Study for Diabetes
ELISA	Enzyme-linked immunosorbent assay
EPA	Eicosapentaenoic acid
ERK	Extracellular signal-regulated kinase
FAAH	Fatty acid amide hydrolase
FACS	Fluorescence-activated cell sorting
FBS	Foetal bovine serum
FFAR	Free fatty acid receptor

FITC	Fluorescein isothiocyante
GABA	γ-aminobutyric acid
GDP	Guanosine diphosphate
GFP	Green fluorescent protein
GIP	Glucose-dependent insulinotropic polypeptide
GLP-1	Glucagon-like peptide-1
GLUT	Glucose transporter
Gly-pro AMC	Gly-Pro-7-amido-4-methylcoumarin
GPCR	G-protein coupled receptor
GTP	Guanosine triphosphate
HBSS	Hank's buffered saline solution
HbA_{1c}	Glycated haemoglobin A1c
HCl	Hydrochloric acid
HEPES	4-(2-hydroxyethyl)-1-piperazineethanesulphonic acid
HDL	High density lipoproteins
HHS	Hyperglycaemic hyperosmolar syndrome
IFG	Impaired fasting glucose
IGT	Impaired glucose tolerance
IP_3	Inositol trisphosphate

K^{ATP}	Potassium ATP
KCl	Potassium chloride
KH_2PO_4	Potassium dihydrogen orthophosphate
KRBB	Krebs Ringer bicarbonate buffer
LDH	Lactate dehydrogenase
LDL	Low density lipoproteins
LPC	Lysophosphatidylcholine
LPI	L-α-lysophosphatidylinositol
$MgSO_4.7H_2O$	Magnesium sulphate
NaCl	Sodium chloride
$NaHCO_3$	Sodium bicarbonate
NaOH	Sodium hydroxide
NEDH	New England Deaconess Hospital
NHEJ	Non-homologous end joining
NIH	National Institute of Health
NPY	Neuropeptide Y
NSB	Non-specific binding
OD	Optical density
OEA	Oleoylethanolamide

OGTT	Oral glucose tolerance test
OXM	Oxyntomodulin
PAF	Platelet activating factor
PBS	Phosphate buffered saline
PEA	Palmitoylethanolamide
PFA	Paraformaldehyde
PKA	Protein kinase A
PKB	Protein kinase B
PKC	Protein kinase C
PLC	Phospholipase C
PP	Pancreatic polypeptide
PPAR	Peroxisome proliferator activation receptor
PYY	Peptide YY
RIA	Radioimmunoassay
RLU	Relative light units
RFU	Relative fluorescence units
SGLT	Sodium glucose co-transport
sgRNA	Single guide RNA
shRNA	Small hairpin RNA

siRNA	Small interfering RNA
SSTR	Somatostatin receptor
STZ	Streptozotocin
SUR	Sulphonylurea receptor
TALEN	Transcription activator-like effector nuclease
THC	Δ-9-tetrahydrocannabinol
TZD	Thiazolidinedione
VIP	Vasoactive intestinal polypeptide

Declaration

"I hereby declare that for 2 years following the date on which this thesis is deposited in the library of Ulster University, the thesis shall remain confidential with access or copying prohibited. Following expiry of this period, I permit the librarian of the university to allow the thesis to be copied in whole or in part without reference to me on the understanding that such authority applies to the provision of single copies made for study purposed or for the inclusion within the stock of another library.

This restriction does not apply to the British Library Thesis Service (which subject to the expiry of confidentiality, is permitted to copy the thesis on demand for loan or sale under the terms of a separate agreement) nor to the copying publication of the title or abstract of the thesis.

IT IS A CONDITION OF USE OF THIS THESIS THAT ANYONE WHO CONSULTS IT MUST RECOGNISE THAT THE COPYRIGHT RESTS WITH THE AUTHOR AND THAT NO QUOTATION FROM THE THESIS AND NO INFORMATION DERIVED FROM IT MAY BE PUBLISHED UNLESS THE SOURCE IS PROPERLY ACKNOWLEDGED".

Publications arising from Thesis

Publications

McCloskey, A. G., Flatt, P. R., Moore, C. B. T., Nesbit, M.A., Christie, K. A., McKillop, A. M.

CRISPR/Cas9 gene editing and studies in high fat fed mice demonstrate metabolic importance of GPR55 in islet and enteroendocrine cell function

Diabetologia (Submitted)

McCloskey, A. G., Miskelly, M. G., Flatt, P. R., McKillop, A. M.

Acute metabolic actions of selective GPR120 agonists on islet and enteroendocrine cell function and glucose homeostasis in diabetic mice

BBA – General Subjects (Submitted)

Abstracts

McCloskey, A. G., Miskelly, M. G., Flatt, P. R., McKillop, A. M. (2018). Evaluation of the acute metabolic effects and specificity of GPR55 agonists (Abn-CBD and AM251) on islet and enteroendocrine cell function. *Diabetologia*, 61(1): S73-S73 (Oral presentation)

McCloskey, A. G., Miskelly, M. G., MacDonald, M., Flatt, P. R., McKillop, A. M. (2018). Acute metabolic effects and specificity of putative GPR55 agonists using CRISPR/Cas9 gene editing and diabetic mice. *Irish J Med Sci*, 187(5): S183-S183 (Oral presentation)

McCloskey, A. G., Miskelly, M. G., Flatt, P. R., McKillop, A. M. (2018). Acute metabolic effects of activation of GPR120 with selective long-chain fatty acid agonists on islet and enteroendocrine cell function. *Diabetic Medicine,* 35(1): 78-79 (Oral presentation)

McCloskey, A. G., Miskelly, M. G., Flatt, P. R., McKillop, A. M. (2017). Evaluation of the functional role of GPR120 on islet cell function upon biological activation with selective long chain fatty acid agonists. *Irish J Med Sci*, 186(9): S350-S351 (Poster presentation)

McCloskey, A. G., Gormley, N.M., Flatt, P. R., McKillop, A. M. (2017). Expression and regulatory role of G-protein coupled receptor-120 (GPR120) on pancreatic function and Type 2 diabetes. *Diabetic Medicine,* 34(1): 46-46 (Poster presentation)

McCloskey, A. G., Gormley, N.M., Flatt, P. R., McKillop, A. M. (2016). Investigation of the regulatory role of GPR120 receptor on islet function and glucose homeostasis. *Irish J Med Sci*, 185(7): 373-373 (Oral presentation)

Chapter 1

General Introduction

1.1: Pancreas

The pancreas is a vital organ of gastrointestinal system that is located behind the stomach in the abdominal cavity and is composed of both endocrine and exocrine tissue (Bertelli & Bendayan 2005). The functionality of the pancreas includes the regulation of food digestion and energy metabolism (Roder *et al.* 2016). The exocrine pancreas releases digestive enzymes and pancreatic juice that facilitates the breakdown and absorption of nutrients in the gastrointestinal tract (Roder *et al.* 2016). Pancreatic juice contains bicarbonates which can neutralise the acidity of chyme, whilst the secretion of digestive enzymes can help breakdown proteins, lipids and carbohydrates (Lee & Kim 2000).

The endocrine pancreas comprises 1-2% of total pancreatic mass and is referred to as the 'islets of Langerhans' (Steiner *et al.* 2010). Islets are arranged in small clusters and are comprised of 5 different cell types; insulin producing beta cells, glucagon secreting alpha cells, pancreatic polypeptide secreting PP cells, somatostatin secreting delta cells and ghrelin secreting epsilon cells (Steiner *et al.* 2010).

1.1.1: Insulin

Insulin is a peptide hormone that is produced, stored and secreted from the beta cells of the endocrine pancreas (Steiner *et al.* 2010). Insulin is released in response to hormones, glucose, neurotransmitters and other nutrients (Gerber & Rutter 2017). Upon release, insulin regulates the metabolism of glucose, complex carbohydrates, fats and proteins, whilst promoting the absorption of glucose from the circulatory system to peripheral tissues (i.e. muscle, adipose) (Gerber & Rutter 2017). Upon insulin signalling in peripheral tissues, glucose is absorbed then converted to glycogen and/or triglycerides via

glycogenesis and lipogenesis, respectively. Subsequently, insulin is considered the primary anabolic hormone of the body (Otero *et al.* 2014).

Insulin is a 51 amino acid polypeptide that is synthesised within the ribosomes of the endoplasmic reticulum (ER) (Vargas & Sepulveda 2018). Insulin begins synthesis as a large biologically inactive precursor, known as preproinsulin, which is cleaved to form proinsulin within the ER, then transported to the Golgi apparatus (Vargas & Sepulveda 2018). Prohormone convertase 1/3 (PC1/3) and prohormone convertase 2 (PC2) further cleave proinsulin into equal concentrations of both C-peptide and the biologically active insulin (Hoshino *et al.* 2011). Insulin is then densely stored in granules within pancreatic beta cells, prior to the stimulation of insulin release (Rorsman & Renstrom 2003).

The release of insulin from pancreatic beta cells is primarily driven by circulating glucose concentrations (MacDonald *et al.* 2005). Glucose stimulated insulin secretion (GSIS) begins with the absorption of glucose into the pancreatic beta cell by glucose transporter 2 (GLUT2) (MacDonald *et al.* 2005). During the anabolic glycolysis of glucose within the beta cells via the Schiff pathway, the ATP:ADP ratio is increased. Subsequently, potassium ATP (K_{ATP}) channels are closed within the cell resulting in cellular depolarisation (MacDonald *et al.* 2005). In response, voltage dependent Ca^{2+} channels are opened to re-polarise the cell, which results in insulin exocytosis from intracellular insulin storage granules through Ca^{2+} specific protein signalling (MacDonald *et al.* 2005).

Circulating insulin secreted from the pancreas facilitates the absorption of glucose in peripheral tissues by binding to the insulin receptor which mediates the translocation of glucose transporter 4 (GLUT4), thus enabling glucose to enter the cell (Brewer *et al.* 2014)

1.1.2: Glucagon

Glucagon is 29 amino acid peptide hormone that is secreted from the alpha cells of the endocrine pancreas (Wewer-Albrechtsen *et al.* 2016). Alpha cells comprise 15-20% of islet mass and augment glucagon secretion in response to hypoglycaemic blood glucose concentrations (Baetens *et al*. 1979, Briant *et al.* 2017). Upon secretion, glucagon stimulates glycogenesis and gluconeogenesis in the liver, whilst also reducing lipogenesis and triglyceride production (Kalra & Gupta 2016). Glucagon is synthesised from a large precursor peptide called proglucagon (Dhanvantari *et al.* 1996). Proglucagon is differentially cleaved within various cell types to produce a diverse range of bioactive hormones (GLP-1, GLP-2, glicentin, oxyntomodulin, glucagon) (Dhanvantari *et al.* 1996). Within the pancreatic alpha cell, proglucagon is cleaved by PC2 to form glucagon. Secretion of glucagon from alpha cells is mediated by voltage dependent Ca^{2+} channels, which augment glucagon exocytosis in response to low circulating glucose concentrations (Dhanvantari *et al.* 1996, Briant *et al.* 2016).

1.1.3: Somatostatin

Also known as growth hormone-inhibiting hormone (GHIH), somatostatin is secreted by the delta cells of the endocrine pancreas (Steiner *et al.* 2010). Upon secretion, somatostatin is a paracrine inhibitor of insulin, glucagon and PP secretion from pancreatic islet cells (Strowski *et al.* 2000, Henquin *et al.* 2017). The release of somatostatin from the pancreatic islet is triggered by hyperglycaemic glucose concentrations (Ribes *et al.* 1987). In a similar manner to insulin release from beta cells, high glucose concentrations increase the ATP:ADP ratio and augments exocytotic somatostatin release by increasing intracellular Ca^{2+} concentrations (Gopel *et al.* 2000). Somatostatin regulates islet cell function through six different specific somatostatin receptors (sstr), sstr1, sstr2A, sstr2B,

sstr3, sstr4, and sstr5 on the beta, alpha and PP cells, whilst the expression of somatostatin receptor is downregulated in type 2 diabetic islets (Portela-Gomes *et al.* 2010, Henquin *et al.* 2017). GPR120 activation was previously shown to inhibit somatostatin secretion from pancreatic delta cells (Stone *et al.* 2014). Aside from the inhibitory effects of somatostatin towards pancreatic hormone release, somatostatin also decreases the rate of gastric emptying, reduces intestinal motility and supresses the release of other gastrointestinal hormones, including gastrin, cholecystokinin (CCK), secretin, motilin and vasoactive intestinal peptide (VIP) (Krejs 1986, ElSayed & Bhimji 2018).

1.1.4: Pancreatic polypeptide

Pancreatic polypeptide (PP) is a 36 amino acid peptide that is secreted from islet PP cells, which account for approximately 2% of total islet cells and are primarily located at the head of the pancreas (Steiner *et al.* 2010). PP belongs to a family of peptides including neuropeptide Y (NPY) and peptide YY (PYY) (Holzer *et al.* 2013). PP is released postprandial and remains elevated for several hours in humans (Koska *et al.* 2004). Studies have revealed that PP reduces food intake, intestinal motility and decreases exocrine secretions (Koska *et al.* 2004, Schmidt *et al.* 2005). Interestingly, PP responses are blunted in obese children with Prader-Willi syndrome (Zipf *et al.* 1981). Moreover, circulating PP concentrations are greatly reduced in in both rodents and humans with obesity, whilst abnormal circulating concentrations are also associated with eating disorders (Reinehr *et al.* 2006, Yulyaningish *et al.* 2014). PP secretion is almost entirely dependent on the PP cells of the islet and is released via the Ca^{2+} and K_{ATP} channels (Liu *et al.* 1999).

1.2: Gastrointestinal hormones

The gastrointestinal hormones are comprised by a group of hormones that are secreted by the enteroendocrine cells of the stomach and small intestine and purpose to regulate food digestion and energy homeostasis (Rehfeld 2014). Moreover, studies have also demonstrated that gut hormones such as secretin substance P and cholecystokinin can act as neuromodulators in both the central nervous system (CNS) and peripheral nervous system (PNS) (Wank *et al.* 1992, Madva & Granstein 2013). Several gut hormones are known to play a pivotal role in the maintenance of glucose homeostasis, including glucagon-like peptide 1 (GLP-1), glucose-dependent insulinotropic polypeptide (GIP), peptide YY (PYY), oxyntomodulin (OXM), pancreatic polypeptide (PP) and ghrelin (Drucker 2007).

1.2.1: Glucagon-like peptide 1 (GLP-1)

Glucagon-like peptide 1 (GLP-1) is a gastrointestinal hormone secreted from the enteroendocrine L-cells of the duodenum and ileum (Sun *et al.* 2017). GLP-1 synthesised is derived from the proglucagon peptide that undergoes tissue specific posttranslational processing (Sandoval & D'Alessio 2015). The full-length product, produced by the L-cells, is GLP-1 (1-37) that is highly susceptible to proteolytic cleavage and amination which results in the formation of two truncated yet bioactive peptides; GLP-1 (7-36) and GLP-1 (7-37) (Deacon 2004). The shorter bioactive forms of GLP-1 have potent insulinotropic properties in response to glucose (Deacon 2004). In addition, GLP-1 inhibits glucose release, decreases food intake and delays gastric emptying (Gutzwiller *et al.* 1999). The bioactive forms of GLP-1 play a key role in pancreatic beta cell function

and modulate insulin release through the adenylate cyclase pathway increasing cAMP through the phosphorylation of protein kinase A (PKA) (Leech *et al.* 2011). Moreover, GLP-1 increases beta cell mass and increases insulin synthesis whilst inducing cytoprotective effects towards beta cells (Vilsboll 2009, Vasu *et al.* 2014). Although the active forms of GLP-1 play a key role in pancreatic function, they are readily degraded by dipeptidyl peptidase IV (DPP-IV) to the biologically inactive GLP-1 (9-36) and GLP-1 (9-37), which are subsequently excreted by the kidneys (Deacon 2004).

1.2.2: Glucose-dependent insulinotropic polypeptide (GIP)

Glucose-dependent insulinotropic polypeptide (GIP) is a 42 amino acid peptide that is secreted by the enteroendocrine K-cells of the jejunum and duodenum (Deacon 2004). The biologically active form of GIP (1-42) is derived from a 153 amino acid precursor proprotein encoded by the GIP gene (Inagaki *et al.* 1989). PC1/3 cleaves GIP proprotein within the endocrine K-cells to form the bioactive GIP molecule (Ugleholdt *et al.* 2006). Like GLP-1, GIP is also an incretin hormone and enhances GSIS within the pancreatic islet (Gault *et al.* 2003, Rehfeld 2014). In addition, GIP has been shown to play a role in islet cell regeneration through the reduction of beta cell apoptosis and the promotion of beta cell proliferation (Vasu *et al.* 2014). Similar to GLP-1, GIP also modulates insulin release through the adenylyl cyclase and cAMP pathway (McIntosh *et al.* 2012). Aside from effects towards insulin release, GIP is also a weak inhibitor of gastric acid secretin and has only minor effects on gastric emptying (Meier *et al.* 2006). The active form of GIP (1-42) is readily cleaved at the alanine residue at position two by DPP-IV to form the truncated and biologically inactive isoform GIP (3-42) (Deacon 2004).

1.2.3: Peptide YY (PYY)

Peptide YY (PYY) is a short 36 amino acid peptide that is secreted by the L-cells of the colon and ileum postprandial (Ballantyne 2006). The primary physiological function of PYY is to attenuate appetite and reduce food intake (Ballantyne 2006). The circulating concentration of PYY increases after food intake and lowers when fasting. There are two isoforms of PYY; PYY (1-36) and PYY (3-36). PYY (1-36) is directly secreted from the enteroendocrine cells of the gut then cleaved to form PYY (3-36) by DPP-IV (Batterham & Bloom 2003). Interestingly, the shorter isoform PYY (3-36) is the most biologically active form of PYY and activates the Y2 receptor to induce appetite suppression (Hung *et al.* 2004). In addition, PYY demonstrates effects in pancreatic beta cells within the endocrine pancreas (Lafferty *et al.* 2018). Although, PYY has no effect towards insulin release, it has been shown to increase beta cell proliferation and enhance beta cell mass (Lafferty *et al.* 2018).

1.2.4: Cholecystokinin (CCK)

Cholecystokinin (CCK) is a peptide hormone that is secreted from the I-cells of the gut and exhibits similar structure to the gastrointestinal hormone gastrin (Rehfeld *et al.* 2007). Gastrin and CCK share the same five amino acid residues at the C-terminus, however CCK can be composed of a various number of amino acids based on the posttranslational modification of the 150 amino acid CCK precursor, preprocholecystokinin (Rehfeld *et al.* 2007). Resultingly, CCK can exist in several isoforms, including CCK5, CCK7, CCK8 and CCK12 (Rehfeld 2017). In the gut, CCK has a range of physiological functions including satiety and digestion (Rehfeld 2017). Medium chain fatty acids are the most potent stimulators of CCK secretion from the mucosal lining of the small intestine, however, its half-life is very short when in circulation (McLaughlin *et al.* 1998). With

respect to the endocrine pancreas, CCK stimulates insulin release from pancreatic beta cells through the activation of phospholipase C (PLC) and protein kinase C (PKC) (Ning *et al.* 2015).

1.2.5: Oxyntomodulin (OXM)

Oxyntomodulin (OXM) is a short 37 amino acid peptide that is secreted from the enteroendocrine L-cells of the intestine, with synthesis deriving from the proglucagon precursor polypeptide (Pocai 2013). OXM is released from the gut in response to nutrient ingestion and is cleaved by DPP-IV for clearance (Yi *et al.* 2015). Although the mechanistic function of OXM is not fully understood, studies have shown it to bind to both the GLP-1 and glucagon receptors (Pocai 2013). OXM decreases body weight, increases energy expenditure, attenuates appetite and improves glucose tolerance in humans (Pocai 2013, Pathak *et al.* 2015). Interestingly, OXM stimulates weight loss beyond the capabilities of selective GLP-1 agonists (Pocai 2013).

1.3 Diabetes mellitus

Diabetes mellitus (DM) is a chronic metabolic disease that is associated with hyperglycaemic blood glucose concentrations over an extended period (Lebovitz 2001). Healthy, non-diabetic individuals maintain glucose homeostasis through glucose stimulated insulin secretion (GSIS) from the endocrine pancreas (Lebovitz 2001). Insulin secreted from pancreatic beta cells facilitates the absorption of circulating glucose to peripheral tissues (i.e. muscle and adipose tissue), thus lowering blood glucose concentrations (Briant *et al.* 2017). In diabetic patients, hyperglycaemic blood glucose

concentrations are a symptomatic result of pancreatic beta cell dysfunction resulting in insufficient insulin release and/or impaired insulin signalling in peripheral tissues, resulting in reduced glucose absorption (Cerf 2013).

Common symptoms associated with diabetes include polyuria, polyphagia polydipsia, impaired eyesight and fatigue (Hharroubi & Darwish 2015). Moreover, various health complications may arise as the prognosis of the disease deteriorates. Acute complications most commonly linked with diabetes includes hypoglycaemia, hyperglycaemia hyperosmolar syndrome (HHS) and diabetic ketoacidosis (DKA) (Gosmanov *et al.* 2000). In addition, adverse chronic health complications can develop in severe circumstances, including chronic kidney failure, diabetic retinopathy, cardiovascular disease, stroke, amputations and foot ulcers (Hung *et al.* 2017).

At present, diabetes is prevalent in all ethnical backgrounds and is associated with individuals of all ages (Zheng *et al.* 2018). Clinical studies have demonstrated that the incidence of diabetes is typically higher in African-Americans and Hispanic-Americans, when compared to Non-Hispanic Whites (Mercader & Florez 2017). Studies presenting these findings have indicated that genetic predisposition correlates with the incidence of the disease within ethnicities (Mercader & Florez 2017). However, studies have also indicated that the prevalence of diabetes in is strongly linked with dietary and lifestyle choices, which are typified by the consumption of high-sugar/high-fat food coupled with exceedingly low levels of exercise (Appuhamy *et al.* 2014).

Diagnosis of a pre-diabetic individual can be identified by impaired glucose tolerance and impaired fasting blood glucose concentrations (Lebovitz 2001). In accordance to the American Diabetes Association (ADA), criteria used to diagnose the disease include a non-fasting blood glucose concertation >11.1 mmol/l, fasting blood glucose >7.0 mmol/l,

>11.1 mmol blood glucose post two-hour oral glucose tolerance test (OGTT) and >48 mmol/l HbA1c (American Diabetes Association 2014).

Recent figures demonstrate that diabetes is a global epidemic with 3.3 million sufferers diagnosed within the United Kingdom alone (Howells *et al.* 2016). Over the past two decades, data trends have documented the incidence of the disease to be increasing at an alarming rate, with a projection of 5 million patients with diabetes to be diagnosed within the United Kingdom by 2025 (Howells *et al.* 2016). Subsequent treatment costs cast a substantial financial burden towards government expenditure and the NHS (Elbich *et al.* 2017). Although the onset of diabetes is not linked with one origin, factors including diet, exercise, genetic predisposition, general health and environmental factors greatly contribute (Fletcher *et al.* 2002).

1.3.1: Type 1 diabetes

Type 1 diabetes is characterised by hyperglycaemia and low circulating insulin concentrations due to auto-immune destruction of pancreatic beta cells which are responsible for the production and release of insulin (Paschou *et al.* 2018). Type 1A (autoimmune) and type 1B (idiopathic) are two further subdivisions of type 1 diabetes (Paschou *et al.* 2018). Type 1B diabetes involves destruction of pancreatic beta cells with no evidence of autoimmunity. This classification is due to genetic inheritance and is strongly linked associated with individuals of African and Asian descent (Paschou *et al.* 2018).

Type 1A diabetes is derived from autoimmune destruction of insulin-producing pancreatic beta cells (Michels & Gottlieb 2000). The onset of this disease can occur at any age; however, it is commonly diagnosed at early developmental stages. Globally, type

1 diabetes accounts for 5-10% of all diabetes (Michels & Gottlieb 2000). Two predominant antibodies are responsible for the autoimmune destruction of beta cells; anti-insulin antibodies (IAA) and anti-islet cell antibodies (ICA) and are expressed in 50% and 70-80% of type 1A diabetic patients, respectfully (Michels & Gottlieb 2000).

Current therapies for type 1 diabetes are limited and patients are typically required to frequently administer synthetic insulin to maintain glucose homeostasis (McCall & Farhy 2013). Currently, the restoration of endocrine-pancreatic function, including the production of endogenous insulin in patients with type 1 diabetes requires pancreatic transplantation (Lerner 2008). The frequency and success rate of this method has improved drastically in recent years; however, the cost of the procedure and donor availability remain substantial limitations (Lerner 2008).

1.3.2: Gestational diabetes

Currently, gestational diabetes (GDM) is a metabolic disorder that affects 13.2% of pregnant woman worldwide (Melchior *et al.* 2017). Women that are genetically linked with the onset of diabetes and/or have previously experienced pregnancy complications are at an increased risk for the development of GDM (Melchior *et al.* 2017). Obesity, large foetal development and late-age pregnancies are factors that contribute to the pathophysiology of the disease, however, only 50% of pregnant woman display the predominant risk factors associated with GDM (Melchior *et al.* 2017).

Due to the prevalence of GDM, women are typically screened for the disease at week 24 of pregnancy for signs of impaired glucose tolerance (Rani & Begum 2016). Biochemical characteristics of GDM include hyperglycaemia, dyslipidaemia and hyperinsulinemia (Rani & Begum 2016). Following diagnosis, patients are typically treated with dietary

intervention rather than anti-diabetic medications (Hernandez *et al.* 2013). Nutritional plans ensure the preservation of maternal and neonatal health, whilst preventing the incidence of hyperglycaemia and ketosis (Hernandez *et al.* 2013). Patients that experience GDM are at a 4- to 7- fold greater risk of developing type 2 diabetes within 5-10 years prior diagnosis (Herath *et al.* 2017).

1.3.3: Type 2 diabetes

Type 2 diabetes is the most prevalent class of type of diabetes and accounts for 90-95% of all diabetes worldwide (American Diabetes Association 2009). Characteristics of type 2 diabetes include hyperglycaemia, insulin resistance and increased hepatic glucose production (Petersen *et al.* 2017). Increased production of glucose from the liver accompanied with increased insulin resistance promotes the production of insulin form pancreatic beta cells (Cerf 2013). The production of insulin beyond normal physiological concentrations results in beta exhaustion after an extended period. Ultimately, pancreatic beta cell exhaustion leads to inadequate insulin production and hyperglycaemia (Cerf 2013).

Numerous studies have correlated prevalence of diabetes with other metabolic diseases, including obesity, cardiovascular disease (CVD) and kidney failure, with findings demonstrating 85% of patients with type 2 diabetes to be above the recommended body mass index (BMI) (Leon & Maddox 2015, Jerant *et al.* 2015). The link between diabetes and obesity has become an area of interest in the development of novel anti-diabetic therapeutics. Type 2 diabetics typically display other symptoms of metabolic syndrome including hypertension and dyslipidaemia, which greatly increases the risk of CVD (Leon & Maddox 2015).

Pre-diabetic and moderate cases of type 2 diabetes are commonly counteracted with dietary intervention and exercise (Senechal *et al.* 2014). However, anti-diabetic pharmaceuticals are often required to improve the prognosis of the disease (Rojas & Gomes 2013). At present, orally available biguanides are the first line of treatment, accompanied with dietary intervention (Rojas & Gomes 2013). In more severe circumstances, administration of synthetic insulin is often required, however, the frequency of the treatment and route of administration (parental) is undesirable for many patients (Swinnen *et al.* 2009).

1.3.3.1: Pancreatic beta cell dysfunction

Type 2 diabetes is typified by beta cell dysfunction reduced beta cell mass (Cerf 2013). Chronic exposure to hyperglycaemia directly affects beta cell function by impairing insulin synthesis and insulin secretion through the disruption of gene transcription and cell secretory mechanics (Cernea & Dobreanu 2013). Upon absorption into the beta cell via GLUT1/GLUT2, glucose undergoes anaerobic glycolysis and produces reactive oxygen species (ROS); a direct bi-product that impairs gene transcription at super-physiological concentrations (Gerber & Rutter 2017). ROS and reactive nitrogen species (RNS) can induce DNA damage, form glycated end products and generate alternate ATP production in the beta cell, which can directly affect cellular insulin responses to glucose (Gerber & Rutter 2017). In addition, increased oxidative stress derived from hyperglycaemia causes increased intra-islet peroxide concentrations which overload the anti-oxidant capabilities of the pancreatic beta, resulting in beta cell failure (Robertson & Harmon 2007). Moreover, elevated intra-islet peroxide concentrations are correlated with defects in PDX-1 transcription; an essential factor for proinsulin processing (Robertson & Harmon 2007).

The multi-factorial process of beta cell dysfunction remains not fully understood; however, studies have demonstrated that increased oxidative stress, cytokines, free fatty acid (FFA), inflammation and cellular organelle stress play a key role in its onset (Cerf 2013). Pro-inflammatory cytokines have been heavily linked with beta cell dysfunction and have been shown to potentiate defective insulin release and increase beta cell apoptosis, through the induction of mitochondrial stress (Nordmann *et al.* 2017).

Chronic exposure to elevated circulating concentrations of FFA as a result of a high-fat/high-sugar diet can directly disrupt the glycolysis pathway, thus impairing insulin biosynthesis, insulin secretion and cellular proliferation (Acosta-Montano & Garcia-Gonzalez 2018). Moreover, increased concentrations of exocrine and intra-islet fat deposits derived from FFAs can directly de-sensitise GSIS and increase islet inflammation and beta cell apoptosis (Murakami *et al.* 2017).

1.3.3.2: Insulin resistance

Insulin resistance in peripheral tissues is a predominant characteristic of type 2 diabetes, which results in reduced glucose absorption to peripheral tissues (muscle, adipose, liver) (Cerf 2013). In response to impaired glucose absorption, pancreatic beta cells produce additional concentrations of insulin to maintain glucose homeostasis, which can ultimately result in beta cell exhaustion (Cerf 2013). Circulating insulin binds to the insulin receptor on peripheral tissues, a tyrosine kinase receptor that stimulates an intracellular signalling cascade within the cell (Ijuin & Takenawa 2012). Upon activation, insulin receptor substrate 1 (IRS-1) is phosphorylated and mediates the translocation of glucose transporter 4 (GLUT4) (Ijuin & Takenawa 2012). The translocation of GLUT4 from the cytosol to the cell surface involves the inactivation of intracellular Rab proteins, which function to withhold GLUT4 within the cytosol (Sano *et al.* 2003). Once

translocated to the cell membrane, GLUT4 facilitates the absorption of glucose from the bloodstream into the cell (Sano *et al.* 2003). In type 2 diabetes, the translocation of GLUT4 to the cell surface is reduced due to impaired insulin-receptor activation (Cerf 2013). Although the exact pathophysiology of insulin resistance is not fully understood, high-fat/high-calorie diets, reduced physical activity and weight gain are correlated with its pathophysiology (Cerf 2013).

1.4: Current therapies for type 2 diabetes

Maintaining glucose homeostasis is the primary objective for all anti-diabetic therapeutics. The prognosis of type 2 diabetes can be improved with dietary intervention and lifestyle changes (Senechal *et al*. 2014). Studies have shown that calorie restriction diets and exercise can greatly improve the symptoms and onset of the disease (Senechal *et al*. 2014). However, in more severe instances, pharmaceuticals are required to maintain physiological glucose concentrations. At present, metformin (Glucophage) is the first line of treatment with diet and exercise (Rojas & Gomes 2013). Alternative types of treatment are then considered for non-responders or when adverse side effects are observed, including sulphonylureas, incretin mimetics and DPP-IV inhibitors (Figure 1.1).

1.4.1: Alpha-glucosidase inhibitors

Alpha-glucosidase inhibitors are a range of oral anti-diabetic drugs that inhibit the digestion of complex carbohydrates and sugars into monosaccharides (Kalra 2014). Acarbose, Miglitol and Voglibose are approved examples of this drug classification that inhibit that action of the alpha-glucosidase enzymes of the small intestine, thus reducing

glucose elevations postprandial (Derosa & Maffioli 2012). Although considered safe, this drug class is not commonly prescribed for the treatment of type 2 diabetes. Common side effects of alpha-glucosidase inhibitors include abdominal bloating, flatulence and diarrhoea, whilst the risk of hypoglycaemia is also presented (Derosa & Maffioli 2012).

1.4.2: Biguanides

Biguanides including metformin (Glucophage), buphormin and phenformin are a class of anti-diabetic drugs that reduce hepatic glucose production, thus lowering blood glucose concentrations (Bailey 1992). At present, metformin is the first line of treatment for type 2 diabetic patients accompanied with dietary intervention and exercise (Rojas & Gomes 2013, American Diabetes Association 2014). In addition, biguanides enhance insulin sensitivity and lower the absorption rate of glucose, with beneficial effects also demonstrated towards macrovascular complications such as dyslipidaemia and CVD risk (Palumbo 1998). Although the exact mechanism of metformin remains elusive, the primary effect of this drug is to acutely decrease hepatic glucose production, predominately mediated through mild and transient inhibition of the mitochondrial respiratory-chain complex 1 (Viollet *et al.* 2012). Studies have demonstrated metformin to enhance insulin receptor activation and GLUT4 translocation in peripheral tissues (Lee *et al.* 2012). Further findings have also shown metformin to lower plasma DPP-IV activity and enhance exogenous GLP-1 action, thus indirectly enhancing GSIS and islet cell function.

Aside from potent antihyperglycaemic properties, metformin is also exhibits numerous additional beneficial effects including improvements in endothelial dysfunction, hemostasis and oxidative stress, insulin resistance, lipid profiles and fat redistribution

(Rojas & Gomes 2013). Metformin is typically prescribed as a monotherapy and omits the risk of hypoglycaemia (Rojas & Gomes 2013, Chaudhury *et al.* 2017).

1.4.3: Sulphonylureas

Sulphonylureas are a common class of anti-diabetic drug used to treat patients with chronic hyperglycaemia (Rendell 2004). Glipizide and Glimepiride are examples of sulphonylureas that target the sulphonylurea receptor (SUR) on pancreatic beta cells to stimulate insulin release (Rendell 2004). Upon activation of the SUR receptor, K_{ATP} are closed which influences an influx of Ca^{2+} leading to insulin exocytosis from intracellular storage granules (Rendell 2004). Hypoglycaemia is the major risk factor associated with this class of pharmaceuticals as activation of the SUR receptor is not glucose dependent (Sola *et al.* 2015). In addition, a range of adverse side effects may also be displayed, including excessive weight gain, beta cell apoptosis and increased CVD risk (Sola *et al.* 2015).

1.4.4: Meglitinides:

Functionally similar to sulphonylureas, meglitinides are a class of anti-diabetic drug that enhances insulin release from pancreatic beta cells through cellular depolarisation with the K_{ATP} channels (Black *et al.* 2007). Repaglinide (Prandin) and nateglinide (Starlix) are examples of meglitinides that present a decreased risk of hypoglycaemia due to a shorter circulating half-life of 4-6 hours (Black *et al.* 2007). Administration of meglitinides occurs pre-prandial to facilities the clearance of glucose from the bloodstream postprandial (Guardado-Mendoza *et al.* 2013). Side effects include weight gain and

gastrointestinal discomfort, whilst the onset of hypoglycaemia is also possible (Stein *et al.* 2013).

1.4.5: Thiazolidinediones

The glucose lowering effect of thiazolidinediones (TZDs), also known as Glitazones is derived from increased insulin sensitivity in peripheral tissues and decreased glycogenolysis in the liver (Diamant & Heine 2003). TZDs bind to the PPAR-gamma receptor which stimulates the activation of several genes that promote glucose uptake in peripheral cells, whilst reducing hepatic glucose production (Diamant & Heine 2003). Additional beneficial effects of this drug class include improved lipid profile and reduced hypertension (Barnett 2009). However, a range of adverse effects are also associated with TZDs, including water retention, weight gain and liver/kidney toxicity (Quinn *et al.* 2008).

1.4.6: Sodium glucose co-transport 2 inhibitors

Sodium glucose co-transport 2 inhibitors (SGLT2 inhibitors) are used to treat type 2 diabetes by reducing glucose reabsorption in the kidney (Hattersley & Thorens 2015). SGLT2 is highly expressed in the epithelial cells of the proximal tubule and depends on GLUT1/GLUT2 for glucose excretion. Inhibiting SGLT2 lowers blood glucose concentrations by increasing urinary glucose excretion (Hattersley & Thorens 2015). As this mechanism is insulin-independent, the risk of hypoglycaemia is very low (Monica-Reddy & Inzucchi 2016). Currently, SGLT2 inhibitors such as Dapagliflozin and Canagliflozin are second- or third-line treatments for type 2 diabetes as other drugs (e.g. metformin) have longer safety records and are less expensive (Johnston *et al.* 2017). Side

effects of SGLT2 inhibitors include urinary tract infections, mycotic infections and osmotic diuresis (Singh & Kumar 2018).

1.4.7: Incretin mimetics

The endogenous GLP-1 and GIP enteroendocrine hormones play a pivotal role in the maintenance of glucose homeostasis by enhancing GSIS and reducing hyperglucagonemia (Green & Flatt 2007). However, both peptides are readily cleaved by DPP-IV and have very short half-lives in circulation (Tarantola *et al.* 2012). Incretin mimetics, primarily GLP-1 analogues, have been designed to avoid enzymatic degradation, thus prolonging their circulating half-life and bioactivity (Green & Flatt 2007). Liraglutide (Victoza) and exenatide (Byetta) are the two most common synthetic GLP-1 analogues currently available for the treatment of type 2 diabetes (Jackson *et al.* 2010). Victoza has 97% sequence homology with the human GLP-1 sequence with an Arg^{34}Lys amino acid replacement accompanied with a glutamic acid and C-16 free fatty acid linkage to Lys26. The structural design promotes non-covalent binding to albumin and prolongs the biological half-life so that only one dose daily is required (Jackson *et al.* 2010). Byetta is derived from salivary glands of the Gila monster and displays 53% sequence homology with human GLP-1 sequence, with once daily administration required (Furman 2012). Longer acting analogues of exenatide and liraglutide are also available with once weekly administration (Christensen & Knop 2010). The major limitation associated with incretin mimetics is the route of administration (subcutaneous), which is unfavourable for many patients with diabetes. Aside from improving glucose homeostasis, GLP-1 mimetics have been also shown to improve weight loss and insulin sensitivity without the risk of hypoglycaemia (Green & Flatt 2007). However, adverse effects such as vomiting, nausea and gastrointestinal discomfort have been reported in

with GLP-1 mimetics (Gupta 2013). Recently, a once weekly dual GIP/GLP-1 agonist (LY3298176) has shown clinical promise in patients with type 2 diabetes and may emerge as a leading therapeutic (Frias *et al.* 2018).

1.4.8: DPP-IV inhibitors

DPP-IV inhibitors are a novel class of orally available anti-diabetic therapeutics that inhibit the function of DPP-IV. DPP-IV is involved in the degradation of several glucoregulatory hormones and is expressed in numerous tissues throughout the body (Tarantola *et al.* 2012). Inhibition of DPP-IV impairs the rapid degradation of the key incretin hormones GLP-1 and GIP. DPP-IV cleaves both GLP-1 (7-36) and GIP (1-42) at the Pro and Ala amino acids at the second position on the N-terminus, resulting in biologically inactive truncated peptides (Deacon 2004). Approved DPP-IV inhibitors such Sitagliptin, Vidagliptin and Saxagliptin are typically used as a second or third line of medication after metformin and sulphonylureas. In addition to the beneficial effects towards glycaemic control, DPP-IV inhibitors have been shown to enhance weight loss and induce appetite suppression without the risk of hypoglycaemia (Ahren 2009). Side effects associated with DPP-IV inhibitors include flu-like symptoms, skin reactions and gastrointestinal discomfort (Ahren 2009).

1.4.9: Combinational therapies

Due to the limitations of current therapies for the treatment of type 2 diabetes and complications associated with the disease, combinational therapies are often utilised to improve patient prognosis (American Diabetes Association 2018). Dual therapies are often considered to reduce the risk of major adverse cardiovascular events. Metformin in

combination with incretin mimetics and DPP-IV inhibitors are most commonly prescribed dual therapies as they are anti-hyperglycaemic agents that reduce the risk of hypoglycaemia and cardiovascular disease, whilst enhancing islet cell regeneration (American Diabetes Association 2018). In addition, dual and triple agonist therapies have also become a promising therapeutic approach with interest focusing on synergistic activation of the incretin receptors (Naylor *et al.* 2016, Frais *et al.* 2018).

1.5: G-protein coupled receptors (GPCRs)

G-protein coupled receptors (GPCRs), also known as seven transmembrane domain receptors (7TM) are the largest family of membrane bound receptors expressed within the human genome (Rosenbaum *et al.* 2009). In recent years, research has intensified on discovering the structure and function of novel GPCRs, mainly through GPCR sequencing and cloning. Findings from the Human Genome Project in 2001 revealed that the number of GPCRs expressed in humans was greatly underestimated (Takeda *et al.* 2002). Subsequently, research investigating the biological function of orphan GPCRs was spurred. Due to the independent downstream signalling cascades stimulated upon receptor activation, GPCRs have been recognised as potential therapeutic targets (Fang *et al.* 2015). GPCRs play a key role at a cellular level and regulate a diverse range of physiological functions, including cell secretions, immune responses, neurological signalling and cellular growth (Fang *et al.* 2015). At present, GPCRs are the direct target of over 700 FDA approved drugs, which account for approximately 35% of all drugs currently prescribed (Sriram & Insel 2018). Non-olfactory GPCRs are primarily targeted by small molecule and peptide ligands, however, the biological function of numerous GPCRs remains largely unknown (Laschet *et al.* 2018).

1.5.1: GPCR classifications

GPCRs can be divided into six separate classifications (A-F) based on their structure and biological function; rhodopsin-like (class A), secretin-like (class B), metabotropic glutamate (class C), pheromone (class D), cAMP (class E) and frizzled (class F) (Peng *et al.* 2010). Rhodopsin-like, secretin-like, metabotropic glutamate and frizzed GPCRs are expressed within mammalian systems, whilst pheromone and cAMP GPCRs are exclusively found in fungal species and amoeba (*Dictyostelium discoideum*), respectively (Peng *et al.* 2010). Further sub-divisions of GPCRs can be made within primary classifications based on ligand binding and biological functionalities (Peng *et al.* 2010).

The rhodopsin-like (Class A) family represents the largest class of GPCRs expressed in mammalian organisms and is comprised of 701 independent receptors (Zhang *et al.* 2015). These receptors are abundantly expressed in numerous tissues, particularly within sensory organs such as the eye (Palczewski 2006). Subsequently, rhodopsin-like GPCRs have been previously isolated from bovine retina and have been characterised with respect to structure more than the other GPCR classifications (Palczewski 2006). Moreover, rhodopsin-like GPCRs are the most structurally stable, enabling extensive characterisation through experimental endurance (Palczewski 2006).

The secretin-like (Class B) family of GPCRs are typically activated by peptides and other large protein-based ligands leading to Gαq and Gαs signalling (Hollenstein *et al.* 2014). Class B receptors are involved in the detection of numerous pancreatic and gastrointestinal hormones, including glucagon, incretins (GLP-1, GIP), vasoactive intestinal hormone (VIP), secretin, parathyroid hormone and calcitonin (Nordstrom *et al.* 2009). Secretin-like receptors are important regulators of energy metabolism and glucose homeostasis (Nordstrom *et al.* 2009).

Metabotropic glutamate (Class C) receptors function as neurotransmitters and are the family of GPCRs responsible for indirect metabotropic signalling, mediating through the associated glutamate residue (Wu *et al.* 2014). This family of GPCRs are abundantly expressed in pre-synaptic and post-synaptic neurons of the cerebral cortex, cerebellum and hippocampus (Niswender & Conn 2010). Subsequently, Class C GPCRs regulate responses within both the peripheral and central nervous systems with receptor activation controlling memory, learning, mood and pain sensitisation (Javitt *et al.* 2011). Studies have identified the pathophysiological role and therapeutic potential of metabotropic glutamate receptors in neurodegenerative diseases such as Parkinson's disease, schizophrenia and generalised anxiety disorder (Chun *et al.* 2012).

Frizzled (Class F) GPCRs are the family of receptors that modulate Wnt signal transduction that facilitates the transfer of cellular responses from cell surface receptors (Katanaev 2012). Frizzled receptors stimulated on the cell membrane activate the cytoplasmic dishevelled phosphoprotein through both canonical and non-canonical Wnt signalling pathways (Gonzalez-Sancho *et al.* 2004). Activation of frizzled receptor signalling can regulate a range of cellular responses, including gene transcription, intracellular calcium concentrations and cytoskeleton dynamics (Huang & Klein 2004).

There are a total of 1265 GPCRs expressed in the human genome, however, the physiological function of only 800 is understood (Kobilka 2007, Insel *et al.* 2012). The endogenous ligands for many GPCRs remains elusive yet the number of orphan receptors is in constant decline due to progressing research utilising GPCR targeting therapeutics (Insel *et al.* 2012). Recent studies have suggested that the majority of human GPCRs act as olfactory receptors by inducing responses to taste, sight and smell. However, approximately 342 non-olfactory GPCRs are also expressed and have been recognised as potential therapeutic targets (Fredriksson *et al.* 2003).

1.5.2 GPCR structure and signalling cascades

All GPCRs are comprised of 7 hydrophobic transmembrane domains accompanied with an intracellular carboxyl terminus and an extracellular amino terminus (Peng *et al.* 2010). The extracellular loops of the membrane bound receptor are stabilised by disulphide bonds formed between two cysteine amino acid residues (Rosenbaum *et al.* 2009). An intact G-protein comprised of three individual subunits (Gα, Gβ, Gγ) completes the intracellular portion of the receptor (Rosenbaum *et al.* 2009). The subunits of the G-protein can be further subdivided with Gα containing 4 classes, Gβ containing 5 classes and Gγ containing 12 classes (Syrovatkina *et al.* 2016). Upon ligand binding and GPCR activation, receptor dependent G-protein subunits are phosphorylated, thus inducing the activation of downstream receptor signalling through secondary messenger pathways (Syrovatkina *et al.* 2016).

The transmembrane domains within all classifications of GPCRs exhibit similar sequence homology, whilst variations are notably present in the extracellular amino terminus and in the TM5/TM6 loops of the intracellular carboxyl terminus (Kobilka 2007). Overall, the greatest degree of structural diversity between independent GPCRs exists in the extracellular amino terminus, with sequence length ranging from 10-600 amino acid residues (Kobilka 2007). Short 10-15 amino termini are typically associated with peptide and small molecule binding, whilst longer 350-600 amino acid termini are linked with glutamate and glycoprotein GPCRs (Kobilka 2007).

Agonist binding typically stimulates downstream GPCR signalling, whilst constitutive phosphorylation of intracellular G-protein subunits may also occur in unbound receptors (Syrovatkina *et al.* 2016). In most cases, the downstream response induced by GPCR activation is directly proportional to the potency of the ligand at the receptor binding sites (Rozenfeld & Devi 2011). Numerous ligands can exist for the activation of an individual

GPCR; ligands inducing full activation of the receptor are referred to as 'agonists', whilst ligands that influence submaximal stimulation of a given receptor are known as 'partial agonists' (Basith *et al.* 2018). Contrastingly, antagonist binding inhibits receptor activation by competitively blocking receptor binding sites and demonstrates no effect towards basal activity (Basith *et al.* 2018). The downstream signalling cascade stimulated by a given receptor directly correlates to the efficacy of the bound ligand (Basith *et al.* 2018).

Upon agonist binding, receptor activation begins with a conformational change within the membrane bound G-protein that catalyses the generation of guanosine triphosphate (GTP) in exchange for guanosine diphosphate (GDP) (Yen *et al.* 2017). As a result of this exchange, the Gα subunit is dissociated from the intact G-protein at the cell membrane into the cytosol and stimulates the receptor dependent signalling cascade (Kobilka 2007). The four independent Gα subunits (Gαq, Gαs, Gαi, Gα12/13) determine the secondary messenger signalling pathway upon receptor activation (Figure 1.2) (Syrovatkina *et al.* 2016).

Activation of Gαq primarily couples to the beta isoform of phospholipase C (PLC), resulting in inositol trisphosphate (IP_3) and diacylglycerol (DAG) secondary messenger signalling, which can lead to mitogen activation protein kinase (MAPK) phosphorylation and/or release of intracellular Ca^{2+} from the ER (Figure 1.4) (Zhang & Shi 2016). The Gα12/13 subunit generates no effects towards secondary messenger signalling pathways; instead activates RhoGEFs such as Rho-, Rac- and Cdc42-like GTPases (Figure 1.5) (Siehler 2009). The Gαs intracellular subunit directly stimulates adenylyl cyclase signalling, resulting in cAMP production and PKA activation (Billington & Penn 2003). In contrast, the Gαi subunit inhibits adenylyl cyclase leading to attenuated cAMP production (Billington & Penn 2003). Coupling to other secondary messenger molecules

including PLC and K_{ATP} is also linked with Gαi signalling (Billington & Penn 2003). Although lesser understood, the Gβ and Gγ subunits have also been shown to modulate PLC, PKA and adenylyl cyclase signalling (Syrovatkina *et al.* 2016). Following agonist dissociation and receptor deactivation, GTP is hydrolysed to GDP and the G-protein re-associates to the cell membrane (Figure 1.3) (Yen *et al.* 2017).

1.5.3: GPCRs involved in energy homeostasis

Numerous GPCRs play a pivotal role in the maintenance of glucose homeostasis by controlling glucoregulatory and gastrointestinal hormone release (Moran *et al.* 2016). At present, 293 GPCRs have been identified in human islets with activation mediated by a wide range of structurally diverse ligands, including lipids, peptides, macromolecules and monatomic ions (Amisten *et al.* 2013). Activation of specific GPCRs on pancreatic islet cells can potentiate insulin, glucagon and somatostatin secretion, thus controlling circulating blood glucose concentrations (Amisten *et al.* 2013). In addition, GPCRs present on the enteroendocrine cells of the gut can regulate the release of incretins (GLP-1, GIP) and other gastrointestinal hormones in response to the influx of carbohydrates, proteins and lipids (Moran *et al.* 2016).

1.5.4: GLP-1 receptor

The GLP-1 receptor (GLP1R) is a GPCR abundantly expressed in pancreatic islet cells. GLP1R is expressed on chromosome 6 of the human genome and encodes 463 amino acids upon translation (Lee & Lee 2017). With respect to receptor binding, GLP1R contains two binding domains; one transmembrane domain that binds to the N-terminal region of GLP-1 and one extracellular domain that binds to the C-terminal helix of GLP-

1 (Dods & Donnelly 2015). Upon GLP1R agonism, the Gαs subunit is phosphorylated leading to cAMP production through the adenylyl cyclase pathway (Green *et al.* 2004). Pancreatic activation of GLP1R augments insulin release from beta cells whilst attenuating glucagon secretion from alpha cells (Green *et al.* 2004). Moreover, studies have shown that GLP-1 enhances beta cell proliferation and impairs beta cell apoptosis by upregulating pancreas duodenal homebox-1 (PDX-1) expression (Li *et al.* 2005). GLP-1 mimetics exenatide and liraglutide are longer lasting analogues of GLP-1 that activate the GLP-1 receptor, whilst exendin (9-39) is an antagonist (Gupta 2013). GLP1R is expressed in numerous tissues including the intestines, brain, kidneys, nervous system and lungs (Muscogiuri *et al.* 2014). Interestingly, activation of the GLP1R promotes weight loss and exhibits neuroprotective effects in the brain (McIntyre *et al.* 2013, Muscogiuri *et al.* 2014).

1.5.5: GIP receptor

The GIP receptor (GIP-R) gene is expressed on chromosome 19 and encodes a 466 amino acid protein (Gremlich *et al.* 1995). Similar to the GLP-1 receptor, GIP agonism results in activation of Gαs signalling which increases cAMP production and PKA phosphorylation (Green *et al.* 2004). GIP-R is expressed in numerous tissues throughout the body including the pancreas, intestines brain, bone, heart, adipose and circulatory vasculature (Baggio & Drucker 2007). Activation of GIP-R in pancreatic beta cells augments insulin release, hence GIP is categorised as an incretin (Green *et al.* 2004). In patients with type 2 diabetes, the biological activity of GIP is greatly impaired with GIP-R desensitisation suspected as the primary pathophysiological source (Knop *et al.* 2007). The native 42 amino acid GIP molecule exhibits an unfavourable pharmacokinetic profile due to its weak biological activity and effectiveness in the treatment of type 2 diabetes

(Irwin *et al.* 2006). Subsequently, longer acting GIP analogues with increased enzymatic stability have been synthesised to enhance the actions of the GIP receptor (Irwin *et al.* 2006). GIP-R activation also plays a key role in fat deposition and lipid metabolism (Gault *et al.* 2003). Interestingly, antagonism of the GIP-R can alleviate obesity-associated metabolic impairments that are commonly linked with type 2 diabetes (McClean *et al.* 2007).

1.5.6: Glucagon receptor

The glucagon receptor (GCGR) is a 477 amino acid protein that is expressed on chromosome 17 of the human genome (Menzel *et al.* 1994). Agonism of GCGR primarily stimulates activation of the Gαs intracellular G-protein, accompanied with Gαq activation to a lesser extent (Li & Zhuo 2007). Subsequently, glucagon binding stimulates cAMP production and PKA activation through the adenylyl cyclase pathway (Li & Zhuo 2007). Glucagon receptors are abundantly expressed within the endocrine-pancreas, liver and kidney (Brubaker & Drucker 2002). Lower expression is also found in intestine, heart, spleen, brain and adipose tissues (Brubaker & Drucker 2002). Hepatic GCGR activation result in PKA phosphorylation and augments glycogenolysis to increase blood glucose concentrations (Brubaker & Drucker 2002). Native glucagon is a full agonist for GCGR activation, whilst OXM acts as a partial-agonist (Kerr *et al.* 2010). Adomeglivant and L-168,049 are potent GCGR antagonists and emit glucose-lowering effects *in-vivo* (Casieri *at al.* 1999).

1.5.7: Neuropeptide Y receptors

Neuropeptide Y receptors including Y1, Y2, Y4 and Y5 are a family of receptors expressed in pancreatic islets that are activated by endogenous peptide hormones neuropeptide Y (NPY), PP and PYY (Amisten *et al.* 2013). In addition, the Y6 receptor expressed in primates contains a frameshift mutation producing a non-functional truncated gene (Starback *et al.* 2000). Activation of Y1, Y4 and Y5 induces Gαi signalling, thus inhibiting adenylyl cyclase and cAMP, whereas Y2 augments intracellular Ca^{2+} concentrations through Gαq signal transduction (Gao *et al.* 2004). Within the pancreatic islet, PYY has been shown to attenuate insulin release primarily through Y2 activation (Gao *et al.* 2004). NPY, PP and PYY (1-36) have been shown to activate all neuropeptide Y receptors (Lafferty *et al.* 2018). Interestingly, the DPP-IV cleaved isoform PYY (3-36) is selective for Y2 activation and induces appetite suppression and promotes beta cell proliferation (Lafferty *et al.* 2018).

1.6: Cannabinoid receptors

Cannabinoid receptors comprise part of the endocannabinoid system (ECS) and are responsible numerous physiological responses including pain sensitisation, appetite, memory and mood (Manzanares *et al.* 2006). Ligands that activate cannabinoid receptors can be grouped into three primary classifications; plant cannabinoids (e.g. cannabidiol), endocannabinoids and synthetic cannabinoids (Fine & Rosenfeld 2013). Endocannabinoids are produced naturally in mammalian systems whereas synthetic cannabinoids are typically structural analogues of existing cannabinoids (Fine & Rosenfeld 2013). CB1 and CB2 are the primary receptors of the ECS and are heavily

expressed in the CNS, liver and immune system (Mouslech & Valla 2009). The CB1 and CB2 subtypes are involved in the regulation of neurological signalling and the generation of immune responses (Mouslech & Valla 2009). Recently, previously considered orphan receptors GPR18, GPR55 and GPR119 have been shown to mediate the non-CB1/CB2 effects of the endocannabinoid ligands (Irving *et al.* 2017). These novel receptors are linked with the regulation of energy metabolism, whilst exhibiting no psychoactive properties (Table 1.1) (Irving *et al.* 2017).

1.6.1: CB1 receptor

CB1 is a 472 amino acid protein encoded from chromosome 6 in the human genome and is one of the most abundantly expressed receptors in the brain (Laprairie *et al.* 2012). The natural endogenous ligands for CB1 activation are anandamide (AEA) and 2-arachidonoylglycero (2-AG) (Laprairie *et al.* 2012). Activation of CB1 results in Gαi signalling, attenuating cAMP and PKC by inhibition of adenylyl cyclase (Howlett *et al.* 2010). However, ion channel regulation and MAPK signalling are also associated with CB1 agonism (Howlett *et al.* 2010). Hepatic activation of CB1 has been shown to mediate lipogenesis, whilst activation in the nervous system modulates neurotransmitter release (Kunos *et al.* 2008). CB1 receptor knockout mice display numerous physiological alterations, including hypophagia, hypoalgesia and hypoactivity (Wiley *et al.* 2005). In addition, the psychoactive component of marijuana delta9-tetrahydrohydrocannabinol (THC) mediates through CB1 receptors by coupling to inhibitory G-protein subunits (Wiley *et al.* 2005).

1.6.2: CB2 receptor

CB2 is 360 amino acid protein encoded from chromosome 1 of the human genome with high expression found in the peripheral nervous system and immune cells (Liu *et al.* 2009). Activation of CB2 is primarily linked with anti-inflammatory and immunoregulatory responses whilst other studies have demonstrated its involvement in appetite control (Fine & Rosenfeld 2013). Similar to CB1, CB2 also couples to the intracellular Gαi subunit leading to adenylyl cyclase inhibition and cAMP attenuation (Kaminski 1998). In addition, the same endogenous ligands (AEA, 2-AG) are shared between CB1 and CB2 (Fine & Rosenfeld 2013). Interestingly, CB2 was previously targeted for the treatment of obesity with Rimonabant once used as an inverse agonist prior to its withdrawal due to mood altering side effects (Sam *et al.* 2011).

1.6.3: GPR18 and GPR119

Recently, GPR18 and GPR119 have been identified as endocannabinoid receptors (Irving *et al.* 2017). Although structurally dissimilar to CB1 and CB2, these receptors contain endocannabinoid binding sites within extracellular and transmembrane domains (Irving *et al.* 2017). The functionality of GPR18 remains largely unknown as it is still considered as an orphan receptor, although endogenous AEA metabolite N-arachidonoylglycine (NAGly) has been shown to upregulate intracellular Ca^{2+} concentrations in GPR18-transfecrted cells (Burstein *et al.* 2011). GPR18 activation mediates both Gαi and Gαq signal transduction which can regulate cAMP and Ca^{2+} production intracellularly. In contrast, the biological function of GPR119 is further understood with studies revealing its role as a lipid biosensor. N-oleoylethanolamide (OEA) has been recognised as the primary endogenous ligand (Hassing *et al.* 2016). Upon activation, GPR119 couples to Gαs which stimulates cAMP production through adenylyl cyclase signalling (Hassing *et*

al. 2016). GPR119 is highly expressed in pancreatic beta cells and induces GSIS and incretin release upon activation (Moran *et al.* 2014). GPR119 agonist GSK-1292263 (GlaxoSmithKline) has completed stage II clinical trials for the treatment of type 2 diabetes (Polli *et al.* 2013).

1.6.4: GPR55

GPR55 is a 319 amino acid rhodopsin-like receptor that is expressed on chromosome 2q36.3 in the human genome (Sharir & Abood 2010). Previously, GPR55 was considered an orphan receptor prior to research revealing its interactions with endocannabinoid ligands (Sharir & Abood 2010). GPR55 is abundantly expressed in the endocrine-pancreas, intestines, CNS, adipose tissue and spleen (Simcocks *et al.* 2014). Interestingly, GPR55 displays limited sequence homology with other cannabinoid receptors, including CB1 and CB2. Whilst other GPCRs such as CCR4, GPR35 and GPR23 exhibit the closest structural similarities with GPR55 (Sharir & Abood 2010). Recently, studies have demonstrated that GPR55 activation modulates numerous responses involved in energy metabolism, including GSIS, insulin sensitivity, appetite, lipogenesis and gastric emptying (Tuduri *et al.* 2017). Downstream of GPR55 activation, Gαq and Gα12/13 subunits are activated. Gαq augments intracellular Ca^{2+} concentrations and MAPK phosphorylation through PLC signalling, whereas Gα12/13 activation influences RhoGEFs signalling leading to Rho/ROCK, cdc42 and rac activation (Shi *et al.* 2017).

At present, there are a wide range of endogenous and synthetic ligands available for the activation of GPR55. Moreover, several GPR55 endocannabinoids (lysophosphatidylinositol, palmitoylethanolamide, OEA, AEA, 2-AG) and synthetic cannabinoid ligands (Abn-CBD, AM251, O-1602) have been shown to induce insulinotropic and glucoregulatory effects in clonal pancreatic BRIN-BD11 cells and

diabetic mice (McKillop *et al.* 2013). In addition, naturally occurring cannabidiol have been previously used to antagonise GPR55 (McKillop *et al.* 2013).

1.7: Free fatty acid receptors

The free fatty acid family of GPCRs act as lipid biosensors to short, medium and long chain fatty acid molecules (Yonezawa *et al.* 2013). There are five subclasses of free fatty acid receptors that are differentiated based on the carbon length of their corresponding fatty acid ligands (Yonezawa *et al.* 2013). GPR41 (FFAR3) and GPR43 (FFAR2) sense short chain fatty acid (C2-C6) molecules, GPR84 is activated by medium fatty acids (C9-C14), whereas GPR40 (FFAR1) and GPR120 (FFAR4) are long chain fatty acid (C15-C22) sensing GPCRs (Yonezawa *et al.* 2013). Free fatty acid receptors are known to modulate numerous biological functions such as inflammatory responses and energy metabolism (Hara *et al.* 2013). Recently, research has intensified on the involvement of free fatty acid receptors in type 2 diabetes, with the GPR40 agonist Fasiglifam (TAK-875) recently undergoing stage III clinical trials prior to its withdrawal due to signs of liver toxicity (Marcinak *et al.* 2017). In addition, long chain fatty molecules have been previously shown to regulate insulin and GLP-1 release from pancreatic and enteroendocrine cells, respectively (Table 1.1) (Martin *et al.* 2012).

1.7.1: GPR40

Free fatty acid receptor 1 (FFAR1), also known as GPR40 is a 300 amino acid membrane bound protein expressed on chromosome 19q13.1 that senses saturated and unsaturated long chain fatty acid (C12-C16) molecules (Vangaveti *et al.* 2010). GPR40 is expressed

on immune cells, regions of the brain and pancreatic islet cells and potentiates GSIS upon activation (Swaminath 2008). In addition, GPR40 is highly expressed in enteroendocrine I-, K, and L-cells of the gut with effects towards GLP-1, GIP and CCK secretion linked with receptor activation (Hauge *et al.* 2014). GPR40 primarily couples to Gαq which increases intracellular Ca^{2+} through PLC and IP_3 signalling (Hauge *et al.* 2014). Currently, a range of naturally occurring (long chain carboxylic acids) and synthetic (GW9508, TAK-875, TUG-905) agonists exist for the activation of GPR40, whilst GW1100 is recognised as a potent antagonist (Milligan *et al.* 2015). The specificity of endogenous GPR40 agonists remain uncertain, however, several synthetic agonists such as TAK-875 and TUG-905 exhibit selectivity towards GPR40 (Hudson *et al.* 2013). Although GPR40 stimulates insulin release, GPR40 knockout mice are protected from hyperinsulinemia, hypertriglyceridemia, hyperglycaemia and increased hepatic glucose production (Stenenerg *et al.* 2005). However, overexpression of GPR40 in beta cells via the PDX-1 promoter improves insulin secretion and glucose tolerance (Nagasumi *et al.* 2009).

1.7.2: GPR41

Free fatty acid receptor 3 (FFAR3), also referred to as GPR41 is expressed at chromosome 19q13.1 which encodes a 346 amino acid protein (Vangaveti *et al.* 2010). GPR43 is activated by short chain fatty acid (C3-C5) molecules such as propanoic acid, pentanoic acid, butyric acid and 1-methylcyclopropanecarboxylic acid (Swaminath 2008, Vangaveti *et al.* 2010). Expression of GPR41 has been demonstrated in pancreatic islets, enteroendocrine L-cells, spleen, lymph nodes and bone marrow (Swaminath 2008). Studies have shown GPR41 to regulate inflammatory and immune responses, whilst other findings demonstrated GPR41 activation augment leptin production (Kim *et al.* 2014).

GPR41 knockout mice display increased fat mass, attenuated expression of PYY and impaired sympathetic nervous signalling to short chain fatty acids (Inoue *et al.* 2014).

1.7.3: GPR43

GPR43, also known as free fatty acid receptor 2 (FFAR2) is a 330 amino acid protein that is expressed on chromosome 19q13.1 likewise to GPR40 and GPR41 (Vangaveti *et al.* 2010). Activation of GPR43 results in Gαq which generates an increase on intracellular Ca^{2+} concentrations through PLC and IP_3 signalling (Talukdar *et al.* 2011). GPR43 is activated by a range of short chain fatty acids (C2-C3), including propanoic acid, acetic acid and butyric acid (Vangaveti *et al.* 2010). Endogenous acetic acid exhibits selectivity towards GPR43 over GPR41. In addition, synthetic GLPG0974 is a potent antagonist of GPR43 and displays the highest affinity for the receptor (Namour *et al.* 2016). GPR43 has been shown to control inflammatory and immune responses, with GLPG0974 undertaking stage II clinical trials for ulcerative colitis (Namour *et al.* 2016). GPR43 knockout mice display reduced bodyweight, impaired insulin sensitivity and reduced gastrointestinal inflammation (Nakajima *et al.* 2017).

1.7.4: GPR120

GPR120, also known as free fatty acid receptor 4 (FFAR4) is expressed on chromosome 10q23.33 and encodes a 377 rhodopsin-like receptor upon translation (Stone *et al.* 2014). Abundant expression of GPR120 have been identified in pro-inflammatory macrophages, intestines, endocrine-pancreas, lungs, spleen and adipose tissue (Miyauchi *et al.* 2009, Song *et al.* 2017). Moreover, GPR120 is heavily expressed in both human and rodent pancreatic beta and delta cells, with expression also demonstrated on pancreatic beta cell

lines such as BRIN-BD11, MIN6, INS-1 and RINm5f (Moran *et al.* 2014, Stone *et al.* 2014). GPR120 is a long chain fatty acid receptor that senses endogenous omega 3 fatty acids (α-linolenic acid, docosahexaenoic acid, eicosapentaenoic acid) and other structurally similar synthetic analogues (GW9508, GSK137647 and Compound A) (Sparks *et al.* 2014, Oh *et al.* 2014). AH-7614 is a potent antagonist for GPR120 and exhibits no affinity for the other free fatty acid receptors (Sparks *et al.* 2014). Many of the endogenous ligands for long chain fatty acid sensing receptors, such as omega 3 fatty acids DHA and ALA have previously demonstrated insulinotropic and anti-inflammatory properties that are of interest for the treatment of obesity and type 2 diabetes (Oh *et al.* 2010, Moran *et al.* 2014).

Upon agonist binding and receptor activation, GPR120 activates the intracellular Gαq subunit which modulates an increase in intracellular Ca^{2+} from the ER through PLC and IP_3 signalling (Moran *et al.* 2014, Sanchez-Fernandez *et al.* 2014). The Gαq subunit can also augment MAPK (ERK1/2, p38 and JNK) phosphorylation through PKC activation (Sanchez-Fernandez *et al.* 2014). GPR120 activation plays a regulatory role in glucoregulatory hormone release from the endocrine-pancreas (insulin, somatostatin) and the enteroendocrine cells of the gut (GLP-1, CCK) (Martin *et al.* 2012, Moran *et al.* 2014). Aside from hormone release, GPR120 is also linked with anti-inflammatory responses and insulin sensitisation (Oh *et al.* 2014). Interestingly, GPR120 knockout mice demonstrated glucose intolerance and were more susceptible to the effects of a high fat diet, including obesity, fatty liver and increased lipogenesis (Ichimura *et al.* 2012).

1.8: Aims and objectives

GPCRs are responsible for mediating the secretion of numerous glucoregulatory hormones from the pancreatic islet and enteroendocrine cells of the gut, including insulin, GLP-1 and GIP. Recently, novel GPCRs from the cannabinoid and free fatty acids families have been identified as potential therapeutic targets for the treatment of type 2 diabetes and other obesity related complications. Namely, GPR55 and GPR120 have shown pre-clinical promise and may be utilised to counteract beta cell dysfunction, dyslipidaemia and obesity. The present study aims to investigate the specificity, mechanistic function and efficacy of GPCR agonists as novel therapeutic agents using *in-vitro* studies, CRISPR/Cas9 gene editing and diabetic mice studies.

The primary aims of the thesis are as follows:

- To investigate the expression and cellular localisation of GPR55 and GPR120 in clonal BRIN-BD11 cells and islets of lean and diabetic rodent models of diabetes as assessed by qPCR, western blotting and double immunofluorescent staining.
- To determine the role of several GPR55 and GPR120 ligands on insulin and incretin (GLP-1, GIP) release using clonal BRIN-BD11 cells and high fat fed-induced diabetic mice.
- To examine the specificity of putative GPR55 and GPR120 ligands on beta cell function using CRISPR/Cas9 gene editing in clonal BRIN-BD11 cells.
- To explore the intracellular signalling events of insulin secretion activated downstream of GPR55 and GPR120 agonism using western blotting, flow cytometry, ELISA and fluorometric assays.
- To evaluate the chronic therapeutic effectiveness of GPCR agonist monotherapy and combinational therapy (DPP-IV inhibition) in high fat fed-induced diabetic mice.

Table 1.1: Biological function, agonists and signalling mechanism of cannabinoid and free fatty acid GPCRS.

Family	Receptor	G-protein	Biological function	Agonists
Cannabinoid receptors	CB1	Gαi	Neurotransmitter release, anti-inflammatory	Anandamide, 2-arachidonoylglycerol Cannabinol, Δ9-tetrahydrocannabinol,
	CB2	Gαi	Anti-inflammatory, immune regulation	AM7499, Δ9-tetrahydrocannabinol, HU-210, APD371
	GPR18	Gαi Gαq	-	-
	GPR55	Gα12/13 Gαq	Insulin release, Anti-inflammatory	Abn-CBD, O-1602, AM251, OEA, PEA
	GPR119	Gαs	Insulin release, appetite suppression	AS-1269574, PSN-375963, AR-231453
Free fatty acid receptors	GPR40	Gαq	Glucose stimulated insulin secretion	TAK-875, GW9508
	GPR41	Gαi	Anti-inflammatory, Leptin release	Short chain fatty acids (C3-C5)
	GPR43	Gαi Gαq	Immune response Attenuates lipolysis	Short chain fatty acids (C2-C3)
	GPR84	Gαi	Anti-inflammatory	Medium chain fatty acids (C9-C14)
	GPR120	Gαq	Anti-inflammatory, insulin release	ALA, DHA, EPA, GSK137647, Compound A

(Adapted from Swaminath 2008, Amisten *et al.* 2013)

Figure 1.1: Target organs and examples of current therapies for the treatment of type 2 diabetes.

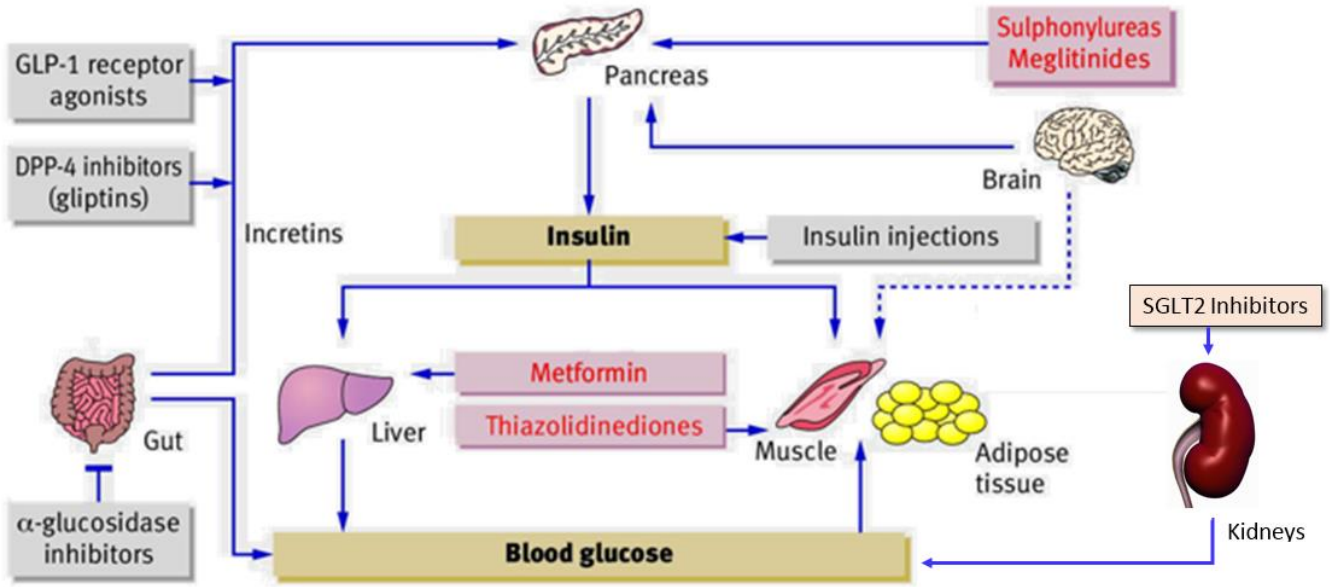

(Adapted from Evans *et al.* 2000)

Figure 1.2: Mechanism of GPCR activation upon agonist binding.

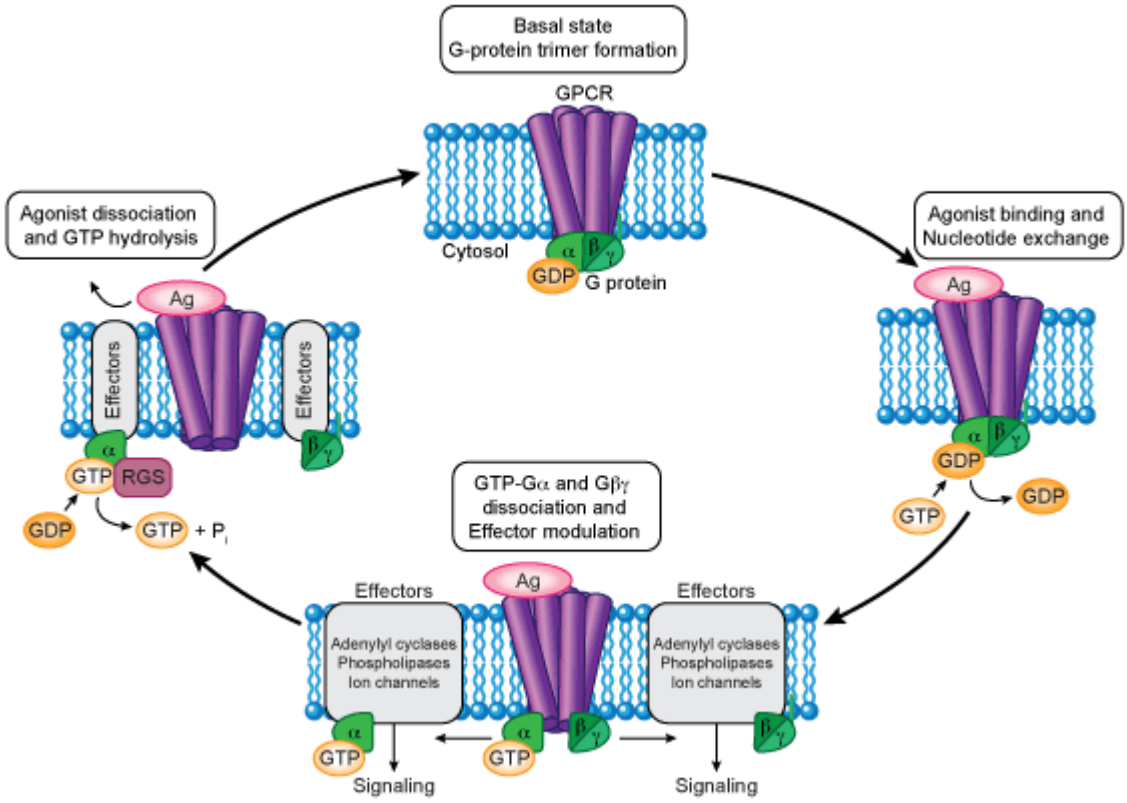

(Adapted from Wettschureck & Offermanns 2005)

Figure 1.3: Intracellular G-protein signalling pathways (Gαq, Gαs, Gαi, Gα12/13) stimulated upon GPCR activation.

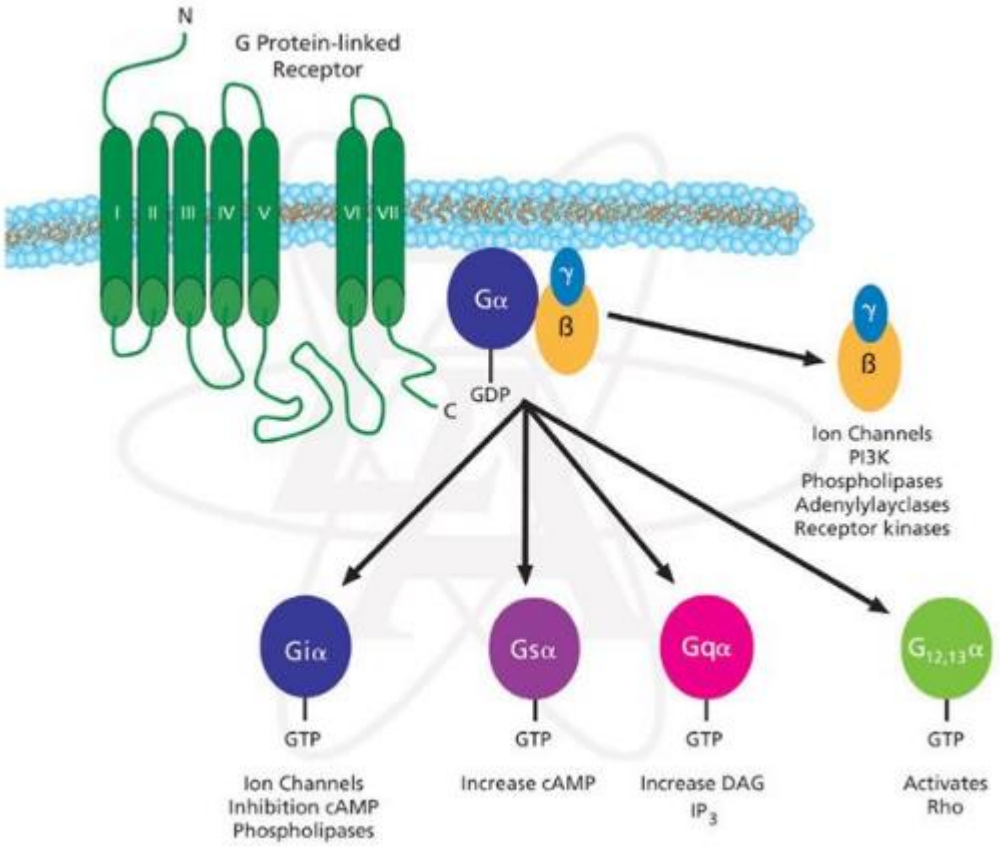

(Adapted from Wu *et al.* 2012)

Figure 1.4: Gαq signalling upon GPCR activation (GPR55 and GPR120 signalling pathways)

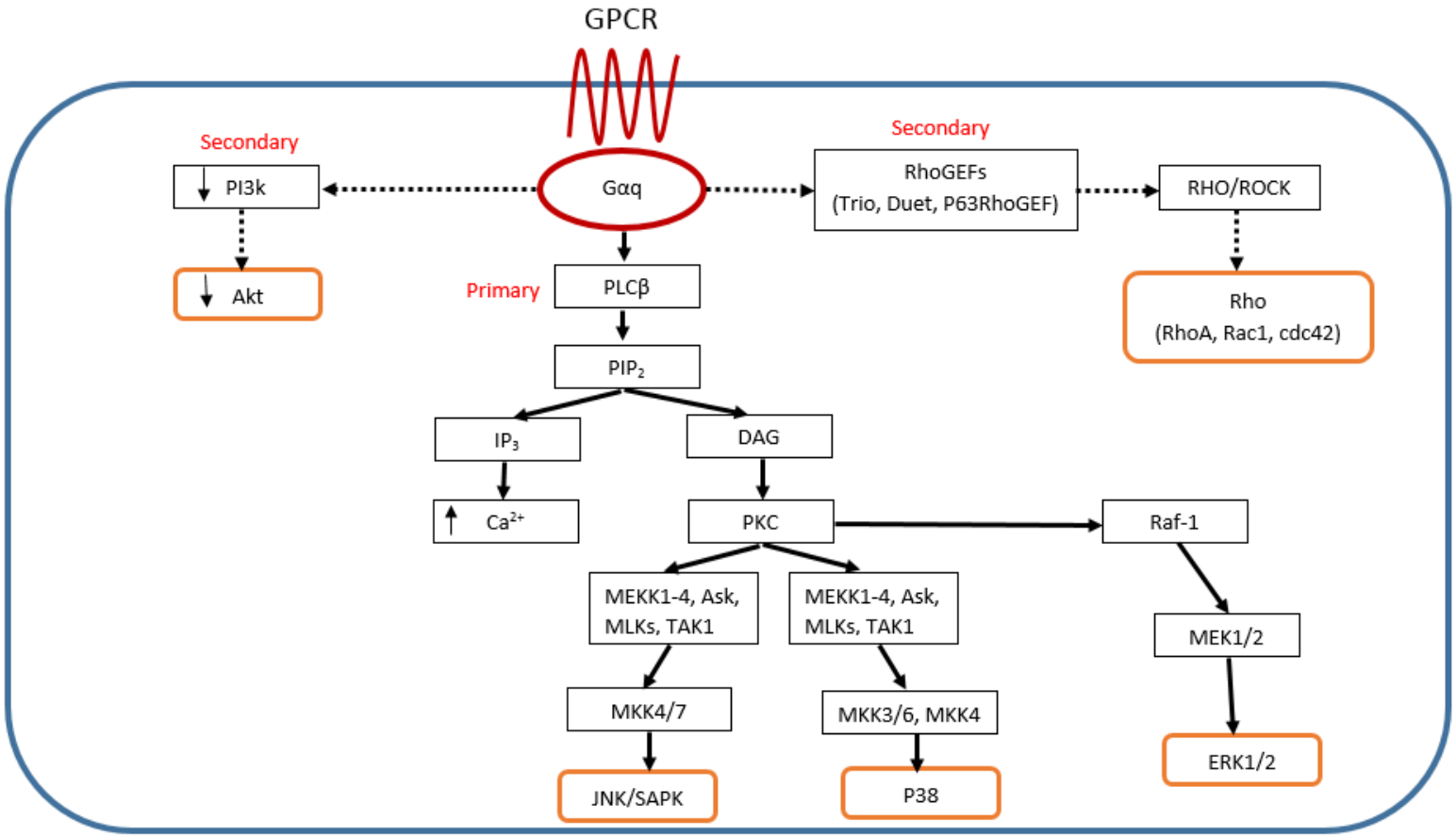

(Adapted from Mizuno & Itoh 2009, Sanchez-Fernandez *et al.* 2014)

Figure 1.5: Gα12/13 signalling upon GPCR activation (GPR55 signalling pathway)

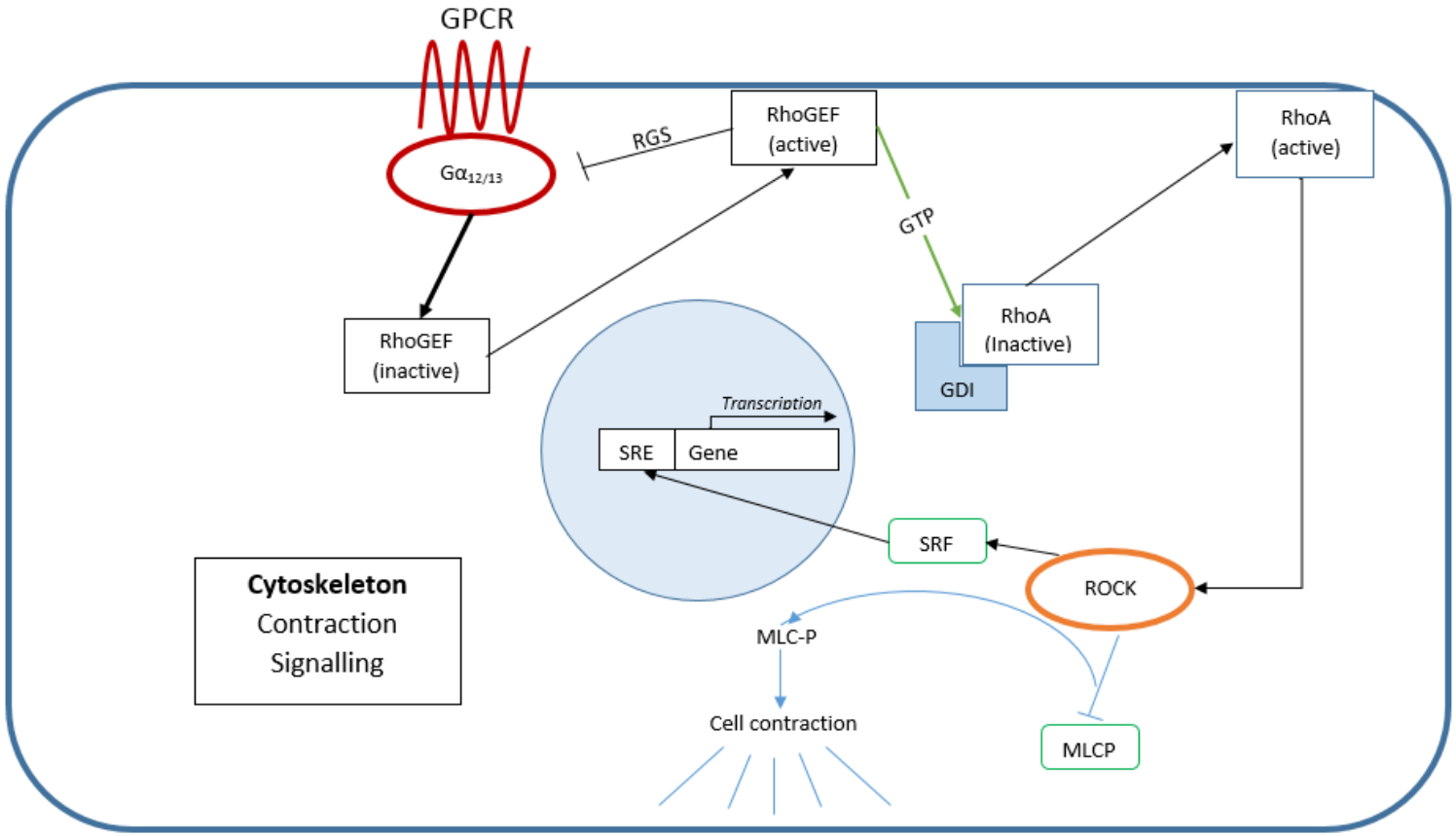

GDI: guanine nucleotide dissociation inhibitor
RGS: Regulator of G-protein signalling
GEF: Guanine nucleotide exchange factor
SRF: Serum response factor
MLC: myosin light chain

(Adapted from Siehler 2009)

Chapter 2

Materials and Methods

2.1: Tissue Culture

2.1.1: Materials

RPMI 1640 medium, foetal bovine serum (FBS), penicillin/streptomycin (100 U/ml; 0.1 mg/ml), trypsin/EDTA and Hanks Buffered Saline Solution (HBSS) were purchased from Gibco Life Technologies (Paisley, Strathclyde, UK). HEPES, sodium chloride (NaCl), potassium chloride (KCl), calcium chloride dihydrate ($CaCl_2.2H_2O$), sodium hydroxide (NaOH), dimethylsulphoxide (DMSO), bovine serum albumin (BSA) and hydrogen peroxide (H_2O_2) were sourced from Sigma-Aldrich (Poole, Dorset, UK). D-glucose, hydrochloric acid (HCL), sodium bicarbonate ($NaHCO_3$), magnesium sulphate ($MgSO_4.7H_2O$) and trypan blue were obtained from BDH Chemicals (Poole, Dorset, UK). Sterile 96-well, 24-well, 12-well and 6-well tissue culture plates were obtained from Nunclon (Roskilde, Denmark).

2.1.2: Culture of clonal BRIN-BD11 cells

Clonal pancreatic BRIN-BD11 cells were derived from the electrofusion of RINm5F cells with New England Deaconess Hospital (NEDH) rat pancreatic beta cells, as previously described (McClenaghan *et al.* 1996). BRIN-BD11 cell stocks, containing 1 million cells, were cryopreserved in 1 ml of freezing medium (80% FBS (v/v), 10% RPMI-1640 (v/v), 10% DMSO (v/v)) and stored in 1.5 ml cryovials (Sterilin, Houslow, UK). Cryovials containing stocks were stored at -20˚C for 4 h, -80˚C for 24 h, followed by long-term storage in liquid nitrogen. BRIN-BD11 cells (passages 15-45) were cultured in RPMI-1640 media with 1% antibiotics (v/v), 10% FBS (v/v) at a glucose concentration of 11.1 mM. Cells were grown in 20 ml of media in 75 cm^3 vented sterile

tissue culture flasks at 37˚C in 5% CO_2 and 95% air inside a LEEC incubator (Laboratory Technical Engineering, Nottingham, UK).

When the cells reached confluency (75-90%) they were harvested by washing with 10 ml of HBSS then incubated with pre-warmed 0.025% (w/v) trypsin/EDTA at 37˚C for 5 min. Confirmation of detachment was performed by visual inspection using a phase contrast microscope (Zeiss, Germany). Cells were resuspended in 10 ml of RPMI-1640 media, transferred to a 50 ml sterilin tube (Sterilin, Houslow, UK) and centrifuged at 900 rpm for 5 min using a bench centrifuge (MSE Mistral 200, RHYS International, Manchester, UK). Supernatant was decanted and the cell pellet resuspended in a known volume of media. An aliquot of cell suspension (100 µl) was stained by adding to trypan blue (100 µl, 1:2 dilution), mixed thoroughly and added to a Neubauer haemocytometer (Scientific Supplies Co, Middlesex, UK) for counting.

2.1.3: Culture of human 1.1B4 cells

The hybrid cell line1.1B4 was formed by the electrofusion of a primary culture of human pancreatic islets with PANC-1, a human pancreatic ductal carcinoma cell line. The generation and characterisation of these cells was previously described (Vasu *et al.* 2013, Green *et al.* 2015). 1.1B4 cell stocks, containing 1 million cells, were cryopreserved in 1 ml of freezing medium (80% FBS (v/v), 10% RPMI-1640 (v/v), 10% DMSO (v/v)) and stored in 1.5 ml cryovials (Sterilin, Houslow, UK). Cryovials containing stocks were stored at -20˚C for 4 h, -80˚C for 24 h, followed by long-term storage in liquid nitrogen. 1.1B4 cells (passages 15-35) were cultured in RPMI-1640 media with 1% antibiotics (v/v), 10% FBS (v/v) at a glucose concentration of 11.1 mM. Cells were grown in 20 ml of media in 75 cm^3 vented sterile tissue culture flasks at 37˚C in 5% CO_2 and 95% air inside a LEEC incubator (Laboratory Technical Engineering, Nottingham, UK).

When the cells reached confluency (75-90%) they were harvested by washing with 10 ml of HBSS then incubated with pre-warmed 0.025% (w/v) trypsin/EDTA at 37˚C for 5 min. Confirmation of detachment was performed by visual inspection using a phase contrast microscope (Zeiss, Germany). Cells were resuspended in 10 ml of RPMI-1640 media, transferred to a 50 ml sterilin tube (Sterilin, Houslow, UK) and centrifuged at 900 rpm for 5 min using a bench centrifuge (MSE Mistral 200, RHYS International, Manchester, UK). Supernatant was decanted and the cell pellet resuspended in a known volume of media. An aliquot of cell suspension (100 µl) was stained by adding to trypan blue (100 µl, 1:2 dilution), mixed thoroughly and added to a Neubauer haemocytometer (Scientific Supplies Co, Middlesex, UK) for counting.

2.1.4: Culture of α-TC1.9 cells

Alpha TC1 cell line was generated from an adenoma produced in transgenic mice expressing SV40 large T antigen controlled under rat preproglucagon promoter (Powers *et al.* 1990). Alpha TC1 clone 9 was cloned from alpha TC1 cell line with no expression of insulin or preproinsulin mRNA (Powers *et al.* 1990). The cell line was a gift from Professor Kevin Doherty, University of Aberdeen. α-TC1.9 cell stocks, containing 1 million cells, were cryopreserved in 1 ml of freezing medium (80% FBS (v/v), 10% Dulbecco's modified Eagle medium (DMEM) (v/v), 10% DMSO (v/v)) and stored in 1.5 ml cryovials (Sterilin, Houslow, UK). Cryovials containing stocks were stored at -20˚C for 4 h, -80˚C for 24 h, followed by long-term storage in liquid nitrogen. α-TC1.9 cells were cultured in DMEM media with 1% antibiotics (v/v), 10% FBS (v/v) at a glucose concentration of 25 mM. Cells were grown in 20 ml of media in 75 cm^3 vented sterile tissue culture flasks at 37˚C in 5% CO_2 and 95% air inside a LEEC incubator (Laboratory Technical Engineering, Nottingham, UK).

When the cells reached confluency (75-90%) they were harvested by washing with 10 ml of HBSS then incubated with pre-warmed 0.025% (w/v) trypsin/EDTA at 37˚C for 5 min. Confirmation of detachment was performed by visual inspection using a phase contrast microscope (Zeiss, Germany). Cells were resuspended in 10 ml of DMEM media, transferred to a 50 ml sterilin tube (Sterilin, Houslow, UK) and centrifuged at 900 rpm for 5 min using a bench centrifuge (MSE Mistral 200, RHYS International, Manchester, UK). Supernatant was decanted and the cell pellet resuspended in a known volume of media. An aliquot of cell suspension (100 µl) was stained by adding to trypan blue (100 µl, 1:2 dilution), mixed thoroughly and added to a Neubauer haemocytometer (Scientific Supplies Co, Middlesex, UK) for counting. For all experiments, cells were used between passages 34 and 42.

2.1.5: Acute insulin secretory tests in BRIN-BD11 and 1.1B4 cells

Confluent BRIN-BD11 or 1.1B4 (70-90%) cells were cultured and harvested as described in Sections 2.1.2 and 2.2.3, respectively. Cells were seeded into 24 well plates at a density of 150,000 cell per well (Nunclon, Roskilde, DK), supplemented with 1ml of RPMI-1640 media then incubated at 37˚C in 5% CO_2 and 95% air overnight to allow for the development of monolayers. Prior to the acute test, media was decanted from each well then 1 ml of 1.1 mM glucose in Krebs Ringer Bicarbonate Buffer pre-incubation buffer (KRBB, 4.7 mM KCl, 115 mM NaCl, 1.28 mM $CaCl_2.2H_2O$, 25 mM $NaHCO_3$, 0.1% BSA (w/v), 1.2 mM KH_2PO_4, 1.2 mM $MgSO_4.7H_2O$, 20 mM HEPES (pH 7.4) was added for 40 min at 37˚C in 5% CO_2 and 95% air. Following pre-incubation, 1.1 mM glucose was decanted and cells were incubated with ranging concentrations (10^{-12}-10^{-4} M) of GPCR agonists at both 5.6 mM and 16.7 mM glucose in KRBB for 20 min at 37˚C in 5% CO_2 and 95% air. After 20 min incubation, cell

supernatants (900 µl) were collected stored at -20˚C until insulin measurement by radioimmunoassay.

2.1.6: 3-(4,5-dimethylthiazol-2-Yl)-2,5-diphenyltetrazolium bromide (MTT) assay

BRIN-BD11 cells were cultured as previously described (Sections 2.1.2) and seeded into 96-well plates at a density of 30,000 cells per well. BRIN-BD11 cells were then incubated overnight at 37˚C in 5% CO_2 and 95% air. After overnight incubation, media was decanted and test solutions consisting of ranging concentrations (10^{-12}-10^{-4} M) of GPCR agonists were added at both 5.6 mM and 16.7 mM glucose supplemented KRBB and incubated for 20 min at 37˚C in 5% CO_2 and 95% air. Following exposure to GPCR treatments, test solutions were decanted and 1 mg/ml of working MTT solution prepared in normal culture media was added for 2 h and incubated at 37˚C in 5% CO_2 and 95% air. Working MTT was decanted and 100µl of DMSO was added to each well, followed by 5 min mixing on a horizontal orbital microplate shaker at 500 rpm (Titramax 1000, Heidolph Instruments, Schwabach, DE). Absorbances were measured at 570 nm and 630 nm using the FlexStation 3 (Molecular Devices, CA, USA).

2.2: Insulin Radioimmunoassay (RIA)

2.2.1: Materials

Thimerosal, iodogen (1,3,4,6-tetrachloro-3α,6α-diphenylglycoluril), BSA, activated charcoal, sequencing grade TFA, dextran T-70 and insulin were purchased from Sigma-Aldrich (Poole, Dorset, UK). Dichloromethane (CH_2Cl_2) and HPLC grade acetonitrile

were sourced from Rathburn (Walkersburn, UK). Radiolabelled sodium iodide ($Na^{125}I$) was supplied by Amersham Pharmacia Biotech (Buchinghamshire, UK). Rat insulin standards were purchased from Novo Industria (Copenhagen, Denmark). All other chemicals used were obtained from BHD chemicals (Poole, Dorset, UK).

2.2.2: Preparation of iodinated insulin

Iodogen was dissolved in dichloromethane (100 μg/ml) and 100 μl aliquots were transferred to the bottom of microcentrifuge tubes (Sarstedt, Germany) and evaporated using a gentle stream of helium for a uniform layer of iodogen. A 20 μl solution of insulin (125 μg/ml in 500 mM sodium phosphate buffer, pH 7.4) and 5 μl of Na^{125} I (100 mCi/ml) were added to these iodogen coated reaction tubes in a designated controlled area with a lead Perspex shielding. The iodination mixture was left on ice for 15 min with 3-4 gentle agitations per min. The reaction was stopped by removing the mixture from the reaction tube into a fresh microcentrifuge tube, washing the reaction tube with 500 μl of 50 mM sodium phosphate buffer which was also transferred to the fresh microcentrifuge tube. This iodination mixture is kept on ice until RP-HPLC separation of bound and unbound fractions.

RP-HPLC was performed using a Spectra Series P200 TSP HPLC gradient pump system (CA, USA) with a Vydac C-8 analytical column (4.6 x 250mm, Phenomenex, Macclesfield, UK). The column was equilibrated using 0.12% (v/v) TFA/H2O and eluted with 0.1% (v/v) TFA in 70% acetonitrile/H2O from 0-40% over 10 min, from 40-80% over 40 min and 80-100% over 10 min. A LKB2112 Redirac fraction collector (Bromma, Sweeden) was set to collect 1 ml fractions in 72 x 12mm polypropylene tubes (Sarstedt, Germany) of which 5 μl aliquots were transferred to plastic LP3 tubes (Sarstedt, Germany) and measured using a gamma counter (1470 Wizard multigamma

counter, PerkinElmer, USA). The fractions with the highest count per min (CPM) were selected for antibody binding and similar binding fractions pooled. Fractions were double diluted with 40 mM sodium phosphate buffer (pH 7.4) composed of 1% BSA (w/v), 1.2 mg/ml thiomersal and stored at 4˚C. A typical RP-HPLC elution profile of the iodination reaction with CMP versus time (min) as displayed in Fig. 2.1.

2.2.3: Determination of insulin by radioimmunoassay

Insulin was determined using a modified dextran-coated charcoal radioimmunoassay (RIA) as previously described (Flatt & Bailey 1981). Stock assay buffer was prepared from 40 mM disodium hydrogen orthophosphate with 0.3% NaCl (w/v) and 0.02% thimersol (w/v) and titrated with 40 mM sodium dihydrogen orthophosphate to pH 7.4. Working assay buffer was prepared composed of 40 mM sodium phosphate buffer (pH 7.4) supplemented with 0.5% BSA (w/v) which was used to dilute guinea-pig anti-porcine insulin antibody, rat insulin standards and ^{125}I labelled insulin. The standard curve (0.039-20 ng/ml) was prepared by serial dilution of rat insulin standard and assayed in triplicate. Guinea-pig anti-porcine insulin antibody was diluted using working assay buffer (1:40,000) and 100 µl added to each standard or unknown sample with the exception of total and non-specific binding tubes. ^{125}I labelled insulin was diluted in assay buffer to 10,000 cpm/ 100 µl which was added to all tubes.

After 48 h at 4˚C, a 1 ml solution of 1:5 dilution of dextran T-70 coated charcoal in working assay buffer was added to all tubes except the total tubes for 20 min at 4˚C. All tubes were centrifuged using a Model J-6B Centrifuge (Beckman Instruments, UK) for 20 min at 2,500 rpm (4˚C), the supernatant decanted and the unbound ^{125}I labelled insulin fraction remained as a black pellet which were counted on the gamma counter (1470 Wizard Multigamma Counter, PerkinElmer, USA). Counts bound to the antibody (total

CPM minus CPM bound to charcoal) were inversely proportional to the concentration of insulin in standards or unknown samples. The rat insulin standard curve was constructed with spline curve fitting algorithm and the unknown samples interpolated from the curve. The rat insulin standard stock of 1 ng/ml insulin is equal to 173 pM and conversion from ng/ml to pM was performed by multiplication by a factor of 173. A typical rat insulin standard curve is shown with CPM versus log insulin concentrations in Fig 2.2.

2.3: Intracellular Ca^{2+} measurement

2.3.1: Materials

FLIPR calcium assay kits were purchased from Molecular Devices (CA, USA). Black walled, clear bottom, 96 well plates were obtained from Greiner Bio-One (Gloucestershire, UK). Probenecid and L-alanine were sourced from Sigma-Aldrich (Poole, Dorset, UK).

2.3.2: Determination of intracellular Ca^{2+} in BRIN-BD11 cells

FLIPR calcium assay kits employ a calcium specific dye that is absorbed into the cell cytoplasm during the incubation. Following agonist-receptor activation, intracellular calcium bound to the dye is released from the cells increasing the fluorescence intensity. BRIN-BD11 cells were seeded at a density of 80,000 cells per well into 96 well black walled, clear bottom plate and incubated overnight at 37°C as previously described (Section 2.1.2). The assay plate was washed with 1.1 mM glucose KRBB solution

composed of 4.7 mM KCl, 115 mM NaCl, 1.28 mM $CaCl_2.2H_2O$, 25 mM $NaHCO_3$, 0.1% BSA (w/v), 1.2 mM KH_2PO_4, 1.2 mM $MgSO_4.7H_2O$, 25 mM HEPES, supplemented with probenecid (500 μM). Probenecid prevents the transport of unbound dye out of the cells by organic anion transporters. The assay plate was incubated with the dye prepared with KRBB at 5.6 mM or 16.7 mM glucose for 1 h at 37°C. The FlexStation 3 (Molecular Devices, CA, USA) was set to run for 5 min at 485 nm excitation, 525 nm emission, 515 nm cut-off filter with 2.5 sec intervals. Test solutions (x5) were transferred (50 μl) at 60 s from the start of the acquisition at a rate of 78 ml/s. Alanine (10 mM) a known modulator of intracellular calcium was used as the positive control for all calcium assays.

2.4: Cyclic AMP assay

2.4.1: Materials

cAMP enzyme immunoassay kits were purchased from Sigma-Aldrich (Poole, Dorset, UK). Sterile, flat bottom, 96-well tissue culture plates were obtained from Nunc (Roskilde, Denmark).

2.4.2: Measurement of cAMP production in BRIN-BD11 cells

The assay utilises a polyclonal anti-cAMP antibody to competitively bind to cAMP in the sample or alkaline phosphatase with a cAMP molecule attached. This enzymatic reaction is based on the colour intensity which is inversely proportional to the concentration of cAMP in the standards or samples. BRIN-BD11 cells were seeded into 96-well plates at a density of 30,000 cells per well and incubated overnight at 37°C as previously outlined

(Section 2.1.2). The contents of the kit were allowed to reach room temperature before use and the assay kit was performed as per the manufacturer's protocol. For standard curve preparation, cAMP standards ranging from 0.78-200 pM/ml were diluted in 0.1 M HCl which were used within 60 min (Fig. 2.3). Wash buffer was prepared by diluting 10ml of the concentrated wash buffer in 90 ml of distilled water. RPMI-1640 media was aspirated from the plate and cells washed in 300 µl of 1.1 mM KRB buffer for 40 min. Test solutions (150 µl) were added to the cells for 20 min incubation at 37°C. After acute incubation all test solutions were removed from the plate and 150 µl of 0.1M HCl was added to lyse the cells. To ensure adequate lysis had occurred, cells were incubated at 37°C for 10 min and inspected using a phase contrast microscope (Zeiss, Germany). Incubation for a further 10 min was performed if adequate lysis had not occurred and once adequate lysis had occurred supernatants were aliquoted into labelled tubes.

Neutralising reagent (50 µl) was added to all wells of the assay plate except the total and blank wells while 100 µl of 0.1M HCl was added to the non-specific binding (NSB) and standard 0 (0 pM/ml) wells. Unknown samples (100 µl) were added to the corresponding wells and 50 µl of 0.1M HCl to the NSB wells. Blue cAMP-alkaline phosphatase conjugate (50 µl) and cAMP-EIA antibody (50 µl) was added to all wells except the total and blank wells. The assay plate was incubated at room temperature on an orbital plate shaker set at 500 rpm for 2 h. Contents of the plate were removed and washed 3 times with 200 µl of the wash buffer. cAMP-alkaline phosphatase (5 µl) was transferred to the total wells and 200 µl of p-Nitrophenyl phosphate was added to all wells of the assay plate which was incubated for 1 h at room temperature. The stop solution (50 µl) was added to all wells and read immediately on the Flexstation 3 plate reader (Molecular Devices, CA, USA). The plate was read at 405 nm with corrections between 570 nm and 590 nm and the mean blank value was subtracted from all readings.

2.5: Determination of BRIN-BD11 cell proliferation and apoptosis upon GPCR agonist treatment.

2.5.1: Materials

ApoLive-Glo™Multiplex Assay was purchased from Promega (Wisconsin, US)

2.5.2 Measurement of cell proliferation and apoptosis

ApoLive-Glo multiplex assay was used to assess BRIN-BD11 cell proliferation and apoptosis. Cells were seeded at a density of 20,000 cells per well in a 96 well plate and allowed to attach overnight (Section 2.1.2). Agonist test solutions (10^{-4} mol/l) and cytokine cocktail solution (TNF-α [200 U/ml], IFN-γ [20 U/ml], IL-1β [100 U/ml]) were prepared in RPMI media to a final volume of 100 µl per well, then added to the cells and incubated for 20 h at 37ºC. After the test incubation period, 20 µl of Viability Reagent was added to each well and briefly mixed by orbital shaking (300–500 rpm for ~30 seconds), then incubated for 30 min at 37°C. Fluorescence was then measured at the following wavelength set: $400_{Ex}/505_{Em}$ using the Flexstation 3 plate reader (Molecular Devices, CA, USA). To determine caspase 3/7 activity, 100µl of Caspase-Glo® 3/7 Reagent was to all wells, and briefly mixed by orbital shaking (300–500 rpm for ~30 s), then incubated for 30 min at room temperature. Luminescence was then determined using the FlexStation 3 plate reader (Molecular Devices, CA, USA).

2.6: Determination of mRNA expression in BRIN-BD11 cells and Swiss TO mouse pancreas

2.6.1: Materials

TRIzol reagent, propan-2-ol and chloroform was supplied by Sigma (Poole, Dorset, UK). Superscript II reverse transcriptase RNase H kit was supplied by Invitrogen (Paisley, UK). Eppendorf real-time PCR tube strips & masterclear cap strips were sourced from Bio-Rad Laboratories (Herrtfordshire, UK). LightCycler® 480 SYBR Green I Master was obtained from Roche (Basel, CH).

2.6.2: mRNA extraction and conversion to cDNA

mRNA was extracted from all cell lines and tissue using the phenol chloroform method as described previously (Chomczynski, Sacchi 1987) Briefly, cells and tissue were harvested as previously mentioned (Sections 2.1.2). Tissue was homogenised and lysed in 1 ml of TRIzol reagent. Cells were seeded in 6-well plates, treated with test solutions for the appropriate time and lysed using TRIzol on ice for 10 min. Cells were agitated with gentle stirring. Tissue and cells were transferred to a fresh microcentrifuge tube and 200 µl of chloroform was added. This suspension was agitated and incubated at room temperature for 10 min before undergoing centrifugation at 12,000g for 15 min at 4°C (MIKRO 200R, Hettich Zentrifugen, Germany). The clear upper aqueous phase containing mRNA was transferred to a new microcentrifuge tube and 0.5 ml of propan-2-ol was added. The interphase and organic phase were discarded. The mixture was agitated and incubated at room temperature for 10 min before centrifugation at 12,000g for 10 min at 4°C. The supernatant was discarded, and 70 % ethanol was used to wash

the pellet of mRNA then centrifuged at 12,000g for 10 min at 4°C. This was repeated for a total of 3 times. The supernatant was then discarded and pellets air dried at room temperature for 10 min. Following air drying, the pellet was suspended in 30 µl of RNase free water and heated at 70°C for 5 min before determination of the mRNA yield using a nanophotometer (Implen, version 2.0). The quality of mRNA was determined by 260/280 ratios with ratios between 1.9 and 2.1 being deemed of sufficient quality. From this mRNA, 1-5 µg was converted to cDNA using the superscript II reverse transcriptase – Rnase H kit as per suppliers' instructions. mRNA samples were stored long term at -80°C while cDNA was stored at -20°C.

2.6.3: Quantitative real-time PCR (qPCR)

qPCR was performed using LightCycler® 480 SYBR Green I Master. Reactions were performed using 4.5 µl of 2x concentrated SYBR green, 1 µl of forward and reverse primers (Table 2.3), 1 µl of cDNA and 3 µl of RNase free water (n=3). All reactions included a negative template control with RNase free water added instead of cDNA (n=3). The reactions were carried out in 8-well real-time PCR Tube Strips and Masterclear™ Cap Strips (Eppendorf, HAM, DE). Amplification conditions were 5 min initial denaturation at 95°C, followed by 40 cycles of 30 s denaturation at 95°C, 30sec annealing at 58°C and 30 s extension at 72°C and a final elongation step for 5min at 72°C. Reactions included melting curve analysis with temperature range of 60°C to 90°C. All reactions were carried out using the MiniOpticon two colour real time PCR detection system (BioRad, UK). Analysis of results was performed using the Livak method and the mRNA levels of all genes were normalised using the housekeeping gene GAPDH. Primer sequences for qPCR are listed in Table 2.3.

2.7: Protein expression in BRIN-BD11 cells using western blotting

Cells were seeded at a density of 1,000,000 cells per well in 6-well plates and allowed to attach overnight. After treatment, total protein was extracted at 4^{o}C for 10 min using RIPA buffer containing 150 mM NaCl, 1.0% Nonidet P-40, 0.5% sodium deoxycholate, 0.1% SDS, 50 mM Tris HCl, pH 7.6, protease inhibitor cocktail (Sigma, UK) and phosphatase inhibitor cocktails 1 + 2 (Abcam, UK). Total protein concentration was determined using Bradford reagent (Sigma, UK). Equal amounts of protein were aliquoted with Laemmli buffer (1µg/µl), then boiled at 95^{o}C for 10 min. Samples (25µg per well) were loaded onto pre-cast gels (NUPAGE 4–12 % Bis–Tris gels, Invitrogen, UK) and subjected to SDS-PAGE (70V, 90 min). After transfer to nitrocellulose membrane for 16 h at 90 mA, membranes were blocked with 5% skimmed milk and probed with primary antibodies (Table 2.2). Membranes were probed with ECL horseradish peroxidase donkey anti-rabbit IgG/ECL horseradish peroxidase sheep anti-mouse IgG (1:10000) (GE Healthcare, UK) and detected using Luminata Forte HRP substrate (Millipore, UK). Data were normalised to β-actin and presented relative to untreated control.

2.8: Histology

2.8.1: Materials

BSA, paraformaldehyde (PFA), 4’ 6-diamidino-2-phenylindole **(**DAPI**)** nuclear stain and ethanol were purchased from Sigma-Aldrich (Poole, Dorset, UK). PBS tablets were obtained from Analab (Dublin, Ireland), while xylene was obtained from VWR (Dublin, Ireland). All other chemicals used were obtained from BHD chemicals (Poole, Dorset,

UK). Suppliers of all primary and secondary antibodies used for immunohistochemical staining are shown in Table 2.1.

2.8.2: Immunofluorescence staining of BRIN-BD11 cells

BRIN-BD11 cells were seeded overnight at 60,000 cells per polylysine-coated slide (25 x 75 x 1 mm, VWR) and incubated in sterile petri dishes with 25 ml of RPMI-1640 at 37˚C. Slides were washed twice in PBS for 5 min and cells fixed in 4% PFA/PBS (v/v) for 20 min at room temperature. After fixation, slides were washed 3 times in PBS and antigen retrieval achieved by incubation in 50 mM sodium citrate (pH 6.0) at 90˚C for 20 min. Slides were blocked with 1.1% BSA (w/v) for 30 min and primary antibodies added (200 µl per slide) at optimised dilutions, overnight at 4˚C or 1 h at 37˚C (Table 2.1). After incubation with primary antibodies, slides were washed 3 times in PBS and appropriate secondary antibodies added (200 µl per slide) for 45 min at 37˚C, protected from light. Slides were washed 3 times in PBS and DAPI (0.1 µg/ml) added to slides for 15 min at 37˚C. Finally, slides were washed twice in PBS, mounted with a glycerol/ PBS solution (1:1) and fixed with clear nail varnish. Slides were analysed under the 350 nm filter (DAPI), fluorescein isothiocyante (FITC) filter (488 nm) and tetramethylrhodamine isothiocyanate filter (TRITC) filter (594 nm) using a fluorescent microscope (Olympus BX51 microscope, South-on-Sea, UK) and images acquired using the DP70 camera.

2.8.3: Tissue processing and immunofluorescence staining of pancreatic tissue

Non-fasted mice were anesthetised by isoflurane and killed by cervical dislocation. Pancreata were extracted into labelled cassettes and placed in 4% PFA (w/v) for at least 48 h at 4˚C. Tissue samples were embedded in paraffin wax using the automated Leica TP1020 automated tissue processor (Leica Bio systems, Germany) as per manufacturer's guidelines. In brief, labelled cassettes were placed in the metal basket attached to the lid

of the tissue processor which transferred the cassettes between 4% PFA (w/v), increasing concentrations of ethanol, xylene and molten paraffin wax as follows: 70%, 80%, 96% ethanol (v/v) for 2 h each, 100% ethanol 2 changes for 2 h, xylene 2 changes for 1 h 30 min and 2 changes in paraffin wax for 4 h. The following day pancreata were placed in moulds, appropriately orientated, covered in molten paraffin wax and labelled cassettes attached to the top. Paraffin wax blocks were left to set for 24 h, after which blocks were removed from the moulds and stored at room temperature.

Pancreatic sections were cut at 8 μm using a microtome (RM2035, Leica, Germany), floated on a 37˚C water bath and lifted onto polylysine-coated slide (25 x 75 x 1mm, VWR). Slides were dried on a hot plate at 37˚C for 2 h and overnight at room temperature. The slides were dewaxed by 2 changes of xylene for 10 min, rehydrated with 2 changes in 100% ethanol for 5 min, 95% ethanol (v/v) for 5 min, 80% ethanol (v/v) for 5 min and distilled water for 5 min. Antigen retrieval, blocking, staining procedure, mounting and visualisation of slides was performed as outlined above (Section 2.8.2).

2.9: Animal models

All animal experiments were performed in accordance with the UK Animal (Scientific Procedures) Act 1986 and the ARRIVE guidelines for experiments involving animals (Kilkenny *et al.* 2010). All mice were housed in an air-conditioned room maintained at 22 ± 2˚C with a 12 h dark: 12 h light cycle (08:00-20:00).

2.9.1: Swiss TO mice

Male Swiss TO mice (8 wk) were purchased from Envigo (Huntingdon, UK) derived from a nucleus colony originally sourced from the National Institute of Health (Maryland, USA). Mice were single caged with drinking water and standard rodent maintenance diet (60% carbohydrate, 30% protein, 10% fat (12.99 kJ/g), Trouw Nutrition, Cheshire, UK) supplied *ad libitum*. Age-matched, Swiss TO were used as a model of normoglycemia and grouped according to body weight and non-fasting plasma glucose.

2.9.2: Diet induced diabetic mice

Male Swiss TO mice (8-10 wk) were obtained from Envigo (Huntingdon, UK) as described previously (Section 2.10.1). Groups of 3-5 mice (10 wk old) were caged with drinking water and high fat diet (35% carbohydrate, 20% protein, 45% fat (26.15 kJ/g), Special Diet Service, Essex, UK) supplied ad libitum for 4 months to induce obesity-diabetes. Swiss TO mice on a high fat diet exhibited increased body weight, hyperglycaemia and impaired glucose tolerance when compared to mice on the standard rodent maintenance diet as outlined previously (Bailey *et al.* 1986). This form of diet-induced diabetes in mice closely resembles a high fat western diet and several important clinical features identified in human obesity.

2.10: Acute *in-vivo* glucose tolerance tests

2.10.1: Materials

Fluoride/ heparin coated microcentrifuge tubes were purchased from Sarstedt (Germany). D-glucose and NaCl were obtained from BDH Chemicals (Poole, Dorset, UK). Bayer Contour Next glucose meter and strips were sourced from Williams Medical Supplies (Rhymney, UK).

2.10.2: Glucose tolerance tests

Two animal models were utilised in these studies including Swiss TO mice and high fat fed Swiss TO mice. Mice were fasted for 18 h prior to testing. Groups of mice (n=6) were maintained as described in Section 2.9, with food withheld for the duration of the experiment. Blood samples were collected via tail vein bleeding of conscious mice prior to the commencement of testing (0 min). GPCR agonists were administered orally in combination with glucose (18 mmol/kg BW) or in combination with glucose and the DPP IV inhibitor Sitagliptin Phosphate (50 mg/kg BW). Blood (50 µl) was collected at 15, 30, 60, 90 and 120 min post administration and centrifuged at 16,060 × *g* for 3 min at 4ºC. Plasma glucose was measured using an automated glucose oxidase procedure with a Beckman glucose analyser (Rhymney, UK) and insulin was determined by radioimmunoassay. Intestinal hormone secretion was assessed using specific ELISA kits; total GLP-1 (Millipore, UK) and total GIP (Millipore, UK). DPP-IV activity was evaluated by Gly-Pro-AMC cleavage (Sigma, UK).

2.11: Chronic biological effects of ALA and Abn-CBD in high fat fed induced diabetic mice

2.11.1: Materials

ALA and Abn-CBD were purchased from Tocris Bioscience (Bristol, UK). Sitagliptin Phosphate was sourced from Apex Bioscience (Durham, North Carolina, USA). Multi species GLP-1 total and rat/mouse GIP total ELISA kits were supplied by Merck Millipore (Watford, UK). Insulin was purchased from Sigma-Aldrich (Poole, Dorset, UK). D-glucose and NaCl were obtained from BDH Chemicals (Poole, Dorset, UK). Materials for triglyceride assay were purchased from Instrumentation Laboratory

(Warrington, UK) while kits for total cholesterol and HDL were purchased from Randox (Co Antrim, UK). Amylase assay kits were purchased from Abcam (Cambridge, UK).

2.11.2: Treatment procedure and parameters assessed

Long-term daily oral administration of ALA and Abn-CBD (0.1 μmol/kg body weight) monotherapy or combinational therapy (Sitagliptin; 50 mg/kg BW) or saline (0.9% w/v NaCl) were assessed in high fat fed-induced diabetic Swiss TO mice (n=8) (Section 2.9.2). Glucose tolerance was assessed by an OGTT which was performed 4 months after the commencement of the high fat diet and prior to the study on 18 h fasted Swiss TO mice. Food intake, fluid intake, body weight, non-fasted plasma glucose and insulin concentrations were monitored every 3 days as indicated in the figures. Blood samples were collected and analysed for plasma glucose and insulin, GLP-1, GIP and DPP-IV activity. After 21-day oral administration of GPCR agonist-based therapies, glucose tolerance was assessed by an OGTT (18 mmol/kg body weight) on 18 h fasted as previously outlined (Section 2.10.2).

2.11.3: Insulin sensitivity

Blood glucose was measured from the cut tail vein tip of non-fasted Swiss TO mice using the handheld Acensia Countour glucose meter (Bayer Healthcare, UK) prior to the injection of insulin. Following the intraperitoneal injection of insulin (40 U/kg) prepared in saline (0.9% v/v), blood glucose was measured at 30, 60 min post injection.

2.11.4: Dual energy X-ray absorption (DEXA)

Non-fasted mice were anesthetised by isoflurane, killed by cervical dislocation and placed on the specimen tray taking care to extend limbs from the body. Calibration and quality control were achieved by 25 measures of the aluminium/lucite phantom (0.069 g/cm^2,

12.0% fat) using a Lunar PIXImus Dual energy X-ray absorption (DEXA) system (software version 1.4x). DEXA scanning was performed on all carcasses as per manufacturer's guidelines. The Lunar PIXImus DEXA system calculates percentage body fat and the fully integrated densitometer estimates bone mineral density (BDM, g/cm^3) and bone mineral content (BMC, g). A representative DEXA scan of a lean Swiss TO mouse and a high fat fed-induced diabetic mouse are shown in Fig. 2.4.

2.11.4: Measurement of plasma hormones and biomarkers

Blood was collected via tail vein bleed on conscious mice every 3 days for biochemical analysis. Plasma glucose determination was performed using a Bayer Contour Next meter (Leverkusen, DE) every 3 days. Plasma insulin was quantified using insulin radioimmunoassay as previously described in Section 2.2.3. Rat/mouse GIP total ELISA kit (Millipore, Watford, UK) was used to measure total GIP concentrations in mouse plasma following chronic treatment. Multi species GLP-1 total ELISA was used to measure total GLP-1 content of mouse plasma. Rodent alpha amylase and C-reactive protein ELISA kits were performed using terminal plasma samples following 21-day treatment. DPP-IV activity was assessed on terminal plasma by Gly-Pro-AMC cleavage.

2.11.5: Assessment of plasma lipid profiles

Plasma triglyceride and HDL cholesterol and total cholesterol concentrations were measured using an I-lab 650 clinical chemistry instrument (Instrumentation Laboratory, Warrington, UK). Reagents for triglyceride assay were purchased from Instrumentation Laboratory (Warrington, UK) while kits for total cholesterol and HDL were purchased from Randox (Co Antrim, UK). LDL cholesterol (mM) was calculated using the Friedewald equation:

$$\text{LDL cholesterol} = \text{Total cholesterol} - \text{HDL cholesterol} – 2.2/\text{Triglycerides}$$

2.11.6: Tissue extraction and immunofluorescence staining

Pancreases were extracted in 4% PFA (w/v) for immunohistochemistry examination or snap frozen in liquid nitrogen for measurement of pancreatic insulin content. Pancreatic tissues were processed, cut (as previously outlined Section 2.8.3) and stained for insulin, glucagon, GPR55, GPR120 and Ki-67 at the dilutions recorded in Table 2.1. Relative quantification was performed on >50 islets per treatment group using Cell F software.

2.11.7: Pancreatic insulin content

Pancreatic tissues were placed in -80˚C for storage prior to the determination of pancreatic insulin content. Tissue was thawed and rinsed in ice cold PBS before being weighed homogenised in a bijou tube with 5 ml (50 mg tissue) of ice cold RIPA buffer (150 mM sodium chloride, 1.0% Triton X-100, 0.5% sodium deoxycholate, 0.1% SDS, 50 mM Tris, pH 8.0). Samples were centrifuged at 3000 rpm for 20 min using a Beckman microcentrifuge (Beckman Instruments, UK) and supernatant transferred to a fresh tube. Samples were measured by insulin radioimmunoassay (Section 2.2.3) and normalised to total protein content.

2.11.8: Measurement of Amylase activity

Multi-species Amylase Assay Kit (Colorimetric) was used to quantify plasma amylase activity. Amylase Assay kit (Colorimetric) (ab102523) detects activity of α-amylase through a two-step reaction. α-Amylase will cleave the substrate ethylidene-pNP-G7 to produce smaller fragments that are eventually modified by α-glucosidase, causing the release of a chromophore that can then be measured at OD = 405 nm. The assay can detect α-amylase content as low as 0.2 mU. Plasma (20 µl) was used for analysis. Each kit contained one 96 well plate.

Components of the kit were pre-warmed to room temperature before commencing the assay as per manufacturer's protocol. A 0-20 nmol amylase standard and positive controls were prepared following manufacturers protocol. An aliquot (100 µl) of reaction mix was prepared for each reaction by mixing 50 µl of assay buffer with 50 µl of substrate buffer. Samples, standards and controls were added to each well, followed by 100 µl of reaction mix. The plate was then mixed on an orbital shaker for 1 min at 400 rpm. The absorbance was then immediately determined at OD=405 in a kinetic mode, every 2 min for 60 min at 25^{o}C using a FlexStation 3. Two time points (T1 and T2) within the linear range of the standard were chosen to calculate the amylase activity, as per manufacturer's protocol.

2.12: DPP-IV assay

2.12.1: Materials

All water used was purified using Milli-Q Water Purification System (Millipore Corporation, Milford, MA, USA). 4-(2-hydroxyethyl)-1-piperazineethanesulfonic acid (HEPES), N, N-Dimethyl-formamide (DMF), Gly-Pro-7-amido-4-methylcoumarin (Gly-

pro AMC), 7-amino-4-methylcoumarin (AMC) and acetic acid were purchased from Sigma-Aldrich (Poole, Dorset, UK). Black, flat bottom, 96-well plates were obtained from Greiner Bio-One (Gloucestershire, UK).

2.12.2: Measurement of plasma DPP-IV activity

This fluorometric method is based on the liberation of AMC from the substrate Gly-Pro-AMC by the enzyme DPP-IV in plasma or tissue. A stock solution of 50 mM AMC was dissolved in DMF and from this stock 100 µl was added to 5 ml of distilled water. This provides a 1 mM AMC solution which is used to prepare the standard curve ranging from 0.24-15.6 µM dissolved in 1 mM HEPES buffer (pH 7.4) (Fig. 2.5). Standards were performed in triplicate by adding 35 µl to each well. Unknown samples were also performed in triplicate by the addition of 10 µl sample with 25 µl of 1 mM HEPES containing Gly-pro AMC substrate (1.8 mM). The 384 well plate was incubated at 37˚C for 60 min and reaction stopped by adding 70 µl of 3M acetic acid (pH 2.6). AMC was measured on the FlexStation 3 (Molecular Devices, CA, USA) using excitation wavelength of 370 nm with 9 nm slit-width and emission of 440 nm with 2.5 nm slit-width. Unknown samples were interpolated from the curve and one unit of DPP-IV activity was defined as the enzyme activity which produced 1 µM of AMC per 10 µl of plasma in 1 min (µM/ml/min).

2.13: Enzyme-linked immunosorbent assay (ELISA)

2.13.1: Materials

Multi species GLP-1 total ELISA and rat/mouse GIP total ELISA kits were purchased from Merck Millipore (Watford, UK). Mouse C-reactive Protein was purchased from Abcam (Cambridge, UK)

2.13.2: Measurement of GLP-1

Multi species GLP-1 total ELISA kits were used to quantify the GLP-1 content of both plasma and cell culture supernatant samples. This is a sandwich-based ELISA which measures both the 7-36 and 9-36 forms of GLP-1. Plasma (20 µl) was used for analysis. Each kit contained one 96 well plate.

Components of the ELISA were pre-warmed to room temperature before commencing the assay as per manufacturer's protocol. A 4.1-100 pM GLP-1 standard was prepared from 1000 pM GLP-1 standard. Quality control 1 and quality control 2 were reconstituted in H_2O. Blank, standard and quality control wells were tested in duplicate while unknown samples were assayed in triplicate. Following plate preparation as per manufacturer's protocol, 50 µl of standards, quality controls and unknown samples were added and incubated at room temperature for 1.5 h on a horizontal orbital microplate shaker at 450 rpm. Solutions were decanted and wells washed 3 times with wash buffer (300 µl). Detection antibody (100 µl) was added and plate incubated for 1 h on a horizontal orbital microplate shaker at room temperature at 450 rpm. Detection antibody was decanted and wells washed 3 times with 300 µl of wash buffer before the addition of 100 µl of enzyme solution and incubation for 30 min on a horizontal orbital microplate

shaker at 450 rpm. Enzyme solution was decanted, wells washed 3 times with wash buffer (300 µl) and 100 µl of substrate solution added. The plate was incubated on a horizontal orbital microplate shaker at 450 rpm until a blue colour was formed. Stop solution (100 µl) was added and absorbance read at 450 nm and 590 nm using a FlexStation 3. A typical GLP-1 standard curve is shown with absorbance versus log GLP-1 concentrations in Fig. 2.6.

2.13.3: Measurement of GIP

Rat/mouse GIP total ELISA kits were used to quantify plasma GIP concentrations. This is a sandwich-based ELISA which measures both the 1-42 and 3-42 forms of GIP. Plasma (20µl) was used for analysis. Each kit contained one 96 well plate.

Components of the ELISA were pre-warmed to room temperature before commencing the assay as per manufacturer's protocol. An 8.2 to 2000 pM GIP standard was prepared from a 2000 pM GIP standard. Quality control 1 and quality control 2 were reconstituted in H_2O. Blank, standard and quality control wells were tested in duplicate while unknown samples were assayed in triplicate. Following plate preparation as per manufacturer's protocol, 10 µl of standards, quality controls and unknown samples were added to the appropriate wells and incubated at room temperature for 1.5 h on a horizontal orbital microplate shaker at 450 rpm. Solution were decanted and wells washed 3 times with wash buffer (300 µl). Detection antibody (100 µl) was added for 1 h on a horizontal orbital microplate shaker at room temperature at 450 rpm. Detection antibody was decanted and wells washed 3 times with 300 µl of wash buffer before the addition of 100 µl of enzyme solution and incubation for 30min on a horizontal orbital microplate shaker at 450 rpm. Enzyme solution was decanted, wells were washed 3 times with wash buffer (300 µl) and 100 µl of substrate solution was added. The plate

was incubated on a horizontal orbital microplate shaker at 450 rpm until a blue colour was formed. Stop solution (100 µl) was added then absorbance was read at 450 nm and 590 nm using a FlexStation 3. A typical GIP standard curve is shown with absorbance versus log GIP concentrations in Fig. 2.7.

2.13.4 Measurement of C-Reactive Protein

Mouse C-Reactive Protein (CRP) ELISA kits were used to quantify plasma CRP concentrations. Plasma (20 µl) was used for analysis. Each kit contained one 96 well plate.

Components of the ELISA were pre-warmed to room temperature before commencing the assay as per manufacturer's protocol. A 156.25 to 40000 pg/ml CRP was prepared from a 4000 pg/ml standard (Fig. 2.8). Each well was incubated for 5 min in 300 µl of wash buffer. Wash buffer was decanted and wells received 50 µl of sample or standard. Blank, standard and quality control wells were tested in duplicate while unknown samples were assayed in triplicate. Following plate preparation, 50 µl of antibody solution was added to each well and incubated at room temperature for 1 h on a horizontal orbital microplate shaker at 400 rpm. Solutions were decanted and wells washed 3 times with wash buffer (300 µl). TMB substrate solution (100 µl) was added to the plate and incubated for 10 min on a horizontal orbital microplate shaker at room temperature at 400 rpm in the dark. Stop solution (100 µl) a was added to each well and mixed on a horizontal orbital microplate shaker at 400 rpm for 1 min. Optical density was read at 450 nm using a FlexStation 3.

2.14: Statistics

Data are expressed as the mean ± the standard error of the mean (SEM). Results were compared using the Student's t-test or one-way ANOVA followed by Newman-Keuls *pos-hoc* test as appropriate on Prism graph pad version 5.0. Incremental area under the curve (AUC) with baseline subtraction, were calculated using Prism graph pad. Differences in data were considered to be statistically significant for $p<0.05$.

Table 2.1: Primary and secondary antibodies used for immunohistochemical staining.

Primary Antibodies	Host Species	Dilution	Source
Insulin	Guinea pig	1:500	Abcam (Cambridge, UK)
Glucagon	Guinea pig	1:200	Raised in-house
GPR120	Rabbit	1:100	Santa Cruz Biotechnology (CA, USA)
GPR55	Rabbit	1:100	Cayman Chemical (Michigan, US)
Ki-67	Rabbit	1:200	Abcam (Cambridge, UK)

Secondary Antibodies	Host Species	Dilution	Source
Anti-guinea pig Alexafluor 488 nm	Goat	1:400	Molecular probes, Life Technologies (Paisley, UK)
Anti-Rabbit Alexafluor 488 nm	Goat	1:400	Molecular probes, Life Technologies (Paisley, UK)
Anti-guinea pig Alexafluor 594 nm	Donkey	1:400	Molecular probes, Life Technologies (Paisley, UK)
Anti-Rabbit Alexafluor 594 nm	Donkey	1:400	Molecular probes, Life Technologies (Paisley, UK)

Table 2.2: Primary and secondary antibodies used for western blotting.

Primary Antibodies	Host Species	Dilution	Source
Total ERK1/2	Rabbit	1:1000	Cell Signalling (MA, USA)
Phospho ERK1/2	Rabbit	1:1000	Cell Signalling (MA, USA)
Total JNK	Rabbit	1:200	Santa Cruz Biotechnology (CA, USA)
Phospho JNK	Rabbit	1:200	Santa Cruz Biotechnology (CA, USA)
Total p38	Rabbit	1:200	Santa Cruz Biotechnology (CA, USA)
Phospho p38	Rabbit	1:200	Santa Cruz Biotechnology (CA, USA)
GPR120	Rabbit	1:150	Santa Cruz Biotechnology (CA, USA)
GPR55	Rabbit	1:150	Cayman Chemical (Michigan, US)
B-actin	Mouse	1:2500	Cell Signalling (MA, USA)

Secondary Antibodies	Host Species	Dilution	Source
Anti-Rabbit IgG	Donkey	1:10000	GE Healthcare (IL, USA)
Anti-Mouse IgG	Sheep	1:10000	GE Healthcare (IL, USA)

Table 2.3: Primers used for qPCR.

Rat:

Gene nomenclature	Name/Alias	Primer Sequence (5' – 3')
GAPDH	Glyceraldehyde 3-phosphate dehydrogenase	Sense- GCATCTTCTTGTGCAGTGCC Anti-sense - GAGAAGGCAGCCCTGGTAAC
Ffar4	GPR120	Sense - AAGTCAATCGCACCCACTTC Anti-sense - GAAGAGGTTGAGCACCAAGC
Gpr55	GPR55	Sense - GGGATACAAGTGCTTCCACA Anti-sense - AAAGGAGACCACGAAGACGA
INS	Insulin	Sense - GCCCAGGCTTTTGTCAAACA Anti-sense - CTCCCCACACACCAGGTAGAG

Mouse:

Gene nomenclature	Name/Alias	Primer Sequence (5' – 3')
GAPDH	Glyceraldehyde 3-phosphate dehydrogenase	Sense- GGACCTCATGGCCTACATGG Anti-sense - TAGGGCCTCTCTTGCTCAGT
Ffar4	GPR120	Sense - CTGGGGCTCATCTTTGTCGT Anti-sense - ACGACGAGCACTAGAGGGAT
Gpr55	GPR55	Sense - ATTTGGAGCAGAGGCACGAA Anti-sense - AGGTTGAGAACCAGGCCAAG
INS	Insulin	Sense - CTGGTGGGCATCCAGTAACC Anti-sense - CAAAAGCCTGGGTGGGTTTG

Figure 2.1: Typical HPLC profile representing iodinated insulin.

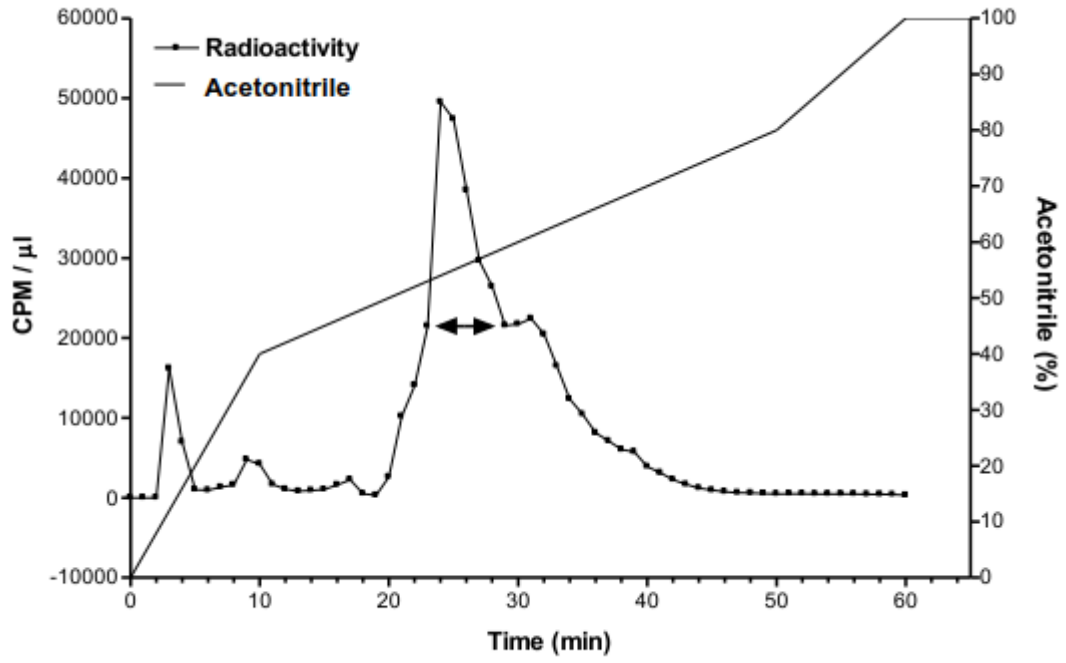

Insulin labelled with $Na^{125}I$ was prepared using the iodogen method described in Section 2.2.2. Separation of bound and unbound fractions was achieved by RP-HPLC using a Vydac C-8 column. Elution of the iodination reaction mixture occurred using 70% acetonitrile/H_2O (v/v) increased to 40% after 10 min, to 80% over 40 min and 80-100% over 10 min. Unbound $Na^{125}I$ was initially eluted between 3-6 min while insulin labelled with $Na^{125}I$ was eluted between 24-30 min as indicated by the black arrows on the graph. Fractions with the highest CPM underwent antibody binding testing and fractions with similar binding were pooled and stored at 4˚C.

Figure 2.2: Typical standard curve obtained for insulin RIA from rat insulin standards.

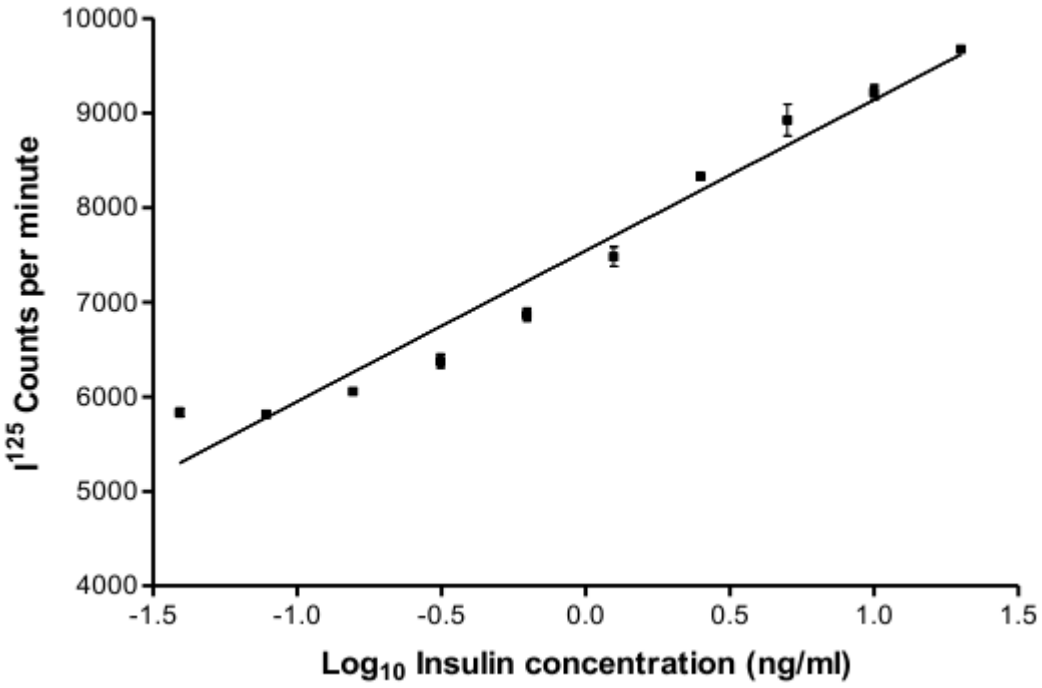

A rat insulin standard curve ranging from 0.039-20 ng/ml by serial dilutions of the stock standard (R^2 = 0.96). Unknown values were interpolated from the standard curve and insulin concentrations anti-logged into ng/ml. Values are ± SEM (n=3).

Figure 2.3: A typical standard curve obtained from a cAMP assay.

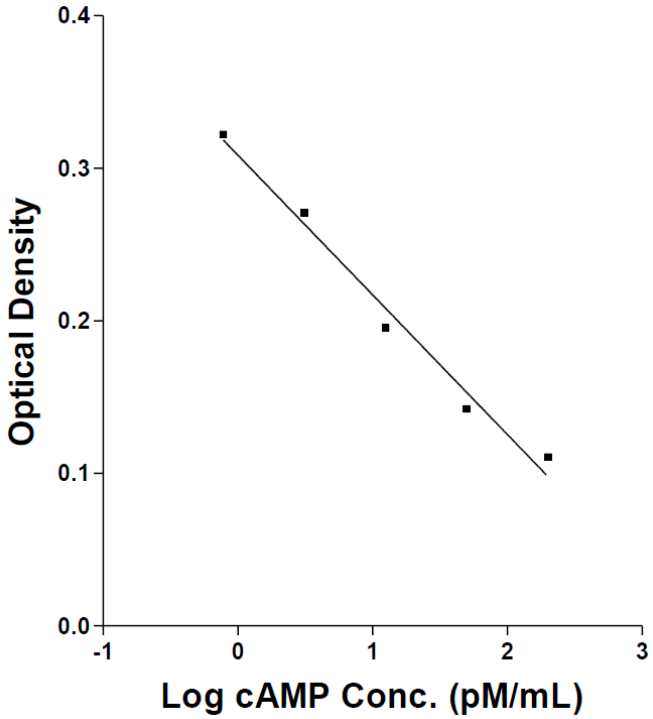

A cAMP curve with standard concentrations of 0.78-200 pM/ml by serial dilution of a 2,000 pM/ml stock (R2 = 0.984). Unknown values are interpolated for the determination of cAMP concentration and anti-logged into pM/ml. Values are ± SEM (n=3).

Figure 2.4: Representative Dual energy X-ray absorption (DEXA) images of (A) a lean Swiss TO mouse and (B) high fat fed-induced diabetic Swiss TO mouse.

A

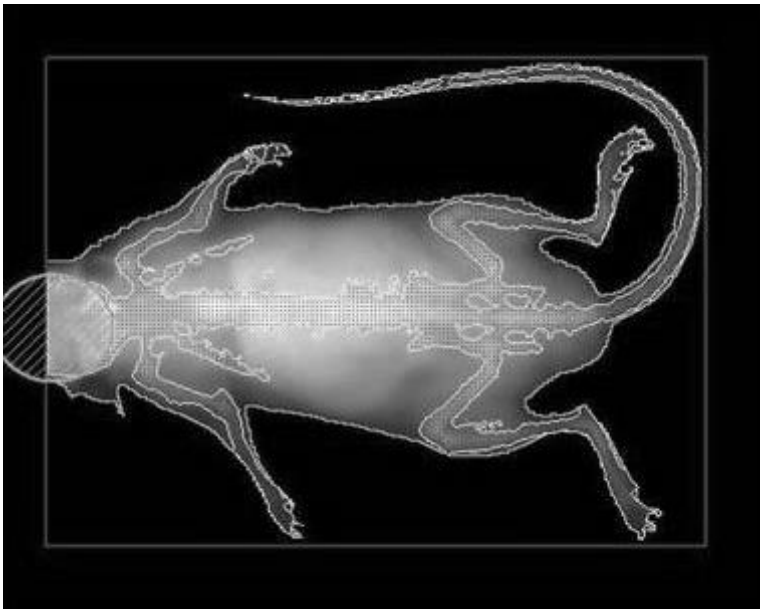

B

Mice were analysed after prior calibration and quality control with the aluminium/lucite phantom (0.069 g/cm2, 12.0% fat) obtained by DEXA using a PIXImus system (software version 1.4x).

Figure 2.5: A typical standard curve obtained from a DPP-IV activity assay.

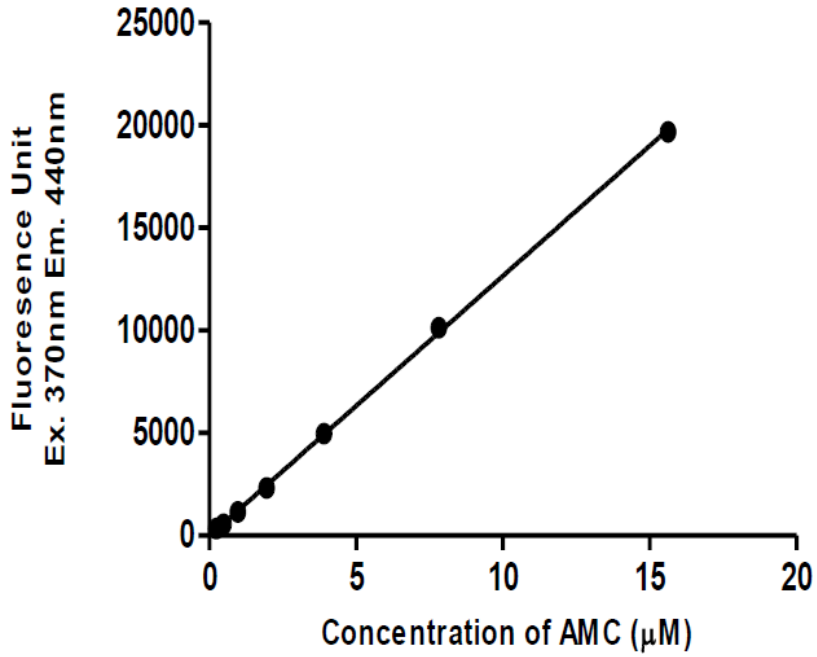

A DPP-IV standard curve with standard concentrations of AMC ranging from 0.24-15.6 μM (R2 = 0.999). Unknown values are interpolated for the determination of AMC concentration and DPP-IV activity calculated as μM/ml/min. Values are ± SEM (n=3).

Figure 2.6: Typical standard curve obtained for multi species GLP-1 total ELISA.

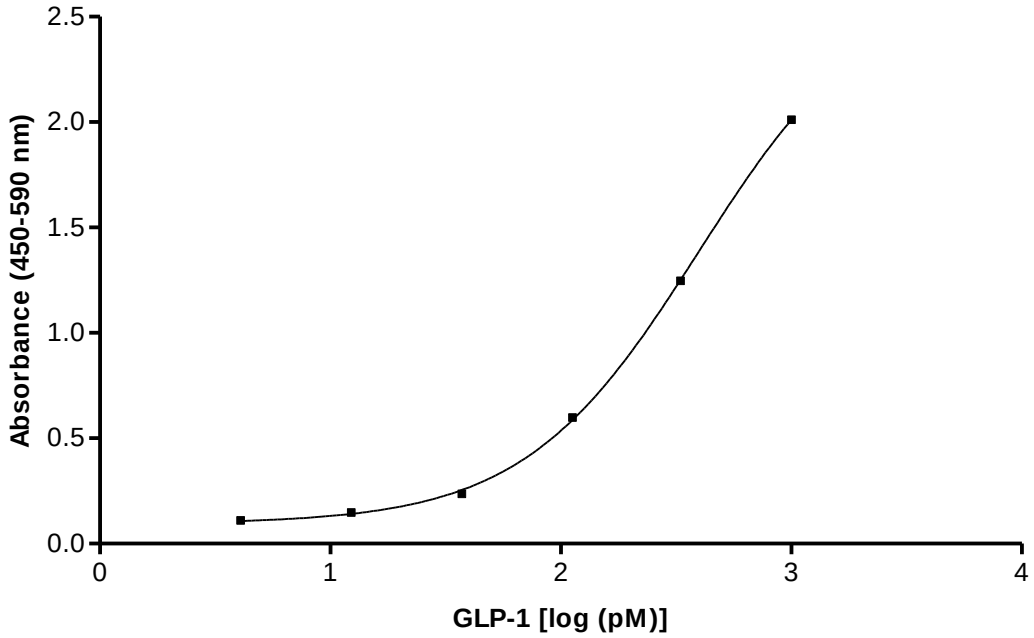

A GLP-1 standard curve with standard concentrations of 4.1-1000 pM by serial dilution of a 1000 pM stock. Absorbance of unknown values was used to interpolate their concentration from the standard curve to quantify GLP-1 concentration. Quality control samples (QC1, QC2) which both fell within the recommended range were provided by the supplier and used to validate the assay. Values are ± SEM (n=2).

Figure 2.7: Typical standard curve obtained for rat/mouse GIP total ELISA.

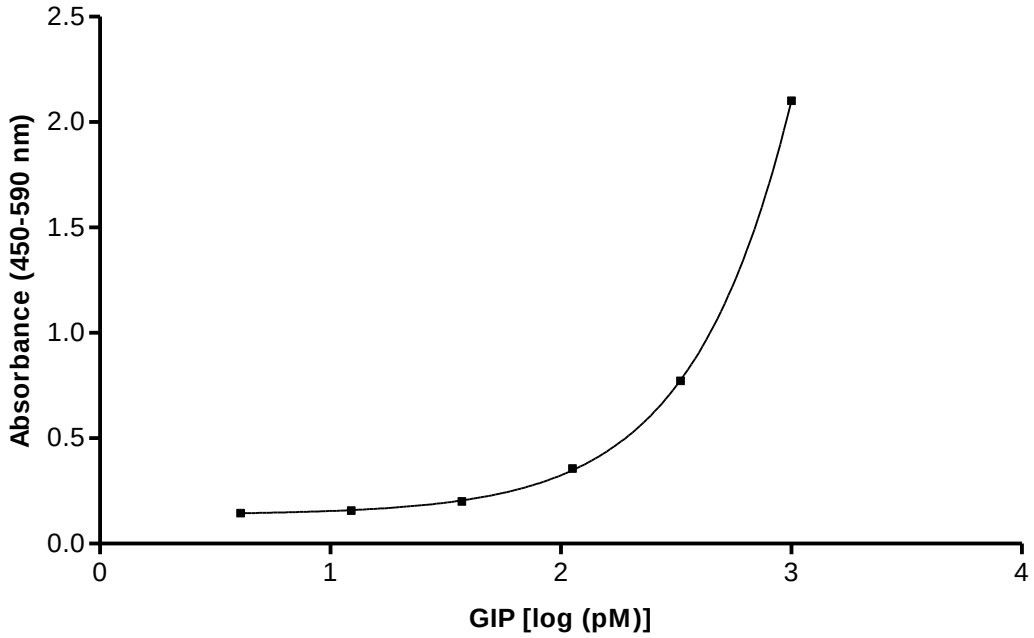

A GIP standard curve with standard concentrations of 8.2-2000 pM by serial dilution of a 2000 pM stock. Absorbance of unknown values was used to interpolate their concentration from the standard curve to quantify GIP concentration. Quality control samples (QC1, QC2) which both fell within the recommended range were provided by the supplier and used to validate the assay. Values are ± SEM (n=2).

Figure 2.8: Typical standard curve obtained for mouse C-reactive protein ELISA.

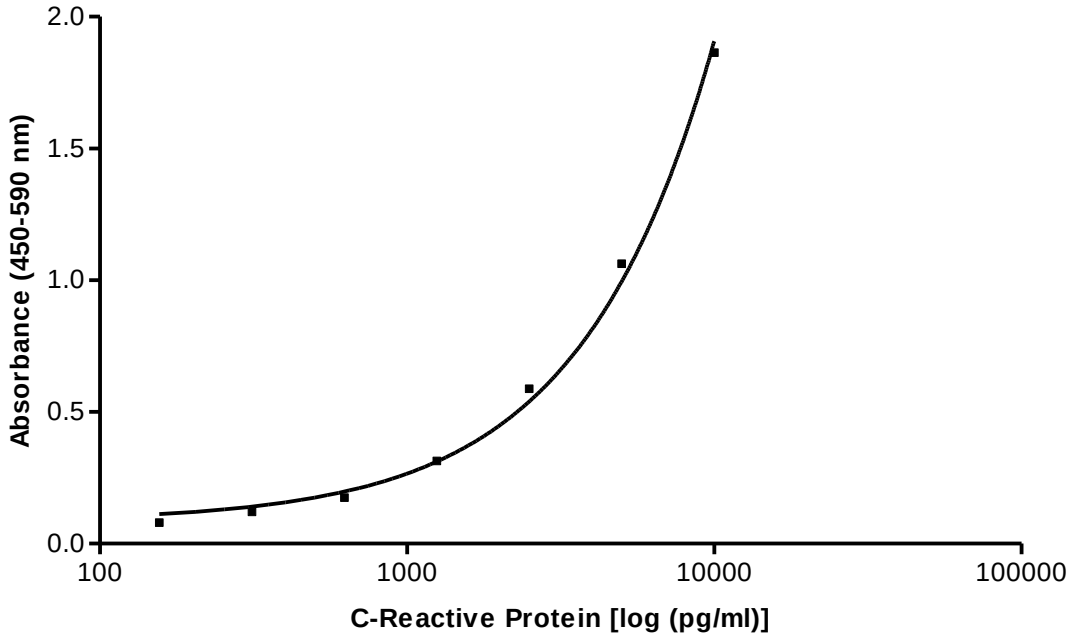

A CRP standard curve with standard concentrations of 1.56-40000 pg/ml by serial dilution of a 40000 pg/ml stock. Absorbance of unknown values was used to interpolate their concentration from the standard curve to quantify CRP concentration. Values are ± SEM (n=2).

Chapter 3

Evaluation of the effects of GPR120 activation on insulin secretion and islet cell function *in-vitro*

3.1: Summary

Long-chain fatty acid (LCFA) sensing G-protein coupled receptors (GPCRs) have been identified as potential anti-diabetic targets, through the enhancement of islet and intestinal cell function. The acute metabolic effects of GPR120 activation towards insulin secretion and islet cell regeneration was evaluated by utilising a range of endogenous and synthetic GPR120 agonists.

Insulinotropic activity and specificity of GPR120 agonists were assessed in rodent (BRIN-BD11) and human (1.1B4) pancreatic cells, with agonist cytotoxicity assessed by MTT analysis. Secondary messenger signalling pathways intracellular Ca^{2+}, cAMP and MAPKs were investigated upon GPR120 activation. Effects of GPR120 agonist treatment on islet cell proliferation and apoptosis were assessed in BRIN-BD11 and α-TC1.9 cells. Expression of GPR120 mRNA and protein were evaluated by qPCR and western blotting in BRIN-BD11 cells upon agonist treatment in both normoglycaemic and hyperglycaemic conditions.

A range of GPR120 agonists (ALA, DHA, EPA, GW9508, Compound A, GSK137647) demonstrated insulinotropic capabilities in pancreatic BRIN-BD11 ($p<0.05$-$p<0.001$) and 1.1B4 ($p<0.05$-$p<0.001$) cells, with endogenous ALA demonstrating the most potent effect ($p<0.05$-$p<0.001$) from BRIN-BD11 cells at 5.6 mmol/l (2-fold; EC_{50} = 9.25 x 10^{-9} mol/l) and 16.7 mmol/l (1.9-fold; EC_{50} = 6.886 x 10^{-8} mol/l) glucose. Potent GPR120 antagonist (AH-7614) impaired the insulinotropic response of GSK137647 ($p<0.05$-$p<0.001$) and Compound-A ($p<0.05$-$p<0.001$) in BRIN-BD11 cells. GPR40 antagonist (GW1100) had no effect on the potency of GSK137647 and Compound A. GPR120 agonist had no effect on cAMP production, whilst antagonising the IP_3 receptor reduced the insulinotropic response of ALA and GSK137647 by 69-84% ($p<0.01$-$p<0.001$) in

BRIN-BD11 cells. GPR120 agonists induced ERK1/2 and p38 phosphorylation, whilst reducing JNK phosphorylation *in-vitro.* Overall, GPR120 agonists improved beta cell viability ($p<0.05$-$p<0.01$) and reduced beta apoptosis ($p<0.05$-$p<0.01$), with opposing effects demonstrated towards pancreatic alpha cells. Incubation of BRIN-BD11 cells with GPR120 agonists increased GPR120 ($p<0.01$) gene expression at 16.7 mM glucose, with a corresponding increase in GPR120 ($p<0.05$-$p<0.01$) protein expression confirmed by western blotting. GPR120 upregulation was attenuated under normoglycaemic conditions ($p<0.05$).

These findings indicate that targeting GPR120 has therapeutic potential for the treatment of type 2 diabetes by potentiating insulin secretion and islet cell regeneration.

3.2: Introduction

G-protein coupled receptor 120 (GPR120), also known as FFAR4, is a G-protein coupled receptor that is agonised by long chain saturated fatty acids (C14-18) and unsaturated fatty acid molecules (C16-22) (Lagerstrom & Schioth 2008, Hara *et al.* 2011). The genomic sequence for the human GPR120 gene is expressed on chromosome 10 at position q23.3 (Ichimura *et al.* 2009). The translated GPR120 protein is expressed in numerous tissues throughout the body including the lungs, spleen, intestines, pro-inflammatory macrophages and peripheral tissues (Moore *et al.* 2009). In addition, recent studies have identified the extensive expression of GPR120 in the pancreatic islet, with further experimentation demonstrating expression within pancreatic beta cell lines (BRIN-BD11, RINm5f, INS-1E, MIN6) (Dhayal *et al.* 2008, Moran *et al.* 2014).

Previous reports have identified that free fatty acid (FFA) molecules are the endogenous agonists for GPR40 (FFAR1), GPR41 (FFAR3), GPR43 (FFAR2), GPR84 and GPR120 (FFAR4) (Ichimura *et al.* 2009, Hara *et al.* 2012, Houthuijzen et al. 2017). Short chain fatty acid molecules exhibit specificity towards GPR41 and GPR42, medium chain fatty acids stimulate GPR84 activation, whereas long chain fatty acid molecules potentiate GPR120 and GPR40 activation (Ichimura *et al.* 2009, Hara *et al.* 2012, Houthuijzen *et al.* 2017). Furthermore, GPR40 and GPR120 display 10% sequence homology and both can be agonised by ligands sharing structural similarities. As the functional role of GPR40 is well understood, it has been attributed to the beneficial effects associated with long chain fatty acid molecules, particularly omega-3 fatty acids (Itoh, *et al.* 2003, Moran *et al.* 2014, Moran *et al.* 2016). The function of the recently discovered GPR120 receptor remains elusive and warrants further investigation.

Many studies have identified GPR120 to act as a lipid sensor in the body, through the biological regulation of adipogenesis, inflammation and glucose homeostasis. Moreover, a recent report demonstrated that a mutated variant of GPR120 (p.R270H) impairs the signalling response of the receptor upon agonist binding. Subsequently, defects were observed towards GPR120-mediated intracellular calcium mobilisation and GLP-1 secretion from intestinal L-cells (Ichimura *et al.* 2012, Bonnefond *et al.* 2015). An additional study demonstrated that siRNA mediated GPR120 gene disruption impaired the protective effects of omega-3 fatty acid agonists in serum starved STC-1 cells (Iaboubov *et al.* 2006).

GPR120 has been shown to have a regulatory function within the gastrointestinal (GI) tract and controls the release of intestinal hormones from intestinal L-cells and K-cells, such as glucagon-like peptide-1 (GLP-1), gastric inhibitory polypeptide (GIP) and cholecystokinin (CCK). In addition, high expression of GPR120 was observed in

intestinal cell lines, including STC-1 and GLUT-ag cells (Hirasawa *et al.* 2005, Iaboubov *et al.* 2006, Sankoda *et al.* 2017). Another study demonstrated GPR120 activation with endogenous agonist alpha-linolenic acid (ALA) to mediate GLP-1 secretion in rats (Hirasawa *et al.* 2005). However, conflicting studies have also indicated that GPR120 has no secretory effect towards GLP-1 in the intestines (Paulsen *et al.* 2014).

Although, the functional role of GPR120 in the GI tract has been heavily documented, the metabolic effect of GPR120 activation in the pancreatic beta cell has remained elusive until recently (Moran *et al.* 2014). GPR120 activation was demonstrated to have a regulatory effect on glucose stimulated insulin secretion (GSIS) from clonal pancreatic beta cells and mouse islets with a range of endogenous and synthetic agonists, including docosahexaenoic acid (DHA), eicosapentaenoic acid (EPA), alpha-linolenic acid (ALA) and GW-9508 (Moran *et al.* 2014). Furthermore, these agonists demonstrated glucose lowering and insulinotropic actions *in-vivo* (Moran *et al.* 2014).

Upon agonist binding and receptor activation, GPR120 stimulates an array of downstream signalling events mediated through the Gαq intracellular subunit. Gαq phosphorylation stimulates a range of secondary signalling events through phospholipase C (PLC), including intracellular calcium mobilisation and mitogen-activated protein kinase (MAPK) phosphorylation (Hirasawa *et al.* 2005, Burns *et al.* 2014, Gerbino & Colella 2018). At present, the mechanism of GPR120-mediated insulin secretion from the pancreatic beta cell remains inconclusive. However, initial studies have shown a range of GPR120 agonists to augment intracellular calcium, which indicates involvement of inositol trisphosphate (IP_3) on intracellular calcium stores through PLCβ signalling (Moran *et al.* 2014). ALA and DHA have been shown to promote the transient and rapid phosphorylation of the receptor in HEK293 cells (Burns *et al.* 2014). Although, the PLC and protein kinase C (PKC) pathways are predominately associated with GPR120

signalling, DHA has also been shown to stimulate G-protein coupled receptor kinase (GPK6) through GPR120 activation (Burns *et al.* 2014). Thr(347), Ser(350) and Ser(357) have been identified as the primary phosphorylation sites of GPR120 in the C-terminal tail (Burns *et al.* 2014).

Recently, novel long chain fatty acid molecules with high specificity for GPR120 have become available. Oh *et al.,* have developed an orally available, selective, high affinity, small GPR120 agonist (Compound A) that exhibits a range of anti-diabetic effects, with initial studies showing oral administration to improve glucose tolerance, increase insulin sensitivity and exert anti-inflammatory effects *in-vivo* (Oh *et al.* 2014). In addition, Sparks *et al.,* identified a potent GPR120 agonist GSK137647 that exhibited secretory effects towards insulin and GLP-1 *in-vitro* (Sparks *et al.* 2014). In addition, *in-vivo* findings showed that GSK137647 induced GLP-1 release by mouse circumvallate papillae (Martin *et al.* 2012, Sparks *et al.* 2014)

The extensive expression of GPR120 in numerous tissues with metabolic function (pancreatic islet, intestines, adipose) indicates that it may have therapeutic potential in the maintenance of glucose homeostasis (Hirasawa *et al.* 2005, Tanaka *et al.* 2008, Moran *et al.* 2014). This present study aims to evaluate the acute metabolic effects and intracellular signalling events of GPR120 activation in the pancreatic beta cell using a range of endogenous and synthetic ligands.

3.3: Materials and methods

3.3.1: Materials

ALA, GW9508, DHA, EPA, alanine and AH7614 were purchased from Sigma-Aldrich (Poole, Dorset). GSK137647 was purchase from Tocris (Bristol, UK) and Compound A from Cayman Chemical (Michigan, US). All other materials were purchased from suppliers as detailed in Section 2.

3.3.2: Acute insulin secretion studies from pancreatic BRIN-BD11 cells

BRIN-BD11 cells were sub-cultured and seeded into 24-well plates at a density of 150,000 cells per well, then supplemented with 1 ml of RPMI media and allowed to attach overnight, as outlined in Section 2.1.2. ALA, GW9508, DHA, EPA, GSK137647, Compound A (10^{-12}-10^{-4} mol/l) and AH7614 (10^{-5} mol/l) were added to KRBB buffer, supplemented with 5.6 mmol/l or 16.7 mmol/l glucose. Cells were pre-treated with 1.1 mmol/l glucose KRBB for 40 min at 37^{o}C. After pre-incubation, test solutions were added and incubated for 20 min at 37^{o}C. Aliquots (900 µl) of cell supernatant were removed and stored at -20^{o}C until determination of insulin concentrations by radioimmunoassay, as outlined in Section 2.2.3. MTT cytotoxicity analysis was conducted with identical test parameters as insulin secretory studies previous detailed in Section 2.1.6.

3.3.3: Determination of GPR120 mRNA expression in pancreatic BRIN-BD11 cells

BRIN-BD11 cells were sub-cultured and seeded into 6-well plates at a density of 1,000,000 cells per well, then supplemented with 2 ml of RPMI media and allowed to

attach overnight, as outlined in Section 2.1.2. Cell were pre-incubated with 1.1 mmol/l glucose for 1 h min at 37^{o}C. Agonist test solutions (10^{-4} mol/l) were prepared in KRBB buffer at 5.6 mmol/l or 16.7 mmol/l glucose. Test solutions were incubated for 4 h at 37^{o}C. After incubation, cells were lysed and RNA harvested with TRIzol reagent (Sigma, UK). RNA was purified then converted to cDNA as previously described in Section 2.6.2. SYBR green PCR kit (Roche, UK) was used for qPCR as previously detailed in Section 2.6.3.

3.3.4: Immunofluorescence staining of BRIN-BD11 cells

As detailed in Section 2.8.2.

3.3.5: Determination of cAMP production in pancreatic BRIN-BD11 cells

BRIN-BD11 cells were sub-cultured and seeded into 6-well plates at a density of 1,000,000 cells per well, then supplemented with 2 ml of RPMI media and allowed to attach overnight, as outlined in Section 2.1.2. Cells were pre-incubated with 1.1 mmol/l glucose for 40 min at 37^{o}C. Agonist test solutions (10^{-4} mol/l) and IBMX (10 mmol/l) were prepared in KRBB buffer at 16.7 mmol/l glucose and assessed for cAMP production. After incubation, cells were lysed and cAMP detected with the cAMP ELISA kit as previously described in Section 2.4.2.

3.3.6: MAPK signalling and GPR120 expression analysis by western blotting in pancreatic BRIN-BD11 cells

BRIN-BD11 cells were sub-cultured and seeded into 6-well plates at a density of 1,000,000 cells per well, then supplemented with 2 ml of RPMI media and allowed to attach overnight, as outlined in Section 2.1.2. Cells were pre-incubated with 1.1 mmol/l glucose for 40 min at 37^{o}C. Agonist test solutions (10^{-4} mol/l) and PMA (200 nmol/l) were prepared in KRBB buffer at 5.6 mmol/l or 16.7 mmol/l glucose. After incubation, cells were lysed at various timepoints with RIPA buffer, supplemented with protease and phosphatase inhibitors. Cell lysates (25 µg) were prepared and separated by SDS-PAGE and transferred to a nitrocellulose membrane, as previously described in Section 2.7. Membranes were probed with total and phosphorylated anti-ERK1/2, anti-JNK and anti-p38 antibodies for MAPK signalling and anti-GPR120 for receptor expression. β-actin was used as a control to normalise data. Images were captured using a G:BOX Chemi XX9 imager (Syngene, UK) and densitometry analysis performed using ImageJ.

3.3.7: ERK1/2 signalling analysis by flow cytometry in pancreatic BRIN-BD11 cells

BRIN-BD11 cells were sub-cultured and seeded into 6-well plates at a density of 1,000,000 cells per well, then supplemented with 2 ml of RPMI media and allowed to attach overnight, as outlined in Section 2.1.2. Cells were pre-incubated with 1.1 mmol/l glucose for 40 min at 37^{o}C. Agonist test solutions (10^{-4} mol/l) and PMA (200 nmol/l) were prepared in KRBB buffer at 16.7 mmol/l glucose. After incubation, cells were detached with trypsin, pelleted by centrifugation then re-suspended in 600µl of flow cytometry staining buffer, supplemented with anti-phospho-ERK1/2 antibodies. Samples were conjugated with an AlexaFluor488 secondary antibody. Samples were gated prior to FITC-GFP expression analysis by flow cytometry.

3.3.8: Cellular viability and apoptosis studies on pancreatic BRIN-BD11 and α-TC1.9 cells

BRIN-BD11 and α-TC1.9 cells were sub-cultured and seeded into a clear 96-well plate at a density of 40,000 cells per well and allowed to attach overnight, as previously outlined in Sections 2.1.2 and 2.1.4. Agonist test solutions (10^{-4} mol/l) and cytokine cocktail solution (TNF-α [200 U/ml], IFN-γ [20 U/ml], IL-1β [100 U/ml]) were prepared in RPMI/DMEM media, then added to the cells and incubated for 20 h at 37^{o}C. Cell viability and apoptosis was determined with Apo-Live-Glo multiplex analysis as per manufacturer's protocol; cell viability by protease activity, cell apoptosis by caspase 3/7 activity (Promega, USA).

3.4: Results

3.4.1: Effect of GPR120 agonists on insulin secretion from clonal pancreatic BRIN-BD11 cells.

The insulinotropic effect of a range of naturally occurring (ALA, EPA, DHA) and synthetic (GW9508, Compound A, GSK137647) GPR120 agonists was assessed in the clonal pancreatic BRIN-BD11 cell line. Essential omega-3 fatty acid ALA (10^{-9}-10^{-4} mol/l) stimulated insulin secretion at 5.6 mmol/l glucose ($p<0.001$) (Fig. 3.1A). At stimulatory glucose concentrations of 16.7 mmol/l, ALA (10^{-8}-10^{-4} mol/l) stimulated insulin secretion ($p<0.05$-$p<0.001$), with a 2.2-fold increase observed at the highest concentration (10^{-4} mol/l) (Fig. 3.2A).

Non-essential omega-3 fatty acid DHA (10^{-10}-10^{-4} mol/l) augmented insulin release ($p<0.01$-$p<0.001$) from BRIN-BD11 cells at 5.6 mmol/l glucose (Fig. 3.3A). The

insulinotropic response of DHA (10^{-9}-10^{-4} mol/l) was also observed at stimulatory glucose concentrations, with a 2.5-fold increase exhibited at the highest concentration (10^{-4} mol/l) (Fig. 3.4A). Naturally occurring EPA (10^{-9}-10^{-4} mol/l) stimulated a 1.3-1.7-fold ($p<0.05$-$p<0.001$) increase on insulin secretion at 5.6 mmol/l glucose (Fig. 3.5A). At a stimulatory glucose concentration of 16.7 mmol/l, EPA (10^{-8}-10^{-4} mol/l) demonstrated a 1.4-1.9-fold ($p<0.01$-$p<0.001$) increase on insulin secretion, with an 85% increase demonstrated at the highest concentration tested (10^{-4} mol/l) (Fig. 3.6A).

Chemically synthetic GW9508 (10^{-8}-10^{-4} mol/l) stimulated insulin secretion ($p<0.01$-$p<0.001$) at a basal glucose concentration with a 2.2-fold increase observed at the highest concentration (Fig. 3.7A). At hyperglycaemic glucose concentrations (16.7 mmol/l glucose) GW9508 augmented insulin release by 1.7-3.4-fold ($p<0.05$-$p<0.001$) (Fig. 3.8A).

Novel synthetic agonist GSK137647 (10^{-8}-10^{-4} mol/l) stimulated insulin secretion ($p<0.05$-$p<0.001$) at 5.6 mmol/l glucose (Fig. 3.9A). GSK137647 augmented a 1.6-2.8-fold ($p<0.01$-$p<0.001$) increase on insulin secretion at 16.7 mmol/l glucose (Fig. 3.10A). The recently discovered GPR120 ligand Compound A (10^{-10}-10^{-4} mol/l) augmented an insulinotropic response ($p<0.05$-$p<0.001$) from BRIN-BD11 cells at 5.6 mmol/l glucose (Fig. 3.11A). The insulin secretory effect ($p<0.05$-$p<0.001$) of Compound A (10^{-7}-10^{-4} mol/l) was also observed at stimulatory 16.7 mmol/l glucose (Fig. 3.12A).

At basal glucose concentrations of 5.6 mmol/l, agonist potency towards insulin secretion was as follows in descending order: EPA (2.11×10^{-9} mol/l), GW9508 (4.97×10^{-9} mol/l), ALA (9.25×10^{-9} mol/l), DHA (1.36×10^{-7} mol/l), GSK137647 (1.36×10^{-7} mol/l), Compound A (2.97×10^{-7} mol/l). At hyperglycaemic glucose concentrations of 16.7 mmol/l, agonist potency towards insulin secretion was as follows in descending order:

GW9508 (5.55 x 10^{-8} mol/l), Compound A (6.57 x 10^{-8} mol/l), ALA (6.88 x 10^{-8} mol/l), DHA (7.37 x 10^{-7} mol/l), EPA (1.21 x 10^{-6} mol/l), GSK137647 (3.69 x 10^{-6} mol/l).

The positive control (alanine) augmented insulin secretion ($p<0.001$) for all insulin secretory analysis (Fig. 3.1-12A). Cytotoxicity analysis by MTT demonstrated no adverse effects towards BRIN-BD11 cell viability at 5.6 mmol/l and 16.7 mmol/l glucose upon incubation with all agonists at a range of concentrations (Fig. 3.1-12B).

3.4.2: Effect of GPR120 agonists on insulin secretion from clonal human pancreatic 1.1B4 cells

The insulin secretory effect of naturally occurring (ALA) and synthetic (GW9508, Compound A) agonists was further assessed in the human clonal pancreatic 1.1B4 cell line at 5.6 mmol/l and 16.7 mmol/l glucose concentrations. Endogenous omega-3 fatty acid ALA (10^{-8}-10^{-4} mol/l) stimulated insulin secretion by 1.3-2.0-fold ($p<0.05$-$p<0.001$) at 5.6 mmol/l glucose (Fig. 3.13A). The insulinotropic action of ALA (10^{-8}-10^{-4} mol/l) was also observed at 16.7 mmol/l glucose, with a 77% ($p<0.001$) increase demonstrated at the highest concentration tested (10^{-4} mmol/l) (Fig. 3.13B).

Synthetic agonist GW9508 augmented insulin secretion by 1.3-1.6-fold ($p<0.05$-$p<0.01$) at 5.6 mmol/l (Fig. 3.14A). At a stimulatory glucose concentration of 16.7 mmol/l glucose, GW9508 (10^{-7}-10^{-4} mol/l) increased insulin secretion ($p<0.05$-$p<0.01$), with a 46% ($p<0.01$) increase observed at the highest agonist concentration tested (10^{-4} mol/l) (Fig. 3.13B). Novel synthetic Compound A (10^{-8}-10^{-4} mol/l) stimulated insulin secretion ($p<0.05$-$p<0.001$) at a basal glucose concentration (Fig. 3.14A). At 16.7 mmol/l, Compound A (10^{-8}-10^{-4} mol/l) augmented insulin secretion ($p<0.05$-$p<0.001$), with a 192% ($p<0.001$) increase towards insulin secretion (Fig. 3.14B).

ALA was the most potent agonist at 5.6 mmol/l with an EC_{50} value of 5.059 x 10^{-8} mol/l, followed by GW9508 (1.15 x 10^{-7} mol/l) then Compound A (1.22 x 10^{-6} mol/l). In order of potency at 16.7 mmol/l glucose; GW9508 (9.98 x 10^{-7} mol/l), ALA (1.15 x 10^{-6} mol/l) and Compound A (7.97 x 10^{-6} mol/l) (Table. 3.1).

3.4.3: Effect of GPR120 antagonist (AH7614) and GPR40 antagonist (GW1100) on Compound A and GSK137647 induced insulin secretion from clonal pancreatic BRIN-BD11 cells

Compound A and GSK137647 were co-incubated with GPR120 antagonist (AH7614 and GPR40 antagonist (GW1100). The insulin secretory effect of Compound A and GSK137647 was not influenced upon co-incubation with the GPR40 antagonist GW1100 (10^{-5} mol/l), as a similar insulinotropic response was observed in the presence of the antagonist, compared to agonist only (Figure 3.16 A, B; Figure 3.17 A, B).

Co-incubation of the GPR120 antagonist AH-7614 (10^{-5} mol/l) significantly reduced the insulin secretory response of Compound A and GSK137647. At 5.6 mmol/l glucose, in the presence of the GPR120 antagonist, Compound A (10^{-6}-10^{-4} mol/l) augmented insulin secretion by 1.25- to 1.3-fold ($p<0.05$), resulting in a 65% reduction at 10^{-4} mol/l. GSK137647 demonstrated no significant insulin secretory effect in the presence of the antagonist (Fig. 3.16B). At 16.7 mmol/l glucose in the presence of the GPR120 antagonist, Compound A (10^{-5}-10^{-4} mol/l) augmented insulin secretion by 1.7- to 1.8-fold ($p<0.05$), resulting in a 65% reduction compared to agonist only (10^{-4} mol/l) (Fig. 3.17A). GSK137647 at 10^{-7}-10^{-4} mol/l increased insulin secretion by 1.7- to 2.1-fold. ($P<0.01$) (Fig. 3.17B), exhibiting a 40% reduction compared to agonist only at 10^{-4} mol/l.

3.4.4: Expression and distribution of GPR120 and insulin in clonal pancreatic BRIN-BD11 cells

Immunocytochemistry analysis was employed to determine the distribution of (A) DAPI, (B) insulin, (C) GPR120 in BRIN-BD11 cells (Fig. 3.18) High expression of GPR120 and insulin was present in the BRIN-BD11 cell line, with areas of co-localisation displayed between GPR120 and insulin observed upon double immuno-fluorescence staining (Fig. 3.18D).

3.4.5: Effects of GW9508, ALA, Compound A and GSK137647 on GPR120 expression in clonal pancreatic BRIN-BD11 cells

Western blotting and qPCR were employed to determine GPR120 protein and mRNA expression in BRIN-BD11 cells upon agonist treatment at 5.6 mmol/l and 16.7 mmol/l glucose. (Fig. 3.19; Fig. 3.20). GW9508 and ALA reduced GPR120 mRNA expression by 23-39% ($p<0.05$) at 5.6 mmol/l glucose (Fig. 3.19A), compared to 5.6 mmol/l glucose control. Complimentary western blotting showed GW9508 to reduce GPR120 protein expression ($p<0.05$), whilst ALA had no effect on receptor protein expression (Fig. 3.19C). At 16.7 mmol/l glucose, GW9508 and ALA increased GPR120 mRNA expression by 1.7-2.3-fold ($p<0.01$), with complimentary western blotting demonstrating GW9508 (3.4-fold) and ALA (4.8-fold) to increase GPR120 protein expression ($p<0.01$) (Fig. 3.19B; Fig. 3.19D).

At normoglycaemic (5.6 mmol/l glucose) Compound A and GSK137647 down-regulated GPR120 receptor mRNA expression ($p<0.05$) in BRIN-BD11 cells, compared to 5.6 mmol/l glucose (Fig. 3.20A). When exposed to 16.7 mmol/l glucose, Compound A and

GSK137647 incubation increased GPR120 mRNA expression ($p<0.01$), compared to 16.7 mmol/l glucose control (Fig. 3.20B).

Complimentary western blotting demonstrated GSK137647 to upregulate ($p<0.05$) GPR120 protein expression by 1.9-fold ($p<0.05$) in hyperglycaemic conditions, whilst Compound A had no significant effect (Fig. 3.20D). GPR120 protein expression was not altered upon agonist incubation in normoglycaemic conditions (Fig. 3.20C).

3.4.6: Effect of GPR120 agonists on cAMP production and intracellular Ca^{2+} modulated insulin secretion from clonal pancreatic BRIN-BD11 cells

BRIN-BD11 cells were incubated with ALA, GW9508 and GSK137647 (10^{-4} mol/l) and IBMX (10 mmol/l) for 20 min in KRBB supplemented with 16.7 mmol/l glucose. All agonists demonstrated no effects on cAMP production, whilst the positive control (IBMX) stimulated a 19-fold ($p<0.001$) increase (Figure 3.21A).

To investigate intracellular Ca^{2+}-modulated insulin secretion, pancreatic BRIN-BD11 cells were co-incubated with GPR120 agonists (ALA, GSK137647) and Xestospongin C (IP_3 receptor antagonist), resulting in impaired insulin secretory effects ($p<0.01$-$p<0.001$). Xestospongin C reduced the insulinotropic effects of ALA and GSK137647 by 69-86% ($p<0.01$-$p<0.001$) at 10^{-4} mol/l. At 10^{-5} mol/l, Xestospongin C abolished the insulinotropic effects of ALA and GSK137647 ($p<0.001$) (Figure 3.21B).

3.4.7: Effect of GSK137647, GW9508, ALA and PMA on ERK1/2 (p44/42) signalling in clonal pancreatic BRIN-BD11 cells

SDS-PAGE western blotting demonstrated GSK137647, GW9508 and ALA to stimulate ERK1/2 phosphorylation after 15 min incubation in BRIN-BD11 cells (Fig. 3.22). GSK137647 also induced ERK1/2 phosphorylation after 5 min incubation. PMA was used as a positive control and subsequently induced ERK1/2 phosphorylation in a time dependent manner at 10, 15, 30 and 60 min incubation. Total-ERK1/2 concentrations remained unaffected compared to the non-treated control upon agonist treatment at all timepoints.

In addition, flow cytometry demonstrated similar findings, with GSK137647, GW9508, ALA and PMA stimulating ERK1/2 phosphorylation in BRIN-BD11 cells after 15 min incubation (Fig. 3.23). PMA emitted the most potent effect, with 19% ERK1/2 phosphorylation of total cells observed (Fig. 3.23B). In descending order of potency, GPR120 agonists ALA (17%; Fig. 3.23E), GW9508 (8%; Fig. 3.23C) and GSK137647 (7%; Fig. 3.23D) stimulated ERK1/2 phosphorylation after 15 min incubation.

3.4.8: Effect of GSK137647 on JNK, p38 and ERK1/2 MAPK signalling in clonal pancreatic BRIN-BD11 cells

The effect of GSK137647 on mitogen-activated protein kinase (MAPK) signalling was assessed by western blotting in BRIN-BD11 cells (Fig. 3.24). Positive control PMA (200 nm) induced JNK and p38 phosphorylation at 20 min and ERK1/2 phosphorylation at 30 min. GSK137647 treatment from 5-30 min reduced JNK phosphorylation compared to the non-treated control, whilst total-JNK remained unchanged. GSK137647 induced p38 phosphorylation after 5 min incubation, with the response reduced to baseline after 10

min. Total-p38 concentrations were unaffected upon agonist treatment at all timepoints. GSK137647 augmented ERK1/2 phosphorylation at 5- and 15-min incubation, with total-ERK1/2 concentrations remaining unchanged at all timepoints (Fig. 3.24).

3.4.9: Effect of GW9508, ALA and GSK137647 on clonal pancreatic BRIN-BD11 cell viability and apoptosis

BRIN-BD11 cells were incubated with GPR120 agonists for 20 h. Cell viability was determined by protease activity and apoptosis by caspase3/7 activity (Fig. 3.25). At 10^{-6} mol/l, GW9508 increased cell viability by 15% ($p<0.05$), whilst ALA and GSK137647 had no effect. At a higher agonist concentration (10^{-4} mol/l), GW9508 ($p<0.01$) and ALA ($p<0.01$) increased cell viability by 23% with GSK137647 having no effect. Cytokine cocktail incubation reduced cell viability by 13% after 20 h (Fig. 3.25A).

At 10^{-6} mol/l, ALA and GSK137647 reduced caspase3/7 activity by 50% ($p<0.01$) and 27% ($p<0.05$) respectively, whilst GW9508 had no significant effect. At 10^{-4} mol/l, GW9508 ($p<0.05$) and GSK137647 ($p<0.05$) increased caspase3/7 activity by 26-40% with ALA having no effect. Cytokine cocktail incubation increased caspase3/7 by 47% ($p<0.01$) after 20 h (Fig. 3.25B).

3.4.10: Effect of GW9508, ALA and GSK137647 on clonal pancreatic α-TC1.9 cell viability and apoptosis

α-TC1.9 cells were incubated with GPR120 agonists for 20 h. Cell viability was determined by protease activity and apoptosis by caspase3/7 activity (Fig. 3.26). At 10^{-6} mol/l, GW9508, ALA and GSK137647 had no effect towards cell viability. At a higher agonist concentration (10^{-4} mol/l), GW9508, ALA and GSK137647 reduced cell viability

by 23-46% ($p<0.01$-$p<0.001$). Cytokine cocktail incubation reduced cell viability by 32% after 20 h (Fig. 3.26A).

At 10^{-6} mol/l, ALA (18%) and GSK137647 (20%) reduced caspase3/7 activity ($p<0.01$-$p<0.001$), whilst ALA had no significant effect. At a higher agonist concentration (10^{-4} mol/l), ALA and GSK137647 increased caspase3/7 activity by 16-28% ($p<0.001$) with GW9508 having no significant effect. Cytokine cocktail incubation increased caspase3/7 by 15% ($p<0.01$) after 20 h (Fig. 3.26B).

3.5: Discussion

In recent years, research focusing on long chain fatty acids receptors has intensified due to their regulatory role in the maintenance of glucose and lipid homeostasis, including GPR40, GPR120, GPR55 and GPR119 (Hara *et al.* 2011, McKillop *et al* 2013, McKillop *et al.* 2016). Many of the endogenous ligands for long chain fatty acid sensing receptors, such as omega 3 fatty acids DHA and ALA have previously demonstrated insulinotropic and anti-inflammatory properties that are of interest for the treatment of obesity and type 2 diabetes (Oh *et al.* 2010, Moran *et al.* 2014). Interestingly, a GPR40 agonist Fasiglifam (TAK-875) recently underwent stage III clinical trials. During the trial, Fasiglifam demonstrated insulinotropic capabilities to the same potency of the current sulphonylurea Glimepiride, whilst omitting the risk of hypoglycaemia (Otieno *et al.* 2017).

GPR120, also known as free fatty acid receptor 4 (FFAR4) is a class A (rhodopsin) GPCR that has been shown to exert a range of glucose lowering properties (Moran *et al.* 2014). With particular interest, GPR120 was recently shown to be highly expressed in pancreatic islet cells with insulin secretory capabilities upon activation (Moran *et al.* 2014). The

ability of GPR120 to stimulate GLP-1 from intestinal L-cells, accompanied with its regulatory role in islet cell function makes it an attractive therapeutic target (Martin *et al.* 2012). Furthermore, as GPR120 and GPR40 can be activated by similar ligands, such as synthetic GW9508, specific agonists are essential to evaluate the anti-diabetic potential of GPR120.

In this present study, the functional role of GPR120 was assessed in the pancreatic BRIN-BD11 cell line, using a range of endogenous (ALA, DHA, EPA) and synthetic (GW9508, Compound A, GSK137647) agonists. The biological effects of these agonists towards insulin secretion, islet cell regeneration and downstream receptor signalling were evaluated. The insulinotropic activities of the GPR120 agonists were assessed in the pancreatic BRIN-BD11 cell line at both normoglycaemic and hyperglycaemic glucose concentrations. At normoglycemia, ALA and EPA demonstrated the most potent insulin secretory effect for the endogenous agonists (EC_{50} ~10^{-9} mol/l), whereas, GW9508 was the most potent synthetic agonist (EC_{50} 4.97 x 10^{-9} mol/l). At stimulatory glucose concentrations, ALA (EC_{50} = 6.88 x 10^{-8} mol/l) and GW9508 (5.55 x 10^{-8} mol/l) remained the most potent endogenous and synthetically derived agonists.

Complimentary analysis using the human 1.1B4 cell line was employed to validate the insulinotropic capability of GPR120 activation in human beta cells. Endogenous (ALA) and synthetic (GW9508, Compound A) induced insulin secretion from the human cell line at a similar potency to rodent cells, whilst previous studies have also demonstrated glucoregulatory effects of omega 3 fatty acids in humans (Bhaswant *et al.* 2015). With respect to cytotoxicity, previous studies demonstrated ALA, DHA, EPA and GW9508 to have no effects on lactate dehydrogenase (LDH) release from pancreatic cells (Moran *et al.* 2014). Whilst LDH is a marker that requires breakage of the cell membrane for

detection, the present study also revealed that GPR120 agonists demonstrate no cytotoxic effects when assessed by cellular metabolic activity (Bopp & Lettieri *et al.* 2008).

As GPR120 and GPR40 can be activated by similar ligands, the specificity of many endogenous and synthetic GPR120 agonists remains uncertain. Therefore, it is difficult to attribute the biological effects of these putative agonists solely to GPR120 activation. Recently, selective GPR120 agonists (Compound A and GSK137647) have become commercially available (Oh *et al*. 2014, Sparks *et al.* 2014). To demonstrate the selectivity of the novel agonists towards GPR120, potent antagonists for GPR120 and GPR40 were used in insulin secretory studies. In the presence of GPR40 antagonist (GW1100), the insulin secretory response of both Compound A and GSK137647 was relatively unaffected. In contrast, the GPR120 antagonist (AH-7614) impaired the insulinotropic properties of both Compound A and GSK137647, suggesting that these novel agonists stimulate glucose dependent insulin secretion through the mechanics of GPR120 and not GPR40 in the pancreatic beta cell.

Immunocytochemistry demonstrated high expression and co-localisation of GPR120 and insulin in pancreatic BRIN-BD11 cells, which further elucidates the role of GPR120 in insulin secretion from the pancreatic beta cell. Upon agonist treatment, expression analysis demonstrated an upregulation of GPR120 in BRIN-BD11 cells exposed to hyperglycaemia, suggesting that GPR120 may have a regulatory role in the pancreatic islet when exposed to diabetic stress factors. In contrast, agonist treatment under normoglycaemic conditions significantly attenuated GPR120 expression. Thus, revealing the glucose responsive properties of GPR120 expression and the suitability of GPR120 as an anti-diabetic target. In harmony with these findings, previous studies have also demonstrated GPR120 expression to be upregulated in the gut of diet induced obese mice (Paulsen *et al.* 2014).

The mechanism of GPR120-mediated insulin secretion from BRIN-BD11 cells was investigated by assessing cyclic adenosine monophosphate (cAMP) and intracellular Ca^{2+} modulation. GPR120 activation results in the phosphorylation of the intracellular Gαq subunit, whereas GPR40 has been shown to activate both Gαq and Gαs with some agonists (Moran *et al.* 2016). ALA, GSK137647 and GW9508 had no effect on cAMP production in BRIN-BD11 cells, potentially suggesting the involvement of intracellular Ca^{2+} modulation through Gαq activation, with previous studies also showing a range of putative agonists to augment intracellular Ca^{2+} in BRIN-BD11 cells (Moran *et al.* 2014). To correlate this GPR120-induced increase in intracellular Ca^{2+} with insulin secretion, an inositol 1,4,5-trisphosphate (IP_3) receptor antagonist (Xestospongin C) was utilised to block calcium release from the endoplasmic reticulum upon receptor activation. Antagonising the IP_3 receptor impaired the insulinotropic capabilities of endogenous ALA and selective GSK137647, which compliments previous findings and suggests that GPR120-induced insulin secretion is primarily potentiated through Gαq/PLC/IP_3 signalling.

As phospholipase C (PLC) phosphorylation occurs upon GPR120 activation, the diacylglycerol (DAG) branch of the PLC pathway was also investigated. Downstream of DAG, protein kinase C (PKC) can be activated, resulting in the phosphorylation of mitogen-activated protein kinases (MAPK) ERK1/2, JNK and p38. (Putney 2012). MAPK pathways are critical for the regulation of cell survival and growth, whilst also regulating a range of cellular responses, such as proliferation, apoptosis, differentiation and development (Mebratu, 2009, Stewart *et al.* 2015). ERK1/2 activation is associated with cell proliferation and survival, whilst JNK and p38 activation are linked with cell apoptosis and cell death (Mebratu 2009, Stewart *et al.* 2015).

Subsequently, the effect of GPR120 agonists towards ERK1/2, JNK and p38 were investigated. GSK137647, GW9508 and ALA induced ERK1/2 phosphorylation after 15 min when assessed by western blotting and flow cytometry. Interestingly, ALA was the most potent agonist assessed, which mirrors the insulin secretory potency findings and indicates the involvement of ERK1/2 activation in GPR120-indued insulin release. Moreover, GPR120 activation reduced the stress related JNK pathway after 5 min with the effect prolonged throughout the experimental timeframe, indicating a cytoprotective effect of GPR120 activation as JNK activation has been previously linked with beta cell apoptosis (Hou *et al.* 2008, Zhou *et al.* 2014). Previous studies also demonstrated that ERK1/2 phosphorylation is key regulator of insulin synthesis and beta cell proliferation, thus indicating the role of downstream GPR120 signalling in beta cell survival and regeneration (Lawerence *et al.* 2008, Stewart *et al.* 2015).

To assess the effects of GW9508, ALA and GSK137647 on beta cell survival and apoptosis, protease and caspase 3/7 activities were determined upon agonist treatment. ALA and GW9508 at super-physiological concentrations increased cell viability, revealing a proliferative effect of GPR120 activation in the pancreatic beta cell. Complimentary analysis investigating apoptosis showed that ALA and GSK137647 at physiological concentrations markedly reduced apoptosis. Unlike the synthetic agonists tested (GW9508, GSK137647), the endogenous agonist (ALA) exhibited positive effects towards both cell viability and cell apoptosis, therefore revealing the therapeutic potential of ALA in the regeneration of beta cell mass.

Although GPR120 expression has been heavily documented in beta cells, expression has also been shown in glucagon producing alpha cells, whilst endogenous DHA has been shown to potentiate GPR120-dependent glucagon secretion in mice (Whalley *et al.* 2011, Suckow *et al.* 2014). Subsequently, the present study also investigated the proliferative

effects of GPR120 activation in α-TC1.9 cells. GW9508, ALA and GSK137647 had no effect on alpha cell proliferation at physiological concentrations, whilst an overall reduction was observed at super-physiological concentrations. Complimentary analysis showed that super-physiological concentrations of ALA and GSK137647 induced alpha cell apoptosis, whilst physiological concentrations of GW9508 and GSK37647 reduced alpha cell apoptosis. Interestingly, in direct contrast to the analysis in BRIN-BD11 cells, endogenous (ALA) increased alpha cell apoptosis and reduced alpha cell viability.

The study has shown a range of endogenous and synthetic GPR120 agonists to enhance glucose stimulated insulin secretion in rodent and human pancreatic beta cell lines. The biological activation of GPR120 with endogenous and selective agonists potentiates intracellular calcium and MAPK signalling, with increases in beta cell survival also observed. Finally, receptor expression analysis demonstrated the glucose responsive properties of GPR120 under hyperglycaemic stress, a characteristic which may be utilised in the future development of an anti-diabetic agent targeting GPR120.

Table 3.1: Half maximal effective concentration (EC_{50}) of GPR120 agonists in rodent BRIN-BD11 and human 1.1B4 cells at 5.6 mM and 16.7 mM glucose.

Rodent BRIN-BD11 cells

Agonist	5.6 mM glucose	16.7 mM glucose
ALA	9.25×10^{-9} mol/l	6.88×10^{-8} mol/l
DHA	1.36×10^{-7} mol/l	7.37×10^{-7} mol/l
GW9508	4.97×10^{-9} mol/l	5.55×10^{-8} mol/l
GSK137467	1.36×10^{-7} mol/l	3.69×10^{-6} mol/l
EPA	2.11×10^{-9} mol/l	1.21×10^{-6} mol/l
Compound A	2.97×10^{-7} mol/l	6.57×10^{-8} mol/l

Human 1.1B4 cells

Agonist	5.6 mM glucose	16.7 mM glucose
ALA	5.05×10^{-8} mol/l	1.15×10^{-6} mol/l
GW9508	1.15×10^{-7} mol/l	9.98×10^{-7} mol/l
Compound A	1.22×10^{-6} mol/l	7.97×10^{-6} mol/l

Figure 3.1: Acute effect of ALA on insulin secretion and cell viability from clonal pancreatic BRIN-BD11 cells at 5.6 mM glucose.

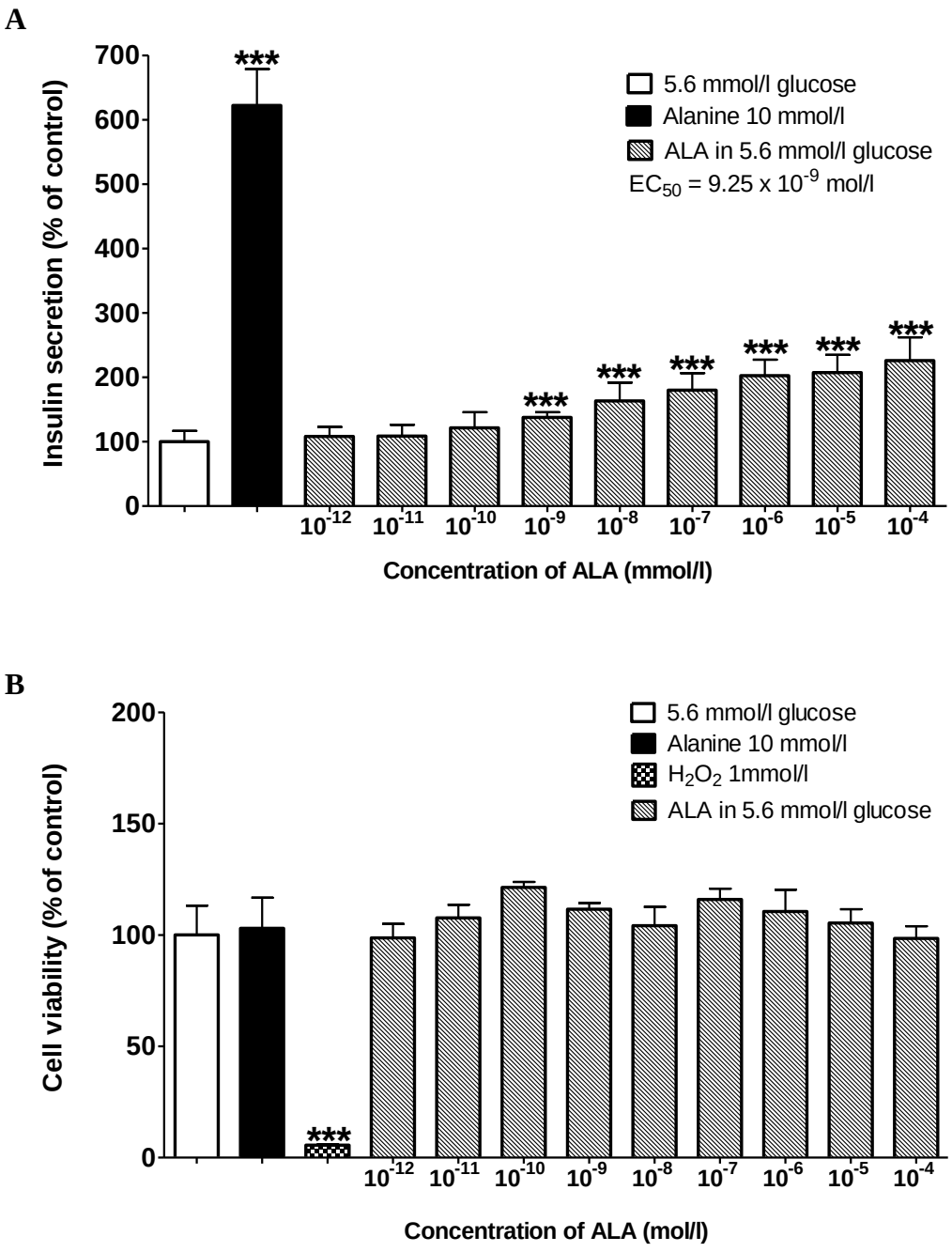

Acute effects of ALA (10^{-12}-10^{-4} M) and alanine (10 mM) on (A) insulin secretion and (B) cell viability (MTT) from clonal pancreatic BRIN-BD11 cells at 5.6 mM glucose. Results are the mean ± SEM (n=8) for insulin secretion and (n=3) for cell viability. ***p<0.001 compared to glucose control.

Figure 3.2: Acute effect of ALA on insulin secretion and cell viability from clonal pancreatic BRIN-BD11 cells at 16.7 mM glucose.

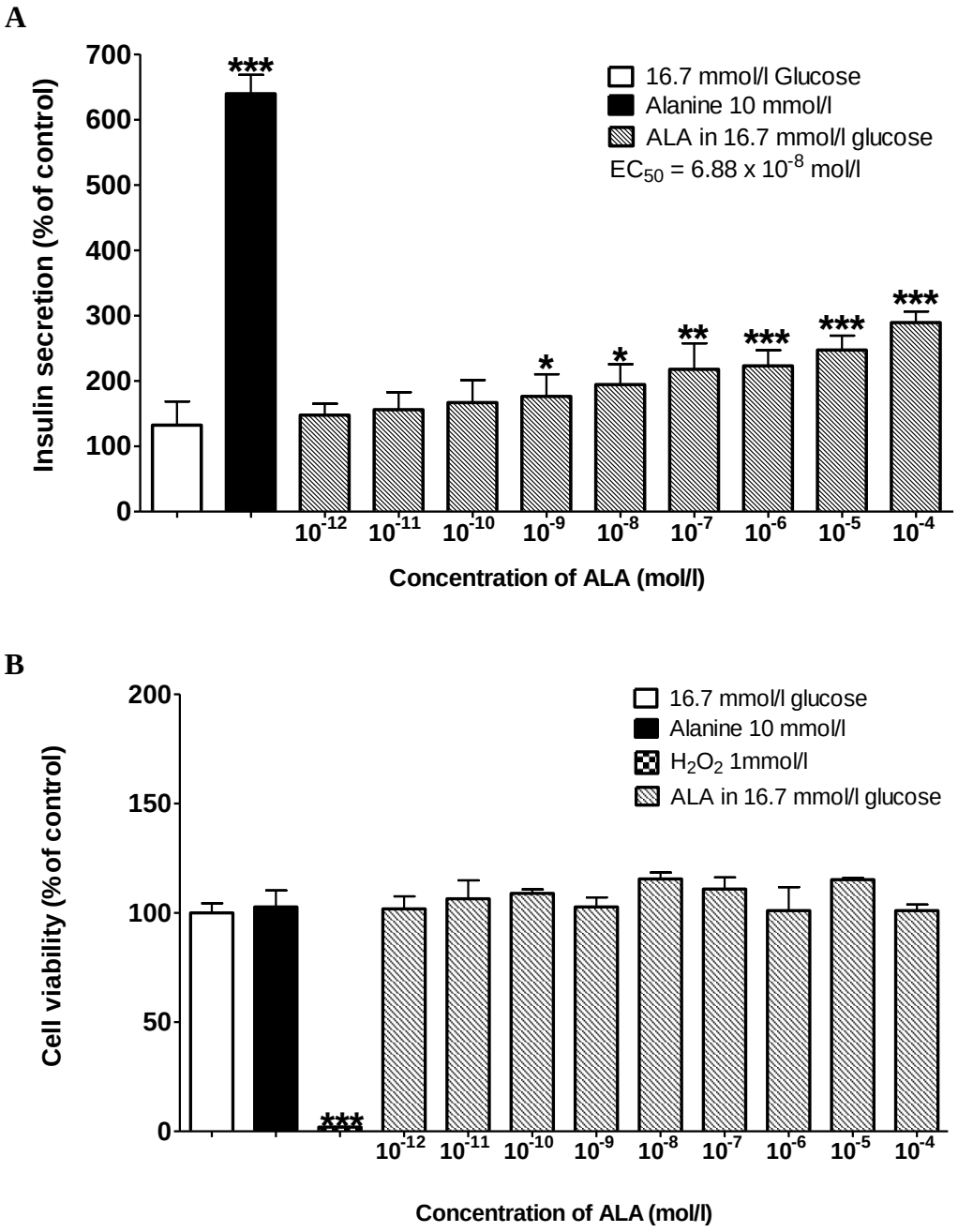

Acute effects of ALA (10^{-12}-10^{-4} M) and alanine (10 mM) on (A) insulin secretion and (B) cell viability (MTT) from clonal pancreatic BRIN-BD11 cells at 16.7 mM glucose. Results are the mean ± SEM (n=8) for insulin secretion and (n=3) for cell viability. *p<0.05, **p<0.01, ***p<0.001 compared to glucose control.

Figure 3.3: Acute effect of DHA on insulin secretion and cell viability from clonal pancreatic BRIN-BD11 cells at 5.6 mM glucose.

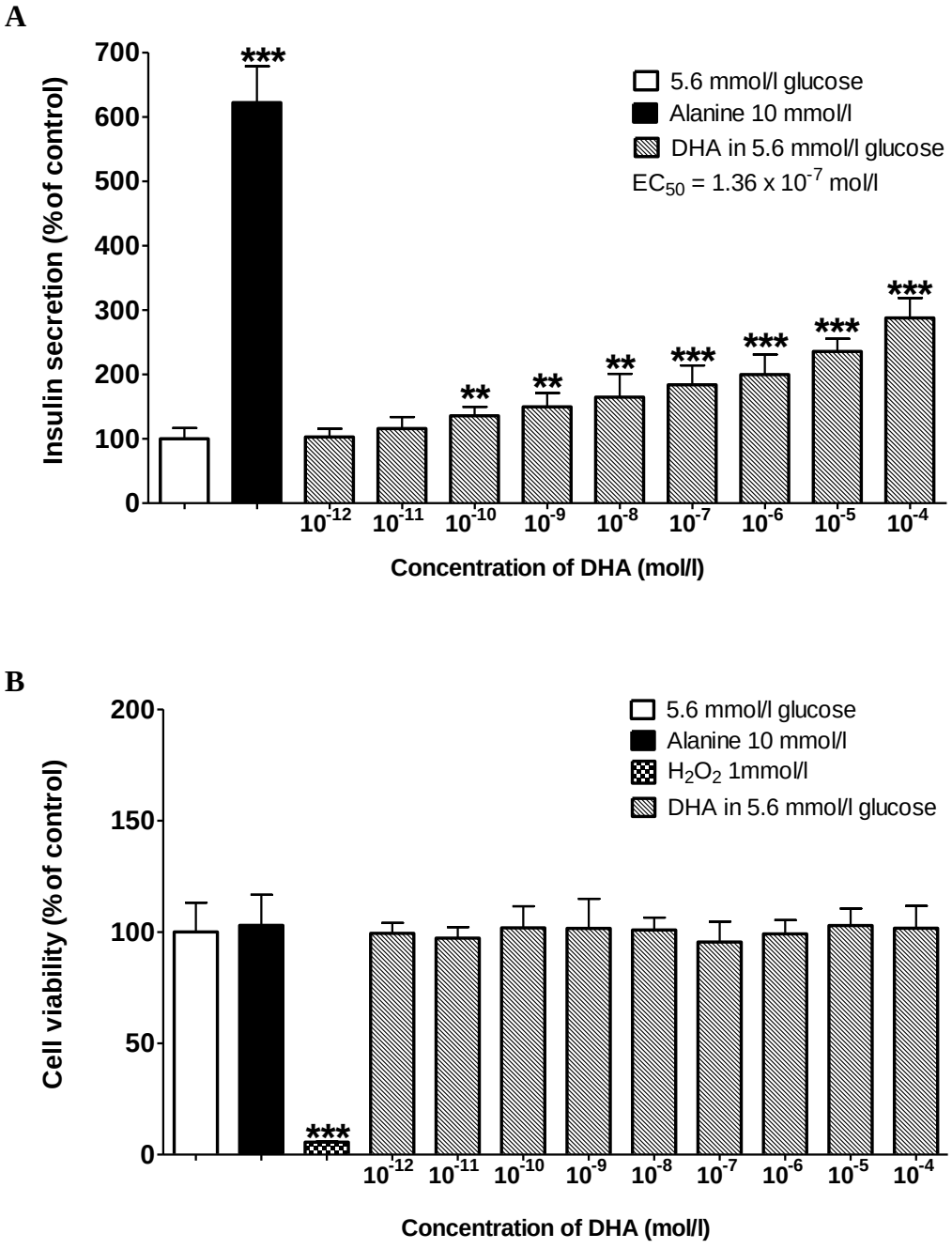

Acute effects of DHA (10^{-12}-10^{-4} M) and alanine (10 mM) on (A) insulin secretion and (B) cell viability (MTT) from clonal pancreatic BRIN-BD11 cells at 5.6 mM glucose. Results are the mean ± SEM (n=8) for insulin secretion and (n=3) for cell viability. **p<0.01, ***p<0.001 compared to glucose control.

Figure 3.4: Acute effect of DHA on insulin secretion and cell viability from clonal pancreatic BRIN-BD11 cells at 16.7 mM glucose.

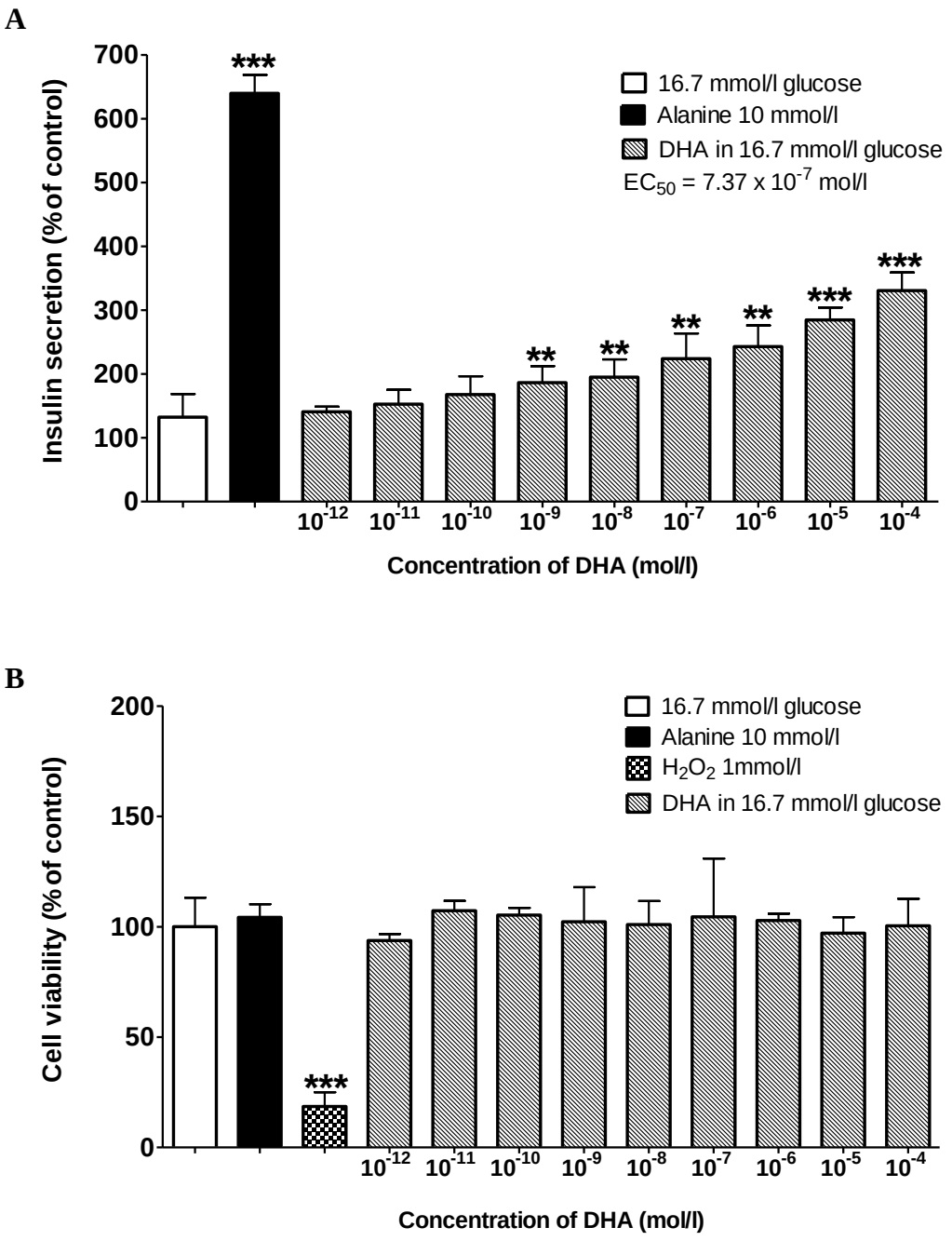

Acute effects of DHA (10^{-12}-10^{-4} M) and alanine (10 mM) on (A) insulin secretion and (B) cell viability (MTT) from clonal pancreatic BRIN-BD11 cells at 16.7 mM glucose. Results are the mean ± SEM (n=8) for insulin secretion and (n=3) for cell viability. **p<0.01, ***p<0.001 compared to glucose control.

Figure 3.5: Acute effect of EPA on insulin secretion and cell viability from clonal pancreatic BRIN-BD11 cells at 5.6 mM glucose.

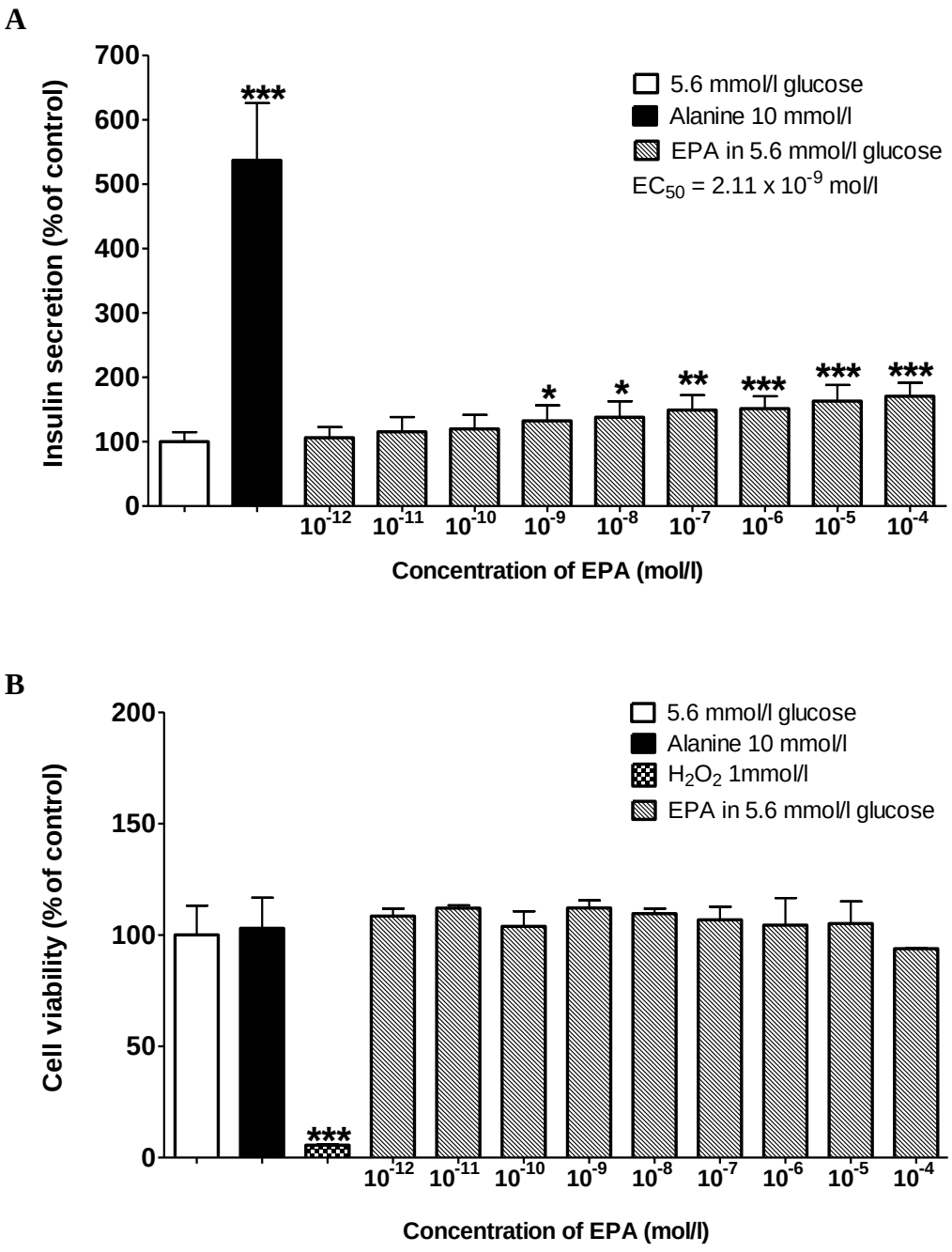

Acute effects of EPA (10^{-12}-10^{-4} M) and alanine (10 mM) on (A) insulin secretion and (B) cell viability (MTT) from clonal pancreatic BRIN-BD11 cells at 5.6 mM glucose. Results are the mean ± SEM (n=8) for insulin secretion and (n=3) for cell viability. *p<0.05, **p<0.01, ***p<0.001 compared to glucose control.

Figure 3.6: Acute effect of EPA on insulin secretion and cell viability from clonal pancreatic BRIN-BD11 cells at 16.7 mM glucose.

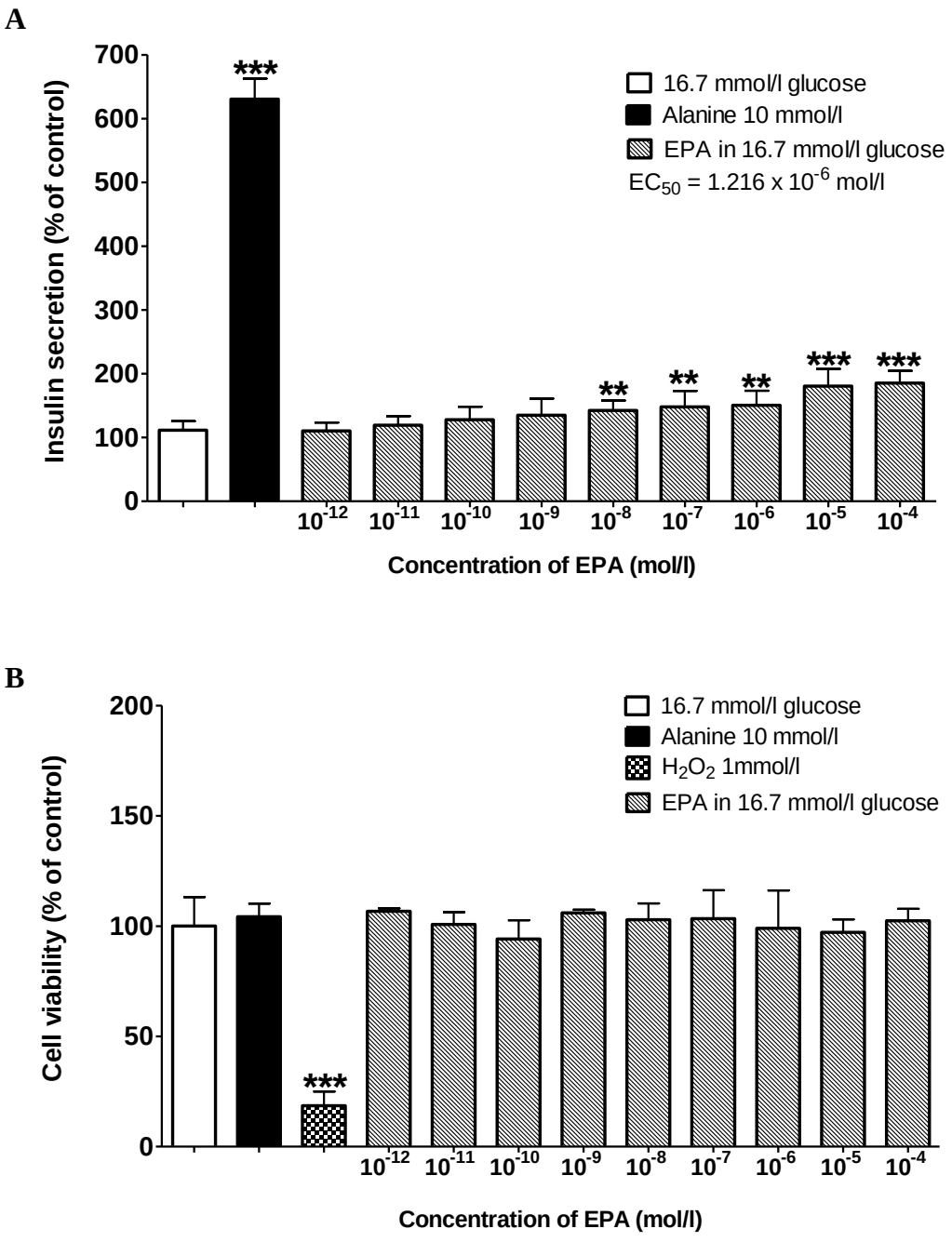

Acute effects of EPA (10^{-12}-10^{-4} M) and alanine (10 mM) on (A) insulin secretion and (B) cell viability (MTT) from clonal pancreatic BRIN-BD11 cells at 16.7 mM glucose. Results are the mean ± SEM (n=8) for insulin secretion and (n=3) for cell viability. **p<0.01, ***p<0.001 compared to glucose control.

Figure 3.7: Acute effect of GW9508 on insulin secretion and cell viability from clonal pancreatic BRIN-BD11 cells at 5.6 mM glucose.

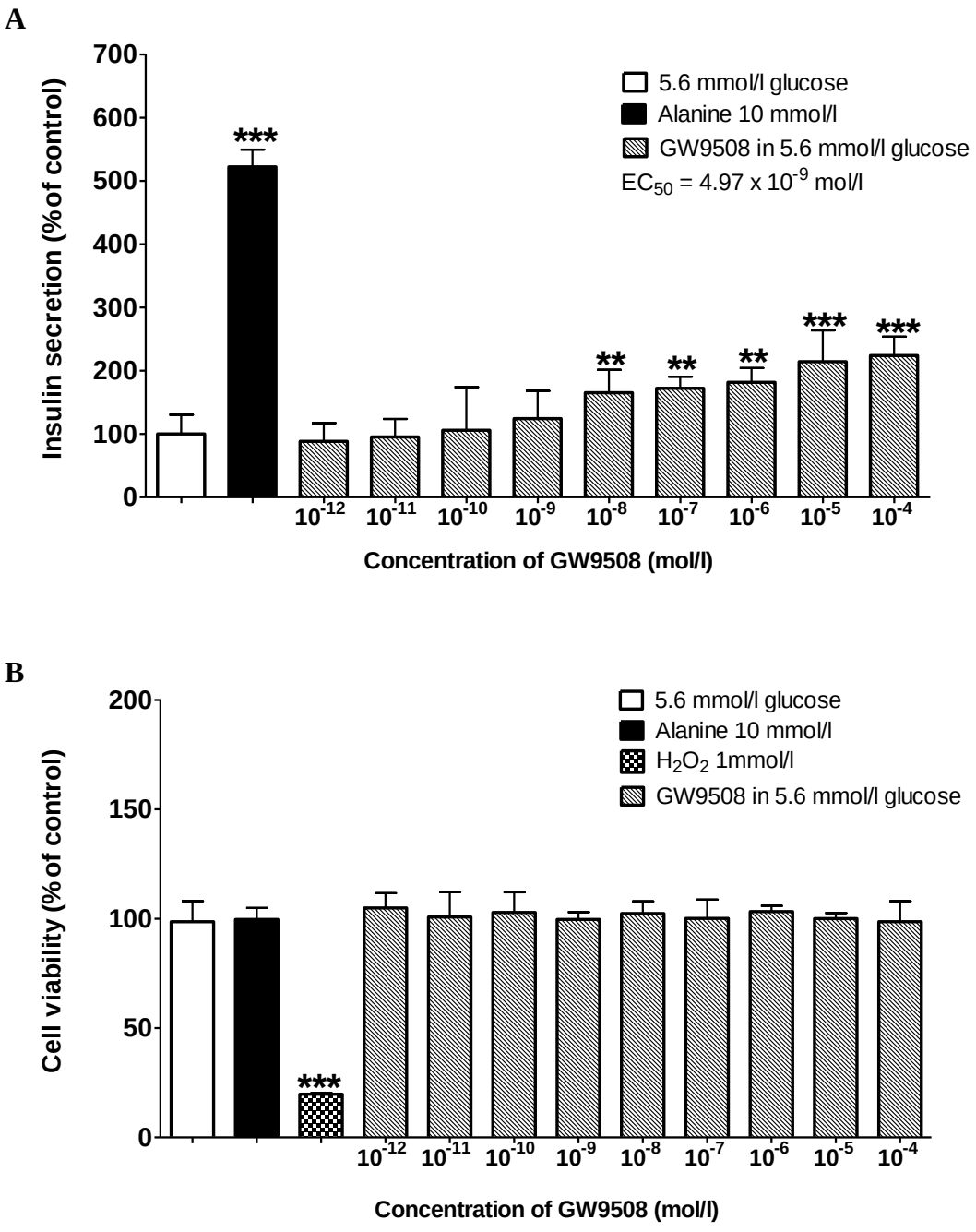

Acute effects of GW9508 (10^{-12}-10^{-4} M) and alanine (10 mM) on (A) insulin secretion and (B) cell viability (MTT) from clonal pancreatic BRIN-BD11 cells at 5.6 mM glucose. Results are the mean ± SEM (n=8) for insulin secretion and (n=3) for cell viability. **p<0.01, ***p<0.001 compared to glucose control.

Figure 3.8: Acute effect of GW9508 on insulin secretion and cell viability from clonal pancreatic BRIN-BD11 cells at 16.7 mM glucose.

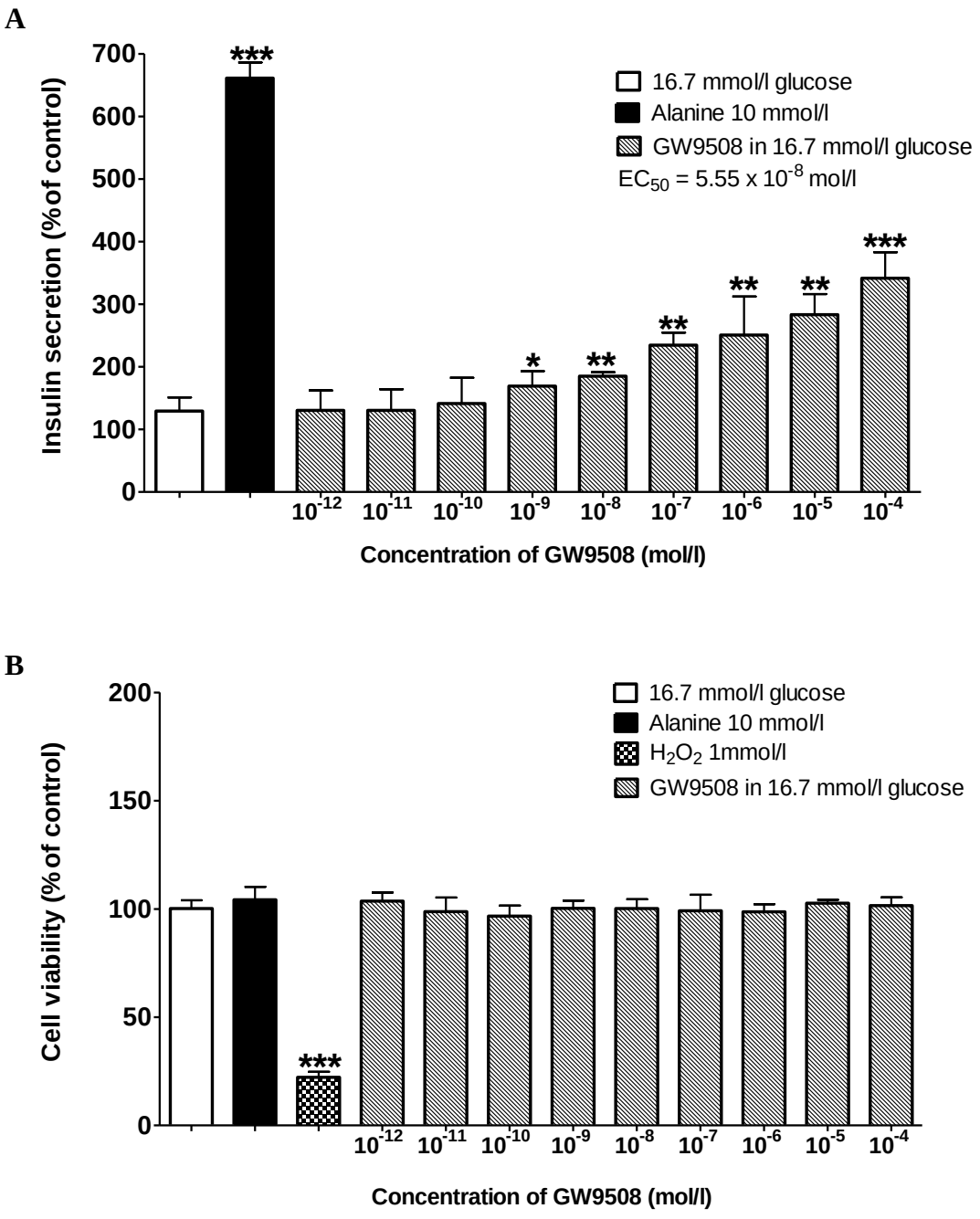

Acute effects of GW9508 (10^{-12}-10^{-4} M) and alanine (10 mM) on (A) insulin secretion and (B) cell viability (MTT) from clonal pancreatic BRIN-BD11 cells at 16.7 mM glucose. Results are the mean ± SEM (n=8) for insulin secretion and (n=3) for cell viability. *p<0.05, **p<0.01, ***p<0.001 compared to glucose control.

Figure 3.9: Acute effect of GSK137647 on insulin secretion and cell viability from clonal pancreatic BRIN-BD11 cells at 5.6 mM glucose.

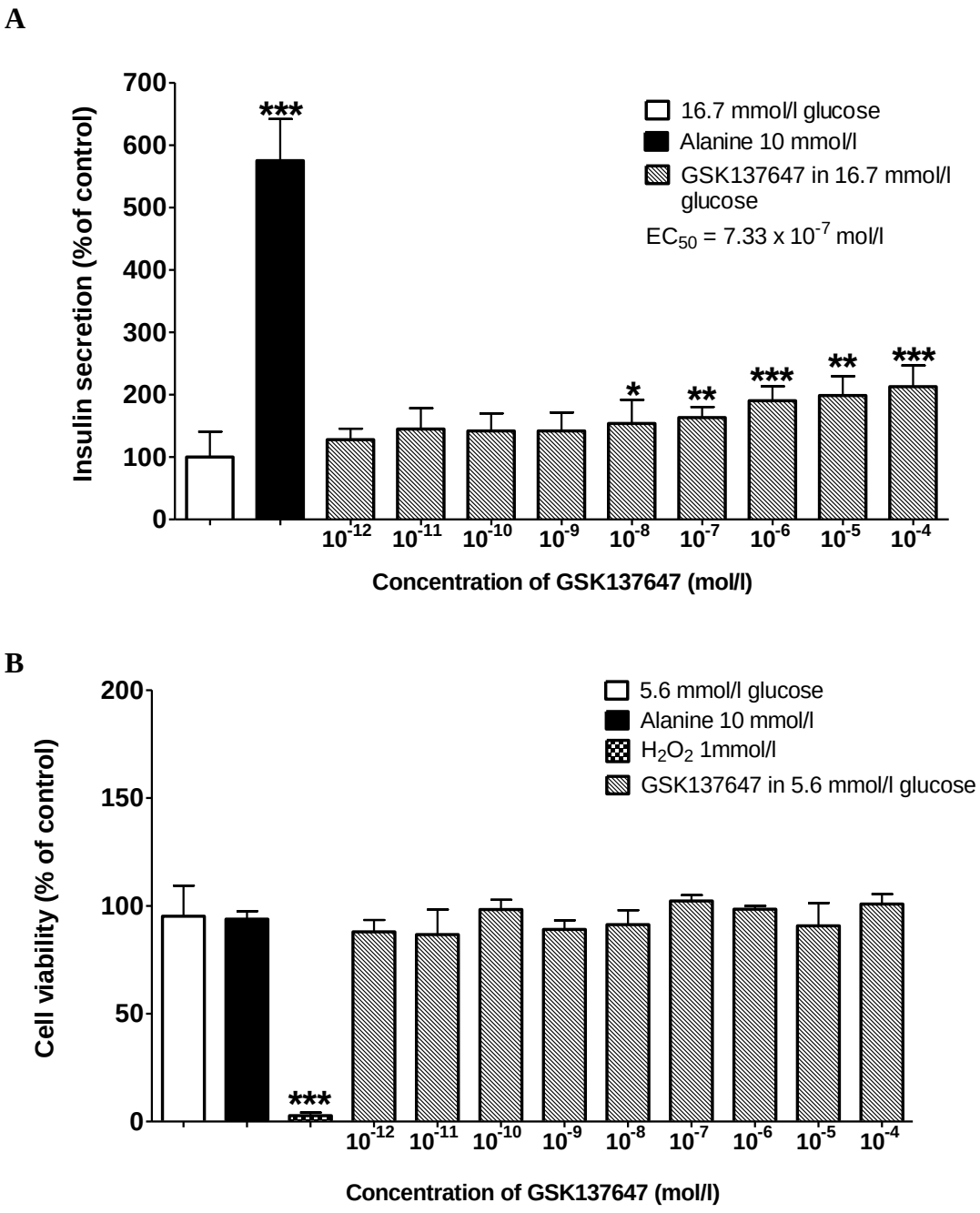

Acute effects of GSK137647 (10^{-12}-10^{-4} M) and alanine (10 mM) on (A) insulin secretion and (B) cell viability (MTT) from clonal pancreatic BRIN-BD11 cells at 5.6 mM glucose. Results are the mean ± SEM (n=8) for insulin secretion and (n=3) for cell viability. *p<0.05, **p<0.01, ***p<0.001 compared to glucose control.

Figure 3.10: Acute effect of GSK137647 on insulin secretion and cell viability from clonal pancreatic BRIN-BD11 cells at 16.7 mM glucose.

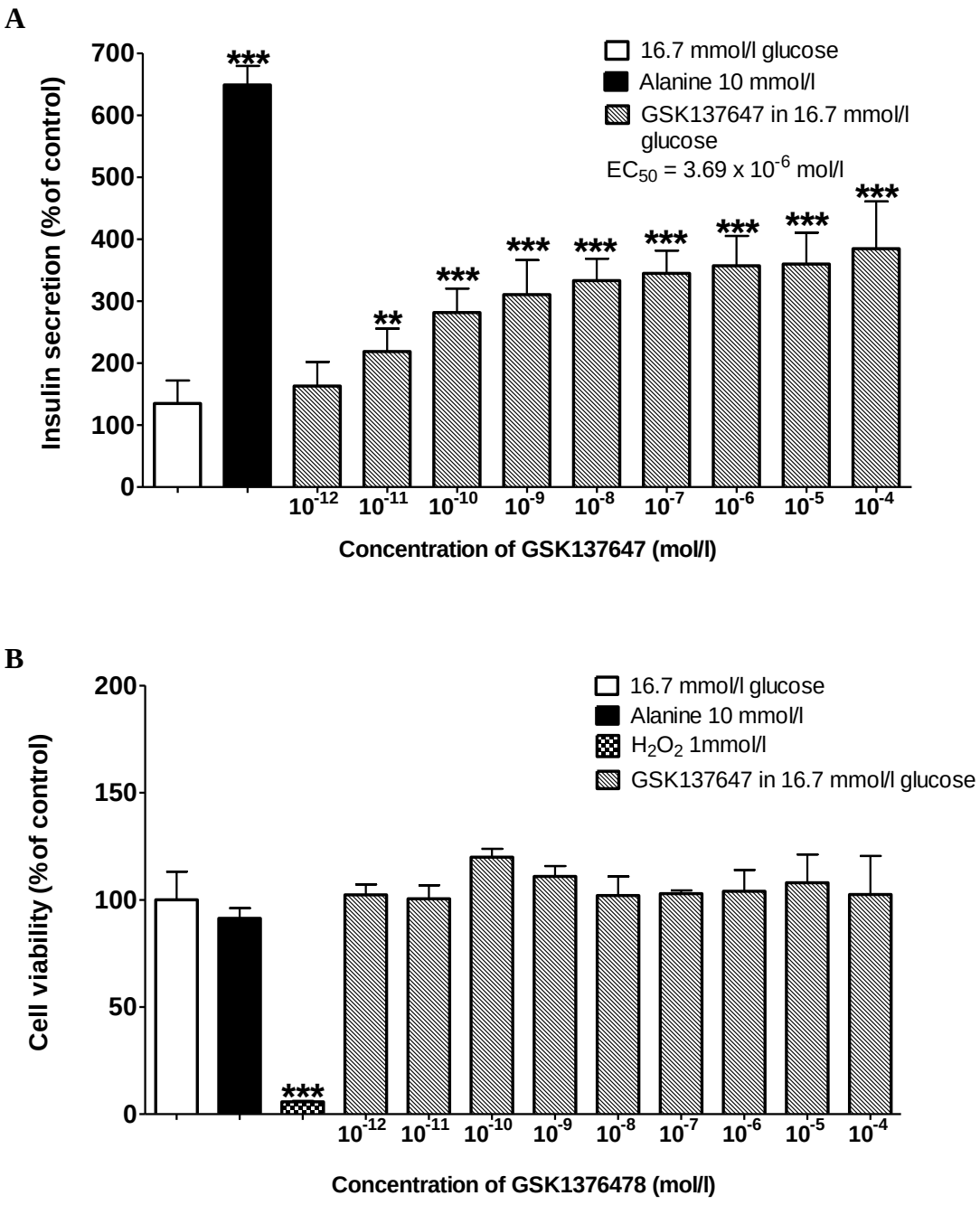

Acute effects of GSK137647 (10^{-12}-10^{-4} M) and alanine (10 mM) on (A) insulin secretion and (B) cell viability (MTT) from clonal pancreatic BRIN-BD11 cells at 16.7 mM glucose. Results are the mean ± SEM (n=8) for insulin secretion and (n=3) for cell viability. **p<0.01, ***p<0.001 compared to glucose control.

Figure 3.11: Acute effect of Compound A on insulin secretion and cell viability from clonal pancreatic BRIN-BD11 cells at 5.6 mM glucose.

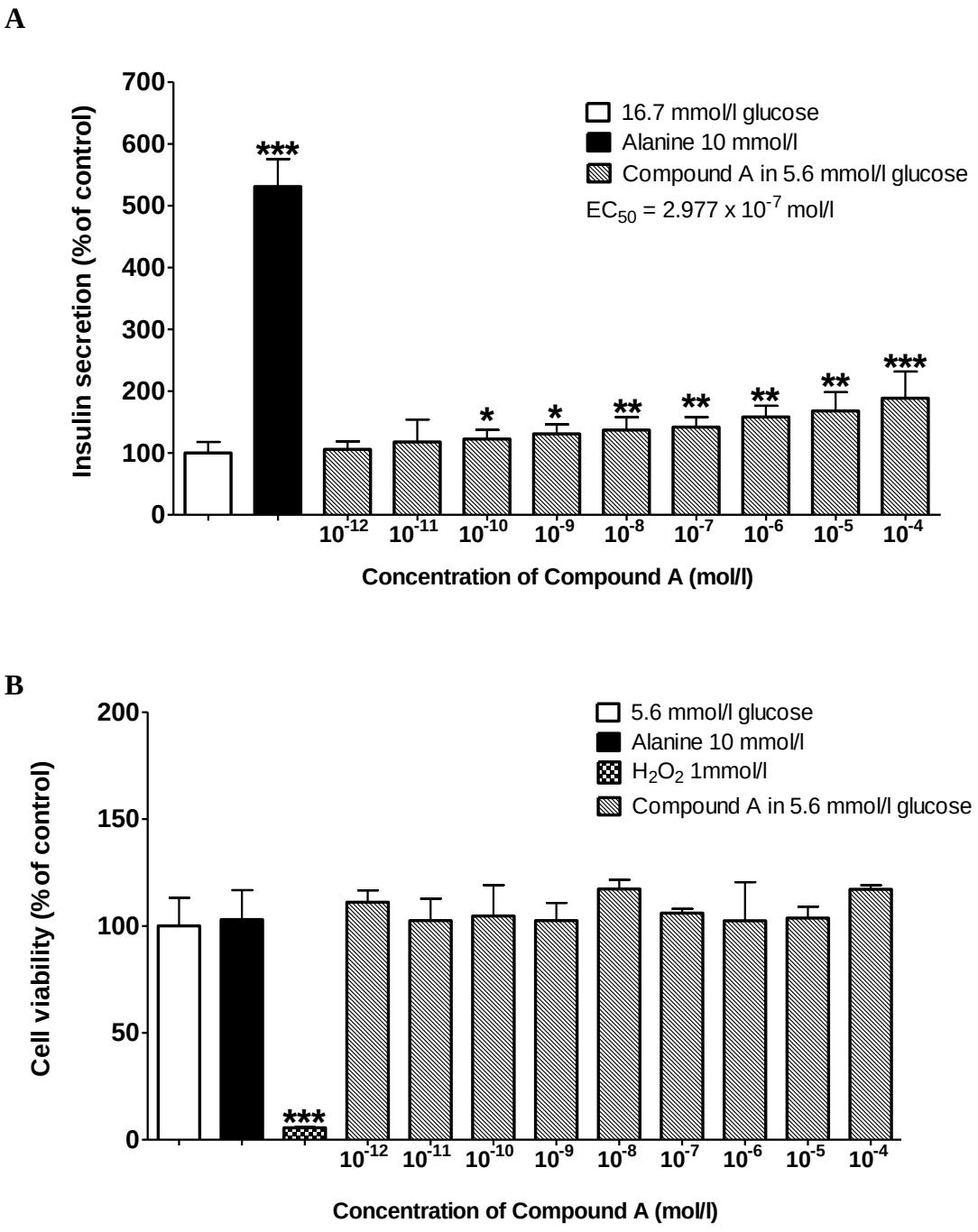

Acute effects of Compound A (10^{-12}-10^{-4} M) and alanine (10 mM) on (A) insulin secretion and (B) cell viability (MTT) from clonal pancreatic BRIN-BD11 cells at 5.6 mM glucose. Results are the mean ± SEM (n=8) for insulin secretion and (n=3) for cell viability. *p<0.05, **p<0.01, ***p<0.001 compared to glucose control.

Figure 3.12: Acute effect of Compound A on insulin secretion and cell viability from clonal pancreatic BRIN-BD11 cells at 16.7 mM glucose.

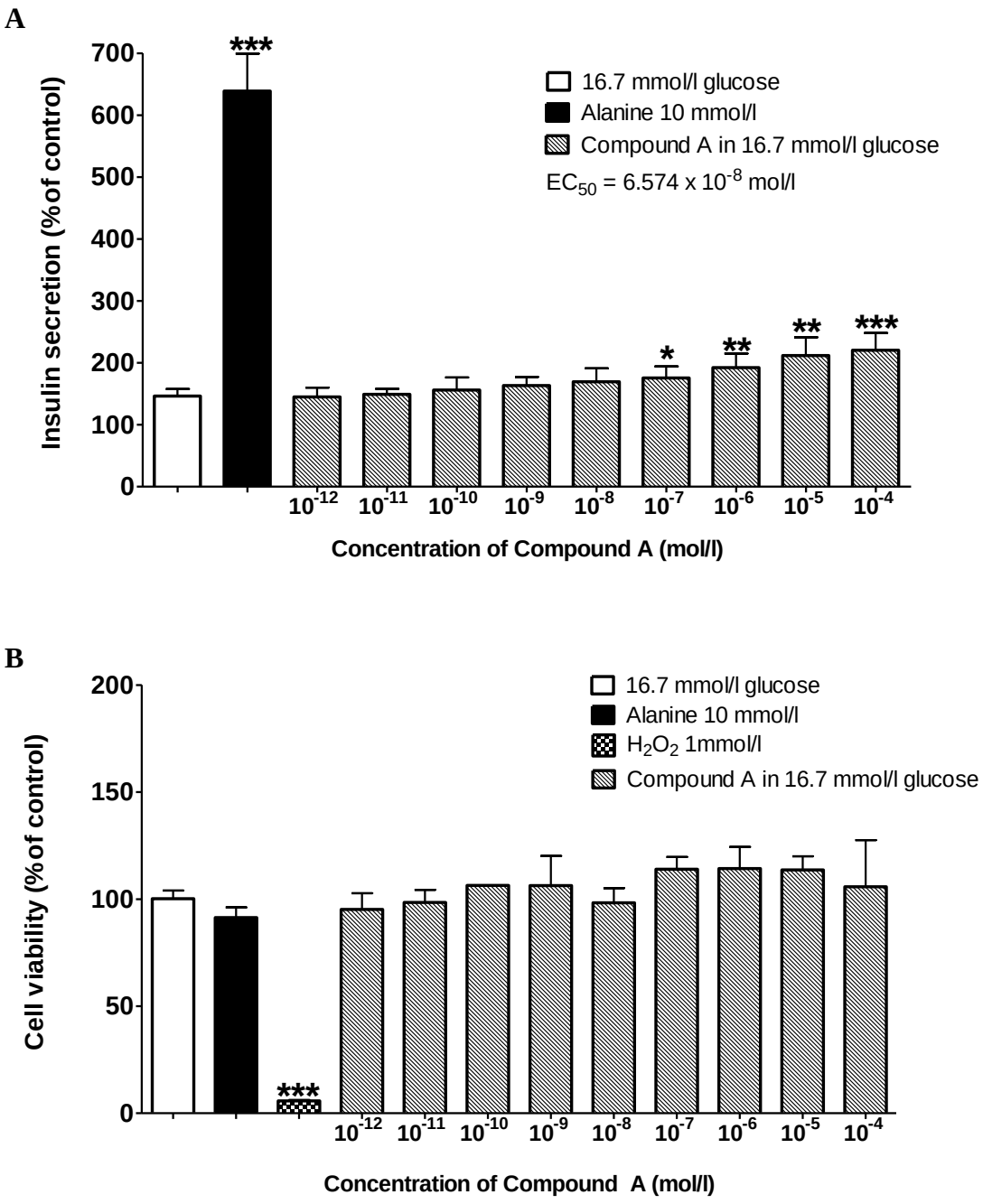

Acute effects of Compound A (10^{-12}-10^{-4} M) and alanine (10 mM) on (A) insulin secretion and (B) cell viability (MTT) from clonal pancreatic BRIN-BD11 cells at 16.7 mM glucose. Results are the mean ± SEM (n=8) for insulin secretion and (n=3) for cell viability. *p<0.05, **p<0.01, ***p<0.001 compared to glucose control.

Figure 3.13: Acute effect of ALA on insulin secretion from clonal human pancreatic 1.1B4 cells at 5.6 mM and 16.7 mM glucose.

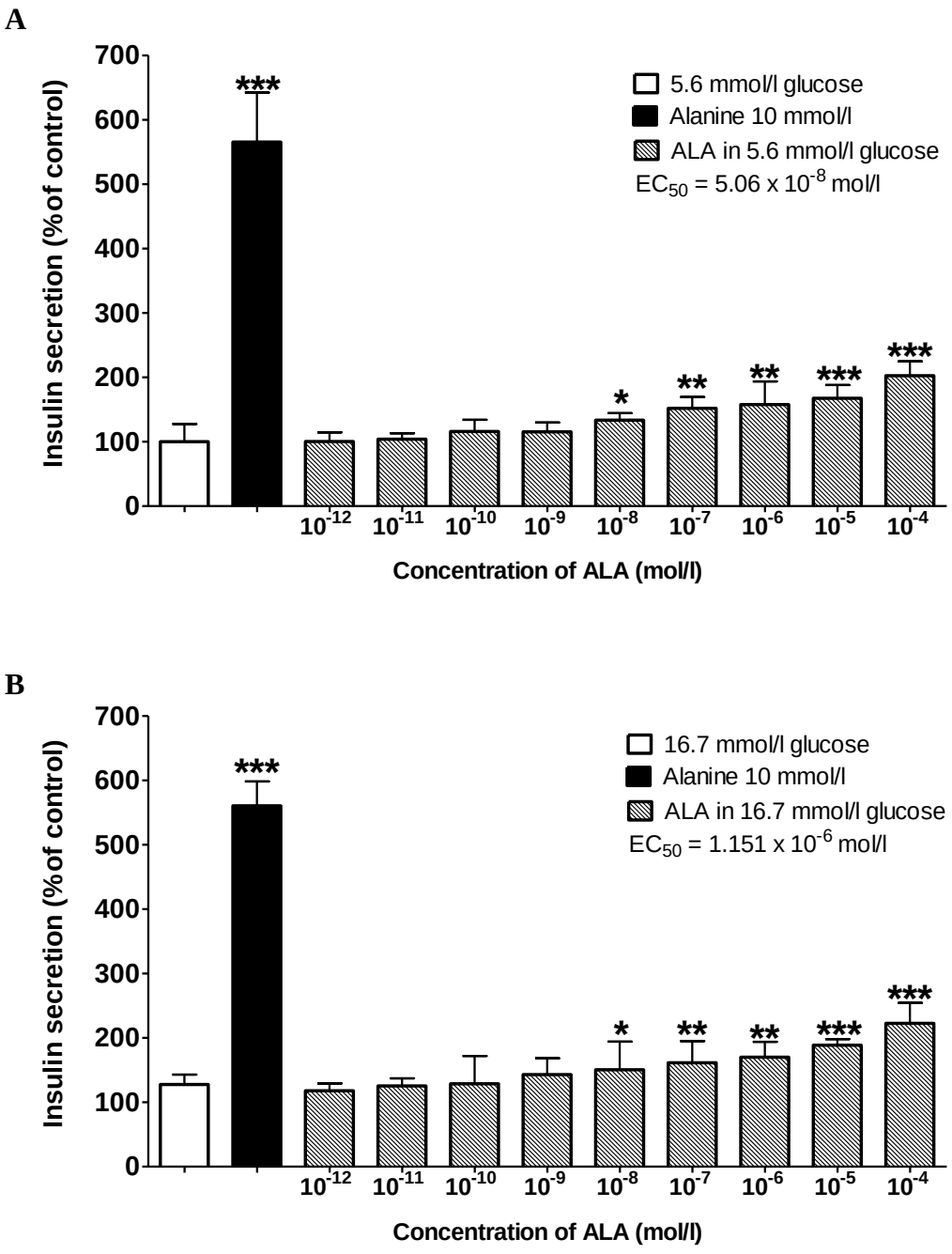

Acute effects of ALA (10^{-12}-10^{-4} M) and alanine (10 mM) on insulin secretion at (A) 5.6 mM and (B) 16.7 mM glucose from human pancreatic 1.1B4 cells. Results are the mean ± SEM (n=8) for insulin secretion. *p<0.05, **p<0.01, ***p<0.001 compared to glucose control.

Figure 3.14: Acute effect of GW9508 on insulin secretion from clonal human pancreatic 1.1B4 cells at 5.6 mM and 16.7 mM glucose.

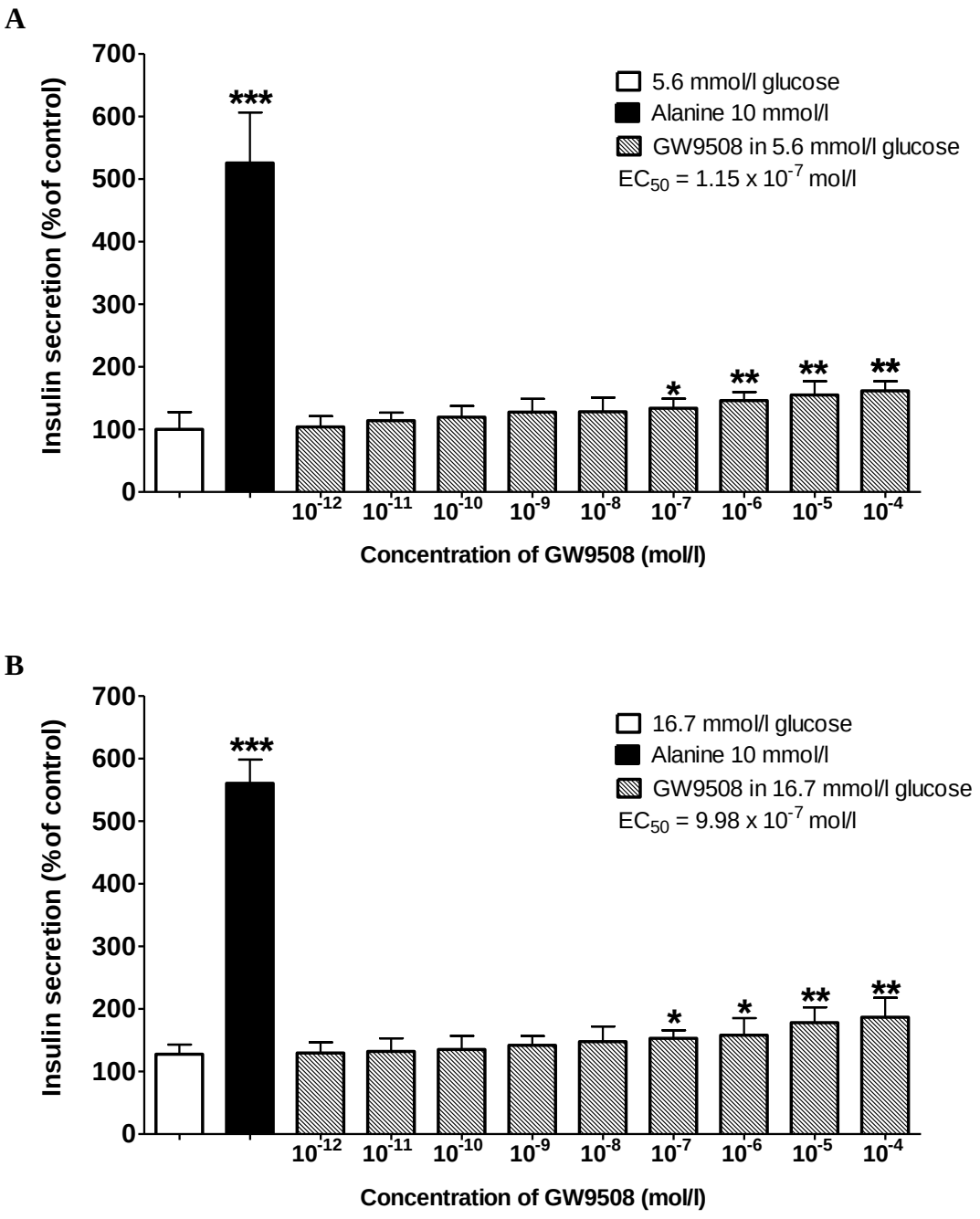

Acute effects of GW9508 (10^{-12}-10^{-4} M) and alanine (10 mM) on insulin secretion at (A) 5.6 mM and (B) 16.7 mM glucose from human pancreatic 1.1B4 cells. Results are the mean ± SEM (n=8) for insulin secretion. *p<0.05, **p<0.01, compared to glucose control.

Figure 3.15: Acute effect of Compound A on insulin secretion from clonal human pancreatic 1.1B4 cells at 5.6 mM and 16.7 mM glucose.

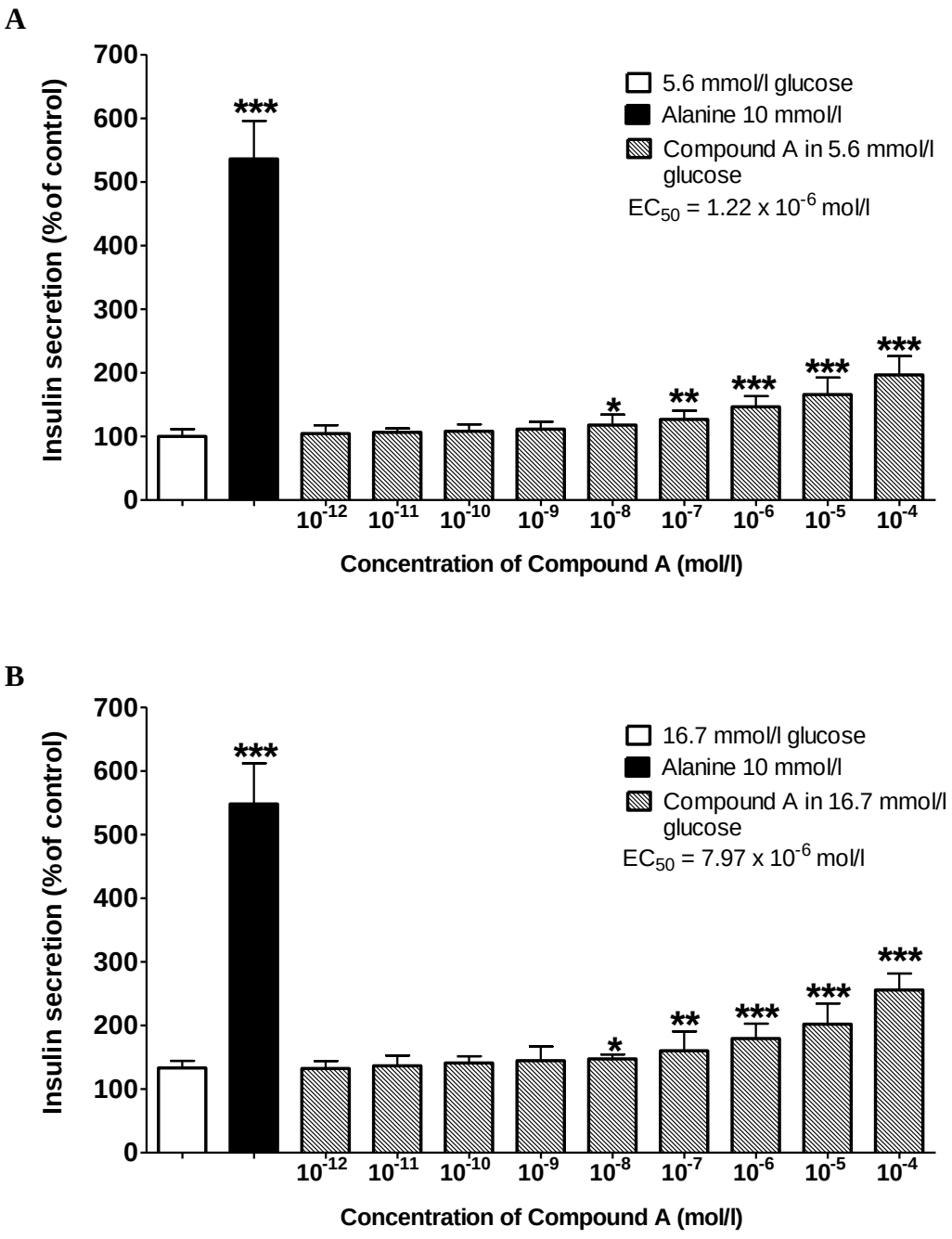

Acute effects of Compound A (10^{-12}-10^{-4} M) and alanine (10 mM) on insulin secretion at (A) 5.6 mM and (B) 16.7 mM glucose from human pancreatic 1.1B4 cells. Results are the mean ± SEM (n=8) for insulin secretion. *p<0.05, **p<0.01, ***p<0.001, compared to glucose control.

Figure 3.16: Effect of GPR120 antagonist (AH7614) and GPR40 antagonist (GW1100) on Compound A and GSK137647 induced insulin secretion from clonal pancreatic BRIN-BD11 cells at 5.6 mM glucose.

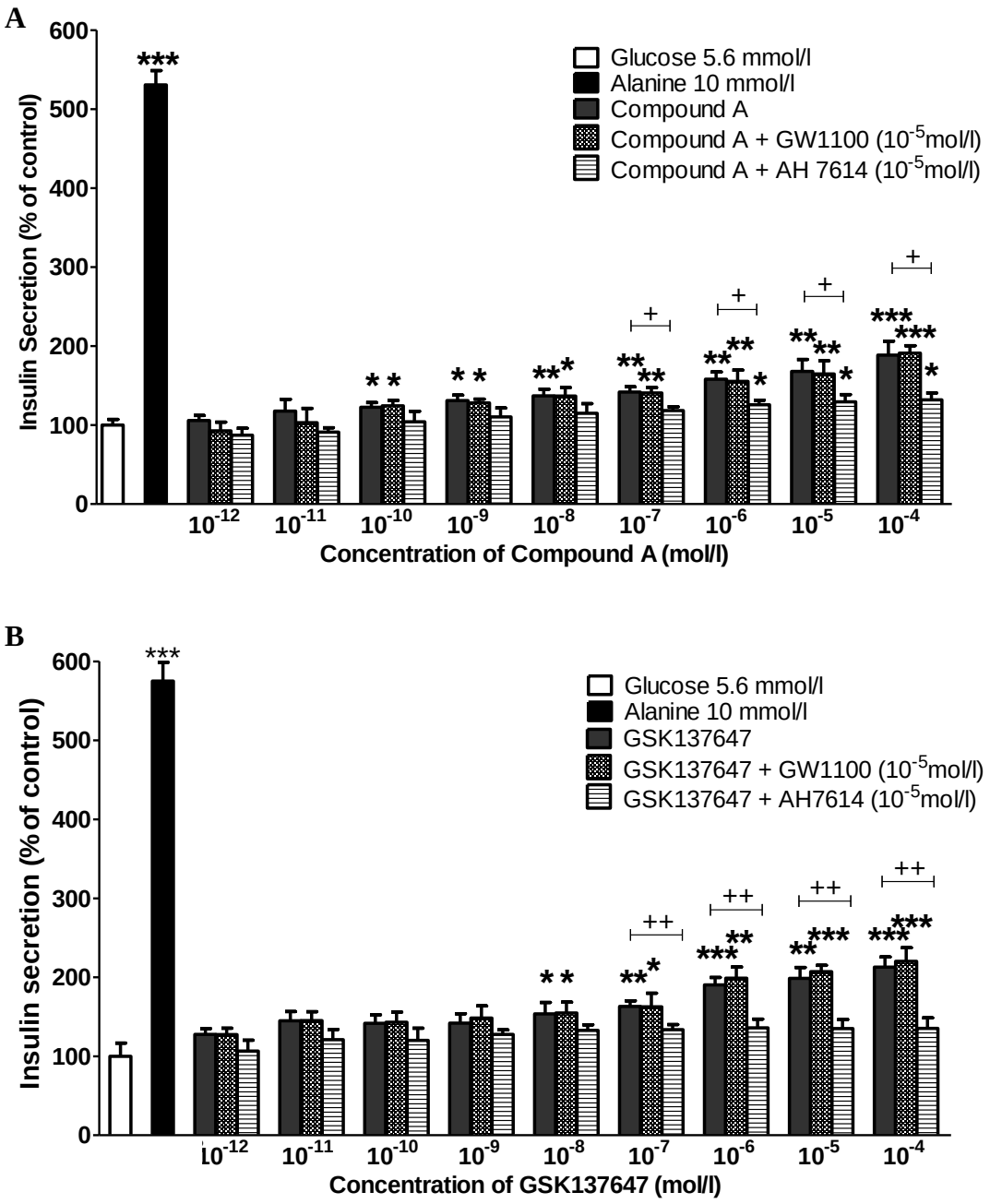

Effect of AH7614 (10^{-5} M) and GW1100 (10^{-5} M) on the insulinotropic effect of (A) Compound A (10^{-12}-10^{-4} M) and (B) GSK137647 at 5.6 mM glucose in clonal pancreatic BRIN-BD11 cells. Results are the mean ± SEM (n=8) for insulin secretion. *p<0.05, **p<0.01, ***p<0.001, compared to glucose control. +p<0.05, ++p<0.01, compared to agonist only.

Figure 3.17: Effect of GPR120 antagonist (AH7614) and GPR40 antagonist (GW1100) on Compound A and GSK137647 induced insulin secretion from clonal pancreatic BRIN-BD11 cells at 16.7 mM glucose.

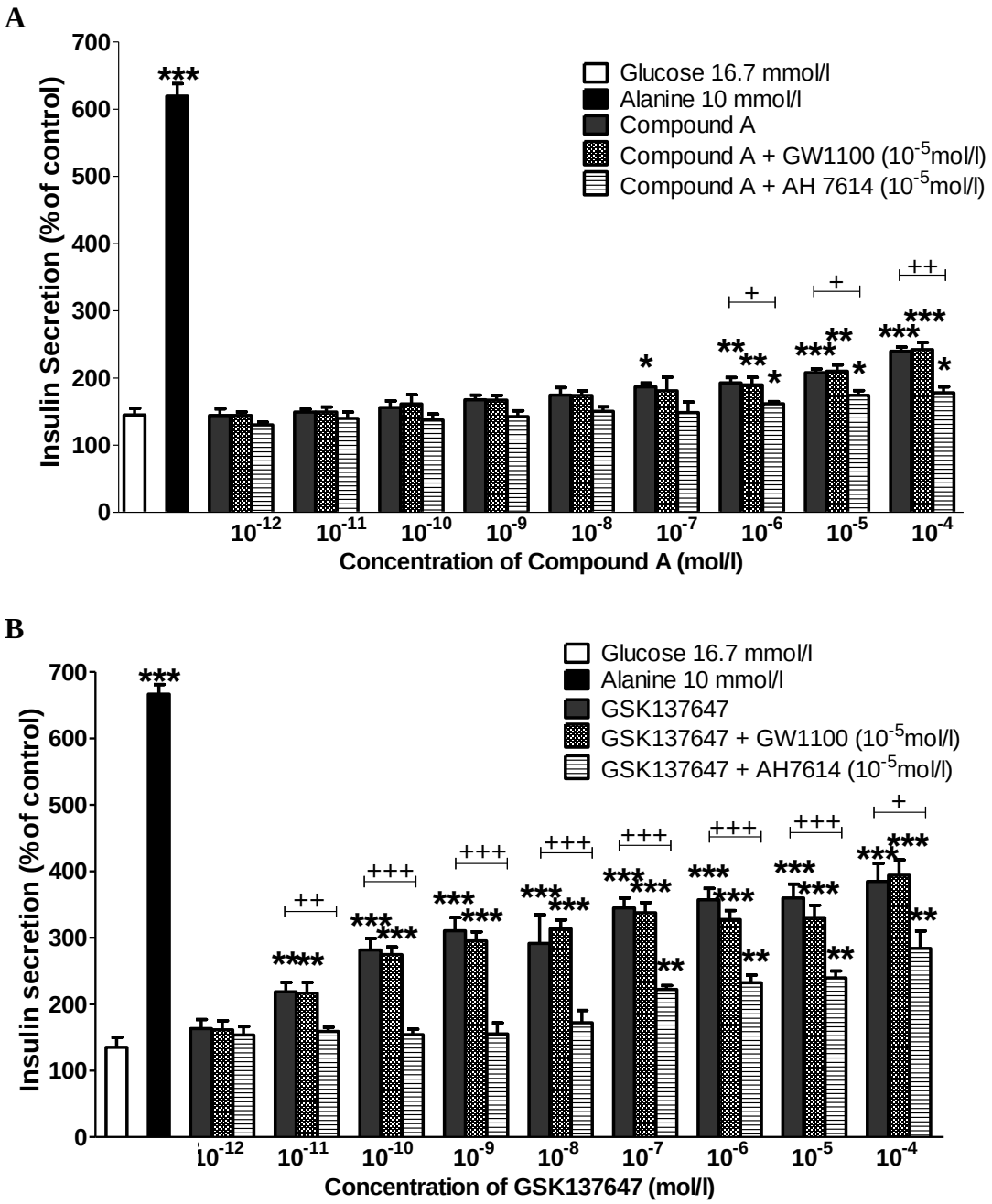

Effect of AH7614 (10^{-5} M) and GW1100 (10^{-5} M) on the insulinotropic effect of (A) Compound A (10^{-12}-10^{-4} M) and (B) GSK137647 at 16.7 mM glucose in clonal pancreatic BRIN-BD11 cells. Results are the mean ± SEM (n=8) for insulin secretion. *p<0.05, **p<0.01, ***p<0.001, compared to glucose control. +p<0.05, ++p<0.01, +++p<0.001, compared to agonist only.

Figure 3.18: Immunocytochemistry staining of GPR120, insulin and DAPI nuclear stain in clonal pancreatic BRIN-BD11 cells.

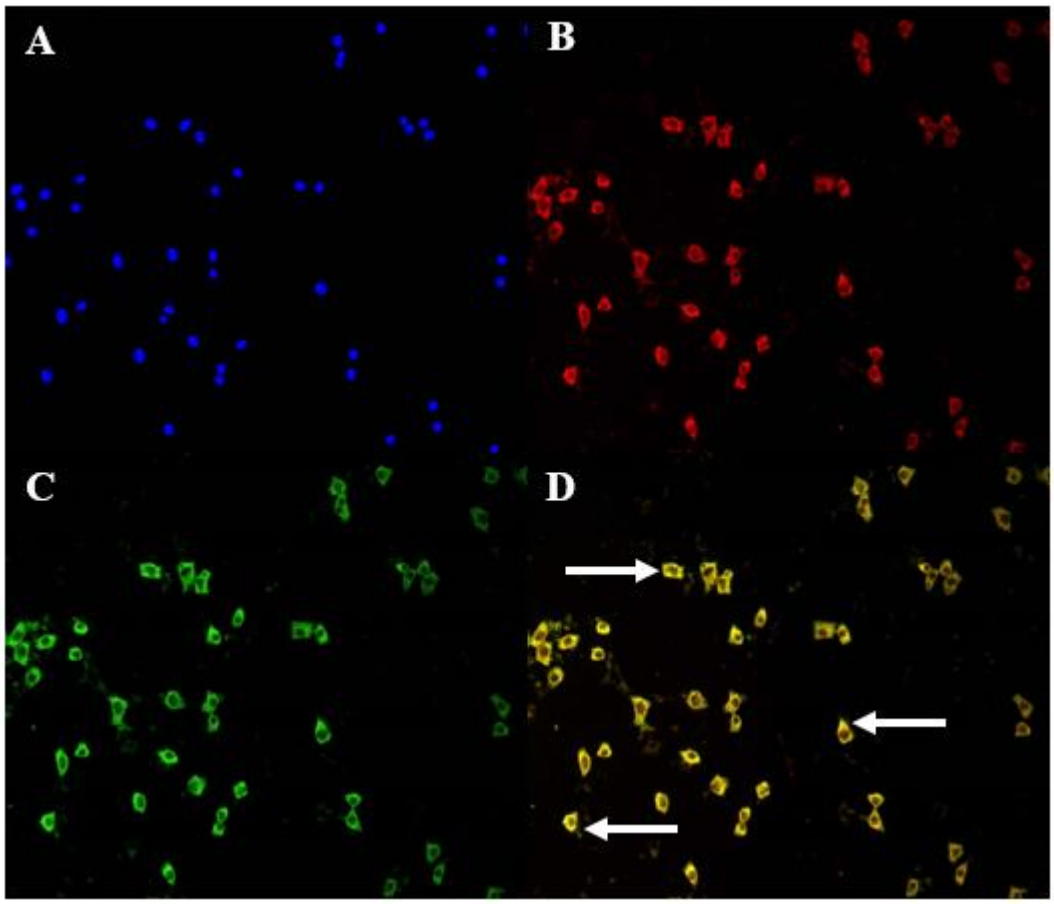

Expression and distribution of (A) DAPI, (B) insulin (C) GPR120 and (D) double antibody immunofluorescence of insulin and GPR120 at 40x magnification in clonal pancreatic BRIN-BD11 cells. Examples of co-localisation between GPR120 and insulin are indicated by white arrows.

Figure 3.19: Effect of GW9508 and ALA on GPR120 mRNA and protein expression in clonal pancreatic BRIN-BD11 cells.

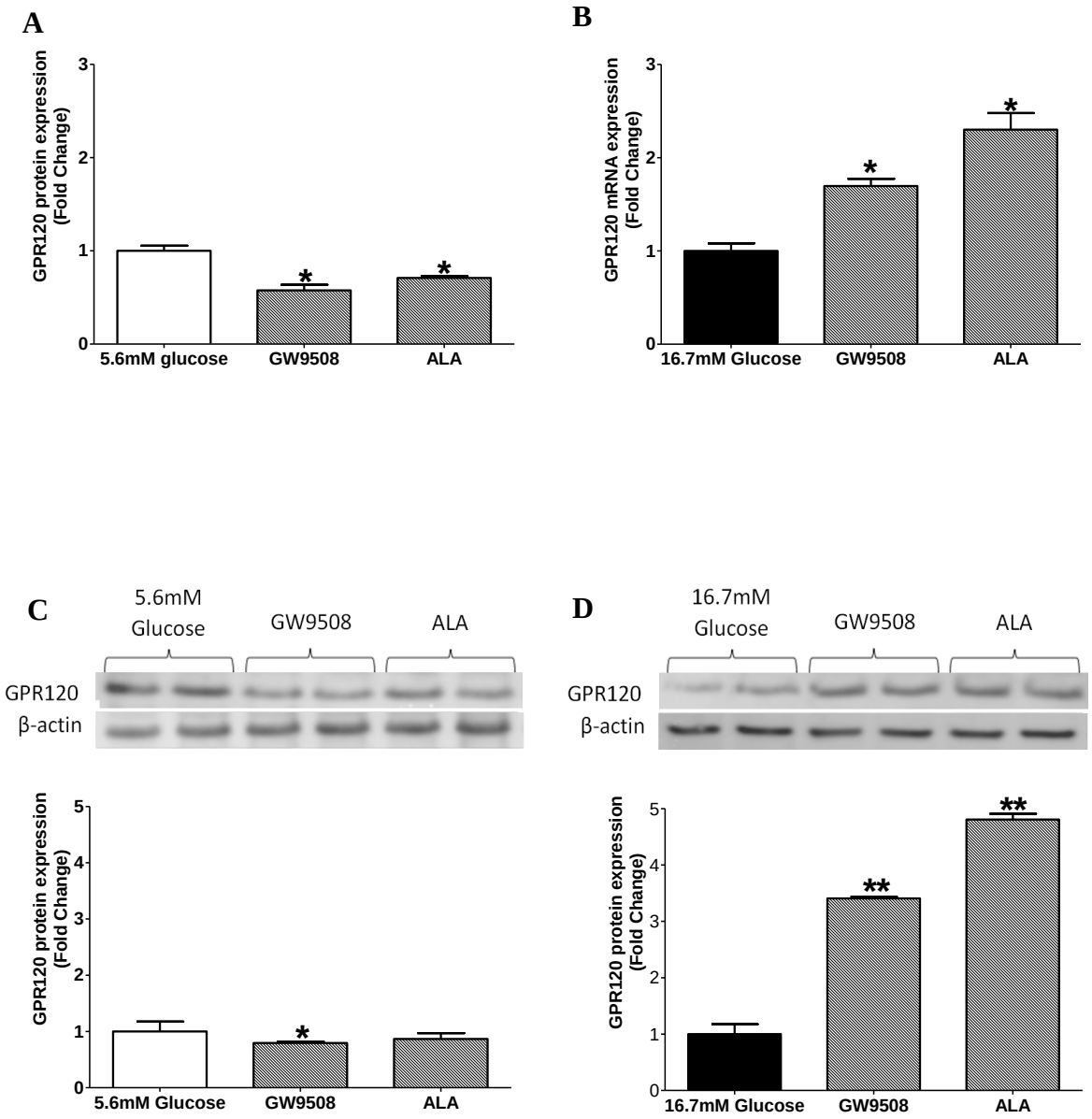

Effect of GW9508 (10^{-4} mol/l) and ALA (10^{-4} mol/l) on GPR120 (A, B) mRNA expression and (C, D) protein expression in clonal pancreatic BRIN-BD11 cells after 4 h incubation at (A, B) 5.6 mM and (C, D) 16.7 mM glucose. Results are the mean ± SEM (n=3) for qPCR and (n=2) for western blotting. *p<0.05, **p<0.01, compared to glucose.

Figure 3.20: Effect of Compound A and GSK137647 on GPR120 mRNA and protein expression in clonal pancreatic BRIN-BD11 cells.

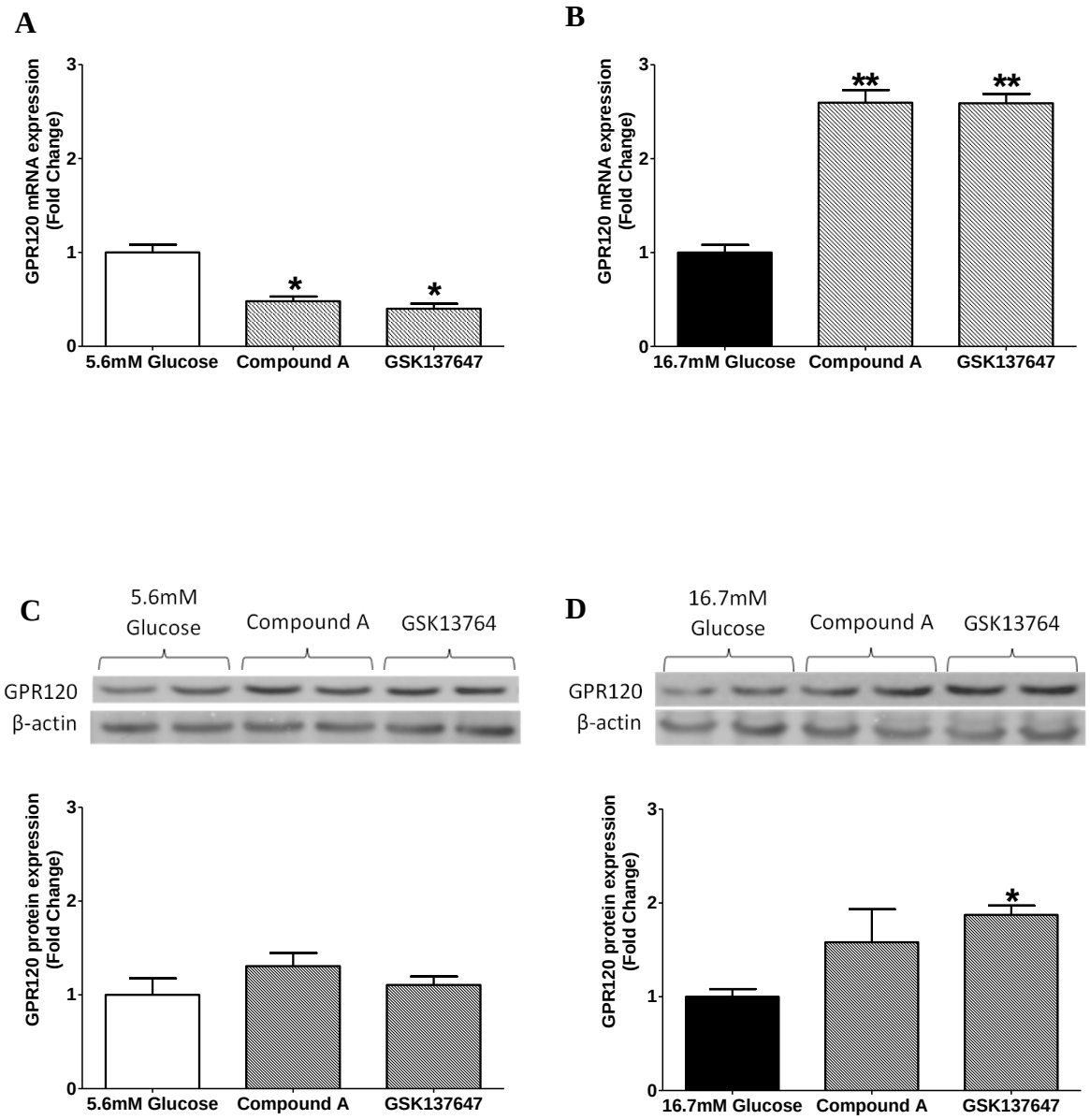

Effect of Compound A (10^{-4} mol/l) and GSK137647 (10^{-4} mol/l) on GPR120 (A, B) mRNA expression and (C, D) protein expression in clonal pancreatic BRIN-BD11 cells after 4 h incubation at (A, B) 5.6 mM and (C, D) 16.7 mM glucose. Results are the mean ± SEM (n=3) for qPCR and (n=2) for western blotting. *$p<0.05$, **$p<0.01$, compared to glucose.

Figure 3.21: Effect of GPR120 agonists on cAMP and intracellular Ca^{2+} modulated insulin secretion from clonal pancreatic BRIN-BD11 cells at 16.7 mM glucose.

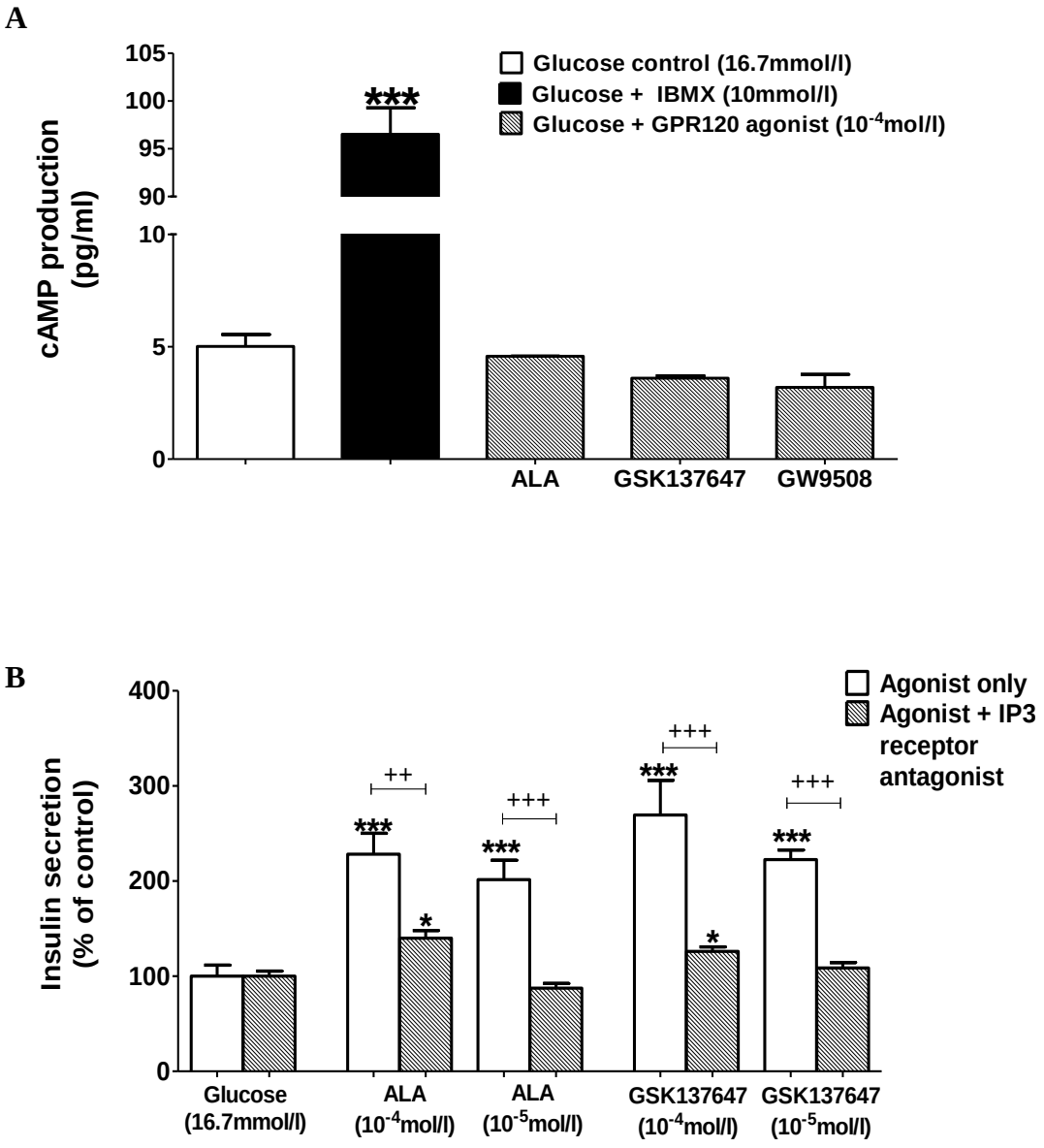

Effect of GPR120 agonists on (A) cAMP production and (C) calcium-induced insulin secretion in clonal pancreatic BRIN-BD11 cells at 16.7 mmol/l glucose. Agonists were co-incubated with inositol trisphosphate receptor antagonist (Xestospongin C, 350 nmol/l) for 20 min for calcium analysis. *p<0.05, **p<0.01, ***p<0.001, compared to glucose control. ++p<0.01, +++p<0.001, compared to agonist only.

Figure 3.22: Western blotting demonstrating the effect of GSK137647, GW9508, ALA and PMA on ERK1/2 (p44/42) signalling in clonal pancreatic BRIN-BD11 cells.

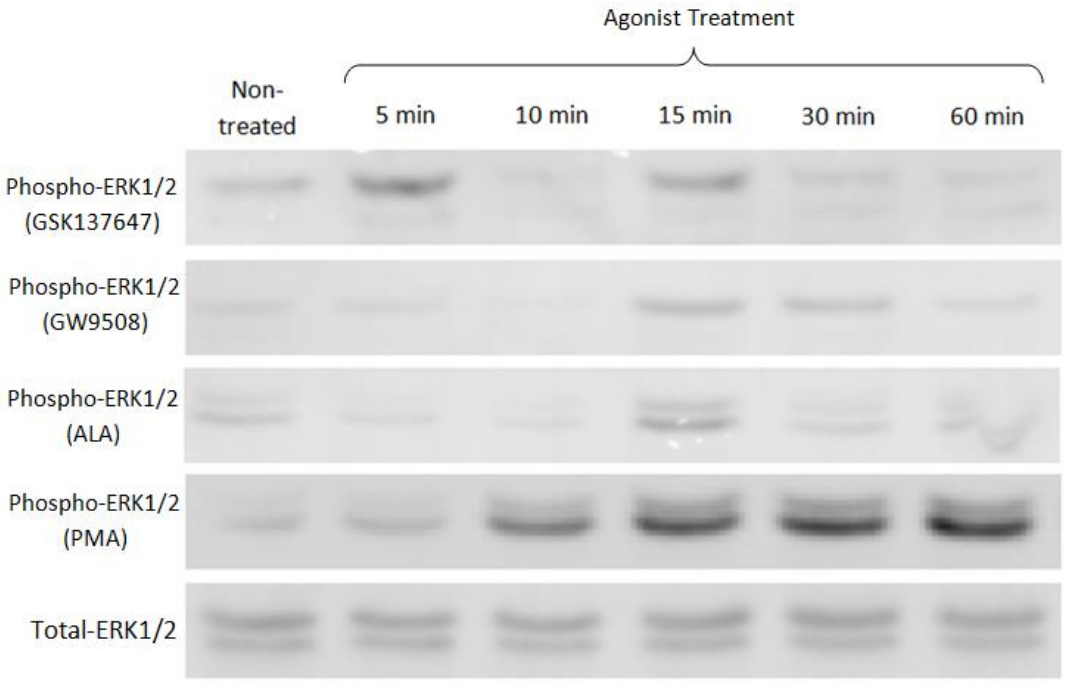

Effect of GSK137647 (10^{-4} mol/l), GW9508 (10^{-4} mol/l), ALA (10^{-4} mol/l) and PMA (200 nm) on ERK1/2 signalling in clonal pancreatic BRIN-BD11 cells at various timepoints (0, 5, 10, 15, 30, 60 min). Following incubation, cell lysates were separated via SDS-PAGE, then probed with antibodies for anti-p-ERK1/2 and anti-t-ERK1/2.

Figure 3.23: Flow cytometry demonstrating the effect of GSK137647, GW9508, ALA and PMA on ERK1/2 (p44/42) signalling in clonal pancreatic BRIN-BD11 cells.

(A) Non-treated

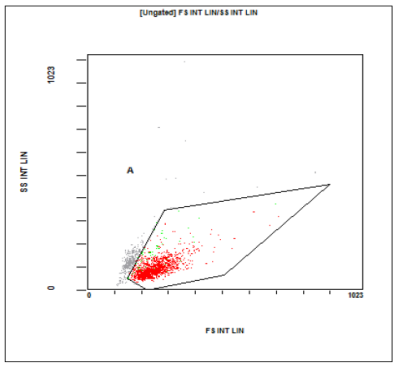

[Ungated] FS INT LIN/SS INT LIN					
Region	Number	%Total	%Gated	X-Mean	Y-Mean
ALL	1569	100.00	100.00	239	106
A	1262	80.43	80.43	254	96.5

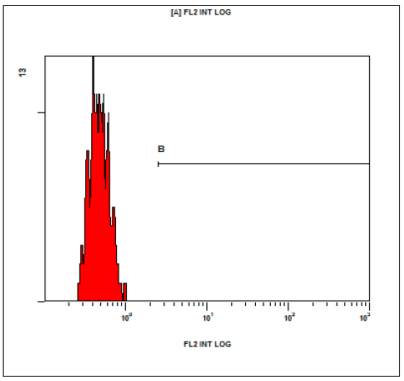

[A] FL2 INT LOG					
Region	Number	%Total	%Gated	X-Mean	Y-Mean
ALL	1262	80.43	100.00	1.19	###
B	68	4.33	5.39	12.6	###

(B) PMA (200 nmol/l)

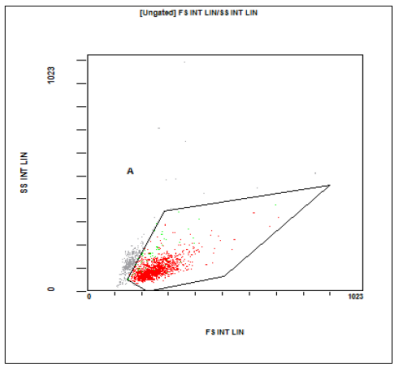

[Ungated] FS INT LIN/SS INT LIN					
Region	Number	%Total	%Gated	X-Mean	Y-Mean
ALL	1569	100.00	100.00	239	106
A	1262	80.43	80.43	254	96.5

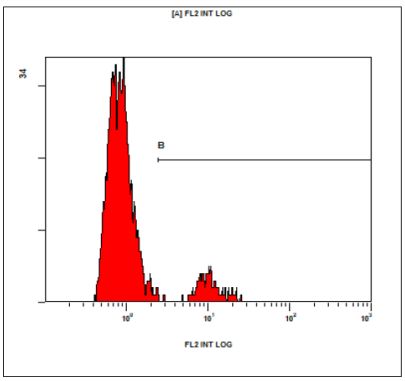

[A] FL2 INT LOG					
Region	Number	%Total	%Gated	X-Mean	Y-Mean
ALL	3960	98.51	100.00	3.28	###
B	755	18.78	19.07	13.4	###

(C) GW9508 (10^{-4} mol/l)

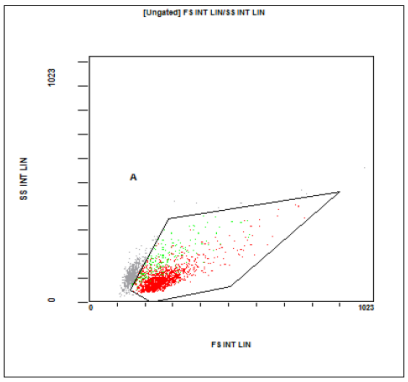

[Ungated] FS INT LIN/SS INT LIN					
Region	Number	%Total	%Gated	X-Mean	Y-Mean
ALL	2372	100.00	100.00	238	110
A	1689	71.21	71.21	266	104

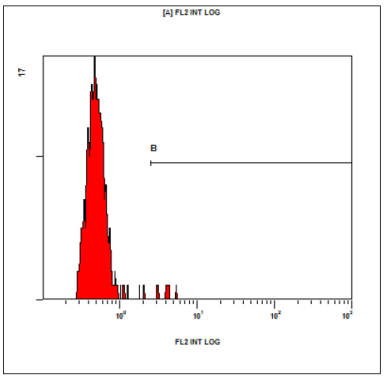

[A] FL2 INT LOG					
Region	Number	%Total	%Gated	X-Mean	Y-Mean
ALL	1689	71.21	100.00	1.52	###
B	209	8.81	12.37	7.93	###

(D) ALA (10^{-4} mol/l)

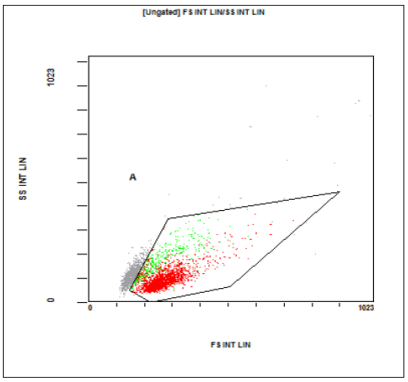

[Ungated] FS INT LIN/SS INT LIN					
Region	Number	%Total	%Gated	X-Mean	Y-Mean
ALL	3392	100.00	100.00	240	113
A	2352	69.34	69.34	269	107

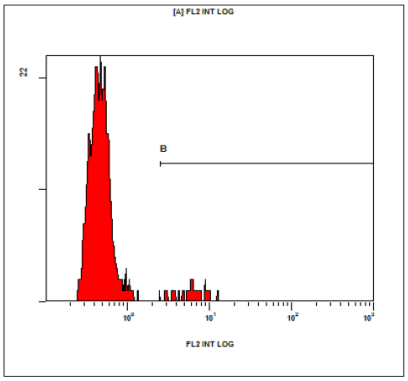

[A] FL2 INT LOG					
Region	Number	%Total	%Gated	X-Mean	Y-Mean
ALL	2352	69.34	100.00	2.08	###
B	389	11.47	16.54	9.8	###

(E) GSK137647 (10^{-4} mol/l)

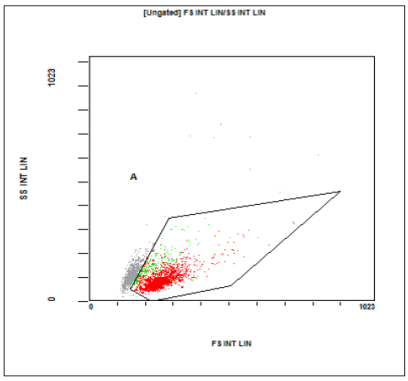

[Ungated] FS INT LIN/SS INT LIN					
Region	Number	%Total	%Gated	X-Mean	Y-Mean
ALL	2505	100.00	100.00	232	120
A	1615	64.47	64.47	259	98.7

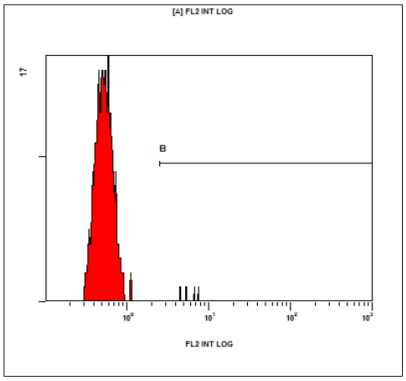

[A] FL2 INT LOG					
Region	Number	%Total	%Gated	X-Mean	Y-Mean
ALL	1615	64.47	100.00	1.37	###
B	184	7.35	11.39	7.35	###

(F)

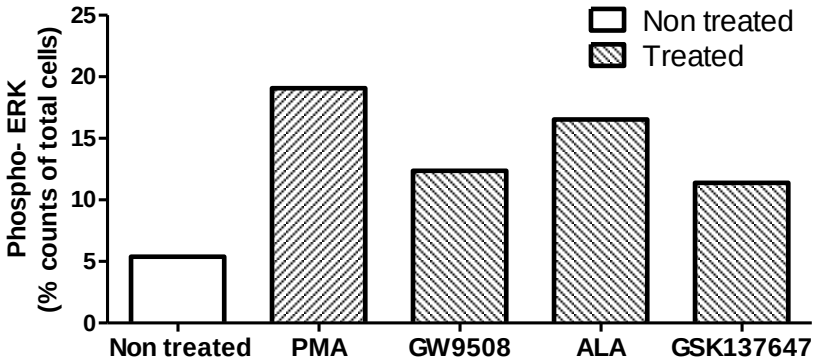

Effects of (B) PMA, (C) GW9508, (D) ALA and (E) GSK137647 on ERK1/2 phosphorylation in clonal pancreatic BRIN-BD11 cells. After 15 min exposure, cells were probed with anti-phospho-ERK1/2 and anti-Alexa Fluor 488 antibodies, then gated for flow cytometry analysis.

Figure 3.24: Effect of GPR120 agonist GSK137647 on mitogen-activated protein kinase (MAPK) signalling in clonal pancreatic BRIN-BD11 cells.

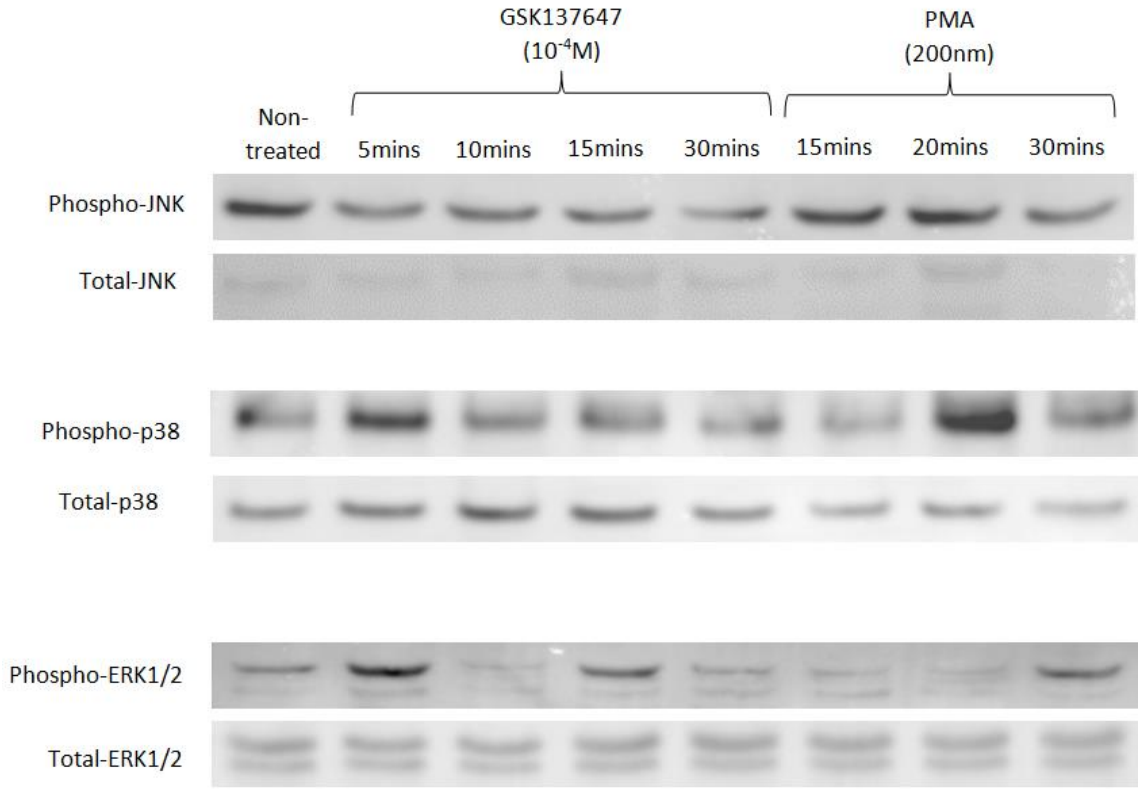

Effect of GPR120 agonist GSK137647 (10^{-4} mol/l) and PMA (200 nm) on JNK, p38 and ERK1/2 (MAPK) signalling in clonal pancreatic BRIN-BD11 cells at various timepoints (0, 5, 10, 15, 30 min). Following incubation, cell lysates were separated via SDS-PAGE, then probed with antibodies for total and phosphorylated ERK1/2, p38 and JNK.

Figure 3.25: Effect of GW9508, ALA and GSK137647 on clonal pancreatic BRIN-BD11 cell viability and apoptosis.

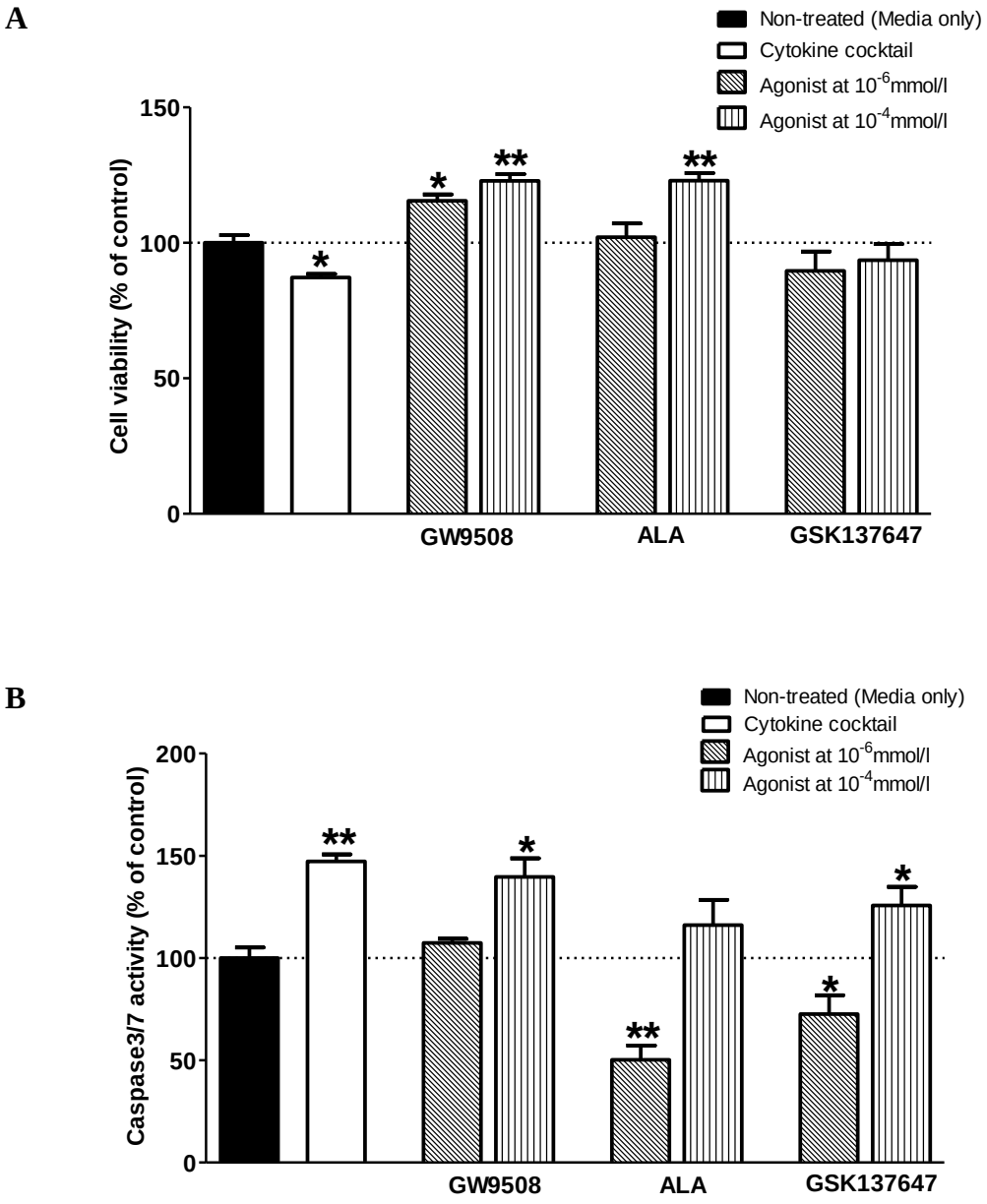

Effects of GW9508, ALA and GSK137647 on clonal pancreatic BRIN-BD11 cell viability and apoptosis after 20 h incubation. Results determined with multiplex analysis; cell viability by protease activity, cell apoptosis by caspase 3/7 activity. Cytokine cocktail (TNF-α [200 U/ml], IFN-γ [20 U/ml], IL-1β [100 U/ml]) was used as a positive control. Results are the mean ± SEM (n=3). *p<0.05, **p<0.01, compared to non-treated control.

Figure 3.26: Effect of GW9508, ALA and GSK137647 on clonal pancreatic α-TC1.9 cell proliferation and apoptosis.

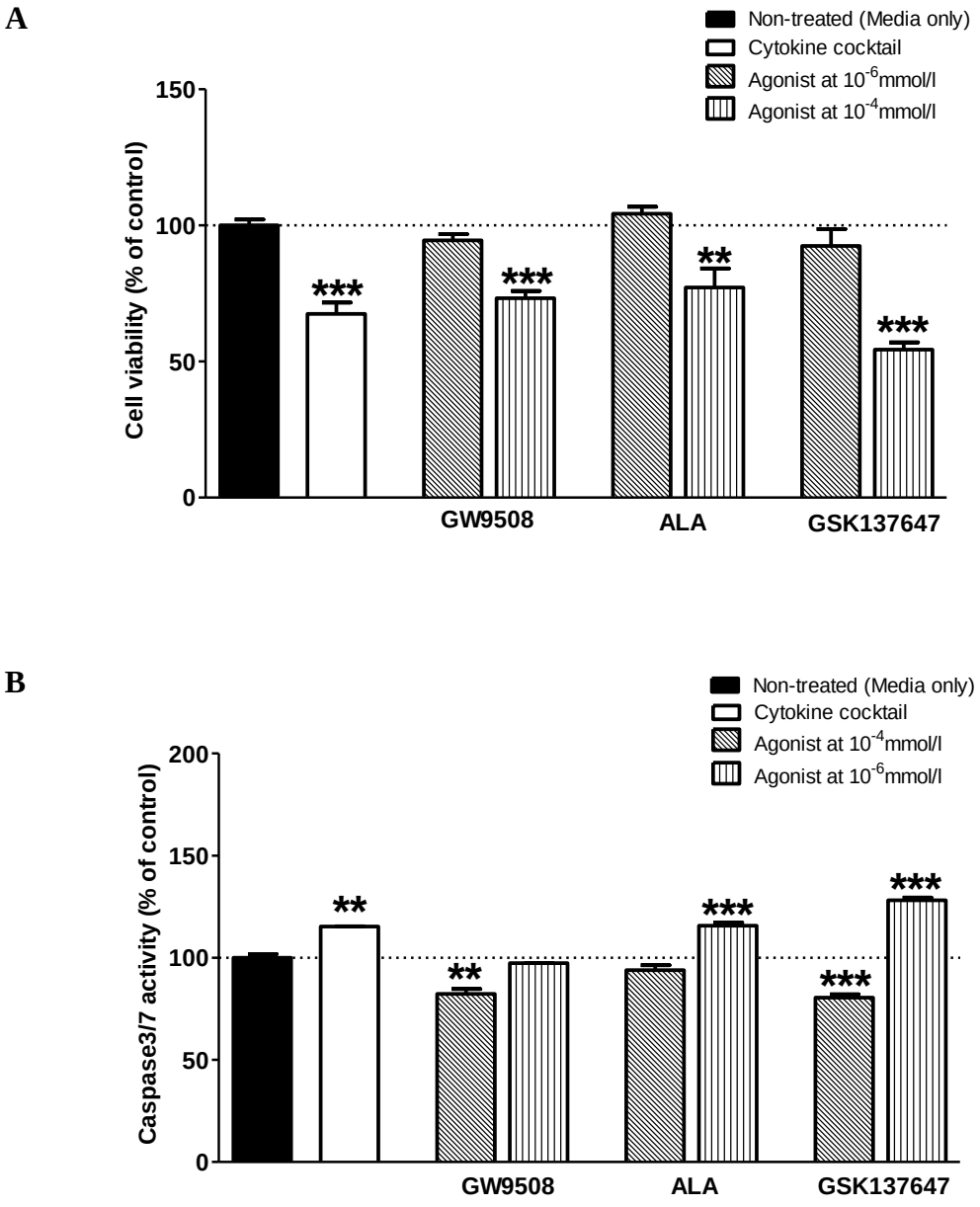

Effect of GW9508, ALA and GSK137647 on clonal pancreatic α-TC1.9 cell viability and apoptosis after 20 h incubation. Results determined with multiplex analysis; cell viability by protease activity, cell apoptosis by caspase 3/7 activity. Cytokine cocktail (TNF-α [200 U/ml], IFN-γ [20 U/ml], IL-1β [100 U/ml]) was used as a positive control. Results are the mean ± SEM (n=3). **p<0.01, ***p<0.001, compared to non-treated control.

Chapter 4

Investigating the effects of GPR55 on insulin secretion, downstream receptor signalling and islet cell regeneration *in-vitro*

4.1: Summary

G-protein coupled receptor 55 (GPR55) has recently been identified as a novel endocannabinoid receptor that is highly expressed in numerous tissues, including the pancreatic islet, intestines, peripheral tissues and the brain. Recent studies have implicated the role of GPR55 in beta cell function and glucose homeostasis. The present study investigates the effect and mechanistic function of GPR55 towards insulin release, downstream receptor signalling and beta cell regeneration using clonal pancreatic islet cells.

Insulinotropic capabilities and cytotoxicity of cannabinoid GPR55 agonists were assessed in rodent pancreatic BRIN-BD11 cells, with secretory effects confirmed in human 1.1B4 cells. Downstream GPR55 signalling pathways including intracellular Ca^{2+}, cAMP and MAPKs were investigated upon receptor activation. Effect of GPR55 agonist treatment towards islet cell proliferation and apoptosis was assessed in insulin secreting BRIN-BD11 and glucagon secreting α-TC1.9 cells. Expression of GPR55 and insulin mRNA and protein concentrations were determined by qPCR and western blotting in BRIN-BD11 cells at both normoglycemia and hyperglycaemia.

Endocannabinoid and atypical cannabinoid GPR55 agonists stimulated insulin secretion ($p<0.05$-$p<0.001$) from pancreatic BRIN-BD11 and 1.1B4 cells, with synthetic Abn-CBD demonstrating the most potent insulinotropic effect ($p<0.05$-$p<0.001$) from BRIN-BD11 cells at 5.6 mmol/l (2.7-fold; EC_{50} = 1.506 x 10^{-8} mol/l) and 16.7 mmol/l (3.1-fold; EC_{50} = 5.18 x 10^{-9} mol/l) glucose. GPR55 agonists prompted an increase in intracellular Ca^{2+} ($p<0.05$-$p<0.001$), with no effects on cAMP production. Abn-CBD, AM251 and OEA had no effect on ERK1/2 phosphorylation, whilst Abn-CBD reduced phospho-JNK and phospho-p38 activation in BRIN-BD11 cells. Abn-CBD and AM251 improved beta cell

viability (14-16%, $p<0.05$), whilst Abn-CBD and O-1602 reduced beta apoptosis (24-39%, $p<0.05$-$p<0.01$). Abn-CBD, AM251 and O-1602 reduced alpha cell viability by 39-52% ($p<0.001$) and increased alpha cell apoptosis by 13-82% ($p<0.0$-$p<0.001$) at super-physiological concentrations. Incubation of BRIN-BD11 cells with Abn-CBD and AM251 reduced GPR55 mRNA ($p<0.01$) expression at 5.6 mmol/l and 16.7 mmol/l glucose.

These findings demonstrate that the novel endocannabinoid receptor GPR55 regulates insulin secretion and beta regeneration, thus promoting the receptor as a therapeutic target for type 2 diabetes.

4.2: Introduction

The previously considered orphan G-protein coupled receptor 55 (GPR55) has been identified as a novel endocannabinoid receptor (Lagerstrom & Schioth 2008, Ryberg *et al.* 2009, Tuduri *et al.* 2017). Although classified as a member of the endocannabinoid system, GPR55 exhibits only 13% and 14% sequence homology with the CB1 and CB2 receptors, respectively (Tuduri *et al.* 2017). Numerous studies have demonstrated the biological activation of GPR55 to be mediated by a range of cannabinoid ligands, including plant (phytocannabinoids), small synthetic cannabinoids and endogenous cannabinoid ligands (McKillop *et al.* 2013, Tuduri *et al.* 2017,). As the functional role of the CB1 and CB2 receptors is well known, it has been hypothesised that GPR55 is accountable for the non-CB1/CB2 effects exerted by the cannabinoid ligands (Shore & Reggio 2015, Tuduri *et al.* 2017).

The gene encoding human-GPR55 is located on chromosome 2 at q37, with the translated GPR55 protein comprised of 319 amino acid residues (Sawzdargo *et al.* 1999). Rat and mouse GPR55 display 78% and 75% sequence homology with human-GPR55, respectively (Tudurí *et al.* 2017). Expression of GPR55 has been reported in many tissues of the human body, with abundant expression observed in adipose tissue, brain, peripheral tissue, central nervous system, endocrine-pancreas and the gastrointestinal (GI) tract (Sawzdargo *et al.* 1999, Ryberg *et al.* 2009, McKillop *et al.* 2013).

GPR55 has a regulatory role in GI tract physiology of both humans and rodents, with high receptor expression demonstrated in the duodenum, jejunum, ileum and colon (Schicho & Storr 2012). The biological function of GPR55 in the GI tract is not fully understood, however, some studies have reported the receptor to potentiate anti-inflammatory and motility functions (Schicho *et al.* 2011, Stancic *et al.* 2015). Furthermore, the endogenous GPR55 agonist OEA is widely produced in the GI tract and exhibits potent inhibitory effects towards food intake (Schicho & Storr 2012). However, conflicting evidence has also demonstrated the atypical GPR55 agonist O-1602 to induce food intake and adiposity in rats (Diaz-Arteaga *et al.* 2012).

The endocannabinoid system is known to exhibit a regulatory role in multiple biological processes, including psychological, cardiovascular and intestinal functions (Pacher & Kunos 2013). However, recent studies have indicated that it may also have a pivotal role in the maintenance of glucose and lipid homeostasis, particularly through GPR55 activation (McKillop *et al.* 2013, McKillop *et al.* 2016, Tudurí *et al.* 2017).

With respect to the endocrine-pancreas, GPR55 is heavily expressed in human and rodent pancreatic islets, with abundant expression demonstrated within insulin secreting beta cells (McKillop *et al.* 2013, Liu *et al.* 2016). In rodent islets, GPR55 expression was shown to be exclusive to pancreatic beta cells, with no expression observed on glucagon

and somatostatin secreting alpha and delta cells, respectively (McKillop *et al.* 2013). However, immunohistochemical analysis using human islets displayed co-expression of GPR55 and glucagon in pancreatic alpha cells (Liu *et al.* 2016).

Accompanied with high expression of GPR55 in pancreatic beta cells, agonising the receptor induces insulin secretion (McKillop *et al.* 2013, Liu *et al.* 2016). In particular, a range of endogenous (OEA, PEA) and atypical (Abn-CBD, O-1602, AM251) ligands were shown to induce glucose stimulated insulin secretion (GSIS) from pancreatic BRIN-BD11 cells (McKillop *et al.* 2013). The insulinotropic effect of the cannabinoid ligands was impaired when co-incubated with a GPR55 antagonist. Furthermore, administration of GPR55 agonists was shown to improve glucose tolerance and enhance insulin secretion in mice (McKillop *et al.* 2013, McKillop *et al.* 2016). Chronic administration of cannabidiol analogue Abn-CBD improved glucose control, increased plasma insulin concentrations and lowered cholesterol in streptozotocin-induced diabetic mice, with reductions in food intake and bodyweight also observed (McKillop *et al.* 2016).

Although, numerous studies have demonstrated the glucose lowering and insulinotropic properties of GPR55, its mechanism of insulin secretion is poorly understood. Upon activation, GPR55 primarily couples to Gα12/13 and Gαq intracellular G-protein subunits, resulting in phospholipase C (PLC) and RhoA signalling (Lauckner *et al.* 2008, Leyva-Illades & DeMorrow 2013). This can stimulate an array of downstream cellular responses, such as myosin contractility, cell cycle maintenance, cellular morphological polarization, cellular secretion, cellular development and transcriptional control (Leyva-Illades & DeMorrow 2013, Yu & Brown 2015). With respect to the pancreatic beta cell, initial studies have demonstrated a range of cannabinoid ligands to augment intracellular Ca^{2+} concentrations, indicating the involvement of inositol trisphosphate (IP_3) on

intracellular calcium stores through PLCβ signalling (McKillop *et al.* 2013, Liu *et al.* 2016).

Another study demonstrated Abn-CBD to exhibit proliferative and cytoprotective effects towards pancreatic mouse islets (Ruz-Maldonado *et al.* 2018). The effects observed were proven to be GPR55 specific with the use of GPR55 knockout mice (Ruz-Maldonado *et al.* 2018). However, the mechanistic function of GPR55-mediated islet cytoprotection and regeneration remains elusive. Interestingly, Abn-CBD has been closely linked with mitogen-activated protein kinase (MAPK) signalling, a highly conserved family of serine/threonine protein kinases that are involved in a range of cellular responses, including differentiation, proliferation, apoptosis, survival, stress response and motility. MAPK pathways (ERK1/2, JNK, p38) can be activated upon G-protein coupled receptor signalling and may contribute to the beneficial effects of GPR55 in the pancreatic islet (Matouk *et al.* 2017).

Currently, there are limited reports on the regulatory role of GPR55 in the pancreatic islet. The present study aims to characterise the mechanistic function of GPR55 with respect to insulin release, islet cell regeneration and receptor expression. Downstream signalling molecules were investigated (intracellular Ca^{2+}, cAMP and MAPKs) to explore the functional role of GPR55, whilst receptor expression analysis further evaluated the therapeutic potential of GPR55 activation.

4.3: Materials and methods

4.3.1: Materials

Abn-CBD, AM251, O-1602, OEA, PEA and alanine were purchased from Tocris Bioscience (Bristol, UK). All other materials were purchased from suppliers as detailed in Section 2.

4.3.2: Acute insulin secretion studies from pancreatic BRIN-BD11 cells

BRIN-BD11 cells were sub-cultured and seeded into 24-well plates at a density of 150,000 cells per well, then supplemented with 1 ml of RPMI media and allowed to attach overnight, as outlined in Section 2.1.2. Abn-CBD, AM251, O-1602, OEA, PEA (10^{-4}-10^{-12} mol/l) were added to KRBB buffer, supplemented with 5.6 mmol/l or 16.7 mmol/l glucose. Cells were pre-treated with 1.1 mmol/l glucose KRBB for 40 min at 37^{o}C. After pre-incubation, test solutions were added and incubated for 20 min at 37^{o}C. Aliquots (900µl) of cell supernatant were removed and stored at -20^{o}C until determination of insulin concentrations by radioimmunoassay, as outlined in Section 2.2.3. MTT cytotoxicity analysis was conducted with identical test parameters as insulin secretory studies previous detailed in Section 2.1.6.

4.3.3: Determination of GPR55 mRNA expression in pancreatic BRIN-BD11 cells

BRIN-BD11 cells were sub-cultured and seeded into 6-well plates at a density of 1,000,000 cells per well, then supplemented with 2 ml of RPMI media and allowed to attach overnight, as outlined in Section 2.1.2. Cell were pre-incubated with 1.1 mmol/l

glucose for 1 h at 37°C. Agonist test solutions (10^{-4} mol/l) were prepared in KRBB buffer at 5.6 mmol/l or 16.7 mmol/l glucose. Test solutions were incubated for 4 h at 37°C. After incubation, cells were lysed and RNA harvested with TRIzol reagent (Sigma, UK). RNA was purified then converted to cDNA as previously described in Section 2.6.2. SYBR green PCR kit (Roche, UK) was used for qPCR as previously detailed in Section 2.6.3.

4.3.4: Immunofluorescence staining of BRIN-BD11 cells

As detailed in Section 2.8.2.

4.3.5: Determination of cAMP production in pancreatic BRIN-BD11 cells

BRIN-BD11 cells were sub-cultured and seeded into 6-well plates at a density of 1,000,000 cells per well, then supplemented with 2 ml of RPMI media and allowed to attach overnight, as outlined in Section 2.1.2. Cells were pre-incubated with 1.1 mmol/l glucose for 40 min at 37°C. Agonist test solutions (10^{-4} mol/l) and IBMX (10 mmol/l) were prepared in KRBB buffer at 16.7 mmol/l glucose and assessed for cAMP production. After incubation, cells were lysed and cAMP detected with the cAMP ELISA kit as previously described in Section 2.4.2.

4.3.6: Intracellular Ca^{2+} measurement

BRIN-BD11 cells were sub-cultured and seeded into 24-well plates at a density of 80,000 cells per well, then supplemented with 1 ml of RPMI media and cultured overnight, as outlined in Section 2.1.2. Alanine (10 mmol/l) and GPR55 agonists (Abn-CBD, AM251, O-1602, OEA, PEA) at 10^{-4} mol/l were added to KRBB buffer, supplemented with 5.6

mmol/l or 16.7 mmol/l glucose. The assay plate was pre-incubated with the dye prepared with KRBB and 50µl of the test solutions were transferred to the plate with fluorescence intensity measured for 5 min using the FlexStation 3 plate reader (Molecular devices, CA, USA), as detailed in Section 2.3.2.

4.3.7: MAPK signalling and GPR55 expression analysis by western blotting in pancreatic BRIN-BD11 cells

BRIN-BD11 cells were sub-cultured and seeded into 6-well plates at a density of 1,000,000 cells per well, then supplemented with 2 ml of RPMI media and allowed to attach overnight, as outlined in Section 2.1.2. Cells were pre-incubated with 1.1 mmol/l glucose for 40 min at 37^{o}C. Agonist test solutions (10^{-4} mol/l) and PMA (200 nmol/l) were prepared in KRBB buffer at 5.6 mmol/l or 16.7 mmol/l glucose. After incubation, cells were lysed at various timepoints with RIPA buffer, supplemented with protease and phosphatase inhibitors. Cell lysates (25µg) were prepared and separated by SDS-PAGE and transferred to a nitrocellulose membrane, as previously described in Section 2.7. Membranes were probed with total and phosphorylated anti-ERK1/2, anti-JNK and anti-p38 antibodies for MAPK signalling and anti-GPR55 for receptor expression. β-actin was used as a control to normalise data. Images were captured using a G:BOX Chemi XX9 imager (Syngene, UK) and densitometry analysis performed using ImageJ.

4.3.8: ERK1/2 signalling analysis by flow cytometry in pancreatic BRIN-BD11 cells

BRIN-BD11 cells were sub-cultured and seeded into 6-well plates at a density of 1,000,000 cells per well, then supplemented with 2 ml of RPMI media and allowed to attach overnight, as outlined in Section 2.1.2. Cells were pre-incubated with 1.1 mmol/l

glucose for 40 min at 37ºC. Agonist test solutions (10^{-4} mol/l) and PMA (200 nmol/l) were prepared in KRBB buffer at 16.7 mmol/l glucose. After incubation, cells were detached with trypsin, pelleted by centrifugation then re-suspended in 600µl of flow cytometry staining buffer, supplemented with anti-phospho-ERK1/2 antibodies. Samples were conjugated with an AlexaFluor488 secondary antibody. Samples were gated prior to FITC-GFP expression analysis by flow cytometry.

4.3.9: Cellular viability and apoptosis studies on pancreatic BRIN-BD11 cells and α-TC1.9 cells

BRIN-BD11 cells were sub-cultured and seeded into a clear 96-well plate at a density of 40,000 cells per well and allowed to attach overnight, as previously outlined in Sections 2.1.2 and 2.1.4. Agonist test solutions (10^{-4} mol/l) and cytokine cocktail solution (TNF-α [200 U/ml], IFN-γ [20 U/ml], IL-1β [100 U/ml]) were prepared in RPMI media, then added to the cells and incubated for 20 h at 37ºC. Cell viability and apoptosis was determined with Apo-Live-Glo multiplex analysis as per manufacturer's protocol; cell viability by protease activity, cell apoptosis by caspase 3/7 activity (Promega, USA).

4.4: Results

4.4.1: Effect of GPR55 agonists on insulin secretion from clonal pancreatic BRIN-BD11 cells

The insulin secretory effect of a range of endogenous (OEA, PEA) and synthetic (Abn-CBD, AM251, O-1602) GPR55 agonists was investigated using the clonal pancreatic

BRIN-BD11 cell line at 5.6 mmol/l and 16.7 mmol/l glucose. Atypical CBD analogue Abn-CBD (10^{-9}-10^{-4} mol/l) stimulated insulin release at 5.6 mmol/l ($p<0.05$-$p<0.001$) (Fig. 4.1A). At 16.7 mmol/l glucose, the insulinotropic effect of Abn-CBD (10^{-9}-10^{-4} mol/l) was increased ($p<0.05$-$p<0.001$), with a 3.1-fold increase observed at the highest concentration tested (10^{-4} mol/l) (Fig. 4.2A). Rimonabant analogue AM251 (10^{-8}-10^{-4} mol/l) induced insulin secretion ($p<0.05$) at 5.6 mmol/l glucose (Fig. 4.3A). At stimulatory glucose concentrations (16.7 mmol/l glucose), AM251 (10^{-5}-10^{-4} mol/l) exhibited insulinotropic capabilities ($p<0.01$-$p<0.001$), with a 68% increase demonstrated at the highest concentration tested (10^{-4} mol/l) (Fig. 4.4A).

The synthetically composed CBD analogue O-1602 (10^{-8}-10^{-4} mol/l) stimulated insulin release at 5.6 mmol/l glucose, with an increase of 83% ($p<0.01$) observed at the highest concentration tested (Fig. 4.5A). At 16.7 mmol/l glucose, O-1602 (10^{-8}-10^{-4} mol/l) demonstrated enhanced insulinotropic capabilities, with a 127% increase observed at the highest agonist concentration investigated (10^{-4} mol/l) (Fig. 4.6A).

Naturally occurring GPR55 agonist PEA (10^{-5}-10^{-4} mol/l) stimulated insulin secretion ($p<0.05$-$p<0.001$) at 5.6 mmol/l glucose (Fig. 4.7A). When incubated at 16.7 mmol/l glucose, PEA (10^{-8}-10^{-4} mol/l) demonstrated enhanced insulinotropic capabilities, whilst omitting a 93% ($p<0.001$) increase at the highest agonist concentration tested (10^{-4} mol/l) (Fig. 4.8A). Endogenous endocannabinoid OEA (10^{-8}-10^{-4} mol/l) induced insulin release ($p<0.05$-$p<0.001$) at 5.6 mmol/l glucose (Fig. 4.9A). At stimulatory glucose concentrations of 16.7 mmol/l glucose, OEA (10^{-7}-10^{-4} mol/l) augmented insulin secretion ($p<0.01$-$p<0.001$), with a 1.8-fold increase demonstrated at the highest agonist concentration tested (10^{-4} mol/l) (Fig. 4.10A).

At basal glucose concentrations (5.6 mmol/l), GPR55-induced insulin release and agonist potencies were as follows (in descending order): Abn-CBD (1.506×10^{-8} mol/l), AM251

(7.6 x 10^{-8} mol/l), O-1602 (1.24 x 10^{-7} mol/l), OEA (4.6 x 10^{-7} mol/l), PEA (3.439 x 10^{-6} mol/l). At hyperglycaemic concentrations of 16.7 mmol/l, agonist potency was as follows (in descending order): Abn-CBD (5.18 x 10^{-9} mol/l), PEA (2.394 x 10^{-8} mol/l), OEA (1.131 x 10^{-6} mol/l), O-1602 (5.87 x 10^{-6} mol/l), AM251 (1.04 x 10^{-5} mol/l) (Table 4.1).

The positive control (alanine) augmented insulin secretion ($p<0.001$) for all insulin secretory analysis (Fig. 4.1-4.10A). Cytotoxicity analysis by MTT demonstrated no adverse effects towards pancreatic BRIN-BD11 cells at 5.6 mmol/l and 16.7 mmol/l glucose upon incubation with all agonists at the range of concentrations tested (Fig. 4.1-4.12B).

4.4.2: Effect of GPR55 agonists on insulin secretion from clonal human pancreatic 1.1B4 cells

The insulinotropic properties of the potent GPR55 agonists (Abn-CBD and AM251) were further investigated in the human clonal pancreatic 1.1B4 cell line at 5.6 mmol/l and 16.7 mmol/l glucose. Atypical cannabinoid Abn-CBD (10^{-9}-10^{-4} mol/l) stimulated insulin secretion by 1.4-2.0-fold at 5.6 mmol/l glucose ($p<0.01$-$p<0.001$) (Fig. 4.11A). At 16.7 mmol/l glucose, Abn-CBD (10^{-6}-10^{-4} mol/l) augmented insulin release ($p<0.05$-$p<0.001$), with an 82% ($p<0.001$) increase observed at the highest concentration tested (10^{-4} mol/l) (Fig. 4.1B).

Rimonabant analogue AM251 (10^{-10}-10^{-4} mol/l) induced insulin secretion by 1.2-2-fold ($p<0.05$-$p<0.001$) at 5.6 mmol/l glucose (Fig. 4.3A). At stimulatory glucose concentrations of 16.7 mmol/l glucose, AM251 (10^{-8}-10^{-4} mol/l) maintained insulinotropic capabilities ($p<0.01$-$p<0.001$), with a 117% increase demonstrated at the

highest concentration tested (10^{-4} mol/l) (Fig. 4.12B). The positive control (alanine) augmented insulin secretion ($p<0.001$) for all insulin secretory analysis (Fig. 4.11-4.12).

AM251was the most potent agonist tested at 5.6 mmol/l with an EC_{50} value of 5.442 x 10^{-7} mol/l, followed by Abn-CBD (1.610 x 10^{-6} mol/l). At 16.7 mmol/l glucose, AM251 remained the most potent with an EC_{50} value of 1.610 x 10^{-6} mol/l, followed by Abn-CBD (3.225 x 10^{-6} mol/l) (Table. 4.1).

4.4.3: Expression and distribution of GPR55 and insulin in clonal pancreatic BRIN-BD11 cells

Immunocytochemistry analysis was employed to determine the distribution of (A) DAPI, (B) insulin, (C) GPR55 in BRIN-BD11 cells (Fig. 4.13). High expression of GPR55 and insulin was demonstrated in BRIN-BD11 cells, with areas of co-localisation observed between GPR55 and insulin using double immuno-fluorescence analysis (Fig. 4.13D).

4.4.4: Effects of Abn-CBD and AM251 on GPR55 and insulin expression in clonal pancreatic BRIN-BD11 cells

qPCR and western blotting were employed to determine GPR55 mRNA and protein expression in BRIN-BD11 cells upon agonist treatment at 5.6 mmol/l and 16.7 mmol/l glucose (Fig. 4.14). Abn-CBD and AM251 reduced GPR55 mRNA expression by 25-40% ($p<0.05$) at 5.6 mmol/l glucose. At 16.7 mmol/l glucose, AM251 reduced GPR55 mRNA expression by 60% ($p<0.05$), whilst Abn-CBD had no effect. Complimentary western blotting demonstrated a down regulation (39-42%) of GPR55 protein expression in the pancreatic BRIN-BD11 cells upon activation with Abn-CBD and AM251 at 16.7 mM glucose (Fig. 4.14C).

At 5.6 mmol/l glucose, Abn-CBD and AM251 up regulated insulin mRNA expression by 2.7-3.0-fold ($p<0.05$-$p<0.01$) (Fig. 4.15A). At 16.7 mmol/l glucose, Abn-CBD and AM251 up regulated insulin mRNA by 1.8-2-fold ($p<0.05$) (Fig. 4.15B).

4.4.5: Effect of GPR55 agonists on intracellular Ca^{2+} and cAMP modulation in clonal pancreatic BRIN-BD11 cells

BRIN-BD11 cells were incubated with GPR55 agonists (Abn-CBD, AM251, O-1602, PEA, AM251) at 10^{-4} mol/l and IBMX or alanine at 10 mmol/l in KRBB supplemented with 16.7 mmol/l glucose. In pancreatic BRIN-BD11 cells AM251 ($p<0.001$), PEA ($p<0.001$), O-1602 ($p<0.05$) and Abn-CBD ($p<0.05$) prompted an increase in intracellular calcium concentrations at 16.7 mmol/l glucose, whilst OEA had no effect (Fig. 4.16)

After 20 min incubation, all GPR55 agonists demonstrated no significant effects on cAMP production, whilst the positive control (IBMX) stimulated a 19-fold ($p<0.001$) increase (Fig. 4.17).

4.4.6: Effect of Abn-CBD, AM251, OEA and PMA on ERK1/2 (p44/42) signalling in clonal pancreatic BRIN-BD11 cells

SDS-PAGE western blotting demonstrated Abn-CBD, AM251 and OEA to have no effect on ERK1/2 phosphorylation at time points ranging from 5-60 min in BRIN-BD11 cells. Whereas, the positive control (PMA) induced ERK1/2 phosphorylation after 30 and 60 min incubation (Fig. 4.18).Further analysis using flow cytometry demonstrated that Abn-CBD (Fig. 4.19C), AM251 (Fig. 4.19D) and OEA (Fig. 4.19E) had no effect on ERK1/2 phosphorylation as each agonist demonstrated a response (7.8-8.7%) similar to the non-treated control (7.8%) (Fig. 4.19A). The positive control (PMA) induced ERK1/2 phosphorylation by 19.9% in BRIN-BD11 cells (Fig. 4.19B).

4.4.7: Effect of Abn-CBD on JNK, p38 and ERK1/2 MAPK signalling in clonal pancreatic BRIN-BD11 cells

The effect of Abn-CBD on mitogen-activated protein kinase (MAPK) signalling was assessed by western blotting in BRIN-BD11 cells (Fig. 4.20). Abn-CBD abolished JNK phosphorylation after 5 min incubation, with JNK phosphorylation returning to basal after further 5 min incubation and continued for the remainder of experimental timeframe (10-30 min). Abn-CBD reduced p38 phosphorylation after 10-30 min incubation. No effect on ERK1/2 phosphorylation was observed throughout the experimental timeframe (5-30min). Total JNK, p38 and ERK1/2 remained constant at all time points. Positive control (PMA) induced JNK, p38 and ERK1/2 phosphorylation within 15-30 min incubation.

4.4.8: Effect of Abn-CBD, AM251 and O-1602 on clonal pancreatic BRIN-BD11 cell viability and apoptosis

BRIN-BD11 cells were incubated with GPR55 agonists for 20 h. Cell viability was determined by protease activity and apoptosis by caspase3/7 activity (Fig. 4.21). Abn-CBD (10^{-4} mol/l and 10^{-6} mol/l) and AM251 (10^{-6} mol/l) increased cell viability by 14-16% ($p<0.05$), whilst O-1602 had no effect at both concentrations (10^{-4} mol/l and 10^{-6} mol/l). Cytokine cocktail incubation reduced cell viability by 13% after 20 h incubation (Fig. 4.21A).

At 10^{-6} mol/l, Abn-CBD, AM251 and O-1602 had no effect on caspase3/7 activity. At a higher agonist concentration (10^{-4} mol/l), Abn-CBD and O-1602 reduced by 24% ($p<0.05$) and 39% ($p<0.01$), respectively, whilst AM251 increased caspase3/7 activity by 97% ($p<0.001$). Cytokine cocktail incubation increased caspase3/7 by 47% ($p<0.01$) after 20 h incubation (Fig. 4.21B).

3.4.9: Effect of Abn-CBD, AM251 and O-1602 on clonal pancreatic α-TC1.9 cell viability and apoptosis

A-TC1.9 cells were incubated with GPR55 agonists for 20 h. Cell viability was determined by protease activity and apoptosis by caspase3/7 activity (Fig. 4.22). At 10^{-6} mol/l, Abn-CBD, AM251 and O-1602 had no effect on cell viability. At a higher agonist concentration (10^{-4} mol/l), Abn-CBD, AM251 and O-1602 reduced cell viability by 39-52% ($p<0.001$). Cytokine cocktail incubation reduced cell viability by 32% after 20 h (Fig. 4.22A).

At 10^{-6} mol/l, Abn-CBD (18%) and O-1602 (15%) reduced caspase3/7 activity ($p<0.01$-$p<0.001$), whilst AM251 had no significant effect. At a higher agonist concentration (10^{-4} mol/l), Abn-CBD, AM251 and O-1602 increased caspase3/7 activity by 13-82% ($p<0.01$-$p<0.001$). Cytokine cocktail incubation increased caspase3/7 by 15% ($p<0.01$) after 20 h (Fig. 4.22B).

4.5: Discussion:

Novel therapeutic strategies that enhance islet cell function and beta cell regeneration are required for the treatment of type 2 diabetes. Recently, research has intensified on the endocannabinoid system upon the discovery of the novel endocannabinoid receptors GPR55, GPR18 and GPR119 (Lagerstrom & Schioth 2008, Ryberg *et al.* 2009). Previous studies have demonstrated a range of beneficial effects exerted by endocannabinoid receptors upon activation with long chain fatty acid agonists, including the regulation of glycaemic control, energy metabolism and anti-inflammatory responses (McKillop *et al.* 2013, McKillop *et al.* 2016, Tudurí *et al.* 2017).

The CB1 and CB2 receptors of the endocannabinoid system are known to modulate a range of physiological functions including appetite, memory, mood and pain-sensitisation (Aizpurua-Olaizola *et al.* 2017). The CB1 receptor is predominately expressed in the brain and the central nervous system, whereas the CB2 receptor is mainly expressed in the immune system and in hematopoietic cells (Pacher and Kunos 2013). Cannabinoid ligands bind stereo-selectively and reversibly to the CB1 and CB2 receptors. Selective subtype cannabinoids have been synthetically composed and present potential for the treatment of obesity and other metabolic diseases, with a CB1 inverse agonist Rimonabant (SR141716) previously used as an anti-obesity drug (Henness *et al.* 2006).

Although categorised as an endocannabinoid receptor, GPR55 is not associated with the control of psychological responses and shares limited sequence homology with the CB1 and CB2 receptors (Morales & Reggio 2017). Recent studies have indicated that GPR55 is responsible for the anti-diabetic effects exerted by cannabinoid ligands through the regulation of insulin release and glucose homeostasis (McKillop *et al.* 2013, McKillop *et al.* 2016, Tuduri *et al.* 2017).

The present study utilised a range of endogenous (OEA, PEA) and synthetic (Abn-CBD, AM251, O-1602) GPR55 agonists to investigate the anti-diabetic efficacy of the receptor through the regulation of insulin release and beta cell regeneration. At normoglycemia, endogenous (OEA) and synthetic (Abn-CBD) were the most potent agonists tested, whilst previous complimentary studies also demonstrated the insulinotropic properties of Abn-CBD in human islets (Ruz-Maldonado *et al.* 2018). Interestingly, at hyperglycaemic concentrations, PEA was the most potent endogenous agonist, whilst Abn-CBD remained the most potent synthetic agonist tested. The secretory response of Abn-CBD was enhanced in hyperglycaemia, thus revealing its glucose responsive properties and therapeutic potential for the treatment of hyperglycaemia. Studies using human 1.1B4

cells revealed that GPR55 agonists emit similar potencies in both rodent and human pancreatic beta cells; an important finding for the development and characterisation of future GPR55 targeting therapeutics. Moreover, for the first time, the study revealed that treatment of GPR55 agonists upregulated insulin mRNA expression in beta cells, suggesting that GPR55 may potentiate second phase insulin secretion.

At present, the mechanism of GPR55-induced insulin secretion from pancreatic beta cells is not fully understood; however, initial studies have shown GPR55 agonism to augment intracellular Ca^{2+} concentrations (McKillop *et al.* 2013, Liu *et al.* 2016). The present study explored the effects of GPR55 agonists on intracellular Ca^{2+} modulation, cAMP production and MAPK phosphorylation in beta cells, which are downstream Gαq, Gαs and Gαi secondary signalling molecules linked with all cannabinoid receptor signalling. Complimentary to previous findings, GPR55 agonists increased intracellular Ca^{2+} after 5 min, indicating the stimulatory effect of GPR55 activation on first phase insulin release.

All agonists tested demonstrated no effect on cAMP production, suggesting that the Gαs and Gαi intracellular protein subunits, modulating adenylyl cyclase activity, are not stimulated following GPR55 activation. This also indicates that GPR119 (Gαs mediated), is not responsible for the effects observed. As studies have acknowledged the cardioprotective effects of Abn-CBD mediated by ERK1/2 signalling (Su & Vo 2007, Matouk *et al.* 2018), ERK1/2 phosphorylation was assessed in beta cells upon GPR55 agonism. Interestingly, all agonists demonstrated no effects on ERK1/2 phosphorylation, suggesting that GPR55 signalling may be tissue specific. However, Abn-CBD abolished JNK phosphorylation and reduced p38 phosphorylation, indicating that Abn-CBD promotes beta cell survival by attenuating the activation of the stress-related MAPK pathways. In harmony with this, Abn-CBD has been recently shown to induce beta cell

proliferation in a GPR55-dependent manner, however, the mechanism of action was not assessed in this study (Ruz-Maldonado *et al.* 2018).

Subsequently, the effect GPR55 activation on islet cell viability (protease activity) and apoptosis (caspase 3/7 activity) was investigated in the present study. Abn-CBD and AM251 increased cell viability, elucidating the proliferative role of GPR55 activation in pancreatic beta cells. Abn-CBD and O-1602 reduced beta cell apoptosis (caspase3/7 activity) which compliments findings showing Abn-CBD to down-regulate stress linked JNK and p38 phosphorylation. Thus, for the first time, indicating the role of MAPK phosphorylation in GPR55-induced beta cell proliferation. Although GPR55 is lesser expressed in glucagon-secreting alpha cells, the proliferative effects of GPR55 activation were also assessed in this cell type. Increased alpha cell proliferation is associated with the pathophysiology of type 2 diabetes and may counteract positive proliferative effects demonstrated by GPR55 activation in beta cells. In direct contrast to beta cells, GPR55 agonism induced a marked reduction in alpha cell proliferation, accompanied with an increase of alpha cell apoptosis. Overall, findings suggest that GPR55 activation may encourage beta cell growth/survival, whilst reducing alpha cell population in the pancreatic islet.

In conclusion to the study, GPR55 agonism induces first and second phase insulin release in rodent and human pancreatic beta cells, with no cytotoxicity. The mechanism of GPR55-induced insulin release is predominately mediated by intracellular Ca^{2+}, with no involvement of cAMP and ERK1/2 signalling. Abn-CBD treatment reduced JNK and p38 phosphorylation and promotes regenerative effects in the pancreatic islet exclusive to insulin-producing beta cells. These findings reveal a range of anti-diabetic properties exerted by cannabinoid ligands and promotes GPR55 as a novel therapeutic target.

Table 4.1: Half maximal effective concentration (EC_{50}) of GPR55 agonists in rodent BRIN-BD11 and human 1.1B4 cells at 5.6 mM and 16.7 mM glucose.

Rodent BRIN-BD11 cells

Agonist	5.6 mM glucose	16.7 mM glucose
AM-251	7.6×10^{-8} mol/l	1.04×10^{-5} mol/l
Abn-CBD	1.50×10^{-8} mol/l	5.18×10^{-9} mol/l
O-1602	1.24×10^{-7} mol/l	5.87×10^{-6} mol/l
OEA	4.60×10^{-7} mol/l	1.13×10^{-6} mol/l
PEA	3.43×10^{-6} mol/l	2.39×10^{-8} mol/l

Human 1.1B4 cells

Agonist	5.6 mM glucose	16.7 mM glucose
AM-251	5.44×10^{-7} mol/l	1.61×10^{-6} mol/l
Abn-CBD	1.16×10^{-6} mol/l	3.22×10^{-6} mol/l

Figure 4.1: Acute effect of Abn-CBD on insulin secretion and cell viability from clonal pancreatic BRIN-BD11 cells at 5.6 mM glucose.

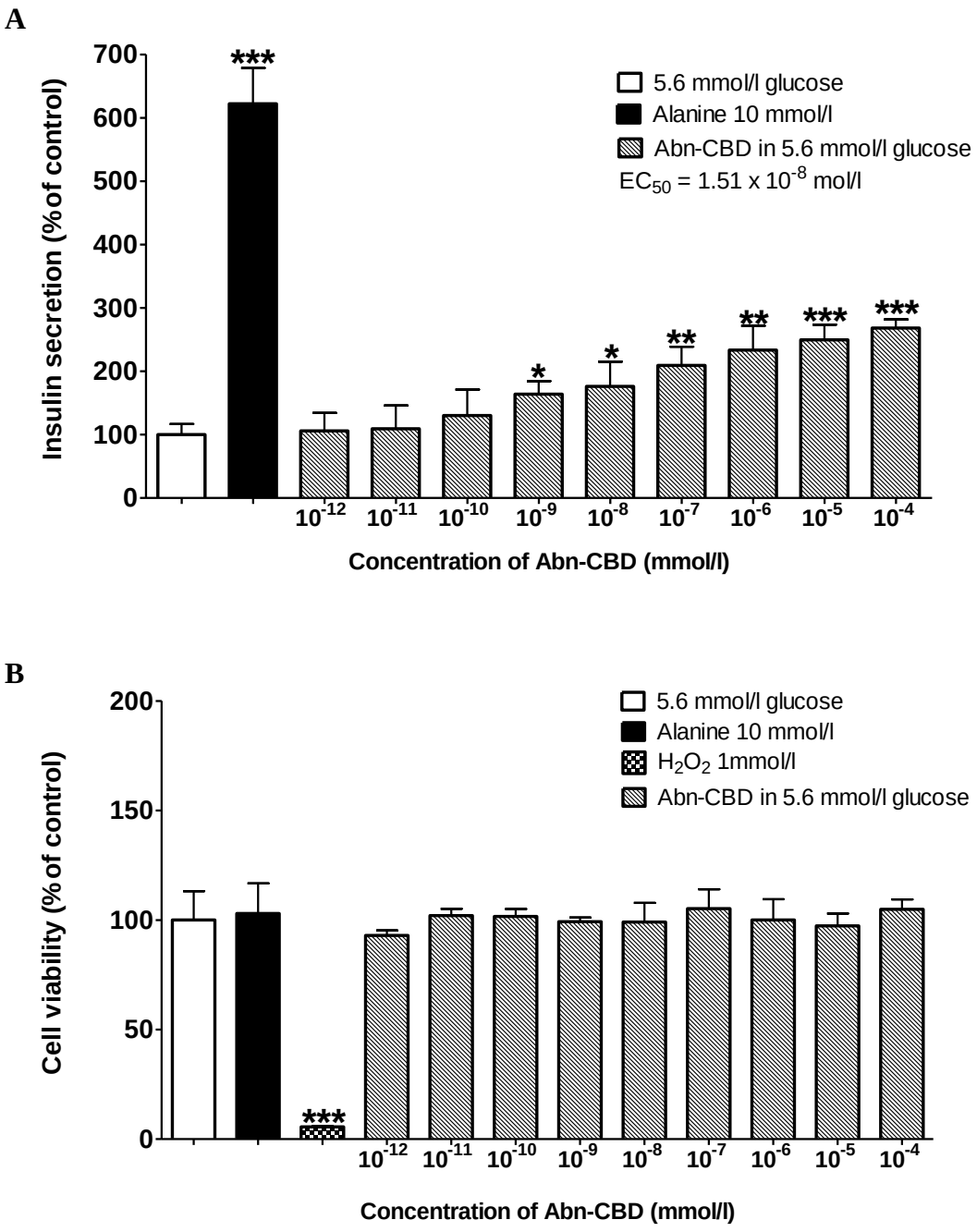

Acute effects of Abn-CBD (10^{-12}-10^{-4} M) and alanine (10 mM) on (A) insulin secretion and (B) cell viability (MTT) from clonal pancreatic BRIN-BD11 cells at 5.6 mM glucose. Results are the mean ± SEM (n=8) for insulin secretion and (n=3) for cell viability. *p<0.05, **p<0.01, ***p<0.001 compared to glucose control.

Figure 4.2: Acute effect of Abn-CBD on insulin secretion and cell viability from clonal pancreatic BRIN-BD11 cells at 16.7 mM glucose.

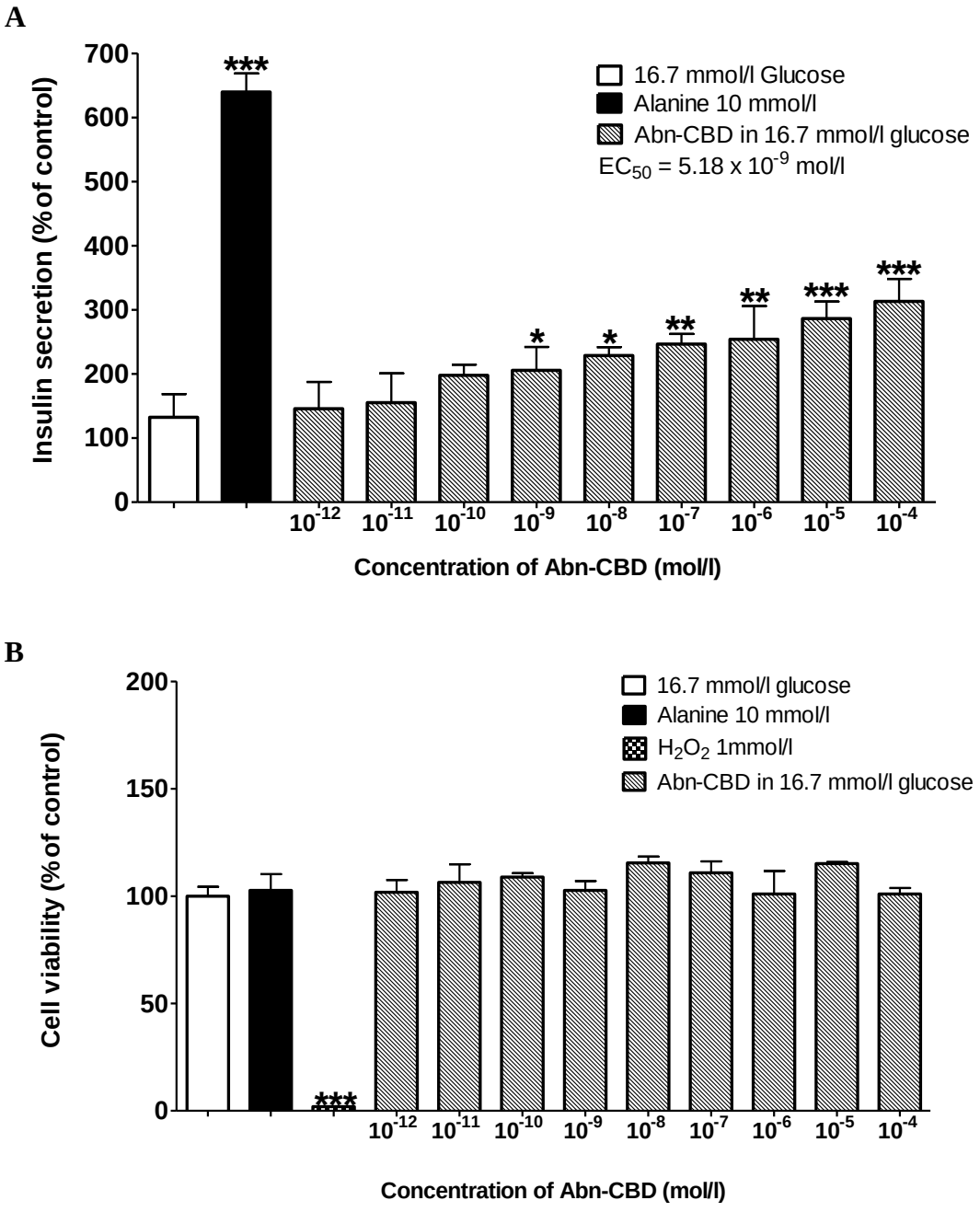

Acute effects of Abn-CBD (10^{-12}-10^{-4} M) and alanine (10 mM) on (A) insulin secretion and (B) cell viability (MTT) from clonal pancreatic BRIN-BD11 cells at 16.7 mM glucose. Results are the mean ± SEM (n=8) for insulin secretion and (n=3) for cell viability. *p<0.05, **p<0.01, ***p<0.001 compared to glucose control.

Figure 4.3: Acute effect of AM251 on insulin secretion and cell viability from clonal pancreatic BRIN-BD11 cells at 5.6 mM glucose.

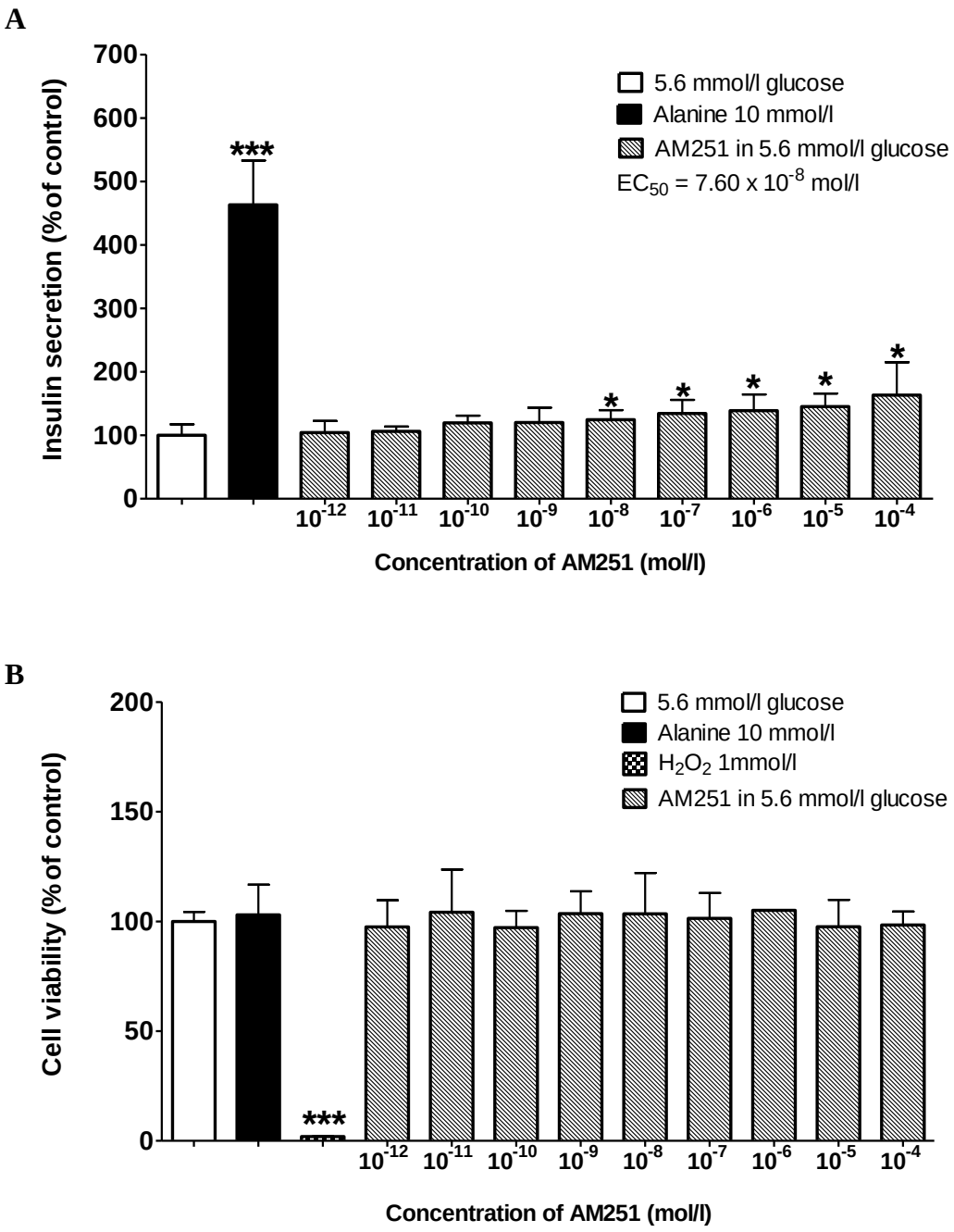

Acute effects of AM251 (10^{-12}-10^{-4} M) and alanine (10 mM) on (A) insulin secretion and (B) cell viability (MTT) from clonal pancreatic BRIN-BD11 cells at 5.6 mM glucose. Results are the mean ± SEM (n=8) for insulin secretion and (n=3) for cell viability. *p<0.05, ***p<0.001 compared to glucose control.

Figure 4.4: Acute effect of AM251 on insulin secretion and cell viability from clonal pancreatic BRIN-BD11 cells at 16.7 mM glucose.

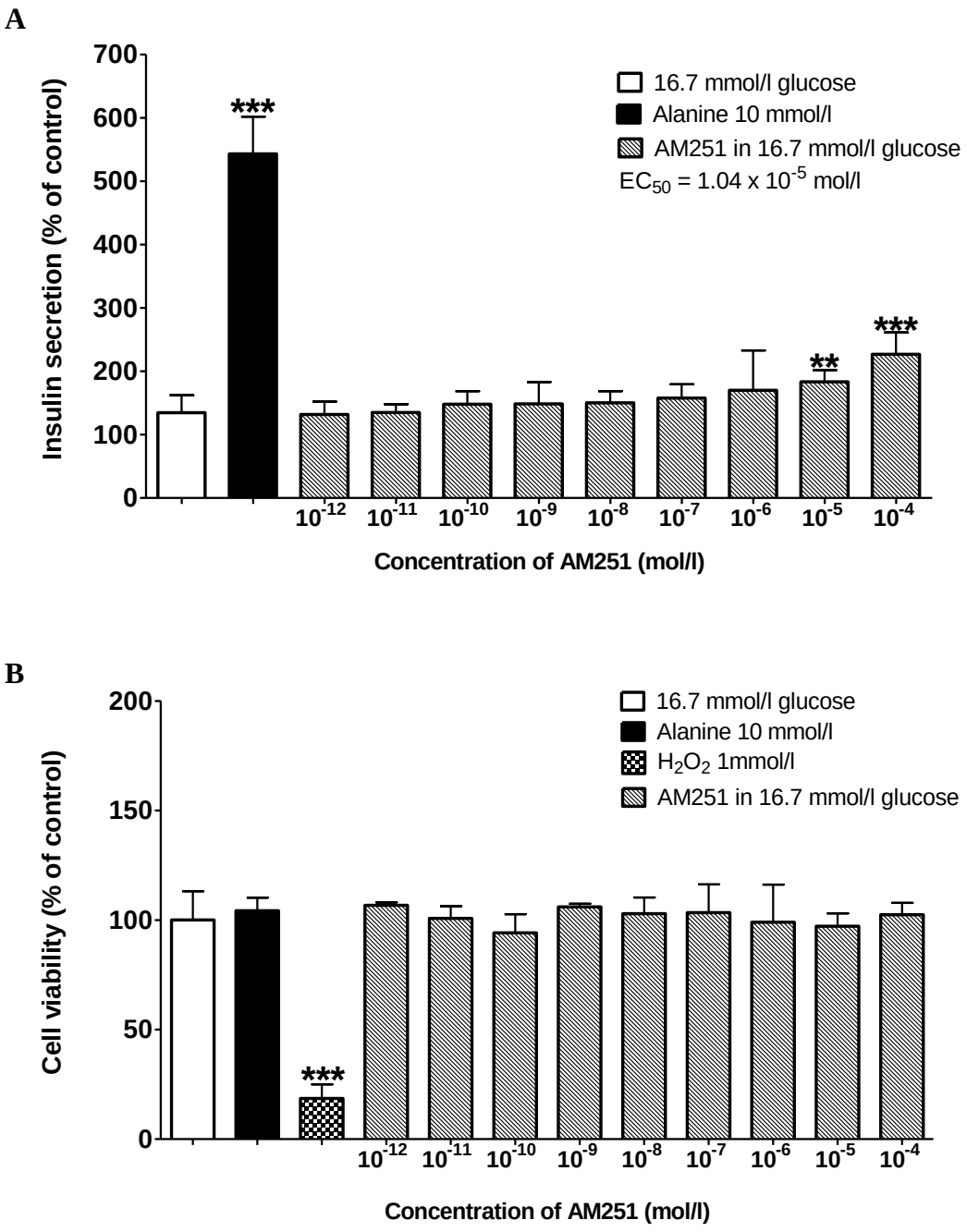

Acute effects of AM251 (10^{-12}-10^{-4} M) and alanine (10 mM) on (A) insulin secretion and (B) cell viability (MTT) from clonal pancreatic BRIN-BD11 cells at 16.7 mM glucose. Results are the mean ± SEM (n=8) for insulin secretion and (n=3) for cell viability. **p<0.01, ***p<0.001 compared to glucose control.

Figure 4.5: Acute effect of O-1602 on insulin secretion and cell viability from clonal pancreatic BRIN-BD11 cells at 5.6 mM glucose.

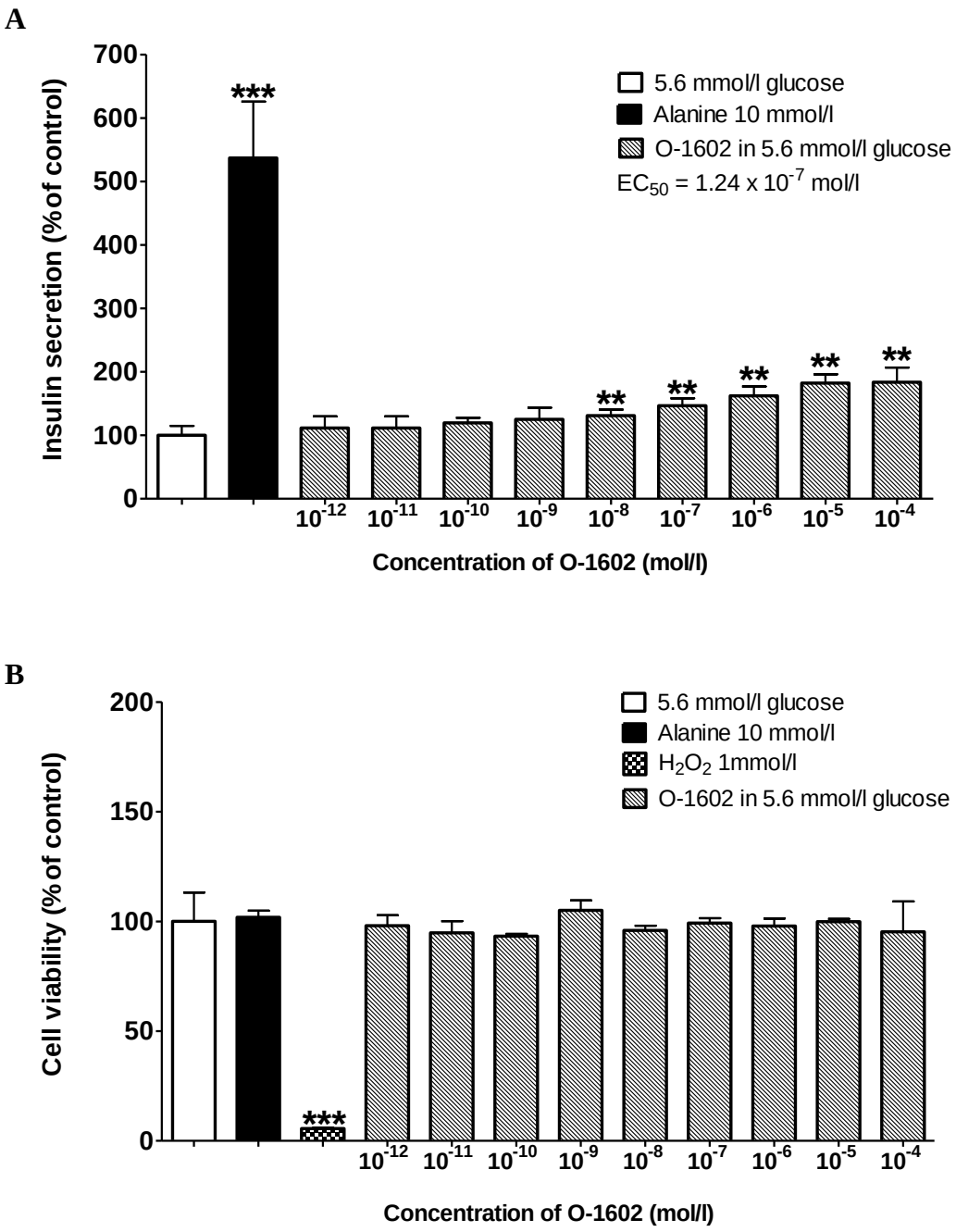

Acute effects of O-1602 (10^{-12}-10^{-4} M) and alanine (10 mM) on (A) insulin secretion and (B) cell viability (MTT) from clonal pancreatic BRIN-BD11 cells at 5.6 mM glucose. Results are the mean ± SEM (n=8) for insulin secretion and (n=3) for cell viability. **p<0.01, ***p<0.001 compared to glucose control.

Figure 4.6: Acute effect of O-1602 on insulin secretion and cell viability from clonal pancreatic BRIN-BD11 cells at 16.7 mM glucose.

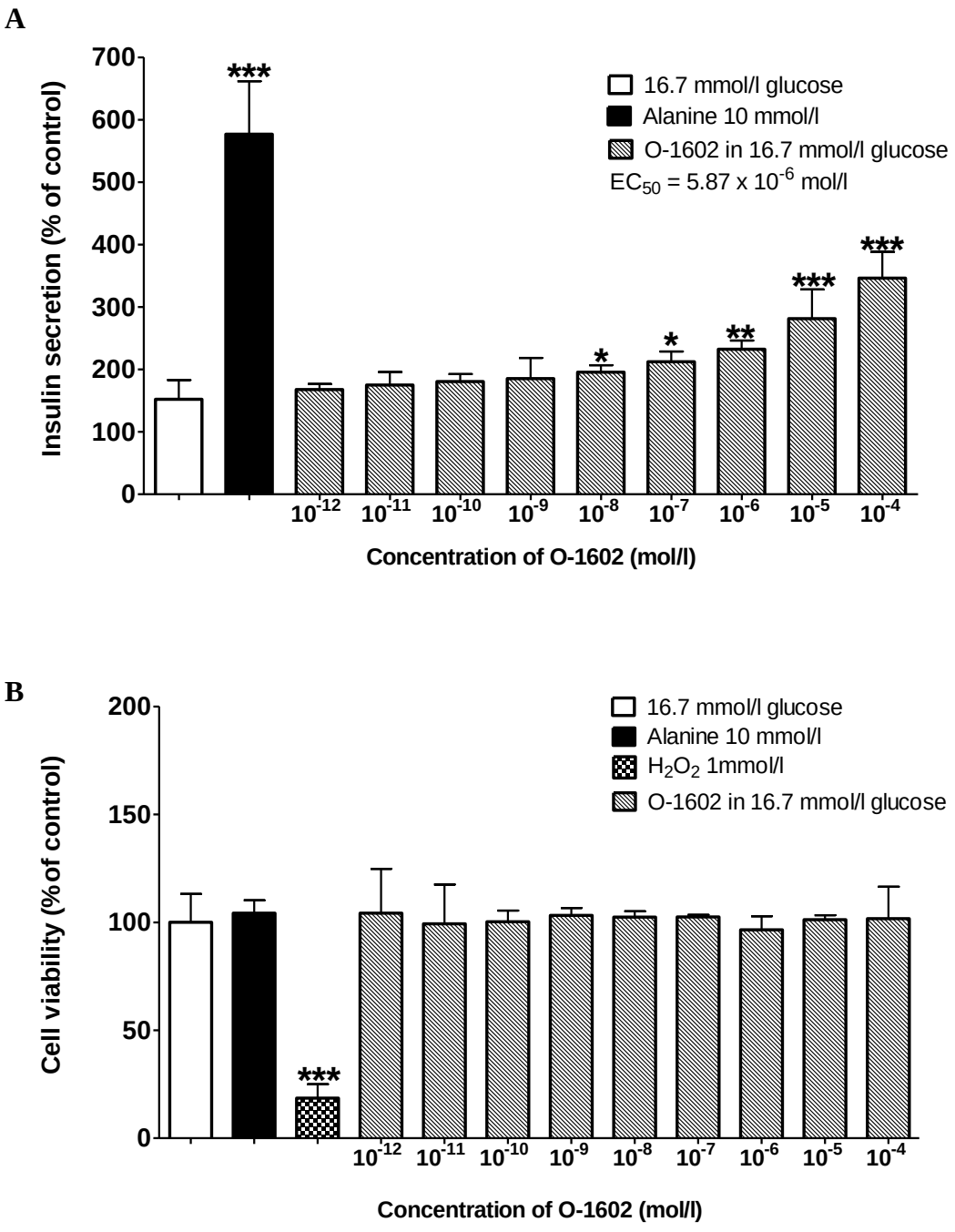

Acute effects of O-1602 (10^{-12}-10^{-4} M) and alanine (10 mM) on (A) insulin secretion and (B) cell viability (MTT) from clonal pancreatic BRIN-BD11 cells at 16.7 mM glucose. Results are the mean ± SEM (n=8) for insulin secretion and (n=3) for cell viability. *p<0.05, **p<0.01, ***p<0.001 compared to glucose control.

Figure 4.7: Acute effect of PEA on insulin secretion and cell viability from clonal pancreatic BRIN-BD11 cells at 5.6 mM glucose.

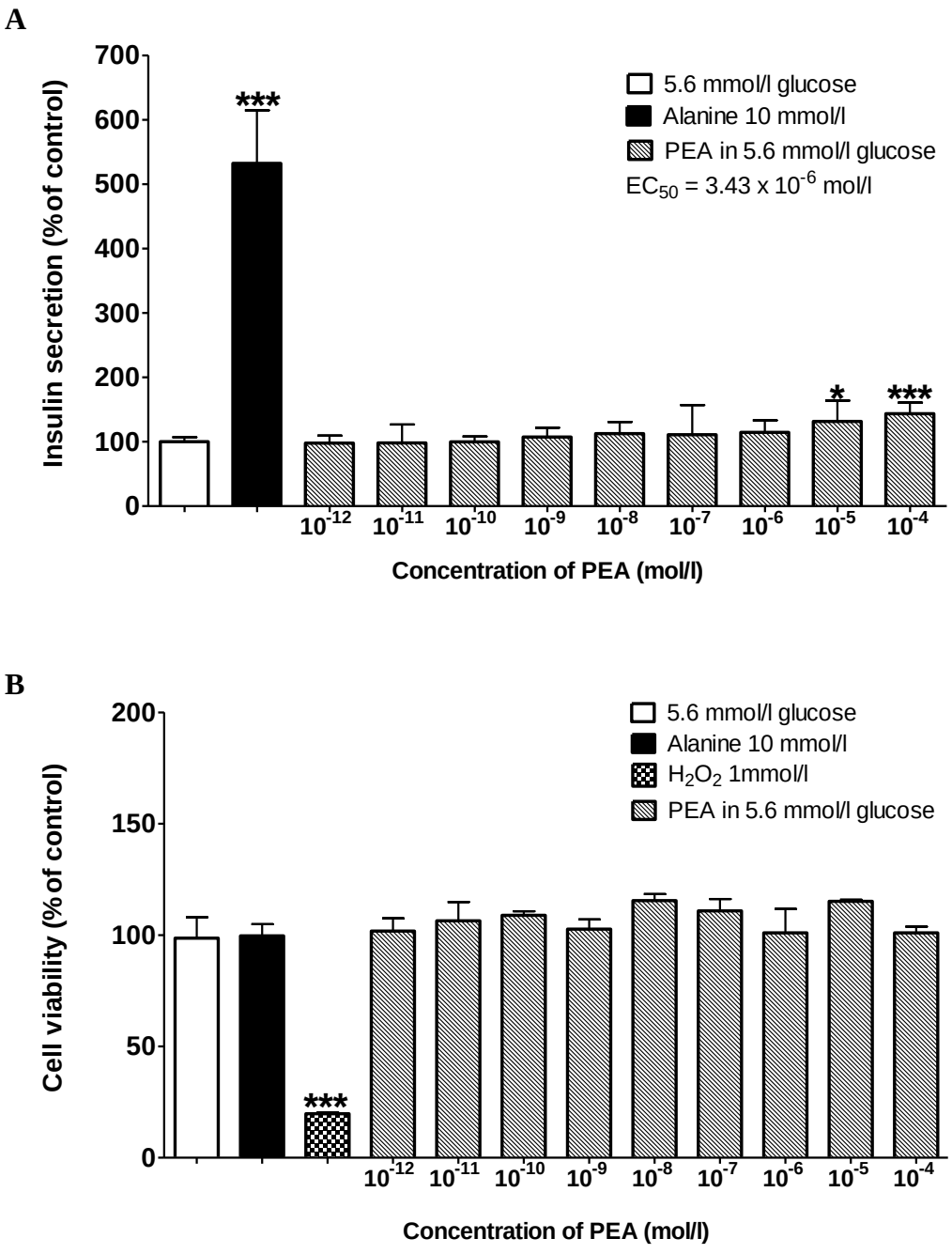

Acute effects of PEA (10^{-12}-10^{-4} M) and alanine (10 mM) on (A) insulin secretion and (B) cell viability (MTT) from clonal pancreatic BRIN-BD11 cells at 5.6 mM glucose. Results are the mean ± SEM (n=8) for insulin secretion and (n=3) for cell viability. *p<0.05, ***p<0.001 compared to glucose control.

Figure 4.8: Acute effect of PEA on insulin secretion and cell viability from clonal pancreatic BRIN-BD11 cells at 16.7 mM glucose.

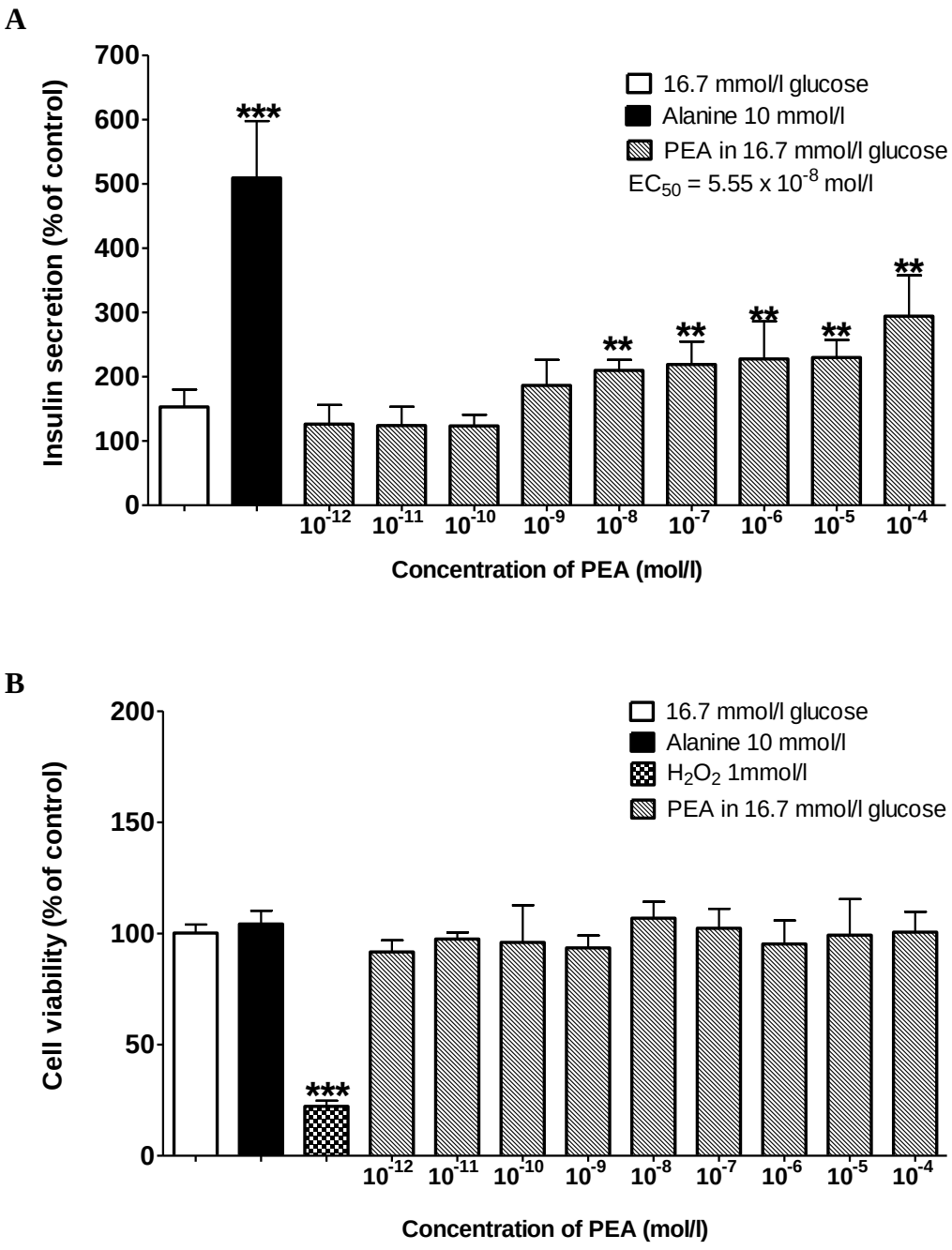

Acute effects of PEA (10^{-12}-10^{-4} M) and alanine (10 mM) on (A) insulin secretion and (B) cell viability (MTT) from clonal pancreatic BRIN-BD11 cells at 16.7 mM glucose. Results are the mean ± SEM (n=8) for insulin secretion and (n=3) for cell viability. **p<0.01, ***p<0.001 compared to glucose control.

Figure 4.9: Acute effect of OEA on insulin secretion and cell viability from clonal pancreatic BRIN-BD11 cells at 5.6 mM glucose.

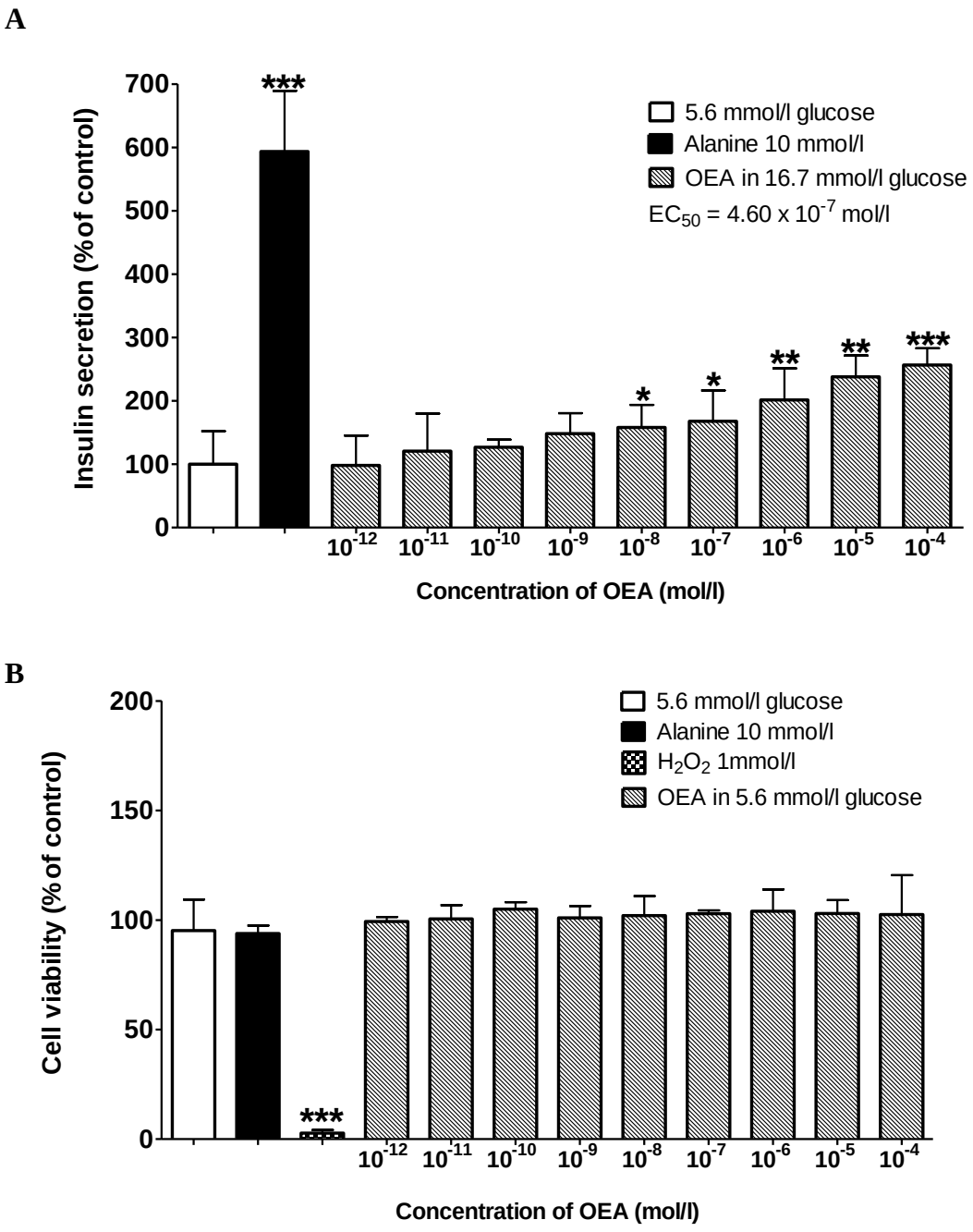

Acute effects of OEA (10^{-12}-10^{-4} M) and alanine (10 mM) on (A) insulin secretion and (B) cell viability (MTT) from clonal pancreatic BRIN-BD11 cells at 5.6 mM glucose. Results are the mean ± SEM (n=8) for insulin secretion and (n=3) for cell viability. *p<0.05, **p<0.01, ***p<0.001 compared to glucose control.

Figure 4.10: Acute effect of OEA on insulin secretion and cell viability from clonal pancreatic BRIN-BD11 cells at 16.7 mM glucose.

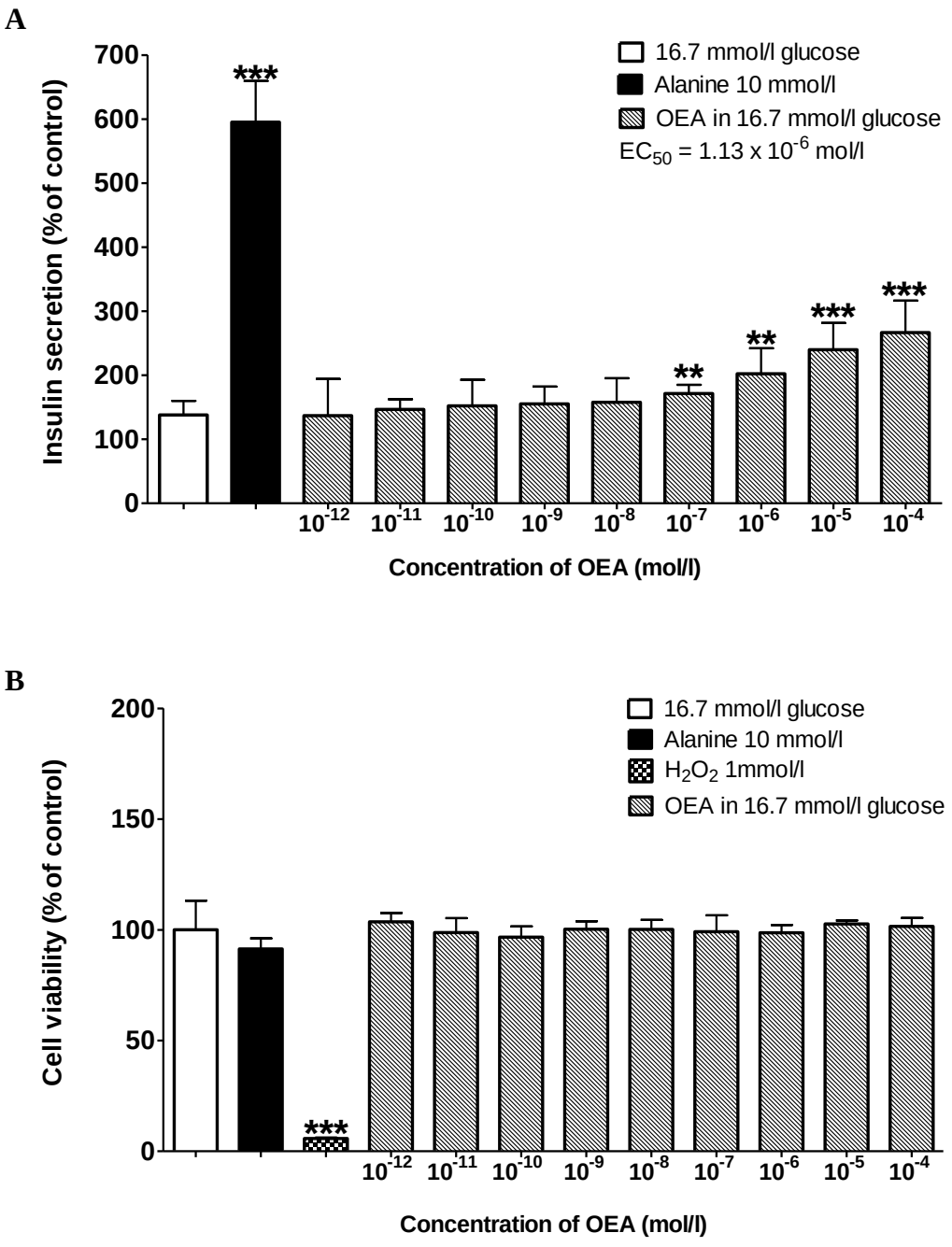

Acute effects of OEA (10^{-12}-10^{-4} M) and alanine (10 mM) on (A) insulin secretion and (B) cell viability (MTT) from clonal pancreatic BRIN-BD11 cells at 16.7 mM glucose. Results are the mean ± SEM (n=8) for insulin secretion and (n=3) for cell viability. **p<0.01, ***p<0.001 compared to glucose control.

Figure 4.11: Acute effect of Abn-CBD on insulin secretion from clonal human pancreatic 1.1B4 cells at 5.6 mM and 16.7 mM glucose.

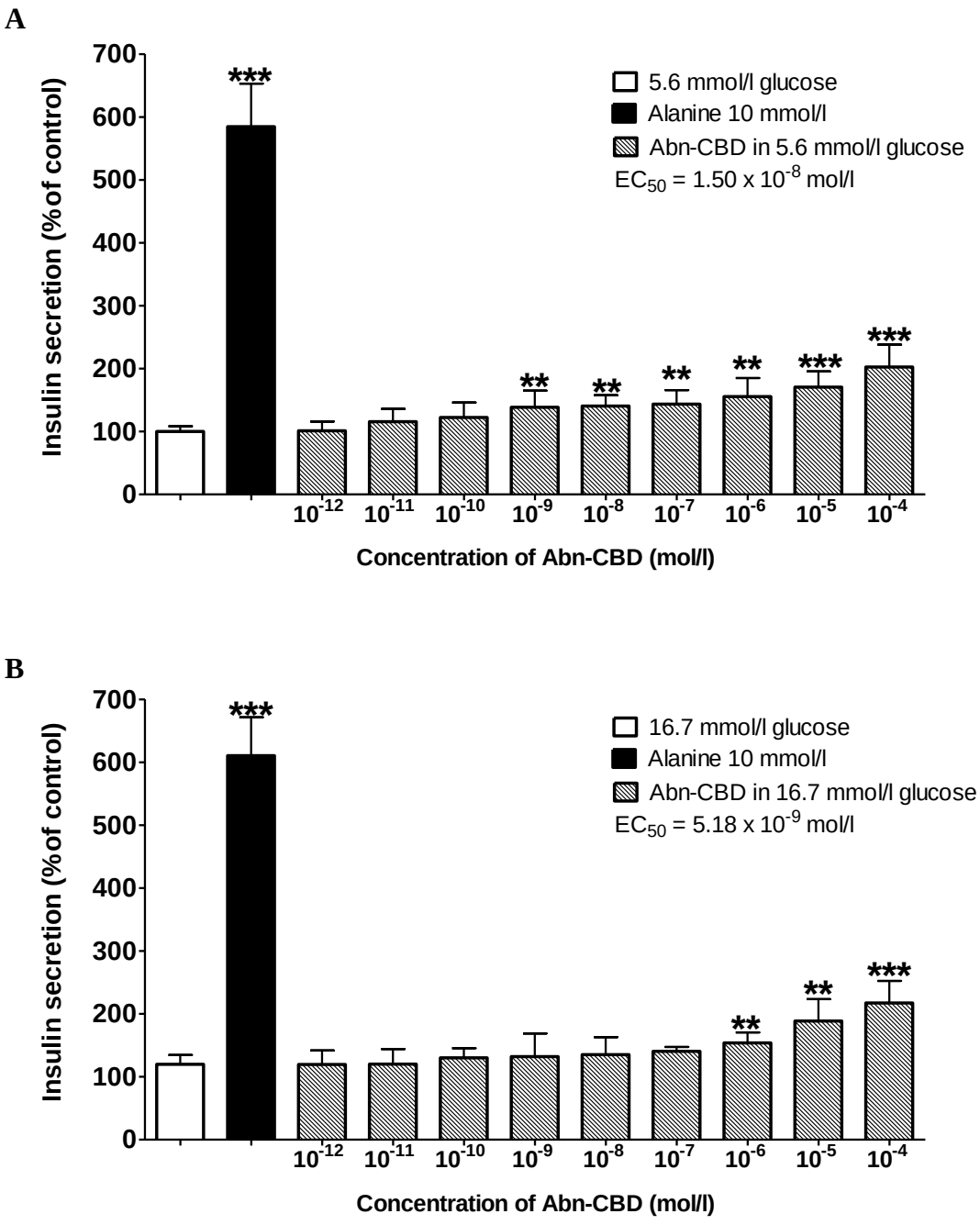

Acute effects of Abn-CBD (10^{-12}-10^{-4} M) and alanine (10 mM) on insulin secretion at (A) 5.6 mM and (B) 16.7 mM glucose from human pancreatic 1.1B4 cells. Results are the mean ± SEM (n=8) for insulin secretion. **p<0.01, ***p<0.001 compared to glucose control.

Figure 4.12: Acute effect of AM251 on insulin secretion from clonal human pancreatic 1.1B4 cells at 5.6 mM and 16.7 mM glucose.

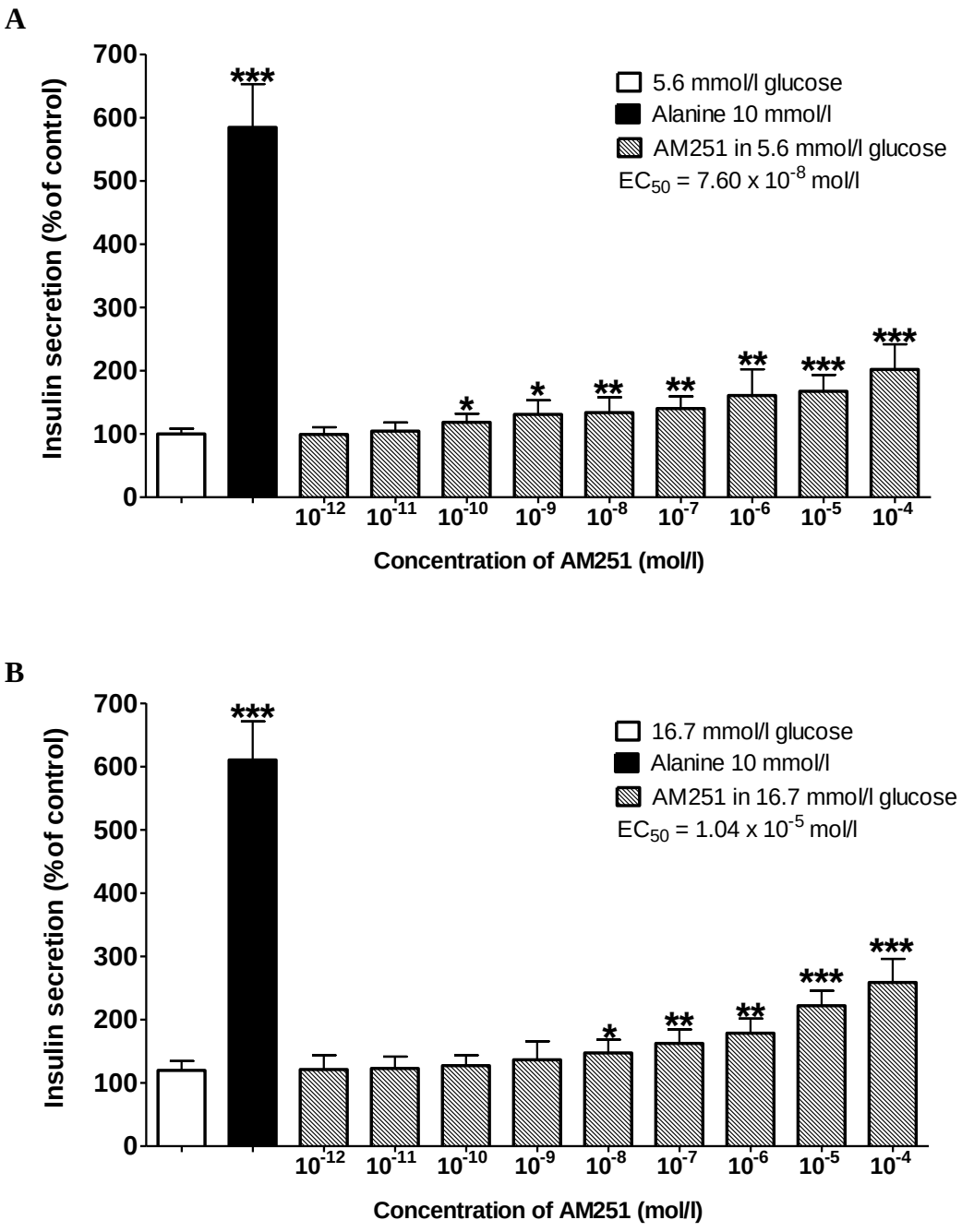

Acute effects of AM251 (10^{-12}-10^{-4} M) and alanine (10 mM) on insulin secretion at (A) 5.6 mM and (B) 16.7 mM glucose from human pancreatic 1.1B4 cells. Results are the mean ± SEM (n=8) for insulin secretion. *p<0.05, **p<0.01, ***p<0.001, compared to glucose control.

Figure 4.13: Immunocytochemistry staining of GPR55, insulin and DAPI nuclear stain in clonal pancreatic BRIN-BD11 cells.

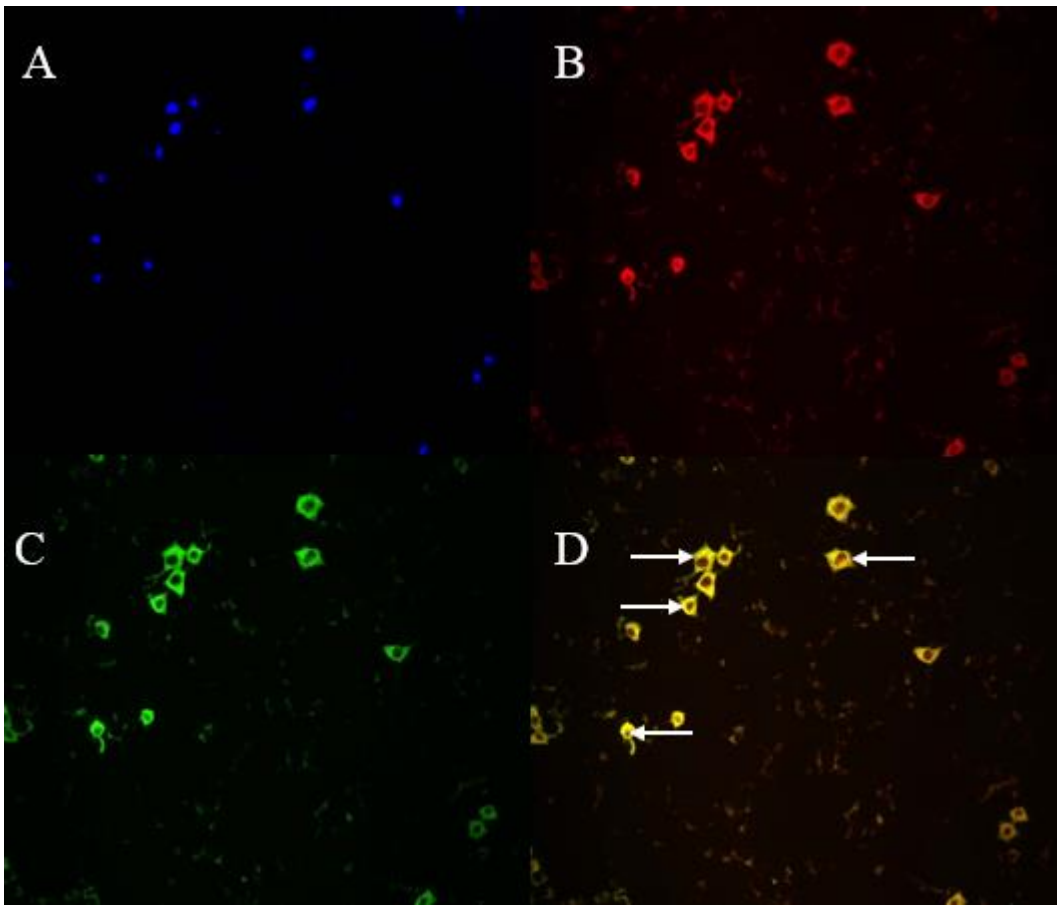

Expression and distribution of (A) DAPI, (B) insulin (C) GPR55 and (D) double antibody immunofluorescence of insulin and GPR55 at 40x magnification in clonal pancreatic BRIN-BD11 cells. Examples of co-localisation between GPR55 and insulin are indicated by white arrows.

Figure 4.14: Effect of Abn-CBD and AM251 on GPR55 mRNA and protein expression in clonal pancreatic BRIN-BD11 cells.

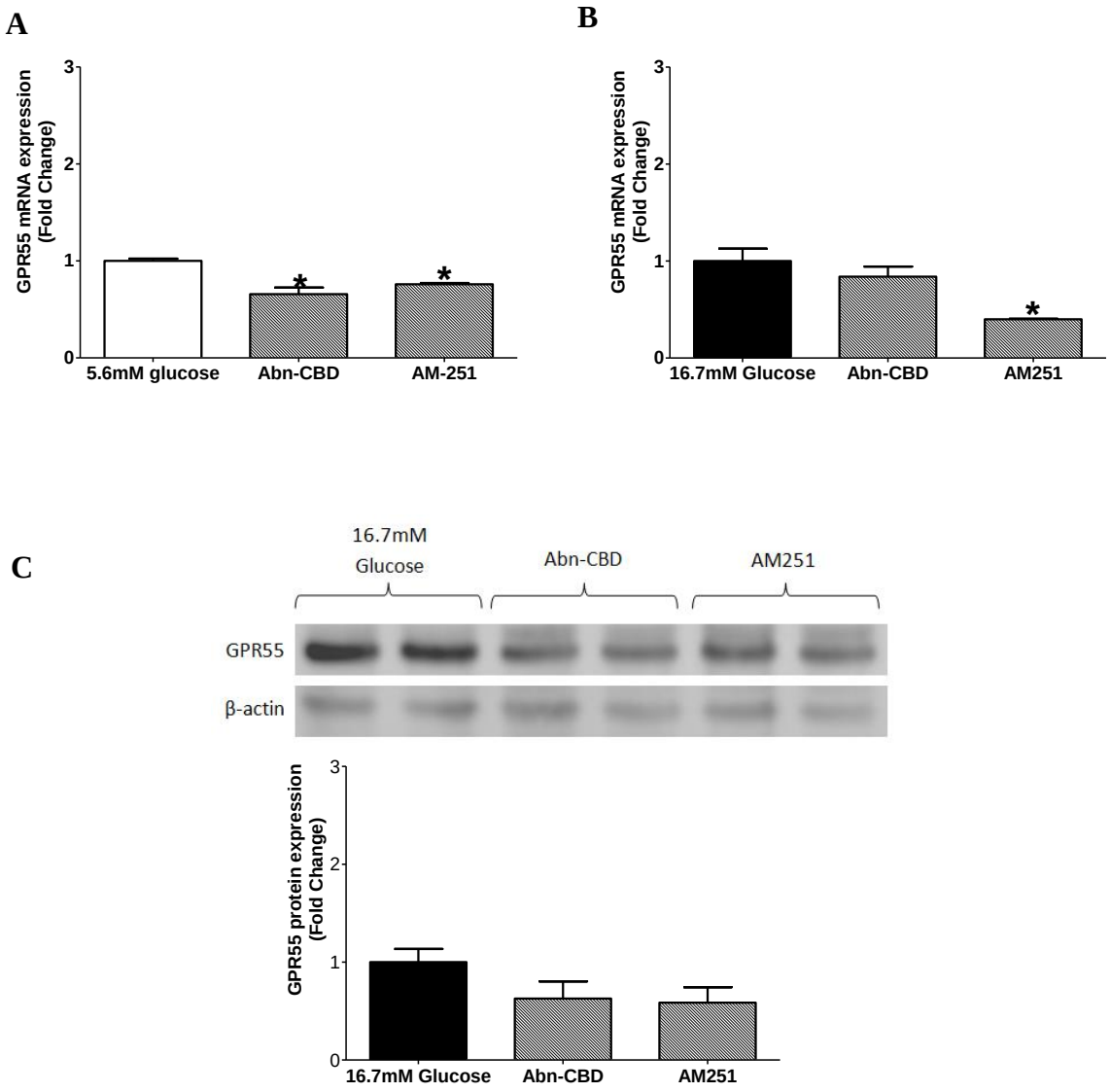

Effect of Abn-CBD (10^{-4} mol/l) and AM251 (10^{-4} mol/l) on GPR55 (A, B) mRNA and (C) protein expression in clonal pancreatic BRIN-BD11 cells after 4 h incubation at (A) 5.6 mM and (B, C) 16.7 mM glucose. Results are the mean ± SEM (n=3) for qPCR and (n=2) for western blotting. *$p<0.05$, compared to glucose control.

Figure 4.15: Effect of Abn-CBD and AM251 on insulin mRNA expression in clonal pancreatic BRIN-BD11 cells.

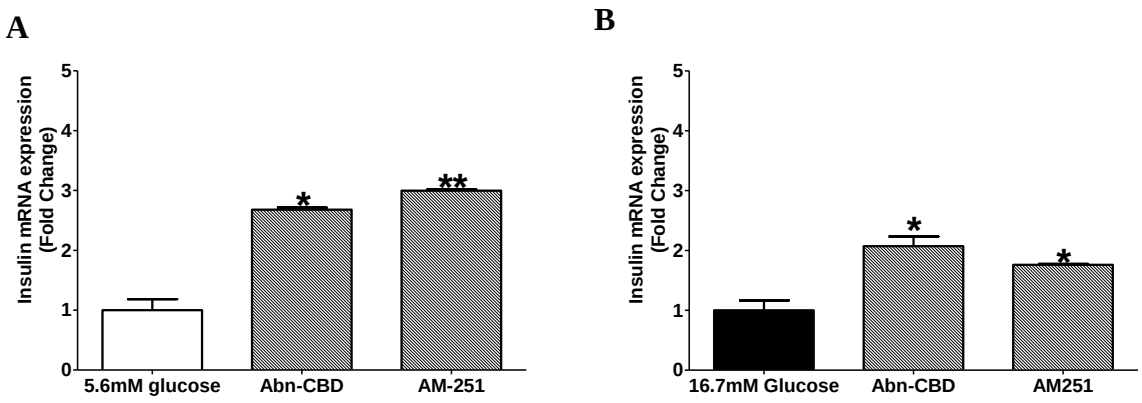

Effect of Abn-CBD (10^{-4} mol/l) and AM251 (10^{-4} mol/l) on insulin mRNA expression in clonal pancreatic BRIN-BD11 cells after 4 h incubation at (A) 5.6 mM and (B) 16.7 mM glucose. Results are the mean ± SEM (n=3) for qPCR and (n=2) for western blotting. *p<0.05, **p<0.01, compared to glucose control.

Figure 4.16: Effect of GPR55 agonists on intracellular Ca^{2+} modulation in clonal pancreatic BRIN-BD11 cells at 16.7 mM glucose.

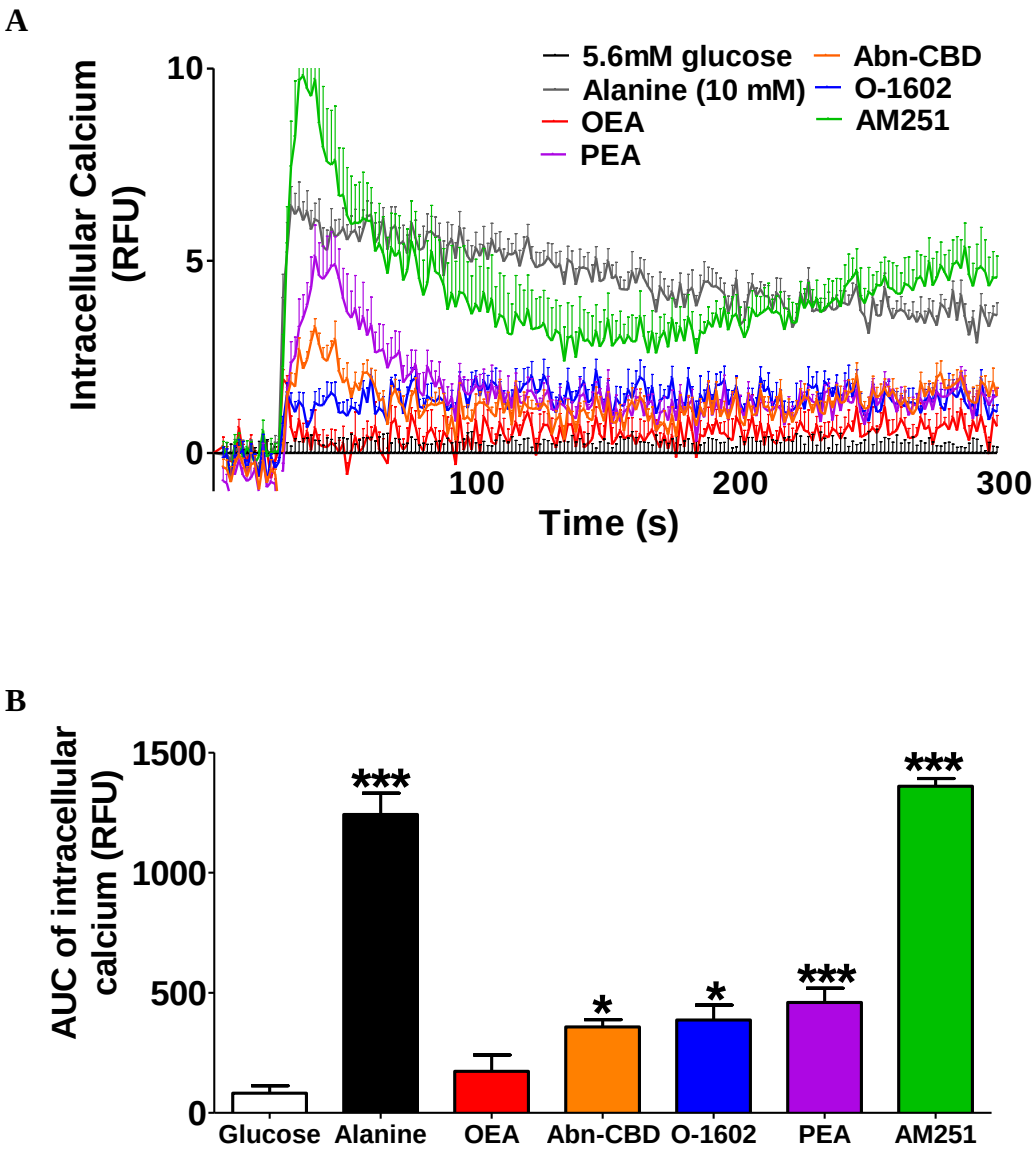

Effect of alanine and GPR55 agonists (OEA, Abn-CBD, O-1602, PEA, AM251) at 10^{-4} mol/l on intracellular Ca^{2+} modulation in clonal pancreatic BRIN-BD11 cells at 16.7 mmol/l glucose with (A) intracellular Ca^{2+} measurements (RFU) for 5 min and (B) corresponding AUC data. Results are the mean ± SEM *p<0.05, ***p<0.001, compared to glucose control.

Figure 4.17: Effect of GPR55 agonists on cAMP production in clonal pancreatic BRIN-BD11 cells at 16.7 mM glucose.

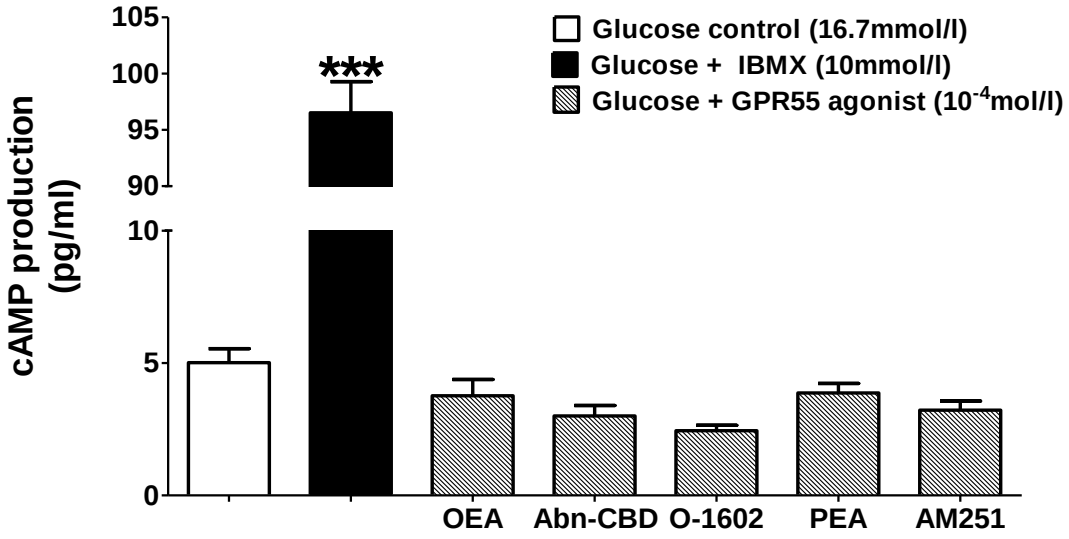

Effect of GPR55 agonists (OEA, Abn-CBD, O-1602, PEA, AM251) and IBMX on cAMP production in clonal pancreatic BRIN-BD11 cells at 16.7 mmol/l glucose. BRIN-BD11 cells were incubated with treatments for 20 min. Result are the mean SEM (n=3). ***p<0.001, compared to glucose control.

Figure 4.18: Western blotting demonstrating the effect of Abn-CBD, AM251, OEA and PMA on ERK1/2 (p44/42) signalling in clonal pancreatic BRIN-BD11 cells.

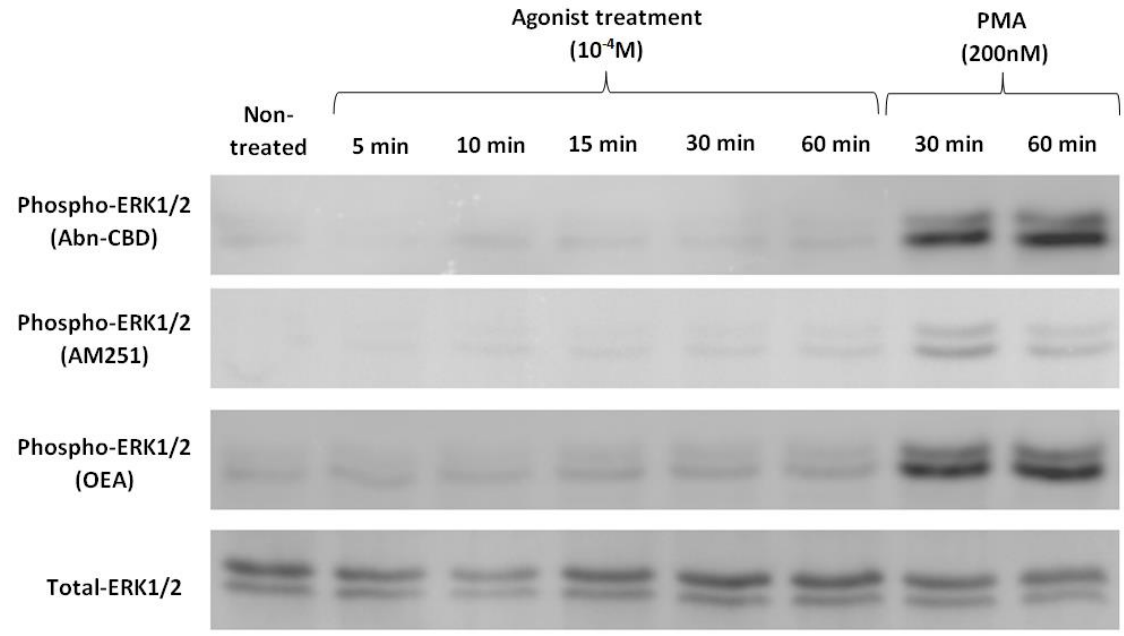

Effect of Abn-CBD (10^{-4} mol/l), AM251 (10^{-4} mol/l), OEA (10^{-4} mol/l) and PMA (200 nM) on ERK1/2 signalling in clonal pancreatic BRIN-BD11 cells at various timepoints (0, 5, 10, 15, 30, 60 min). Following incubation, cell lysates were separated via SDS-PAGE, then probed with antibodies for anti-p-ERK1/2 and anti-t-ERK1/2.

Figure 4.19: Flow cytometry demonstrating the effect of Abn-CBD, AM251, OEA and PMA on ERK1/2 (p44/42) signalling in clonal pancreatic BRIN-BD11 cells.

(A) Non-treated

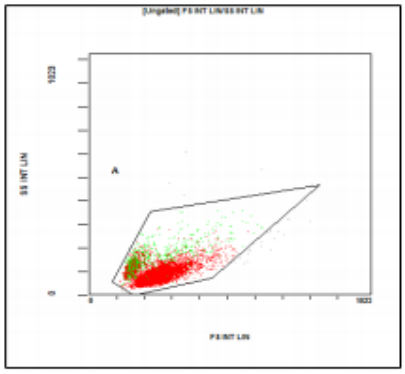

[Ungated] FS INT LIN/SS INT LIN

Region	Number	%Total	%Gated	X-Mean	Y-Mean
ALL	10096	100.00	100.00	243	87.8
A	10060	99.64	99.64	242	86.9

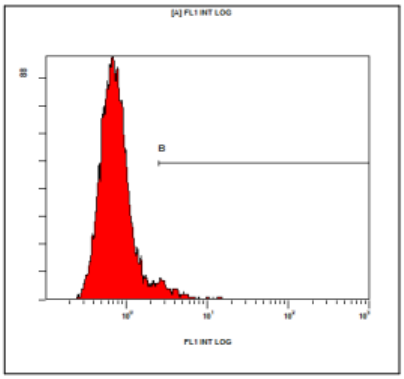

[A] FL1 INT LOG

Region	Number	%Total	%Gated	X-Mean	Y-Mean
ALL	10060	99.64	100.00	1.32	###
B	786	7.79	7.81	7.64	###

(B) PMA (200 nmol/l)

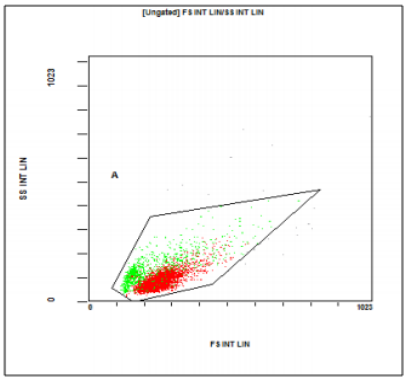

[Ungated] FS INT LIN/SS INT LIN

Region	Number	%Total	%Gated	X-Mean	Y-Mean
ALL	5531	100.00	100.00	249	91.5
A	5499	99.42	99.42	246	89.1

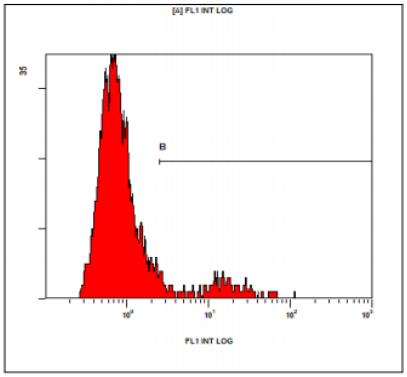

[A] FL1 INT LOG

Region	Number	%Total	%Gated	X-Mean	Y-Mean
ALL	5499	99.42	100.00	6.61	###
B	1094	19.78	19.89	29.8	###

(C) Abn-CBD (10^{-4} mol/l)

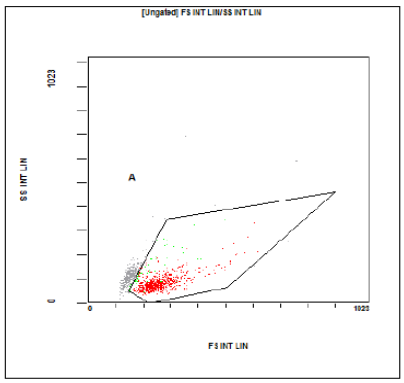

[Ungated] FS INT LIN/SS INT LIN

Region	Number	%Total	%Gated	X-Mean	Y-Mean
ALL	999	100.00	100.00	223	98.2
A	631	63.16	63.16	259	87.2

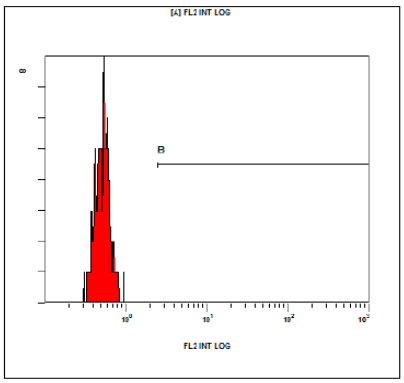

[A] FL2 INT LOG

Region	Number	%Total	%Gated	X-Mean	Y-Mean
ALL	631	63.16	100.00	1.11	###
B	55	5.51	8.72	6.14	###

(D) AM251 (10^{-4} mol/l)

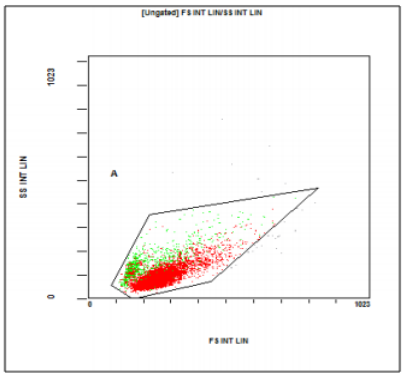

[Ungated] FS INT LIN/SS INT LIN					
Region	Number	%Total	%Gated	X-Mean	Y-Mean
ALL	9985	100.00	100.00	253	90.2
A	9949	99.64	99.64	251	89.1

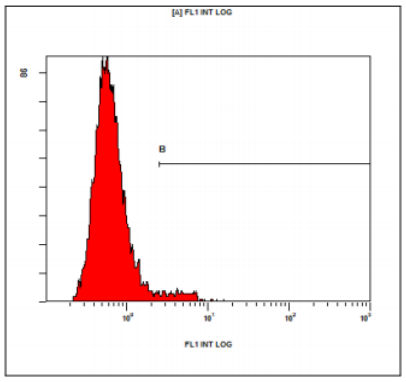

[A] FL1 INT LOG					
Region	Number	%Total	%Gated	X-Mean	Y-Mean
ALL	9949	99.64	100.00	1.33	###
B	773	7.74	7.77	8.99	###

(E) OEA (10^{-4} mol/l)

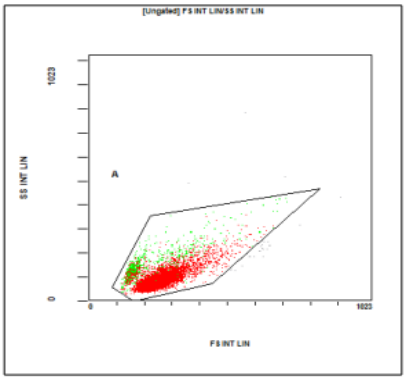

[Ungated] FS INT LIN/SS INT LIN					
Region	Number	%Total	%Gated	X-Mean	Y-Mean
ALL	8773	100.00	100.00	253	91.7
A	8747	99.70	99.70	252	91.2

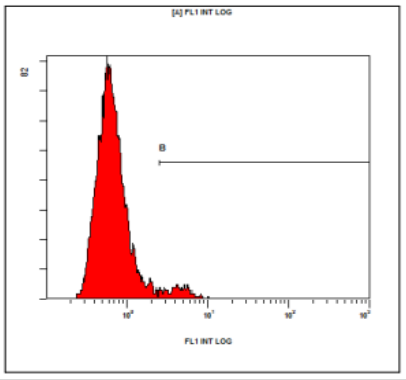

[A] FL1 INT LOG					
Region	Number	%Total	%Gated	X-Mean	Y-Mean
ALL	8747	99.70	100.00	1.15	###
B	685	7.81	7.83	6.33	###

(F)

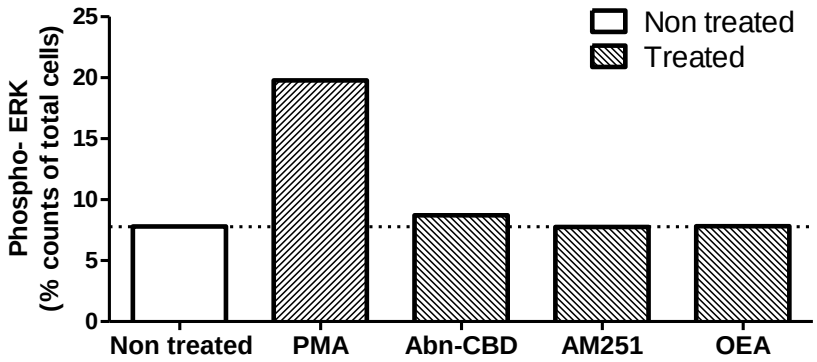

Effects of (B) PMA, (C) Abn-CBD, (D) AM251 and (E) OEA on ERK1/2 phosphorylation in clonal pancreatic BRIN-BD11 cells. After 15 min exposure, cells were probed with anti-phospho-ERK1/2 and anti-Alexa Fluor 488 antibodies, then gated for flow cytometry analysis.

Figure 4.20: Effect of GPR55 agonist Abn-CBD mitogen-activated protein kinase (MAPK) signalling in clonal pancreatic BRIN-BD11 cells.

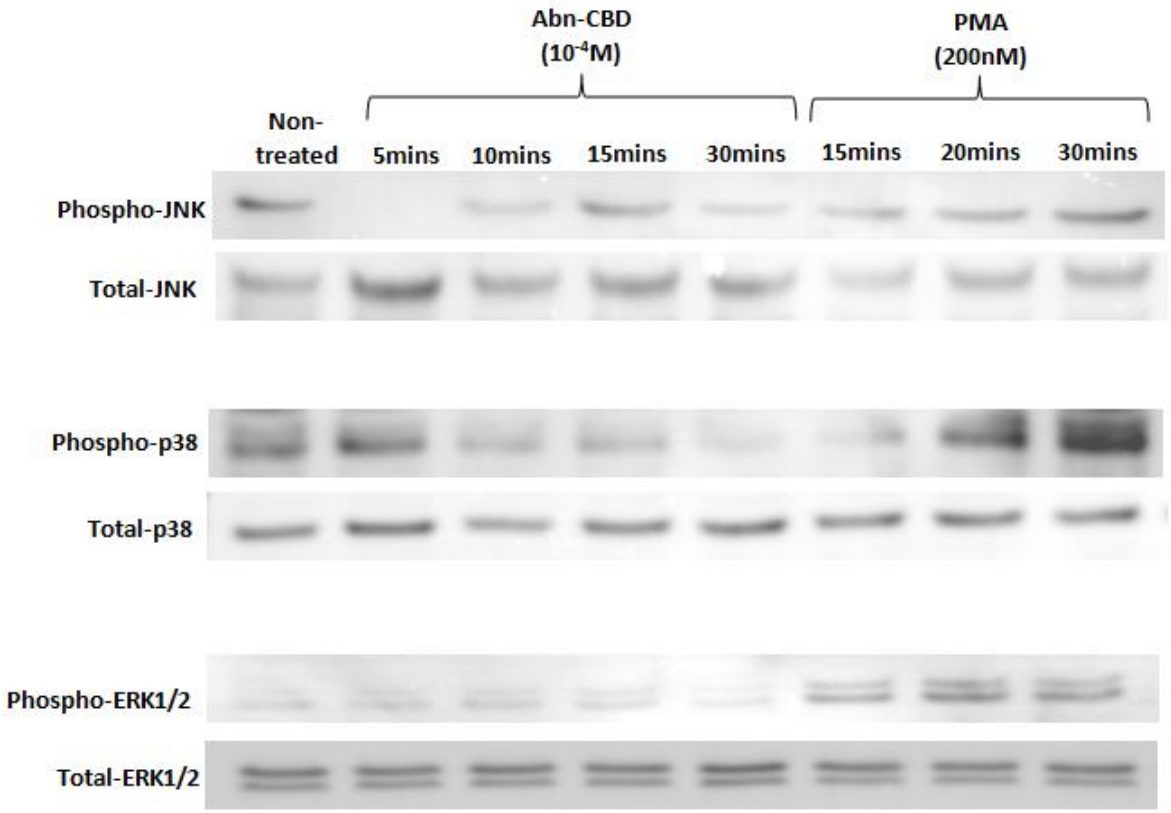

Effect of GPR55 agonist Abn-CBD (10^{-4} mol/l) and PMA (200 nM) on JNK, p38 and ERK1/2 (MAPK) signalling in clonal pancreatic BRIN-BD11 cells at various timepoints (0, 5, 10, 15, 30 min). Following incubation, cell lysates were separated via SDS-PAGE, then probed with antibodies for total and phosphorylated ERK1/2, p38 and JNK.

Figure 4.21: Effect of Abn-CBD, AM251 and O-1602 on clonal pancreatic BRIN-BD11 cell viability and apoptosis.

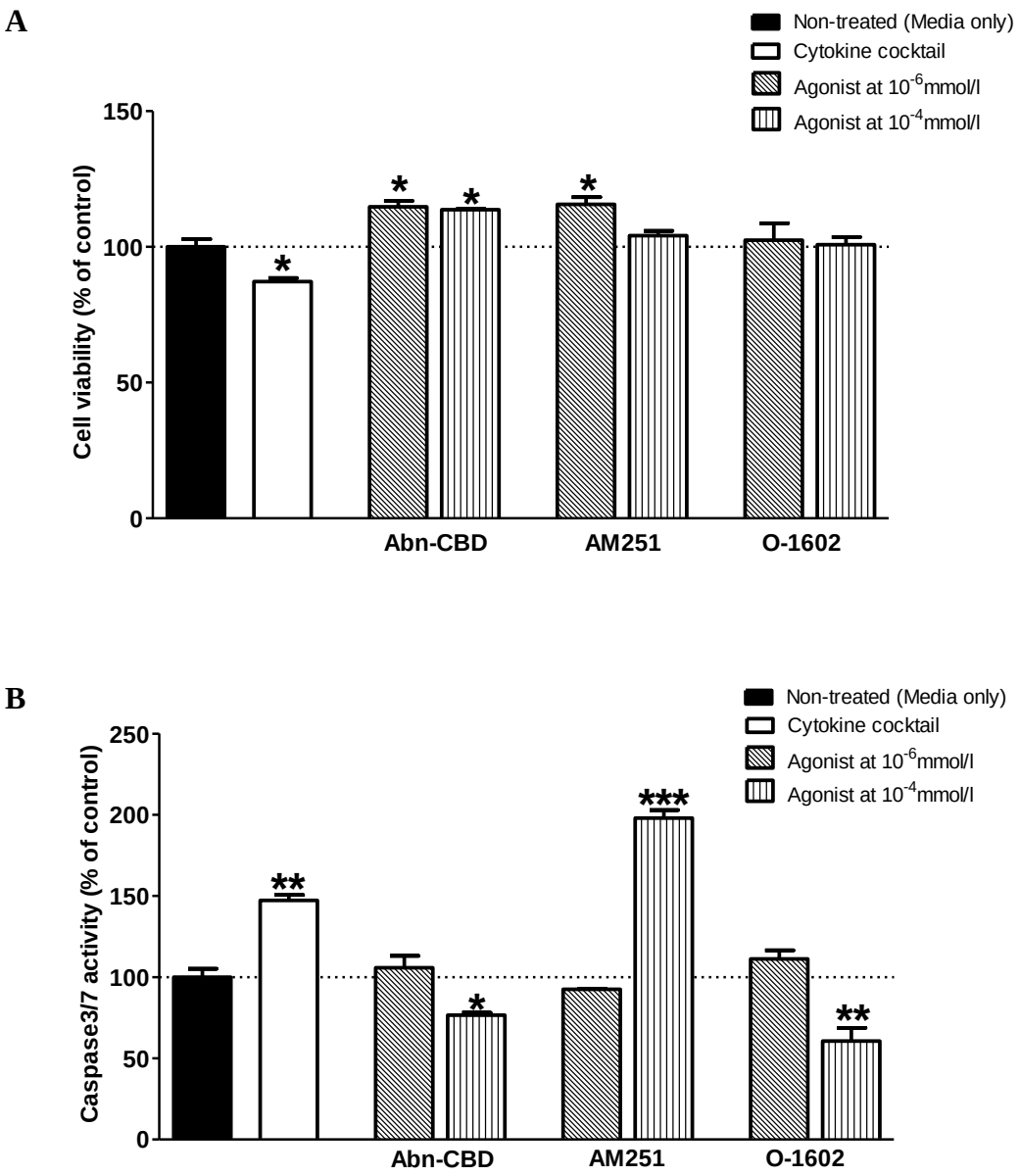

Effects of Abn-CBD, AM251 and O-1602 on clonal pancreatic BRIN-BD11 cell viability and apoptosis after 20 h incubation. Results determined with multiplex analysis; cell viability by protease activity, cell apoptosis by caspase 3/7 activity. Cytokine cocktail (TNF-α [200 U/ml], IFN-γ [20 U/ml], IL-1β [100 U/ml]) was used as a positive control. Results are the mean ± SEM (n=3). *p<0.05, **p<0.01, ***p<0.001, compared to non-treated control.

Figure 4.22: Effect of Abn-CBD, AM251 and O-1602 on clonal pancreatic α-TC1.9 cell proliferation and apoptosis

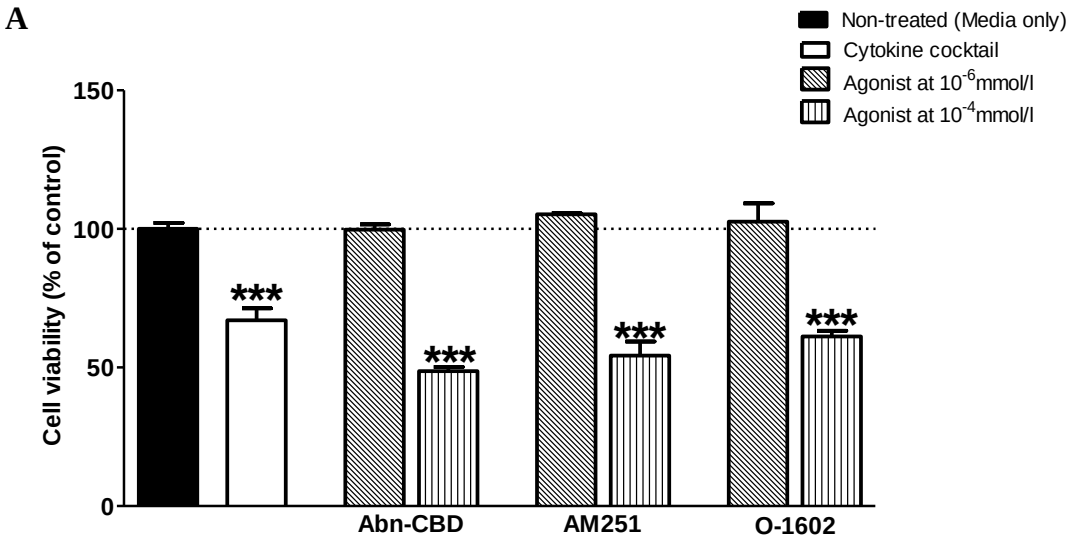

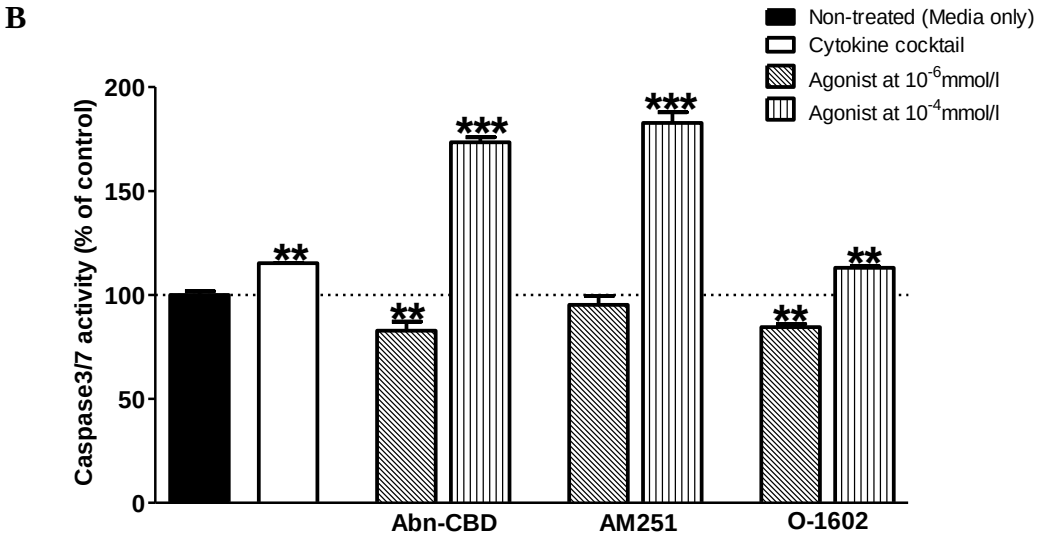

Effects of Abn-CBD, AM251 and O-1602 on clonal pancreatic α-TC1.9 cell viability and apoptosis after 20 h incubation. Results determined with multiplex analysis; cell viability by protease activity, cell apoptosis by caspase 3/7 activity. Cytokine cocktail (TNF-α [200 U/ml], IFN-γ [20 U/ml], IL-1β [100 U/ml]) was used as a positive control. Results are the mean ± SEM (n=3). **p<0.01, ***p<0.001, compared to non-treated control.

Chapter 5

Determining the specificity and pharmacological role of putative GPR55 and GPR120 agonists in islets using innovative CRISPR/Cas9 gene editing.

5.1: Summary

Long chain fatty acid (LCFA) sensing GPR55 and GPR120 are novel anti-diabetic targets which enhance beta cell function and insulin secretion. The specificity of many LCFA ligands acting through GPR55 and GPR120 remains elusive. The aim of this study is to assess metabolic functionality of GPR55/GPR120 agonists in beta cells using innovative CRISPR Cas9 gene editing to elucidate their importance in beta cell function.

Clonal GPR55 and GPR120 knockout insulin secreting beta cells derived from the rat BRIN-BD11 cell line were generated by CRISPR/Cas9 gene editing and used to investigate insulin secretion/expression and downstream receptor signalling (intracellular Ca^{2+} and cAMP).

Atypical (Abn-CBD, O-1602, AM251) and endogenous (PEA, OEA) endocannabinoid ligands (10^{-7}-10^{-4} M) stimulated insulin secretion ($p<0.05$-$p<0.001$) in wild type BRIN-BD11 cells, with 2-2.7-fold ($p<0.001$) increase demonstrated at the highest concentration tested (10^{-4} M). The insulinotropic effect of CBD and Rimonabant analogues Abn-CBD and AM251 was impaired by 42% ($p<0.05$) and 30% respectively in GPR55 knockout BRIN-BD11 cells at 10^{-4}M, with the secretory effect of O-1602 abolished altogether ($p<0.001$). The secretory effect of endogenous PEA was reduced by 53% ($p<0.05$), whilst OEA-induced insulin secretion was retained in GPR55 knockout cells. GPR55 ablation abolished release of intracellular Ca^{2+} upon treatment with O-1602, Abn-CBD and PEA at 10^{-4}M. No effect on cAMP production was observed upon agonist treatment in wild type and GPR55 knockout cells. While treatment of BRIN-BD11 cells with Abn-CBD and AM251 increased insulin mRNA expression at 5.6 mM glucose by 2.7-3-fold ($p<0.01$) and by 1.7-2-fold ($p<0.001$), respectively at 16.7 mM glucose, it was greatly diminished ($p<0.001$) in GPR55 null cells. Endogenous (ALA, DHA, EPA) and synthetic

(GW9508, GSK137647, Compound A) GPR120 agonists at 10^{-7}-10^{-4}M augmented insulin secretion ($p<0.05$-$p<0.001$) in wild type BRIN-BD11 cells, with DHA omitting the most potent effect (3.3 fold; $p<0.001$) at the highest concentration tested (10^{-4} M). At physiological concentrations of 10^{-6}M, the insulinotropic effect of ALA, DHA, GSK137647 and Compound A were abolished in GPR120 knockout BRIN-BD11 cells. The secretory effect of dual agonist GW9508 was reduced by 53% ($p<0.05$), whilst EPA-induced insulin secretion was retained in GPR120 knockout cells. GPR120 deletion abolished release of intracellular Ca^{2+} upon treatment with ALA, EPA, GSK137647 and Compound A at 10^{-4}M.

These findings demonstrate the specificity of several putative GPR55 and GPR120 agonists in the pancreatic beta cell, with Abn-CBD and ALA omitting the most potent and selective properties, respectively.

5.2: Introduction

Several long chain fatty acid (LCFA) receptors have recently been identified as novel therapeutic targets in the treatment of metabolic diseases, including GPR40, GPR41, GPR43, GPR120, GPR18, GPR55 and GPR119 (Lagerstrom & Schioth 2008, Moran *et al.* 2016, Tuduri *et al.* 2017). In particular, current research is now directed towards the biological actions of the novel endocannabinoid receptor GPR55 and long chain fatty acid sensing GPR120 (McKillop *et al.* 2013, Moran *et al.* 2014). Although the specificity of many LCFA ligands remains poorly understood (Stewart *et al.* 2006), the use of specific agonists is essential to accurately characterise the functionality of novel receptors.

The novel endocannabinoid receptor GPR55 is highly expressed in the intestines, endocrine-pancreas, peripheral tissue, brain and central nervous system of the human body (Sawzdargo *et al.* 1999, Ryberg *et al.* 2009, McKillop *et al.* 2013). Upon activation, GPR55 has been shown to demonstrate a wide range of biological effects in the pancreatic islet, including enhanced insulin release and beta cell regeneration (Chapter 4). The insulinotropic effects of some putative GPR55 agonists were diminished upon GPR55 antagonism with cannabidiol (CBD), however, potential synergistic activity and antagonist selectivity may have influenced the findings observed (Chapter 4, McKillop *et al.* 2013).

Studies evaluating the effects of global receptor deletion using GPR55 knockout mice reported a mild impairment in glucose homeostasis, with no effect on glucose stimulated insulin secretion (GSIS) (Tuduri *et al.* 2017). Recently, another study using isolated islets from wild type and GPR55 knockout mice reported that the synthetic agonist O-1602 augmented intracellular Ca^{2+} and insulin secretion, with effects diminished in GPR55 deficient islets, thus demonstrating that the atypical cannabinoids can have a direct effect in the pancreatic islet through GPR55-dependent signalling (Liu *et al.* 2016). In contrast, the cannabinoid agonist Abn-CBD stimulated insulin release from both wild type and GPR55 knockout mouse islets, indicating a GPR55-independent mechanism of action (Ruz-Maldonado *et al.* 2018). However, the same report demonstrated that the positive effects of Abn-CBD treatment on beta cell proliferation were diminished in GPR55 knockout islets, which indicates that Abn-CBD has a GPR55-mediated function in the pancreatic islet (Ruz-Maldonado *et al.* 2018).

At present, the specificity of endogenous endocannabinoids and synthetic cannabinoid ligands towards GPR55 remains unknown as many may also target other novel endocannabinoid receptors, GPR18 and GPR119 (Moran *et al.* 2014, Henstridge *et al.*

2011). Even though GPR18 and GPR119 are linked with the endocannabinoid system, they are still considered orphan receptors as their respective endogenous agonists remain unknown (Henstridge *et al.* 2011).

LCFA sensing GPCRs have been shown to regulate glucose homeostasis upon activation with a range of endogenous and synthetic agonists (Moran *et al.* 2014). In particular, the structurally related GPR40 and GPR120 receptors have been shown to exhibit therapeutic effectiveness for the treatment of type 2 diabetes, with the GPR40 agonist Fasiglifam (TAK-875) recently undertaking stage 3 clinical trials (Marcinak *et al.* 2017).

GPR120 is highly expressed in the pancreatic islet and augments insulin release and beta cell proliferation in pancreatic beta cells through a series of downstream Gαq signalling, including intracellular Ca^{2+} and ERK1/2 (Chapter 3). Recently, chemically synthesised agonists (GSK137647, Compound A) have become commercially available for the selective activation of GPR120 and have also demonstrated insulinotropic and proliferative effects in clonal beta cells (Sparks *et al.* 2014, Oh *et al.* 2014). The secretory effects observed by a range of GPR120 agonists were greatly diminished in the presence of the high affinity GPR120 antagonist (AH7614) (Chapter 3). Although, this range of experimentation is highly dependent on ligand binding affinity and the total biological function of the antagonist.

Endogenous GPR120 omega-3 fatty acid agonists (ALA, DHA, EPA) have been shown to demonstrate a range of biological activity in the maintenance of glucose and lipid homeostasis, however, the specificity of these molecules remains elusive as many have been shown to activate both GPR120 and GPR40 receptors (Bradberry & Hilleman 2013, Moran *et al.* 2014, Hauge *et al.* 2014). Receptor binding studies have demonstrated GPR120 activation with endogenous ALA and DHA in human HEK293 cells. In addition,

these molecules were shown to phosphorylate both isoforms of human GPR120 (Burns & Moniri 2010).

Although numerous studies using knockout mice and receptor antagonists have been performed, the specificity of many putative GPR55 and GPR120 agonists in the pancreatic beta cell remains poorly understood (Liu *et al.* 2016, Houthuijzen 2016). CRISPR/Cas9 gene editing has emerged as a revolutionary gene editing tool that can be employed to disrupt gene transcription and mediate protein deletion, including receptor knockout (Ran *et al.* 2013).

Previously, Naylor *et al.* utilised CRISPR/Cas9 to develop clonal GLP-1 and GIP knockout pancreatic beta cells using the INS-1 832/13 cell line (Naylor *et al.* 2016). Surpassing the capabilities of antagonist binding, these knockout cell lines were used to accurately characterise the functionality and specificity of dual GLP-1/GIP peptides (Naylor *et al.* 2016). Using a similar approach, CRISPR/Cas9 induced deletion of GPR55 and GPR120 greatly contributes to the effective characterisation of the respective receptors within in the pancreatic beta cell.

Numerous methods of gene disruption are available to alter receptor expression, including siRNA, TALEN, RNAi and shRNA (Rao *et al.* 2009, Boettcher & McManus 2015). The major advantage of CRISPR/Cas9 is its ability to generate complete gene knockout rather than gene knockdown, which enables absolute characterisation of a given gene. In addition, CRISPR/Cas9 is the highly favoured method for generating a clonal knockout cell line due to its specificity, efficiency and target design simplicity (Ran *et al.* 2013, Boettcher & McManus 2015). To characterise the role of a receptor in a specific cell type (i.e. beta cell), the development of a clonal knockout cell line is preferred as use of tissues from knockout mice is greatly complicated by induction of complimentary compensatory pathways (Barbaric *et al*. 2007, Ran *et al.* 2013).

The present study, for the first time, has investigated the specificity and downstream signalling of numerous putative GPR55 and GPR120 agonists using wild type and receptor knockout beta cells generated by CRISPR/Cas9 gene editing.

5.3: Materials and methods

5.3.1: Materials

Rabbit anti-GPR55 polyclonal antibody was purchased from Cayman chemical (Michigan, USA) and Rabbit anti-GPR120 from Santa Cruz (Santa Cruz, UK). pSpCas9(BB)-2A-Puro (PX459) V2.0 and pSpCas9(BB)-2A-GFP (PX458) were gifts from Feng Zhang (Addgene plasmids; #62988, #48138).

5.3.2: Constructs

The *S.pyogenes* Cas9 vector plasmid used for the dual luciferase assay was pSpCas9(BB)-2A-Puro (PX459) V2.0. The *S. pyogenes* Cas9 vector plasmid used for FACS sorting was pSpCas9(BB)-2A-GFP (PX458), both plasmids were a gift from Feng Zhang (Broad Institute, MIT; Addgene plasmid #62988). sgRNA specific to GPR55 and GPR120 was designed incorporating the start codon at position 5-8 and 3-6 in the respective guide sequences, hereafter named sgGPR55 and sgGPR120. Guide sequences were cloned into the respective plasmids following a published protocol (Ran *et al*. 2013). briefly, pSpCas9(BB)-2A-Puro and pSpCas9(BB)-2A-GFP were digested with BbsI (NEB, US) and the following oligos, 5′-CACCGGAACATGAGTCAGCTAGACA-3′, 5′-AAACCTTGTACTCAGTCGATCTGTC-3′ for sgGPR55 and 5′-CACCG

CGCACACTCAGGGGACATGC-3′, 5′-AAACGCATGTCCCCTGAGTGTGCGC-3′ for sgGPR120 (Life Technologies, UK), were annealed and ligated into the digested plasmids. To assess Cas9 cleavage efficiency directed by sgGPR55/sgGPR120, a firefly luciferase expression plasmid with a 50bp insert of GPR55/GPR120 sequence encoding the target site were inserted into psiTEST-LUC-Target (York Bioscience Ltd, York, UK), hereafter named as GPR55WT-Luc and GPR120WT-Luc. An expression construct for *Renilla* luciferase (pRL-CMV, Promega, Southampton, UK) was used for the dual-luciferase assay to normalize transfection efficiency.

5.3.3: Dual-luciferase assay

A dual-luciferase assay was used to determine cleavage efficiency of the Cas9-sgGPR55 and Cas9-sgGPR120 expression constructs, using methods previously described (Allen *et al*. 2013, Courtney *et al*. 2014, Atkinson *et al*. 2011). HEK AD293 cells (Life Technologies, UK) were transfected using Lipofectamine 3000 (Life Technologies, UK); the GPR55WT-Luc and GPR120WT-Luc expression constructs were co-transfected with either sgNSC, sgGPR55 or sgGPR120 constructs and a *Renilla* luciferase expression plasmid. Cells were incubated for 72 h before being lysed and the activities of both *Firefly* and *Renilla* luciferase quantified.

5.3.4: Construct transfection and FACS sorting

Wild type insulin secreting BRIN-BD11 cells were transfected with the plasmid co-expressing Cas9, sgGPR55/sgGPR120 and GFP using Lipofectamine 3000 following manufactures recommended protocol. The generation, characteristics and culture of these cells have been previously described (McClenaghan *et al.* 1996). 72 h post-transfection,

cells were detached with trypsin/EDTA and resuspended in sterile PBS. Flow cytometry was employed to detect and FACS sort the cells expressing GFP. Cells emitting the top 1% of FITC-A GFP expression were isolated into single cell populations in a 96-well plate and allowed to expand under normal culture conditions for 3 weeks to form colonies.

5.3.5: Sequencing and determination of GPR55/GPR120 knockout

Upon clonal expansion, gDNA was extracted using DNA extraction kit (Qiagen, UK). Individual samples were then subjected to PCR amplification using the following primers to amplify the targeted region: 5′-AGCCCCTCGTTCTGTGTTTA-3′, 5′-AGGAGGAAGGTGGGAATGTG-3′ for GPR55 and 5′-CAGTGTTGCCAGGCACTT-3′, 5′- GCGGAACAAGATGCAGAGG-3′ for sgGPR120. PCR products were gel purified and ligated into the CloneJet cloning vector (Life Technologies, UK), then transformed into competent DH5α cells (Life Technologies, UK). DNA from 40-50 BRIN-BD11 cell clones were prepared using a plasmid miniprep kit (Life Technologies, UK) following manufacturer's protocol. Isolated DNA was then sequenced (Department of Biochemistry, University of Cambridge) using the forward PCR amplification primer.

5.3.6: Insulin secretion from BRIN-BD11 cells

Wild type, GPR55 and GPR120 knockout BRIN-BD11 cells were used. In brief, cells were seeded (150, 000 cells per well) into 24-well plates and allowed to attach overnight. Following a 40 min pre-incubation (1.1 mmol/l glucose), cells were incubated (20 min; 37^{o}C) in KRB buffer with established stimulators of beta cell function and GPR55/GPR120 agonists (10^{-7}-10^{-4} mol/l). Supernatants were removed, then frozen at -20^{o}C until determination of insulin by radioimmunoassay (Flatt & Bailey 1981).

5.3.7: Determination of cAMP production in pancreatic BRIN-BD11 cells

BRIN-BD11 cells were sub-cultured and seeded into 6-well plates at a density of 1,000,000 cells per well, then supplemented with 2 ml of RPMI media and allowed to attach overnight, as outlined in Section 2.1.2. Cells were pre-incubated with 1.1 mmol/l glucose for 40 min at 37ºC. Agonist test solutions (10^{-4} mol/l) and GLP-1 (10 mmol/l) were prepared in KRBB buffer at 16.7 mmol/l glucose and assessed for cAMP production. After incubation, cells were lysed and cAMP detected with the cAMP ELISA kit as previously described in Section 2.4.2.

5.3.8: Intracellular Ca^{2+} measurement

BRIN-BD11 cells were sub-cultured and seeded into 24-well plates at a density of 80,000 cells per well, then supplemented with 1 ml of RPMI media and cultured overnight, as outlined in Section 2.1.2. Alanine (10 mmol/l) and GPR55 agonists (Abn-CBD, AM251, O-1602, OEA, PEA) at 10^{-4} mol/l were added to KRBB buffer, supplemented with 16.7 mmol/l glucose. The assay plate was pre-incubated with the test dye prepared in KRBB and 50µl of the test solutions were transferred to the plate with fluorescence intensity measured for 5 min using the FlexStation 3 plate reader (Section 2.3.2) (Molecular Devices, San Diego, CA, USA).

5.3.9: Gene expression analysis by qPCR

mRNA was extracted from wild type and GPR55 knockout BRIN-BD11 cells following exposure to agonist treatment for 4 h using the RNeasy Mini kit adhering to manufacturer's protocol (Qiagen, UK). Isolated mRNA (3 µg) was converted to cDNA using SuperScript II Reserve Transcriptase (Life Technologies, UK). SYBR green

amplification parameters for GPR55, GLP-1R and GIPR were set at 95^{o}C for denaturation, 58^{o}C for primer annealing and 72^{o}C for elongation for a total of 40 cycles, followed with melting curve analysis, with temperature range set at 60^{o}C to 90^{o}C. Values were analysed using the Livak 2(-Delta C(T)) method (Livak & Schmittgen 2001) and normalised to *Gapdh* expression.

5.3.10: Protein expression using western blotting

Wild type, GPR55 and GPR120 knockout BRIN-BD11 cells were seeded at a density of 1 x 10^{6} cells per well in 6-well plates and allowed to attach overnight. Total protein was extracted at 4^{o}C for 10 min using RIPA buffer containing 150 mM NaCl, 1.0% Nonidet P-40, 0.5% sodium deoxycholate, 0.1% SDS, 50 mM Tris HCl, pH 7.6 and protease inhibitor cocktail (Sigma, UK). Total protein concentration was determined using Bradford reagent (Sigma, UK). Equal amounts of protein were aliquoted with Laemmli buffer (1µg/µl), then heated at 95^{o}C for 10 min. Samples (25µg per well) were loaded onto pre-cast gels (NUPAGE 4–12 % Bis–Tris gels, Invitrogen, UK) and subjected to SDS-PAGE (70V, 90 min). After transfer to nitrocellulose membrane for 16 h at 90mA, membranes were blocked with 5% skimmed milk and probed with rabbit anti-GPR55 (1:150) (Cayman Chemical, US), rabbit anti-GPR120 (1:150) (Santa Cruz, UK) or mouse anti-β-actin (1:2500) (Cell Signalling, US). Membranes were probed with ECL horseradish peroxidase donkey anti-rabbit IgG/ECL horseradish peroxidase sheep anti-mouse IgG (1:10000) (GE Healthcare, UK) and detected using Luminata Forte HRP substrate (Millipore, UK), with images captured using the G:BOX Chemi XX9 imager (Syngene, UK). Data were normalised to β-actin and presented relative to untreated control.

5.4: Results

5.4.1: Development of a GPR55 null BRIN-BD11 cell line using CRISPR/Cas9 gene editing

The CRISPR/Cas9 construct (px458) used co-expresses GFP, which was utilised to select the cells which had been successfully transfected (Fig. 5.1A). A sgRNA was designed to target 1bp upstream of the GPR55 start codon to induce gene disruption by non-homologous end joining (NHEJ); the sgRNA was targeted early in the transcript, encompassing the ATG start codon at position 5-8 in the guide sequence and is referred to as sgGPR55 (Fig. 5.1A, B). sgGPR55 was shown to have good cleavage efficiency, resulting in a 60% reduction in firefly luciferase activity ($p<0.001$), when assessed with a dual luciferase assay (Fig. 5.1C).

Post-transfection (72h) with the Cas9-sgGPR55-GFP expression construct, cells emitting the top 1% of GFP expression were single cell sorted by FACS, followed by clonal expansion (Fig. 5.2).

To determine which cells had bi-allelic indels, individual PCR products from clonal cell populations were sequenced; for clone 2 sequence analysis revealed a 29 and 33 nucleotide deletion on allele 1 and allele 2 respectively (Fig. 5.3A). In addition, a 2-nucleotide insertion mutation was present on allele 2 (Fig. 5.3A). This indicates a bi-allelic deletion of the GPR55 start codon was present in this cell line that would be predicted to abolish expression of GPR55 protein (Fig. 5.3B).

GPR55 mRNA expression was ablated in GPR55 knockout BRIN-BD11 cells, compared to wild type cells (Fig. 5.4A). Incretin receptor mRNA expression (GLP-1 R and GIP R) were unaffected in the GPR55 knockout cell line, compared to wild type cells (Fig. 4A).

Western blotting demonstrated the absence of GPR55 protein in the GPR55 null cell line, whilst GPR55 protein was demonstrated in wild type cells (Fig. 5.4B). Both wild type ($p<0.05$) and GPR55 knockout ($p<0.05$) BRIN-BD11 cells demonstrated glucose stimulated insulin secretion (GSIS) at 16.7 mM glucose (Fig. 5.4C). Wild type and GPR55 knockout BRIN-BD11 cells also demonstrated identical insulin secretory responses ($p<0.001$) to a wide range of insulinotropic modulators (Fig. 5.4C).

5.4.2: Effects of GPR55 agonists on insulin secretion from wild type and GPR55 knockout BRIN-BD11 cells

The insulinotropic capabilities and specificity of a range of putative GPR55 agonists were assessed using wild type and GPR55 knockout BRIN-BD11 cells. At 16.7 mM glucose, a synthetic CBD analogue (Abn-CBD) augmented insulin secretion at 10^{-7}-10^{-4}M by 0.8-2.7-fold ($p<0.05$-$p<0.001$) in wild type BRIN-BD11 cells (Fig. 5.5A). The secretory response of Abn-CBD was significantly impaired at 10^{-5}-10^{-4}M ($p<0.05$) in GPR55 knockout BRIN-BD11 cells, with a 42% ($p<0.05$) reduction demonstrated at the highest agonist concentration (10^{-4} M) (Fig. 5.5A).

Rimonabant analogue (AM251) stimulated insulin secretion at 10^{-7}-10^{-4}M by 0.3-2.1-fold ($p<0.05$-$p<0.001$) in wild type BRIN-BD11 cells (Fig. 5.5B). AM251-induced insulin secretion was reduced by 30% at 10^{-4}M in GPR55 knockout BRIN-BD11 cells (Fig. 5.5B). Synthetic CBD analogue (O-1602) induced insulin secretion at 10^{-7}-10^{-4}M by 0.6-2.7-fold ($p<0.05$-$p<0.001$) in wild type BRIN-BD11 cells (Fig. 5.6A). The insulinotropic effect of O-1602 was abolished at 10^{-7}-10^{-4}M in GPR55 knockout BRIN-BD11 cells. At the highest agonist concentration (10^{-4} M), an 85% ($p<0.001$) reduction in insulin secretion was observed between wild type and GPR55 knockout cells (Fig. 5.6A).

Endogenous endocannabinoid PEA (10^{-7}-10^{-4} M) augmented insulin secretion by 0.6-2.0-fold ($p<0.01$-$p<0.001$) from wild type BRIN-BD11 cells (Fig. 5.6B). The insulinotropic response of PEA at the highest concentration (10^{-4} M) was impaired by 53% ($p<0.05$) in GPR55 knockout cells (Fig. 5.6B). Endogenous OEA (10^{-7}-10^{-4} M) induced insulin secretion by 0.7-2.2-fold from wild type BRIN-BD11 cells (Fig. 5.7). When assessed in GPR55 knockout cells, the insulinotropic response of OEA was retained at all concentrations tested (Fig. 5.7).

5.4.3: Effects of GPR55 agonists on intracellular Ca^{2+} and cAMP in wild type and GPR55 knockout BRIN-BD11 cells

Exposure of wild type BRIN-BD11 cells to AM251, PEA, O-1602 and Abn-CBD at 10^{-4}M induced a prompt increase in intracellular Ca^{2+} concentrations ($p<0.05$-$p<0.001$) (Fig. 5.8A). Using AUC data, AM251 demonstrated the most potent effect, with a 17-fold increase observed, compared to 5.6 mM glucose alone (Fig. 5.8B). Increases in intracellular Ca^{2+} mediated by PEA, O-1602 and Abn-CBD were abolished when assessed in GPR55 knockout BRIN-BD11 cells, whilst the effect of AM251 was reduced by 43% (Fig. 5.9A, B). None of the agonists affected cAMP production in either wild type nor GPR55 knockout BRIN-BD11 cells (Fig. 5.10).

5.4.4: Effects of GPR55 agonists on insulin mRNA expression in wild type and GPR55 knockout BRIN-BD11 cells

Culture of cells for 4 h with atypical cannabinoid GPR55 agonists Abn-CBD and AM251 induced a 2.8-3.0-fold ($p<0.05$-$p<0.01$) increase of insulin mRNA expression in wild type BRIN-BD11 cells at 5.6 mM glucose, whilst a 1.8-2.1-fold ($p<0.05$) was demonstrated at

16.7 mM glucose (Fig. 5.11A, B). In contrast, incubation Abn-CBD and AM251 greatly diminished ($p<0.001$) insulin mRNA expression in GPR55 KO cells at both 5.6 mM and 16.7 mM glucose (Fig. 5.11C, D).

5.4.5: Development of GPR120 null BRIN-BD11 clonal cell lines using CRISPR/Cas9 gene editing

The CRISPR/Cas9 construct (px458) used co-expresses GFP, which was utilised to select the cells which had been successfully transfected (Fig. 5.12A). A sgRNA was designed to target 1bp downstream of the GPR120 start codon to induce gene disruption by non-homologous end joining (NHEJ); the sgRNA was targeted within the transcript, encompassing the ATG start codon at position 3-6 in the guide sequence and is referred to as sgGPR120. (Fig. 5.12A, B). sgGPR120 was shown to have good cleavage efficiency, resulting in a 65% reduction in firefly luciferase activity ($p<0.001$), when assessed with a dual luciferase assay (Fig. 5.12C).

Using the same approach for GPR55 KO cell line development, 72 h post-transfection with the Cas9-sgGPR120-GFP expression construct, cells emitting the top 1% of GFP expression were single cell sorted by FACS, followed by clonal expansion (Fig. 5.13).

To determine which cells had bi-allelic indels, individual PCR products from clonal cell populations were sequenced; for clone 5 sequence analysis revealed an identical single nucleotide indel on both alleles (Fig. 5.14A). The insertion mutation was positioned within the GPR120 start codon, indicating disruption of transcription initiation that would be predicted to abolish expression of GPR120 protein. (Fig. 5.14B). However, GPR120 protein expression was retained within the Clone 5 (Fig. 5.14C).

Multiple clones were screened for indels upstream of the GPR120 start codon (ATG) by sanger sequencing, followed by western blotting to determine GPR120 protein expression. Clones 13, 14 and 15 revealed null GPR120 expression when assessed by western blotting and were subsequently brought forward for functional analysis (Fig. 5.15B).

5.4.6: Effects of GPR120 agonists on insulin secretion from wild type and GPR120 knockout BRIN-BD11 cells

The insulinotropic capabilities and specificity of a range of putative GPR120 agonists were assessed using wild type and 3 individual GPR120 knockout BRIN-BD11 cell lines. At 16.7 mM glucose, parent omega 3 fatty acid (ALA) augmented insulin secretion at 10^{-7}-10^{-4}M by 2.1-2.9-fold ($p<0.05$-$p<0.001$) in wild type BRIN-BD11 cells (Fig. 5.16A). The secretory response of ALA was ablated at all concentrations tested ($p<0.001$) in GPR120 knockout BRIN-BD11 cells (Fig. 5.16A).

Endogenous DHA stimulated insulin secretion at 10^{-7}-10^{-4}M by 2.2-3.3-fold ($p<0.001$) in wild type BRIN-BD11 cells (Fig. 5.5B). DHA-induced insulin secretion was reduced by 83% ($p<0.001$) when assessed using the GPR120 knockout BRIN-BD11 cells (Fig. 5.16B). Endogenous EPA induced insulin secretion at 10^{-7}-10^{-4}M by 1.5-1.9-fold ($p<0.01$-$p<0.001$) in wild type BRIN-BD11 cells (Fig. 5.17A). The insulinotropic effect of EPA was retained in GPR120 knockout BRIN-BD11 cells (Fig. 5.17A).

Synthetic dual agonist GW9508 (10^{-7}-10^{-4} M) augmented insulin secretion by 2.3-3.4-fold ($p<0.001$) from wild type BRIN-BD11 cells (Fig. 5.17B). The insulinotropic response of GW9508 (10^{-4} M) was impaired by 54% ($p<0.05$) in GPR120 knockout cells (Fig. 5.17B). Synthetic GSK137647 (10^{-7}-10^{-4} M) increased insulin release by 2.5-2.8-

fold in wild type BRIN-BD11 cells (Fig. 5.18A). The secretory effect of GSK137647 was abolished from 10^{-7}-10^{-5}M ($p<0.001$), however, a secretory response of 1.4-fold ($p<0.05$) was observed at the highest concentration tested (10^{-4} M) (Fig. 5.18A). Synthetic Compound A induced insulin secretion (10^{-7}-10^{-4} M) by 1.8-2.2-fold in wild type cells (Fig. 5.18B). The secretory response of Compound A was ablated at 10^{-7}-10^{-5}M ($p<0.001$) in GPR120 knockout cells, however, Compound A induced insulin release by 1.3-fold at the highest concentration tested (10^{-4} M) (Fig. 5.18B).

5.4.7: Effects of GPR120 agonists on intracellular Ca^{2+} in wild type and GPR120 knockout BRIN-BD11 cells

Exposure of wild type BRIN-BD11 cells to endogenous and synthetic agonists (10^{-4} M) at 16.7 mM glucose induced a prominent increase in intracellular Ca^{2+} concentrations ($p<0.05$-$p<0.01$) (Fig. 5.19A, 5.21A). Using AUC data, DHA omitted a 70% ($p<0.01$) increase and was the most potent endogenous agonist, whilst GW9508 demonstrated a 69% ($p<0.01$) was the most potent synthetic agonist (Fig. 5.19B, 5.21B). Increases of intracellular Ca^{2+} mediated by ALA, EPA, Compound A and GSK137647 were abolished when assessed in GPR120 knockout BRIN-BD11 cells, whilst the effect of GW9508 and DHA were reduced by 9% and 32%, respectively (Fig. 5.20, 5.22).

5.5: Discussion

Novel therapies that enhance beta cell function and regeneration are required for the treatment of type 2 diabetes, with interest intensifying on the involvement of two novel long chain fatty acid sensing GPCRs, namely GPR55 and GPR120 (Moran *et al.* 2016,

McKillop *et al.* 2013, Moran *et al.* 2014). GPR55 and GPR120 have recently been shown to omit a range of beneficial effects in the maintenance of glucose homeostasis, including enhanced glucoregulatory hormone secretion and islet cell proliferation (Moran *et al.* 2014, McKillop *et al.* 2016, Liu *et al.* 2016).

Although a range of endogenous and synthetic agonists exist for the activation of each receptor; their specificity remains largely unknown (Hauge *et al.* 2014, Liu *et al.* 2014, Ruz-Maldonado *et al.* 2018). With respect to the endocannabinoid system, the biological activation of other novel receptors GPR18 and GPR119 may be partially responsible for the beneficial effects observed upon GPR55 activation (Irving *et al.* 2017). Likewise, the GPR120 and GPR40 receptor share similar sequence homology and can be activated by similar ligands (Hauge *et al.* 2014). Therefore, determination of agonist specificity is essential to characterise the respective receptors.

GPR55 is a rhodopsin (class A) GPCR that has been previously shown to demonstrate anti-diabetic effects through the regulation of insulin secretion and glycaemic control (McKillop *et al.* 2013, McKillop *et al.* 2016) with no cytotoxicity effects. In the present study, the acute metabolic effects and specificity of several naturally occurring and atypical endocannabinoid ligands were assessed using a clonal GPR55 knockout BRIN-BD11 cell line developed using CRISPR/Cas9 gene editing. Previous studies (Liu *et al.* 2016, Ruz-Maldonado *et al.* 2018) have used islets from GPR55 knockout mice but this study evaluates, for the first time, the functionality of GPR55 solely and specifically within the pancreatic beta cell.

To establish the GPR55 knockout BRIN-BD11 cells, the Cas9 enzyme was directed to cleave immediately adjacent to the GPR55 start codon, stimulating the NHEJ DNA repair machinery which often, as in the selected clone, introduces indel mutations at the cleavage site. The resultant GPR55 knockout clone contained a bi-allelic deletion of the GPR55

start codon, with GPR55 mRNA expression and protein translation abolished. In addition, the knockout cell line displayed identical secretory responses to wild type cells in response to a wide range of insulinotropic modulators, demonstrating the retention of the beta cell phenotype.

Subsequently, the insulin secretory effects and specificity of putative GPR55 agonists were assessed using the wild type and GPR55 knockout BRIN-BD11 cells. Naturally occurring (OEA, PEA) and atypical (Abn-CBD, AM251, O-1602) agonists demonstrated potent insulinotropic effects in wild type cells. The insulin secretory effect of CBD analogue (Abn-CBD) was impaired in the knockout cell line by 42%, indicating the involvement of GPR55 in Abn-CBD mediated insulin secretion. In addition, the secretory response of another CBD analogue (O-1602) was totally abolished in the knockout cell line, suggesting O-1602 as a selective agonist for GPR55 activation in the pancreatic beta cell.

Rimonabant analogue (AM251) demonstrated insulinotropic capabilities in wild type and GPR55 knockout BRIN-BD11 cells. However, the secretory response of AM251 was reduced by 30% in the knockout cell line, indicating that AM251 induced insulin secretion is only partly driven by GPR55 in pancreatic beta cells.

Endogenous cannabinoid ligands (OEA, PEA) augmented insulin secretion in wild type and GPR55 knockout BRIN-BD11 cells, illustrating the non-selective properties of the endogenous endocannabinoids. The secretory response of OEA was fully retained within the knockout cell line, indicating that OEA is not a GPR55 agonist within the pancreatic beta cell. In contrast, the secretory response of PEA was impaired by 53% in the GPR55 deficient cell line, demonstrating that PEA induced insulin secretion is partially mediated through GPR55 with potential synergistic agonism of another endocannabinoid receptor, such as GPR119 and GPR18 (Irving *et al.* 2017).

Intracellular Ca^{2+} and cAMP signalling studies were employed on wild type and GPR55 knockout BRIN-BD11 cells to determine the downstream effects of the endocannabinoid ligands. Complimentary to insulin secretory studies, increases of intracellular Ca^{2+} observed in the wild type cells by O-1602, PEA and Abn-CBD were abolished in GPR55 knockout cells, while response to AM251 was only impaired. No changes in cAMP production were observed in wild type or knockout cells, suggesting that GPR55 signalling is primarily modulated through Gαq activation and release of Ca^{2+} from intracellular stores (Putney & Tomita 2012). However, Gα12/13 activation may also contribute to the actions of GPR55.

Complimentary gene expression analysis by qPCR demonstrated increased insulin mRNA expression upon Abn-CBD and AM251 treatment in normoglycaemic and hyperglycaemic conditions; indicating the role of the cannabinoid ligands in second phase insulin release. Interestingly, Abn-CBD and AM251 treatment greatly diminished insulin mRNA expression in GPR55 knockout cells, thus, revealing the importance of GPR55 in the production of intracellular insulin stores.

To investigate the functional role of GPR120, a similar approach was employed to develop clonal GPR120 knockout cells using CRISPR/Cas9 gene editing. The Cas9 enzyme was directed to cleave directly within the GPR120 start codon, which subsequently initiates the NHEJ repair mechanism that often introduces indels at the cleavage site. As observed in Clone 5, a single nucleotide insertion was observed within the GPR120 start codon, shifting the reading frame and disrupting the transcription initiation site. Interestingly, GPR120 protein expression was retained within Clone 5 when assessed by western blotting. This may be due to the intact kozak consensus sequence directly upstream of the cleavage site, which has a major role in the initiation of the transcription process (Grzegorski *et al.* 2014).

A series of clones transfected with sgGPR120-Cas9 plasmid were then screened for genomic disruptions in GPR120 gDNA by Sanger sequencing. Clones demonstrating mutations were then examined for GPR120 protein expression by western blotting. Clones 13, 14 and 15 were GPR120 null, whilst β-actin expression was retained. Subsequently, these clones were brought forward for functional studies. All functional assays were performed on 3 separate GPR120 knockout clones to validate the findings observed.

At physiological concentrations of 10^{-6}M, the insulinotropic response of ALA, DHA, GSK137647 and Compound A were abolished, indicating their specificity for GPR120. At super physiological concentrations of 10^{-4}M, a slight insulinotropic effect was observed by DHA, GSK137647 and Compound A, which may suggest slight affinity for another LCFA sensing receptor, such as GPR40.

Omega-3 fatty acid agonist EPA was shown to be none specific for GPR120 activation in pancreatic beta cells as identical secretory effects were observed in the wild type and GPR120 null cells. As anticipated, the synthetic GPR120/GPR40 dual agonist GW9508 demonstrated insulinotropic capabilities on both the wild type and GPR120 knockout cells. The secretory response omitted by GW9508 was substantially impaired at all concentrations, with a 54% reduction observed at the top concentration tested, suggesting that the biological effects are partly driven by GPR120.

All endogenous GPR120 agonists (ALA, DHA, EPA) augmented intracellular Ca^{2+} concentrations in wild type BRIN-BD11 cells, with EPA omitting a lesser effect. When assessed using GPR120 null cells, the effects observed by ALA and EPA were abolished, with a reduced effect observed upon DHA treatment. The effects demonstrated by DHA suggest involvement of another Gαq mediating receptor, such as GPR40. Interestingly, EPA demonstrated insulinotropic activity but ablated intracellular Ca^{2+} activity in

GPR120 knockout cells, suggesting that the insulinotropic response observed may be generated by a non-Gαq dependent receptor, such as GPR40.

In conclusion, the specificity of putative LCFA GPR55 and GPR120 agonists were assessed using respective receptor knockout cell lines, generated by CRISPR/Cas9 gene editing. GPR55 agonists O-1602, Abn-CBD, AM251 and PEA demonstrated GPR55-dependent insulin secretion through intracellular Ca^{2+} modulation. GPR120 agonists ALA, DHA, GSK137647 and Compound A were shown to be GPR120 specific and augmented intracellular calcium induced insulin release. Abn-CBD (GPR55) and ALA (GPR120) were the most specific and potent agonists identified and subsequently present therapeutic potential for the treatment of type 2 diabetes. Moreover, the knockout cell lines developed in this study are robust and reliable models that will greatly facilitate future research exploring the mechanistic function and specificity of GPR55 and GPR120 agonists in pancreatic beta cells.

Figure 5.1: Genomic deletion of GPR55 using CRISPR/Cas9 gene editing.

A

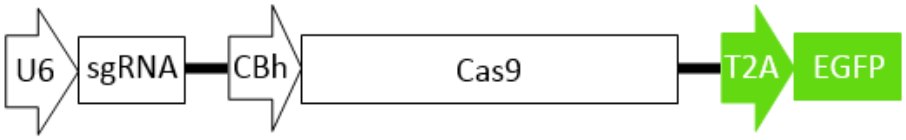

B

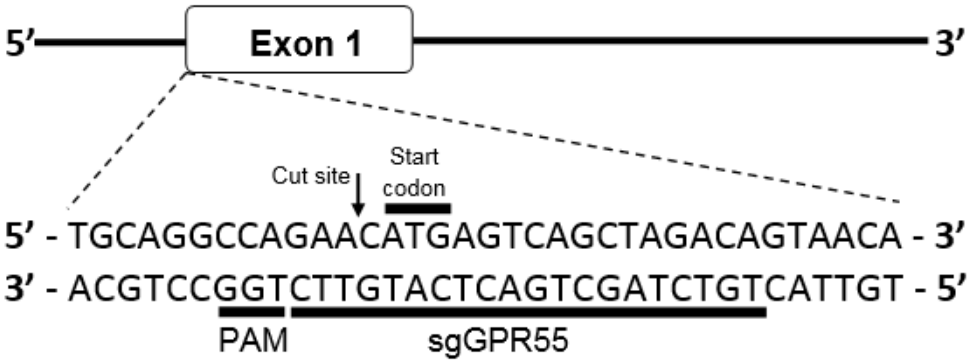

C

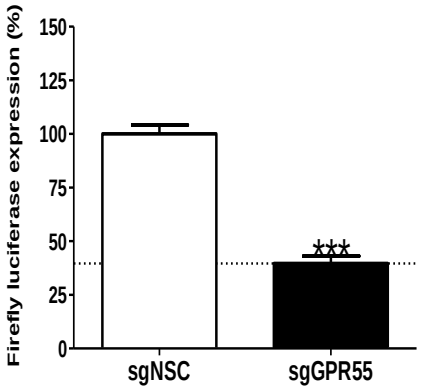

Specific targeting and genomic deletion of GPR55 in BRIN-BD11 cells using CRISPR/Cas9 gene editing. (A) Schematic of px458 construct used. (B) sgRNA and PAM sequences (underlined) and predicted genomic DNA cleavage sites (indicated by arrow) encoding GPR55 exon 1. (C) Dual luciferase assay demonstrating sgGPR55 cutting efficiency compared to non-specific control (sgNSC). Values are mean ± SEM (C: n=8) *** $p<0.001$, compared to non-specific control.

Figure 5.2: Single cell isolation with FACS for clonal GPR55 knockout cell line development.

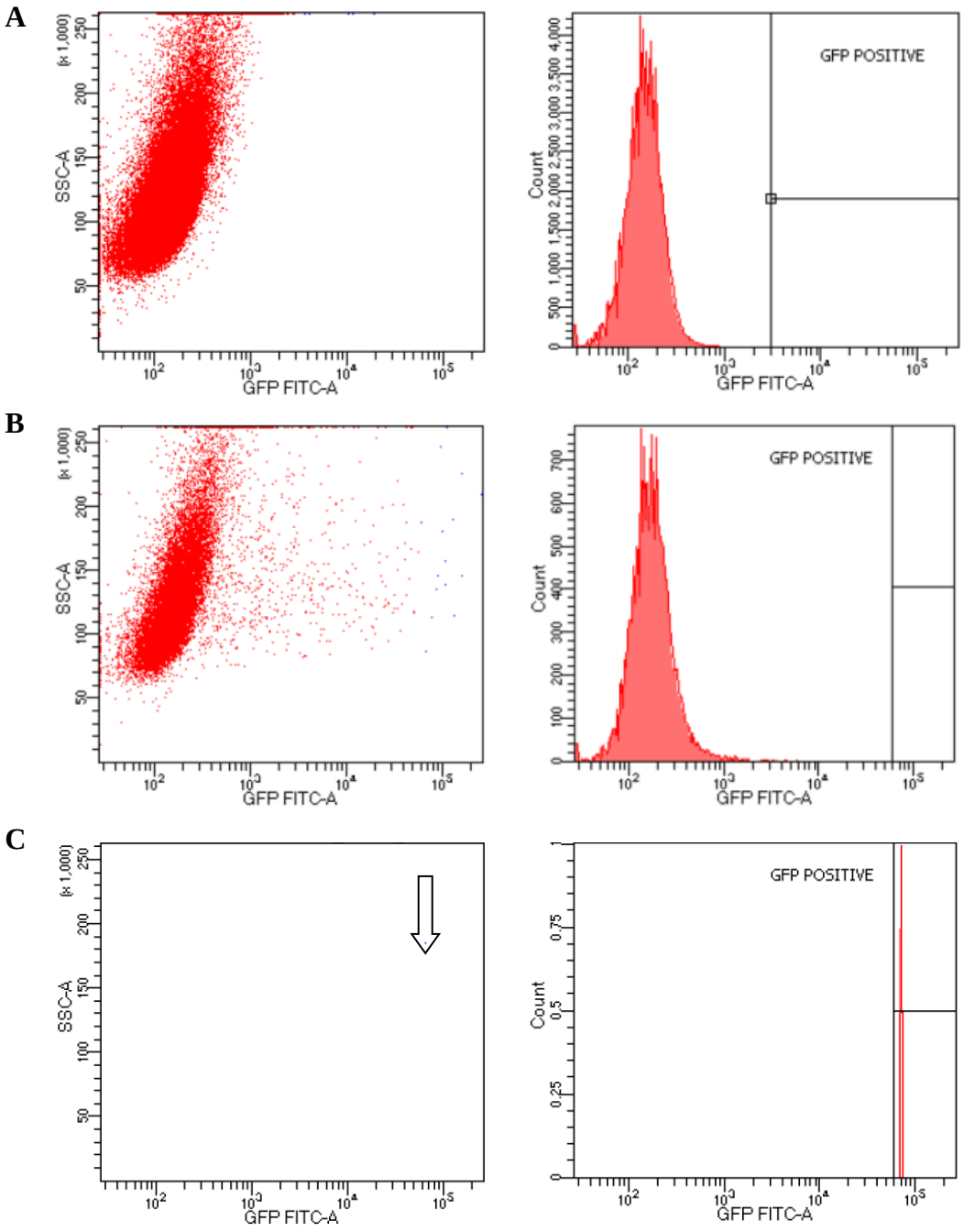

Phase contrast photomicrograph and sorting gate of GFP+ cells 72 h post-lipofection with sgGPR55 construct prior to fluorescence-activated cell sorting (FACS). (A) non-transfected, (B) CRISPR-GFP transfected and (C) single cell CRISPR-GFP FACS

Figure 5.3: Genomic disruption of GPR55 in Clone 2 demonstrated by sanger sequencing.

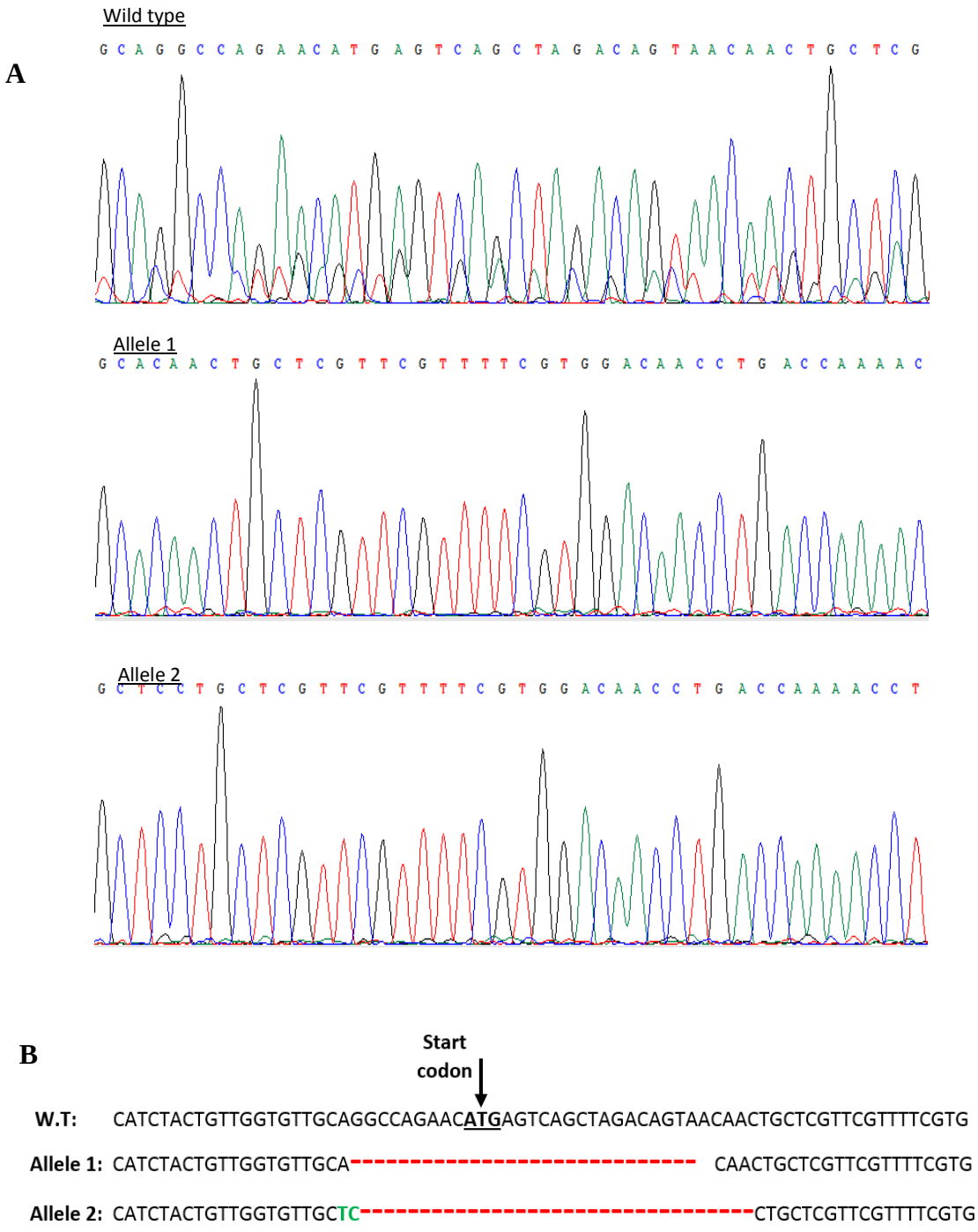

Sanger sequencing analysis displaying (A) Single allele DNA sequencing traces of GPR55 knockout clone 2. (B) Bi-allelic genomic deletion of the GPR55 start codon.

Figure 5.4: Characterisation of clonal GPR55 knockout BRIN-BD11 cell line developed by CRISPR/Cas9 gene editing.

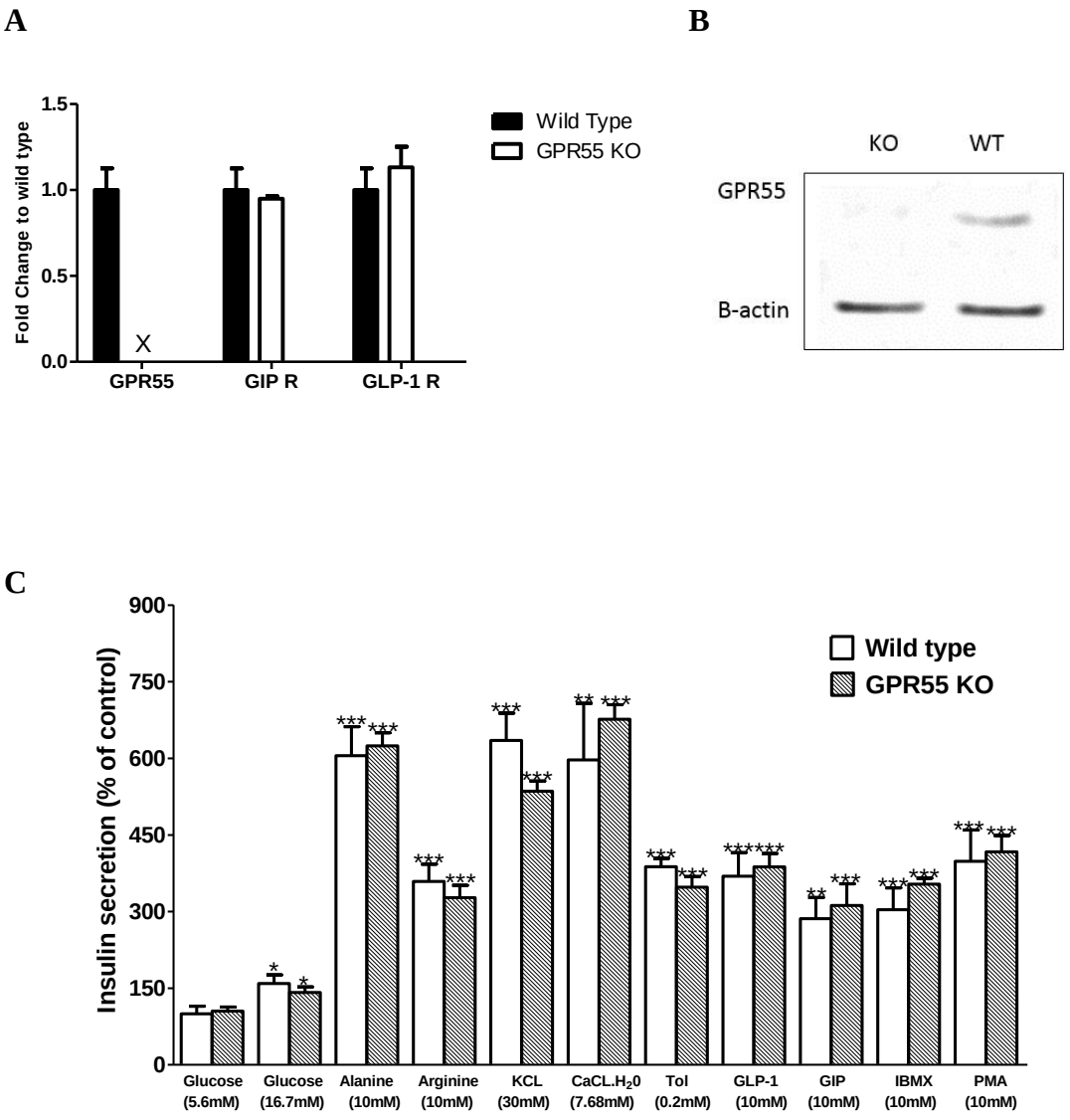

Characterisation of the clonal GPR55 knockout BRIN-BD11 cells. (A) Receptor mRNA expression by qPCR. (B) Western blotting demonstrating GPR55 protein expression in wild type and GPR55 knockout BRIN-BD11 cells. (C) Acute insulin secretory response of wild type and GPR55 knockout BRIN-BD11 cells to a range of insulinotropic modulators at 5.6 mM glucose. Values are mean ± SEM (A: n=3, B; n=2, C: n=8), * $p<0.05$, **$p<0.01$, *** $p<0.001$, compared to 5.6 mM glucose control

Figure 5.5: Acute effect of Abn-CBD and AM251 on insulin secretion from wild type and GPR55 knockout clonal pancreatic BRIN-BD11 cells.

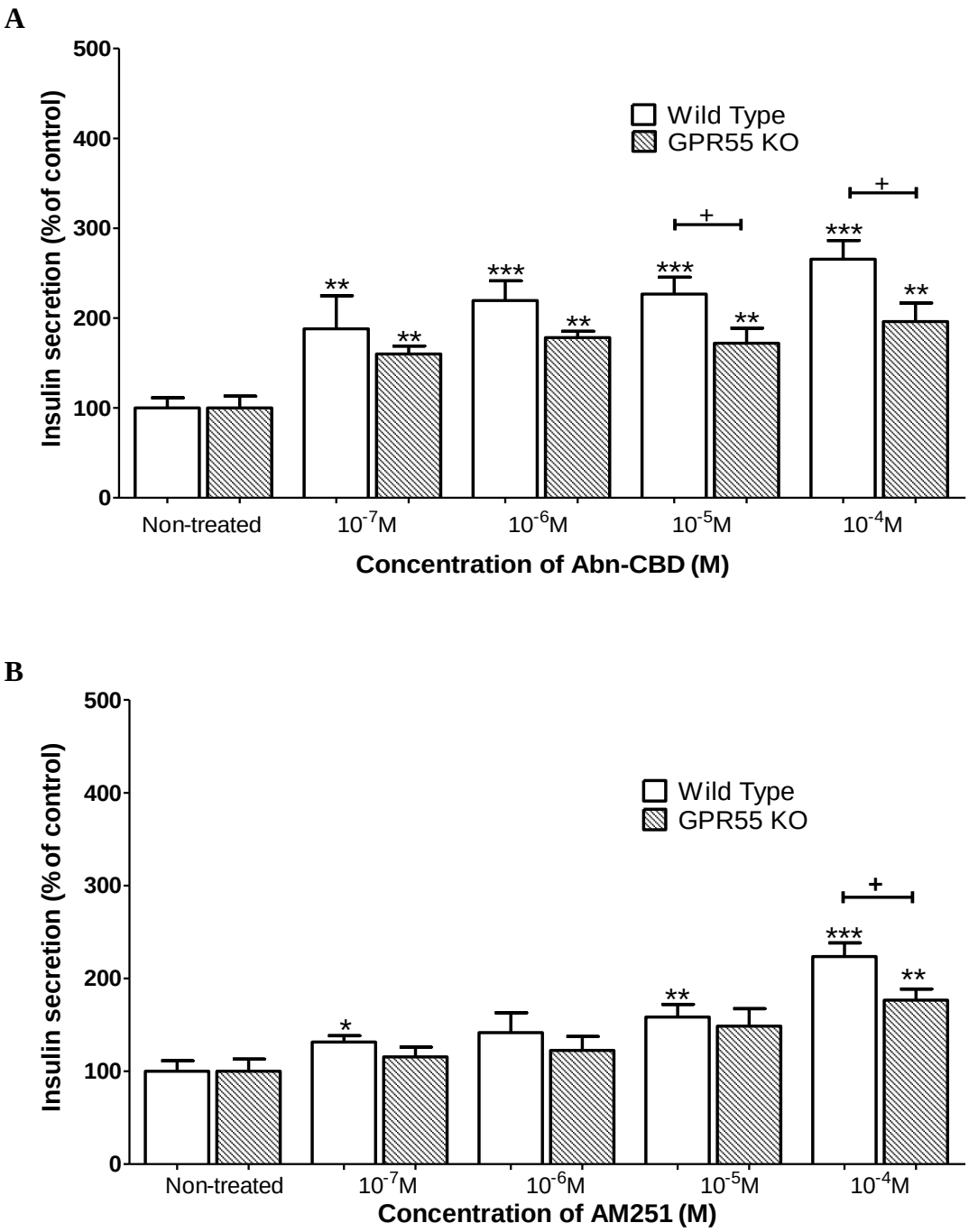

Acute effects of (A) Abn-CBD (10^{-7}-10^{-4} M) and (B) AM251 (10^{-7}-10^{-4} M) on insulin secretion wild type and GPR55 knockout clonal pancreatic BRIN-BD11 cells at 16.7 mM glucose. Results are the mean ± SEM (n=8). *p<0.05, **p<0.01, ***p<0.001, compared to glucose control. +p<0.05, compared to wild type cells.

Figure 5.6: Acute effect of O-1602 and PEA on insulin secretion from wild type and GPR55 knockout clonal pancreatic BRIN-BD11 cells.

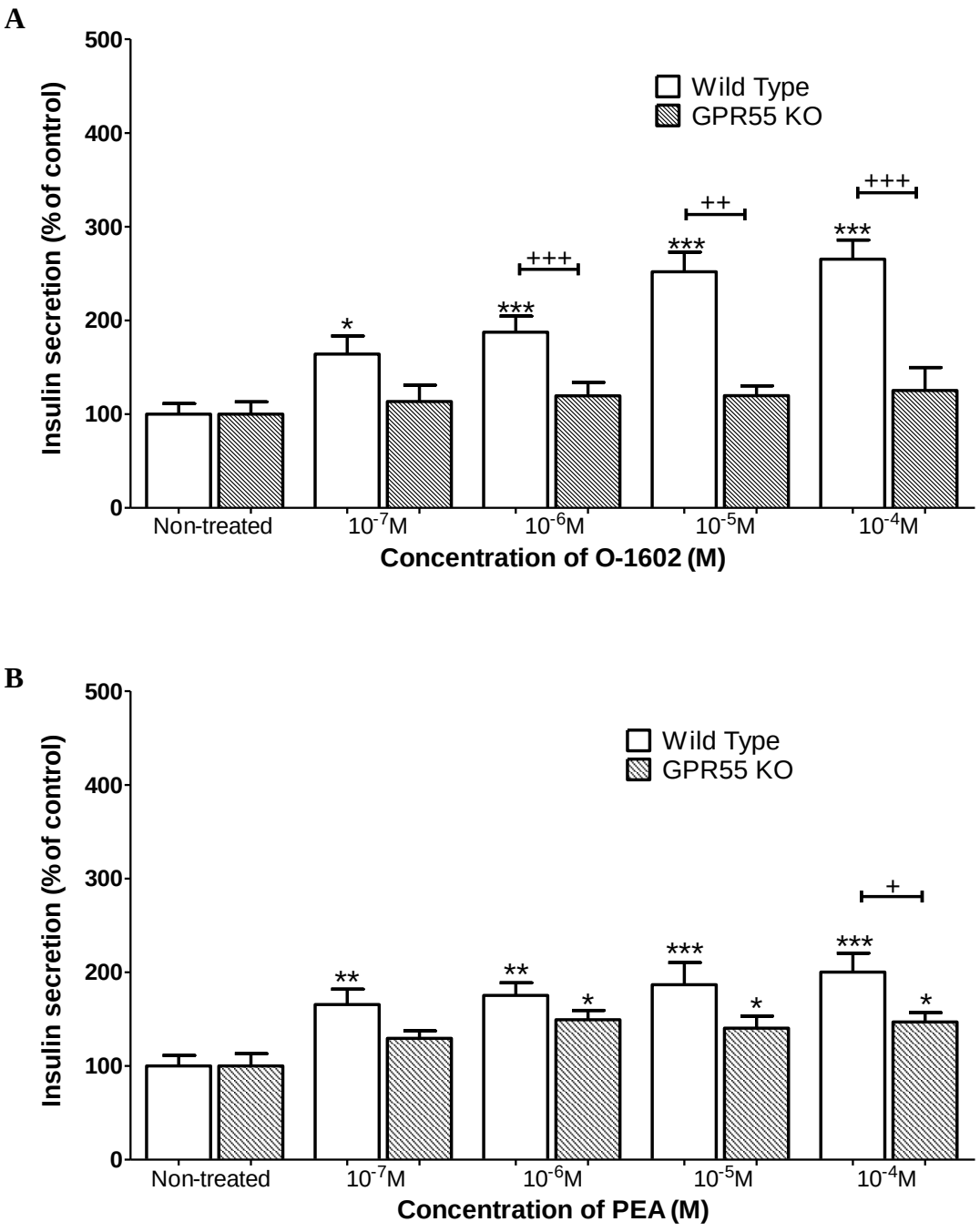

Acute effects of (A) O-1602 (10^{-7}-10^{-4} M) and (B) PEA (10^{-7}-10^{-4} M) on insulin secretion wild type and GPR55 knockout clonal pancreatic BRIN-BD11 cells at 16.7 mM glucose. Results are the mean ± SEM (n=8). *p<0.05, **p<0.01, ***p<0.001, compared to glucose control. +p<0.05, ++p<0.01, +++p<0.001 compared to wild type cells.

Figure 5.7: Acute effect of OEA on insulin secretion from wild type and GPR55 knockout clonal pancreatic BRIN-BD11 cells.

A

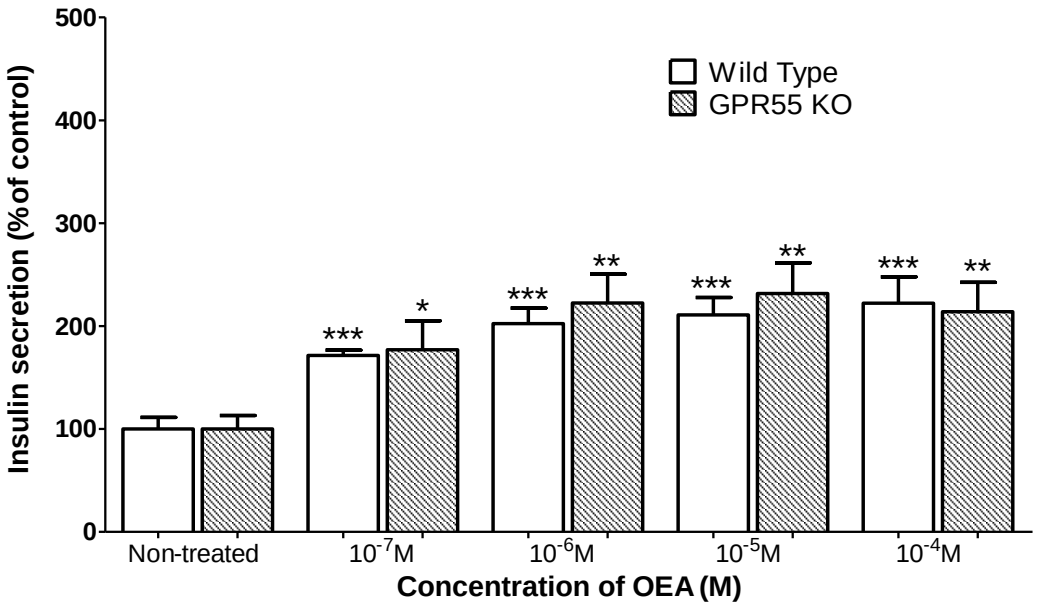

Acute effects of (A) OEA (10^{-7}-10^{-4} M) on insulin secretion wild type and GPR55 knockout clonal pancreatic BRIN-BD11 cells at 16.7 mM glucose. Results are the mean ± SEM (n=8). *p<0.05, **p<0.01, ***p<0.001, compared to glucose control.

Figure 5.8: Acute effect of GPR55 agonists on intracellular Ca^{2+} release from wild type pancreatic BRIN-BD11 cells.

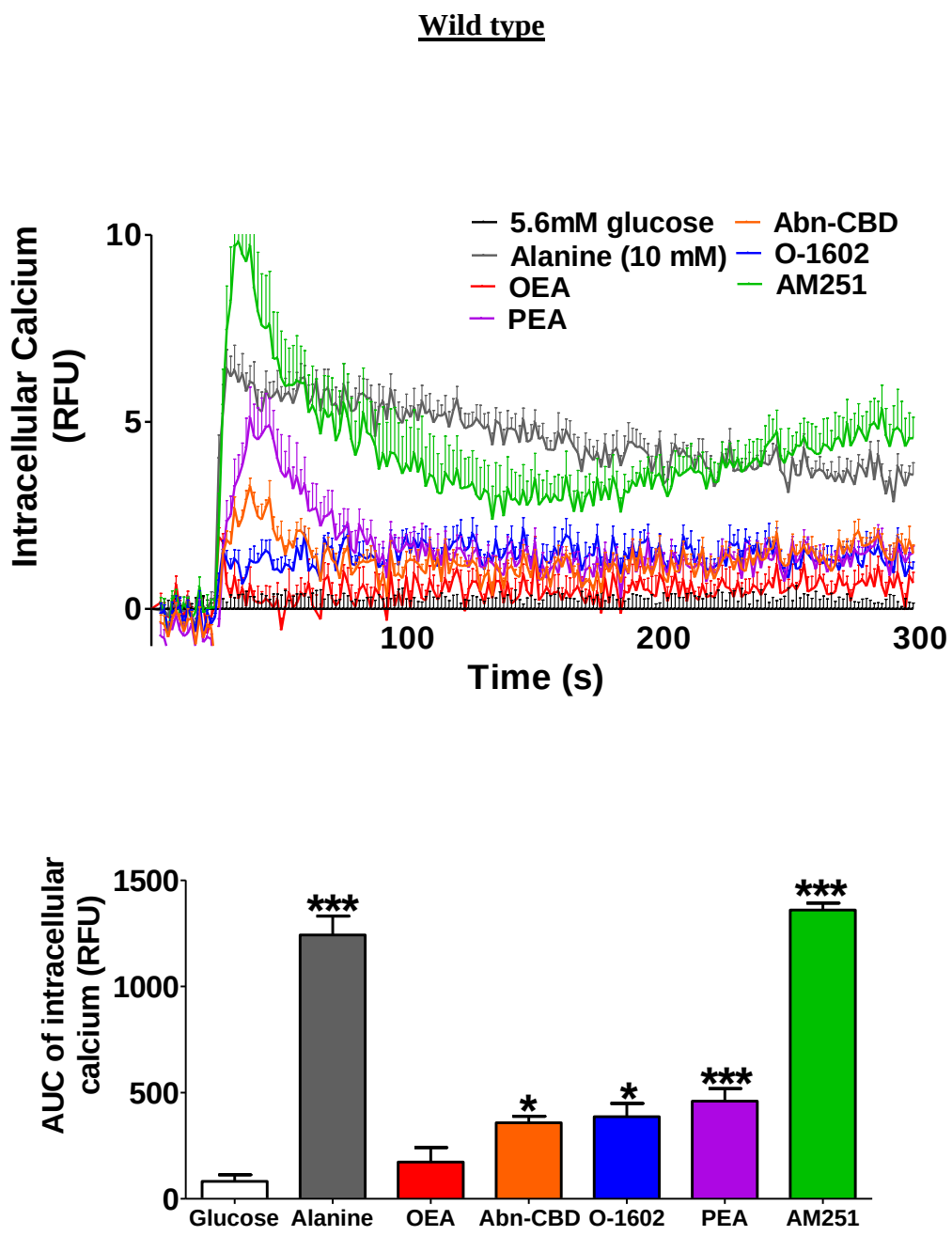

Acute effects of GPR55 agonists (10^{-4} M) on intracellular Ca^{2+} release from pancreatic BRIN-BD11 cells at 16.7 mM glucose. Results are the mean ± SEM (n=8). *p<0.05, ***p<0.001, compared to glucose control.

Figure 5.9: Acute effect of GPR55 agonists on intracellular Ca^{2+} release from clonal GPR55 knockout pancreatic BRIN-BD11 cells.

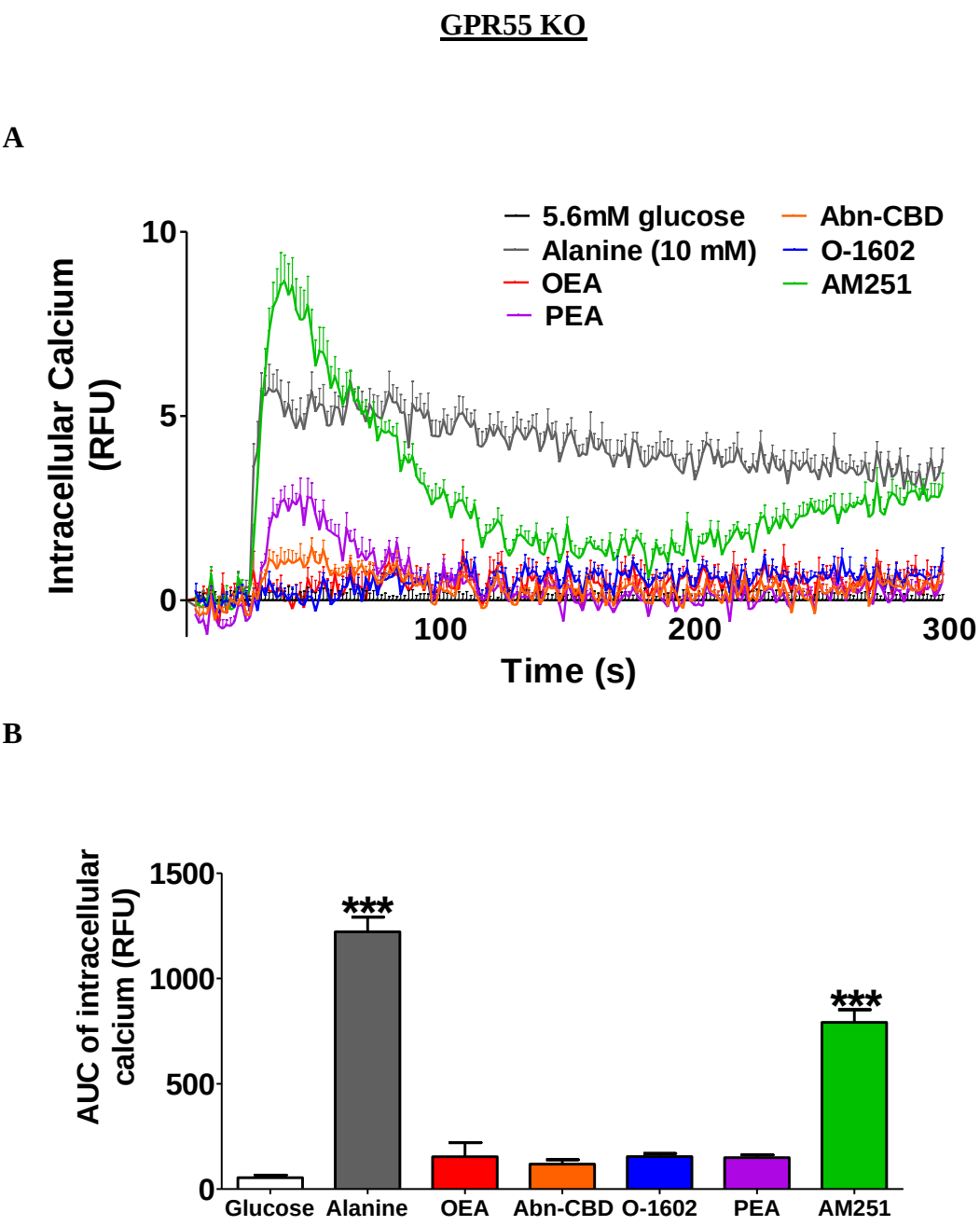

Acute effects of GPR55 agonists (10^{-4} M) on intracellular Ca^{2+} release from pancreatic BRIN-BD11 cells at 16.7 mM glucose. Results are the mean ± SEM (n=8). ***p<0.001, compared to glucose control.

Figure 5.10: Acute effect of GPR55 agonists on cAMP production in wild type and clonal GPR55 knockout BRIN-BD11 cells.

A

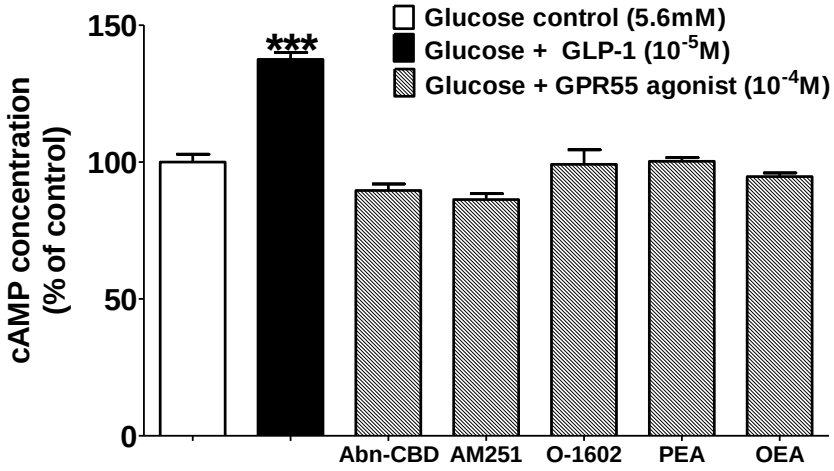

B

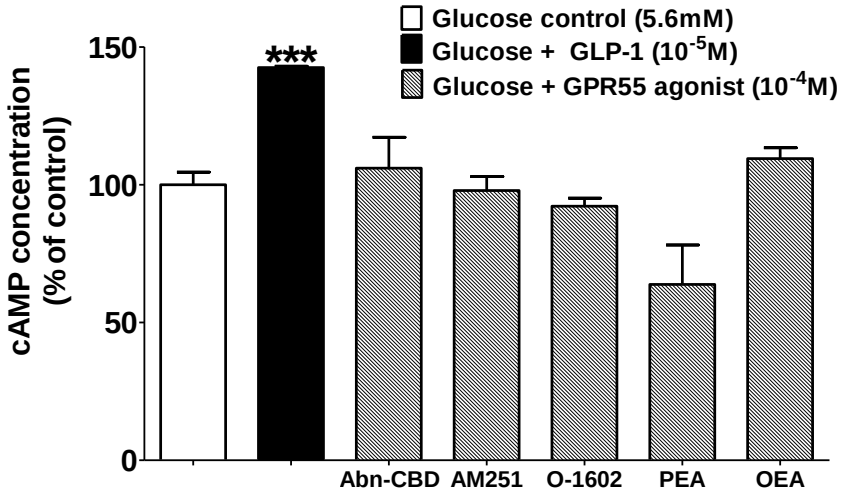

Acute effects of GPR55 agonists (10^{-4} M) and GLP-1 (10^{-5} M) on cAMP production in (A) wild type and (B) clonal GPR55 knockout BRIN-BD11 cells at 16.7 mM glucose. Results are the mean ± SEM (n=4). ***p<0.001, compared to glucose control.

Figure 5.11: Effects of GPR55 agonists on insulin mRNA expression in wild type and GPR55 knockout BRIN-BD11 cells at 5.6 mM and 16.7 mM glucose.

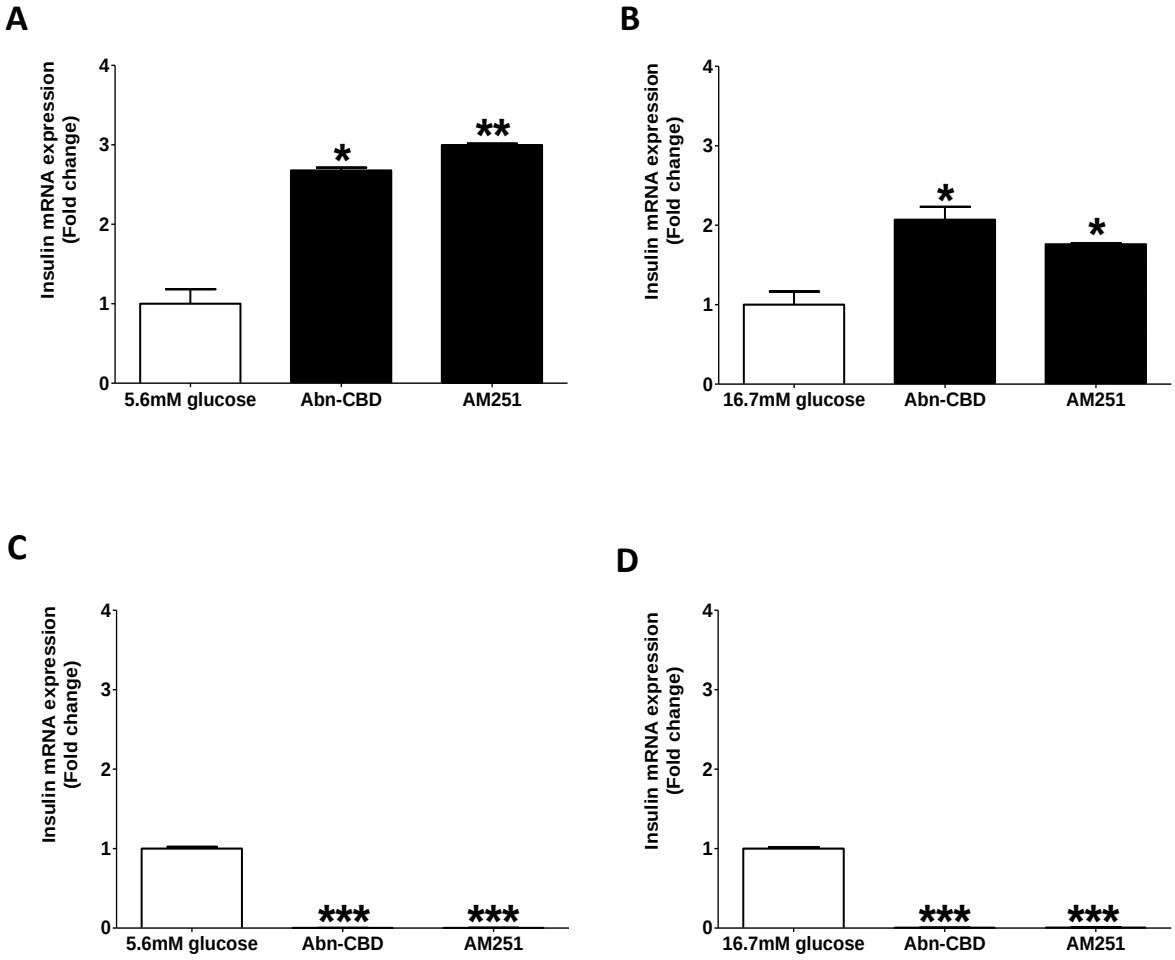

qPCR analysis demonstrating insulin mRNA expression in wild type (A, B) and GPR55 knockout (C, D) BRIN-BD11 cells upon agonist treatment (10^{-4} M) for 4 h at 5.6 mM and 16.7 mM glucose. Values are mean ± SEM (n=3). * $p<0.05$, ** $p<0.01$, *** $p<0.001$, compared to glucose control.

Figure 5.12: Genomic deletion of GPR120 using CRISPR/Cas9 gene editing.

A

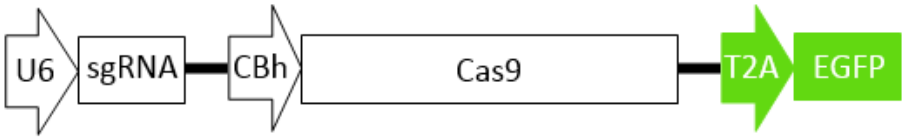

B

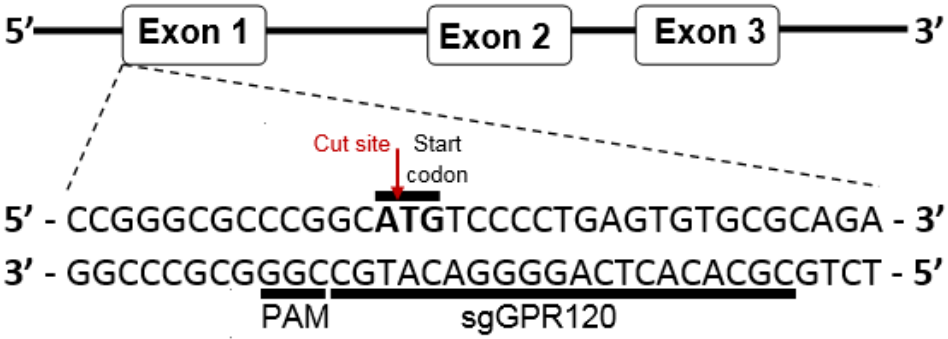

C

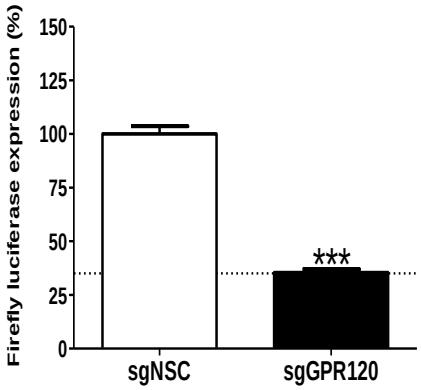

Specific targeting and genomic deletion of GPR120 in BRIN-BD11 cells using CRISPR/Cas9 gene editing. (A) Schematic of px458 construct used. (B) sgRNA and PAM sequences (underlined) and predicted genomic DNA cleavage sites (indicated by red arrow) encoding GPR120 exon 1. (C) Dual luciferase assay demonstrating sgGPR120 cutting efficiency compared to non-specific control (sgNSC). Values are mean ± SEM (C: n=8) *** $p<0.001$, compared to non-specific control.

Figure 5.13: Single cell isolation with FACS for clonal GPR120 knockout cell line development.

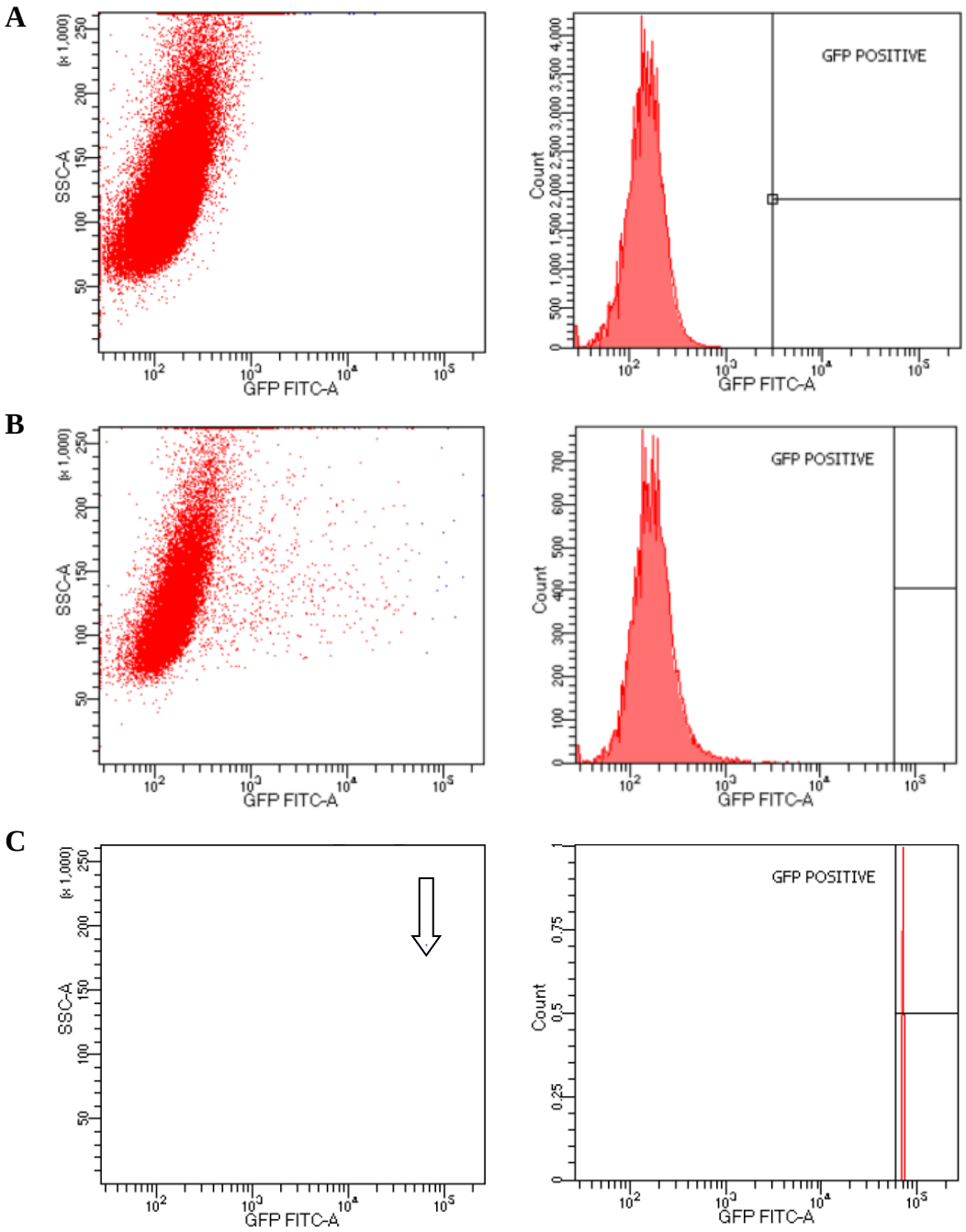

Phase contrast photomicrograph and sorting gate of GFP+ cells 72 h post-lipofection with sgGPR120 construct prior to fluorescence-activated cell sorting (FACS). (A) non-transfected, (B) CRISPR-GFP transfected and (C) single cell CRISPR-GFP FACS

Figure 5.14: Genomic and protein expression of GPR120 in Clone 5 demonstrated by Sanger sequencing and western blotting.

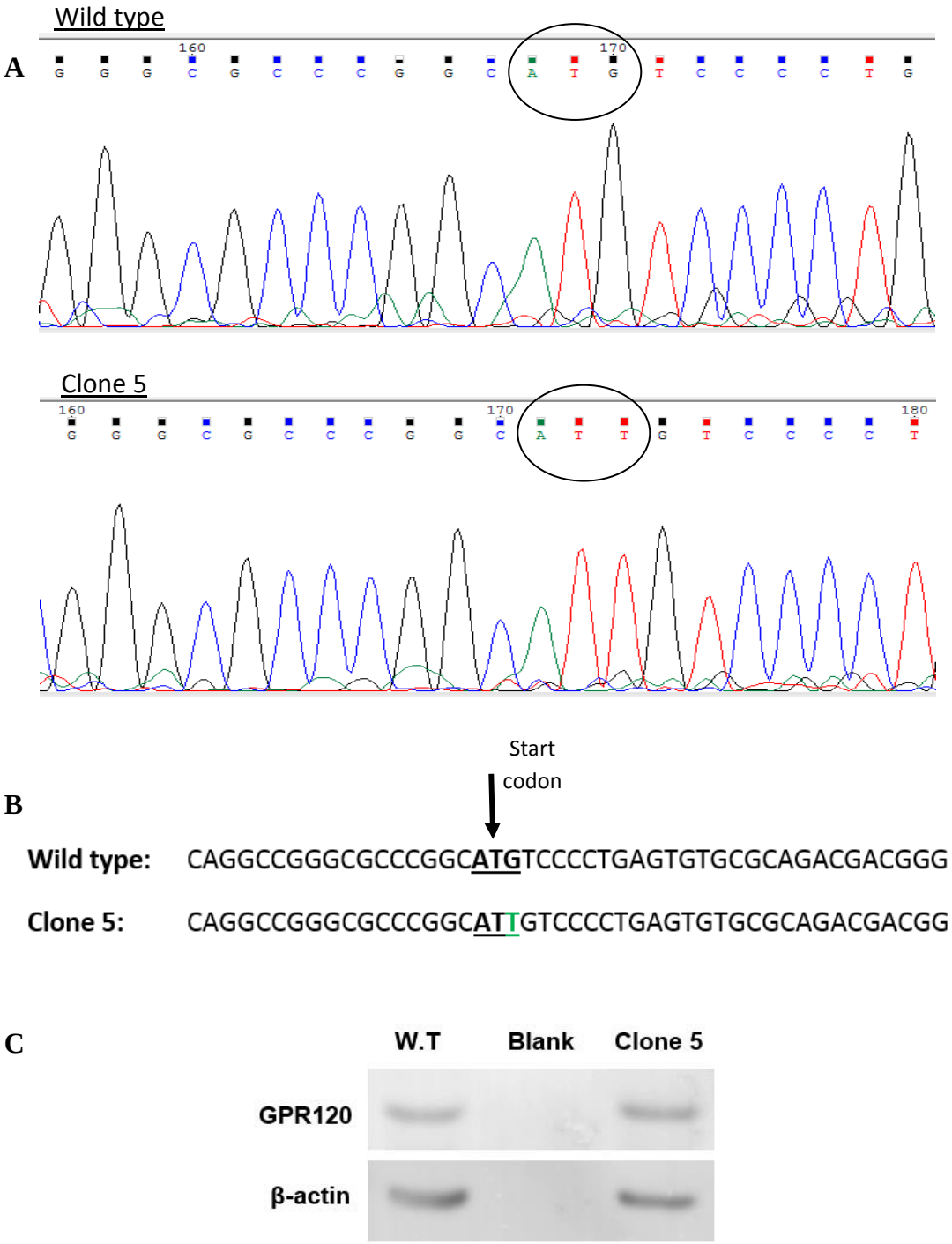

GPR120 expression: (A) DNA sequencing traces of wild type and sgGPR120 transfected clone 5. (B) Genomic disruption of the GPR120 start codon. (C) Western blotting illustrating GPR120 protein expression in wild type and clone 5 transfected cells.

Figure 5.15: Identification of sgGPR120 transfected BRIN-BD11 cell clones with null GPR120 protein expression.

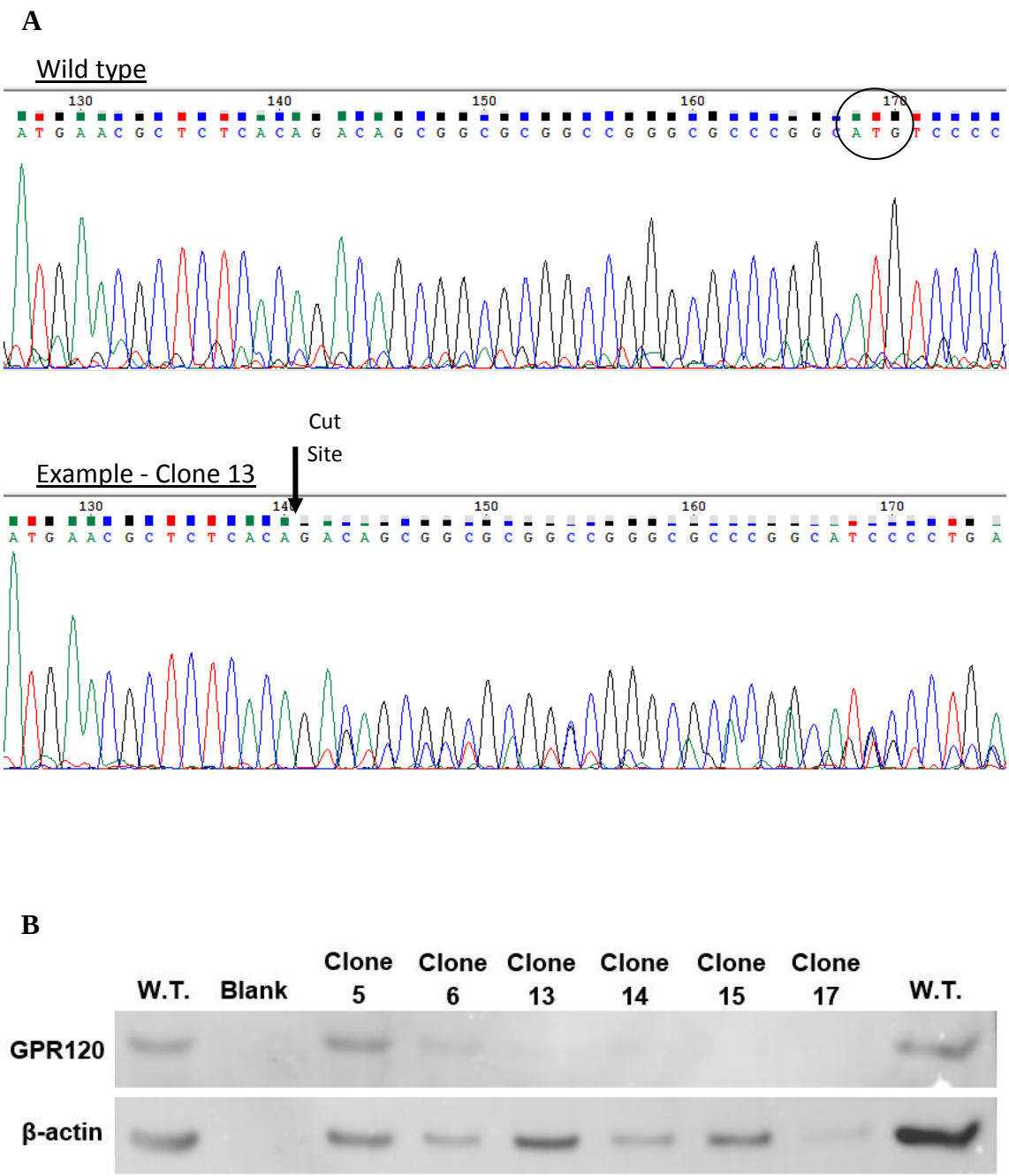

Identification of clonal GPR120 knockout BRIN-BD11 cells with (A) sanger sequencing to screen for genomic mutations in GPR120 coding DNA and (B) western blotting to examine GPR120 protein expression.

Figure 5.16: Acute effect of ALA and DHA on insulin secretion from wild type and GPR120 knockout clonal pancreatic BRIN-BD11 cells.

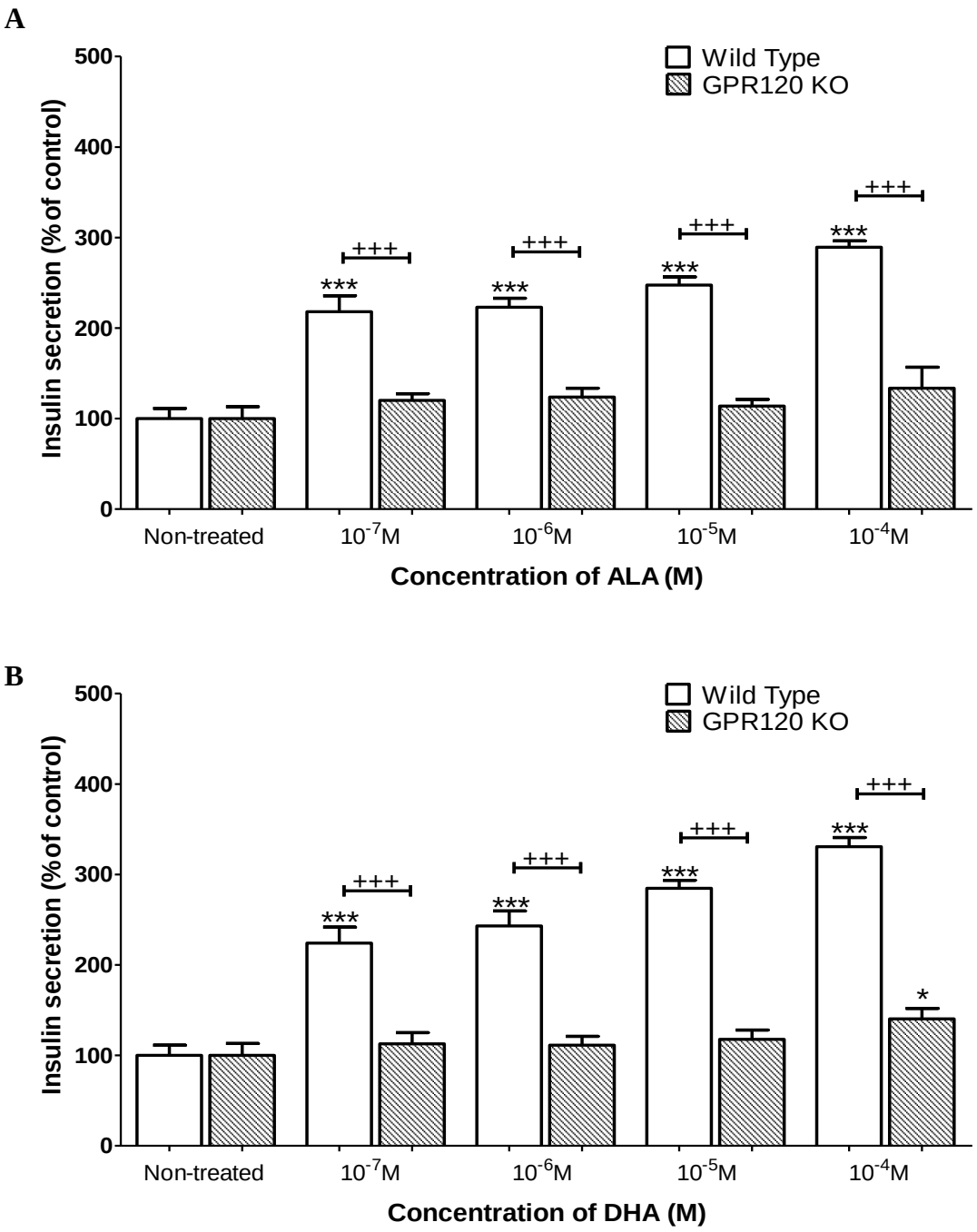

Acute effects of (A) ALA (10^{-7}-10^{-4} M) and (B) DHA (10^{-7}-10^{-4} M) on insulin secretion wild type and GPR120 knockout clonal pancreatic BRIN-BD11 cells at 16.7 mM glucose. Results are the mean ± SEM (n=8). *p<0.05, ***p<0.001, compared to glucose control. ++p<0.01, +++p<0.001, compared to wild type cells.

Figure 5.17: Acute effect of EPA and GW9508 on insulin secretion from wild type and GPR120 knockout clonal pancreatic BRIN-BD11 cells.

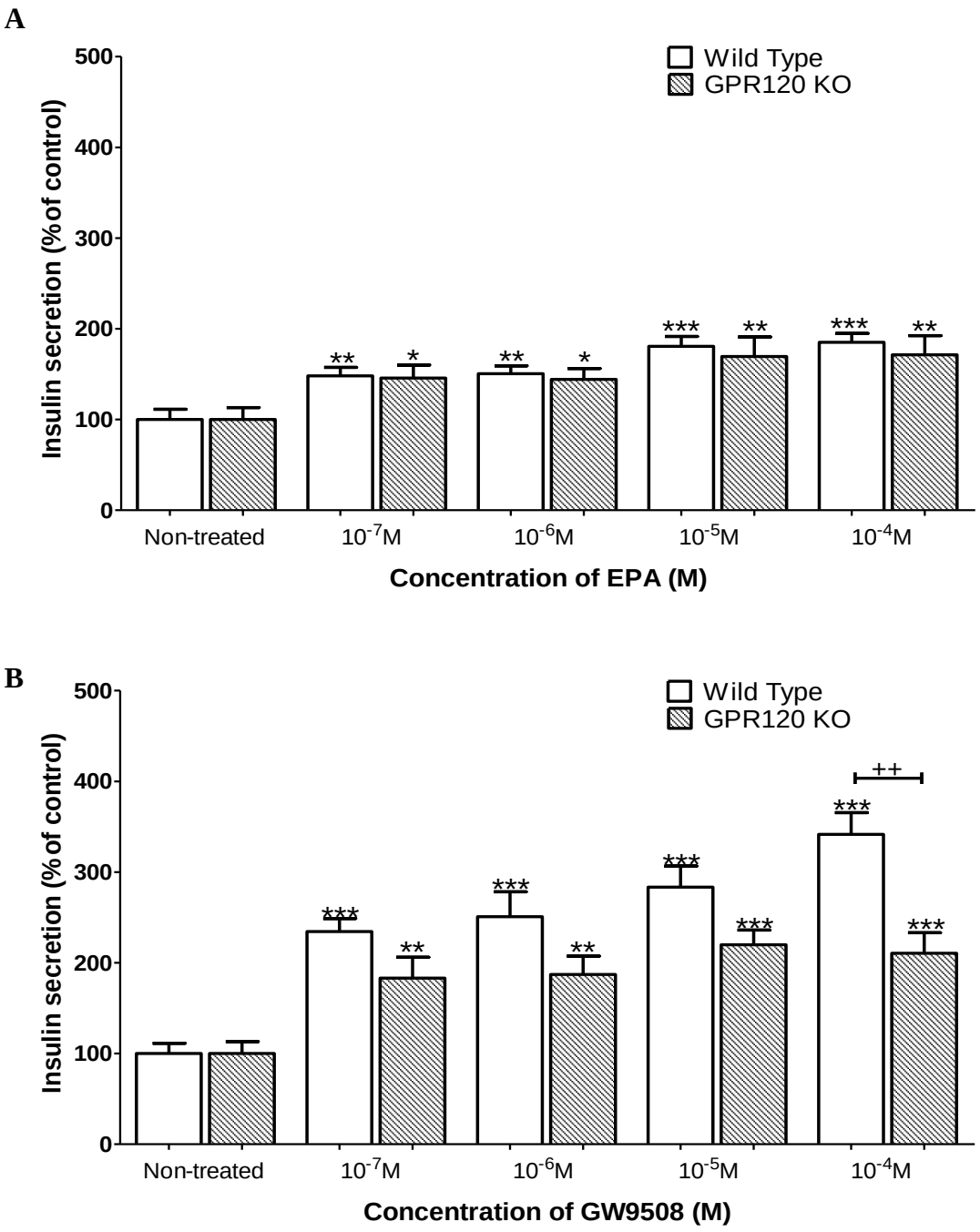

Acute effects of (A) EPA (10^{-7}-10^{-4} M) and (B) GW9508 (10^{-7}-10^{-4} M) on insulin secretion wild type and GPR120 knockout clonal pancreatic BRIN-BD11 cells at 16.7 mM glucose. Results are the mean ± SEM (n=8). *p<0.05, **p<0.01, ***p<0.001, compared to glucose control. ++p<0.01, compared to wild type cells.

Figure 5.18: Acute effect of GSK137647 and Compound A on insulin secretion from wild type and GPR120 knockout clonal pancreatic BRIN-BD11 cells.

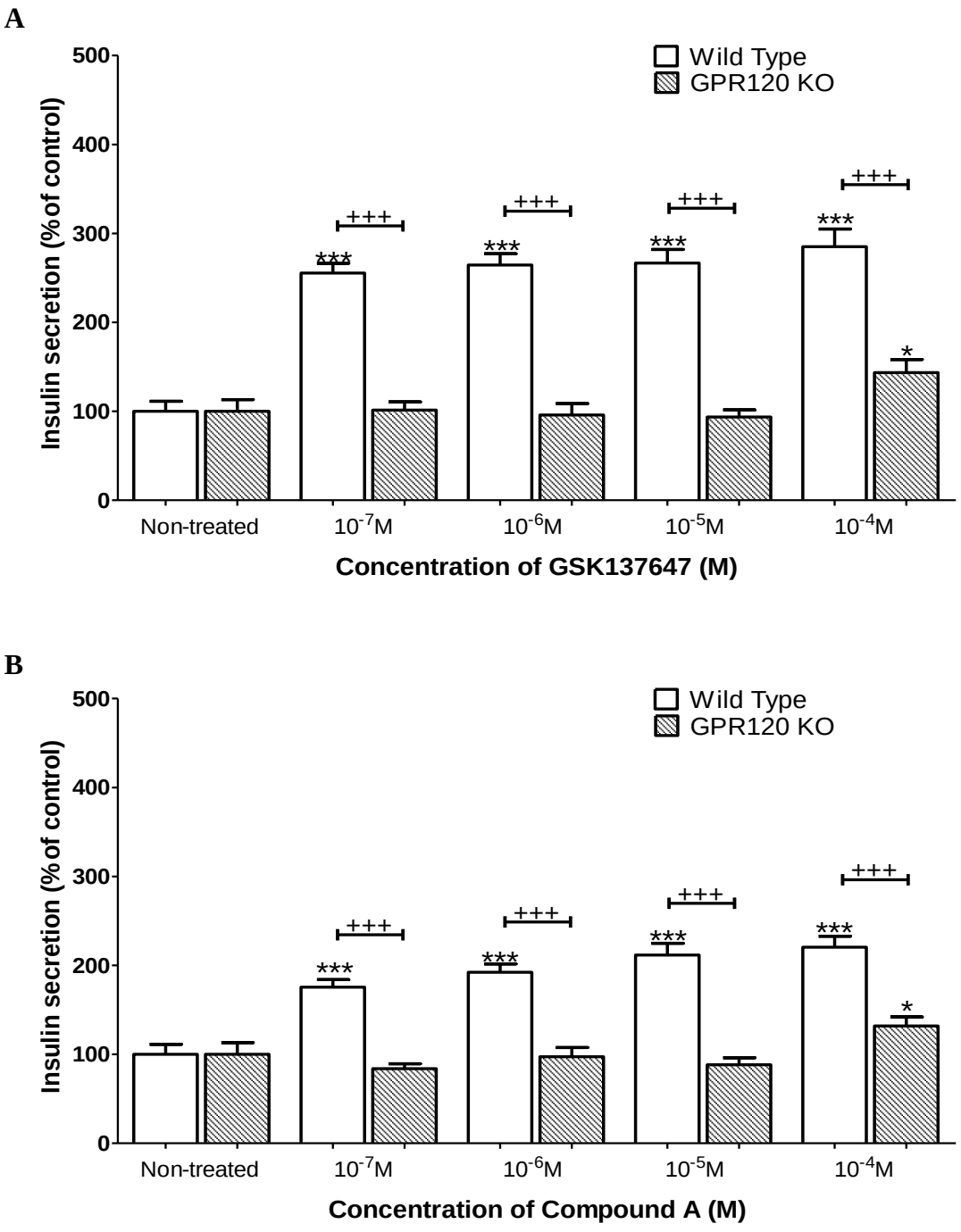

Acute effects of (A) GSK137647 (10^{-7}-10^{-4} M) and (B) Compound A (10^{-7}-10^{-4} M) on insulin secretion wild type and GPR120 knockout clonal pancreatic BRIN-BD11 cells at 16.7 mM glucose. Results are the mean ± SEM (n=8). *p<0.05, ***p<0.001, compared to glucose control. +++p<0.001, compared to wild type cells.

Figure 5.19: Acute effect of endogenous GPR120 agonists on intracellular Ca^{2+} release from wild type pancreatic BRIN-BD11 cells.

Wild type

A

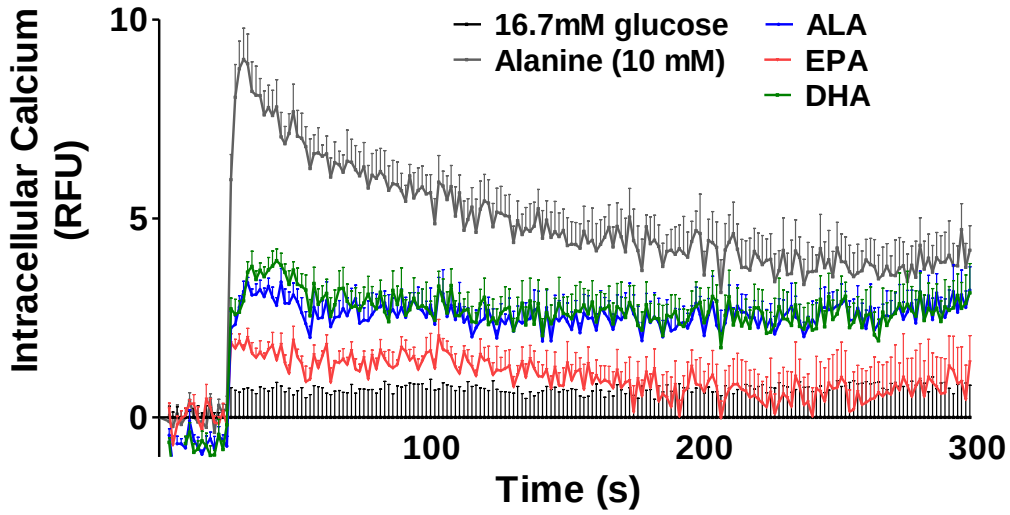

B

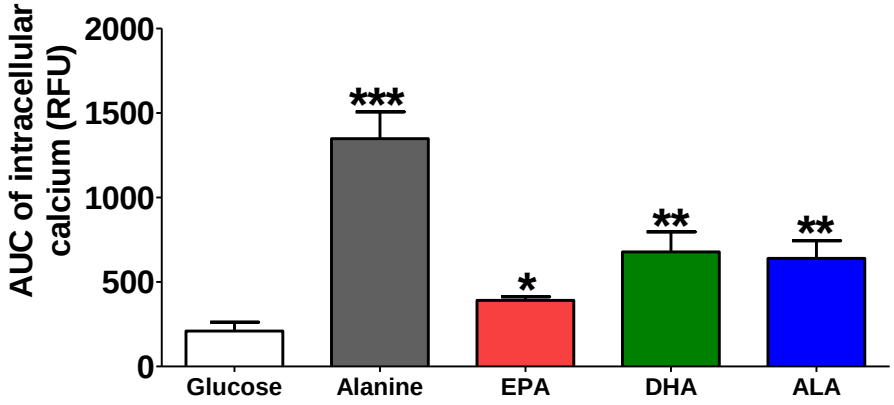

Acute effects of endogenous GPR120 agonists on intracellular Ca^{2+} release from wild type pancreatic BRIN-BD11 cells at 16.7 mM glucose. Results are the mean ± SEM (n=8). *p<0.05, **p<0.01, ***p<0.001, compared to glucose control.

Figure 5.20: Acute effect of endogenous GPR120 agonists on intracellular Ca^{2+} release from clonal GPR120 knockout pancreatic BRIN-BD11 cells.

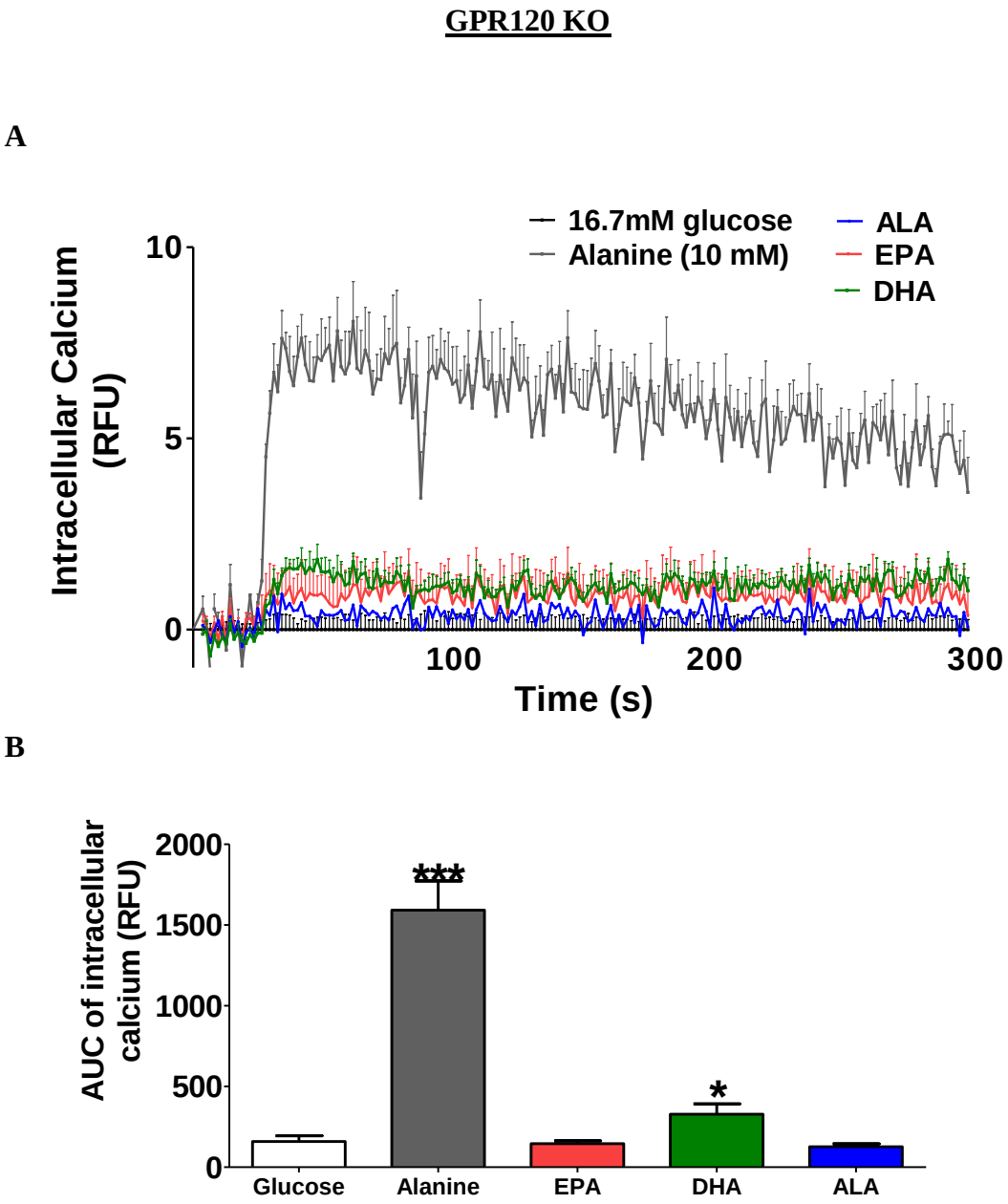

Acute effects of endogenous GPR120 agonists on intracellular Ca^{2+} release from clonal GPR120 knockout pancreatic BRIN-BD11 cells at 16.7 mM glucose. Results are the mean ± SEM (n=8). *p<0.05, ***p<0.001, compared to glucose control.

Figure 5.21: Acute effect of synthetic GPR120 agonists on intracellular Ca^{2+} release from wild type pancreatic BRIN-BD11 cells.

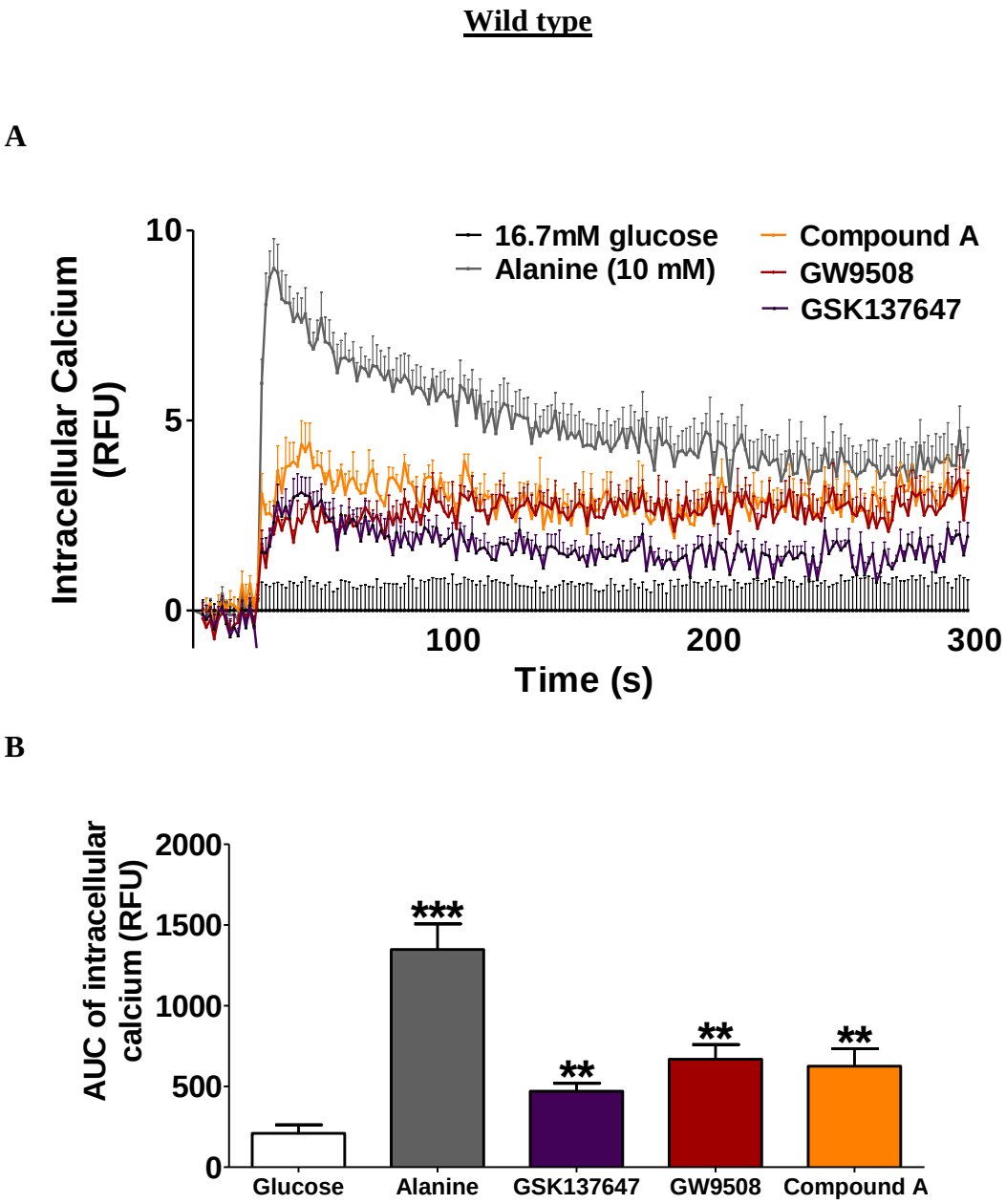

Acute effects of synthetic GPR120 agonists on intracellular Ca^{2+} release from wild type pancreatic BRIN-BD11 cells at 16.7 mM glucose. Results are the mean ± SEM (n=8). **p<0.01, ***p<0.001, compared to glucose control.

Figure 5.22: Acute effect of synthetic GPR120 agonists on intracellular Ca^{2+} release from clonal GPR120 knockout pancreatic BRIN-BD11 cells.

GPR120 KO

A

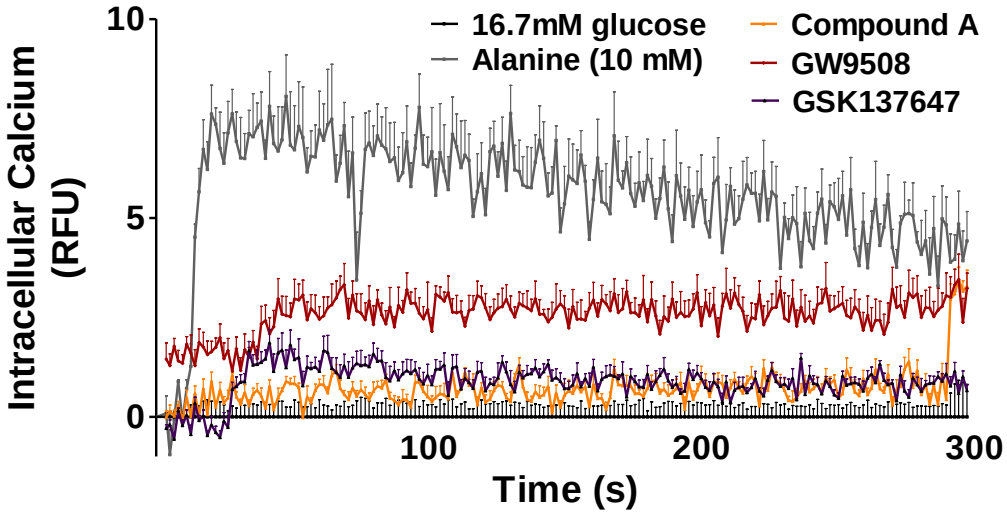

B

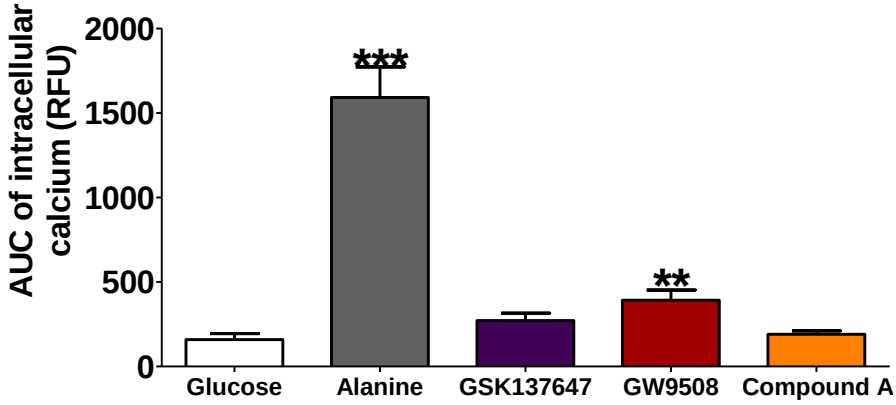

Acute effects of synthetic GPR120 agonists on intracellular Ca^{2+} release from clonal GPR120 knockout pancreatic BRIN-BD11 cells at 16.7 mM glucose. Results are the mean ± SEM (n=8). **p<0.01, ***p<0.001, compared to glucose control.

Chapter 6

Investigating the metabolic actions of GPR120 agonist monotherapy and combinational therapy (Sitagliptin) on glycaemic control and lipid homeostasis *in-vivo*

6.1: Summary

Novel long chain fatty acid (LCFA) GPCRs have been identified with potential to counteract defective insulin release, insulin resistance and low beta cell mass. The present study aims to evaluate the metabolic effects and GPR120 agonist monotherapy and combinational therapy (Sitagliptin) in the maintenance of glucose and lipid homeostasis.

Acute metabolic actions and potency of oral GPR120 agonist treatments were assessed in high fat fed (HFF) induced diabetic obese mice, with hormone release and glucose lowering effects determined. Long term effects investigated once daily oral administration of ALA alone and in combination with Sitagliptin was performed in HFF mice (n=8), with glycaemic control, bodyweight, food intake, insulin, DPP-IV activity, CRP, amylase and lipid profiles assessed. Following 21-day administration, effects towards glucose tolerance, insulin sensitivity, DEXA and islet morphology analysis were examined.

Orally administered GPR120 agonists ALA, GW9508, GSK137647 and Compound A (0.1µmol/kg BW) improved glucose tolerance ($p<0.001$), increased plasma insulin ($p<0.001$), GLP-1 ($p<0.05$) and GIP ($p<0.05$) in HFF mice, with glucose-lowering effects enhanced in combination with DPP-IV inhibitor (Sitagliptin) ($p<0.05$). ALA monotherapy (32%; $p<0.05$) and combinational therapy with Sitagliptin (67%; $p<0.001$) demonstrated the most potent acute glucose lowering effect, with complimentary changes in insulin secretion ($p<0.01$-$p<0.001$). Daily administration of ALA alone and in combination with Sitagliptin reduced non-fasting plasma glucose (83-88%; $p<0.001$) with corresponding increases in circulating insulin (29-33%; $p<0.001$). ALA reduced bodyweight (7%; $p<0.05$) and attenuated cumulative food intake ($p<0.05$).

Following 21-day administration, ALA alone and with Sitagliptin improved glucose tolerance ($p<0.01$-$p<0.001$) by 37% and 47%, respectively and insulin sensitivity by 36-42% ($p<0.05$). Sitagliptin (16%; $p<0.05$), ALA (20%; $p<0.001$) alone and ALA in combination with Sitagliptin (19%; $p<0.05$) reduced fat mass, whilst ALA with Sitagliptin restored bone mineral content (BMC) ($p<0.01$). Sitagliptin (65%; $p<0.001$), ALA (57%; $p<0.001$) alone and ALA in combination with Sitagliptin (57%; $p<0.001$) improved hypertriglyceridaemia and reduced total cholesterol (21-27%; $p<0.001$). ALA monotherapy reduced LDL cholesterol by 17% ($p<0.05$), whilst ALA in combination with Sitagliptin restored elevated CRP concentrations ($p<0.05$). ALA improved beta cell area by 4% ($p<0.001$) and increased beta cell proliferation ($p<0.001$).

The present study reveals the therapeutic potential of targeting GPR120 with ALA monotherapy and combinational therapy (Sitagliptin) and for the treatment of type 2 diabetes, CVD risk and obesity related diseases.

6.2: Introduction

In recent years, research has intensified on the involvement of free fatty acid (FFA) molecules and their ability to activate novel G-protein coupled receptors (GPCRs), with the potential to counteract defective insulin secretion and low beta cell mass in obesity and type 2 diabetes (Vangaveti *et al.* 2010, Moran *et al.* 2016). Islet GPCRs have been shown to have a pivotal role in islet cell function, including the regulation of hormone release and cellular proliferation, which elucidates the potential of GPCRs as novel therapeutic targets (McKillop *et al.* 2013, Moran *et al.* 2014, McKillop *et al.* 2016).

FFA sensing GPCR signalling pathways result in an array of downstream signalling, with alterations in intracellular Ca^{+}, cAMP production and mitogen activated protein kinase phosphorylation, depending on the intracellular G-protein subunit activated (Amisten *et al.* 2013). Long chain fatty acid (LCFA) sensing GPCRs have been heavily reported to play a key role in energy metabolism and glucose homeostasis, namely GPR40 (FFAR1), GPR41 (FFAR3), GPR43 (FFAR2) and GPR120 (FFAR4) (Stoddart *et al.* 2008). Research on the functionality of LCFA receptors is advancing rapidly, with the potent GPR40 agonist TAK-875 (Fasiglifam) recently undergoing stage III clinical trials, before its withdrawal due to signs of liver toxicity (Marcinak *et al.* 2017).

GPR120 (FFAR4) is a class A (rhodopsin) GPCR that exhibits 10% sequence homology with GPR40 (FFAR1), with both demonstrating high affinity for saturated and unsaturated LCFA molecules (Vangaveti *et al.* 2010, Hirasawa *et al.* 2005). Although the signalling mechanism of GPR120 remains largely unknown, studies have demonstrated the involvement of phospholipase C, IP_3 and intracellular Ca^{2+} upon Gαq phosphorylation in the pancreatic beta cell (Sanchez-Reyes *et al.* 2014, Moran *et al.* 2014). However, other underexplored signalling pathways may also have a regulatory role in pancreatic islet cells, including extracellular signal-regulated kinase (ERK), phosphoinositide (PI)-3-kinase and Akt (Hara *et al.* 2011, Sanchez-Reyes *et al.* 2014, Moran *et al.* 2014).

Abundant expression of GPR120 has been identified in the lungs, pro-inflammatory macrophages, adipose tissue, endocrine-pancreas and intestines (Moore *et al.* 2009, Amisten *et al.* 2013). Interestingly, single nucleotide polymorphisms in the GPR120 gene have been shown to modulate circulating insulin concentrations and insulin sensitivity in response to omega-3 fatty acid supplements, including docosahexaenoic acid (DHA) and eicosapentaenoic acid (EPA) (Vallee Marcotte *et al*. 2017). With respect to the

gastrointestinal (GI) tract, studies have demonstrated that agonising GPR120 modulates GLP-1, GIP and CCK secretion from enteroendocrine L-cells and K-cells (Hirasawa *et al.* 2005, Ikoubov *et al.* 2007, Sankoda *et al.* 2017).

GPR120 is activated by micromolar concentrations of circulating omega-3 fatty acid molecules, including docosahexaenoic acid (DHA), eicosapentaenoic acid (EPA) and α-linolenic acid (ALA) (Shimpukade *et al.* 2012, Watson *et al.* 2012). In addition, numerous synthetic agonists have been developed with high affinity for GPR120 activation, including GW9508, Compound A and GSK137647 (Mizuta *et al.* 2015, Oh *et al.* 2010, Sparks *et al.* 2014). The parent omega-3 fatty acid ALA cannot be synthesised and must be acquired from dietary components, such as plants, fish and seeds (Biondeau *et al.* 2015). Once consumed, ALA is broken down into DHA and EPA through the action of the enzyme delta-6-desaturase (Shi *et al.* 2016). The activity of fatty acid desaturation enzymes is altered with diabetic complications, including elevated circulating insulin concentrations (Brenner 2003).

Recent studies demonstrated a range of endogenous (ALA, DHA, EPA) and synthetic (GW9508) GPR120 agonists to enhance glucose stimulated insulin release from clonal beta cells, isolated mouse islets and mice (Moran *et al.* 2014). In addition, acute and chronic administration of ALA has been shown to promote GLP-1 secretion in rats (Tanaka *et al.* 2008). Furthermore, administration of ALA has been shown to omit potent anti-inflammatory effects, through the downregulation of inflammatory COX-2, iNOS and TNF-alpha gene expression mediated by blocking of NF-kappaB and MAPK activation (Ren & Chung 2007). Positive effects of ALA towards insulin resistance have been heavily documented in both pre-clinical studies using rodents and clinical human intervention studies. In an 8-week clinical study, obese participants that received an oral dose of ALA displayed enhanced peripheral insulin sensitivity (Wang *et al.* 2013).

ALA supplementation has been demonstrated to counteract oxidative stress by quenching a range of reactive oxygen species (ROS) (Li *et al.* 2013). As this molecule is soluble in both lipid and aqueous portions of the cell, its biological functionality is not limited by cellular environments (Li *et al.* 2013). In addition, several studies have also revealed the lipid modulating characteristics of ALA, including the lowering of circulating triglycerides, control of hypertension and protection against LDL oxidation (Bradberry *et al.* 2013). Subsequently, ALA supplementation may act as a possible protective agent against risk factors associated with cardiovascular disease (CVD) (Bradberry *et al.* 2013).

Type 2 diabetes is one of the most prevalent metabolic diseases strongly linked with increased risk of CVD (Martin-Timon *et al.* 2014). The risk is derived from counterregulatory bodily functions that coexist with CVD risk factors and complications, including obesity, hypertension and dyslipidaemia (Bradberry *et al.* 2013). In general, the incidence of thrombotic and macrovascular disease is greatly increased in patients with type 2 diabetes. Pro-inflammatory cytokines and inflammation play a key role in the lipotoxic and glucotoxic induced mitochondrial injury, oxidative stress, beta cell apoptosis and insulin resistance in type 2 diabetes (Lathief & Inzucchi 2013). Whilst, the parent omega-3 fatty acid, ALA has the potential to counteract inflammation and adiposity (Todric *et al.* 2006).

Although the anti-inflammatory and lipid lowering properties of GPR120 and ALA are well known, the present study aims to evaluate the glucoregulatory and anti-obesity effects of ALA supplementation in high fat fed (HFF) induced diabetic obese mice. Due to the hypothesised role of GPR120 in the modulation of incretin release from enteroendocrine cells, ALA combinational therapy using the DPP-IV inhibitor (Sitagliptin) was utilised to prolong the circulating half-life of incretin hormones. Acute glucose lowering parameters of ALA monotherapy and combinational therapy

(Sitagliptin) were assessed, including glucose tolerance, insulin secretion, incretin secretion, DPP-IV activity and agonists specificity. In addition, chronic analysis assessed the effects of 21-day oral administration of ALA monotherapy and combinational therapy on bodyweight, food intake, non-fasting plasma glucose, insulin secretion/content, insulin sensitivity, lipid profile, pancreatic islet morphology, amylase activity, C-reactive protein and DEXA analysis.

6.3: Materials and methods

Development of high fat fed induced diabetic obese mice was outlined previously in Section 2.9.2. Materials and methods used to assess the metabolic actions of GPR120 agonist-based therapies are outlined in Sections 2.10 and 2.11. Materials and methodologies for DPP-IV activity analysis and ELISAs used for biochemical analysis are detailed in Sections 2.12 and 2.13, respectively.

6.4 Results

6.4.1: Effect of a high fat fed diet for 4 months on glucose tolerance in Swiss TO mice

To confirm the diabetic phenotype, Swiss TO mice, subjected to a high fat fed diet for four months, were challenged with an oral glucose tolerance test. Using AUC data, the glycaemic control of the high fat fed mice was impaired by 47% ($p<0.001$), compared to the lean control (Fig. 6.1A), with glucose stimulated insulin release impaired by 48% ($p<0.001$; Fig. 6.1D). In addition, mice subjected to the high fat diet demonstrated an average weight gain of 18% ($p<0.001$), compared to the lean control (Fig. 6.1E).

6.4.2: Acute effect of GPR120 agonist monotherapy and combinational therapy (Sitagliptin) on glucose tolerance and insulin secretion in high fat fed diabetic mice

An oral glucose tolerance test (OGTT) was performed to assess the acute glucose lowering properties of GPR120 agonists (ALA. GW9508, GSK137647, Compound A) in fasted, HFF mice. Agonists were assessed alone or in combination with the DPP-IV inhibitor (Sitagliptin). The GPR120 antagonist AH-7614 was utilised to determine agonist specificity *in-vivo*. Oral administration of all GPR120 agonists improved glucose tolerance ($p<0.05$-$p<0.001$) (Fig. 6.2-6.9 A), with AUC data showing decreases in glucose with ALA (32%; $p<0.05$), GW9508 (16%), Compound A (26%; $p<0.05$) and GSK137647 (18%; $p<0.05$) (Fig. 6.2-6.9 B). In combination with Sitagliptin, synthetic GPR120 agonist GW9508 exhibited a further 22% ($p<0.01$) improvement on glucose excursion, whilst the endogenous agonist ALA demonstrated an additive 35% ($p<0.05$) effect in combination (Fig. 6.2-6.9 B). The GPR120 antagonist impaired the glucose lowering properties of ALA (31%), GW9508 (6%), Compound A (77%; $p<0.05$) and GSK137647 (89%; $p<0.05$) (Fig. 6.2-6.9 B). The acute glucose lowering effect of the GPR120/GPR40 dual agonist GW9508 was also impaired by 31% in the presence of the GPR40 antagonist (GW1100).

These effects on blood glucose control were accompanied by relative changes in insulin secretion. Agonising GPR120 with ALA (23%; $p<0.01$), GW9508 (21%; $p<0.05$), Compound A (17%; $p<0.05$) and GSK137647 (35% $p<0.001$) increased plasma insulin when assessed with AUC data (Fig. 6.2-6.9). ALA in combination with Sitagliptin demonstrated an additive 16% ($p<0.05$) insulinotropic effect compared to agonist monotherapy (Fig. 6.2-6.9). The GPR120 antagonist AH-7614 abolished the insulinotropic effect of ALA and GW9508 (Fig. 6.3B, 6.5B), whilst the effects of

Compound A and GSK137647 were impaired by 30% ($p<0.001$) and 76% ($p<0.001$), respectively (Fig. 6.7B, 6.9B).

6.4.3: Acute effect of GPR120 agonist monotherapy and combinational therapy (Sitagliptin) on incretin secretion and DPP-IV activity in high fat fed diabetic mice

In response to an oral glucose tolerance test, all GPR120 agonists increased GLP-1 secretion by 20-25% ($p<0.05$-$p<0.01$) (Fig. 6.10). ALA (41%; $p<0.01$), GW9508 (30%; $p<0.05$) and GSK137647 (31%; $p<0.01$) stimulated GIP secretion, whilst Compound had no significant effect (Fig. 6.11). GSK137647 ($p<0.01$) and ALA ($p<0.01$) reduced DPP-IV activity, with activity further diminished when administered in combination with Sitagliptin ($p<0.001$) (Figure 6.12).

6.4.4: Chronic effect of once daily oral administration of ALA monotherapy and combinational therapy (Sitagliptin) on body weight, non-fasting plasma glucose, insulin, pancreatic insulin content, circulating incretin concentrations, DPP-IV activity and food intake

Once daily oral administration of Sitagliptin, ALA alone and combination with Sitagliptin demonstrated no significant effect towards bodyweight in HFF mice when measured every consecutive 3 days (Fig. 6.13A, B). However, when assessed by percentage weight change, ALA alone and in combination with Sitagliptin influenced a 7% ($p<0.05$) reduction in bodyweight (Fig. 6.13C).

HFF-induced hyperglycaemia was reduced by Sitagliptin (56%; $p<0.01$), ALA alone (83%; $p<0.001$) and ALA in combination with Sitagliptin (88%; $p<0.001$) during the 21-day treatment period (Fig. 6.14). Administration of ALA and Sitagliptin in HFF mice

resulted in a greater reduction (32%; $p<0.05$) of glucose when compared to Sitagliptin alone.

Corresponding increases in plasma insulin concentrations were observed upon treatment with Sitagliptin (24%; $p<0.001$), ALA alone (29%; $p<0.001$) and ALA in combination with Sitagliptin (33%; $p<0.001$) (Fig. 6.15A, B). ALA or Sitagliptin administration resulted in a similar insulin response to combination therapy. Terminal pancreatic tissue analysis demonstrated that insulin content was reduced by 70% ($p<0.01$) in HFF-induced diabetic mice. Treatment with Sitagliptin and ALA alone in HFF mice increased insulin content by 48% ($p<0.05$), whilst ALA in combination with Sitagliptin had no effect (Fig. 6.15C).

HFF mice treated with Sitagliptin and ALA alone and ALA in combination with Sitagliptin demonstrated no effect in circulating total-GLP-1 (Fig. 6.16) and total-GIP (Fig. 6.17). DPP-IV activity was elevated by 42% ($p<0.01$) in HFF-induced diabetic mice, whilst administration of Sitagliptin alone and ALA in combination with Sitagliptin reduced DPP-IV activity by 26-34% ($p<0.05$) (Fig. 6.18).

When assessed by consecutive 3-day measurements, no significant changes in food intake were identified upon treatment with Sitagliptin, ALA alone and ALA in combination with Sitagliptin (Fig. 6.19). However, upon the assessment of cumulative food intake, ALA monotherapy reduced food intake at day 21 ($p<0.05$), whilst Sitagliptin monotherapy and ALA combination with Sitagliptin demonstrated no change in food intake (Fig. 6.20A). Cumulative energy intake demonstrated that HFF-induced diabetic mice consumed higher energy intake from days 3-21 ($p<0.01$-$p<0.001$), compared to lean control (Fig. 6.20B). Corresponding to food intake analysis, ALA treated mice demonstrated reduced cumulative energy intake at day 21 ($p<0.05$) (Fig. 6.20B).

6.4.5: Chronic effect of once daily oral administration of ALA monotherapy and combinational therapy (Sitagliptin) on glucose tolerance and insulin sensitivity

Administration of Sitagliptin, ALA alone and ALA in combination with Sitagliptin for 21 days improved glucose tolerance ($p<0.05$-$p<0.001$), as assessed by an oral glucose tolerance test (Fig. 6.21A). Overall, using AUC data, Sitagliptin, ALA and ALA in combination with Sitagliptin improved glucose tolerance by 37-47% ($p<0.01$-$p<0.001$), with ALA combinational therapy demonstrating the most potent effect (47%; $p<0.001$) (Fig. 6.21C). Corresponding insulin secretory responses were observed in response to the glucose lowering effects observed by ALA ($p<0.001$) from 15-60 min, whilst Sitagliptin alone having no effect on insulin release (Fig. 6.21B). ALA alone augmented insulin release by 18% ($p<0.01$), whilst ALA in combination with Sitagliptin demonstrated an additive insulin secretory response of 51% ($p<0.001$) (Fig. 6.21B, D). In addition, 21-day oral administration of ALA alone and ALA in combination with Sitagliptin lowered blood glucose ($p<0.05$-$p<0.01$) following exogenous insulin injection, compared to non-treated HFF mice (Fig. 6.22A). Overall, using AOC data, HFF mice treated with ALA and ALA in combination with Sitagliptin demonstrated enhanced glucose lowering capabilities by 36-42% ($p<0.05$) upon insulin injection, whilst Sitagliptin alone had no effect (Fig. 6.22B).

6.4.6: Chronic effect of once daily oral administration of ALA monotherapy and combinational therapy (Sitagliptin) on DEXA measurements, lipid profile, plasma C-reactive protein and amylase activity

Post 21-day oral administration, Sitagliptin, ALA alone and ALA in combination with Sitagliptin demonstrated reductions in bodyweight 11-14% ($p<0.05$) in HFF-induced diabetic mice, as measured by DEXA analysis (Fig. 6.23A). HFF mice demonstrated

increased fat mass by 32% ($p<0.001$), whilst administration of Sitagliptin, ALA alone and ALA in combination with Sitagliptin reduced fat mass by 16-20% ($p<0.05$-$p<0.01$) in HFF mice (Fig. 6.23B). No effects on lean mass was observed in all groups (Fig. 6.23C).

DEXA analysis revealed that HFF mice demonstrated reduced total bone mineral content ($p<0.05$; Fig. 6.24A) and femur bone mineral content ($p<0.05$; Fig. 6.24A) compared to lean controls. Administration of Sitagliptin alone and ALA in combination with Sitagliptin increased total bone mineral content by 10-11% ($p<0.01$), whilst ALA alone had no effect (Fig. 6.24A). When localised to the femur, Sitagliptin reduced bone mineral content ($p<0.05$), whilst ALA monotherapy and combinational therapy increased bone mineral content by 9-13% ($p<0.05$-$p<0.01$) (Fig. 16.25A). All groups had no effect on total bone mineral density nor femur bone mineral density (Fig. 6.24B; 6.25B).

Lipid profile analysis on terminal plasma revealed that HFF-induced diabetic mice exhibited increased triglycerides ($p<0.001$), total cholesterol ($p<0.001$) and LDL cholesterol ($p<0.001$) concentrations, with no change in HDL cholesterol, compared to lean mice (Fig. 6.26, 6.27). Administration of Sitagliptin alone (65%; $p<0.001$), ALA (57%; $p<0.001$) alone and ALA in combination with Sitagliptin (57%; $p<0.001$) improved hypertriglyceridemia and reduced total cholesterol (21-27%; $p<0.001$). (Fig. 6.26). Sitagliptin treated HFF mice demonstrated reduced HDL cholesterol (5%; $p<0.05$) and increased LDL cholesterol (17%; $p<0.01$). ALA demonstrated no effect on HDL cholesterol, however, ALA monotherapy reduced LDL cholesterol by 17% ($p<0.05$) (Fig. 6.27B).

Mice subjected to a HFF diet displayed elevated plasma CRP concentrations by 37% ($p<0.05$), compared to lean control. Administration of ALA in combination with Sitagliptin reduced plasma CRP by 46% ($p<0.05$), whereas ALA and Sitagliptin alone had no effect (Fig. 6.28A). HFF mice demonstrated elevated plasma amylase activity by

18% ($p<0.01$), whilst administration of Sitagliptin, ALA alone and ALA in combination with Sitagliptin all reduced amylase activity by 12-16% ($p<0.01$) (Fig. 6.28B).

6.4.7: Chronic effect of once daily oral administration of ALA monotherapy and combinational therapy (Sitagliptin) on islet morphology

Immunohistochemistry was utilised to examine insulin and glucagon expression in lean, HFF and treated mouse pancreatic islets (Fig. 6.29). HFF mice revealed increased islet size by 62% ($p<0.001$), whilst treatment with Sitagliptin and ALA alone resulted in no change to islet size. Treatment with ALA in combination with Sitagliptin reduced islet size by 65% ($p<0.001$) (Fig. 6.28A, 6.29). Mice subjected to a HFF diet demonstrated major islet abnormalities, including reduced insulin-positive beta cell percentage ($p<0.05$; Fig.6.30B) and increased glucagon-positive alpha cell percentage ($p<0.05$; Fig.6.30D). However, complimentary to islet size, HFF mice demonstrated increased beta cell mass ($p<0.05$; Fig.6.30C) and alpha cell mass ($p<0.01$; Fig.6.30E). Administration of ALA alone increased percentage beta cell area ($p<0.001$; Fig.6.30B) and beta cell mass ($p<0.05$; Fig.6.30C), whilst reducing percentage alpha cell area ($p<0.01$; Fig.6.30D) and alpha cell mass ($p<0.05$; Fig.6.30E). ALA in combination with Sitagliptin reduced percentage alpha cell area ($p<0.05$; Fig.6.30D) and alpha cell mass ($p<0.05$; Fig.6.30E). Administration of Sitagliptin alone to HFF mice demonstrated no effects towards islet morphology (Fig.6.30).

Administration on ALA in HFF mice increased beta cell proliferation by 3.1% ($p<0.001$), as assessed by Ki-67 immunohistochemistry (Fig 6.31). In addition, abundant expression of both GPR120 and insulin was demonstrated on islets from lean and HFF mice (Fig. 6.32), with areas of double-immunofluorescent staining between both GPR120 and insulin observed (Fig. 6.32G, H).

6.5: Discussion

Novel therapeutics that improve defective insulin secretion and beta cell mass are required, with recent interest focusing on the role of long chain fatty acid sensing GPCRs (Vangaveti *et al.* 2010, Moran *et al.* 2016). The functional role of many of the 293 GPCRs on the pancreatic islet remains largely unknown (Amisten *et al.* 2013). However, recent studies have demonstrated several LCFA GPCRs to exhibit therapeutic potential for the treatment of type 2 diabetes, CVD and obesity related diseases (Stoddart *et al.* 2008). Namely, GPR119, GPR55, GPR40, GPR41, GPR43 and GPR120 have been shown to regulate glucose homeostasis mediated through enhanced hormone release and cellular proliferation (Stoddart *et al.* 2008, Marcinak *et al.* 2017).

Previous studies have demonstrated insulinotropic and anti-inflammatory properties of GPR120 (FFAR4) with a range of endogenous (ALA, DHA, EPA) and synthetic (GW9508, GSK137647, Compound A) agonists (Moran *et al.* 2014). Recently, novel synthetic agonists (GSK137647, Compound A) have been developed with high specificity for GPR120, thus enabling accurate characterisation of the receptor by diminishing the risk of off-target receptor activation (Oh *et al.* 2010, Sparks *et al.* 2014).

The present study firstly investigates the acute metabolic actions and compares the potency of several naturally occurring and synthetic GPR120 agonists in HFF-induced diabetic obese mice. HFF mice have been extensively reported to be a robust model of obesity and type 2 diabetes with characteristics including weight gain, glucose intolerance, insulin resistance, dyslipidaemia, hyperinsulinemia, hyperglucagonemia and alterations to pancreatic islet morphology (Heydemann 2016). To confirm the diabetic phenotype prior to analysis, HFF mice challenged to an oral glucose tolerance test displayed glucose intolerance and defective insulinotropic actions.

Oral administration of GPR120 agonists (ALA, GW9508, GSK137647, Compound A) improved glucose excursion and insulin release when given in combination with glucose to the diabetic animal model, thus demonstrating the glucoregulatory role of GPR120 activation in the pancreatic islet. Complimentary studies have also demonstrated the acute glucose lowering and insulinotropic actions of GPR120 activation in streptozotocin-induced diabetic mice (Moran *et al.* 2014).

To investigate the specificity of putative GPR120 agonists, the high affinity GPR120 antagonist (AH7614) was employed to block the respective receptor. The glucose lowering and insulinotropic effects of ALA, GSK137637 and Compound A were greatly diminished in the presence of the GPR120 antagonist, demonstrating their selectivity towards GPR120. In contrast, the effect omitted by the synthetic GPR120/GPR40 dual agonist GW9508 was impaired by 37% in the presence of the GPR120 antagonist, suggesting that the glucose lowering and insulinotropic responses observed were only partly driven by GPR120.

Conflicting results have been reported of the effect of GPR120 activation on GLP-1 secretion (Tanaka *et al.* 2008, Paulsen *et al.* 2014). In the present acute study, ALA, GW9508, GSK137647 and Compound A were shown to induce GLP-1 secretion, whilst only ALA and GSK137647 stimulated GIP secretion. Interestingly, ALA and GSK137647 enhanced both GLP-1 and GIP secretion and omitted the most potent glucose lowering and insulinotropic effects. To prolong the bioactivity of endogenously released incretins, the DPP-IV inhibitor Sitagliptin was examined in combination with the GPR120 agonists (Drucker *et al.* 2007). Under these conditions, GPR120 agonists exhibited enhanced glucose lowering capabilities by stimulating incretin (GLP-1, GIP) and insulin secretion through GPR120 activation, supplemented with prolonged incretin action through DPP-IV inhibition. Although ALA and GSK137647 slightly attenuated

DPP-IV activity, the activity of DPP-IV was completely abolished when administered in combination with Sitagliptin. ALA demonstrated the greatest additive effect towards both glucose tolerance and insulin secretion when administered in combination with Sitagliptin, further elucidating its role in incretin release.

Upon assessment of acute GPR120 agonist potency and efficacy, the second phase of this study investigated the effect of 21-day oral administration of ALA monotherapy and combinational therapy (Sitagliptin) in HFF-induced diabetic obese mice. In the study, ALA alone and in combination with Sitagliptin demonstrated marked improvements on the prognosis of the diabetic animal model, surpassing the capabilities of Sitagliptin alone. A range of beneficial effects were demonstrated, including improvements towards glucose tolerance, circulating insulin, insulin sensitivity, weight loss, hyperlipidaemia and islet morphology.

Administration of ALA reduced bodyweight by 7%, implicating the involvement of ALA in energy homeostasis and bodyweight management. With respect to glucose tolerance, ALA alone and in combination (Sitagliptin) improved glycaemic control beyond the capabilities on Sitagliptin only, with ALA combinational therapy omitting the most potent effect. These effects on blood glucose control were accompanied by relative changes in insulin secretion with ALA combination (Sitagliptin) proving most potent towards circulating insulin concentrations. As anticipated, Sitagliptin alone and in combination with ALA reduced DPP-IV activity. DPP-IV inhibition however countered the inhibitory effects of ALA on feeding activity. Further studies are required to fully understand the mechanism but inhibition of DPP-IV-mediated degradation of PYY(1-36) to the active form PYY(3-36) seems likely (Batterham & Bloom 2003).

Post 21-day oral administration of Sitagliptin, ALA alone and ALA in combination with Sitagliptin improved glucose tolerance when subjected to an OGTT. Interestingly, ALA

combinational therapy (Sitagliptin) demonstrated the greatest insulin secretory effect in response to the glucose challenge, with insulinotropic actions enhanced from 15-60 min, suggesting involvement of the incretin hormones. Complimentary to previous findings, ALA based therapies attenuated insulin resistance (Oh *et al.* 2010), whilst Sitagliptin alone had no effect.

DEXA analysis revealed reduced bone mineral content in HFF mice. Interestingly, the actions of Sitagliptin appeared to restore total bone mineral content, whilst ALA restored bone mineral content when analysis was localised to the femur. Consistently, ALA combinational therapy restored bone mineral content for each analysis. Preservation of bone quality and strength is strongly linked with GLP-1 and GIP receptor activation, which may implicate the mechanism of action for ALA and Sitagliptin based therapies on bone mineral content restoration (Irwin & Flatt 2015).

Terminal plasma analysis demonstrated that Sitagliptin, ALA alone and ALA in combination with Sitagliptin greatly improved total cholesterol and triglyceride concentrations. Interestingly, Sitagliptin alone attenuated HDL cholesterol, however, increased LDL cholesterol. Previous studies have demonstrated omega-3 fatty acids DHA and EPA to reduce triglycerides but elevate LDL cholesterol (Bradberry 2013). In contrast, administration of the parent omega-3 fatty (ALA) reduced LDL cholesterol and diminished hypertriglyceridemia, revealing the regulatory role of ALA in cardiovascular health. In this study, administration of ALA in combination with Sitagliptin restored elevated C-reactive protein concentrations in HFF mice, which further implicates the beneficial effects of ALA based therapies on CVD risk and obesity related diseases. In harmony with these findings, previous have also demonstrated the cardioprotective effects of omega-3 fatty acids (Clearfield 2005, Bahadursingh *et al.* 2009).

HFF mice demonstrated elevated circulating amylase activity due to pancreatic islet cell damage (Vasudevan *et al.* 2018). Administration of Sitagliptin, ALA alone and ALA in combination with Sitagliptin all restored amylase activity, implicating pancreatic cytoprotection. Terminal analysis revealed that HFF mice demonstrated major islet abnormalities, including increased islet size and alpha percentage area with reduced percentage beta cell area. Due to an increase in islet size, HFF islets displayed increased alpha and beta cell mass. Administration of ALA increased beta cell area and beta cell mass, whilst reducing alpha cell area and mass. Interestingly, ALA in combination with Sitagliptin reduced islet size, alpha cell area and alpha cell mass, however, no effects were observed towards the beta cell population. Thus, revealing the beneficial effects of this treatment in the restoration of non-diabetic islet architecture. When exploring the positive effects observed by ALA administration, Ki-67 staining revealed that ALA increased beta cell proliferation, which contributes to the increase in beta cell population. Furthermore, upon exploring the expression of GPR120 lean and HFF islets, abundant regions of co-localisation between GPR120 and insulin were observed, which further implicates the importance of GPR120 in beta cell function.

In conclusion, oral administration of GPR120 agonist monotherapy and combinational therapy (Sitagliptin) improved glycaemic control in HFF-induced diabetic obese mice, with positive effects towards CVD risk and obesity related diseases also observed. Biological effects included attenuated plasma glucose with increased insulin and incretin secretion. In addition, long term administration of ALA improved glucose tolerance, insulin sensitivity and hyperlipidaemia, whilst restoring CRP, amylase activity and islet cell morphology. Beneficial effects observed were predominantly enhanced in the presence of the DPP-IV inhibitor Sitagliptin, with particular benefits observed in the restoration of islet morphology. These findings promote GPR120 agonist monotherapy

and combinational therapy (Sitagliptin) as a novel therapeutic approach for the treatment of type 2 diabetes and obesity related diseases.

Figure 6.1: Effect four-month high fat fed diet on glucose tolerance and insulin secretion in 18 h fasted Swiss TO mice.

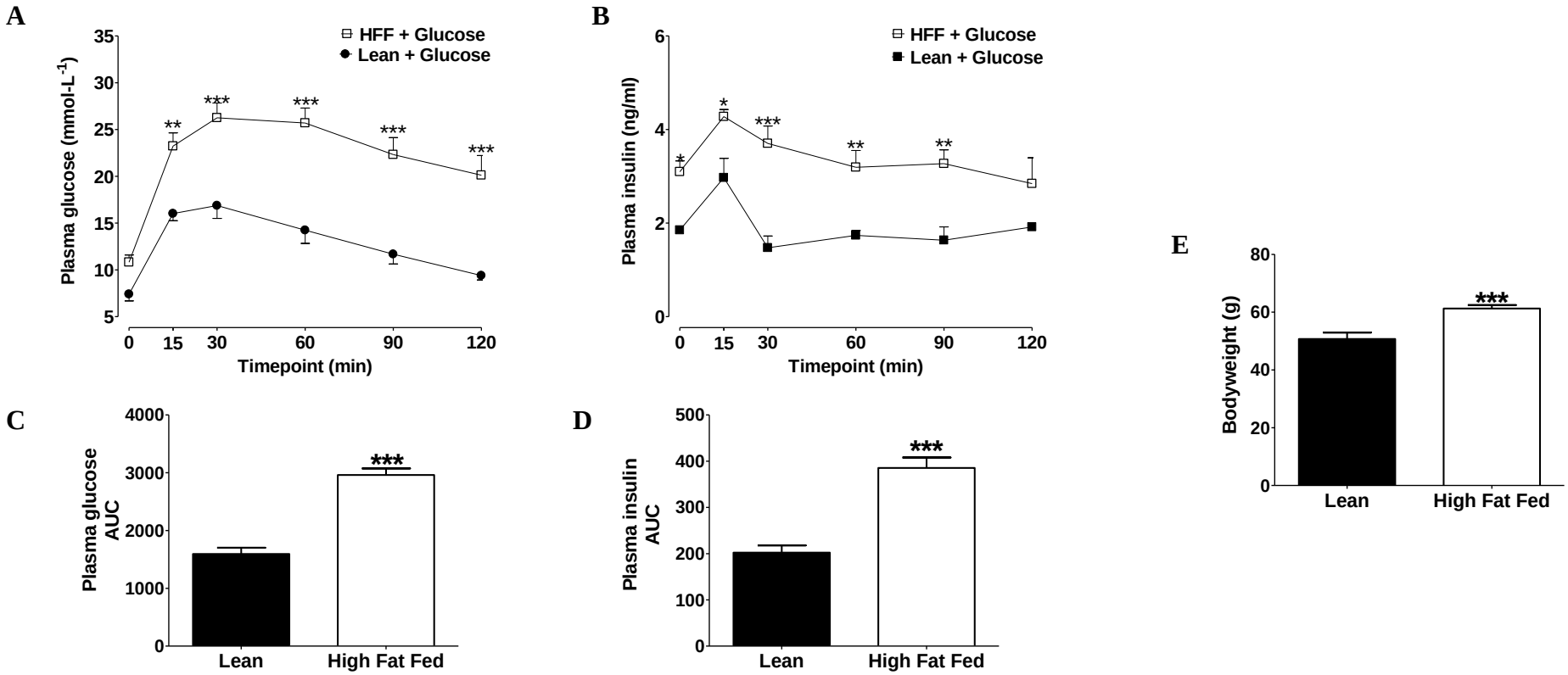

Swiss TO mice were subjected to a high fat fed (HFF) diet for four months to induce an insulin resistance and glucose intolerance. To confirm the diabetic phenotype of the model, animals were subjected to an oral glucose tolerance test (18 mmol/kg bw) with (A, C) glucose tolerance, (B, D) insulin secretory response and (E) bodyweight determined. Results are the mean ± SEM (n=6). *p<0.05, **p<0.01, ***p<0.001 compared to lean control.

Figure 6.2: Acute effect of ALA on plasma glucose in 18 h fasted high fat fed diabetic mice.

A

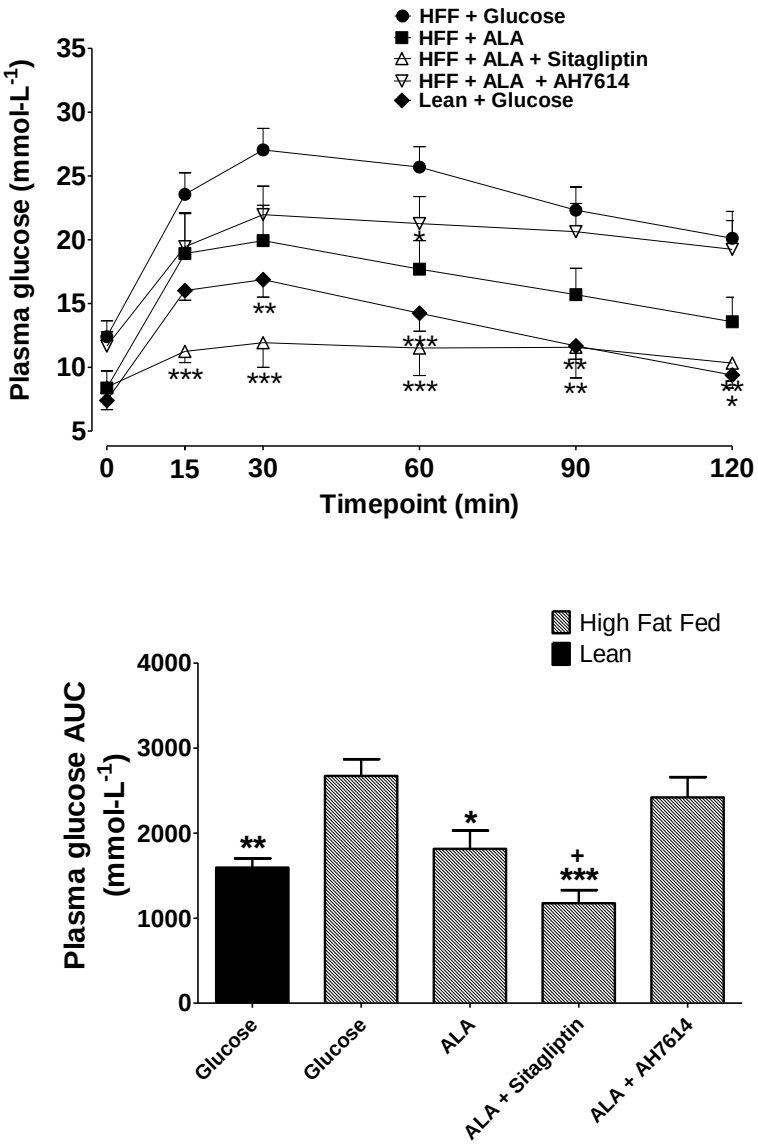

Acute effect of ALA on plasma glucose (A) and respective AUC (B). Glucose (18 mmol/kg bw) was administered orally alone or in combination with ALA (0.1µmol/kg bw) and either the GPR120 antagonist AH7614 (0.1µmol/kg bw) or Sitagliptin (50 mg/kg bw) to HFF mice (n = 6). Values are presented as mean ± SEM. *p<0.05, **p<0.01, ***p<0.001, compared to HFF glucose control. +p<0.05, compared to agonist alone.

Figure 6.3: Acute effect of ALA on plasma insulin in 18 h fasted high fat fed diabetic mice.

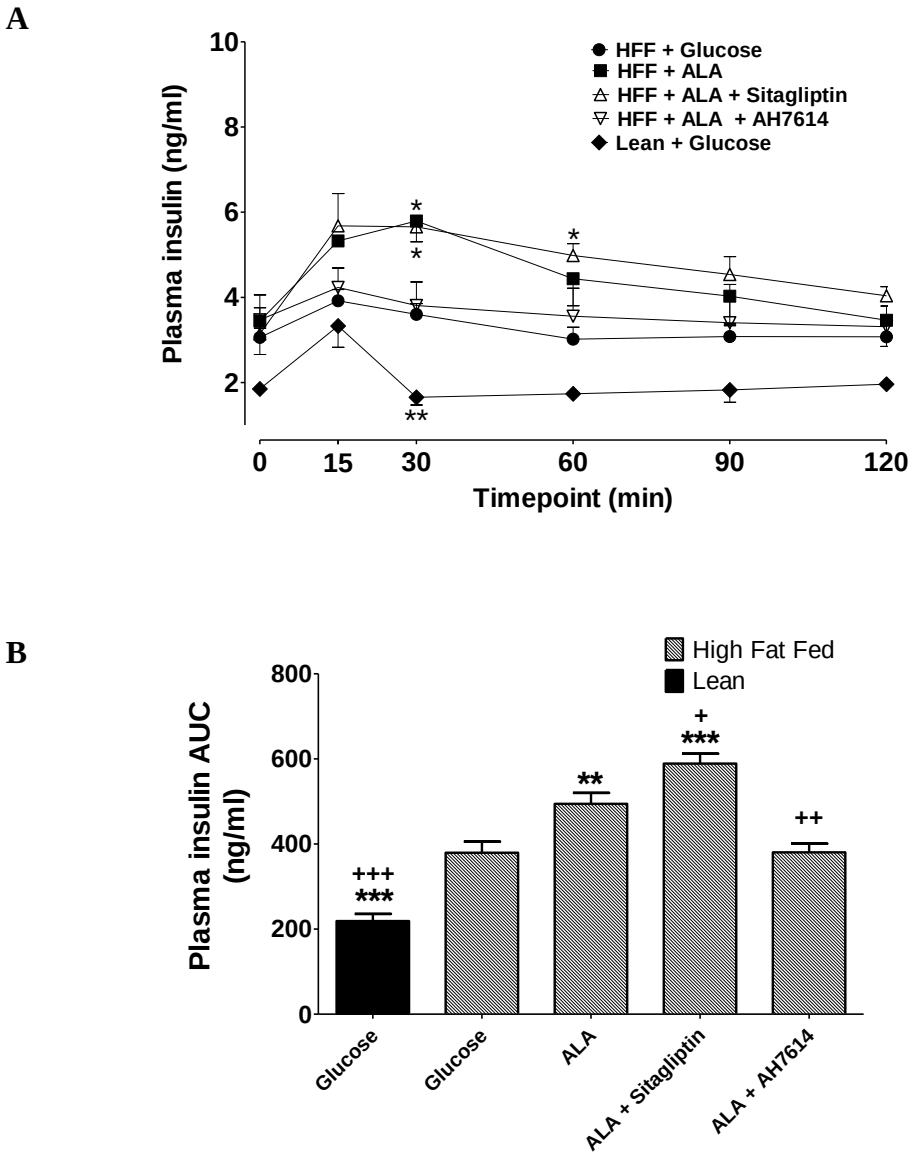

Acute effect of ALA on plasma insulin (A) and respective AUC (B). Glucose (18 mmol/kg bw) was administered orally alone or in combination with ALA (0.1µmol/kg bw) and either the GPR120 antagonist AH7614 (0.1 µmol/kg bw) or Sitagliptin (50 mg/kg bw) to HFF mice (n = 6). Values are presented as mean ± SEM. *p<0.05, **p<0.01, ***p<0.001, compared to HFF glucose control. +p<0.01, ++p<0.05, +++p<0.001, compared to agonist alone.

Figure 6.4: Acute effect of GW9508 on plasma glucose in 18 h fasted high fat fed diabetic mice.

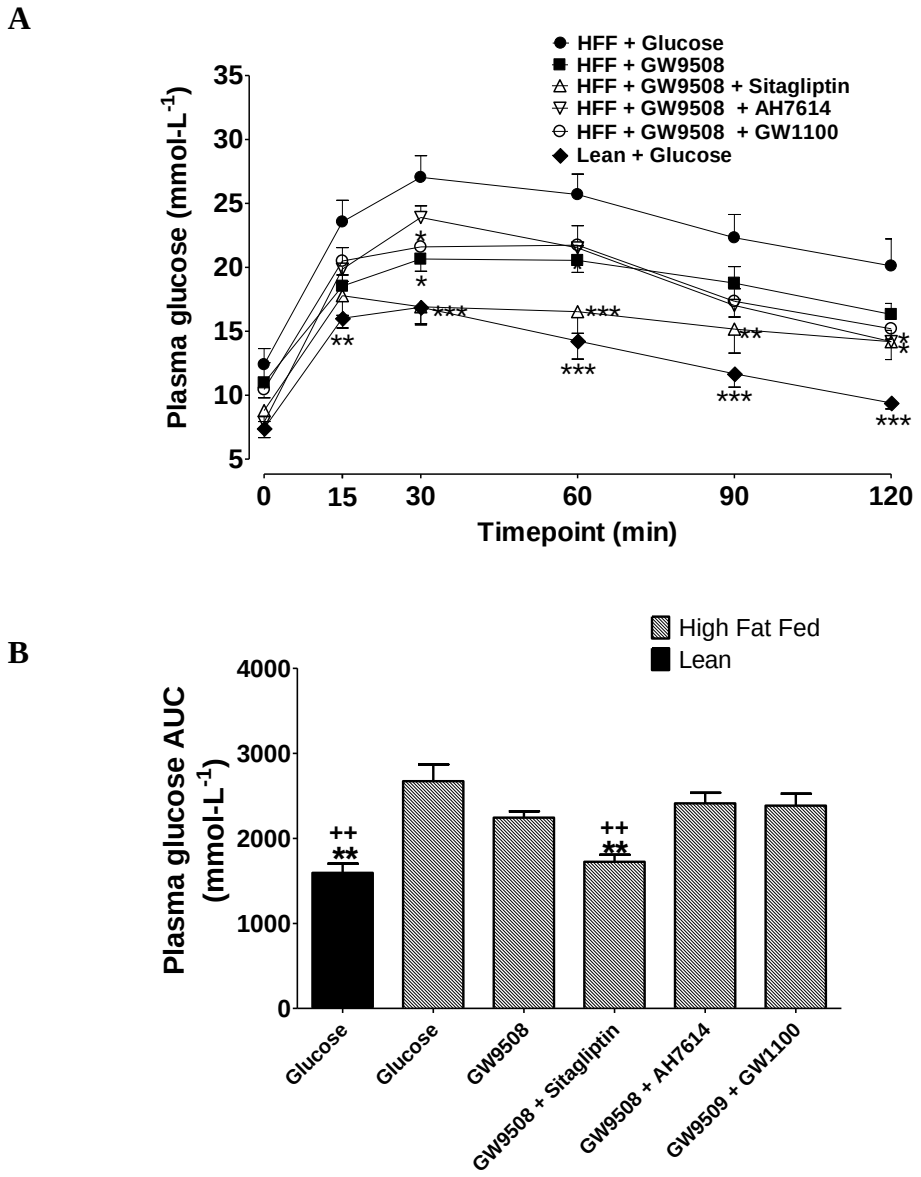

Acute effect of GW9508 on plasma glucose (A) and respective AUC (B). Glucose (18 mmol/kg bw) was administered orally alone or in combination with GW9508 (0.1µmol/kg bw) and either the GPR120 antagonist AH7614 (0.1µmol/kg bw), GPR40 antagonist GW1100 (0.1µmol/kg bw) or Sitagliptin (50 mg/kg bw) to HFF mice (n = 6). Values are presented as mean ± SEM. *p<0.05, **p<0.01, ***p<0.001, compared to HFF glucose control. ++p<0.01, compared to agonist alone.

Figure 6.5: Acute effect of GW9508 on plasma insulin in 18 h fasted high fat fed diabetic mice.

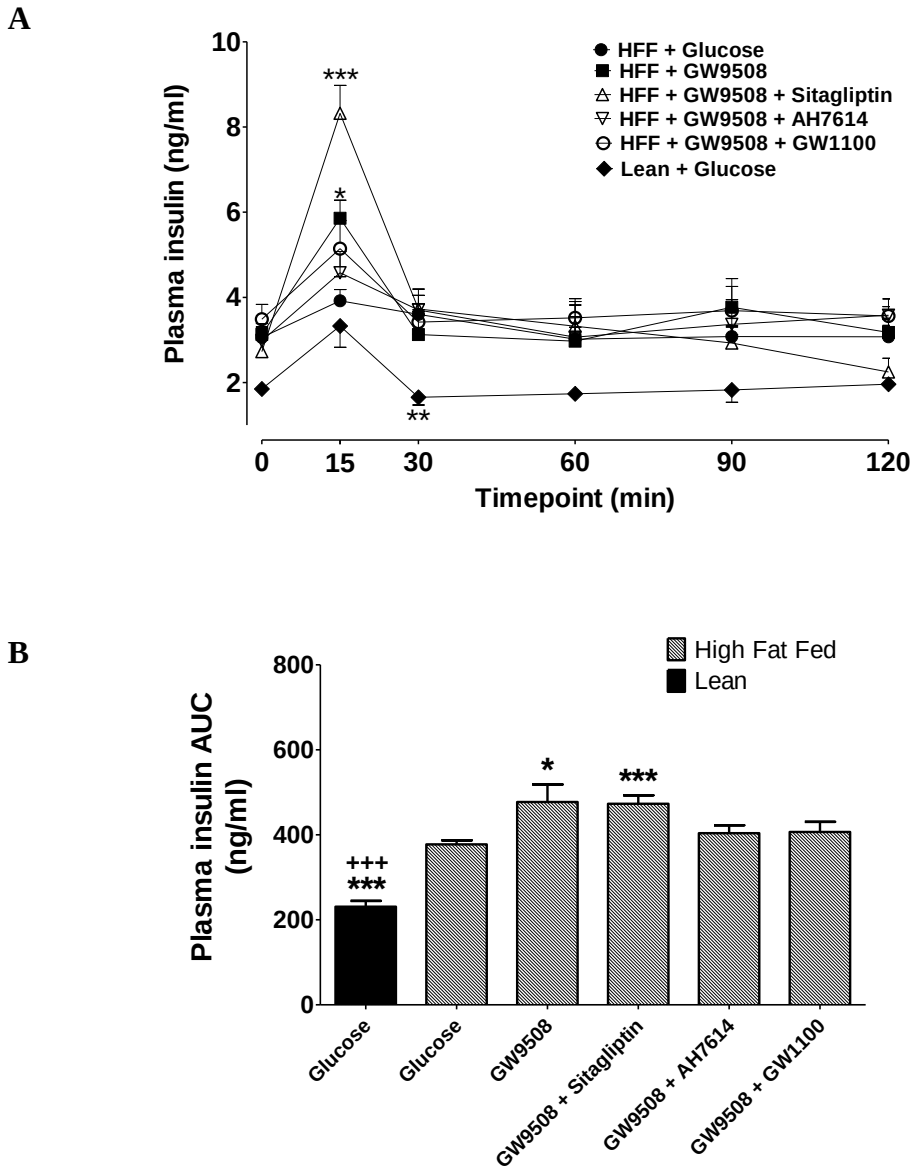

Acute effect of GW9508 on plasma insulin (A) and respective AUC (B). Glucose (18 mmol/kg bw) was administered orally alone or in combination with GW9508 (0.1µmol/kg bw) and either the GPR120 antagonist AH7614 (0.1µmol/kg bw), GPR40 antagonist GW1100 (0.1µmol/kg bw) or Sitagliptin (50 mg/kg bw) to HFF mice (n = 6). Values are presented as mean ± SEM. *p<0.05, **p<0.01, ***p<0.001, compared to HFF glucose control. +++p<0.001, compared to agonist alone.

Figure 6.6: Acute effect of GSK137647 on plasma glucose in 18 h fasted high fat fed diabetic mice.

A

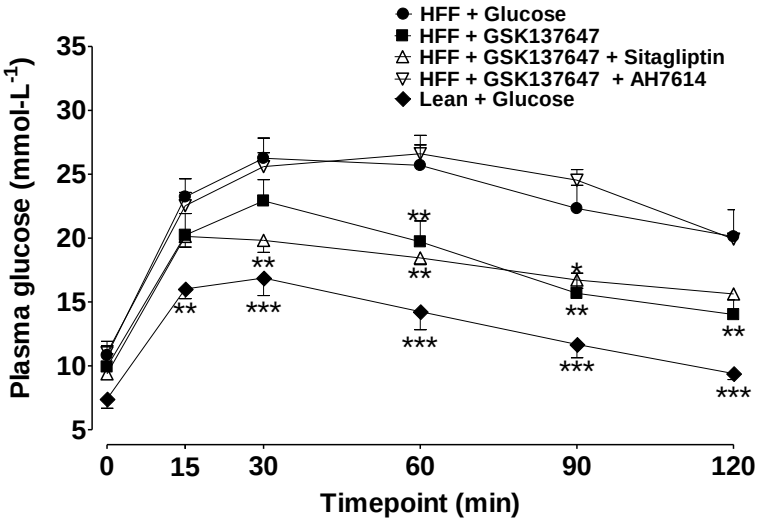

B

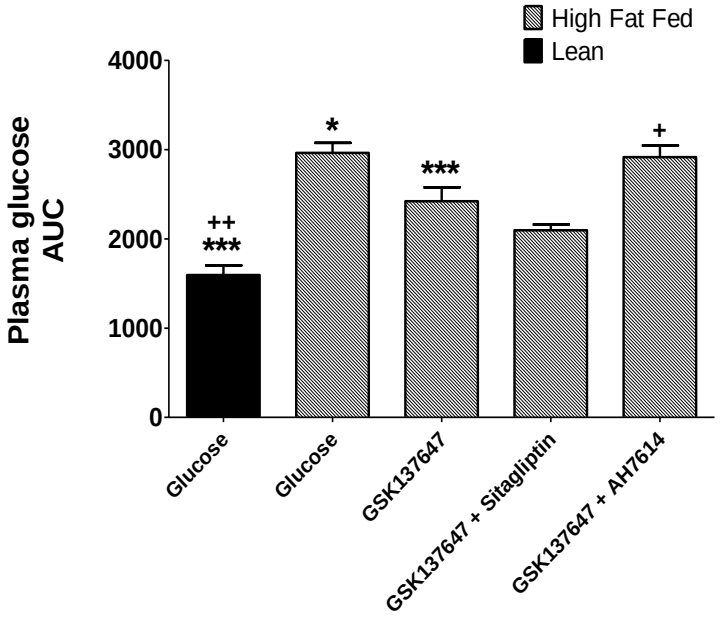

Acute effect of GSK137647 on plasma glucose (A) and respective AUC (B). Glucose (18 mmol/kg bw) was administered orally alone or in combination with GSK137647 (0.1µmol/kg bw) and either the GPR120 antagonist AH7614 (0.1µmol/kg bw) or Sitagliptin (50 mg/kg bw) to HFF mice (n = 6). Values are presented as mean ± SEM. *p<0.05, **p<0.01, ***p<0.001, compared to HFF glucose control. +p<0.05, ++p<0.01, compared to agonist alone.

Figure 6.7: Acute effect of GSK137647 on plasma insulin in 18 h fasted high fat fed diabetic mice.

A

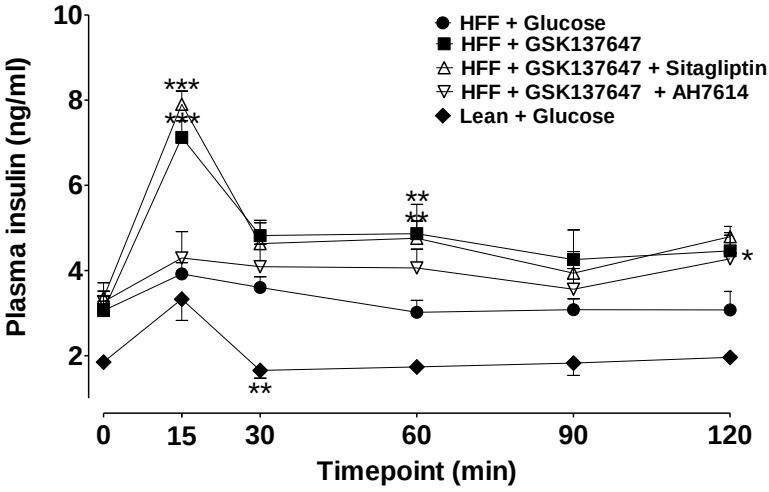

B

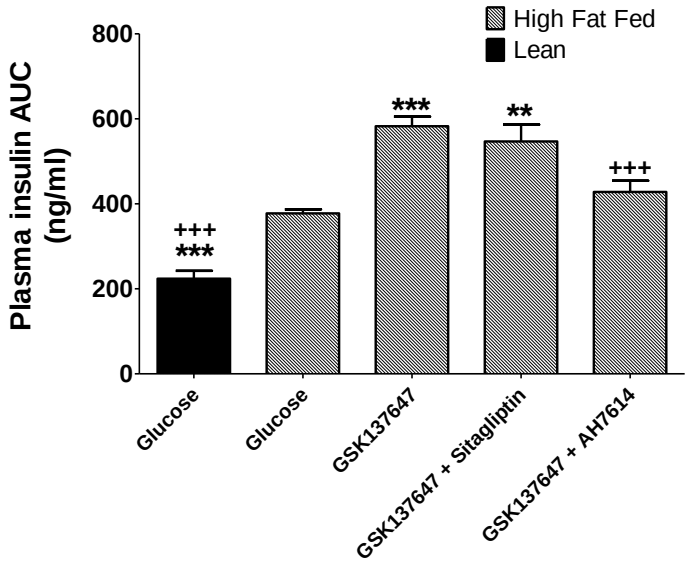

Acute effect of GSK137647 on plasma insulin (A) and respective AUC (B). Glucose (18 mmol/kg bw) was administered orally alone or in combination with GSK137647 (0.1µmol/kg bw) and either the GPR120 antagonist AH7614 (0.1µmol/kg bw) or Sitagliptin (50 mg/kg bw) to HFF mice (n = 6). Values are presented as mean ± SEM. *p<0.05, **p<0.01, ***p<0.001, compared to HFF glucose control. +++p<0.001, compared to agonist alone.

Figure 6.8: Acute effect of Compound A on plasma glucose in 18 h fasted high fat fed diabetic mice.

A

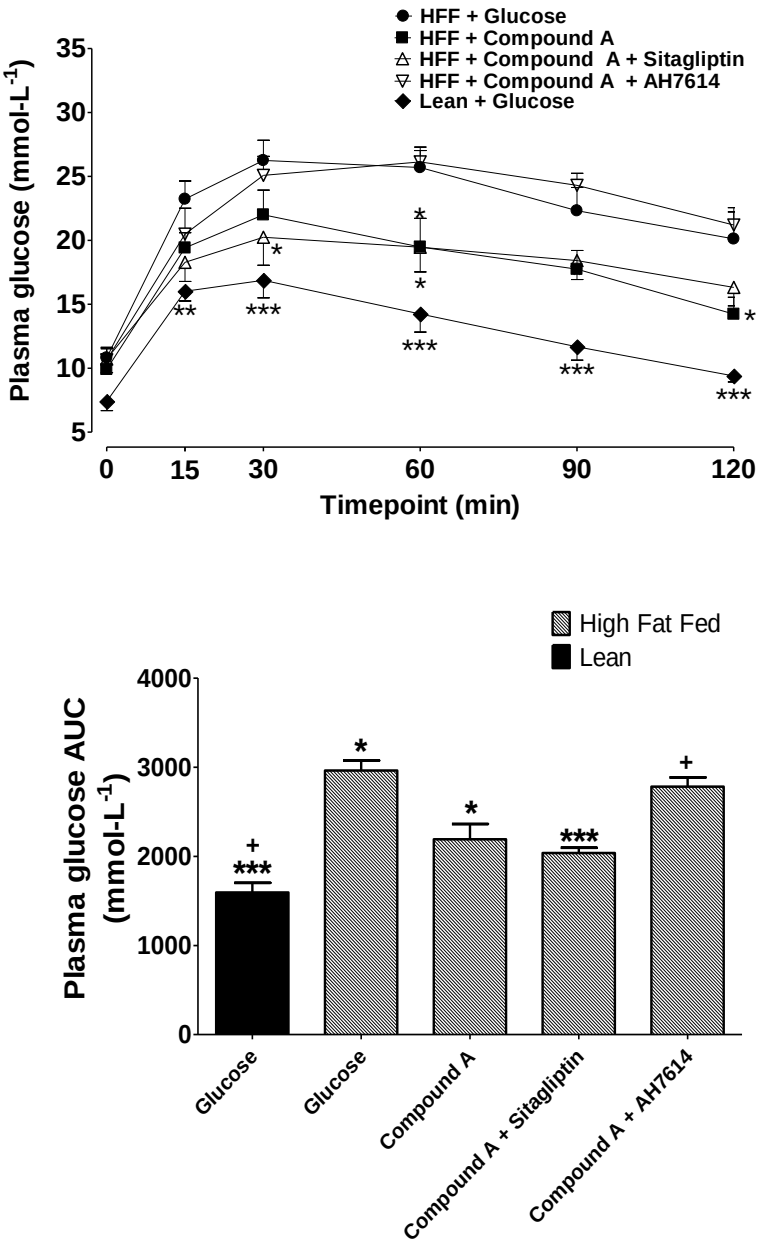

Acute effect of Compound A on plasma glucose (A) and respective AUC (B). Glucose (18 mmol/kg bw) was administered orally alone or in combination with GSK137647 (0.1µmol/kg bw) and either the GPR120 antagonist AH7614 (0.1µmol/kg bw) or Sitagliptin (50 mg/kg bw) to HFF mice (n = 6). Values are presented as mean ± SEM. *p<0.05, **p<0.01, ***p<0.001, compared to HFF glucose control. +p<0.05, compared to agonist alone.

Figure 6.9: Acute effect of Compound A on plasma insulin in 18 h fasted high fat fed diabetic mice.

A

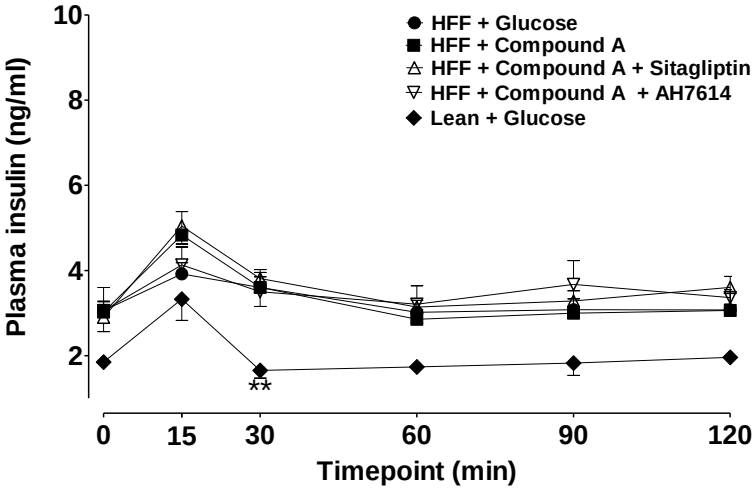

B

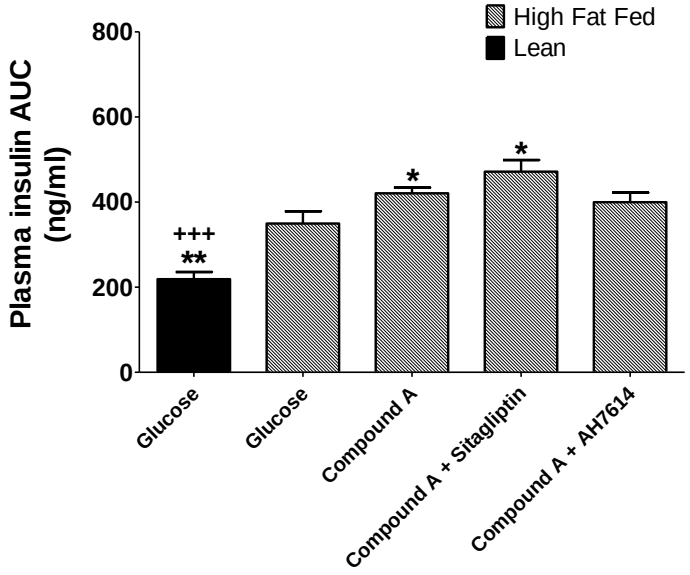

Acute effect of Compound A on plasma insulin (A) and respective AUC (B). Glucose (18 mmol/kg bw) was administered orally alone or in combination with Compound A (0.1µmol/kg bw) and either the GPR120 antagonist AH7614 (0.1µmol/kg bw) or Sitagliptin (50 mg/kg bw) to HFF mice (n = 6). Values are presented as mean ± SEM. *p<0.05, **p<0.01, compared to HFF glucose control. +++p<0.001, compared to agonist alone.

Figure 6.10: Acute effects of GPR120 agonists on total plasma GLP-1 in 18 h fasted high fat fed diabetic mice.

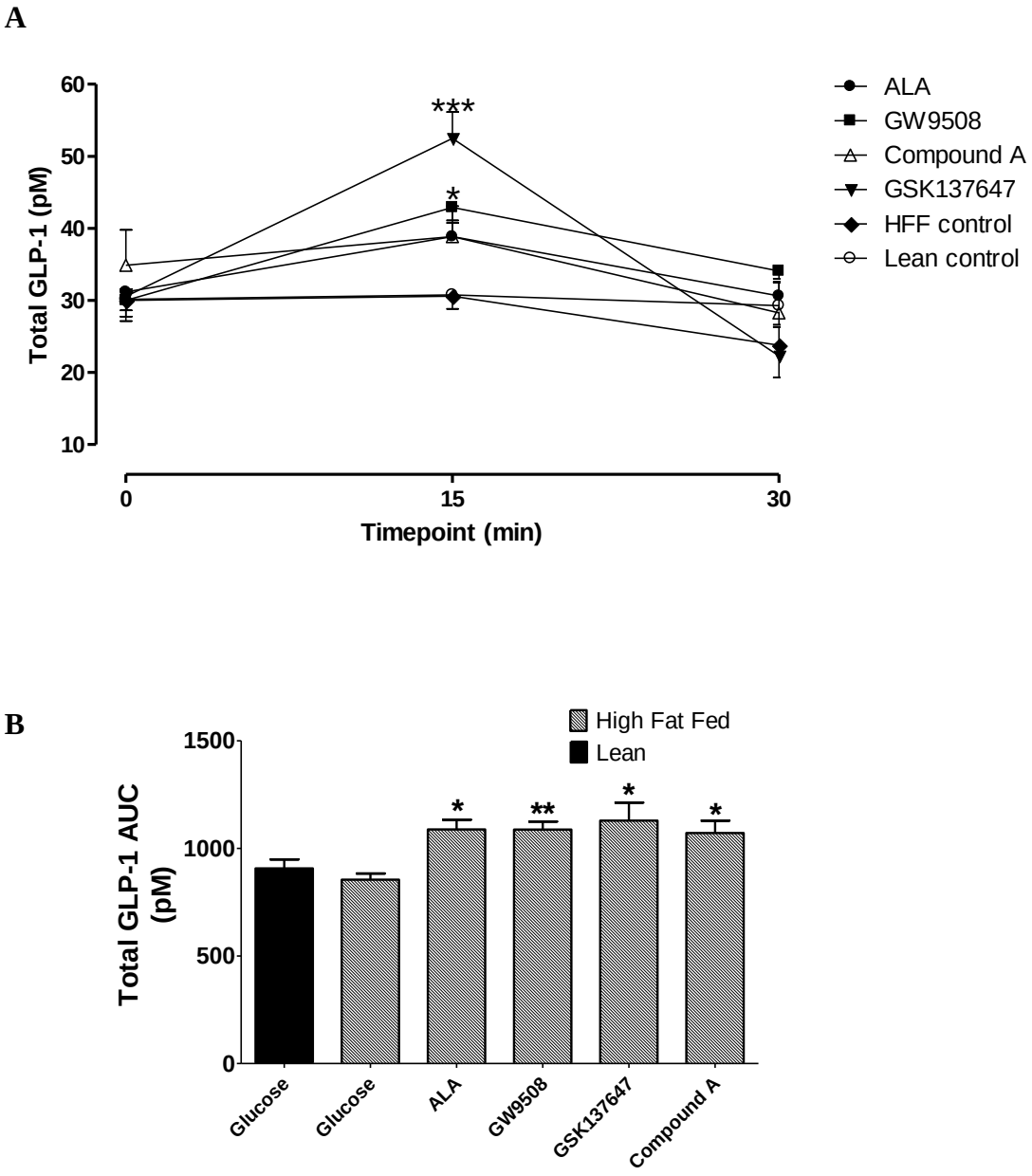

Acute effects of GPR120 agonists on total plasma GLP-1 (A) and respective AUC (B). Glucose (18 mmol/kg bw) was administered orally alone or in combination with GPR120 agonists (0.1µmol/kg bw) to HFF mice (n = 6). Values are presented as mean ± SEM. *p<0.05, **p<0.01, ***p<0.001, compared to HFF glucose control.

Figure 6.11: Acute effects of GPR120 agonists on total plasma GIP in 18 h fasted high fat fed diabetic mice.

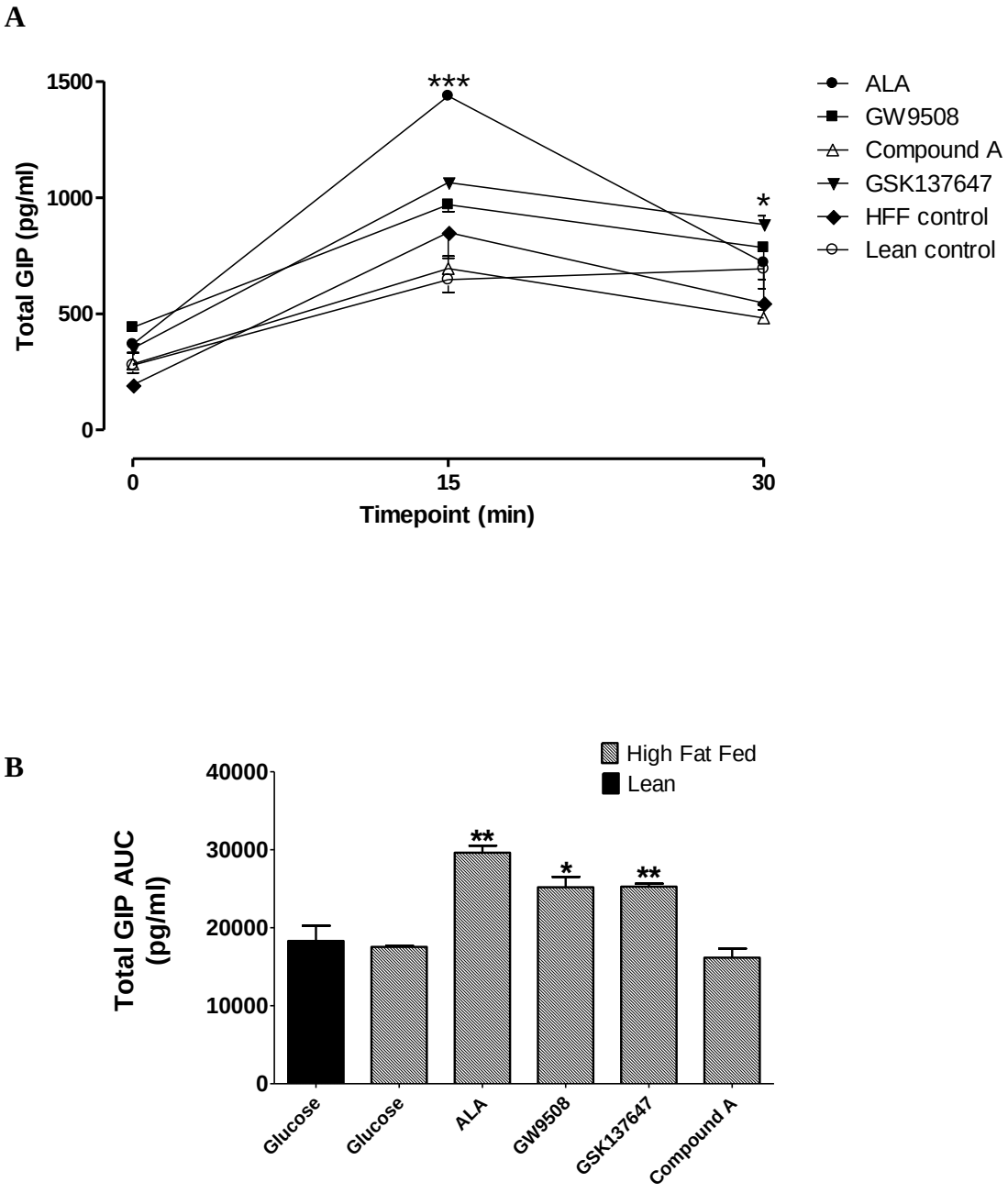

Acute effects of GPR120 agonists on total plasma GIP (A) and respective AUC (B). Glucose (18 mmol/kg bw) was administered orally alone or in combination with GPR120 agonists (0.1µmol/kg bw) to HFF mice (n = 6). Values are presented as mean ± SEM. *p<0.05, **p<0.01, ***p<0.001, compared to HFF glucose control.

Figure 6.12: Acute effects of GPR120 agonists and Sitagliptin on DPP-IV activity in 18 h fasted high fat fed diabetic mice.

A

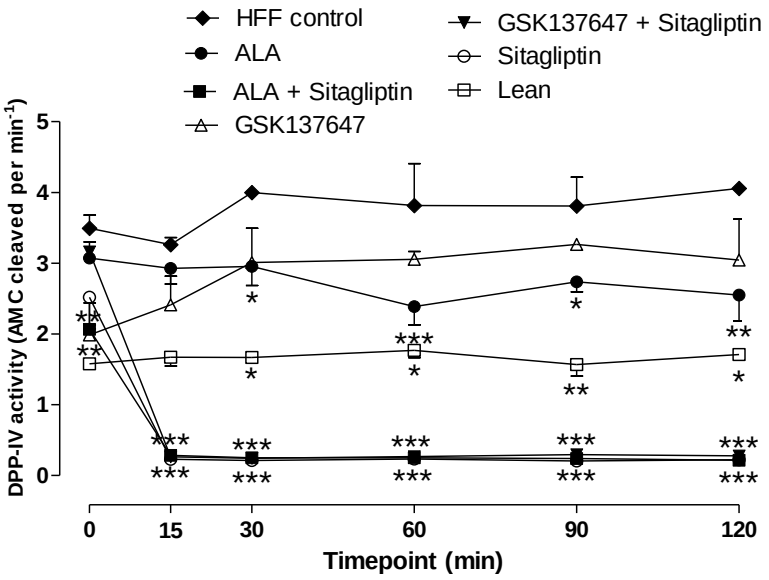

B

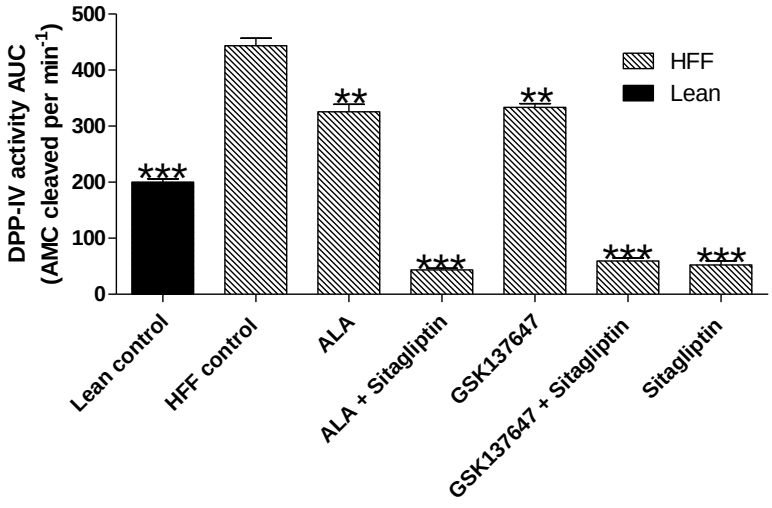

Acute effects of GPR120 agonists on DPP-IV activity (A) and respective AUC (B). Glucose (18 mmol/kg bw) was administered orally alone or in combination with GPR120 agonists (0.1µmol/kg bw) to HFF mice (n = 6). Values are presented as mean ± SEM. *p<0.05, **p<0.01, ***p<0.001 compared to HFF glucose control.

Figure 6.13: Chronic effect of once daily oral administration of ALA monotherapy and combinational therapy (sitagliptin) on bodyweight in high fat fed diabetic mice.

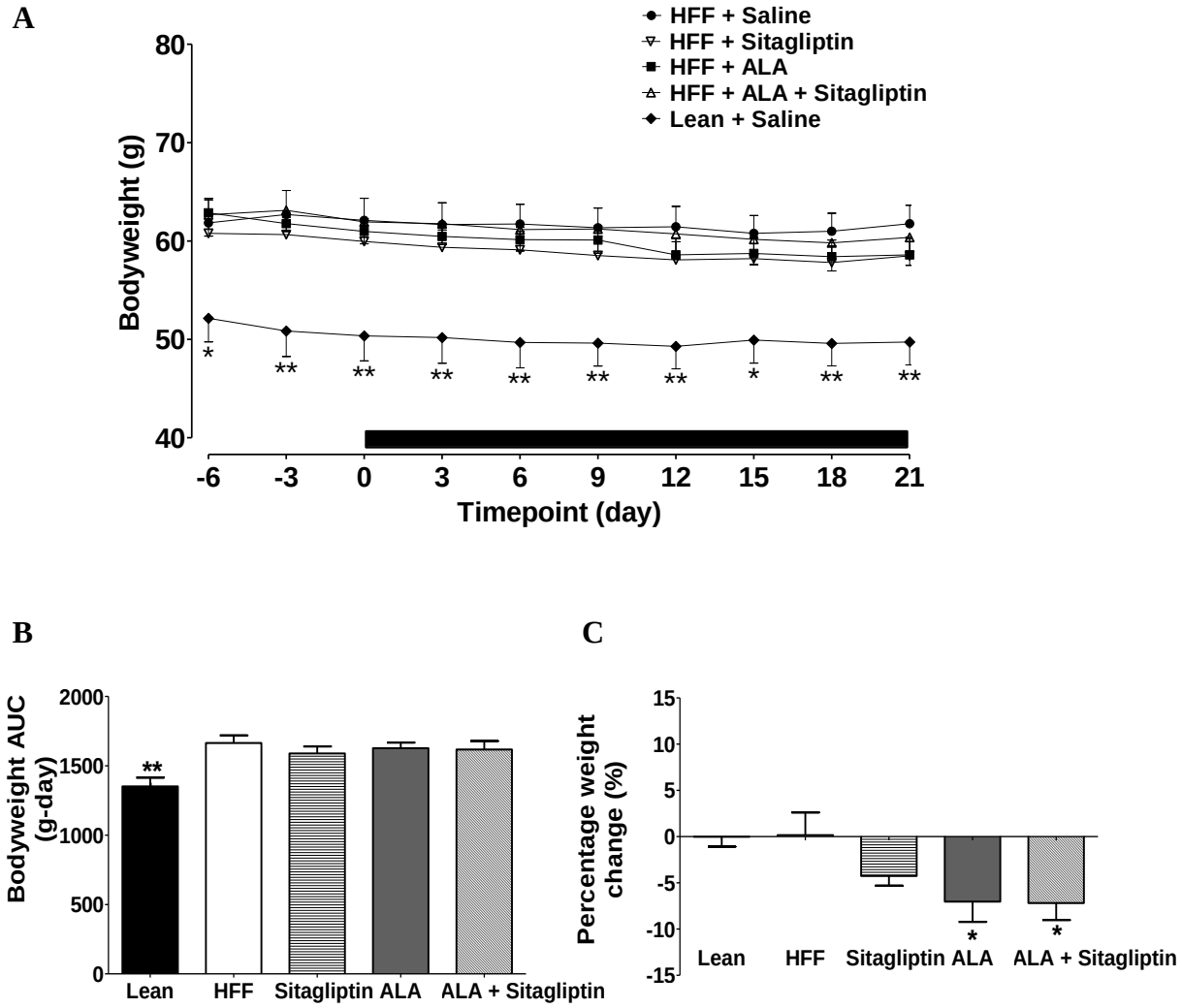

Chronic effect of ALA alone and in combination with Sitagliptin on (A) bodyweight, (B) respective AUC and (C) percentage weight change. Bodyweight measurements were obtained before and during ALA (0.1 µmol/kg bw) and Sitagliptin (50 mg/kg bw) therapies (indicated by the black bar). Values are presented as mean ± SEM (n = 8). *p<0.05, **p<0.01, compared to HFF control.

Figure 6.14: Chronic effect of once daily oral administration of ALA monotherapy and combinational therapy (Sitagliptin) for 21 days on plasma glucose in high fat fed diabetic mice.

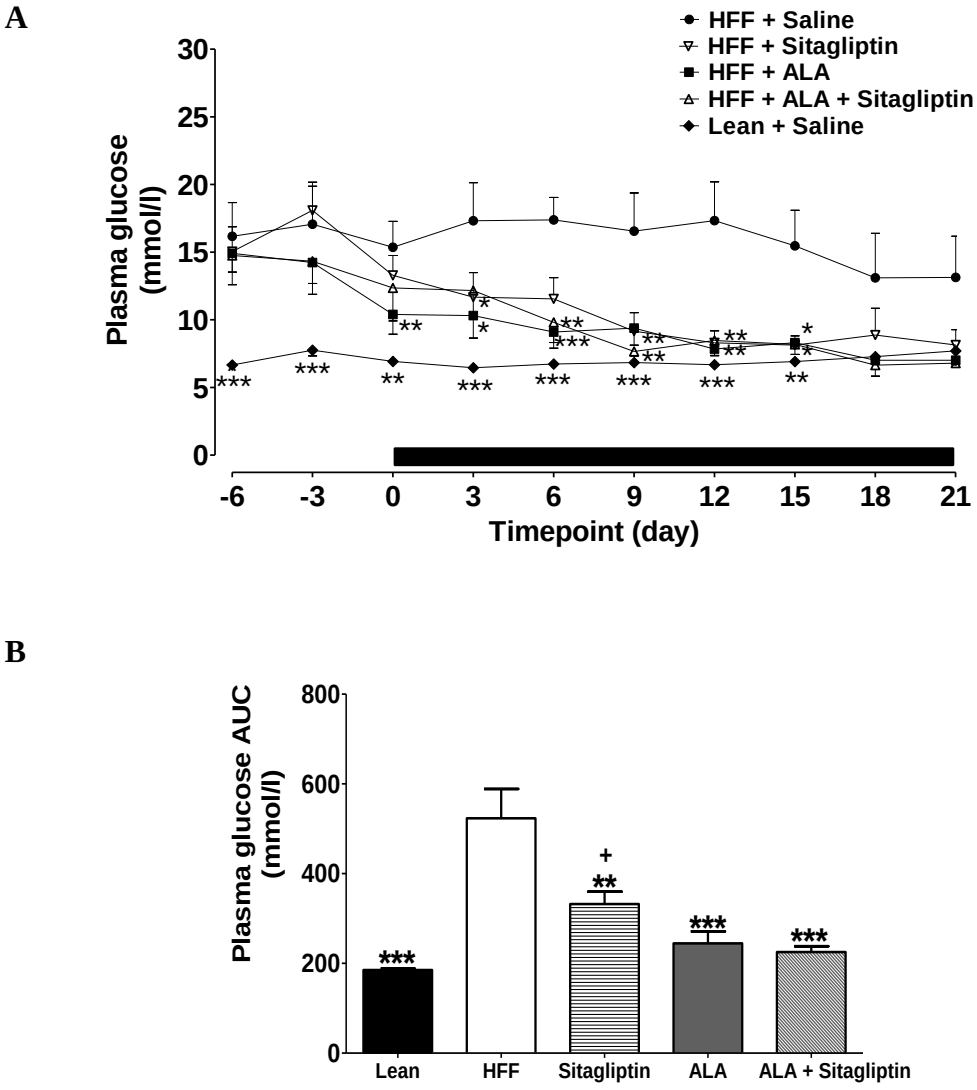

Chronic effect of ALA alone and in combination with Sitagliptin on (A) plasma glucose and (B) respective AUC. Parameters were obtained before and during ALA (0.1µmol/kg bw) and Sitagliptin (50 mg/kg bw) therapies (indicated by the black bar). Values are presented as mean ± SEM (n = 8). *p<0.05, **p<0.01, ***p<0.001, compared to HFF control. +p<0.05, compared to ALA alone.

Figure 6.15: Chronic effect of once daily oral administration of ALA monotherapy and combinational therapy (Sitagliptin) for 21 days on plasma insulin concentrations in high fat fed diabetic mice.

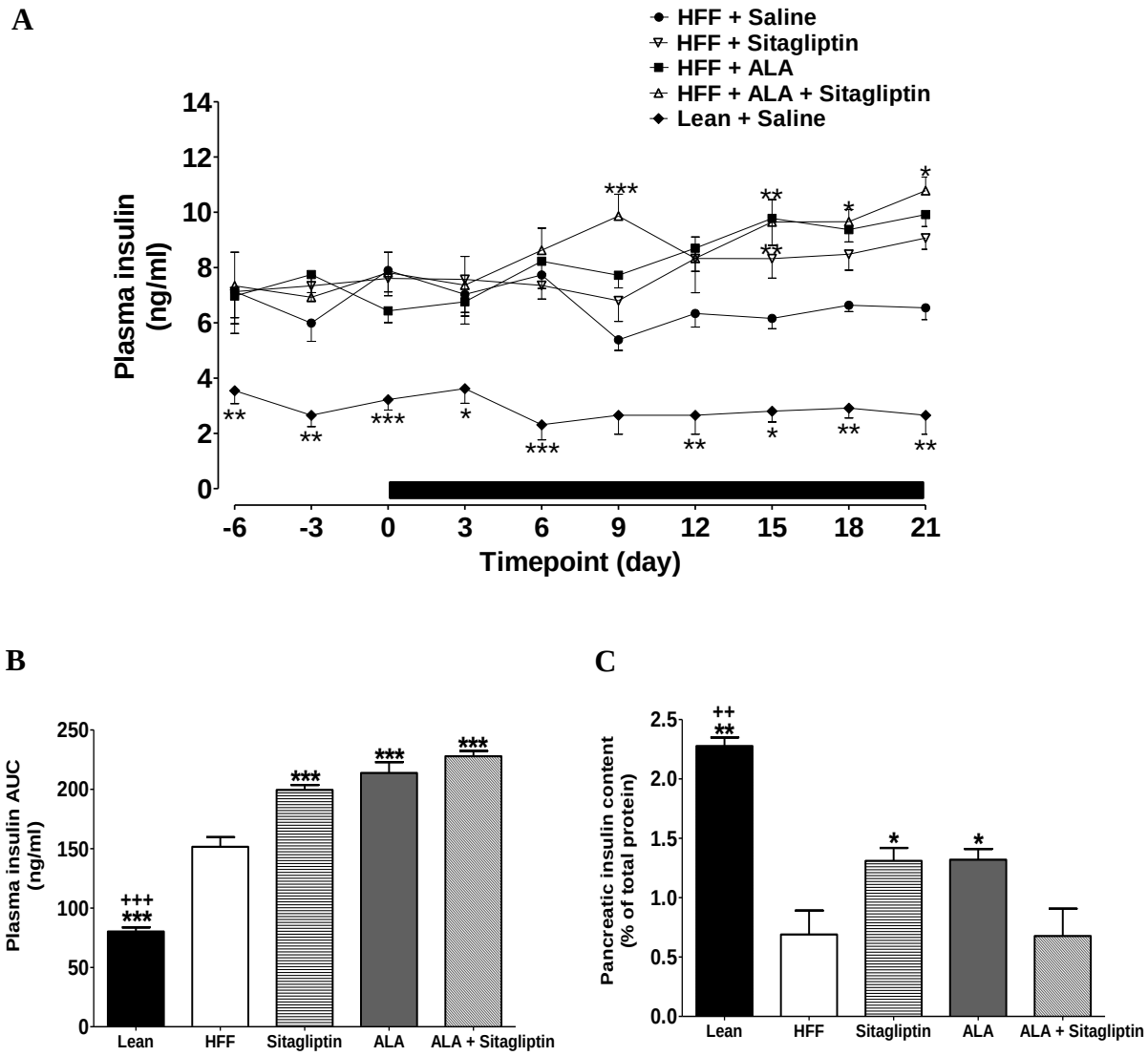

Chronic effect of ALA alone and in combination with Sitagliptin on (A) plasma insulin, (B) respective AUC and (C) pancreatic insulin content. Parameters were obtained before and during ALA (0.1µmol/kg bw) and Sitagliptin (50 mg/kg bw) therapies (indicated by the black bar). Insulin content was determined after 21-day treatment. Values are presented as mean ± SEM (n = 8). *p<0.05, **p<0.01, ***p<0.001, compared to HFF control. +++p<0.001, compared to ALA alone.

Figure 6.16: Chronic effect of once daily oral administration of ALA monotherapy and combinational therapy (Sitagliptin) for 21 days on circulating total-GLP-1 in high fat fed diabetic mice.

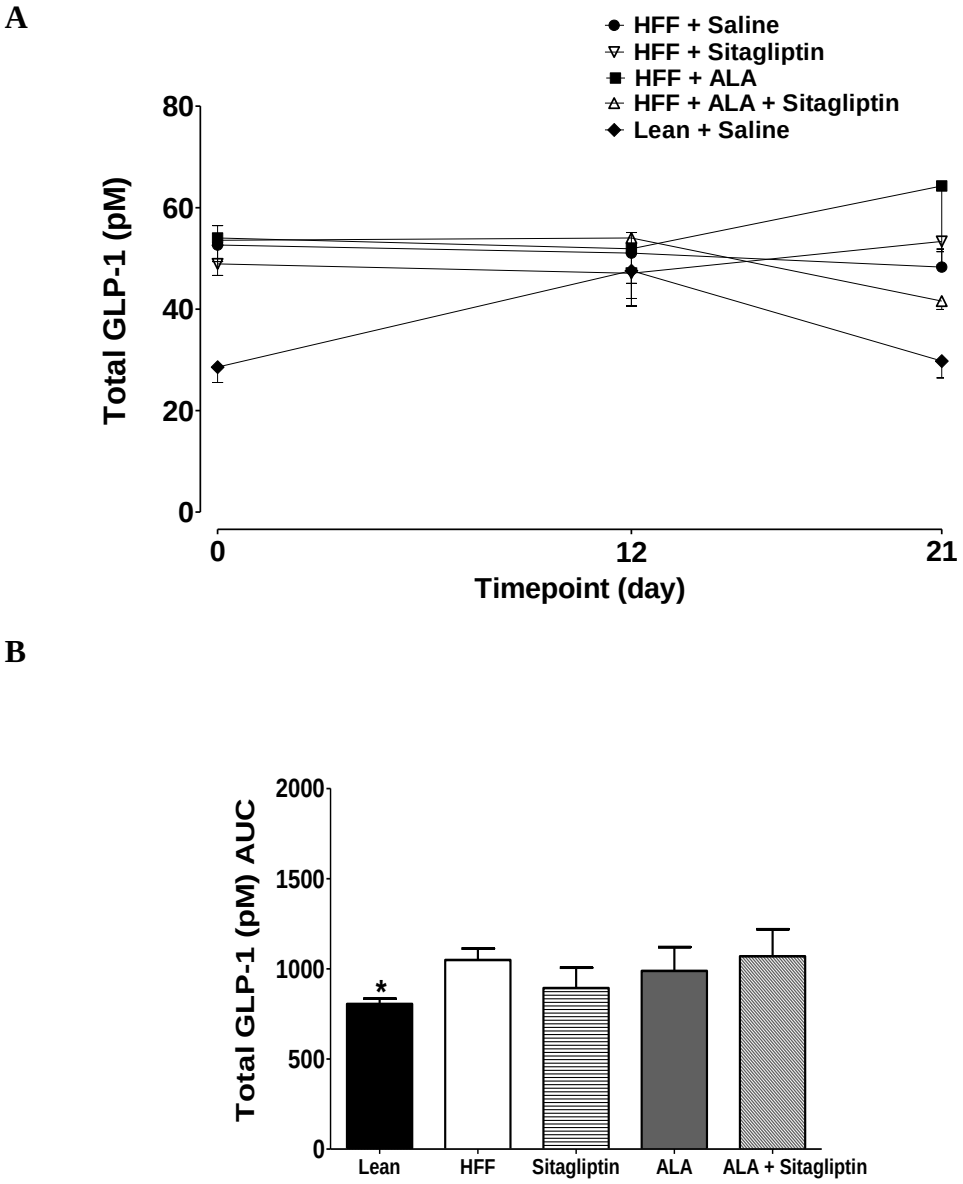

Chronic effect of ALA alone and in combination with Sitagliptin on (A) total-GLP-1 and (B) respective AUC. Parameters were obtained before and during ALA (0.1 µmol/kg bw) and Sitagliptin (50 mg/kg bw) therapies. Values are presented as mean ± SEM (n = 6). *p<0.05, compared to HFF control.

Figure 6.17: Chronic effect of once daily oral administration of ALA monotherapy and combinational therapy (Sitagliptin) for 21 days on circulating total-GIP in high fat fed diabetic mice.

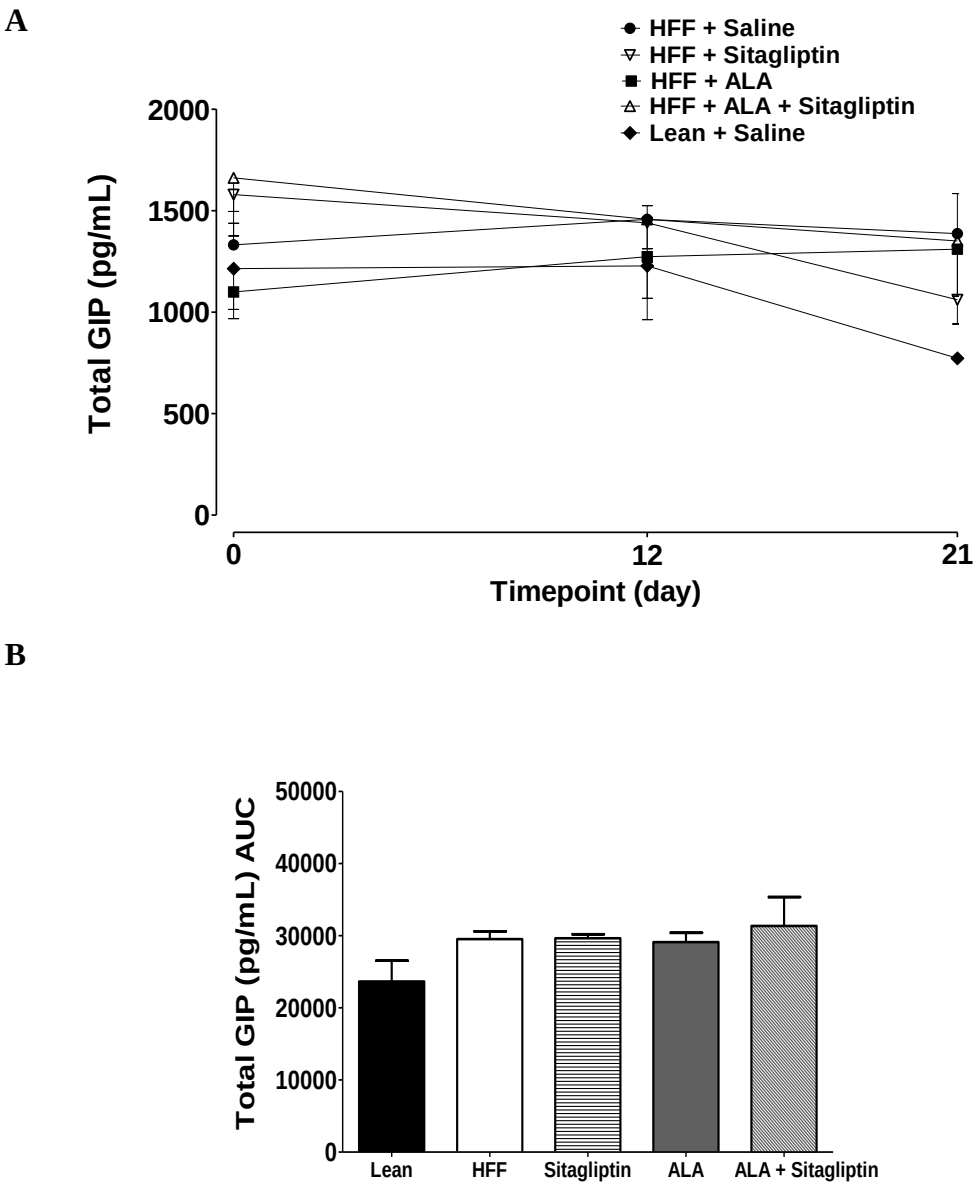

Chronic effect of ALA alone and in combination with Sitagliptin on (A) total-GIP and (B) respective AUC. Parameters were obtained before and during ALA (0.1 µmol/kg bw) and Sitagliptin (50 mg/kg bw) therapies. Values are presented as mean ± SEM (n = 6).

Figure 6.18: Chronic effect of once daily oral administration of ALA monotherapy and combinational therapy (Sitagliptin) for 21 days on DPP-IV activity in high fat fed diabetic mice.

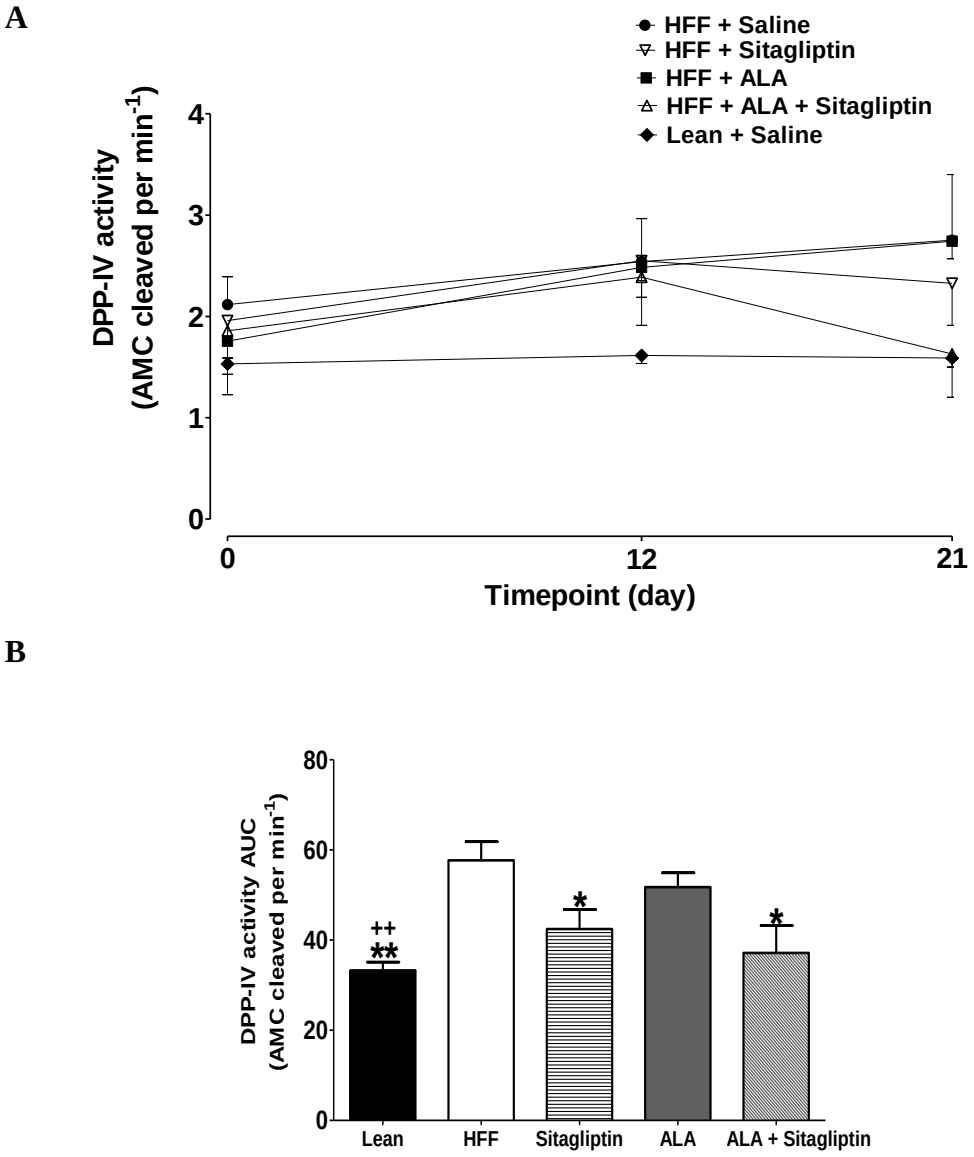

Chronic effect of ALA alone and in combination with Sitagliptin on (A) DPP-IV activity and (B) respective AUC. Parameters were obtained before and during ALA (0.1 µmol/kg bw) and Sitagliptin (50 mg/kg bw) therapies (indicated by the black bar). Values are presented as mean ± SEM (n = 8). *p<0.05, **p<0.01, compared to HFF control. ++p<0.05, compared to ALA alone.

Figure 6.19: Chronic effect of once daily oral administration of ALA monotherapy and combinational therapy (Sitagliptin) for 21 days on food intake in high fat fed diabetic mice.

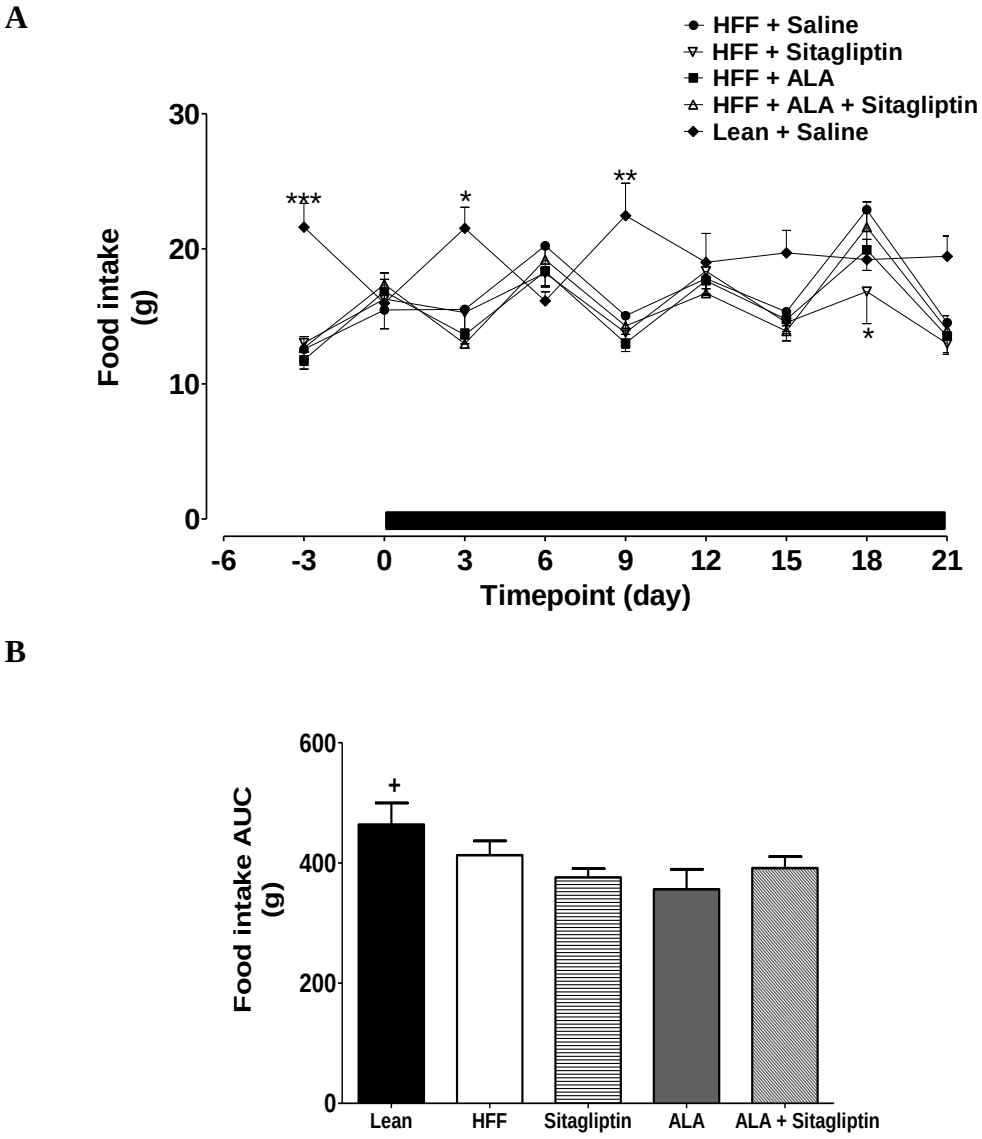

Chronic effect of ALA alone and in combination with Sitagliptin on (A) food intake and (B) respective AUC. Parameters were obtained before and during ALA (0.1µmol/kg bw) and Sitagliptin (50 mg/kg bw) therapies (indicated by the black bar). Values are presented as mean ± SEM (n = 8). *p<0.05, **p<0.01, ***p<0.001, compared to HFF control. +p<0.05, compared to ALA alone.

Figure 6.20: Chronic effect of once daily oral administration of ALA monotherapy and combinational therapy (Sitagliptin) for 21 days on cumulative food and energy intake in high fat fed diabetic mice.

A

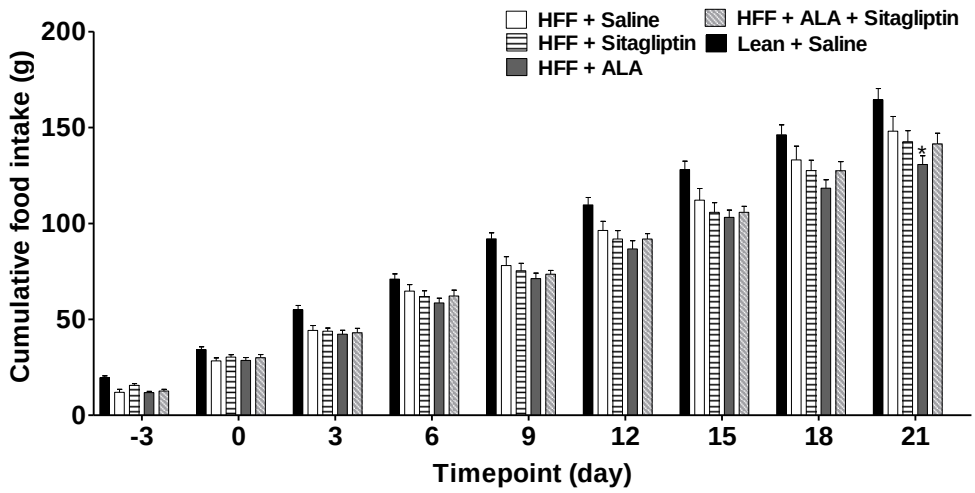

B

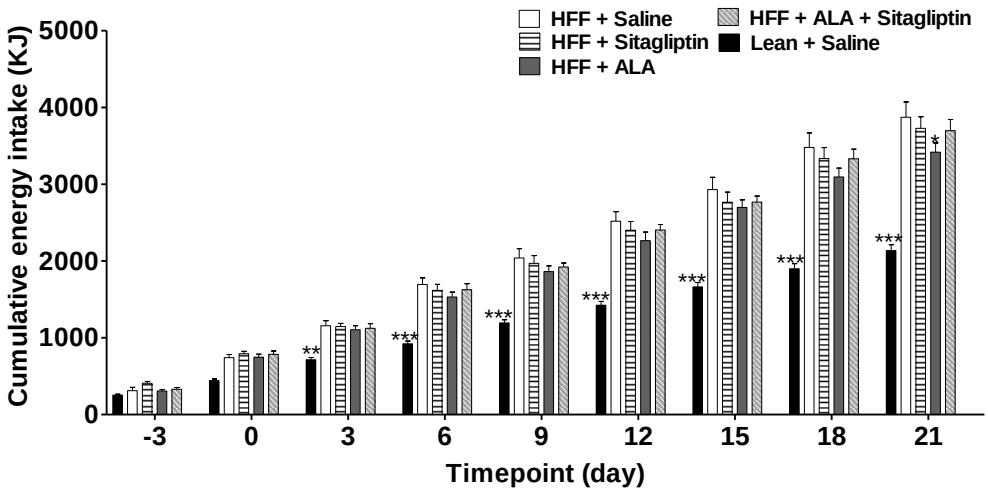

Chronic effect of ALA alone and in combination with Sitagliptin on (A) food intake and (B) energy intake. Parameters were obtained before and during ALA (0.1µmol/kg bw) and Sitagliptin (50 mg/kg bw) therapies (indicated by the black bar). Values are presented as mean ± SEM (n = 8). *p<0.05, **p<0.01, ***p<0.001, compared to HFF control.

Figure 6.21: Chronic effect of 21-day oral administration of ALA monotherapy and combinational therapy (Sitagliptin) on glucose tolerance and insulin secretion in high fat fed diabetic mice.

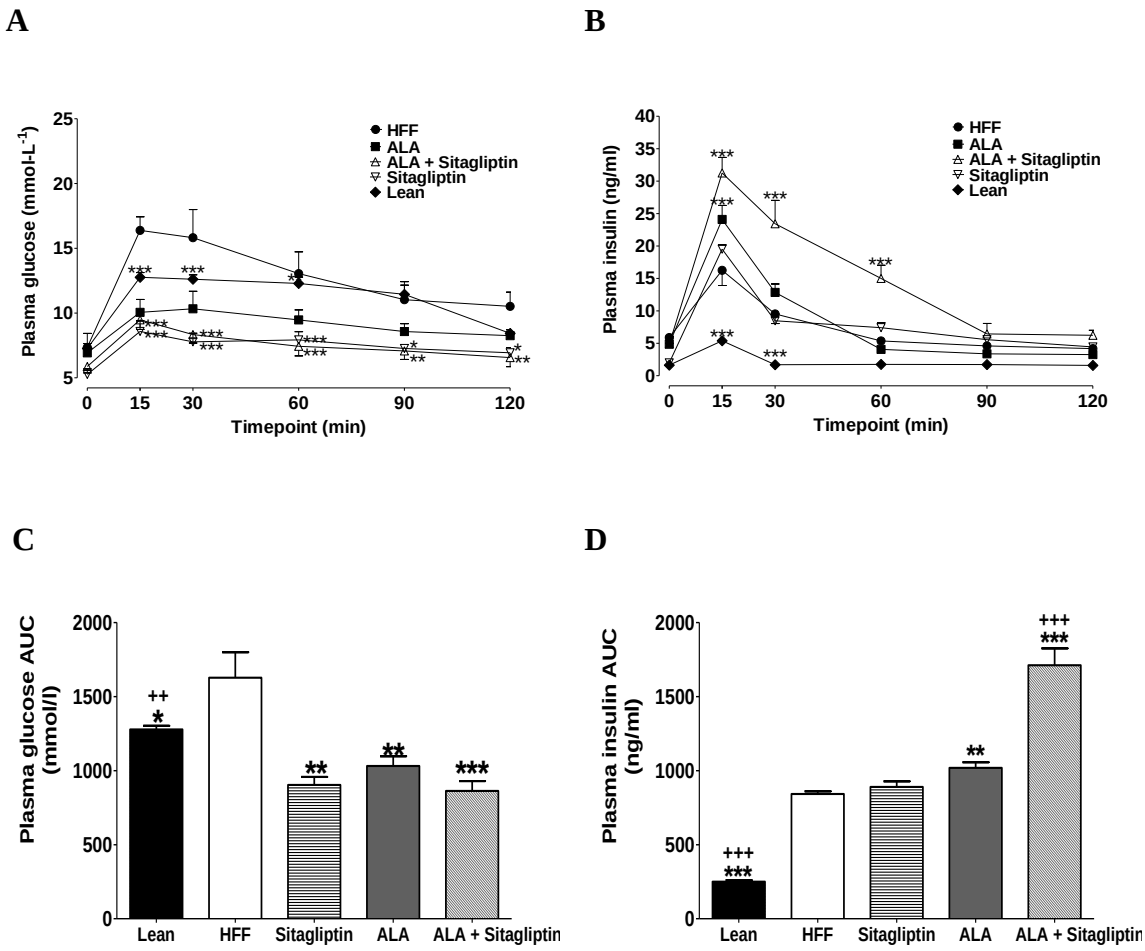

Oral glucose tolerance test (18 mmol/kg bw) was conducted on HFF mice following 21-day treatment with ALA (0.1µmol/kg bw) and/or Sitagliptin (50 mg/kg bw). (A, C) Plasma glucose and (B, D) plasma insulin were determined. Results are mean ± SEM (n=6). *p<0.05, **p<0.01, ***p<0.001, compared to HFF glucose control. ++p<0.01, +++p<0.001, compared to ALA alone.

Figure 6.22: Chronic effect of 21-day oral administration of ALA monotherapy and combinational therapy (Sitagliptin) on insulin sensitivity in high fat fed diabetic mice.

A

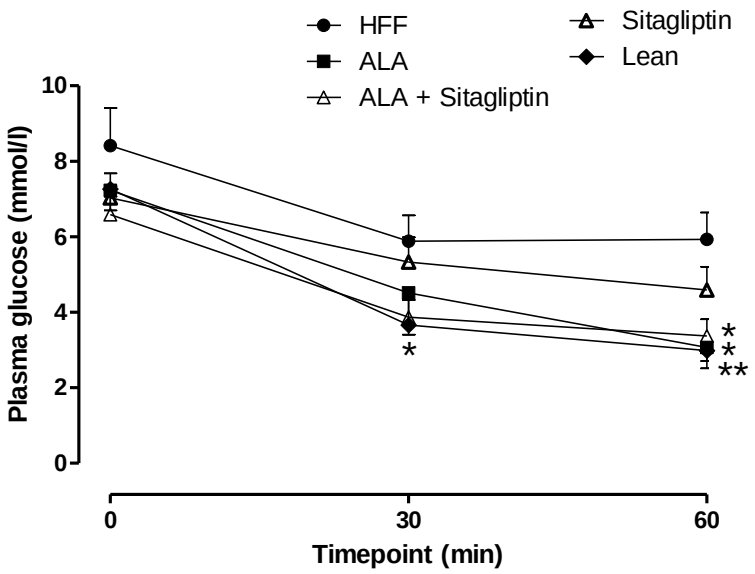

B

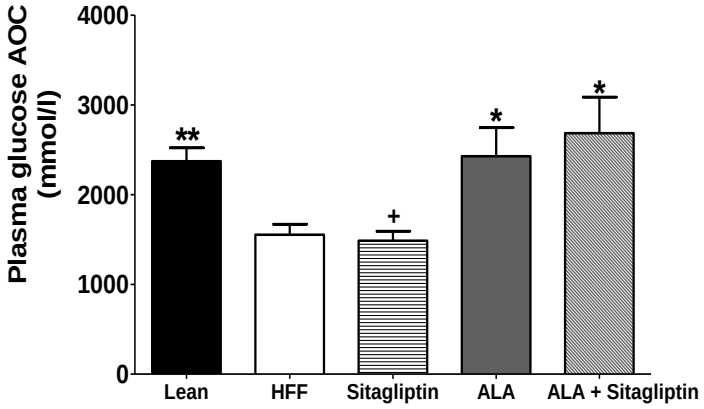

Insulin sensitivity (40U/kg bodyweight; dissolved in 0.9% saline, i.p. injection) test was conducted following 21-day treatment with ALA alone (0.1 µmol/kg bw) or in combination with Sitagliptin (50 mg/kg bw) to HFF diabetic mice. (A) Blood glucose and (B) respective AOC are shown. Results are mean ± SEM (n=8). *p<0.05, **p<0.01, compared to HFF control. +p<0.05, compared to ALA alone.

Figure 6.23: Chronic effect of 21-day oral administration of ALA monotherapy and combinational therapy (Sitagliptin) on bodyweight, fat mass and lean mass as measured by DEXA in high fat fed diabetic mice.

A

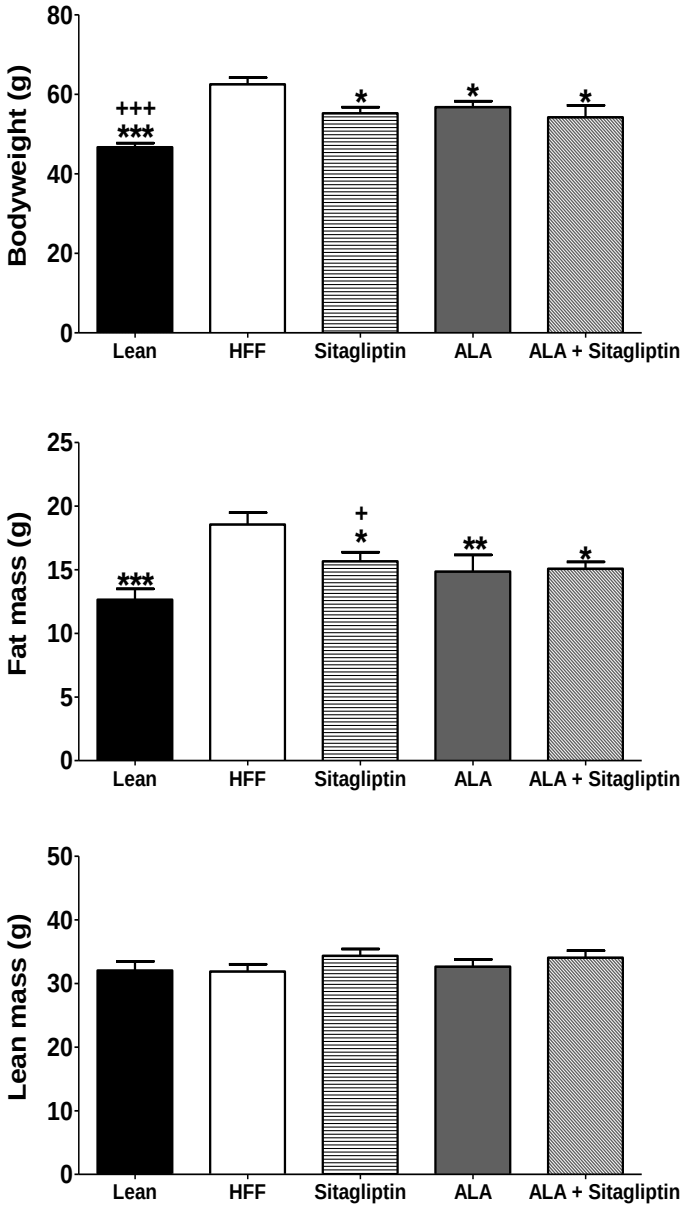

Chronic effect of 21-day oral administration of ALA (0.1 µmol/kg bw) alone and in combination with Sitagliptin (50 mg/kg bw) on (A) bodyweight, (B) fat mass and (C) lean mass in HFF diabetic mice. Values are presented as mean ± SEM (n = 8). *p<0.05, **p<0.01, ***p<0.001, compared to HFF control. +p<0.05, compared to ALA alone.

Figure 6.24: Chronic effect of 21-day oral administration of ALA monotherapy and combinational therapy (Sitagliptin) on total bone mineral content and bone mineral density as measured by DEXA in high fat fed diabetic mice.

A

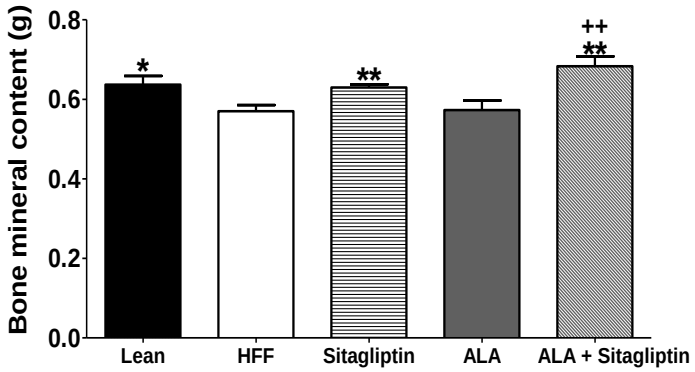

B

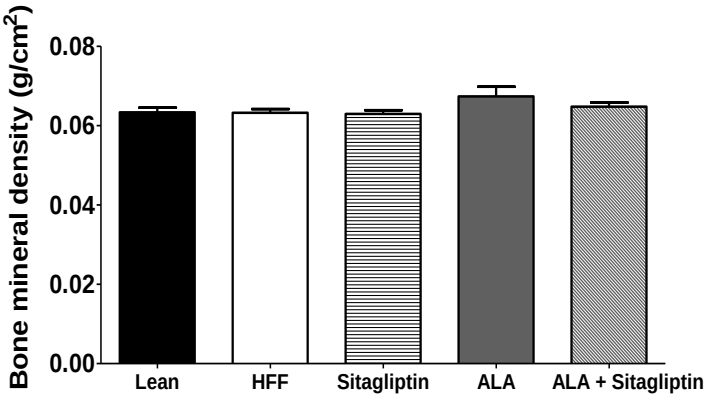

Chronic effect of 21-day oral administration of ALA (0.1 µmol/kg bw) alone and in combination with Sitagliptin (50 mg/kg bw) on (A) bone mineral content, (B) bone mineral density in HFF diabetic mice. Values are presented as mean ± SEM (n = 8). *p<0.05, **p<0.01, compared to HFF control. ++p<0.01, compared to ALA alone.

Figure 6.25: Chronic effect of 21-day oral administration of ALA monotherapy and combinational therapy (Sitagliptin) on total bone mineral content and bone mineral density as measured by DEXA in the femur of high fat fed diabetic mice.

A

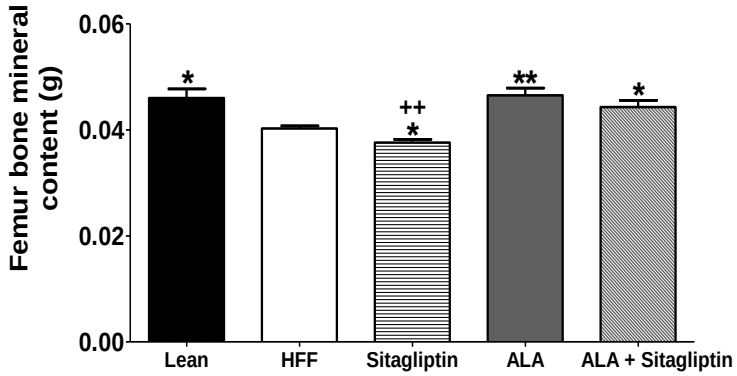

B

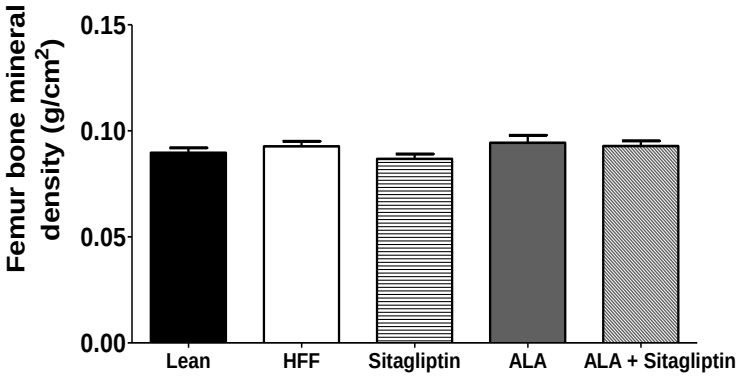

Chronic effect of 21-day oral administration of ALA (0.1 µmol/kg bw) alone and in combination with Sitagliptin (50 mg/kg bw) on (A) bone mineral content, (B) bone mineral density in the femur of HFF diabetic mice. Values are presented as mean ± SEM (n = 8). *p<0.05, **p<0.01, compared to HFF control. ++p<0.01, compared to ALA alone.

Figure 6.26: Chronic effect of 21-day oral administration of ALA monotherapy and combinational therapy (Sitagliptin) on plasma triglycerides and total cholesterol in high fat fed diabetic mice.

A

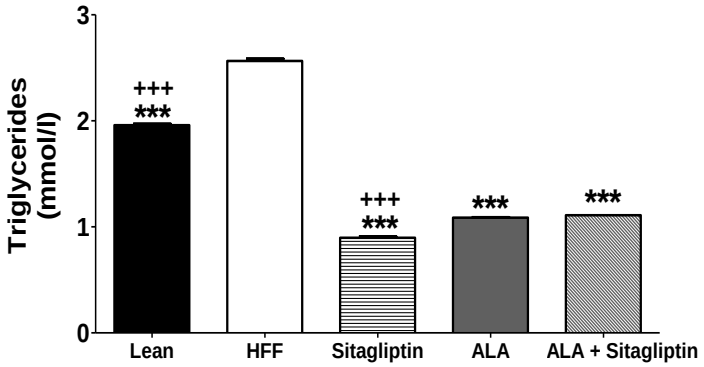

B

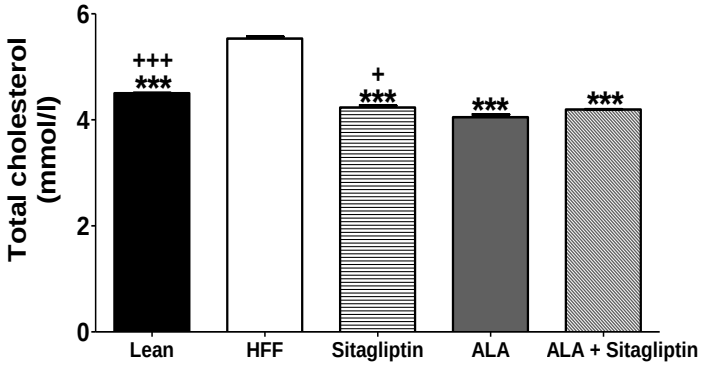

Chronic effect of 21-day oral administration of ALA (0.1 µmol/kg bw) alone and in combination with Sitagliptin (50 mg/kg bw) on (A) plasma triglyceride, (B) total cholesterol in HFF diabetic mice. Values are presented as mean ± SEM (n = 8). ***p<0.001, compared to HFF control. +p<0.05, +++p<0.001, compared to ALA alone.

Figure 6.27: Chronic effect of 21-day oral administration of ALA monotherapy and combinational therapy (Sitagliptin) on plasma HDL cholesterol and LDL cholesterol in high fat fed diabetic mice.

A

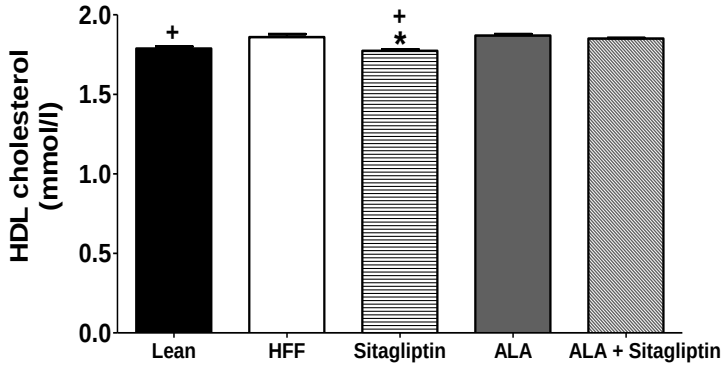

B

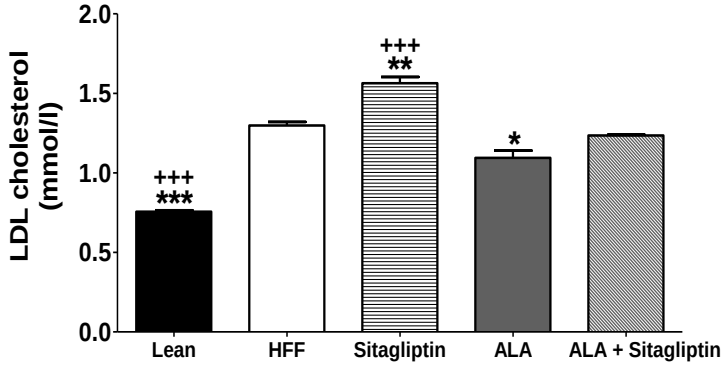

Chronic effect of 21-day oral administration of ALA (0.1µmol/kg bw) alone and in combination with Sitagliptin (50 mg/kg bw) on plasma (A) triglycerides and (B) total cholesterol in HFF diabetic mice. Values are presented as mean ± SEM (n = 8). *p<0.05, **p<0.01, ***p<0.001, compared to HFF control. +p<0.05, +++p<0.001, compared to ALA alone.

Figure 6.28: Chronic effect of 21-day oral administration of ALA monotherapy and combinational therapy (Sitagliptin) on plasma C-reactive protein and amylase activity in high fat fed diabetic mice.

A

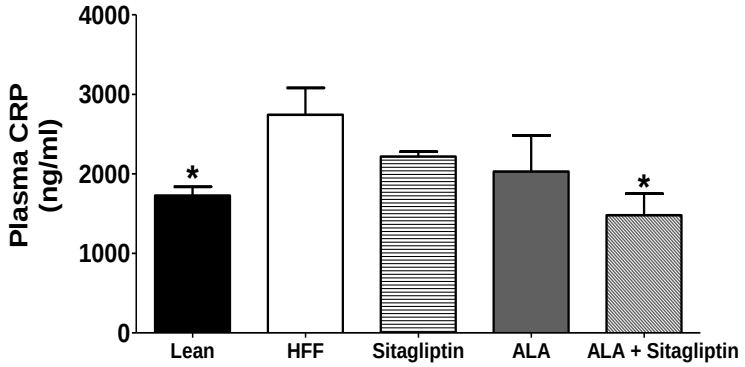

B

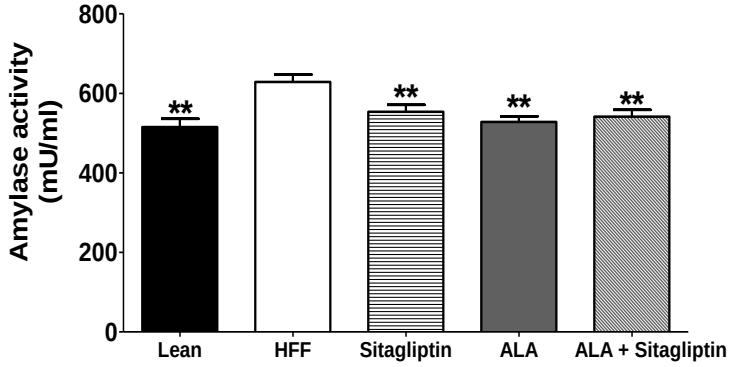

Chronic effect of 21-day oral administration of ALA (0.1µmol/kg bw) alone and in combination with Sitagliptin (50 mg/kg bw) on plasma (A) C-reactive protein and (B) amylase activity in HFF diabetic mice. Values are presented as mean ± SEM (n = 6). *p<0.05, **p<0.01, compared to HFF control.

Figure 6.29: Distribution of islet insulin and glucagon, following 21-day oral administration of ALA monotherapy and combinational therapy (Sitagliptin) in high fat fed diabetic mice.

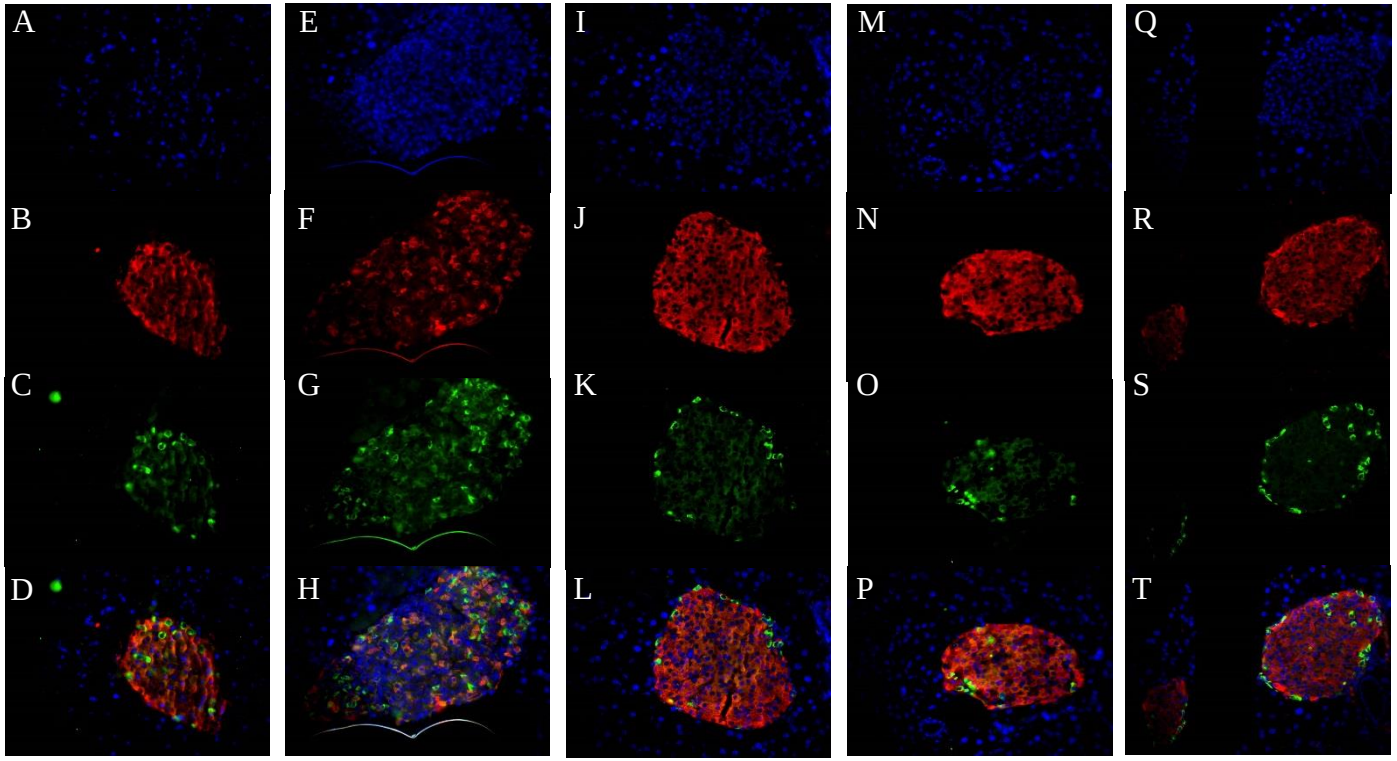

Representative images for distribution of DAPI (blue), insulin (red) and glucagon (green) in pancreatic islets of HFF mice at x40 magnification, following 21-day treatment of (A-D) lean control, (E-H) HFF, (I-L) Sitagliptin, (M-P) ALA and (Q-T) ALA + Sitagliptin.

Figure 6.30: Effect of 21-day oral administration of ALA monotherapy and combinational therapy (Sitagliptin) on islet morphology in high fat fed diabetic mice.

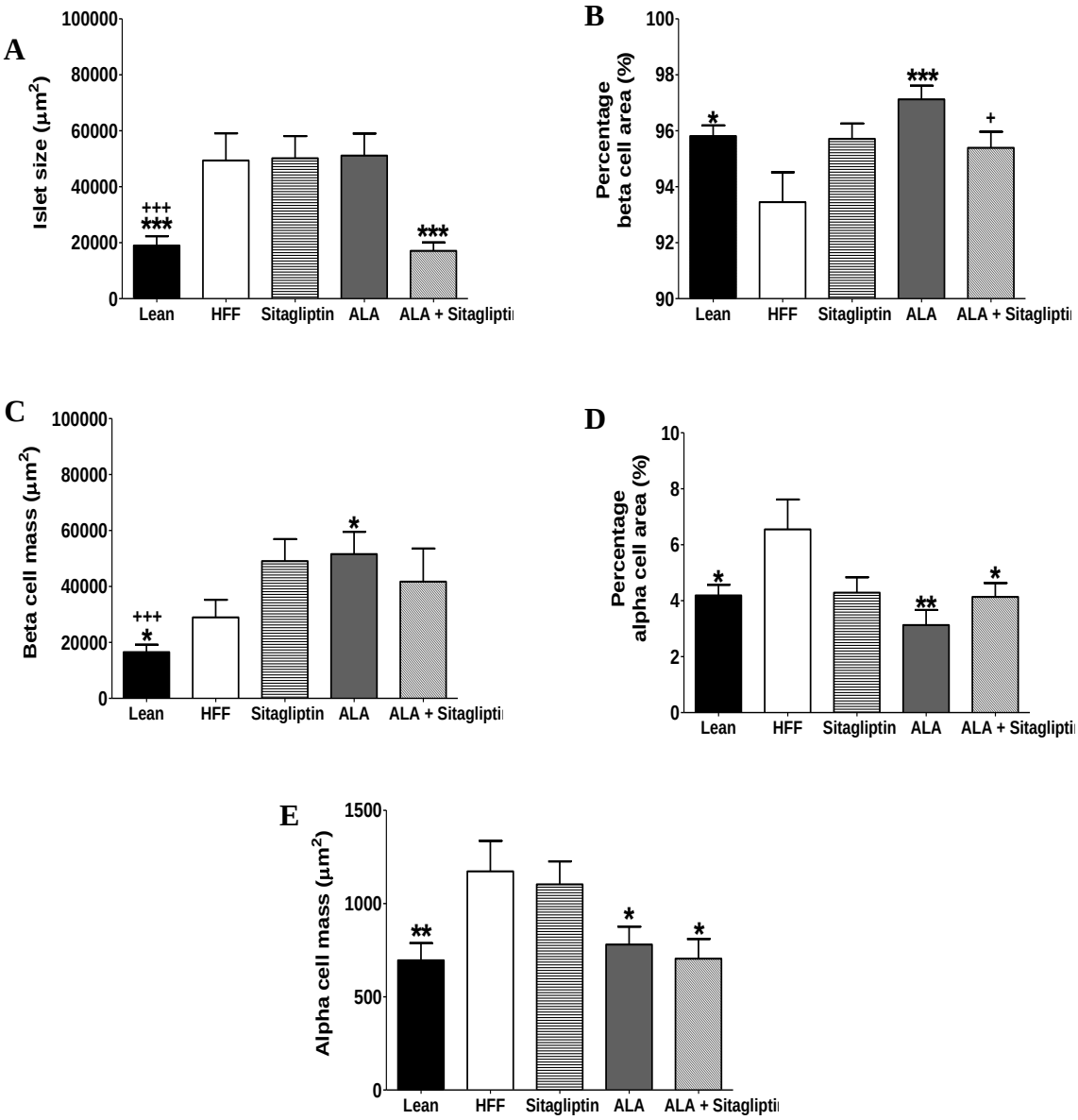

Immunohistochemistry demonstrating the effect of ALA monotherapy and combinational therapy (Sitagliptin) on (A) islet size, (B) beta cell area, (C) beta cell mass, (D) alpha cell area and (E) alpha cell mass in HFF mice. Values are mean ± SEM (n = 8), with 30 islets per group. *p<0.05, **p<0.01, ***p<0.001, compared to HFF. +p<0.05, +++p<0.001, compared to ALA alone. (Representative images as per Fig 6.29).

Figure 6.31: Effect of 21-day oral administration of ALA on beta cell proliferation (Ki-67) in high fat fed diabetic mice.

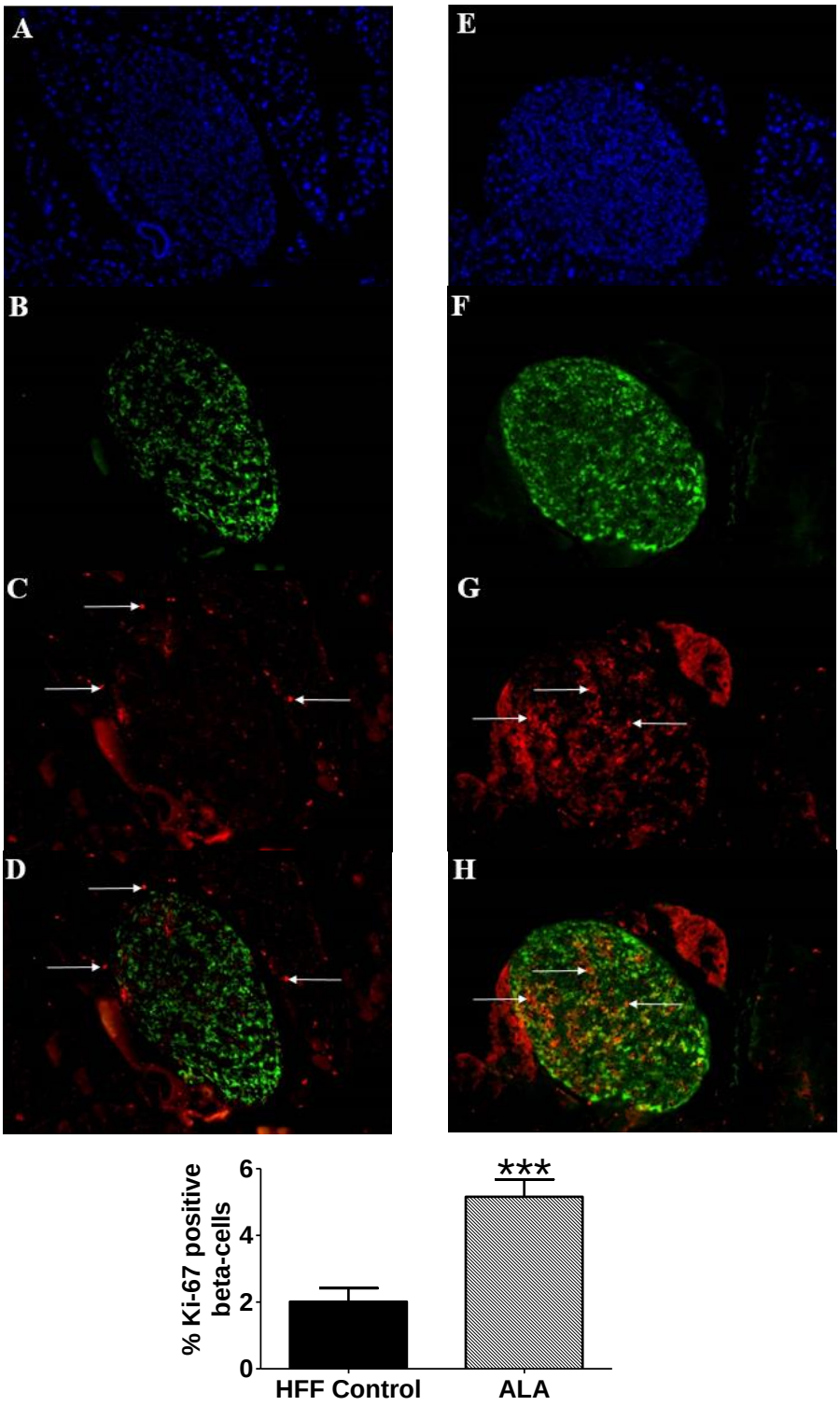

Representative images for DAPI (blue), insulin (green) and Ki-67 (red) in pancreatic islets of HFF mice at x40 magnification, following 21-day treatment with (A-D) HFF control and (E-H) ALA. Values are mean ± SEM (n = 8), with 50 islets per group. ***p<0.001, compared to HFF. Positive Ki-67 staining indicated by arrows.

Figure 6.32: Distribution of GPR120 and insulin in pancreatic islets from lean and high fat fed mice.

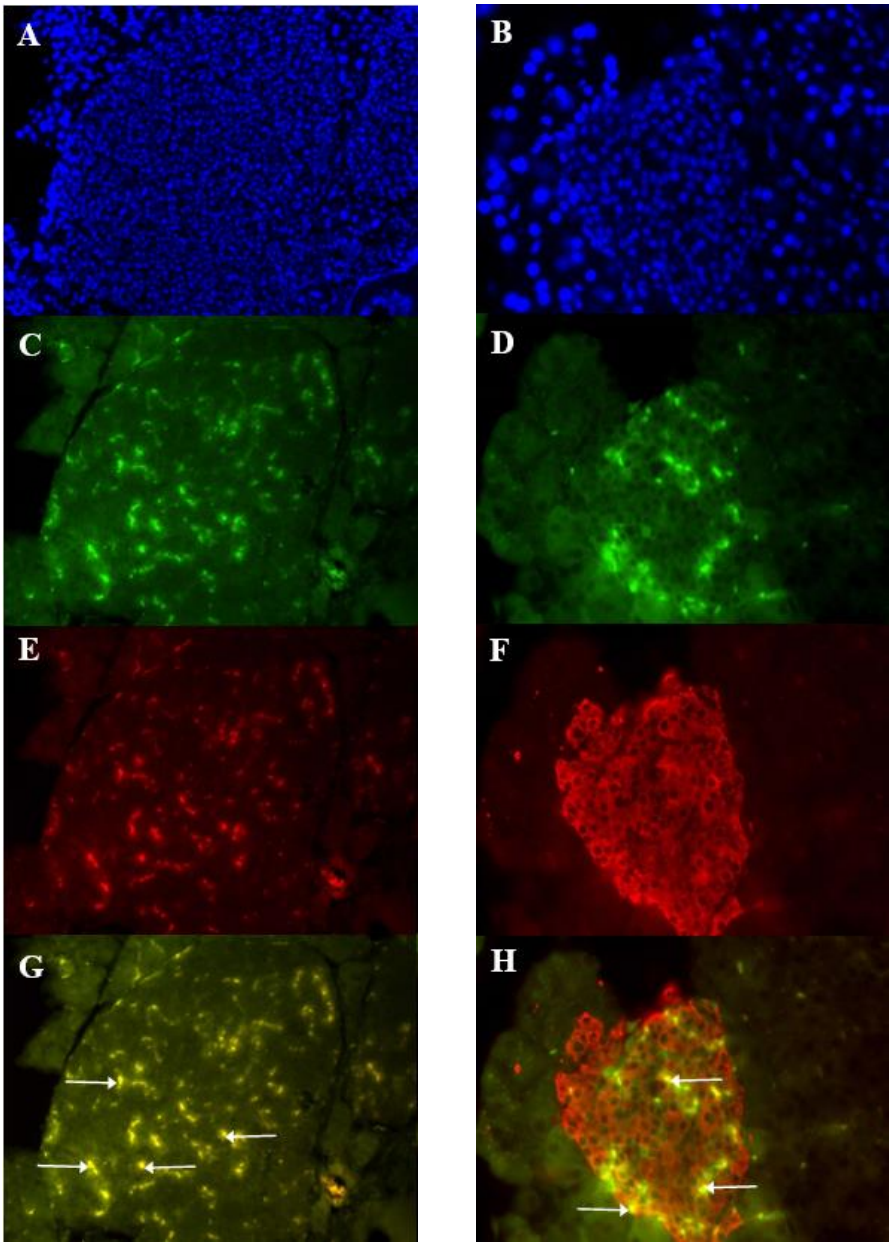

Immunohistochemistry demonstrating the distribution of DAPI (blue), GPR120 (green) and insulin (red) in HFF (A, C, E, G) and lean (B, D, F, H) pancreatic islets at x40 magnification. Areas of double immunofluorescent staining indicated by white arrows. Images are representative of several tissue sections.

Chapter 7

Assessing the therapeutic actions of GPR55 agonist monotherapy and combinational therapy (Sitagliptin) on glucose intolerance, dyslipidaemia and bodyweight control *in-vivo*

7.1: Summary

Recent studies have recognised GPR55 as a novel anti-diabetic target through enhancement of beta cell function and beta cell mass. The present study aims to evaluate the metabolic actions and therapeutic efficacy of GPR55 agonist monotherapy and combinational therapy (Sitagliptin) in islet and enteroendocrine cell function.

Acute glucose lowering effects of agonist monotherapy and combinational therapy (DPP-IV inhibitor) were investigated in HFF-induced diabetic mice, followed by biochemical assessment of plasma glucose and glucoregulatory hormone release. Chronic effect of 21-day oral administration of Abn-CBD (0.1 μmol/kg bw) monotherapy and combinational therapy with Sitagliptin (50 mg/kg bw) were assessed in HFF mice (n=8). Biochemical and anthropometric assessments of plasma glucose, circulating insulin, DPP-IV activity, CRP, amylase, lipids, body weight and food intake were conducted. Glucose tolerance, insulin sensitivity, DEXA scanning and islet morphology analysis were performed post 21-day administration.

Abn-CBD (31%; $p<0.01$) and AM251 (28%; $p<0.01$) improved glucose tolerance in HFF mice. Plasma insulin concentrations were enhanced by 27-39% ($p<0.001$), with further increases in GLP-1 ($p<0.05$-$p<0.001$) and GIP ($p<0.05$) release. When accompanied with DPP-IV inhibition (Sitagliptin), glucose lowering capabilities of Abn-CBD were enhanced by 22% ($p<0.05$). Chronic administration of Abn-CBD alone (54%; $p<0.001$) and in combination with Sitagliptin (57%; $p<0.001$) attenuated plasma glucose and enhanced circulating insulin concentrations by 18 and 24% ($p<0.001$), respectively. Abn-CBD and Abn-CBD in combination with the DPP-4 inhibitor reduced bodyweight by 9% ($p<0.05$-$p<0.01$). Post 21-day administration, Abn-CBD alone (23%; $p<0.01$) and with Sitagliptin (47%; $p<0.01$) improved glucose tolerance, whilst enhancing insulin

sensitivity by 42-43% ($p<0.05$). Abn-CBD increased islet area (43%; $p<0.05$), beta cell mass ($p<0.001$) and beta cell proliferation (3.5%; $p<0.001$), whilst Abn-CBD in combination with Sitagliptin reduced islet area (44%; $p<0.05$). Abn-CBD alone reduced plasma triglycerides by 34% ($p<0.001$) and both total cholesterol and LDL cholesterol by 15% ($p<0.01$). Abn-CBD in combination with Sitagliptin further reduced triglycerides ($p<0.001$) and total cholesterol ($p<0.001$) by 22% and 10%, respectively. Abn-CBD in combination with Sitagliptin reduced fat mass by 22% ($p<0.05$) and restored elevated CRP concentrations (48%; $p<0.05$).

These findings promote Abn-CBD monotherapy and combinational therapy (Sitagliptin) as a novel therapeutic approach for the treatment of glucose intolerance, bodyweight control and dyslipidaemia in patients with type 2 diabetes.

7.2: Introduction

The endocannabinoid system (ECS) has been shown to exhibit a wide range of physiological functions upon activation with small lipid-based retrograde neurotransmitter molecules (Reggio 2010). The ECS is responsible for the pharmacological effects of cannabis, whilst also mediating effects towards appetite, pain-sensation, memory, mood and energy metabolism (Donvito *et al.* 2018, Manzanares *et al.* 2006, McKillop *et al.* 2013). The physiological functions of the CB1 and CB2 cannabinoid receptors have been extensively reported, with functionality primarily associated within the brain, central nervous system and peripheral nervous system (Svizenska *et al.* 2018). Recently, GPR55 has been identified as a novel endocannabinoid

receptor and has been hypothesised to be responsible for the non CB1/CB2 physiological effects omitted by cannabinoid ligands (Morales & Reggio 2017).

G-protein coupled receptor 55 (GPR55) was first identified and cloned in 1999 (Sawzdargo *et al.* 1999). Later studies revealed GPR55 to be a cannabinoid receptor due to similar amino acid sequence identity in the binding sites of the receptor (Baker *et al.* 2006). Initial characterisation of GPR55 focused on its function in blood pressure control upon activation with cannabinoid ligands (Johns *et al.* 2007). Although several cannabinoids were shown to demonstrate blood pressure lowering properties, these actions were shown to be independent of GPR55 activation (Johns *et al.* 2007). At present, the entire physiological function of GPR55 remains unclear, with GPR55 knockout mice displaying no specific phenotype (Johns *et al.* 2007). However, studies have demonstrated the receptor to play a role in energy metabolism, whilst exhibiting pharmacological potential for metabolic diseases (McKillop *et al.* 2013, McKillop *et al.* 2016, Liu *et al.* 2016)

Activation of GPR55 is mediated by a range of natural and synthetic ligands, including endocannabinoids, phytocannabinoid plant components and long chain fatty acid molecules (McKillop *et al.* 2013, Tudurí *et al.* 2017). Lysophosphatidylinositol (LPI) has been generally accepted as the endogenous ligand of GPR55, however, one recent study utilising GPR55 knockout mice demonstrated LPI to act through a GPR55-independent mechanism in pancreatic islets (Tudurí *et al.* 2017, Liu *et al.* 2016). Interestingly, increased circulating concentrations of LPI is associated with obesity and type diabetes with concentrations correlating with BMI and fat percentage (Moreno-Navarrete *et al.* 2012). Furthermore, increased plasma LPI concentrations have also been shown to be a prognostic indicator of cardiac arrest and ovarian cancer (Arifin & Falasca 2016). Due to the undefined specificity of LPI and its correlation with poor prognosis of obesity and

inflammatory related diseases, studies have favoured LPI as a prognostic biomarker rather than a therapeutic agent (Kim *et al.* 2017).

GPR55 is expressed widely throughout the body, with abundant expression in the brain, intestines, osteoblasts and endocrine-pancreas (Ryberg *et al.* 2009, McKillop *et al.* 2013, Sawzdargo *et al.* 1999). Recent results from the genome wide association study (GWAS) revealed that a variant of the GPR55 gene displayed the phenotype of type 2 diabetes and coronary artery calcification (Divers *et al.* 2017). The variant displayed a single nucleotide polymorphism (SNP) on an intronic region of the GPR55 gene at chromosome 2q37.1 (Divers *et al.* 2017).

Current research is now heavily investigating the therapeutic potential of GPR55 in the treatment of type 2 diabetes and other obesity related diseases (Tudurí *et al.* 2017). GPR55 has been shown to demonstrate insulinotropic actions in clonal pancreatic beta cells upon activation with a range of endogenous (OEA, PEA) and synthetic (Abn-CBD, AM251) agonists (McKillop *et al.* 2013). In the same study, antagonising the receptor impaired the stimulatory effect of the agonists, with Abn-CBD omitting the potent and selective properties (McKillop *et al.* 2013).

Chronic administration of Abn-CBD was previously reported to induce glucose lowering and insulinotropic effects in multiple low dose streptozotocin mice, with further improvements towards insulin sensitivity, glucose tolerance and lipid balance also observed (McKillop *et al.* 2016). In addition, immunohistochemical analysis revealed abundant GPR55 expression in mouse and human pancreatic islet cells (McKillop *et al.* 2013, Liu *et al.* 2016). Interestingly, GPR55 expression was demonstrated to be solely expressed in beta cells in rodent rodents, however, one recent study identified moderate GPR55 expression in alpha cells of human islets also (Liu *et al.* 2016).

Previous reports resulted in discrepancies over the specificity of Abn-CBD in the pancreatic islet, particularly with respect to insulin-producing beta cells (McKillop *et al.* 2013, Ruz-Maldonado *et al.* 2018). Recently, the insulinotropic actions of Abn-CBD in mouse islets were demonstrated to be independent of GPR55 activation when assessed using isolated GPR55 knockout islets (Ruz-Maldonado *et al.* 2018). However, the same report revealed the proliferative effects of Abn-CBD in beta cells to be GPR55-dependent using the same model (Ruz-Maldonado *et al.* 2018). The use of knockout tissues to determine specificity may be unreliable as numerous compensatory pathways may be introduced. Studies using a clonal GPR55 knockout beta cell line, developed using innovative CRISPR/Cas9 gene editing, revealed that Abn-CBD induced insulin release is predominately GPR55-dpenednatnt, with potential synergistic activity with other cannabinoid receptors such as GPR18 (Chapter 5).

Chronic administration of Abn-CBD has also been shown to confer cardioprotection in diabetic rats by alleviating defective ventricle function and myocardial oxidative stress, through the restoration of impaired nitric oxide (NO) and adiponectin (ADN) concentrations (Matouk *et al.* 2018).

Given the known insulinotropic and cardioprotective function of Abn-CBD, the present study aims to evaluate the glucoregulatory and anti-obesity effects of Abn-CBD in high fat fed (HFF) induced diabetic obese mice. Due to abutment expression of GPR55 incretin-releasing enteroendocrine cells, Abn-CBD combinational therapy using the DPP-IV inhibitor (Sitagliptin) was explored and utilised to prolong the circulating half-life of incretin hormones (Drucker *et al.* 20017). Acute glucose lowering parameters of Abn-CBD monotherapy and combinational therapy (Sitagliptin) were assessed, including glucose tolerance, insulin secretion, incretin secretion, DPP-IV activity and agonist specificity. In addition, chronic analysis assessed the effects of 21-day oral administration

of Abn-CBD monotherapy and combinational therapy on bodyweight, food intake, non-fasting plasma glucose, insulin secretion/content, insulin sensitivity, lipid profile, pancreatic islet morphology, amylase activity, C-reactive protein and DEXA analysis.

7.3: Materials and methods

Development of high fat fed induced diabetic obese mice were outlined previously in Section 2.9.2. Materials and methods used to assess the metabolic actions of GPR55 agonist-based therapies are outlined in Sections 2.10 and 2.11. Materials and methodologies for DPP-IV activity analysis and ELISAs used for biochemical analysis are detailed in Sections 2.12 and 2.13, respectively.

7.4: Results

7.4.1: Effect of four-month high fat fed diet on glucose tolerance in Swiss TO mice

To confirm the diabetic phenotype, Swiss TO mice subjected to a high fat fed diet for four months were challenged with an oral glucose tolerance test. Using AUC data, the glycaemic control of the high fat fed mice was impaired by 47% ($p<0.001$), compared to the lean control (Fig. 7.1A), with glucose stimulated insulin release impaired by 48% ($p<0.001$; Fig. 7.1D). In addition, mice subjected to the high fat diet demonstrated an average weight gain of 18% ($p<0.001$), compared to the lean control (Fig. 7.1E).

7.4.2: Acute effect of GPR55 agonist monotherapy and combinational therapy (Sitagliptin) on glucose tolerance and insulin secretion in high fat fed mice

An oral glucose tolerance test (OGTT) was performed to assess the acute glucose lowering properties of GPR55 agonists Abn-CBD and AM251 in fasted, HFF mice. Agonists were assessed alone or in combination with the DPP-IV inhibitor (Sitagliptin). The GPR55 antagonist CBD was utilised to determine agonist specificity *in-vivo*. Oral administration of both GPR55 agonists improved glucose tolerance ($p<0.05$-$p<0.001$) (Fig. 7.2, 7.4 A), with AUC data showing decreases in glucose with Abn-CBD (28%; $p<0.01$) and AM251 (31%; $p<0.01$) (Fig. 7.2, 7.4 B). In combination with Sitagliptin, both GPR55 agonists exhibited a further improvement on glucose excursion by 8-22%, whilst Abn-CBD demonstrating the most potent glucose lowering effect (50%; $p<0.001$) in combination (Fig. 7.2). The GPR55 antagonist impaired the glucose lowering capabilities of Abn-CBD and AM251 by 47% and 2%, respectively (Fig. 7.2, 7.4 B). Effects on blood glucose control were accompanied by relative changes in insulin secretion. Agonising GPR55 with Abn-CBD (27%; $p<0.001$) and AM251 (39%; $p<0.001$) increased plasma insulin when assessed with AUC data (Fig. 7.3, 7.5 B). Abn-CBD combination with Sitagliptin demonstrated an additive 15% insulinotropic effect compared to agonist monotherapy (Fig. 7.3, 7.5). The GPR55 antagonist CBD impaired the insulinotropic effect of Abn-CBD by 55% (Fig. 7.3B), whilst the effects of AM251 were greatly diminished by 80% ($p<0.001$) (Fig. 7.5B).

7.4.3: Acute effect of GPR55 agonist monotherapy and combinational therapy (Sitagliptin) on incretin secretion and DPP-IV activity in high fat fed mice

In response to an oral glucose tolerance test, Abn-CBD and AM251 agonists increased GLP-1 secretion ($p<0.05$-$p<0.001$) at 15 min (Fig. 7.6). After 15 min, AM251 stimulated

GIP secretion ($p<0.01$), whilst Abn-CBD had no significant effect (Fig. 7.7). Overall, using AUC data for the 30 min treatment period, both Abn-CBD ($p<0.001$) and AM251 ($p<0.05$) stimulated GLP-1 release, whilst Abn-CBD ($p<0.05$) and AM251 ($p<0.05$) also augmented GIP secretion. (Fig. 7.7B). DPP-IV activity was diminished through the actions of Sitagliptin only ($p<0.001$; Fig. 7.8).

7.4.4: Chronic effect of once daily oral administration of Abn-CBD monotherapy and combinational therapy (Sitagliptin) on body weight, non-fasting plasma glucose, insulin, pancreatic inulin content, circulating incretin concentrations, DPP-IV activity and food intake

Once daily oral administration of Sitagliptin, Abn-CBD alone and combination with Sitagliptin demonstrated no significant effect towards bodyweight in HFF mice when measured every consecutive 3 days (Fig. 7.9A, B). However, when assessed by percentage weight change, Abn-CBD alone and in combination with Sitagliptin influenced a 9-10% ($p<0.05$-$p<0.01$) reduction in bodyweight (Fig. 7.9C). HFF-induced hyperglycaemia was reduced by Sitagliptin (37%; $p<0.01$), Abn-CBD alone (54%; $p<0.001$) and Abn-CBD in combination with Sitagliptin (57%; $p<0.001$) during the 21-day treatment period (Fig. 7.10). Abn-CBD alone surpassed the glucose lowering capabilities of Sitagliptin by 17% ($p<0.05$).Corresponding increases in plasma insulin concentrations were observed upon treatment with Sitagliptin (24%; $p<0.001$), Abn-CBD alone (18%; $p<0.001$) and Abn-CBD in combination with Sitagliptin (24%; $p<0.001$) (Fig. 7.11A, B). Terminal pancreatic tissue analysis demonstrated that insulin content was reduced by 70% ($p<0.01$) in HFF-induced diabetic mice. Treatment with Sitagliptin alone increased insulin content by 48% ($p<0.05$), whilst Abn-CBD alone and in combination with Sitagliptin had no effect (Fig. 7.11C).

Chronic administration of Abn-CBD and Abn-CBD in combination with Sitagliptin enhanced circulating GLP-1 concentrations by 27% ($p<0.05$; Fig.7.12) and 30% ($p<0.01$, Fig. 7.13), respectively. No effects on circulating GIP concentrations were observed. DPP-IV activity was elevated by 42% ($p<0.01$) in HFF-induced diabetic mice, whilst administration of Sitagliptin and Abn-CBD in combination with Sitagliptin reduced DPP-IV activity by 26-35% ($p<0.05$) (Fig. 7.14). When assessed by consecutive 3-day measurements, no significant changes in food intake nor cumulative food intake were identified upon treatment with Sitagliptin, Abn-CBD alone and Abn-CBD in combination with Sitagliptin (Fig. 7.15, 7.16). Cumulative energy intake demonstrated that HFF-induced diabetic mice consumed higher energy intake from days 3-21 ($p<0.01$-$p<0.001$), compared to lean control (Fig. 7.16B). Corresponding to food intake analysis, no effects towards cumulative food intake were observed with all treatment groups (Fig. 7.16B).

7.4.5: Chronic effect of once daily oral administration of Abn-CBD monotherapy and combinational therapy (Sitagliptin) on glucose tolerance and insulin sensitivity

Administration of Sitagliptin, Abn-CBD alone and Abn-CBD in combination with Sitagliptin for 21 days improved glucose tolerance ($p<0.05$-$p<0.001$), as assessed by an oral glucose tolerance test (Fig. 7.17A). Overall, using AUC data, Sitagliptin, Abn-CBD and Abn-CBD in combination with Sitagliptin improved glucose tolerance by 23-47% ($p<0.01$) (Fig. 7.17C). Corresponding insulin secretory responses were observed in response to the glucose lowering effects observed by Abn-CBD combinational therapy with Sitagliptin ($p<0.001$) at 15 min, whilst Sitagliptin and Abn-CBD alone having no effect on insulin release (Fig. 7.17B). Abn-CBD in combination with Sitagliptin demonstrated an additive insulin secretory response of 30% ($p<0.01$) (Fig. 7.17B, D). In addition, 21-day oral administration of Abn-CBD alone and Abn-CBD in combination

with Sitagliptin lowered blood glucose ($p<0.05$-$p<0.01$) following exogenous insulin injection, compared to non-treated HFF mice (Fig. 7.18A). Overall, using AOC data, HFF mice treated with Abn-CBD and Abn-CBD in combination with Sitagliptin demonstrated enhanced glucose lowering capabilities by 42-43% ($p<0.05$) upon insulin injection, whilst Sitagliptin alone had no effect (Fig. 7.18B).

7.4.6: Chronic effect of once daily oral administration of Abn-CBD monotherapy and combinational therapy (Sitagliptin) on DEXA measurements, lipid profile, plasma C-reactive protein and amylase activity

Post 21-day oral administration, Sitagliptin, Abn-CBD alone and Abn-CBD in combination with Sitagliptin demonstrated reductions in bodyweight 11-18% ($p<0.05$-$p<0.01$) in HFF-induced diabetic mice, as measured by DEXA analysis (Fig. 7.19A). HFF mice demonstrated increased fat mass by 32% ($p<0.001$), whilst administration of Sitagliptin, Abn-CBD alone and Abn-CBD in combination with Sitagliptin reduced fat mass by 14-22% ($p<0.05$) in HFF mice (Fig. 7.19B). No effects towards lean mass was observed in all groups (Fig. 7.19C). DEXA analysis revealed that HFF mice demonstrated reduced total bone mineral content ($p<0.05$; Fig. 7.20A) and femur bone mineral content ($p<0.05$; Fig. 7.21A). Administration of Sitagliptin and Abn-CBD increased total bone mineral content by 12% ($p<0.01$) (Fig. 7.20A). When localised to the femur, Sitagliptin reduced bone mineral content ($p<0.05$), whilst Abn-CBD combinational therapy increased bone mineral content by 17% ($p<0.01$) (Fig. 7.21A). All groups had no effect on total bone mineral density nor femur bone mineral density (Fig. 7.20B; 7.21B).

Lipid profile analysis on terminal plasma revealed that HFF-induced diabetic mice exhibited increased triglycerides ($p<0.001$), total cholesterol ($p<0.001$) and LDL

cholesterol ($p<0.001$) concentrations, with no change in HDL cholesterol (Fig. 7.22, 7.23). Administration of Sitagliptin, Abn-CBD alone and Abn-CBD in combination with Sitagliptin lowered triglycerides by 34-65% ($p<0.001$) and total cholesterol concentrations by 15-25% ($p<0.001$) (Fig. 7.22). Sitagliptin treated HFF mice demonstrated reduced HDL cholesterol (5%; $p<0.05$) and increased LDL cholesterol (17%; $p<0.01$). Abn-CBD alone demonstrated no effect towards HDL cholesterol, however, reduced LDL cholesterol by 15% ($p<0.01$). Abn-CBD in combination with Sitagliptin reduced HDL cholesterol by 7% ($p<0.05$), whilst having no effect on LDL cholesterol (Fig. 7.23).

Mice subjected to a HFF diet displayed elevated plasma CRP concentrations by 37% ($p<0.05$), compared to lean control. Administration of Abn-CBD in combination with Sitagliptin reduced plasma CRP by 48% ($p<0.05$), whereas Abn-CBD and Sitagliptin alone had no effect (Fig. 7.24A). HFF mice demonstrated elevated plasma amylase activity by 18% ($p<0.01$), whilst administration of Sitagliptin and Abn-CBD in combination with Sitagliptin reduced amylase activity by 10-12% ($p<0.05$-$p<0.01$) (Fig. 7.24B).

7.4.7: Chronic effect of once daily oral administration of Abn-CBD monotherapy and combinational therapy (Sitagliptin) on islet morphology

Immunohistochemistry was utilised to examine insulin and glucagon expression in lean, HFF and treated mouse pancreatic islets (Fig. 7.25). HFF mice revealed increased islet size by 62% ($p<0.001$). Treatment with Abn-CBD alone increased islet size by 43% ($p<0.05$) whilst Abn-CBD in combination with Sitagliptin reduced islet size by 44% ($p<0.01$) (Fig. 7.26A). Mice subjected to a HFF diet demonstrated major islet abnormalities, including reduced insulin-positive beta cell percentage ($p<0.05$;

Fig.7.26B) and increased glucagon-positive alpha cell percentage ($p<0.05$; Fig.7.26D). However, complimentary to islet size, HFF mice demonstrated increased beta cell mass ($p<0.05$; Fig.7.26C) and alpha cell mass ($p<0.01$; Fig.7.26E). Administration of Abn-CBD alone increased beta cell mass ($p<0.001$; Fig.7.26C) and alpha cell mass ($p<0.01$; Fig.7.26E). All treatment groups demonstrated no effects towards percentage beta and alpha cell area (Fig.7.26B, D).

Administration on Abn-CBD in HFF mice increased beta cell proliferation by 3.5% ($p<0.001$), as assessed by Ki-67 immunohistochemistry (Fig 7.27). In addition, abundant expression of both GPR55 and insulin was demonstrated on islets from lean and HFF mice (Fig. 7.28), with areas of double-immunofluorescent staining between both GPR55 and insulin observed (Fig. 7.28D, H).

7.5: Discussion

It has been estimated that 34% current FDA approved drugs are mediating through GPCRs, with characterisation and specific targeting of novel GPCRs revealing a promising approach for future drug discovery (Hauser *et al.* 2018). In particular, research has intensified on the potential pharmacological capabilities of novel endocannabinoid receptors in metabolic control, with the CB1 inverse agonist Rimonabant once used as an anti-obesity drug (Sam *et al.* 2011). Recently, the novel endocannabinoid receptor GPR55 has been identified as a potential therapeutic target for the treatment of obesity and type 2 diabetes (Tuduri *et al.* 2017). Interestingly, pre-clinical studies have demonstrated GPR55 activation to omit insulinotropic and glucoregulatory effects in clonal beta cells, diabetic mice and human islets (McKillop *et al.* 2013, Liu *et al.* 2016).

However, further investigations are warranted to fully understand the functionality of GPR55 activation and evaluate its potential as a novel therapeutic target.

The present study investigates the acute and chronic effects of GPR55 agonist monotherapy and combinational therapy with the DPP-IV inhibitor Sitagliptin in HFF-induced diabetic obese mice. The acute metabolic actions of potent GPR55 agonists Abn-CBD and AM251 on glucose excursion, insulin release, incretin release and DPP-IV activity were investigated. Oral administration of Abn-CBD and AM251 improved glucose tolerance and insulin secretion when administered in combination with glucose to HFF mice, revealing the glucoregulatory role of GPR55 activation in an obese insulin resistant model of type 2 diabetes. This compliments previous reports which demonstrated glucose lowering and insulinotropic actions of GPR55 agonists in multiple low dose streptozotocin-induced diabetic mice (McKillop *et al.* 2016). Cannabidiol (CBD) was employed to antagonise the GPR55 receptor and demonstrate agonist specificity *in-vivo*. In harmony with previous findings using GPR55 knockout cells generated by CRISPR/Cas9 gene editing (Chapter 5), the glucose lowering effect and insulinotropic response of Abn-CBD was abolished upon GPR55 antagonism, suggesting that the actions of Abn-CBD are GPR55-dependent *in-vitro* and *in-vivo*. Although the GPR55 antagonist abolished the insulinotropic response of AM251, an attenuated glucose lowering effect was still observed, suggesting that the actions of AM251 are only partly driven by GPR55 in the beta cell.

Abundant GPR55 expression has been extensively reported in the intestines, with previous studies demonstrating its role in inflammatory responses and motility (Schicho & Storr 2012, Shore & Reggio 2015). The present study revealed, for the first time, that Abn-CBD and AM251 augments both GLP-1 and GIP secretion from enteroendocrine cells; greatly encouraging GPR55 as an anti-diabetic target. Upon the discovery of the

incretin secretory effect of GPR55 activation, the DPP-IV inhibitor Sitagliptin was administered in combination with Abn-CBD and AM251 to prolong the circulating half-life of the incretin hormones (Drucker *et al.* 2007). As anticipated, the actions of Sitagliptin when administered alone or in combination with the GPR55 agonists abolished DPP-IV activity, whilst Abn-CBD and AM251 alone had no effect. When accompanied with DP-IV inhibition through Sitagliptin, Abn-CBD and AM251 demonstrated enhanced glucose lowering and insulinotropic capabilities, through GPR55- induced incretin release, supplemented with prolonged incretin action through DPP-IV inhibition. Abn-CBD demonstrated the most potent glucoregulatory effects in combination with Sitagliptin.

21-day oral administration Abn-CBD alone and in combination with Sitagliptin greatly improved glycaemic control and dyslipidaemia in HFF mice and surpassed the capabilities of Sitagliptin monotherapy. Abn-CBD based therapies demonstrated a range of anti-diabetic effects, including improvements towards glycaemic control, GSIS, bodyweight, insulin sensitivity, dyslipidaemia and islet architecture. Oral administration of Abn-CBD alone and in combination with Sitagliptin reduced bodyweight by 9% in the obese animal model, whilst terminal DEXA analysis also revealed reduced bodyweight and fat mass with all treatment groups. Interestingly, the CB1 endocannabinoid receptor shares structural similarities with GPR55 and has been previously shown to regulate bodyweight, thus clearly revealing the pivotal role of the endocannabinoid system in bodyweight management (Bergholm *et al.* 2013). With respect to glucose control, Abn-CBD alone and in combination with Sitagliptin improved glucose control beyond the capabilities of Sitagliptin alone, clearly implicating the therapeutic efficacy of GPR55 activation. In response to the glucose lowering effect, relative changes in plasma insulin concentrations were also observed, with Sitagliptin based therapies demonstrating the most potent insulinotropic effect. Sitagliptin alone and in combination with Abn-CBD

augmented pancreatic insulin content, whilst Abn-CBD alone had no effect, indicating the role of prolonged incretin action on insulin production. Correspondingly, Sitagliptin alone and in combination with Abn-CBD reduced circulating DPP-IV activity, complimenting previous findings (Drucker *et al.* 2007).

Although marked reductions in bodyweight were demonstrated by Abn-CBD alone and in combination with Sitagliptin, no effects towards cumulative food intake nor cumulative energy intake were observed, thus indicating an alternative mechanism of weight loss which warrants further investigation. Interestingly, inverse agonism of the structurally related CB2 receptor has also been shown to reduce bodyweight in humans (Sam *et al.* 2011). Post 21-day oral administration of Sitagliptin and Abn-CBD in combination with Sitagliptin improved glucose tolerance when subjected to an OGTT. Interestingly, Abn-CBD combinational therapy (Sitagliptin) demonstrated the greatest insulin secretory effect in response to the glucose challenge, elucidating the beneficial effects of Abn-CBD combinational therapy (Sitagliptin) on the restoration of beta cell function. In addition, Abn-CBD alone and in combination with Sitagliptin improved insulin sensitivity in HFF mice; a novel finding which may be partly driven by the anti-inflammatory properties associated with GPR55 activation (Stancic *et al.* 2015).

Lipid profile analysis post 21-day treatment demonstrated that Abn-CBD, Sitagliptin and Abn-CBD in combination with Sitagliptin improved dyslipidaemia with marked reductions on plasma triglycerides and total cholesterol. Interestingly, Sitagliptin reduced HDL cholesterol and increased LDL cholesterol. In contrast, Abn-CBD alone attenuated LDL cholesterol and had no effect on HDL cholesterol, corresponding with previous studies, which demonstrate the cardioprotective effects of Abn-CBD in type 2 diabetes (Su & Vo 2007, Matouk *et al.* 2018). In addition, Abn-CBD in combination with Sitagliptin ameliorated plasma C-reactive protein concentrations; a biomarker that

correlates with CVD risk and cardiovascular health (Bahadursingh *et al.* 2009, Clearfield 2005).

Complimentary with previous studies (McKillop *et al.* 2013, Ruz-Maldonado *et al.* 2018), expression analysis of GPR55 in lean and HFF islets revealed abundant regions of co-localisation between GPR55 and insulin, which further implicates the importance of GPR55 in beta cell function. As anticipated, examination of islet architecture revealed that HFF mice demonstrated major islet abnormalities, including increased islet size and alpha percentage area with reduced percentage beta cell area. Interestingly, Abn-CBD greatly increased islet area, with further increases of beta and alpha cell mass observed. Previous studies have demonstrated the proliferative and anti-apoptotic effect of Abn-CBD in beta cells, which is likely to account for the effects observed (Ruz-Maldonado *et al.* 2018, Chapter 4). In harmony with this, Ki-67 staining revealed that Abn-CBD increased beta cell proliferation. Although normal islet architecture was restored, Abn-CBD in combination with Sitagliptin greatly reduced islet area to non-diabetic islet specifications. Complimentary with enhanced GSIS post 21-day treatment and reduced plasma amylase activity, these findings suggest that Abn-CBD accompanied with DPP-IV inhibition improves beta cell function and promotes islet cell regeneration.

Collectively, the present study demonstrates that oral administration of GPR55 agonist monotherapy and combinational therapy with Sitagliptin emit potent glucoregulatory and anti-obesity properties in HFF diabetic mice. Biochemical analysis demonstrated that acute and chronic administration of GPR55 agonists regulate glucose homeostasis through both insulin and incretin secretion and through the restoration of islet morphology. In addition, long term administration of Abn-CBD improved bodyweight, dyslipidaemia and plasma CRP concentrations. Overall, revealing the efficacy of GPR55

as novel therapeutic target for the treatment of type 2 diabetes and obesity related disorders.

Figure 7.1: Effect four-month high fat fed diet on glucose tolerance and insulin secretion in 18 h fasted Swiss TO mice.

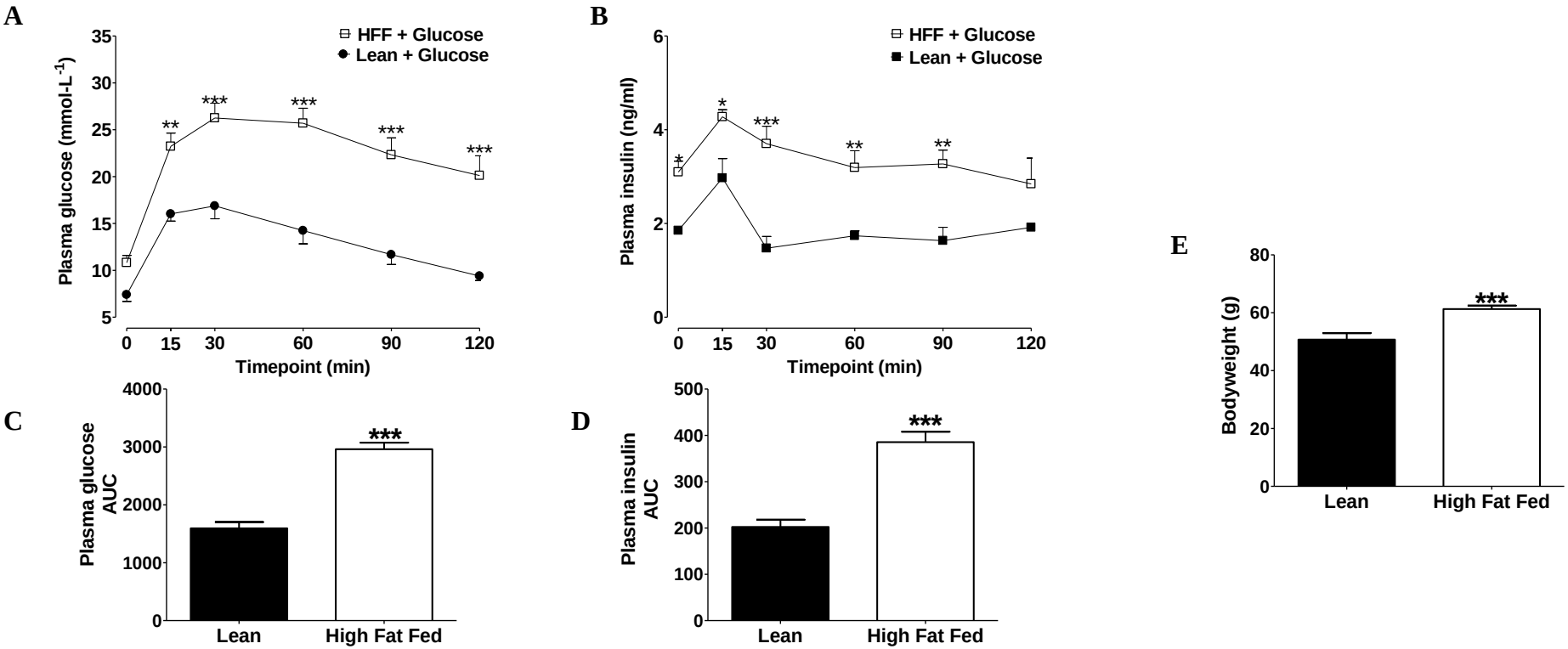

Swiss TO mice were subjected to a high fat fed (HFF) diet for four months to induce an insulin resistance and glucose intolerance. To confirm the diabetic phenotype of the model, animals were subjected to an oral glucose tolerance test (18 mmol/kg bw) with (A, C) glucose tolerance, (B, D) insulin secretory response and (E) bodyweight determined. Results are the mean ± SEM (n=6). *p<0.05, **p<0.01, ***p<0.001 compared to glucose control.

Figure 7.2: Acute effect of Abn-CBD on plasma glucose in 18 h fasted high fat fed diabetic mice.

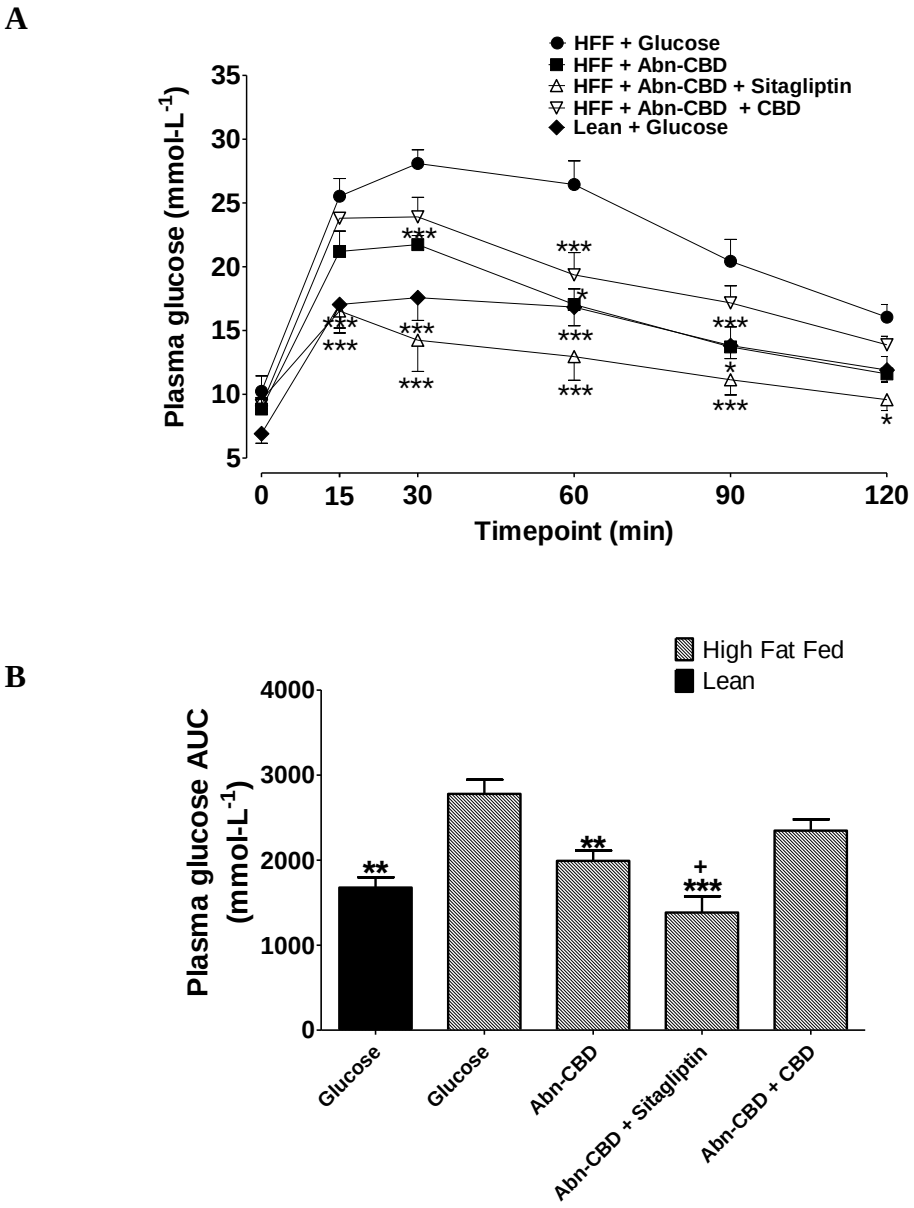

Acute effect of Abn-CBD on plasma glucose (A) and respective AUC (B). Glucose (18 mmol/kg bw) was administered orally alone or in combination with Abn-CBD (0.1µmol/kg bw) and either the GPR55 antagonist CBD (0.1µmol/kg bw) or Sitagliptin (50 mg/kg bw) to HFF mice (n = 6). Values are presented as mean ± SEM. *p<0.05, **p<0.01, ***p<0.001, compared to HFF glucose control. +p<0.05, compared to agonist alone.

Figure 7.3: Acute effect of Abn-CBD on plasma insulin in 18 h fasted high fat fed diabetic mice.

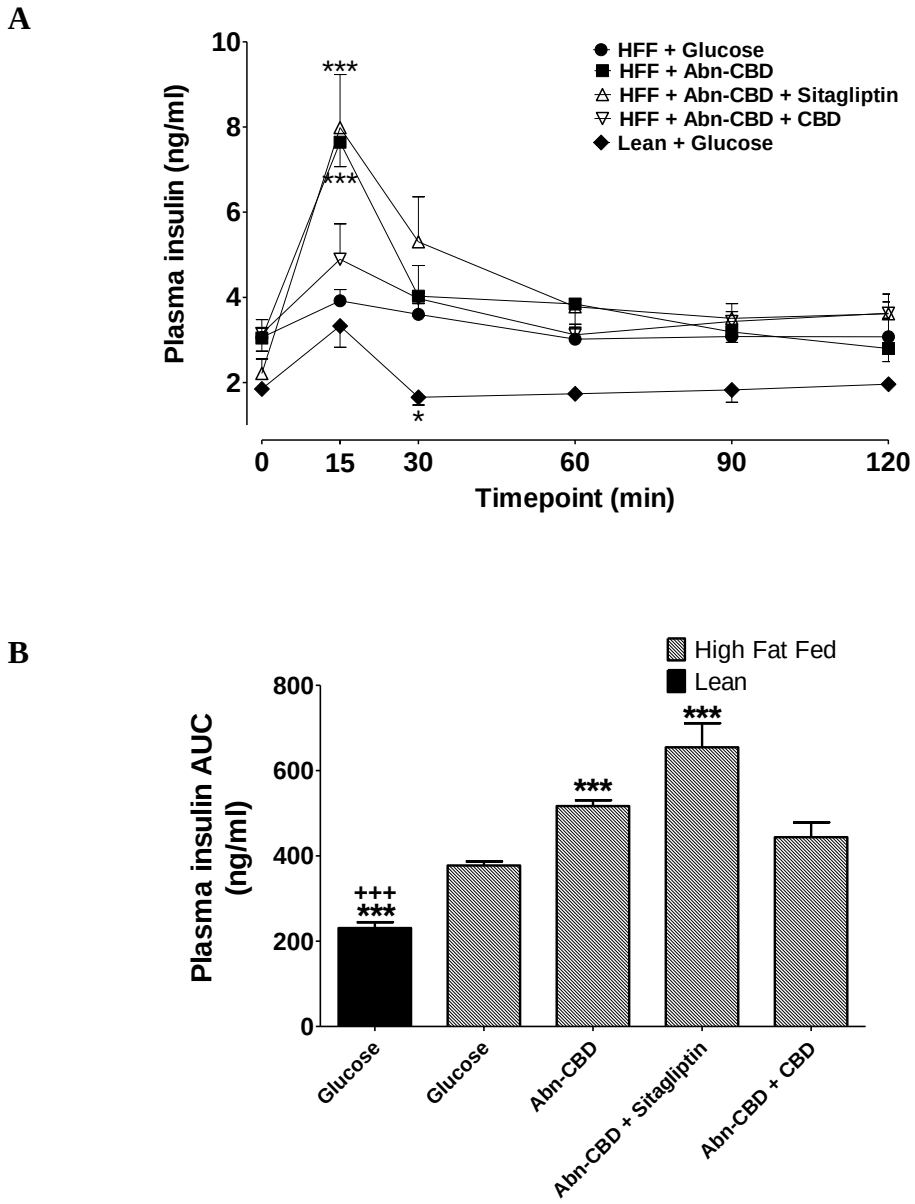

Acute effect of Abn-CBD on plasma insulin (A) and respective AUC (B). Glucose (18 mmol/kg bw) was administered orally alone or in combination with Abn-CBD (0.1µmol/kg bw) and either the GPR55 antagonist CBD (0.1 µmol/kg bw) or Sitagliptin (50 mg/kg bw) to HFF mice (n = 6). Values are presented as mean ± SEM. ***p<0.001, *p<0.05, compared to HFF glucose control.

Figure 7.4: Acute effect of AM251 on plasma glucose in 18 h fasted high fat fed diabetic mice.

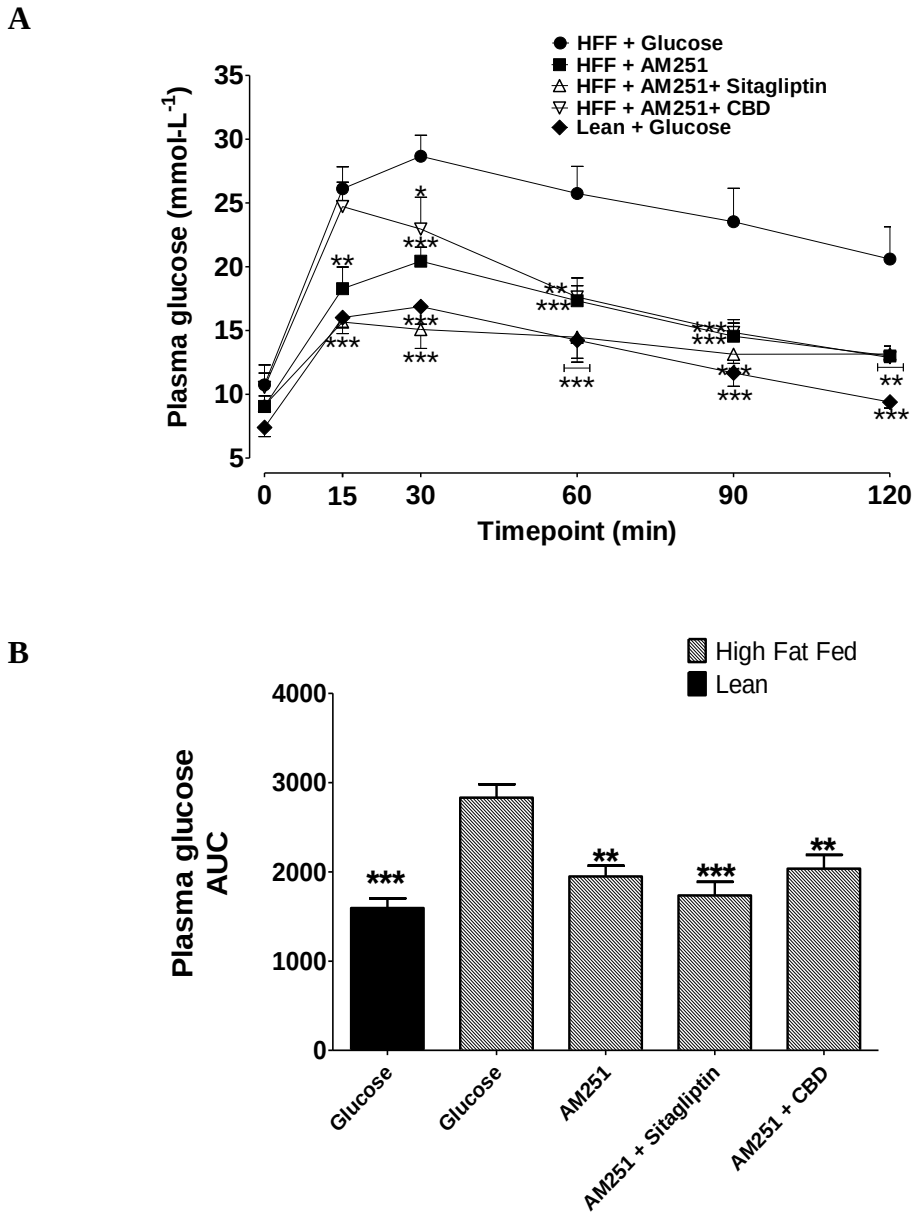

Acute effect of AM251 on plasma glucose (A) and respective AUC (B). Glucose (18 mmol/kg bw) was administered orally alone or in combination with AM251 (0.1 µmol/kg bw) and either the GPR55 antagonist CBD (0.1µmol/kg bw) or Sitagliptin (50 mg/kg bw) to HFF mice (n = 6). Values are presented as mean ± SEM. *p<0.05, **p<0.01, ***p<0.001, compared to HFF glucose control.

Figure 7.5: Acute effect of AM251 on plasma insulin in 18 h fasted high fat fed diabetic mice.

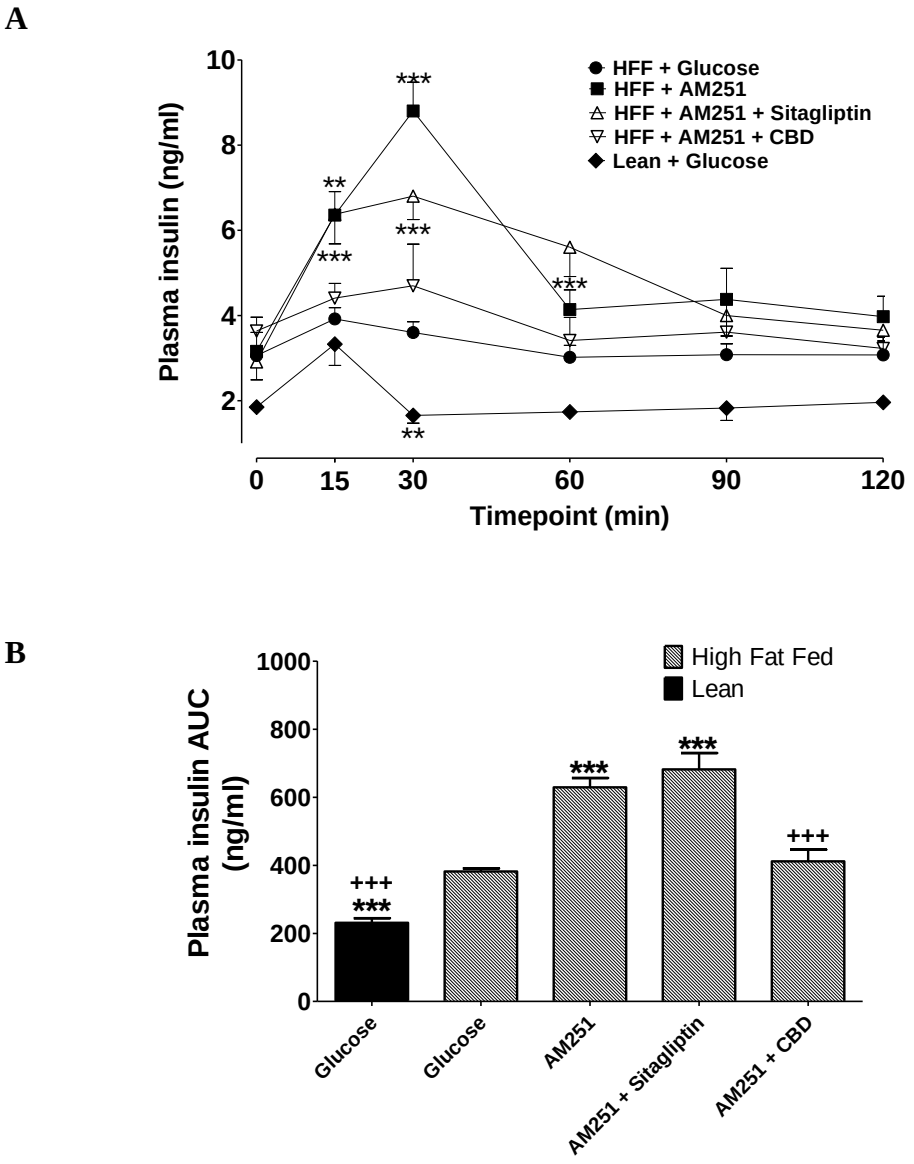

Acute effect of AM251 on plasma insulin (A) and respective AUC (B). Glucose (18 mmol/kg bw) was administered orally alone or in combination with AM251 (0.1 µmol/kg bw) and either the GPR55 antagonist CBD (0.1µmol/kg bw) or Sitagliptin (50 mg/kg bw) to HFF mice (n = 6). Values are presented as mean ± SEM. **p<0.01, ***p<0.001, compared to HFF glucose control. +++p<0.001, compared to agonist alone.

Figure 7.6: Acute effects of GPR55 agonists on total plasma GLP-1 in 18 h fasted high fat fed diabetic mice.

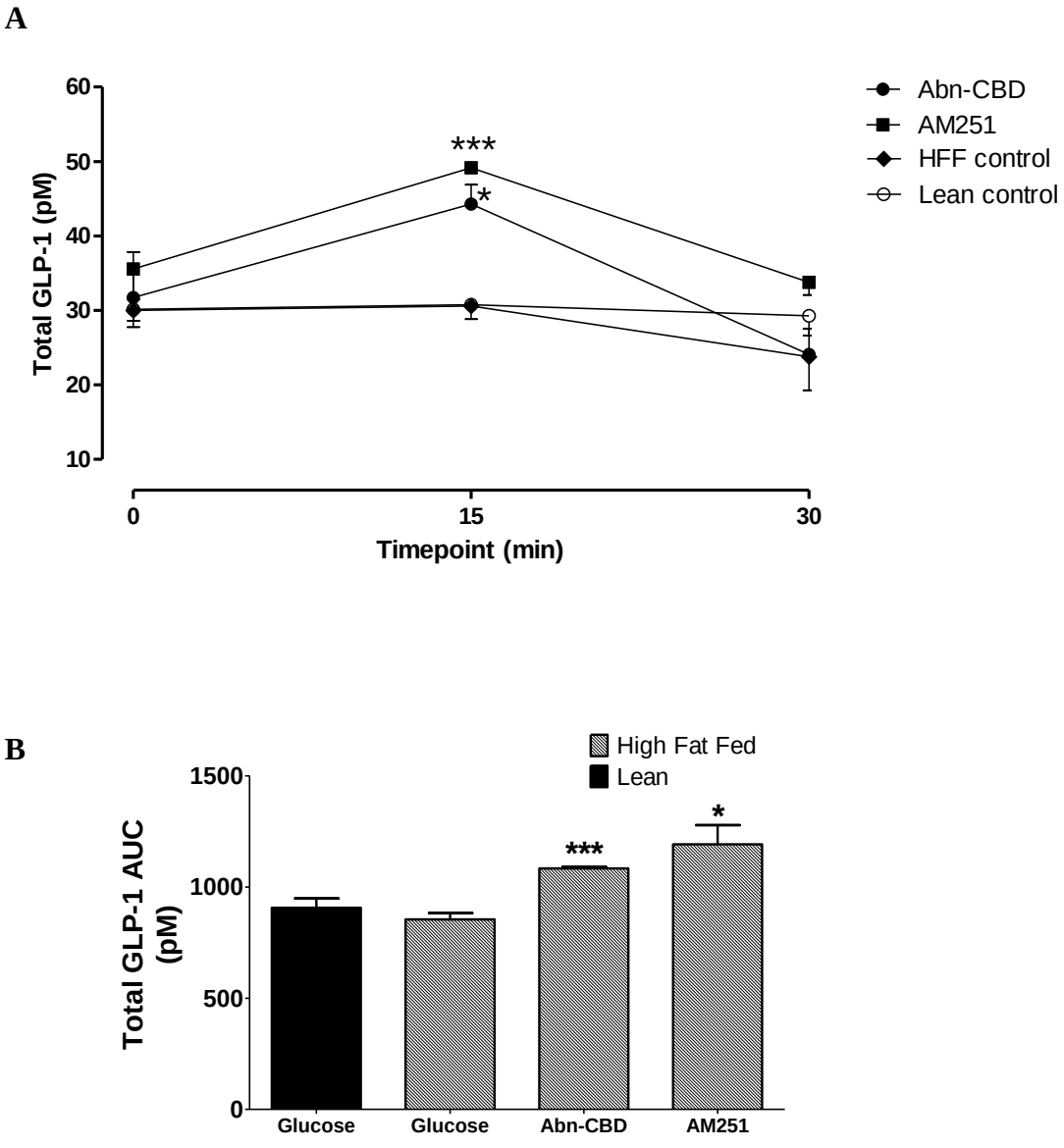

Acute effects of GPR55 agonists on total plasma GLP-1 (A) and respective AUC (B). Glucose (18 mmol/kg bw) was administered orally alone or in combination with GPR55 agonists (0.1 µmol/kg bw) to HFF mice (n = 6). Values are presented as mean ± SEM. *p<0.05, ***p<0.001, compared to HFF glucose control.

Figure 7.7: Acute effects of GPR55 agonists on total plasma GIP in 18 h fasted high fat fed diabetic mice.

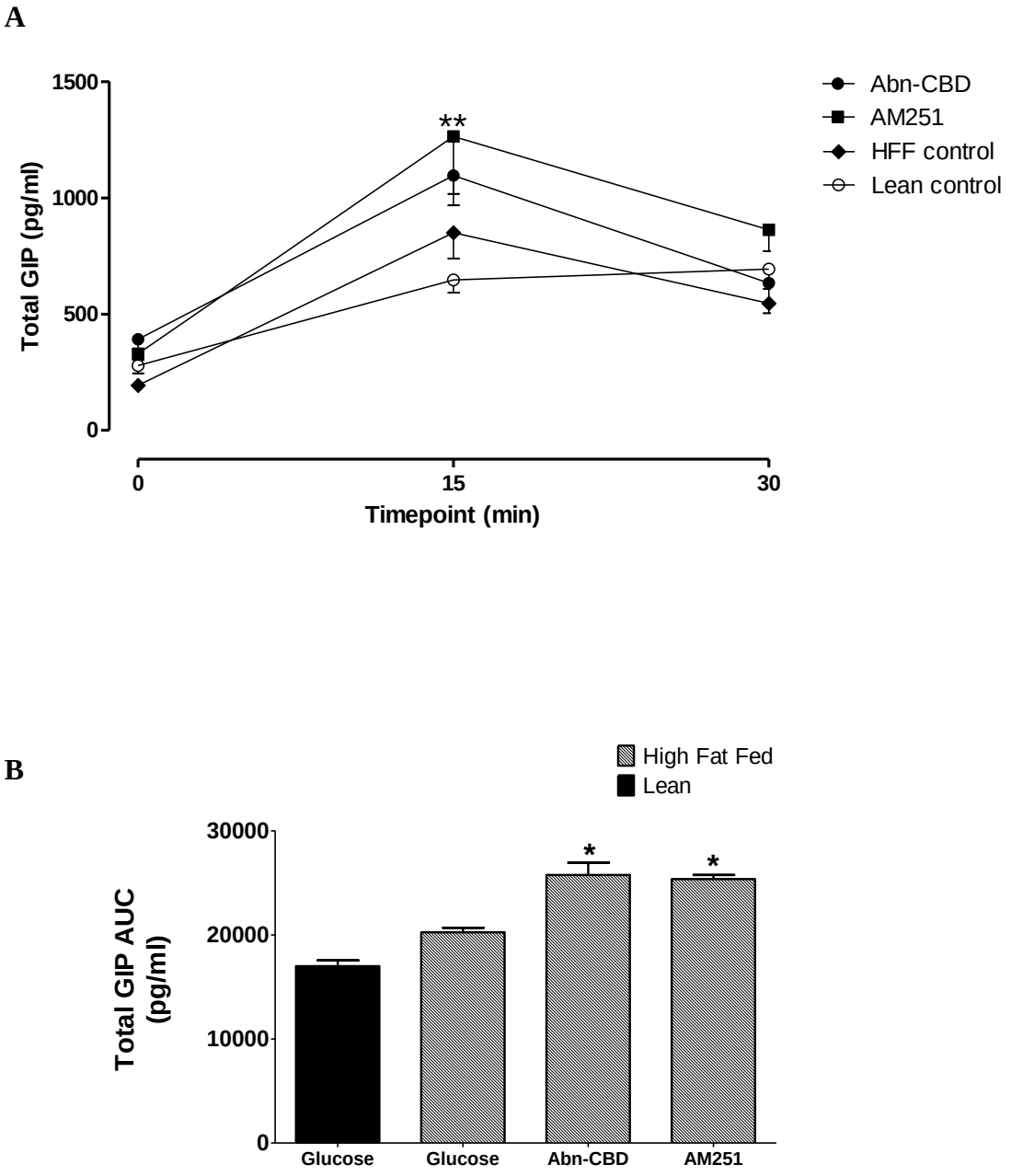

Acute effects of GPR55 agonists on total plasma GIP (A) and respective AUC (B). Glucose (18 mmol/kg bw) was administered orally alone or in combination with GPR55 agonists (0.1µmol/kg bw) to HFF mice (n = 6). Values are presented as mean ± SEM. *p<0.05, **p<0.01, compared to HFF glucose control.

Figure 7.8: Acute effects of GPR55 agonists and Sitagliptin on DPP-IV activity in 18 h fasted high fat fed diabetic mice.

A

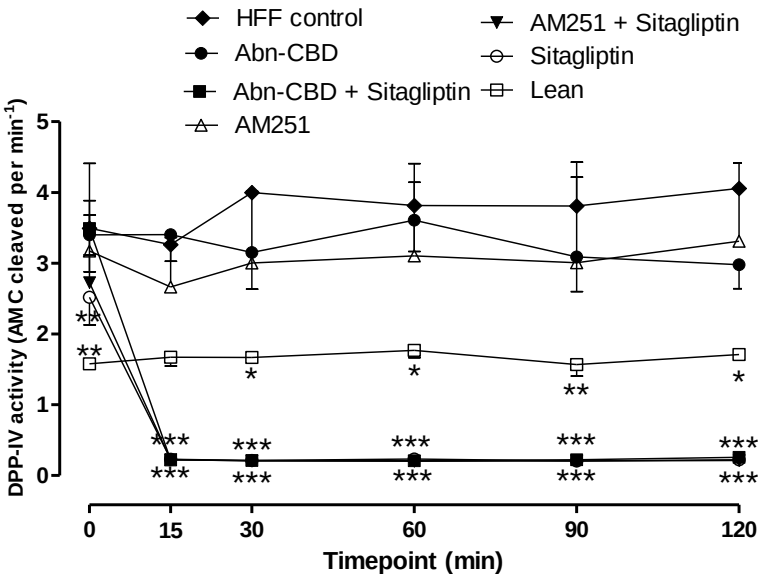

B

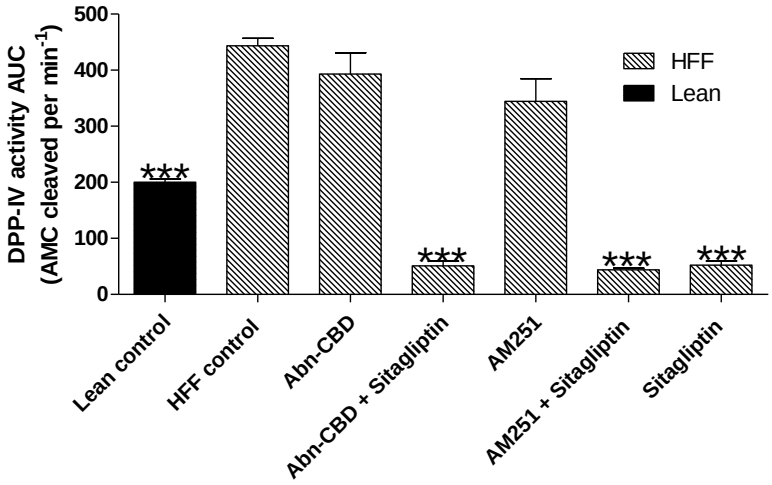

Acute effects of GPR55 agonists on DPP-IV activity (A) and respective AUC (B). Glucose (18 mmol/kg bw) was administered orally alone or in combination with GPR55 agonists (0.1 µmol/kg bw) to HFF mice (n = 6). Values are presented as mean ± SEM. *p<0.05, **p<0.01 ***p<0.001, compared to HFF glucose control.

Figure 7.9: Chronic effect of once daily oral administration of Abn-CBD monotherapy and combinational therapy (sitagliptin) on bodyweight in high fat fed diabetic mice.

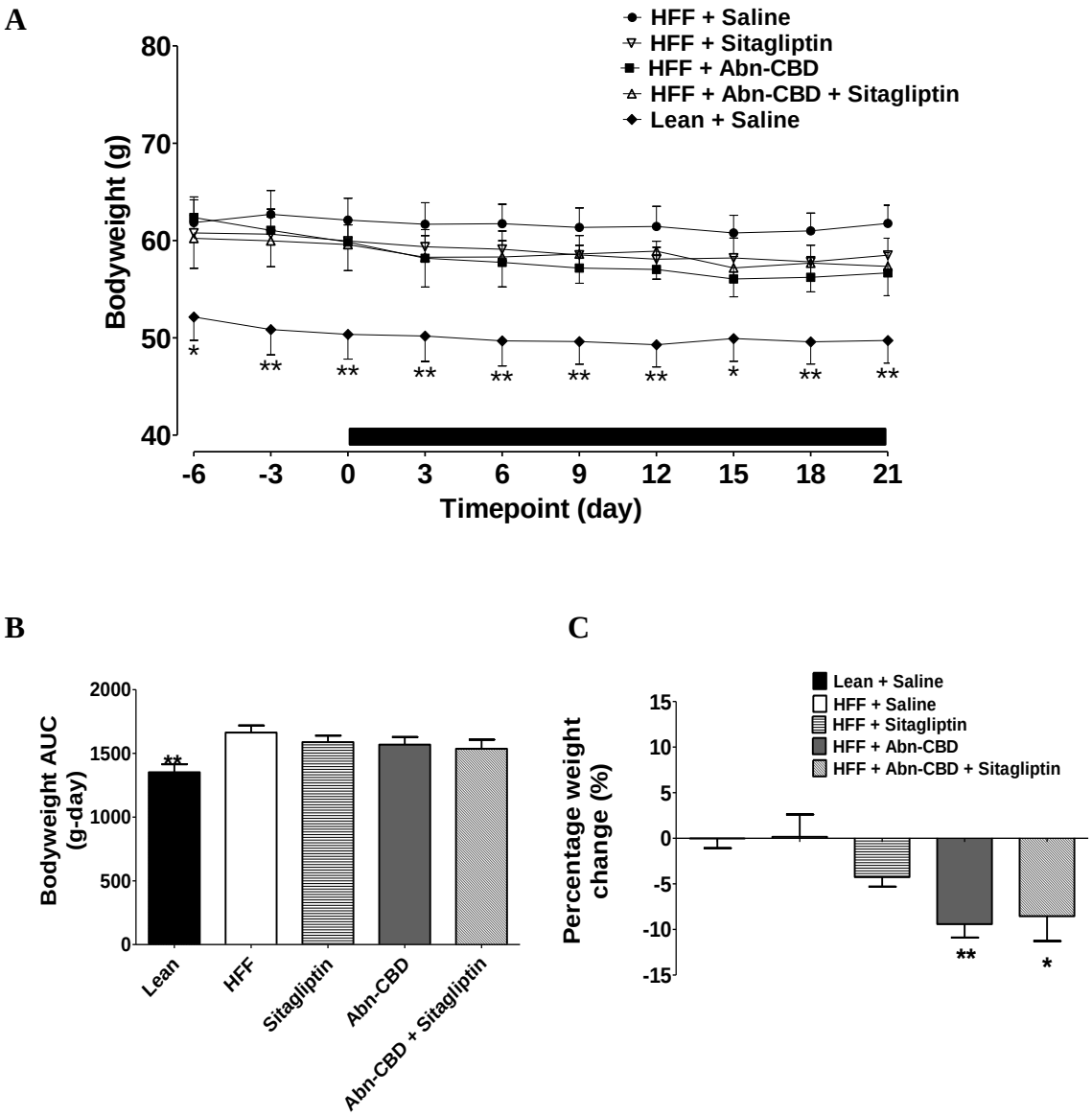

Chronic effect of Abn-CBD alone and in combination with Sitagliptin on (A) bodyweight, (B) respective AUC and (C) percentage weight change. Bodyweight measurements were obtained before and during Abn-CBD (0.1 µmol/kg bw) and Sitagliptin (50 mg/kg bw) therapies (indicated by the black bar). Values are presented as mean ± SEM (n = 8). *p<0.05, **p<0.01, compared to HFF control.

Figure 7.10: Chronic effect of once daily oral administration of Abn-CBD monotherapy and combinational therapy (Sitagliptin) for 21 days on plasma glucose in high fat fed diabetic mice.

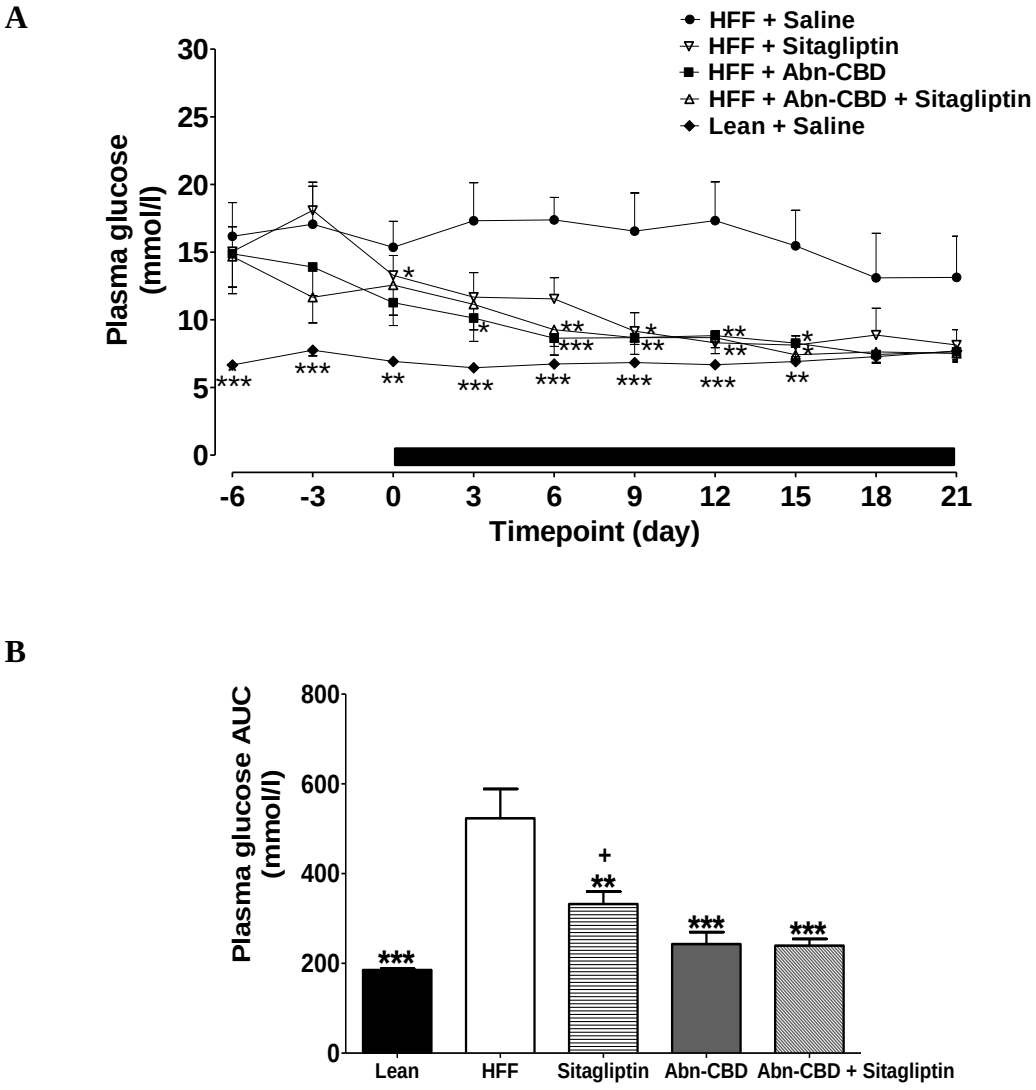

Chronic effect of Abn-CBD alone and in combination with Sitagliptin on (A) plasma glucose and (B) respective AUC. Parameters were obtained before and during Abn-CBD (0.1 µmol/kg bw) and Sitagliptin (50 mg/kg bw) therapies (indicated by the black bar). Values are presented as mean ± SEM (n = 8). *p<0.05, **p<0.01, ***p<0.001, compared to HFF control. +p<0.05, compared to Abn-CBD alone.

Figure 7.11: Chronic effect of once daily oral administration of Abn-CBD monotherapy and combinational therapy (Sitagliptin) for 21 days on plasma insulin concentrations in high fat fed diabetic mice.

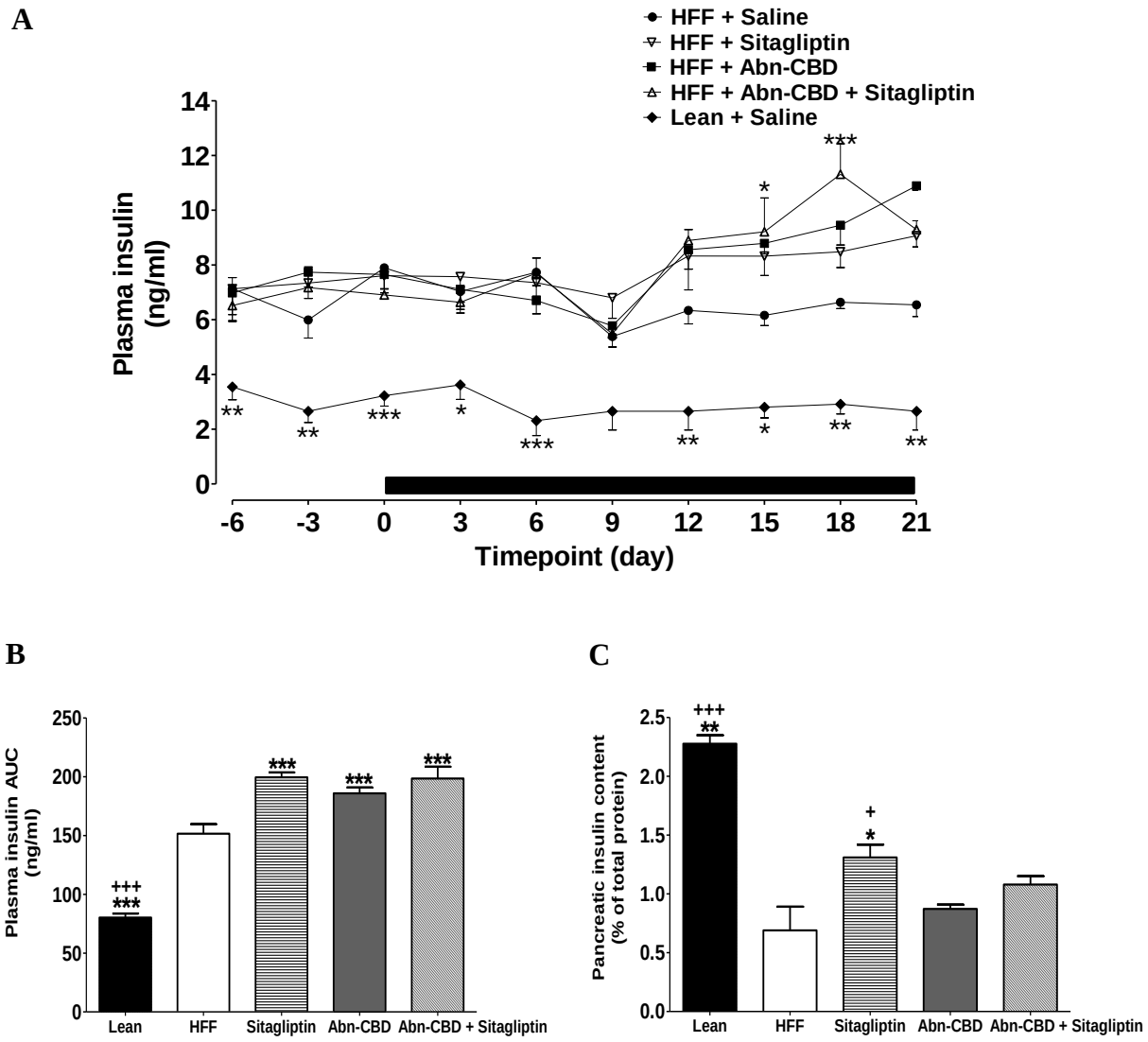

Chronic effect of Abn-CBD alone and in combination with Sitagliptin on (A) plasma insulin, (B) respective AUC and (C) pancreatic insulin content. Parameters were obtained before and during Abn-CBD (0.1 µmol/kg bw) and Sitagliptin (50 mg/kg bw) therapies (indicated by the black bar). Insulin content was determined after 21-day treatment. Values are presented as mean ± SEM (n = 8). *p<0.05, **p<0.01, ***p<0.001, compared to HFF control. +p<0.05, +++p<0.001, compared to Abn-CBD alone.

Figure 7.12: Chronic effect of once daily oral administration of Abn-CBD monotherapy and combinational therapy (Sitagliptin) for 21 days on circulating total-GLP-1 in high fat fed diabetic mice.

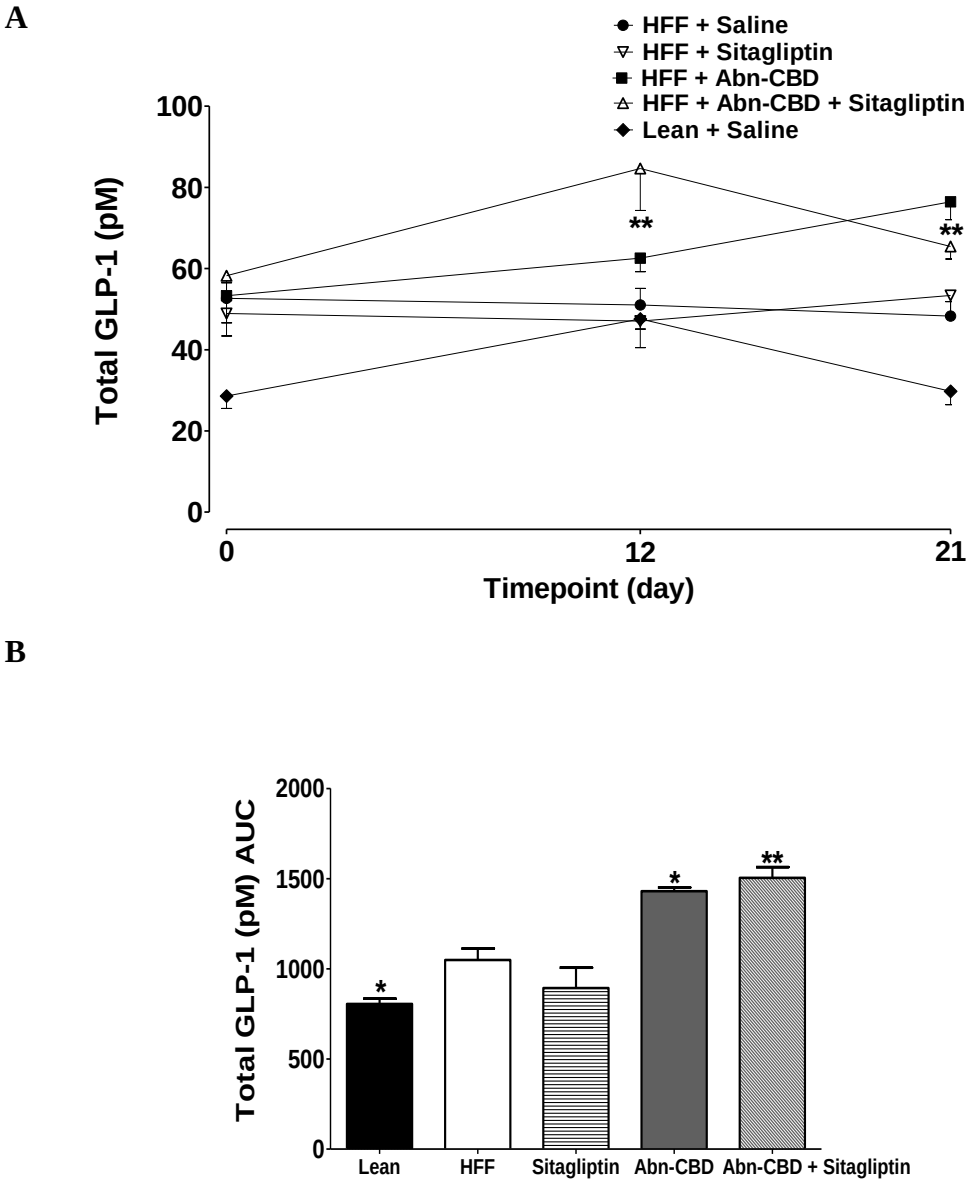

Chronic effect of Abn-CBD alone and in combination with Sitagliptin on (A) total-GLP-1 and (B) respective AUC. Parameters were obtained before and during Abn-CBD (0.1 µmol/kg bw) and Sitagliptin (50 mg/kg bw) therapies. Values are presented as mean ± SEM (n = 6). *p<0.05, **p<0.01, compared to HFF control.

Figure 7.13: Chronic effect of once daily oral administration of Abn-CBD monotherapy and combinational therapy (Sitagliptin) for 21 days on circulating total-GIP in high fat fed diabetic mice.

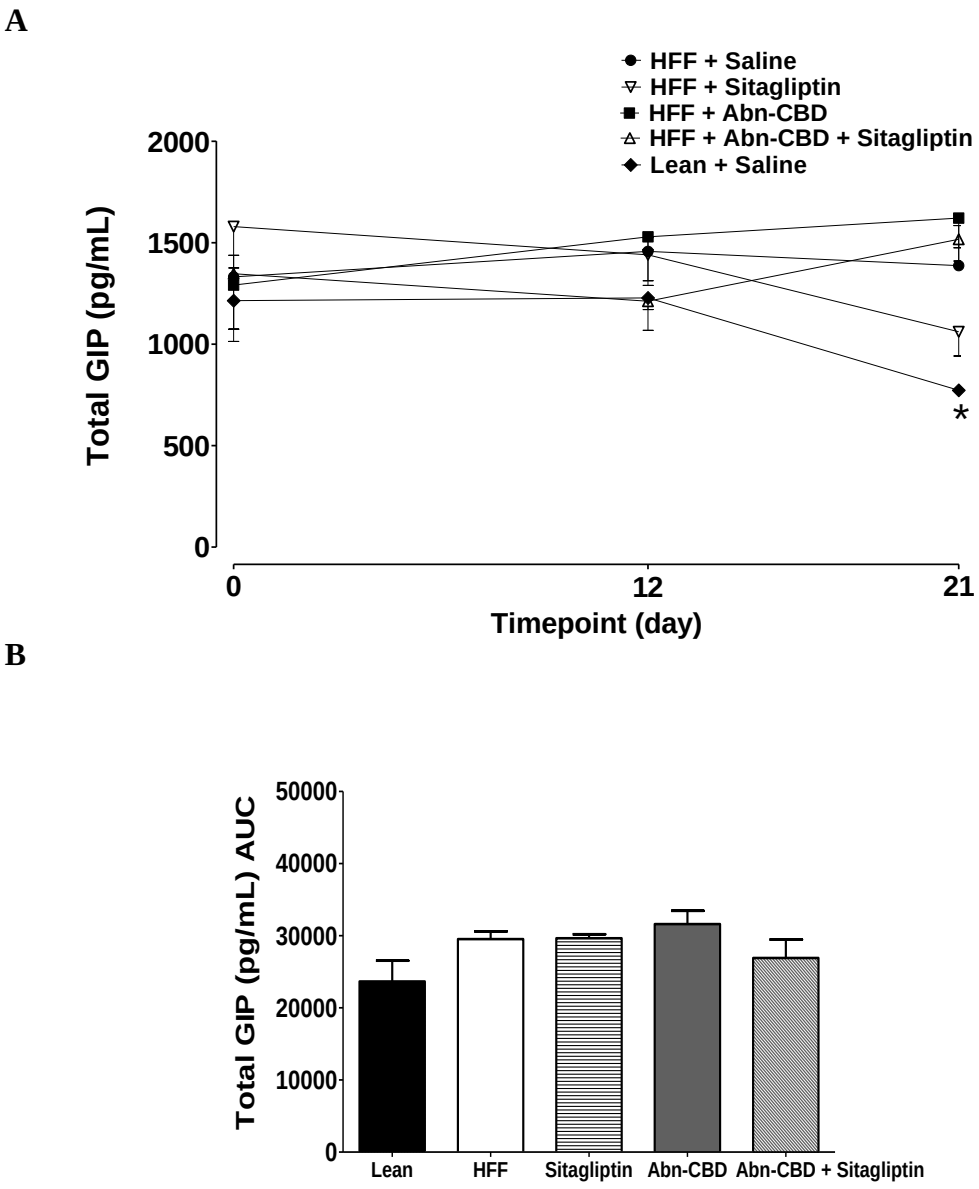

Chronic effect of Abn-CBD alone and in combination with Sitagliptin on (A) total-GIP and (B) respective AUC. Parameters were obtained before and during Abn-CBD (0.1 µmol/kg bw) and Sitagliptin (50 mg/kg bw) therapies. Values are presented as mean ± SEM (n = 6). *p<0.05, compared to HFF control.

Figure 7.14: Chronic effect of once daily oral administration of Abn-CBD monotherapy and combinational therapy (Sitagliptin) for 21 days on DPP-IV activity in high fat fed-induced diabetic mice.

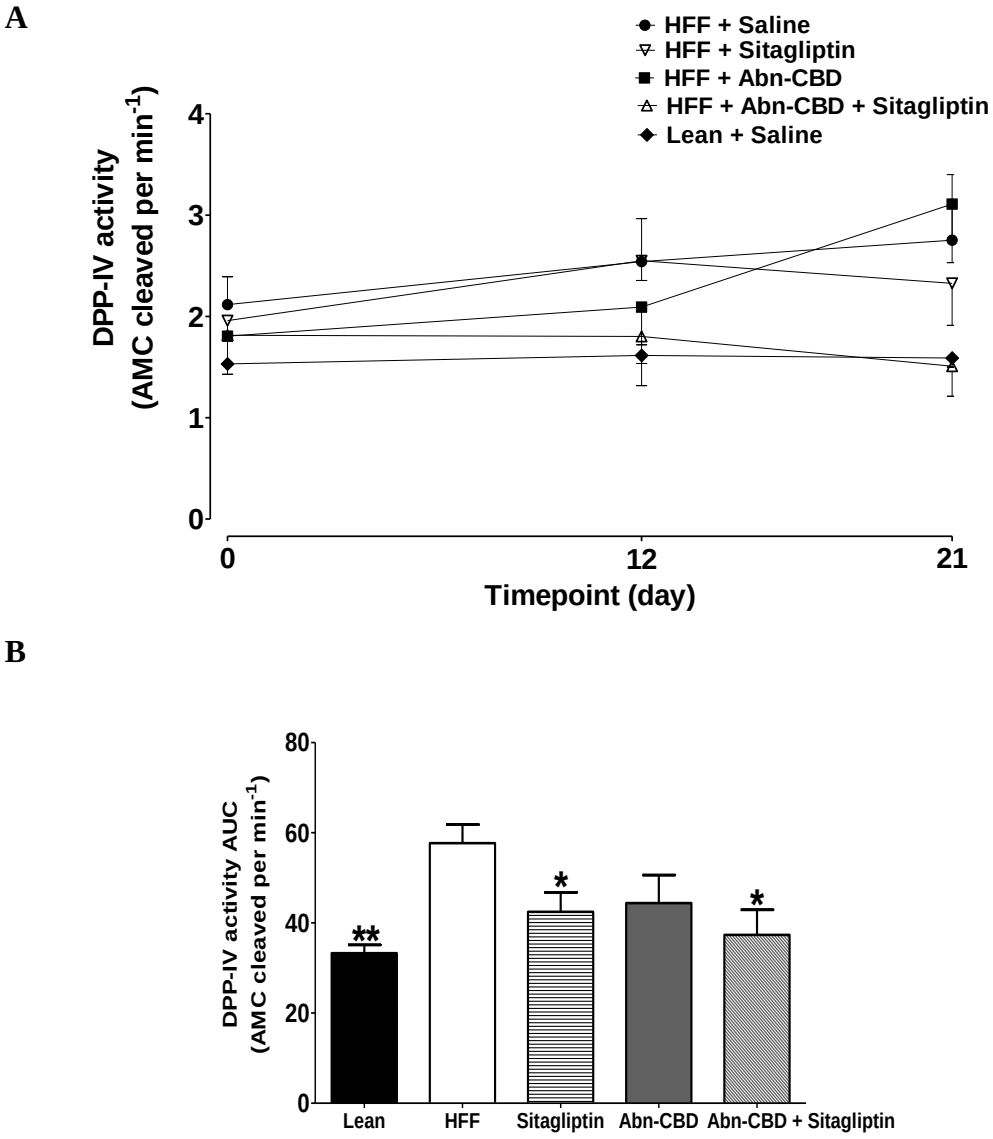

Chronic effect of Abn-CBD alone and in combination with Sitagliptin on (A) DPP-IV activity and (B) respective AUC. Parameters were obtained before and during Abn-CBD (0.1 µmol/kg bw) and Sitagliptin (50 mg/kg bw) therapies (indicated by the black bar). Values are presented as mean ± SEM (n = 8). *p<0.05, **p<0.01, compared to HFF control. +p<0.05, compared to Abn-CBD alone.

Figure 7.15: Chronic effect of once daily oral administration of Abn-CBD monotherapy and combinational therapy (Sitagliptin) for 21 days on food intake in high fat fed diabetic mice.

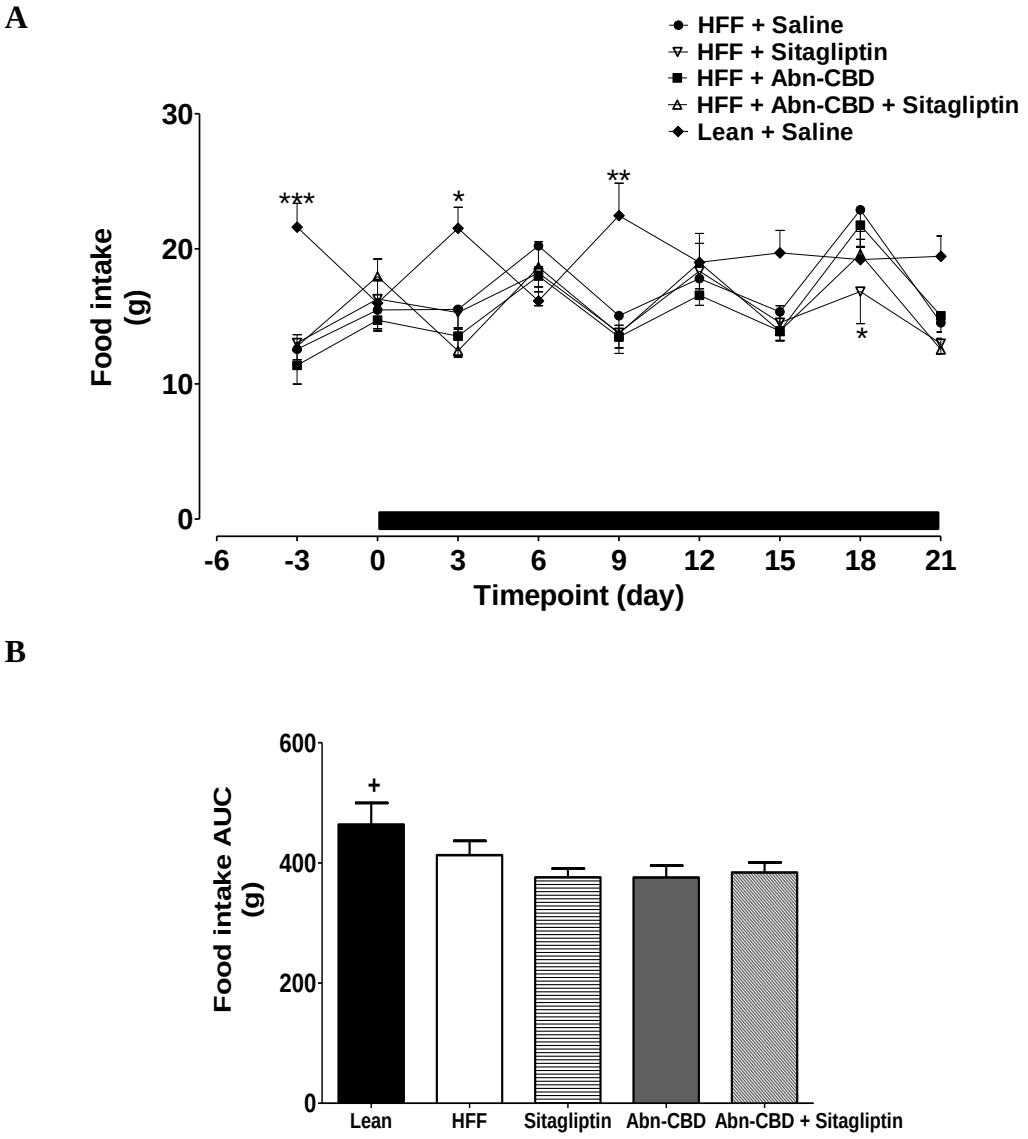

Chronic effect of Abn-CBD alone and in combination with Sitagliptin on (A) food intake and (B) respective AUC. Parameters were obtained before and during Abn-CBD (0.1µmol/kg bw) and Sitagliptin (50 mg/kg bw) therapies (indicated by the black bar). Values are presented as mean ± SEM (n = 8). *p<0.05, **p<0.01, ***p<0.001, compared to HFF control. +p<0.05, compared to Abn-CBD alone.

Figure 7.16: Chronic effect of once daily oral administration of Abn-CBD monotherapy and combinational therapy (Sitagliptin) for 21 days on cumulative food and energy intake in high fat fed diabetic mice.

A

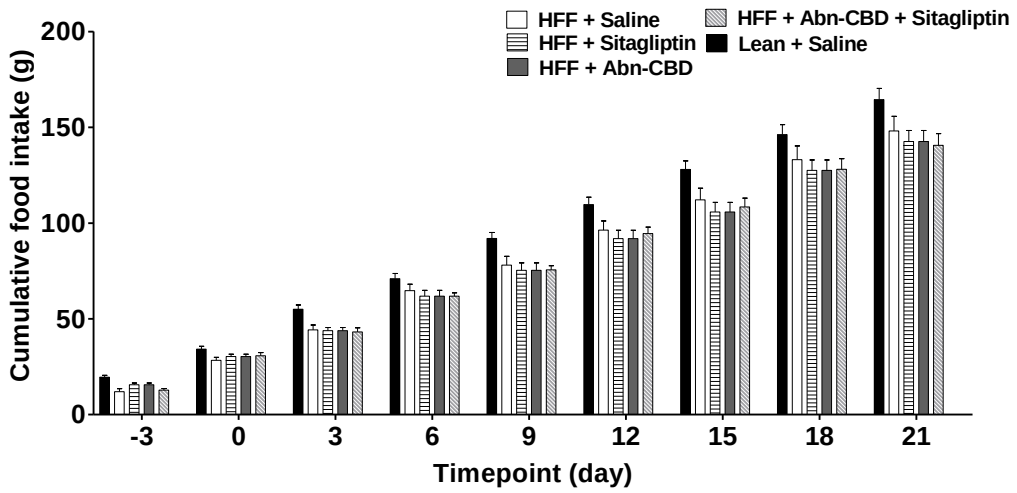

B

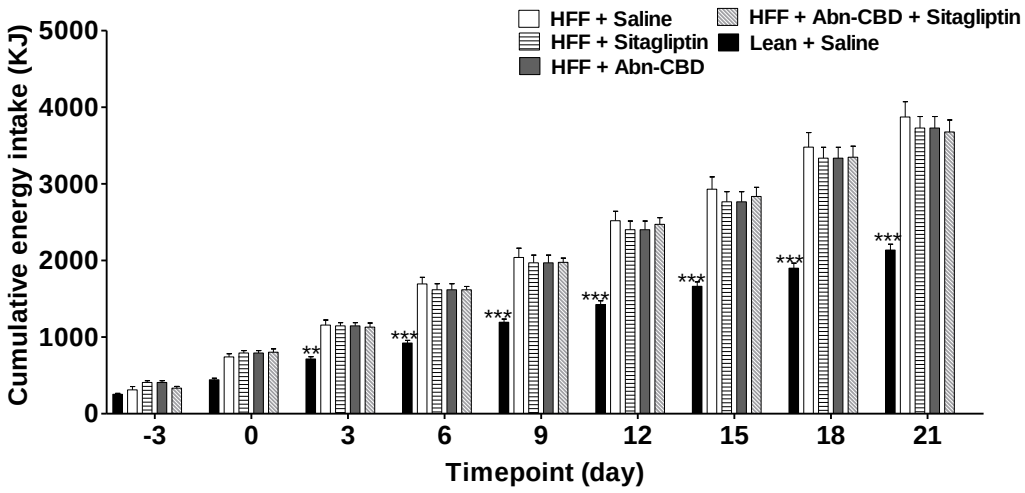

Chronic effect of Abn-CBD alone and in combination with Sitagliptin on (A) food intake and (B) energy intake. Parameters were obtained before and during Abn-CBD (0.1 µmol/kg bw) and Sitagliptin (50 mg/kg bw) therapies (indicated by the black bar). Values are presented as mean ± SEM (n = 8). *p<0.05, **p<0.01, ***p<0.001, compared to HFF control. +p<0.05, compared to Abn-CBD alone.

Figure 7.17: Chronic effect of 21-day oral administration of Abn-CBD monotherapy and combinational therapy (Sitagliptin) on glucose tolerance and insulin secretion in high fat fed diabetic mice.

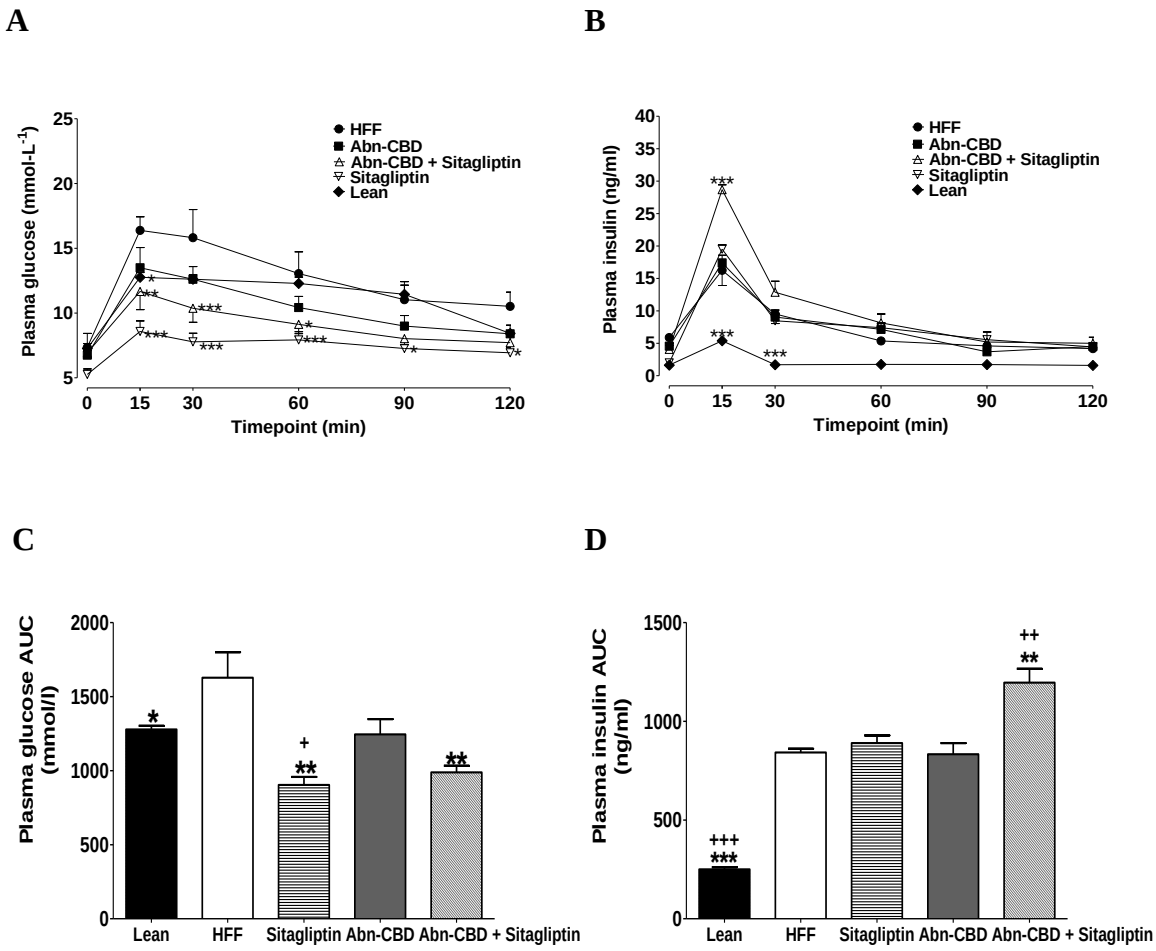

Oral glucose tolerance test (18 mmol/kg bw) was conducted on HFF mice following 21-day treatment with Abn-CBD (0.1µmol/kg bw) and/or Sitagliptin (50 mg/kg bw). (A, C) Plasma glucose and (B, D) plasma insulin were determined. Results are mean ± SEM (n=6). *p<0.05, **p<0.01, ***p<0.001, compared to HFF glucose control. ++p<0.01, +++p<0.001, compared to Abn-CBD alone.

Figure 7.18: Chronic effect of 21-day oral administration of Abn-CBD monotherapy and combinational therapy (Sitagliptin) on insulin sensitivity in high fat fed diabetic mice.

A

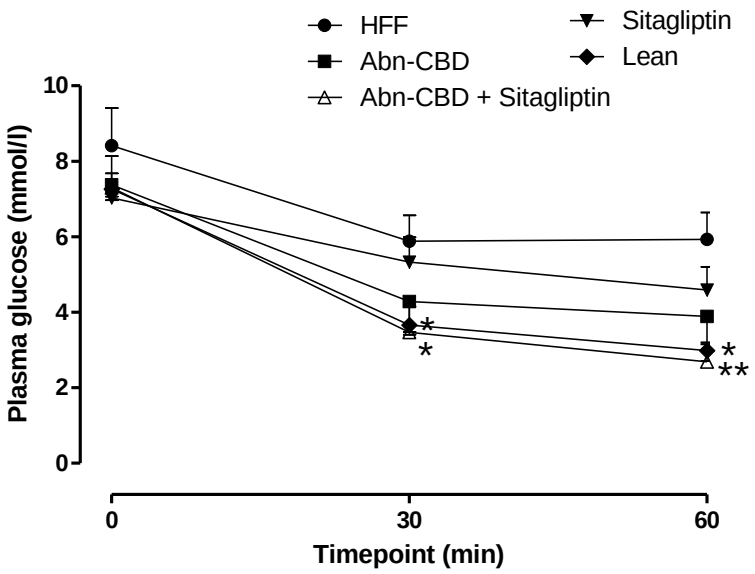

B

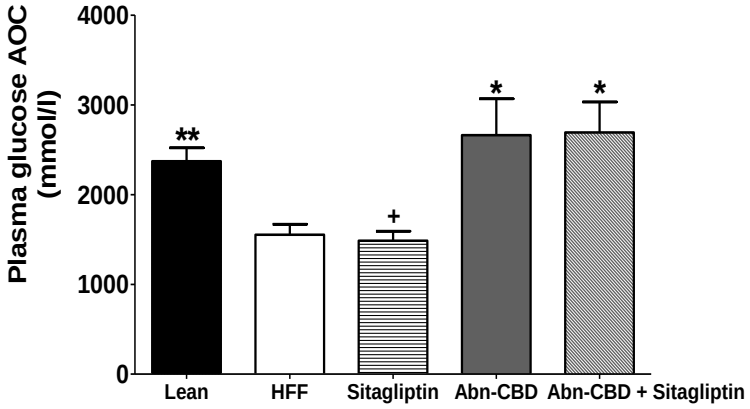

Insulin sensitivity (40U/kg bodyweight; dissolved in 0.9% saline, i.p. injection) test was conducted following 21-day treatment with Abn-CBD alone (0.1 µmol/kg bw) or in combination with Sitagliptin (50 mg/kg bw) to HFF diabetic mice. (A) Blood glucose and (B) respective AOC are shown. Results are mean ± SEM (n=8). *p<0.05, **p<0.01, compared to HFF control. +p<0.05, compared to Abn-CBD alone.

Figure 7.19: Chronic effect of 21-day oral administration of Abn-CBD monotherapy and combinational therapy (Sitagliptin) on bodyweight, fat mass and lean mass as measured by DEXA in high fat fed diabetic mice.

A

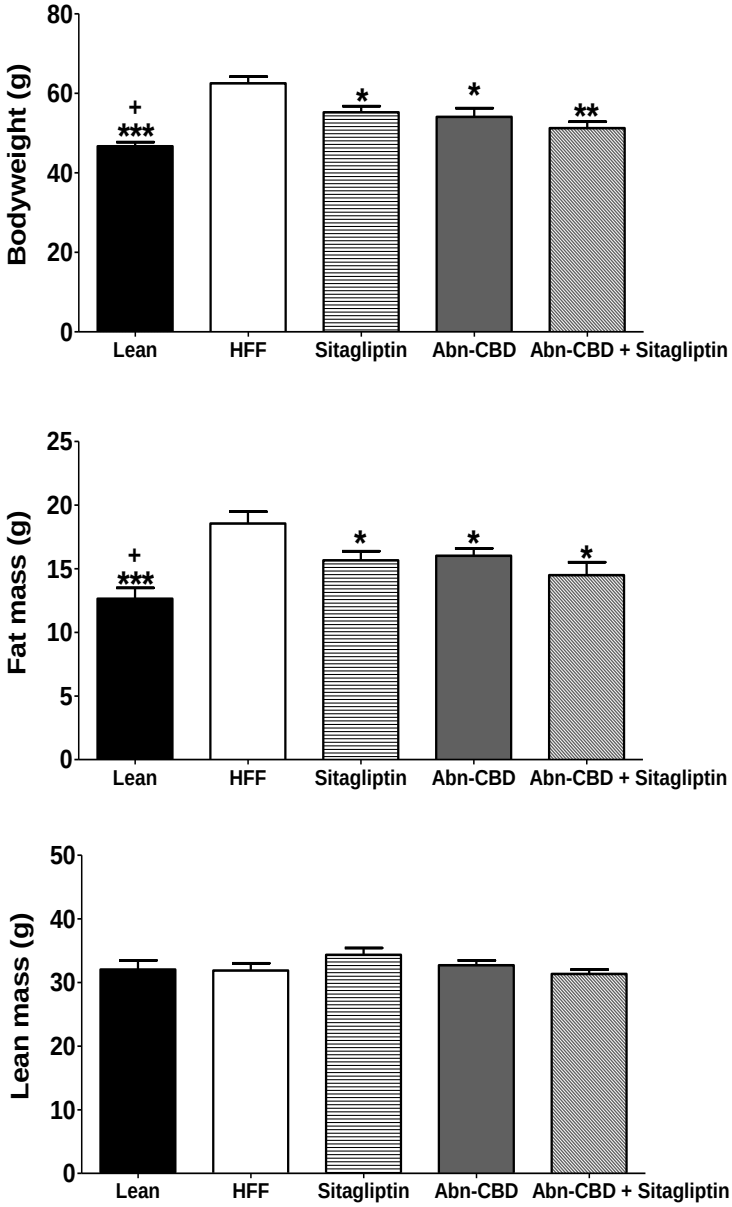

Chronic effect of 21-day oral administration of Abn-CBD (0.1 µmol/kg bw) alone and in combination with Sitagliptin (50 mg/kg bw) on (A) bodyweight, (B) fat mass and (C) lean mass in HFF diabetic mice. Values are presented as mean ± SEM (n = 8). *p<0.05, **p<0.01, ***p<0.001, compared to HFF control. +p<0.05, compared to Abn-CBD alone.

Figure 7.20: Chronic effect of 21-day oral administration of Abn-CBD monotherapy and combinational therapy (Sitagliptin) on total bone mineral content and bone mineral density as measured by DEXA in high fat fed diabetic mice.

A

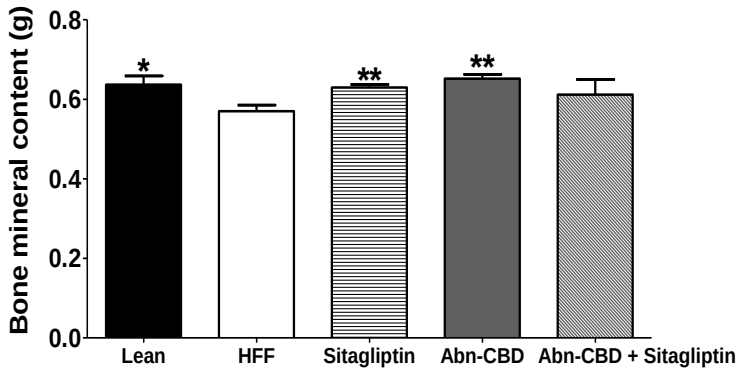

B

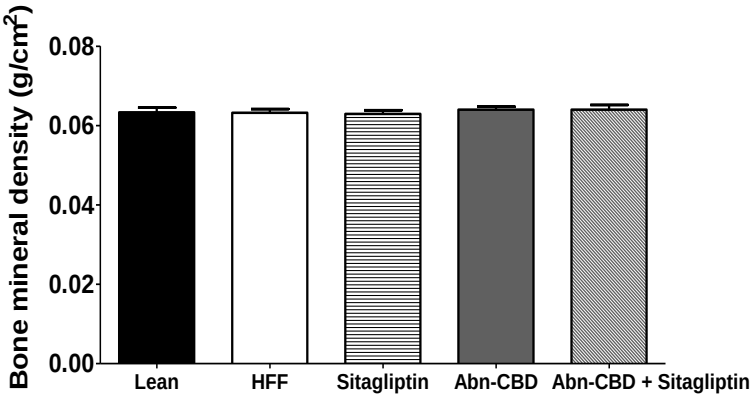

Chronic effect of 21-day oral administration of Abn-CBD (0.1 µmol/kg bw) alone and in combination with Sitagliptin (50 mg/kg bw) on (A) bone mineral content, (B) bone mineral density in HFF diabetic mice. Values are presented as mean ± SEM (n = 8). *p<0.05, **p<0.01, compared to HFF control.

Figure 7.21: Chronic effect of 21-day oral administration of Abn-CBD monotherapy and combinational therapy (Sitagliptin) on total bone mineral content and bone mineral density as measured by DEXA in the femur of high fat fed diabetic mice.

A

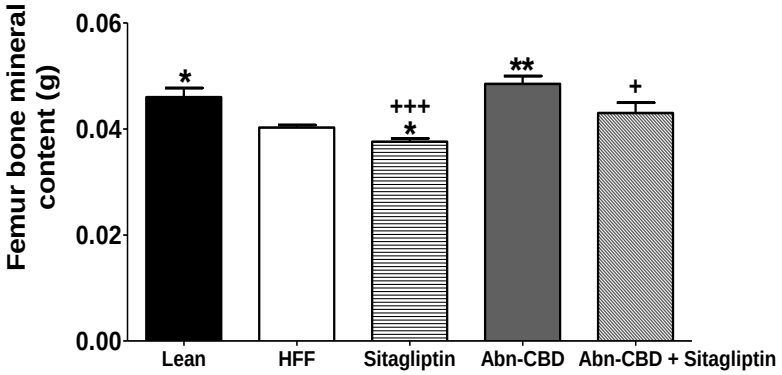

B

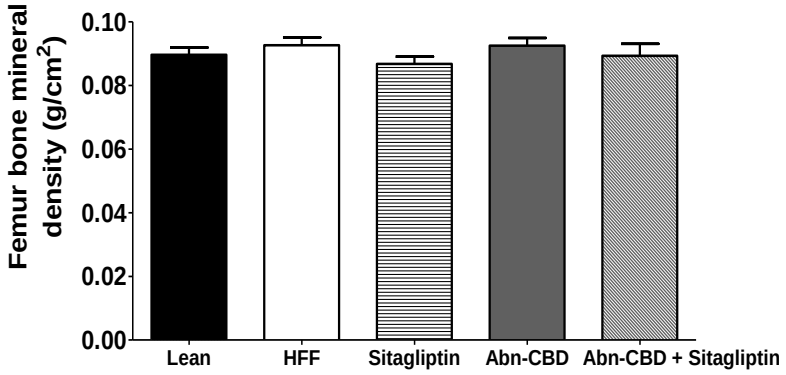

Chronic effect of 21-day oral administration of Abn-CBD (0.1 µmol/kg bw) alone and in combination with Sitagliptin (50 mg/kg bw) on (A) bone mineral content, (B) bone mineral density in the femur of HFF diabetic mice. Values are presented as mean ± SEM (n = 8). *p<0.05, **p<0.01, compared to HFF control. +p<0.05, +++p<0.001, compared to Abn-CBD alone.

Figure 7.22: Chronic effect of 21-day oral administration of Abn-CBD monotherapy and combinational therapy (Sitagliptin) on plasma triglycerides and total cholesterol in high fat fed diabetic mice.

A

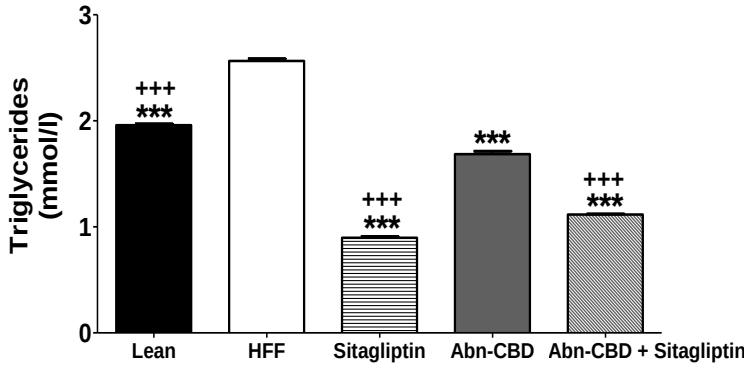

B

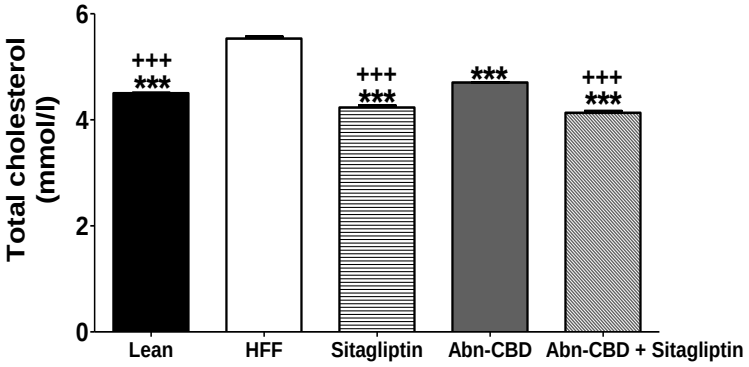

Chronic effect of 21-day oral administration of Abn-CBD (0.1 µmol/kg bw) alone and in combination with Sitagliptin (50 mg/kg bw) on (A) plasma triglyceride, (B) total cholesterol in HFF diabetic mice. Values are presented as mean ± SEM (n = 8). ***p<0.001, compared to HFF control. +++p<0.001, compared to Abn-CBD alone.

Figure 7.23: Chronic effect of 21-day oral administration of Abn-CBD monotherapy and combinational therapy (Sitagliptin) on plasma HDL cholesterol and LDL cholesterol in high fat fed diabetic mice.

A

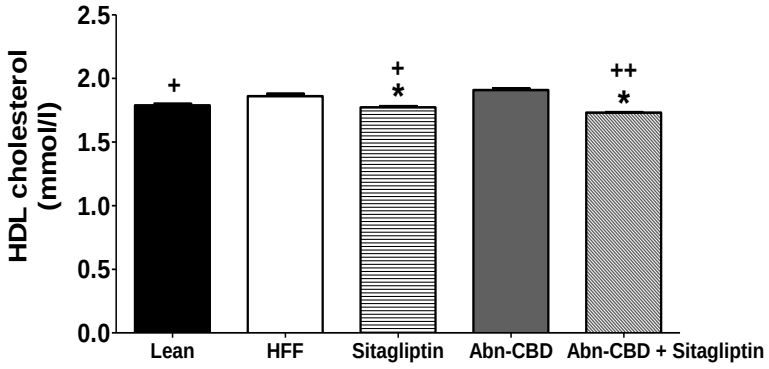

B

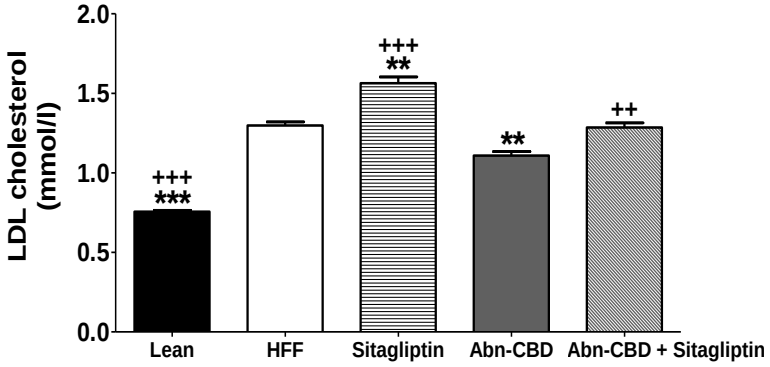

Chronic effect of 21-day oral administration of Abn-CBD (0.1 µmol/kg bw) alone and in combination with Sitagliptin (50 mg/kg bw) on plasma (A) triglycerides and (B) total cholesterol in HFF diabetic mice. Values are presented as mean ± SEM (n = 8). *p<0.05, **p<0.01, ***p<0.001, compared to HFF control. +p<0.05, ++p<0.01, +++p<0.001, compared to Abn-CBD alone.

Figure 7.24: Chronic effect of 21-day oral administration of Abn-CBD monotherapy and combinational therapy (Sitagliptin) on plasma C-reactive protein and amylase activity in high fat fed diabetic mice.

A

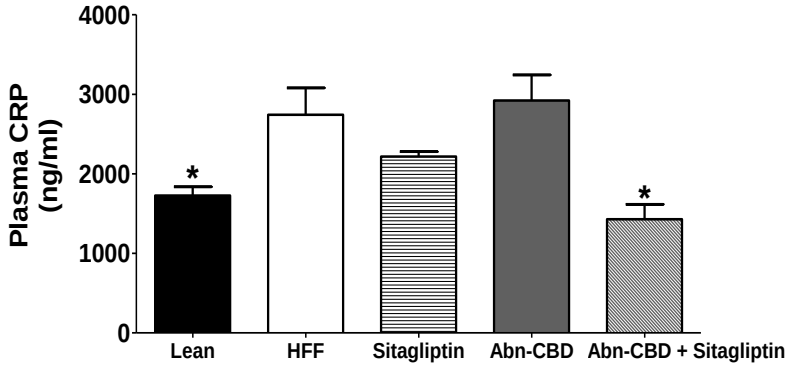

B

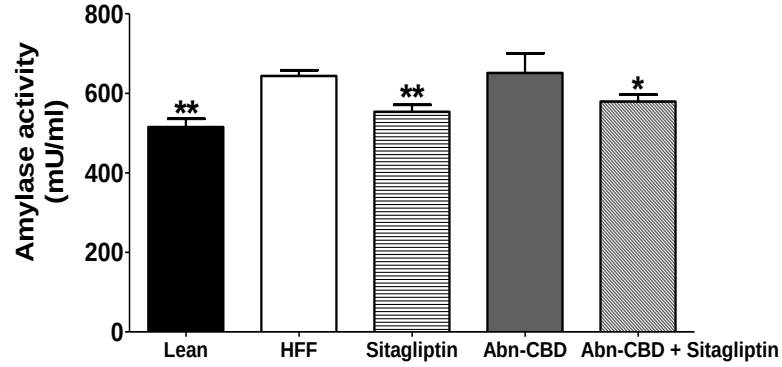

Chronic effect of 21-day oral administration of Abn-CBD (0.1 µmol/kg bw) alone and in combination with Sitagliptin (50 mg/kg bw) on plasma (A) C-reactive protein and (B) amylase activity in HFF diabetic mice. Values are presented as mean ± SEM (n = 6). *p<0.05, **p<0.01, compared to HFF control.

Figure 7.25: Distribution of islet insulin and glucagon, following 21-day oral administration of Abn-CBD monotherapy and combinational therapy (Sitagliptin) in high fat fed-induced diabetic mice.

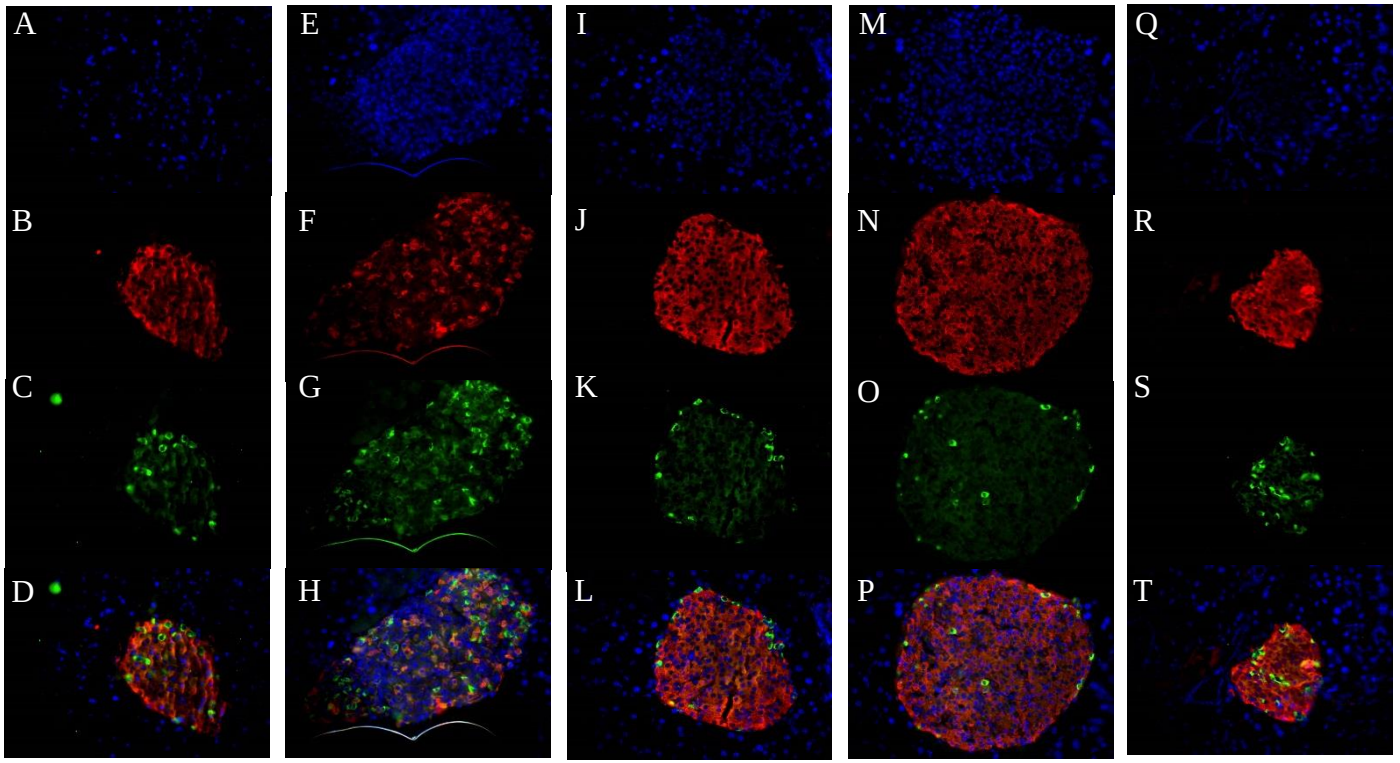

Representative images for distribution of DAPI (blue), insulin (red) and glucagon (green) in pancreatic islets of HFF mice at x40 magnification, following 21-day treatment of (A-D) lean control, (E-H) HFF, (I-L) Sitagliptin, (M-P) Abn-CBD and (Q-T) Abn-CBD + Sitagliptin.

Figure 7.26: Effect of 21-day oral administration of Abn-CBD monotherapy and combinational therapy (Sitagliptin) on islet morphology in high fat fed diabetic mice.

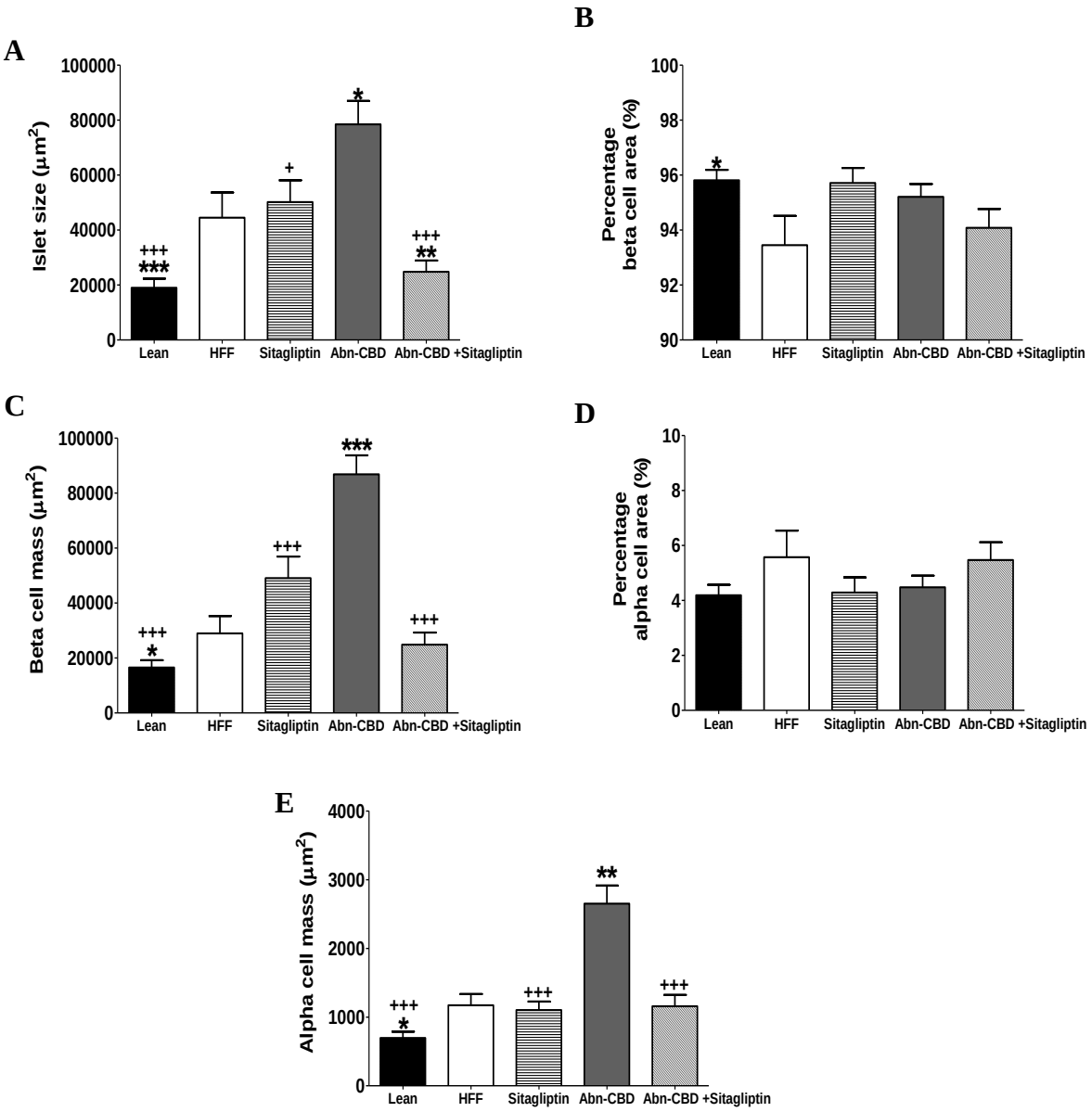

Immunohistochemistry analysis demonstrating the effect of Abn-CBD monotherapy and combinational therapy (Sitagliptin) on (A) islet size, (B) beta cell area, (C) beta cell mass, (D) alpha cell area and (E) alpha cell mass in HFF mice. Values are mean ± SEM (n = 8), with 30 islets per group. *p<0.05, **p<0.01, ***p<0.001, compared to HFF. +p<0.05, +++p<0.001, compared to Abn-CBD alone. (Representative images as per Figure 7.25)

Figure 7.27: Effect of 21-day oral administration of Abn-CBD on beta cell proliferation (Ki-67) in high fat fed diabetic mice.

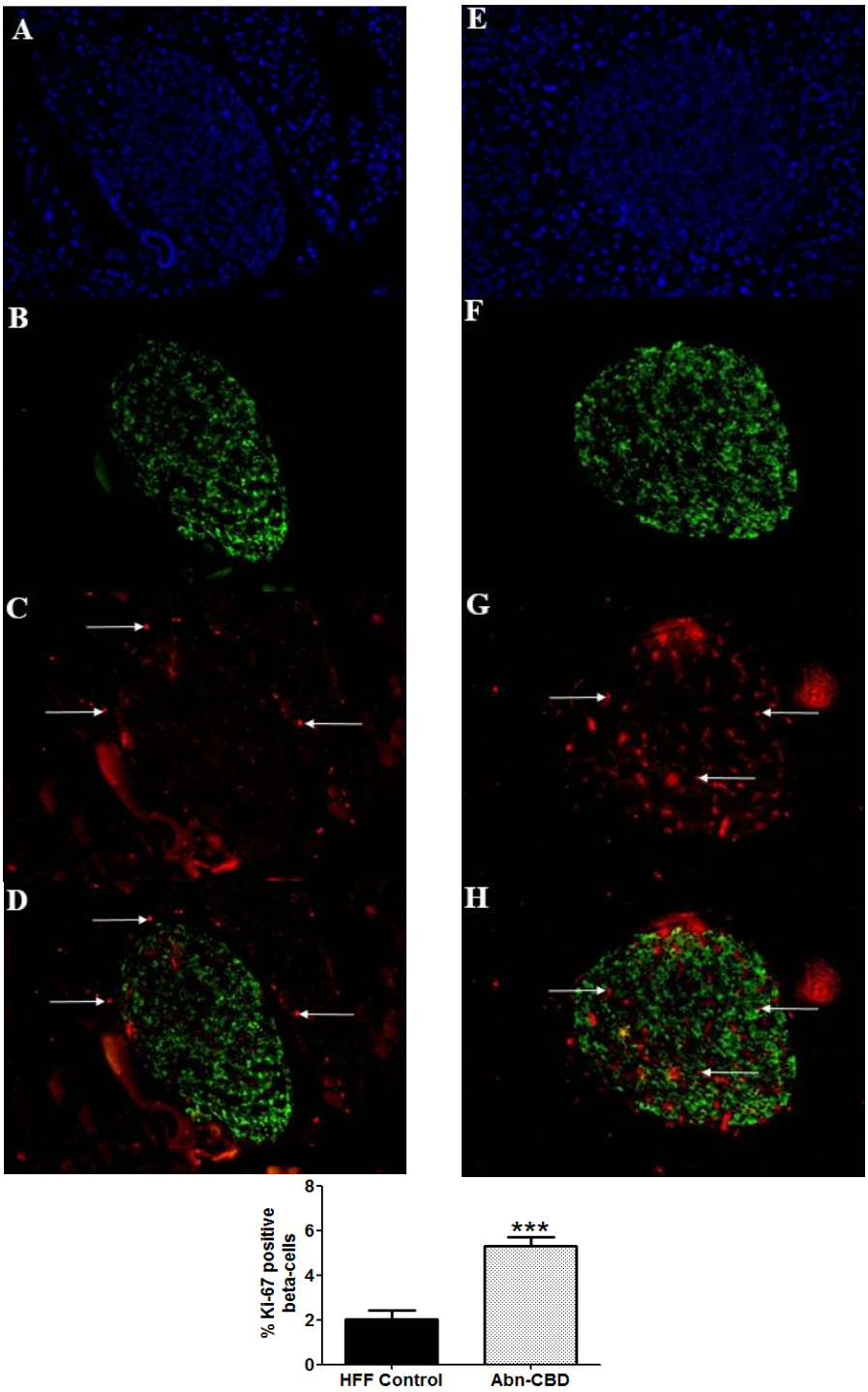

Representative images for DAPI (blue), insulin (green) and Ki-67 (red) in pancreatic islets of HFF mice at x40 magnification, following 21-day treatment with (A-D) HFF control and (E-H) Abn-CBD. Values are mean ± SEM (n = 8), with 50 islets per group. ***p<0.001, compared to HFF. Positive Ki-67 staining indicated by arrows.

Figure 7.28: Distribution of GPR55 and insulin in pancreatic islets from lean and HFF mice.

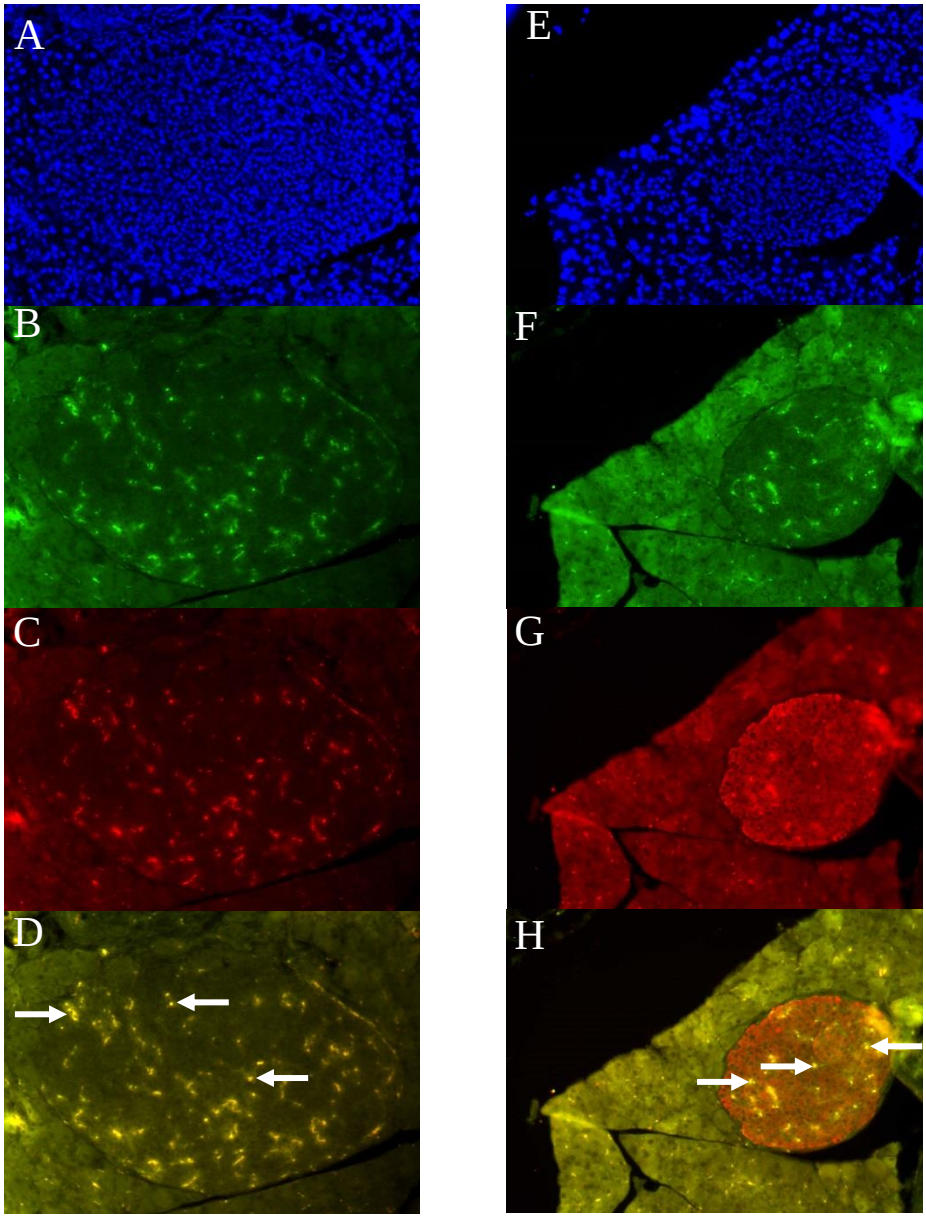

Immunohistochemistry demonstrating the distribution of DAPI (blue), GPR55 (green) and insulin (red) in HFF (A-D) and lean (E-H) pancreatic islets at x40 magnification. Areas of double immunofluorescent staining indicated by white arrows. Images are representative of several tissue sections.

Chapter 8

General Discussion

8.1: Limitations of current anti-diabetic therapeutics

The primary objective for all anti-diabetic therapies is to maintain glucose homeostasis whilst attenuating micro- and macro-vascular complications correlated with the disease (Lebovitz 2011). First line treatments routinely fail to maintain glycaemic control with long-term patient response rates declining over time; warranting combinational therapeutic approaches to retain normoglycemia (Turner *et al.* 1999, Cahn & Cefalu 2016). Moreover, current therapies overlook chronic complications of diabetes including obesity, CVD risk and kidney disease (Molenaar *et al.* 2008, Trudeau & Gilbert 2018). According to ADA/EASD guidelines, metformin monotherapy is the current first line of treatment; however, 20-30% of patients have reported adverse effects with this approach, including gastrointestinal tract discomfort, nausea and vomiting (American Diabetes Association 2015, Schommers *et al.* 2017). In addition, second line therapeutics such as sulphonylureas, meglitinides and TZDs have been shown to favour weight gain, hypoglycaemia, increase ischemic complications and accelerate beta cell exhaustion (Del Prato & Pulizzi 2006, Chaudhury *et al.* 2017).

The pathophysiology of type 2 diabetes is a multifactorial process that involves numerous organs in the body, whilst many current therapies exploit single glucoregulatory responses, such as insulin secretion, insulin resistance or hepatic glucose production (Bailey 2000). Moreover, current oral therapies fail to counteract reduced beta cell mass and impaired beta cell function, ultimately leading to beta cell exhaustion and poor disease prognosis (Cernea & Raz 2011). In recent years, incretin mimetics with increased plasma stability and DPP-IV inhibitors have been identified as promising classes of anti-diabetic drugs due to their ability to maintain glucose homeostasis and enhance beta cell proliferation (Siddigui 2009, Vanderheiden *et al.* 2016). Incretin-based therapies omit the

risk of hypoglycaemia and have been shown to display a range of additional beneficial effects towards cognitive function and cardio-protection (Groeneveld *et al.* 2016).

8.2: GPCR targeting therapeutics

It has been estimated that 108 independent GPCRs are the primary target of 475 FDA approved drugs, accounting for approximately 34% of all drugs (Hauser *et al.* 2017). However, it has been estimated that around 700 FDA approved drugs stimulate GPCR activation (Sriram & Insel 2018). Reports conclude that 321 GPCR ligands are undergoing clinical trials, whilst 66 (20%) of these agents are targeting novel GPCRs with no pre-approved drug (Hauser *et al.* 2017). Subsequently, the number of biological drugs, selective agonists and allosteric modulators have increased (Hauser *et al.* 2017). Disease indications for GPCR agonist therapies have primarily shifted towards obesity, diabetes, Alzheimer's disease and other neurological disorders (Hauser *et al.* 2017, Sriram & Insel 2018). Currently, 56% (224) of non-olfactory GPCRs have not yet been explored in clinical trials and present untapped therapeutic potential for the treatment of metabolic, genetic and immune system disorders (Hauser *et al.* 2017, Sriram & Insel 2018).

Non-olfactory GPCRs (e.g. incretin, cannabinoid and free fatty acid receptors) have presented therapeutic interest due to their regulation by a diverse range of ligands including peptides, fatty acids and monatomic ions (Reimann & Gribble 2016). With respect to obesity and type 2 diabetes, research has intensified on the exploitation of incretin receptors (GLP-1, GIP) due to the effectiveness of the endogenous incretin hormones on glucose homeostasis, bodyweight management and islet cell regeneration

(Siddigui 2009, Vanderheiden *et al.* 2016). The incretin GPCRs are expressed in the gut-brain-pancreatic axis and are key regulators of postprandial metabolism and food intake (Reimann & Gribble 2016). GLP-1 mimetics liraglutide and exenatide are current pharmaceuticals that act through incretin GPCRs, whilst once weekly GLP-1 mimetics (e.g. Semaglutide) have also become available (Madsbad 2009, Andreadis *et al.* 2018). Interestingly, pre-clinical trials using hybrid peptides that simultaneously target multiple glucoregulatory GPCRs have shown promise in diabetic animal models (Gault *et al.* 2013).

Aside from peptide hormones, fatty acid receptors have been shown to play a pivotal role in lipid and glucose homeostasis with recent studies revealing GPCR-dependent effects on islet and enteroendocrine cell secretions (McKillop *et al.* 2013, Moran *et al.* 2014, Moran *et al.* 2016) (Table 8.1). Moreover, several fatty acid ligands have undertaken clinical trials for metabolic, inflammatory and immune system disorders. GPR40 (FFAR1) is a long chain fatty acid sensing receptor that has shown promise for the treatment of type 2 diabetes with Fasiglifam (TAK875) passing both stage I and stage II clinical trials (Marcinak *et al.* 2017). Although Fasiglifam demonstrated effective glucose-dependent insulinotropic responses surpassing the capabilities of the current sulphonylurea Glimepiride, stage III trials proved unsuccessful due to signs of hepatotoxicity (Marcinak *et al.* 2017).

In addition, the long chain fatty acid sensing cannabinoid receptor GPR119 has been shown to act as a lipid biosensor and modulates both lipid and glucose homeostasis (Moran *et al.* 2014, Reimann & Gribble 2016, Ritter *et al.* 2016). Several GPR119 agonists have progressed into clinical trials for the treatment of type 2 diabetes (Reimann & Gribble 2016, Ritter *et al.* 2016). BMS-903452 (Bristol-Myers Squibb) and ZYG-19 (Zydus Cadila) have successfully completed phase I clinical trials with MBX-2982

(Metabolex) also completing phase II clinical trials and exhibiting potent anti-diabetic effects towards glycaemic control and weight loss (Ritter *et al.* 2016). Although, GPR119 agonists have yet to reach stage III clinical trials, results from early studies reveal the therapeutic potential of novel endocannabinoid GPCRs, including GPR55 and GPR18.

Cannabinoid (GPR55, GPR119) and free fatty acid (GPR40, GPR41, GPR43, GPR120) receptors are abundantly expressed in the pancreatic beta cells and enteroendocrine L-, K- and I-cells of the gut, with effects towards insulin, GLP-1, GIP, CCK, leptin and PYY release stimulated upon activation (Moran *et al.* 2016). Pre-clinical studies using clonal beta cells and diabetic mice have demonstrated the effects of fatty acid agonists towards islet cell proliferation and the regeneration of beta cell mass (McKillop *et al*.2016, Ruz-Maldonado *et al.* 2018). Although many GPCRs have been previously shown to regulate glycaemic control (Reimann & Gribble 2016), GPR55 and GPR120 have been identified with promising anti-diabetic potential (McKillop *et al.* 2013, Moran *et al.* 2014). GPR55 and GPR120 are both abundantly expressed in islet and enteroendocrine cells and stimulate insulin secretion upon activation (Moran *et al.* 2016). The known anti-inflammatory effects (Oh *et al.* 2014, Stancic *et al.* 2015) accompanied with hypothesised involvement on incretin release (Martin *et al.* 2012, Tuduri *et al.* 2017) warrants further investigation into the glucoregulatory role and therapeutic efficacy of GPR55 and GPR120.

8.3: Activation of GPR120 in pancreatic islets

In chapter 3, the antidiabetic potential of GPR120 activation with respect to islet cell function was assessed by utilising a range of endogenous (ALA, DHA, EPA) and

synthetic (GW9508, Compound A, GSK137647) agonists (Fig. 8.1). Previously, GPR120 expression was determined in both pancreatic islets and clonal beta cells (Moran *et al.* 2014). The insulinotropic actions of the endogenous omega-3 fatty acids have been well documented using rodent models, however interspecies variation and involvement of GPR40 may have also contributed to the effects observed (Houthuijzen 2016). The present study compared the potency of the endogenous and synthetically-derived selective GPR120 agonists. Insulinotropic responses were observed in BRIN-BD11 cells to the endogenous ligands, with ALA emitting the most potent effect. Although less potent than ALA, recently developed selective agonists (Compound A, GSK137647) augmented insulin release with effects abolished upon simultaneous GPR120 antagonism. ALA was the most potent agonist tested with the degradation profile of ALA possibly contributing to the effects observed (Kaur *et al.* 2014). Upon cleavage by delta-6 desaturase, ALA is broken down to form DHA and EPA which are other GPR120 agonists that may synergistically agonise GPR120 (Kaur *et al.* 2014). The insulinotropic effect observed using rodent BRIN-BD11 cells was replicated on human 1.1B4 cells, ruling out interspecies variation, particularly as minor structural differences exist between rodent and human GPR120.

Literature has documented that GPR120 activation is coupled with Gαq downstream receptor signalling which utilises PLCβ and IP_3 secondary messenger pathways, however, conflicting studies have also indicated the involvement of cAMP in beta cells (Moran *et al.* 2014, Stone *et al.* 2014,). Understanding the downstream signalling mechanism of GPR120 in the beta cell is essential to evaluate the efficacy of GPR120 targeting therapeutics. The present study revealed that intracellular calcium modulation was the primary mechanism of insulin release upon GPR120 activation, whilst the response was abolished upon IP_3 receptor blocking, further eliciting PLCβ and IP_3 signalling. The other arm of PLCβ signalling was subsequently investigated and for the first time, the present

study revealed that GPR120 induces ERK1/2 phosphorylation in beta cells; a key MAPK phosphoprotein that regulates insulin synthesis and beta cell proliferation (Lawrence *et al.* 2008, Stewart *et al.* 2015).

Many current therapies fail to counteract reduced beta cell mass and enhanced alpha cell area in type 2 diabetic islets (Siddigui 2009, Sabir *et al.* 2018). The present study demonstrated that GPR120 activation induces beta cell proliferation and alpha cell apoptosis, thus indicating the beneficial effects of GPR120 in beta cell regeneration. Moreover, both GPR120 and insulin expression were upregulated in hyperglycaemia upon agonist treatment. Previous findings reported that GPR120 downregulation in type 2 diabetes contributes to the onset of high fat diet complications, including weight gain and hyperglycaemia (Ichimura *et al.* 2012). Chapter 3 demonstrated that GPR120 expression is glucose-dependent and is upregulated upon agonist treatment; a property of the receptor that may be exploited by future GPR120-targeting therapeutics. Overall, GPR120 activation augments insulin biosynthesis, insulin release and islet cell regeneration.

8.4: Activation of GPR55 in pancreatic islets

This research study investigated the effect of GPR55 activation on islet cell function using a range of endogenous (OEA, PEA) and synthetic (Abn-CBD, AM251, O-1602) agonists (Chapter 4; Fig. 8.1). Studies have demonstrated the expression of GPR55 in rodent and human islets with abundant expression in beta cells (McKillop *et al.* 2013, Ruz-Maldonado *et al.* 2018). Interestingly, GPR55 is lowly expressed in human alpha cells with some studies implicating that it is null expressed in rodent alpha cells (McKillop *et*

al. 2013). Complimentary with previous reports, the present study demonstrated the insulinotropic effects of endogenous and synthetic GPR55 agonists in rodent beta cells (McKillop *et al.* 2013). This response was retained when assessed using human 1.1B4 cells, validating the use of rodent models for assessment of GPR55 function.

Upon activation, GPR55 couples to both Gαq and Gα12/13 subunits (Shi *et al.* 2017). Initial studies have suggested that GPR55 is primarily driven by intracellular Ca^{2+} modulation, therefore, downstream PLCβ signalling mechanisms were assessed in this study (McKillop *et al.* 2013). As anticipated, GPR55 activation increased intracellular Ca^{2+} levels and had no effect on cAMP, ruling out GPR119 agonism which couples to Gs and modulates adenylyl cyclase signalling (Hassing *et al.* 2016). Investigating the diacylglycerol (DAG) branch of PLCβ signalling revealed that GPR55 activation attenuates the phosphorylation of apoptotic MAPK signalling (JNK, p38) (Hou *et al.* 2008, Zhou *et al.* 2014). Interestingly, previous studies have demonstrated cardioprotective effects of Abn-CBD mediated by ERK1/2 signalling in other cell types (Su & Vo 2007, Matouk *et al.* 2017, Matouk *et al.* 2018), however, the present study in beta cells have indicated that only JNK and P38 are regulated by Abn-CBD treatment. Moreover, GPR55 activation enhanced beta cell proliferation, increased insulin biosynthesis and reduced beta cell apoptosis, with opposing effects demonstrated in alpha cells, thus revealing the effects of GPR55 in beta cell regeneration.

Previous findings demonstrated that Abn-CBD augments beta cell proliferation in a GPR55-dependent manner, however, the mechanism of action remains unclear (Ruz-Maldonado *et al.* 2018). These studies suggest that intracellular Ca^{2+}, JNK and p38 signalling downstream of GPR55 activation may be key modulators in beta cell regeneration and insulin release. These proliferative effects accompanied with

insulinotropic and glucose-lowering actions present GPR55 as a promising therapeutic target for type 2 diabetes.

8.5: Specificity of putative GPR120 and GPR55 agonists in islets

Currently, the specificity of GPR120 and GPR55 agonists remains poorly understood (Moran *et al.* 2016, Tuduri *et al.* 2017, Ruz-Maldonado *et al.* 2018). Long chain fatty acid sensing GPR40 and GPR120 share similar sequence homology and can be activated by similar ligands (Yonezawa *et al.* 2013). Whereas, GPR55 shares structural similarities with other cannabinoid receptors (e.g. GPR119 and GPR18) and can be activated by the same endocannabinoid ligands (Fine & Rosenfeld 2013, Irving *et al.* 2017). Many studies have used antagonists to assess agonist specificity, however, adverse antagonist bioactivity and selectivity may influence findings. In addition, studies using knockout mice typically incorporate multiple cells types which can lead to induction of complimentary compensatory pathways (Barbaric *et al.* 2007). Chapter 5 involves the development of two independent (GPR120 and GPR55) knockout beta cell lines using revolutionary CRISPR/Cas9 gene editing. The major advantage of CRISPR/Cas9 is its ability to generate complete gene knockout rather than gene knockdown, which enables absolute characterisation of a given gene (Ran *et al.* 2013, Boettcher & McManus 2015).

Insulin secretory analysis using both wild type and GPR120 knockout cells revealed that ALA was completely GPR120-dependent whilst DHA, Compound A and GSK137647 were only GPR120-dependent at normal physiological concentrations (10^{-6} M). Complimentary studies utilising GPR120 knockout mice concluded that DHA-induced glucagon release from islets is driven by GPR120, whilst other studies revealed that ALA-

induced GLP-1 release is GPR120-dependent (Martin *et al.* 2012, Suckow *et al.* 2014). As anticipated, the effect of dual-agonist GW9508 was substantially impaired, in support of previous evidence demonstrating the pharmacology of this agonist (Briscoe *et al.* 2006). Moreover, EPA was shown to be GPR120-independent and suggests involvement of another free fatty acid receptor, such as GPR40 (Yonezawa *et al.* 2013). Gαq signalling downstream of GPR120 activation resulting in intracellular Ca^{2+} modulation was then assessed in both wild type and GPR120 knockout cells. In harmony with insulin secretory analysis, ALA, GSK137647 and Compound A demonstrated GPR120-dependent effects on intracellular Ca^{2+} production, which implicates that these long chain fatty acid agonists are acting through GPR120.

Upon assessment of GPR55 agonists on insulin release and intracellular Ca^{2+} production from both wild type and GPR55 knockout cells, it was revealed that Abn-CBD, AM251, PEA and O-1602 were partly driven by GPR55. Thus, corresponding with previous research utilising the GPR55 antagonist (Cannabidiol) (McKillop *et al.* 2013). Contrastingly, OEA-induced insulin release was independent of GPR55. No changes in cAMP production were observed in wild type or knockout cells, suggesting that GPR55 signalling is primarily modulated through Gαq activation and release of Ca^{2+} from intracellular stores (Putney & Tomita 2012). However, Gα12/13 activation may also contribute to the actions of GPR55 and warrants further investigation (Shi *et al.* 2017).

Evaluation of the specificity of agonists is essential to characterise the biological function of a given GPCR. Overall, the present study identified ALA (GPR120) and Abn-CBD (GPR55) as the most potent and receptor-specific modulators of insulin release.

8.6: Biological effect of GPR55/GPR120 agonist monotherapy and combinational therapy

The therapeutic efficacy of GPR55 and GPR120 activation in high fat fed-induced diabetic mice was investigated by examining the effect of several GPR55/GPR120 agonists on glucose tolerance and glucoregulatory hormone release (Fig. 8.1). GPR120 (ALA, GW9508, GSK137647, Compound A) and GPR55 (Abn-CBD, AM251) agonists improved glucose excursion and enhanced GSIS in glucose intolerant obese mice. Complimentary findings also previously reported acute glucose lowering and insulinotropic actions of GPR55 and GPR120 activation in lean mice (McKillop *et al.* 2013, Moran *et al.* 2014). Previous studies have demonstrated abundant GPR55 and GPR120 expression in enteroendocrine cells of the gut with other studies showing GPR120 to modulate GLP-1 release (Martin *et al.* 2012, Simcocks *et al.* 2014). The present study revealed for the first time that GPR55 and GPR120 activation induces both GLP-1 and GIP secretion in high fat fed mice. Moreover, the glucose lowering and insulinotropic effects observed were enhanced in combination with DPP-IV inhibition (Sitagliptin), with Abn-CBD (GPR55) and ALA (GPR120) emitting the most potent effects. In accordance with this, previous GPCR agonist combinational studies have also shown promising anti-diabetic effects such as the GPR40 agonist (AS-2575959), which enhanced insulin and GLP-1 concentrations when in combination with Sitagliptin (Tanaka *et al.* 2014).

Chronic oral administration of Abn-CBD and ALA for 21 days improved glucose homeostasis and dyslipidaemia in high fat fed mice. Biological effects included decreased non-fasting glucose, bodyweight and DPP-IV activity accompanied with enhanced non-fasting insulin and insulin sensitivity. In support of these findings, previous studies also

demonstrated the glucoregulatory effects of Abn-CBD using streptozotocin-induced diabetic mice and potentiation of GSIS by ALA in lean mice (Moran *et al.* 2014, McKillop *et al.* 2016).

Following 21-day treatment, both Abn-CBD and ALA based therapies substantially reduced bodyweight in the obese mouse model, whilst LDL cholesterol, triglycerides and CRP concentrations were greatly improved. Thus, revealing anti-obesity and cardioprotective effects that may be partly driven by anti-inflammatory responses linked with fatty acid GPCR activation (Oh *et al.* 2014). Notably, Abn-CBD emitted the most potent effects towards weight loss, whilst ALA demonstrated the greatest improvement towards GSIS and glycaemic control; highlighting the prospective applications of GPR55 and GPR120 targeting therapeutics.

Treatment of ALA and Abn-CBD therapies restored pancreatic islet architecture in high fat fed-induced diabetic mice by enhancing beta cell proliferation and beta cell mass. The proliferative effects observed may be modulated indirectly of GPCR activation through incretin hormone secretion. Complimentary studies demonstrated the proliferative effect of Abn-CBD in murine islets to be GPR55-dependent (Ruz-Maldonado *et al.* 2018). Whilst both therapeutic approaches in the present study improved islet cell regeneration, Abn-CBD monotherapy induced a vast increase in islet size; a potential characteristic of GPR55 that may be exploited in novel pharmaceutical development. These studies suggest that GPR55 and GPR120 agonist monotherapy and combinational therapy with Sitagliptin are effective therapeutic approaches and may have future clinical applications for the treatment of type 2 diabetes and other obesity related diseases (Fig. 8.1).

8.7: Future studies

GPR55 and GPR120 have been shown to regulate a range of physiological responses involved in the maintenance of glucose and lipid homeostasis and are presented as promising therapeutic targets. To build on the growing body of evidence that demonstrate the efficacy of GPR55- and GPR120-targerting agents, future studies are required to further explore the mechanistic function and specificity of GPCR agonist-based therapies. The use of GPCR knockout mice would greatly aid the investigation of agonist action *in-vivo*. Moreover, GPCR knockout murine islets accompanied with already established clonal knockout cell lines (Chapter 5) could be utilised to further explore agonist specificity and compensatory pathways in response to GPCR ablation. Global receptor knockout mice could be used to evaluate the importance of GPR55 and GPR120 on energy metabolism, glucoregulatory hormone release and islet cell regeneration.

Studies have revealed that GPR55 and GPR120 improved insulin sensitivity in HFF insulin resistant mice (Oh *et al.* 2014, Chapter 6, 7), which may be partly driven by the anti-inflammatory effects emitted by the agonists (Oh *et al.* 2014, Stancic *et al.* 2015). Whilst the insulinotropic properties of GPR55 and GPR120 are well documented (McKillop *et al.* 2013, Moran *et al.* 2014, Moran et al. 2016), agonist effects on insulin action remains poorly understood and may have major impact on the development of future GPCR-based therapies. Therefore, future studies could investigate the effects of GPCR agonism towards insulin sensitivity and glucose uptake using peripheral cell lines such 3T3 and c2c12. Moreover, effects towards insulin sensitivity could be further validated *in-vivo* using knockout animal models.

Due to the known safety and previous clinical analysis of both endogenous omega-3 ALA and Sitagliptin, it would be interesting to implement a placebo-controlled crossover trial

in type 2 diabetic patients to assess the acute glucoregulatory effect of GPR120-targeting agents in humans. Moreover, it would be of interest to compare the effects observed with conventional therapies currently in use. As previous clinical trials with synthetic GPR40 agonists have been conducted (Tanaka *et al.* 2014, Marcinak *et al.* 2017), it would also be of interest for pharmaceutical companies to consider a clinical trial that utilised a synthetic GPR120 agonist (e.g. GSK137647) based on the growing body of pre-clinical evidence supporting its therapeutic efficacy (Sparks *et al.* 2014, Chapter 6). Moreover, a clinical trial could be utilised to assess the biosynthesis and degradation of omega-3 fatty acids as they remain poorly understood in patients with type 2 diabetes. It would be of interest to assess the circulation and breakdown of omega-3 molecules in both healthy and type 2 diabetic patients. Initial biochemical assessment could investigate circulating ALA, DHA, EPA concentrations and other desaturase enzymes involved in their degradation.

Collectively, the studies in the thesis demonstrate that both GPR55 and GPR120 play a key role in metabolic hormone release and glucose homeostasis. Similar to the effects of incretin mimetics and DPP-IV inhibitors, GPR55 and GPR120 agonist monotherapies and combinational therapies have potential to emerge as a leading therapeutic approach for the treatment of type 2 diabetes and other obesity related diseases.

Table 8.1: Summary of GPCRs located in intestinal and pancreatic endocrine cells that have been assessed in clinical trials for the treatment of type 2 diabetes.

Receptor	Natural ligands	Target cell types/tissues	Effect of GPCR agonism
GLP1R	GLP-1, oxyntomodulin	Pancreatic beta and delta cells, brain, vagus nerve	↑ insulin, ↓ glucagon, ↓ gastric emptying
GIPR	GIP	Pancreatic alpha, beta and delta cells, adipose tissue	↑ insulin, ↑ glucagon, ↑ fat storage
GCGR	Glucagon, oxyntomodulin	Pancreatic beta cells, liver, adipose tissue, brain	↑ insulin, ↑ energy expenditure, ↓ food intake
GPR119	Oleoylethanolamide, monooleoylglycerol	Enteroendocrine cells, pancreatic alpha and beta cells	↑ GLP-1, ↑ GIP, ↑ insulin (possible ↑ glucagon)
FFAR1 (GPR40)	Long-chain NEFA	Enteroendocrine cells, pancreatic beta cells	↑ GLP-1, ↑ GIP, ↑ insulin

(Adapted from Reimann & Gribble 2016)

Figure 8.1: Therapeutic action of GPR55 and GPR120 monotherapy and combinational therapy (Sitagliptin) for the treatment of type 2 diabetes

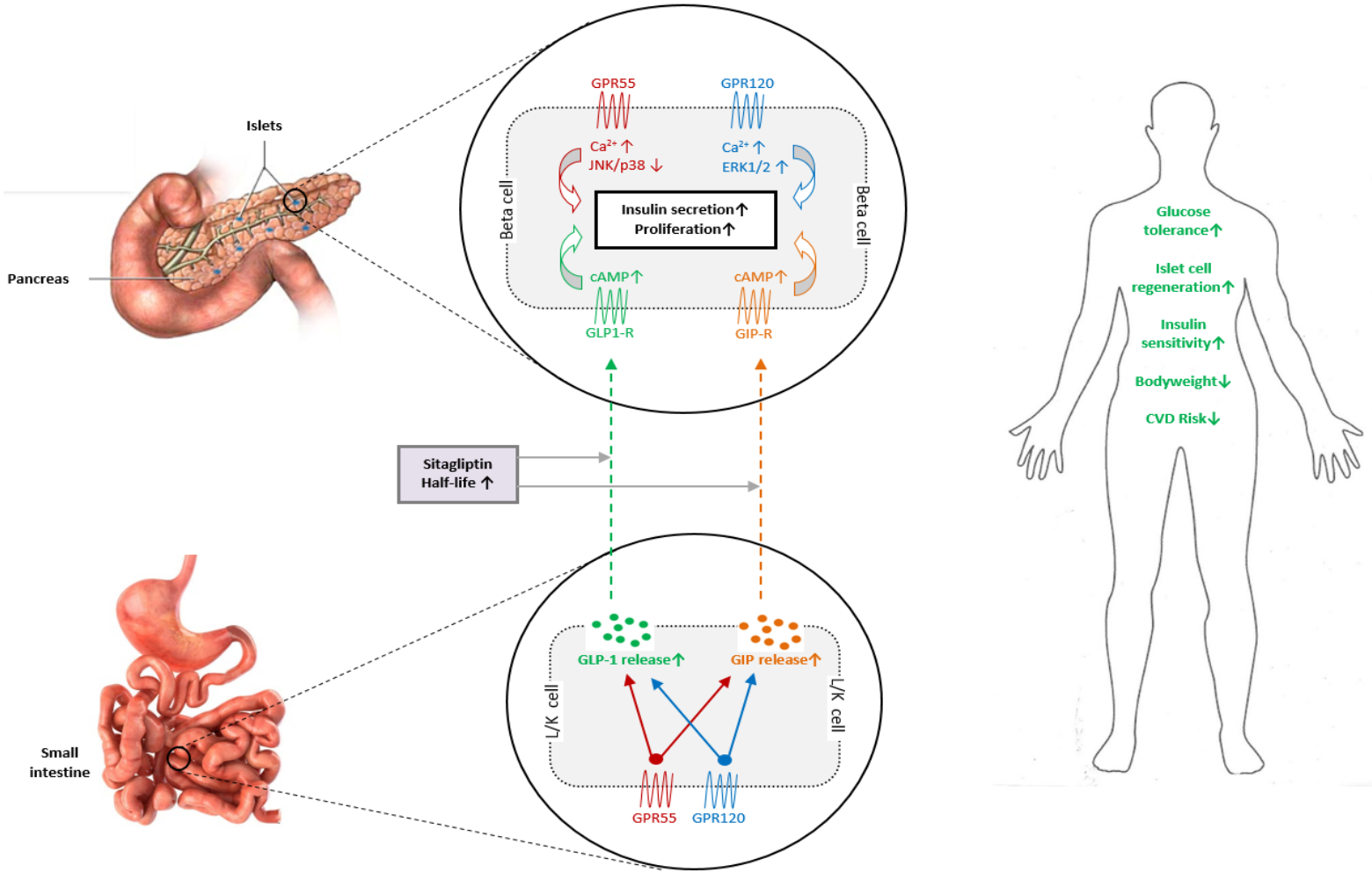

(Adapted from Siddiqui 2009, Chapters 3-7)

Chapter 9

References

Aizpurua-Olaizola, O., Elezgarai, I., Rico-Barrio, I., Zarandona, I., Etxebarria, N. and Usobiaga, A. (2017) Targeting the endocannabinoid system: future therapeutic strategies. *Drug Discovery Today,* 22(1), 105-110.

Allen, E.H.A., Atkinson, S.D., Liao, H., Moore, J.E., Pedrioli, D.M.L., Smith, F.J.D., McLean, W.H.I. and Moore, C.B.T. (2013) Allele-specific siRNA silencing for the common keratin 12 founder mutation in Meesmann epithelial corneal dystrophy. *Investigative Ophthalmology & Visual Science,* 54(1), 494-502.

American Diabetes Association. (2009) Diagnosis and classification of diabetes mellitus. *Diabetes Care,* 32 Suppl 1, S62-7.

American Diabetes Association. (2014) Standards of medical care in diabetes--2014. *Diabetes Care,* 37 Suppl 1, S14-80.

American Diabetes Association. (2015) (5) Prevention or delay of type 2 diabetes. *Diabetes Care,* 38 Suppl, S31-S32.

American Diabetes Association. (2018) 8. Pharmacologic Approaches to Glycemic Treatment: Standards of Medical Care in Diabetes-2018. *Diabetes Care,* 41(Suppl 1), S73-S85.

Amisten, S., Salehi, A., Rorsman, P., Jones, P.M. and Persaud, S.J. (2013) An atlas and functional analysis of G-protein coupled receptors in human islets of Langerhans. *Pharmacology & Therapeutics,* 139(3), 359-391.

Andreadis, P., Karagiannis, T., Malandris, K., Avgerinos, I., Liakos, A., Manolopoulos, A., Bekiari, E., Matthews, D.R. and Tsapas, A. (2018) Semaglutide for type 2 diabetes mellitus: A systematic review and meta-analysis. *Diabetes, Obesity & Metabolism,* 20(9), 2255-2263.

Appuhamy, J.A., Kebreab, E., Simon, M., Yada, R., Milligan, L.P. and France, J. (2014) Effects of diet and exercise interventions on diabetes risk factors in adults without diabetes: meta-analyses of controlled trials. *Diabetology & Metabolic Syndrome,* 6, 127-5996-6-127. eCollection 2014.

Arifin, S.A. and Falasca, M. (2016) Lysophosphatidylinositol Signalling and Metabolic Diseases. *Metabolites,* 6(1), 10.3390/metabo6010006.

Atkinson, S.D., McGilligan, V.E., Liao, H., Szeverenyi, I., Smith, F.J., Moore, C.B. and McLean, W.H. (2011) Development of allele-specific therapeutic siRNA for keratin 5 mutations in epidermolysis bullosa simplex. *The Journal of Investigative Dermatology,* 131(10), 2079-2086.

Baggio, L.L. and Drucker, D.J. (2007) Biology of incretins: GLP-1 and GIP. *Gastroenterology,* 132(6), 2131-2157.

Bahadursingh, S., Beharry, K., Maharaj, K., Mootoo, C., Sharma, P., Singh, J., Teelucksingh, K. and Tilluckdharry, R. (2009) C-reactive protein: adjunct to cardiovascular risk assessment. *The West Indian Medical Journal,* 58(6), 551-555.

Bailey, C.J. (1992) Biguanides and NIDDM. *Diabetes Care,* 15(6), 755-772.

Bailey, C.J. (2000) Potential new treatments for type 2 diabetes. *Trends in Pharmacological Sciences,* 21(7), 259-265.

Baker, D., Pryce, G., Davies, W.L. and Hiley, C.R. (2006) In silico patent searching reveals a new cannabinoid receptor. *Trends in Pharmacological Sciences,* 27(1), 1-4.

Ballantyne, G.H. (2006) Peptide YY(1-36) and peptide YY(3-36): Part I. Distribution, release and actions. *Obesity Surgery,* 16(5), 651-658.

Barbaric, I., Miller, G. and Dear, T.N. (2007) Appearances can be deceiving: phenotypes of knockout mice. *Briefings in Functional Genomics & Proteomics,* 6(2), 91-103.

Barnett, A.H. (2009) Redefining the role of thiazolidinediones in the management of type 2 diabetes. *Vascular Health and Risk Management,* 5(1), 141-151.

Basith, S., Cui, M., Macalino, S.J.Y., Park, J., Clavio, N.A.B., Kang, S. and Choi, S. (2018) Exploring G Protein-Coupled Receptors (GPCRs) Ligand Space via Cheminformatics Approaches: Impact on Rational Drug Design. *Frontiers in Pharmacology,* 9, 128-129.

Batterham, R.L. and Bloom, S.R. (2003) The gut hormone peptide YY regulates appetite. *Annals of the New York Academy of Sciences,* 994, 162-168.

Bergholm, R., Sevastianova, K., Santos, A., Kotronen, A., Urjansson, M., Hakkarainen, A., Lundbom, J., Tiikkainen, M., Rissanen, A., Lundbom, N. and Yki-Jarvinen, H. (2013) CB(1) blockade-induced weight loss over 48 weeks decreases liver fat in proportion to weight loss in humans. *International Journal of Obesity (2005),* 37(5), 699-703.

Bertelli, E. and Bendayan, M. (2005) Association between endocrine pancreas and ductal system. More than an epiphenomenon of endocrine differentiation and development? *The Journal of Histochemistry and Cytochemistry: Official Journal of the Histochemistry Society,* 53(9), 1071-1086.

Bhaswant, M., Poudyal, H. and Brown, L. (2015) Mechanisms of enhanced insulin secretion and sensitivity with n-3 unsaturated fatty acids. *The Journal of Nutritional Biochemistry,* 26(6), 571-584.

Billington, C.K. and Penn, R.B. (2003) Signaling and regulation of G protein-coupled receptors in airway smooth muscle. *Respiratory Research,* 4, 2-2.

Black, C., Donnelly, P., McIntyre, L., Royle, P.L., Shepherd, J.P. and Thomas, S. (2007) Meglitinide analogues for type 2 diabetes mellitus. *The Cochrane Database of Systematic Reviews,* (2):CD004654. doi(2), CD004654.

Blondeau, N., Lipsky, R.H., Bourourou, M., Duncan, M.W., Gorelick, P.B. and Marini, A.M. (2015) Alpha-linolenic acid: an omega-3 fatty acid with neuroprotective properties-ready for use in the stroke clinic? *BioMed Research International,* 2015, 519830.

Boettcher, M. and McManus, M.T. (2015) Choosing the Right Tool for the Job: RNAi, TALEN, or CRISPR. *Molecular Cell,* 58(4), 575-585.

Bonnefond, A., Lamri, A., Leloire, A., Vaillant, E., Roussel, R., Levy-Marchal, C., Weill, J., Galan, P., Hercberg, S., Ragot, S., Hadjadj, S., Charpentier, G., Balkau, B., Marre, M., Fumeron, F. and Froguel, P. (2015) Contribution of the low-frequency, loss-of-function p.R270H mutation in FFAR4 (GPR120) to increased fasting plasma glucose levels. *Journal of Medical Genetics,* 52(9), 595-598.

Bopp, S.K. and Lettieri, T. (2008) Comparison of four different colorimetric and fluorometric cytotoxicity assays in a zebrafish liver cell line. *BMC Pharmacology,* 8, 8-2210-8-8.

Bradberry, J.C. and Hilleman, D.E. (2013) Overview of omega-3 Fatty Acid therapies. *P & T: A Peer-Reviewed Journal for Formulary Management,* 38(11), 681-691.

Brenner, R.R. (2003) Hormonal modulation of delta6 and delta5 desaturases: case of diabetes. *Prostaglandins, Leukotrienes, and Essential Fatty Acids,* 68(2), 151-162.

Brewer, P.D., Habtemichael, E.N., Romenskaia, I., Mastick, C.C. and Coster, A.C. (2014) Insulin-regulated Glut4 translocation: membrane protein trafficking with six distinctive steps. *The Journal of Biological Chemistry,* 289(25), 17280-17298.

Briant, L., Salehi, A., Vergari, E., Zhang, Q. and Rorsman, P. (2016) Glucagon secretion from pancreatic alpha-cells. *Upsala Journal of Medical Sciences,* 121(2), 113-119.

Briant, L.J., Zhang, Q., Vergari, E., Kellard, J.A., Rodriguez, B., Ashcroft, F.M. and Rorsman, P. (2017) Functional identification of islet cell types by electrophysiological fingerprinting. *Journal of the Royal Society, Interface,* 14(128), 10.1098/rsif.2016.0999.

Briscoe, C.P., Peat, A.J., McKeown, S.C., Corbett, D.F., Goetz, A.S., Littleton, T.R., McCoy, D.C., Kenakin, T.P., Andrews, J.L., Ammala, C., Fornwald, J.A., Ignar, D.M. and Jenkinson, S. (2006) Pharmacological regulation of insulin secretion in MIN6 cells through the fatty acid receptor GPR40: identification of agonist and antagonist small molecules. *British Journal of Pharmacology,* 148(5), 619-628.

Brubaker, P.L. and Drucker, D.J. (2002) Structure-function of the glucagon receptor family of G protein-coupled receptors: the glucagon, GIP, GLP-1, and GLP-2 receptors. *Receptors & Channels,* 8(3-4), 179-188.

Burns, R.N. and Moniri, N.H. (2010) Agonism with the omega-3 fatty acids alpha-linolenic acid and docosahexaenoic acid mediates phosphorylation of both the short and long isoforms of the human GPR120 receptor. *Biochemical and Biophysical Research Communications,* 396(4), 1030-1035.

Burns, R.N., Singh, M., Senatorov, I.S. and Moniri, N.H. (2014) Mechanisms of homologous and heterologous phosphorylation of FFA receptor 4 (GPR120): GRK6 and PKC mediate phosphorylation of Thr(3)(4)(7), Ser(3)(5)(0), and Ser(3)(5)(7) in the C-terminal tail. *Biochemical Pharmacology,* 87(4), 650-659.

Cahn, A. and Cefalu, W.T. (2016) Clinical Considerations for Use of Initial Combination Therapy in Type 2 Diabetes. *Diabetes Care,* 39 Suppl 2, S137-45.

Cascieri, M.A., Koch, G.E., Ber, E., Sadowski, S.J., Louizides, D., de Laszlo, S.E., Hacker, C., Hagmann, W.K., MacCoss, M., Chicchi, G.G. and Vicario, P.P. (1999) Characterization of a novel, non-peptidyl antagonist of the human glucagon receptor. *The Journal of Biological Chemistry,* 274(13), 8694-8697.

Cerf, M.E. (2013) Beta cell dysfunction and insulin resistance. *Frontiers in Endocrinology,* 4, 37.

Cernea, S. and Dobreanu, M. (2013) Diabetes and beta cell function: from mechanisms to evaluation and clinical implications. *Biochemia Medica,* 23(3), 266-280.

Cernea, S. and Raz, I. (2011) Therapy in the early stage: incretins. *Diabetes Care,* 34 Suppl 2, S264-71.

Chaudhury, A., Duvoor, C., Reddy Dendi, V.S., Kraleti, S., Chada, A., Ravilla, R., Marco, A., Shekhawat, N.S., Montales, M.T., Kuriakose, K., Sasapu, A., Beebe, A., Patil, N., Musham, C.K., Lohani, G.P. and Mirza, W. (2017) Clinical Review of Antidiabetic Drugs: Implications for Type 2 Diabetes Mellitus Management. *Frontiers in Endocrinology,* 8, 6.

Chomczynski, P. and Sacchi, N. (2006) The single-step method of RNA isolation by acid guanidinium thiocyanate-phenol-chloroform extraction: twenty-something years on. *Nature Protocols,* 1(2), 581-585.

Christensen, M. and Knop, F.K. (2010) Once-weekly GLP-1 agonists: How do they differ from exenatide and liraglutide? *Current Diabetes Reports,* 10(2), 124-132.

Chun, L., Zhang, W.H. and Liu, J.F. (2012) Structure and ligand recognition of class C GPCRs. *Acta Pharmacologica Sinica,* 33(3), 312-323.

Clearfield, M.B. (2005) C-reactive protein: a new risk assessment tool for cardiovascular disease. *The Journal of the American Osteopathic Association,* 105(9), 409-416.

Courtney, D.G., Atkinson, S.D., Moore, J.E., Maurizi, E., Serafini, C., Pellegrini, G., Black, G.C., Manson, F.D., Yam, G.H., Macewen, C.J., Allen, E.H., McLean, W.H. and Moore, C.B. (2014) Development of allele-specific gene-silencing siRNAs for TGFBI Arg124Cys in lattice corneal dystrophy type I. *Investigative Ophthalmology & Visual Science,* 55(2), 977-985.

Davis, J.A., Singh, S., Sethi, S., Roy, S., Mittra, S., Rayasam, G., Bansal, V., Sattigeri, J. and Ray, A. (2010) Nature of action of Sitagliptin, the dipeptidyl peptidase-IV inhibitor in diabetic animals. *Indian Journal of Pharmacology,* 42(4), 229-233.

Deacon, C.F. (2004) Circulation and degradation of GIP and GLP-1. *Hormone and Metabolic Research = Hormon- Und Stoffwechselforschung = Hormones Et Metabolisme,* 36(11-12), 761-765.

Del Prato, S. and Pulizzi, N. (2006) The place of sulfonylureas in the therapy for type 2 diabetes mellitus. *Metabolism: Clinical and Experimental,* 55(5 Suppl 1), S20-7.

Derosa, G. and Maffioli, P. (2012) alpha-Glucosidase inhibitors and their use in clinical practice. *Archives of Medical Science: AMS,* 8(5), 899-906.

Dhanvantari, S., Seidah, N.G. and Brubaker, P.L. (1996) Role of prohormone convertases in the tissue-specific processing of proglucagon. *Molecular Endocrinology (Baltimore, Md.),* 10(4), 342-355.

Dhayal, S., Welters, H.J. and Morgan, N.G. (2008) Structural requirements for the cytoprotective actions of mono-unsaturated fatty acids in the pancreatic beta-cell line, BRIN-BD11. *British Journal of Pharmacology,* 153(8), 1718-1727.

Diamant, M. and Heine, R.J. (2003) Thiazolidinediones in type 2 diabetes mellitus: current clinical evidence. *Drugs,* 63(13), 1373-1405.

Diaz-Arteaga, A., Vazquez, M.J., Vazquez-Martinez, R., Pulido, M.R., Suarez, J., Velasquez, D.A., Lopez, M., Ross, R.A., de Fonseca, F.R., Bermudez-Silva, F.J., Malagon, M.M., Dieguez, C. and Nogueiras, R. (2012) The atypical cannabinoid O-1602 stimulates food intake and adiposity in rats. *Diabetes, Obesity & Metabolism,* 14(3), 234-243.

Divers, J., Palmer, N.D., Langefeld, C.D., Brown, W.M., Lu, L., Hicks, P.J., Smith, S.C., Xu, J., Terry, J.G., Register, T.C., Wagenknecht, L.E., Parks, J.S., Ma, L., Chan, G.C., Buxbaum, S.G., Correa, A., Musani, S., Wilson, J.G., Taylor, H.A., Bowden, D.W., Carr, J.J. and Freedman, B.I. (2017) Genome-wide association study of coronary artery calcified atherosclerotic plaque in African Americans with type 2 diabetes. *BMC Genetics,* 18(1), 105-017-0572-9.

Dods, R.L. and Donnelly, D. (2015) The peptide agonist-binding site of the glucagon-like peptide-1 (GLP-1) receptor based on site-directed mutagenesis and knowledge-based modelling. *Bioscience Reports,* 36(1), e00285.

Donvito, G., Nass, S.R., Wilkerson, J.L., Curry, Z.A., Schurman, L.D., Kinsey, S.G. and Lichtman, A.H. (2018) The Endogenous Cannabinoid System: A Budding Source of Targets for Treating Inflammatory and Neuropathic Pain. *Neuropsychopharmacology: Official Publication of the American College of Neuropsychopharmacology,* 43(1), 52-79.

Drucker, D., Easley, C. and Kirkpatrick, P. (2007) Sitagliptin. *Nature Reviews.Drug Discovery,* 6(2), 109-110.

Drucker, D.J. (2007) The role of gut hormones in glucose homeostasis. *The Journal of Clinical Investigation,* 117(1), 24-32.

Eibich, P., Green, A., Hattersley, A.T., Jennison, C., Lonergan, M., Pearson, E.R. and Gray, A.M. (2017) Costs and Treatment Pathways for Type 2 Diabetes in the UK: A Mastermind Cohort Study. *Diabetes Therapy: Research, Treatment and Education of Diabetes and Related Disorders,* 8(5), 1031-1045.

ElSayed, S.A. and Bhimji, S.S. (2018) Physiology, Pancreas. *In:* Anon.*StatPearls.* Treasure Island (FL): StatPearls Publishing LLC,

Evans, J.L., Balkan, B., Chuang, E. and Rushakoff, R.J. (2000) Oral and Injectable (Non-insulin) Pharmacological Agents for Type 2 Diabetes. *In:* De Groot, L.J., Chrousos, G., Dungan, K., Feingold, K.R., Grossman, A., Hershman, J.M., Koch, C., Korbonits, M., McLachlan, R., New, M., Purnell, J., Rebar, R., Singer, F. and Vinik, A. eds. *Endotext.* South Dartmouth (MA): MDText.com, Inc,

Fine, P.G. and Rosenfeld, M.J. (2013) The endocannabinoid system, cannabinoids, and pain. *Rambam Maimonides Medical Journal,* 4(4), e0022.

Flatt, P.R. and Bailey, C.J. (1981) Abnormal plasma glucose and insulin responses in heterozygous lean (ob/+) mice. *Diabetologia,* 20(5), 573-577.

Fletcher, B., Gulanick, M. and Lamendola, C. (2002) Risk factors for type 2 diabetes mellitus. *The Journal of Cardiovascular Nursing,* 16(2), 17-23.

Fredriksson, R., Lagerstrom, M.C., Lundin, L.G. and Schioth, H.B. (2003) The G-protein-coupled receptors in the human genome form five main families. Phylogenetic analysis, paralogon groups, and fingerprints. *Molecular Pharmacology,* 63(6), 1256-1272.

Frias, J.P., Nauck, M.A., Van, J., Kutner, M.E., Cui, X., Benson, C., Urva, S., Gimeno, R.E., Milicevic, Z., Robins, D. and Haupt, A. (2018) Efficacy and safety of LY3298176, a novel dual GIP and GLP-1 receptor agonist, in patients with type 2 diabetes: a randomised, placebo-controlled and active comparator-controlled phase 2 trial. *Lancet (London, England),*

Furman, B.L. (2012) The development of Byetta (exenatide) from the venom of the Gila monster as an anti-diabetic agent. *Toxicon: Official Journal of the International Society on Toxinology,* 59(4), 464-471.

Gao, J., Ghibaudi, L. and Hwa, J.J. (2004) Selective activation of central NPY Y1 vs. Y5 receptor elicits hyperinsulinemia via distinct mechanisms. *American Journal of Physiology.Endocrinology and Metabolism,* 287(4), E706-11.

Gault, V.A., Bhat, V.K., Irwin, N. and Flatt, P.R. (2013) A novel glucagon-like peptide-1 (GLP-1)/glucagon hybrid peptide with triple-acting agonist activity at glucose-dependent insulinotropic polypeptide, GLP-1, and glucagon receptors and therapeutic potential in high fat-fed mice. *The Journal of Biological Chemistry,* 288(49), 35581-35591.

Gault, V.A., O'Harte, F.P. and Flatt, P.R. (2003) Glucose-dependent insulinotropic polypeptide (GIP): anti-diabetic and anti-obesity potential? *Neuropeptides,* 37(5), 253-263.

Gerber, P.A. and Rutter, G.A. (2017) The Role of Oxidative Stress and Hypoxia in Pancreatic Beta-Cell Dysfunction in Diabetes Mellitus. *Antioxidants & Redox Signaling*, 26(10), 501-518.

Gerbino, A. and Colella, M. (2018) The Different Facets of Extracellular Calcium Sensors: Old and New Concepts in Calcium-Sensing Receptor Signalling and Pharmacology. *International Journal of Molecular Sciences*, 19(4), 10.3390/ijms19040999.

Gonzalez-Sancho, J.M., Brennan, K.R., Castelo-Soccio, L.A. and Brown, A.M. (2004) Wnt proteins induce dishevelled phosphorylation via an LRP5/6- independent mechanism, irrespective of their ability to stabilize beta-catenin. *Molecular and Cellular Biology*, 24(11), 4757-4768.

Gopel, S.O., Kanno, T., Barg, S. and Rorsman, P. (2000) Patch-clamp characterisation of somatostatin-secreting -cells in intact mouse pancreatic islets. *The Journal of Physiology*, 528(Pt 3), 497-507.

Gosmanov, A.R., Gosmanova, E.O. and Kitabchi, A.E. (2000) Hyperglycemic Crises: Diabetic Ketoacidosis (DKA), And Hyperglycemic Hyperosmolar State (HHS). *In:* De Groot, L.J., Chrousos, G., Dungan, K., Feingold, K.R., Grossman, A., Hershman, J.M., Koch, C., Korbonits, M., McLachlan, R., New, M., Purnell, J., Rebar, R., Singer, F. and Vinik, A. eds. *Endotext.* South Dartmouth (MA): MDText.com, Inc,

Gotoh, C., Hong, Y.H., Iga, T., Hishikawa, D., Suzuki, Y., Song, S.H., Choi, K.C., Adachi, T., Hirasawa, A., Tsujimoto, G., Sasaki, S. and Roh, S.G. (2007) The regulation of adipogenesis through GPR120. *Biochemical and Biophysical Research Communications*, 354(2), 591-597.

Green, A.D., Vasu, S., McClenaghan, N.H. and Flatt, P.R. (2015) Pseudoislet formation enhances gene expression, insulin secretion and cytoprotective mechanisms of clonal human insulin-secreting 1.1B4 cells. *Pflugers Archiv: European Journal of Physiology*, 467(10), 2219-2228.

Green, B.D. and Flatt, P.R. (2007) Incretin hormone mimetics and analogues in diabetes therapeutics. *Best Practice & Research.Clinical Endocrinology & Metabolism*, 21(4), 497-516.

Green, B.D., Gault, V.A., Flatt, P.R., Harriott, P., Greer, B. and O'Harte, F.P.M. (2004) Comparative effects of GLP-1 and GIP on cAMP production, insulin secretion, and in vivo antidiabetic actions following substitution of Ala8/Ala2 with 2-aminobutyric acid. *Archives of Biochemistry and Biophysics*, 428(2), 136-143.

Green, B.D., Irwin, N., Duffy, N.A., Gault, V.A., O'Harte, F.P.M. and Flatt, P.R. (2006) Inhibition of dipeptidyl peptidase-IV activity by metformin enhances the antidiabetic effects of glucagon-like peptide-1. *European Journal of Pharmacology*, 547(1-3), 192-199.

Gremlich, S., Porret, A., Hani, E.H., Cherif, D., Vionnet, N., Froguel, P. and Thorens, B. (1995) Cloning, functional expression, and chromosomal localization of the human pancreatic islet glucose-dependent insulinotropic polypeptide receptor. *Diabetes*, 44(10), 1202-1208.

Groeneveld, O.N., Kappelle, L.J. and Biessels, G.J. (2016) Potentials of incretin-based therapies in dementia and stroke in type 2 diabetes mellitus. *Journal of Diabetes Investigation*, 7(1), 5-16.

Grzegorski, S.J., Chiari, E.F., Robbins, A., Kish, P.E. and Kahana, A. (2014) Natural variability of Kozak sequences correlates with function in a zebrafish model. *PloS One*, 9(9), e108475.

Gupta, V. (2013) Glucagon-like peptide-1 analogues: An overview. *Indian Journal of Endocrinology and Metabolism*, 17(3), 413-421.

Gutzwiller, J.P., Goke, B., Drewe, J., Hildebrand, P., Ketterer, S., Handschin, D., Winterhalder, R., Conen, D. and Beglinger, C. (1999) Glucagon-like peptide-1: a potent regulator of food intake in humans. *Gut*, 44(1), 81-86.

Hara, T., Hirasawa, A., Ichimura, A., Kimura, I. and Tsujimoto, G. (2011) Free fatty acid receptors FFAR1 and GPR120 as novel therapeutic targets for metabolic disorders. *Journal of Pharmaceutical Sciences*, 100(9), 3594-3601.

Hara, T., Hirasawa, A., Ichimura, A., Kimura, I. and Tsujimoto, G. (2012) Physiological functions of fatty acid receptors and their therapeutic potential. *Nihon Yakurigaku Zasshi.Folia Pharmacologica Japonica*, 140(6), 275-279.

Hara, T., Kimura, I., Inoue, D., Ichimura, A. and Hirasawa, A. (2013) Free fatty acid receptors and their role in regulation of energy metabolism. *Reviews of Physiology, Biochemistry and Pharmacology*, 164, 77-116.

Hassing, H.A., Fares, S., Larsen, O., Pad, H., Hauge, M., Jones, R.M., Schwartz, T.W., Hansen, H.S. and Rosenkilde, M.M. (2016) Biased signaling of lipids and allosteric actions of synthetic molecules for GPR119. *Biochemical Pharmacology,* 119, 66-75.

Hattersley, A.T. and Thorens, B. (2015) Type 2 Diabetes, SGLT2 Inhibitors, and Glucose Secretion. *The New England Journal of Medicine*, 373(10), 974-976.

Hauge, M., Vestmar, M.A., Husted, A.S., Ekberg, J.P., Wright, M.J., Di Salvo, J., Weinglass, A.B., Engelstoft, M.S., Madsen, A.N., Luckmann, M., Miller, M.W., Trujillo, M.E., Frimurer, T.M., Holst, B., Howard, A.D. and Schwartz, T.W. (2014) GPR40 (FFAR1) - Combined Gs and Gq signaling in vitro is associated with robust incretin secretagogue action ex vivo and in vivo. *Molecular Metabolism,* 4(1), 3-14.

Hauser, A.S., Attwood, M.M., Rask-Andersen, M., Schioth, H.B. and Gloriam, D.E. (2017) Trends in GPCR drug discovery: new agents, targets and indications. *Nature Reviews.Drug Discovery,* 16(12), 829-842.

Hauser, A.S., Chavali, S., Masuho, I., Jahn, L.J., Martemyanov, K.A., Gloriam, D.E. and Babu, M.M. (2018) Pharmacogenomics of GPCR Drug Targets. *Cell*, 172(1-2), 41-54.e19.

Henquin, J.C., Ibrahim, M.M. and Rahier, J. (2017) Insulin, glucagon and somatostatin stores in the pancreas of subjects with type-2 diabetes and their lean and obese non-diabetic controls. *Scientific Reports*, 7(1), 11015-017-10296-z.

Henstridge, C.M., Balenga, N.A., Kargl, J., Andradas, C., Brown, A.J., Irving, A., Sanchez, C. and Waldhoer, M. (2011) Minireview: recent developments in the physiology and pathology of the lysophosphatidylinositol-sensitive receptor GPR55. *Molecular Endocrinology (Baltimore, Md.),* 25(11), 1835-1848.

Herath, H., Herath, R. and Wickremasinghe, R. (2017) Gestational diabetes mellitus and risk of type 2 diabetes 10 years after the index pregnancy in Sri Lankan women-A community based retrospective cohort study. *PloS One*, 12(6), e0179647.

Heydemann, A. (2016) An Overview of Murine High Fat Diet as a Model for Type 2 Diabetes Mellitus. *Journal of Diabetes Research,* 2016, e2902351.

Hirasawa, A., Tsumaya, K., Awaji, T., Katsuma, S., Adachi, T., Yamada, M., Sugimoto, Y., Miyazaki, S. and Tsujimoto, G. (2005) Free fatty acids regulate gut incretin glucagon-like peptide-1 secretion through GPR120. *Nature Medicine,* 11(1), 90-94.

Hollenstein, K., de Graaf, C., Bortolato, A., Wang, M.W., Marshall, F.H. and Stevens, R.C. (2014) Insights into the structure of class B GPCRs. *Trends in Pharmacological Sciences,* 35(1), 12-22.

Holzer, P., Reichmann, F. and Farzi, A. (2012) Neuropeptide Y, peptide YY and pancreatic polypeptide in the gut-brain axis. *Neuropeptides,* 46(6), 261-274.

Hoshino, A., Kowalska, D., Jean, F., Lazure, C. and Lindberg, I. (2011) Modulation of PC1/3 activity by self-interaction and substrate binding. *Endocrinology,* 152(4), 1402-1411.

Hou, N., Torii, S., Saito, N., Hosaka, M. and Takeuchi, T. (2008) Reactive oxygen species-mediated pancreatic beta-cell death is regulated by interactions between stress-activated protein kinases, p38 and c-Jun N-terminal kinase, and mitogen-activated protein kinase phosphatases. *Endocrinology,* 149(4), 1654-1665.

Houthuijzen, J.M. (2016) For Better or Worse: FFAR1 and FFAR4 Signaling in Cancer and Diabetes. *Molecular Pharmacology,* 90(6), 738-743.

Houthuijzen, J.M., Oosterom, I., Hudson, B.D., Hirasawa, A., Daenen, L.G.M., McLean, C.M., Hansen, S.V.F., van Jaarsveld, M.T.M., Peeper, D.S., Jafari Sadatmand, S., Roodhart, J.M.L., van de Lest, C.H.A., Ulven, T., Ishihara, K., Milligan, G. and Voest, E.E. (2017) Fatty acid 16:4(n-3) stimulates a GPR120-induced signaling cascade in splenic macrophages to promote chemotherapy resistance. *FASEB Journal: Official Publication of the Federation of American Societies for Experimental Biology,* 31(5), 2195-2209.

Howells, L., McKay, A.J., Hussain, S. and Majeed, A. (2016) Management of a patient at high risk of type 2 diabetes. *London Journal of Primary Care,* 8(5), 76-79.

Howlett, A.C., Blume, L.C. and Dalton, G.D. (2010) CB(1) cannabinoid receptors and their associated proteins. *Current Medicinal Chemistry*, 17(14), 1382-1393.

Huang, H.C. and Klein, P.S. (2004) The Frizzled family: receptors for multiple signal transduction pathways. *Genome Biology,* 5(7), 234-2004-5-7-234. Epub 2004 Jun 14.

Hudson, B.D., Shimpukade, B., Mackenzie, A.E., Butcher, A.J., Pediani, J.D., Christiansen, E., Heathcote, H., Tobin, A.B., Ulven, T. and Milligan, G. (2013) The pharmacology of TUG-891, a potent and selective agonist of the free fatty acid receptor 4 (FFA4/GPR120), demonstrates both potential opportunity and possible challenges to therapeutic agonism. *Molecular Pharmacology*, 84(5), 710-725.

Hung, C.C., Lin, H.Y., Hwang, D.Y., Kuo, I.C., Chiu, Y.W., Lim, L.M., Hwang, S.J. and Chen, H.C. (2017) Diabetic Retinopathy and Clinical Parameters Favoring the Presence of Diabetic Nephropathy could Predict Renal Outcome in Patients with Diabetic Kidney Disease. *Scientific Reports,* 7(1), 1236-017-01204-6.

Hung, C.C., Pirie, F., Luan, J., Lank, E., Motala, A., Yeo, G.S., Keogh, J.M., Wareham, N.J., O'Rahilly, S. and Farooqi, I.S. (2004) Studies of the peptide YY and neuropeptide Y2 receptor genes in relation to human obesity and obesity-related traits. *Diabetes*, 53(9), 2461-2466.

Iakoubov, R., Izzo, A., Yeung, A., Whiteside, C.I. and Brubaker, P.L. (2007) Protein kinase Czeta is required for oleic acid-induced secretion of glucagon-like peptide-1 by intestinal endocrine L cells. *Endocrinology,* 148(3), 1089-1098.

Ichimura, A., Hirasawa, A., Hara, T. and Tsujimoto, G. (2009) Free fatty acid receptors act as nutrient sensors to regulate energy homeostasis. *Prostaglandins & Other Lipid Mediators*, 89(3-4), 82-88.

Ichimura, A., Hirasawa, A., Poulain-Godefroy, O., Bonnefond, A., Hara, T., Yengo, L., Kimura, I., Leloire, A., Liu, N., Iida, K., Choquet, H., Besnard, P., Lecoeur, C., Vivequin, S., Ayukawa, K., Takeuchi, M., Ozawa, K., Tauber, M., Maffeis, C., Morandi, A., Buzzetti, R., Elliott, P., Pouta, A., Jarvelin, M.R., Korner, A., Kiess, W., Pigeyre, M., Caiazzo, R., Van Hul, W., Van Gaal, L., Horber, F., Balkau, B., Levy-Marchal, C., Rouskas, K., Kouvatsi, A., Hebebrand, J., Hinney, A., Scherag, A., Pattou, F., Meyre, D., Koshimizu, T.A., Wolowczuk, I., Tsujimoto, G. and Froguel, P. (2012) Dysfunction of

lipid sensor GPR120 leads to obesity in both mouse and human. *Nature,* 483(7389), 350-354.

Ijuin, T. and Takenawa, T. (2012) Regulation of insulin signaling and glucose transporter 4 (GLUT4) exocytosis by phosphatidylinositol 3,4,5-trisphosphate (PIP3) phosphatase, skeletal muscle, and kidney enriched inositol polyphosphate phosphatase (SKIP). *The Journal of Biological Chemistry,* 287(10), 6991-6999.

Inagaki, N., Seino, Y., Takeda, J., Yano, H., Yamada, Y., Bell, G.I., Eddy, R.L., Fukushima, Y., Byers, M.G. and Shows, T.B. (1989) Gastric inhibitory polypeptide: structure and chromosomal localization of the human gene. *Molecular Endocrinology (Baltimore, Md.),* 3(6), 1014-1021.

Inoue, D., Tsujimoto, G. and Kimura, I. (2014) Regulation of Energy Homeostasis by GPR41. *Frontiers in Endocrinology,* 5, 81.

Insel, P.A., Snead, A., Murray, F., Zhang, L., Yokouchi, H., Katakia, T., Kwon, O., Dimucci, D. and Wilderman, A. (2012) GPCR expression in tissues and cells: are the optimal receptors being used as drug targets? *British Journal of Pharmacology*, 165(6), 1613-1616.

Irving, A., Abdulrazzaq, G., Chan, S.L.F., Penman, J., Harvey, J. and Alexander, S.P.H. (2017) Cannabinoid Receptor-Related Orphan G Protein-Coupled Receptors. *Advances in Pharmacology (San Diego, Calif.),* 80, 223-247.

Irwin, N. and Flatt, P.R. (2015) New perspectives on exploitation of incretin peptides for the treatment of diabetes and related disorders. *World Journal of Diabetes*, 6(15), 1285-1295.

Irwin, N., O'Harte, F.P., Gault, V.A., Green, B.D., Greer, B., Harriott, P., Bailey, C.J. and Flatt, P.R. (2006) GIP(Lys16PAL) and GIP(Lys37PAL): novel long-acting acylated analogues of glucose-dependent insulinotropic polypeptide with improved antidiabetic potential. *Journal of Medicinal Chemistry,* 49(3), 1047-1054.

Itoh, Y., Kawamata, Y., Harada, M., Kobayashi, M., Fujii, R., Fukusumi, S., Ogi, K., Hosoya, M., Tanaka, Y., Uejima, H., Tanaka, H., Maruyama, M., Satoh, R., Okubo, S., Kizawa, H., Komatsu, H., Matsumura, F., Noguchi, Y., Shinohara, T., Hinuma, S.,

Fujisawa, Y. and Fujino, M. (2003) Free fatty acids regulate insulin secretion from pancreatic beta cells through GPR40. *Nature,* 422(6928), 173-176.

Jackson, S.H., Martin, T.S., Jones, J.D., Seal, D. and Emanuel, F. (2010) Liraglutide (victoza): the first once-daily incretin mimetic injection for type-2 diabetes. *P & T: A Peer-Reviewed Journal for Formulary Management,* 35(9), 498-529.

Javitt, D.C., Schoepp, D., Kalivas, P.W., Volkow, N.D., Zarate, C., Merchant, K., Bear, M.F., Umbricht, D., Hajos, M., Potter, W.Z. and Lee, C.M. (2011) Translating glutamate: from pathophysiology to treatment. *Science Translational Medicine,* 3(102), 102mr2.

Jerant, A., Bertakis, K.D. and Franks, P. (2015) Body mass index and health status in diabetic and non-diabetic individuals. *Nutrition & Diabetes,* 5, e152.

Johns, D.G., Behm, D.J., Walker, D.J., Ao, Z., Shapland, E.M., Daniels, D.A., Riddick, M., Dowell, S., Staton, P.C., Green, P., Shabon, U., Bao, W., Aiyar, N., Yue, T.L., Brown, A.J., Morrison, A.D. and Douglas, S.A. (2007) The novel endocannabinoid receptor GPR55 is activated by atypical cannabinoids but does not mediate their vasodilator effects. *British Journal of Pharmacology,* 152(5), 825-831.

Johnston, R., Uthman, O., Cummins, E., Clar, C., Royle, P., Colquitt, J., Tan, B.K., Clegg, A., Shantikumar, S., Court, R., O'Hare, J.P., McGrane, D., Holt, T. and Waugh, N. (2017) Canagliflozin, dapagliflozin and empagliflozin monotherapy for treating type 2 diabetes: systematic review and economic evaluation. *Health Technology Assessment (Winchester, England),* 21(2), 1-218.

Kalra, S. (2014) Alpha glucosidase inhibitors. *JPMA.the Journal of the Pakistan Medical Association,* 64(4), 474-476.

Kalra, S. and Gupta, Y. (2016) The Insulin:Glucagon Ratio and the Choice of Glucose-Lowering Drugs. *Diabetes Therapy: Research, Treatment and Education of Diabetes and Related Disorders,* 7(1), 1-9.

Kaminski, N.E. (1998) Inhibition of the cAMP signaling cascade via cannabinoid receptors: a putative mechanism of immune modulation by cannabinoid compounds. *Toxicology Letters,* 102-103, 59-63.

Katanaev, V.L. (2010) The Wnt/Frizzled GPCR signaling pathway. *Biochemistry.Biokhimiia,* 75(12), 1428-1434.

Kaur, N., Chugh, V. and Gupta, A.K. (2014) Essential fatty acids as functional components of foods- a review. *Journal of Food Science and Technology,* 51(10), 2289-2303.

Kerr, B.D., Flatt, P.R. and Gault, V.A. (2010) (D-Ser2)Oxm[mPEG-PAL]: a novel chemically modified analogue of oxyntomodulin with antihyperglycaemic, insulinotropic and anorexigenic actions. *Biochemical Pharmacology,* 80(11), 1727-1735.

Kharroubi, A.T. and Darwish, H.M. (2015) Diabetes mellitus: The epidemic of the century. *World Journal of Diabetes,* 6(6), 850-867.

Kim, J., Yin, T., Shinozaki, K., Lampe, J.W. and Becker, L.B. (2017) Potential of lysophosphatidylinositol as a prognostic indicator of cardiac arrest using a rat model. *Biomarkers: Biochemical Indicators of Exposure, Response, and Susceptibility to Chemicals,* 22(8), 755-763.

Kim, S., Kim, J.H., Park, B.O. and Kwak, Y.S. (2014) Perspectives on the therapeutic potential of short-chain fatty acid receptors. *BMB Reports,* 47(3), 173-178.

Knop, F.K., Vilsboll, T., Hojberg, P.V., Larsen, S., Madsbad, S., Holst, J.J. and Krarup, T. (2007) The insulinotropic effect of GIP is impaired in patients with chronic pancreatitis and secondary diabetes mellitus as compared to patients with chronic pancreatitis and normal glucose tolerance. *Regulatory Peptides,* 144(1-3), 123-130.

Kobilka, B.K. (2007) G protein coupled receptor structure and activation. *Biochimica Et Biophysica Acta,* 1768(4), 794-807.

Koska, J., DelParigi, A., de Courten, B., Weyer, C. and Tataranni, P.A. (2004) Pancreatic polypeptide is involved in the regulation of body weight in pima Indian male subjects. *Diabetes,* 53(12), 3091-3096.

Krejs, G.J. (1986) Physiological role of somatostatin in the digestive tract: gastric acid secretion, intestinal absorption, and motility. *Scandinavian Journal of Gastroenterology.Supplement,* 119, 47-53.

Kunos, G., Osei-Hyiaman, D., Liu, J., Godlewski, G. and Batkai, S. (2008) Endocannabinoids and the control of energy homeostasis. *The Journal of Biological Chemistry,* 283(48), 33021-33025.

Lafferty, R.A., Flatt, P.R. and Irwin, N. (2018) Emerging therapeutic potential for peptide YY for obesity-diabetes. *Peptides,* 100, 269-274.

Lagerstrom, M.C. and Schioth, H.B. (2008) Structural diversity of G protein-coupled receptors and significance for drug discovery. *Nature Reviews.Drug Discovery,* 7(4), 339-357.

Laprairie, R.B., Kelly, M.E. and Denovan-Wright, E.M. (2012) The dynamic nature of type 1 cannabinoid receptor (CB(1)) gene transcription. *British Journal of Pharmacology,* 167(8), 1583-1595.

Lathief, S. and Inzucchi, S.E. (2016) Approach to diabetes management in patients with CVD. *Trends in Cardiovascular Medicine,* 26(2), 165-179.

Lauckner, J.E., Jensen, J.B., Chen, H.Y., Lu, H.C., Hille, B. and Mackie, K. (2008) GPR55 is a cannabinoid receptor that increases intracellular calcium and inhibits M current. *Proceedings of the National Academy of Sciences of the United States of America,* 105(7), 2699-2704.

Lawrence, M., Shao, C., Duan, L., McGlynn, K. and Cobb, M.H. (2008) The protein kinases ERK1/2 and their roles in pancreatic beta cells. *Acta Physiologica (Oxford, England),* 192(1), 11-17.

Lebovitz, H.E. (2001) Diagnosis, classification, and pathogenesis of diabetes mellitus. *The Journal of Clinical Psychiatry,* 62 Suppl 27, 5-9; discussion 40-1.

Lebovitz, H.E. (2011) Type 2 diabetes mellitus--current therapies and the emergence of surgical options. *Nature Reviews.Endocrinology,* 7(7), 408-419.

Lee, H.S. and Kim, C.D. (2000) Analysis of human pancreatic juice in tests of pancreatic function. *Journal of Korean Medical Science,* 15 Suppl, S21-S23.

Lee, J.O., Lee, S.K., Kim, J.H., Kim, N., You, G.Y., Moon, J.W., Kim, S.J., Park, S.H. and Kim, H.S. (2012) Metformin regulates glucose transporter 4 (GLUT4) translocation

through AMP-activated protein kinase (AMPK)-mediated Cbl/CAP signaling in 3T3-L1 preadipocyte cells. *The Journal of Biological Chemistry*, 287(53), 44121-44129.

Lee, S. and Lee, D.Y. (2017) Glucagon-like peptide-1 and glucagon-like peptide-1 receptor agonists in the treatment of type 2 diabetes. *Annals of Pediatric Endocrinology & Metabolism*, 22(1), 15-26.

Leech, C.A., Dzhura, I., Chepurny, O.G., Kang, G., Schwede, F., Genieser, H.G. and Holz, G.G. (2011) Molecular physiology of glucagon-like peptide-1 insulin secretagogue action in pancreatic beta cells. *Progress in Biophysics and Molecular Biology*, 107(2), 236-247.

Leon, B.M. and Maddox, T.M. (2015) Diabetes and cardiovascular disease: Epidemiology, biological mechanisms, treatment recommendations and future research. *World Journal of Diabetes*, 6(13), 1246-1258.

Lerner, S.M. (2008) Kidney and pancreas transplantation in type 1 diabetes mellitus. *The Mount Sinai Journal of Medicine, New York*, 75(4), 372-384.

Leyva-Illades, D. and Demorrow, S. (2013) Orphan G protein receptor GPR55 as an emerging target in cancer therapy and management. *Cancer Management and Research*, 5, 147-155.

Li, D.W., Li, G.R., Lu, Y., Liu, Z.Q., Chang, M., Yao, M., Cheng, W. and Hu, L.S. (2013) alpha-lipoic acid protects dopaminergic neurons against MPP+-induced apoptosis by attenuating reactive oxygen species formation. *International Journal of Molecular Medicine*, 32(1), 108-114.

Li, X.C. and Zhuo, J.L. (2007) Targeting glucagon receptor signalling in treating metabolic syndrome and renal injury in Type 2 diabetes: theory versus promise. *Clinical Science (London, England: 1979)*, 113(4), 183-193.

Li, Y., Cao, X., Li, L.X., Brubaker, P.L., Edlund, H. and Drucker, D.J. (2005) beta-Cell Pdx1 expression is essential for the glucoregulatory, proliferative, and cytoprotective actions of glucagon-like peptide-1. *Diabetes*, 54(2), 482-491.

Liu, B., Song, S., Ruz-Maldonado, I., Pingitore, A., Huang, G.C., Baker, D., Jones, P.M. and Persaud, S.J. (2016) GPR55-dependent stimulation of insulin secretion from isolated

mouse and human islets of Langerhans. *Diabetes, Obesity & Metabolism,* 18(12), 1263-1273.

Liu, Q.R., Pan, C.H., Hishimoto, A., Li, C.Y., Xi, Z.X., Llorente-Berzal, A., Viveros, M.P., Ishiguro, H., Arinami, T., Onaivi, E.S. and Uhl, G.R. (2009) Species differences in cannabinoid receptor 2 (CNR2 gene): identification of novel human and rodent CB2 isoforms, differential tissue expression and regulation by cannabinoid receptor ligands. *Genes, Brain, and Behavior,* 8(5), 519-530.

Liu, Y.J., Hellman, B. and Gylfe, E. (1999) Ca2+ signaling in mouse pancreatic polypeptide cells. *Endocrinology,* 140(12), 5524-5529.

Livak, K.J. and Schmittgen, T.D. (2001) Analysis of relative gene expression data using real-time quantitative PCR and the 2(-Delta Delta C(T)) Method. *Methods (San Diego, Calif.),* 25(4), 402-408.

MacDonald, P.E., Joseph, J.W. and Rorsman, P. (2005) Glucose-sensing mechanisms in pancreatic beta-cells. *Philosophical Transactions of the Royal Society of London.Series B, Biological Sciences,* 360(1464), 2211-2225.

Madsbad, S. (2009) Exenatide and liraglutide: different approaches to develop GLP-1 receptor agonists (incretin mimetics)- preclinical and clinical results. *Best Practice & Research.Clinical Endocrinology & Metabolism,* 23(4), 463-477.

Madva, E.N. and Granstein, R.D. (2013) Nerve-derived transmitters including peptides influence cutaneous immunology. *Brain, Behavior, and Immunity,* 34, 1-10.

Manzanares, J., Julian, M. and Carrascosa, A. (2006) Role of the cannabinoid system in pain control and therapeutic implications for the management of acute and chronic pain episodes. *Current Neuropharmacology,* 4(3), 239-257.

Marcinak, J., Cao, C., Lee, D. and Ye, Z. (2017) Fasiglifam for glycaemic control in people with type 2 diabetes: A phase III, placebo-controlled study. *Diabetes, Obesity & Metabolism,* 19(12), 1714-1721.

Martin, C., Passilly-Degrace, P., Chevrot, M., Ancel, D., Sparks, S.M., Drucker, D.J. and Besnard, P. (2012) Lipid-mediated release of GLP-1 by mouse taste buds from circumvallate papillae: putative involvement of GPR120 and impact on taste sensitivity. *Journal of Lipid Research,* 53(11), 2256-2265.

Martin-Timon, I., Sevillano-Collantes, C., Segura-Galindo, A. and Del Canizo-Gomez, F.J. (2014) Type 2 diabetes and cardiovascular disease: Have all risk factors the same strength? *World Journal of Diabetes,* 5(4), 444-470.

Matouk, A.I., Taye, A., El-Moselhy, M.A., Heeba, G.H. and Abdel-Rahman, A.A. (2017) The Effect of Chronic Activation of the Novel Endocannabinoid Receptor GPR18 on Myocardial Function and Blood Pressure in Conscious Rats. *Journal of Cardiovascular Pharmacology,* 69(1), 23-33.

Matouk, A.I., Taye, A., El-Moselhy, M.A., Heeba, G.H. and Abdel-Rahman, A.A. (2018) Abnormal cannabidiol confers cardioprotection in diabetic rats independent of glycemic control. *European Journal of Pharmacology,* 820, 256-264.

McCall, A.L. and Farhy, L.S. (2013) Treating type 1 diabetes: from strategies for insulin delivery to dual hormonal control. *Minerva Endocrinologica,* 38(2), 145-163.

McClean, P.L., Irwin, N., Cassidy, R.S., Holst, J.J., Gault, V.A. and Flatt, P.R. (2007) GIP receptor antagonism reverses obesity, insulin resistance, and associated metabolic disturbances induced in mice by prolonged consumption of high-fat diet. *American Journal of Physiology.Endocrinology and Metabolism,* 293(6), E1746-55.

McClenaghan, N.H., Barnett, C.R., Ah-Sing, E., Abdel-Wahab, Y.H., O'Harte, F.P., Yoon, T.W., Swanston-Flatt, S.K. and Flatt, P.R. (1996) Characterization of a novel glucose-responsive insulin-secreting cell line, BRIN-BD11, produced by electrofusion. *Diabetes,* 45(8), 1132-1140.

McIntosh, C.H., Widenmaier, S. and Kim, S.J. (2012) Glucose-dependent insulinotropic polypeptide signaling in pancreatic beta-cells and adipocytes. *Journal of Diabetes Investigation,* 3(2), 96-106.

McIntyre, R.S., Powell, A.M., Kaidanovich-Beilin, O., Soczynska, J.K., Alsuwaidan, M., Woldeyohannes, H.O., Kim, A.S. and Gallaugher, L.A. (2013) The neuroprotective effects of GLP-1: possible treatments for cognitive deficits in individuals with mood disorders. *Behavioural Brain Research,* 237, 164-171.

McKillop, A.M., Moran, B.M., Abdel-Wahab, Y.H. and Flatt, P.R. (2013) Evaluation of the insulin releasing and antihyperglycaemic activities of GPR55 lipid agonists using clonal beta-cells, isolated pancreatic islets and mice. *British Journal of Pharmacology,* 170(5), 978-990.

McKillop, A.M., Moran, B.M., Abdel-Wahab, Y.H., Gormley, N.M. and Flatt, P.R. (2016) Metabolic effects of orally administered small-molecule agonists of GPR55 and GPR119 in multiple low-dose streptozotocin-induced diabetic and incretin-receptor-knockout mice. *Diabetologia,* 59(12), 2674-2685.

McLaughlin, J.T., Lomax, R.B., Hall, L., Dockray, G.J., Thompson, D.G. and Warhurst, G. (1998) Fatty acids stimulate cholecystokinin secretion via an acyl chain length-specific, Ca2+-dependent mechanism in the enteroendocrine cell line STC-1. *The Journal of Physiology,* 513 (Pt 1), 11-18.

Mebratu, Y. and Tesfaigzi, Y. (2009) How ERK1/2 activation controls cell proliferation and cell death: Is subcellular localization the answer? *Cell Cycle (Georgetown, Tex.),* 8(8), 1168-1175.

Meier, J.J., Nauck, M.A., Kask, B., Holst, J.J., Deacon, C.F., Schmidt, W.E. and Gallwitz, B. (2006) Influence of gastric inhibitory polypeptide on pentagastrin-stimulated gastric acid secretion in patients with type 2 diabetes and healthy controls. *World Journal of Gastroenterology,* 12(12), 1874-1880.

Melchior, H., Kurch-Bek, D. and Mund, M. (2017) The Prevalence of Gestational Diabetes. *Deutsches Arzteblatt International,* 114(24), 412-418.

Menzel, S., Stoffel, M., Espinosa, R.,3rd, Fernald, A.A., Le Beau, M.M. and Bell, G.I. (1994) Localization of the glucagon receptor gene to human chromosome band 17q25. *Genomics,* 20(2), 327-328.

Mercader, J.M. and Florez, J.C. (2017) The Genetic Basis of Type 2 Diabetes in Hispanics and Latin Americans: Challenges and Opportunities. *Frontiers in Public Health,* 5, 329.

Michels, A. and Gottlieb, P. (2000) Pathogenesis of Type 1A Diabetes. *In:* De Groot, L.J., Chrousos, G., Dungan, K., Feingold, K.R., Grossman, A., Hershman, J.M., Koch, C., Korbonits, M., McLachlan, R., New, M., Purnell, J., Rebar, R., Singer, F. and Vinik, A. eds. *Endotext.* South Dartmouth (MA): MDText.com, Inc,

Milligan, G., Alvarez-Curto, E., Watterson, K.R., Ulven, T. and Hudson, B.D. (2015) Characterizing pharmacological ligands to study the long-chain fatty acid receptors GPR40/FFA1 and GPR120/FFA4. *British Journal of Pharmacology,* 172(13), 3254-3265.

Miyauchi, S., Hirasawa, A., Iga, T., Liu, N., Itsubo, C., Sadakane, K., Hara, T. and Tsujimoto, G. (2009) Distribution and regulation of protein expression of the free fatty acid receptor GPR120. *Naunyn-Schmiedeberg's Archives of Pharmacology,* 379(4), 427-434.

Mizuno, N. and Itoh, H. (2009) Functions and regulatory mechanisms of Gq-signaling pathways. *Neuro-Signals,* 17(1), 42-54.

Mizuta, K., Zhang, Y., Mizuta, F., Hoshijima, H., Shiga, T., Masaki, E. and Emala CW, S. (2015) Novel identification of the free fatty acid receptor FFAR1 that promotes contraction in airway smooth muscle. *American Journal of Physiology.Lung Cellular and Molecular Physiology,* 309(9), L970-82.

Molenaar, E.A., Hwang, S.J., Vasan, R.S., Grobbee, D.E., Meigs, J.B., D'Agostino RB, S., Levy, D. and Fox, C.S. (2008) Burden and rates of treatment and control of cardiovascular disease risk factors in obesity: the Framingham Heart Study. *Diabetes Care,* 31(7), 1367-1372.

Moore, K., Zhang, Q., Murgolo, N., Hosted, T. and Duffy, R. (2009) Cloning, expression, and pharmacological characterization of the GPR120 free fatty acid receptor from cynomolgus monkey: comparison with human GPR120 splice variants. *Comparative Biochemistry and Physiology.Part B, Biochemistry & Molecular Biology,* 154(4), 419-426.

Morales, P. and Reggio, P.H. (2017) An Update on Non-CB1, Non-CB2 Cannabinoid Related G-Protein-Coupled Receptors. *Cannabis and Cannabinoid Research,* 2(1), 265-273.

Moran, B.M., Abdel-Wahab, Y.H., Flatt, P.R. and McKillop, A.M. (2014) Activation of GPR119 by fatty acid agonists augments insulin release from clonal beta-cells and isolated pancreatic islets and improves glucose tolerance in mice. *Biological Chemistry,* 395(4), 453-464.

Moran, B.M., Abdel-Wahab, Y.H., Flatt, P.R. and McKillop, A.M. (2014) Evaluation of the insulin-releasing and glucose-lowering effects of GPR120 activation in pancreatic beta-cells. *Diabetes, Obesity & Metabolism,* 16(11), 1128-1139.

Moran, B.M., Flatt, P.R. and McKillop, A.M. (2016) G protein-coupled receptors: signalling and regulation by lipid agonists for improved glucose homoeostasis. *Acta Diabetologica,* 53(2), 177-188.

Moreno-Navarrete, J.M., Catalan, V., Whyte, L., Diaz-Arteaga, A., Vazquez-Martinez, R., Rotellar, F., Guzman, R., Gomez-Ambrosi, J., Pulido, M.R., Russell, W.R., Imbernon, M., Ross, R.A., Malagon, M.M., Dieguez, C., Fernandez-Real, J.M., Fruhbeck, G. and Nogueiras, R. (2012) The L-alpha-lysophosphatidylinositol/GPR55 system and its potential role in human obesity. *Diabetes,* 61(2), 281-291.

Mouslech, Z. and Valla, V. (2009) Endocannabinoid system: An overview of its potential in current medical practice. *Neuro Endocrinology Letters,* 30(2), 153-179.

Muscogiuri, G., Cignarelli, A., Giorgino, F., Prodam, F., Santi, D., Tirabassi, G., Balercia, G., Modica, R., Faggiano, A. and Colao, A. (2014) GLP-1: benefits beyond pancreas. *Journal of Endocrinological Investigation,* 37(12), 1143-1153.

Nagasumi, K., Esaki, R., Iwachidow, K., Yasuhara, Y., Ogi, K., Tanaka, H., Nakata, M., Yano, T., Shimakawa, K., Taketomi, S., Takeuchi, K., Odaka, H. and Kaisho, Y. (2009) Overexpression of GPR40 in pancreatic beta-cells augments glucose-stimulated insulin secretion and improves glucose tolerance in normal and diabetic mice. *Diabetes,* 58(5), 1067-1076.

Nakajima, A., Nakatani, A., Hasegawa, S., Irie, J., Ozawa, K., Tsujimoto, G., Suganami, T., Itoh, H. and Kimura, I. (2017) The short chain fatty acid receptor GPR43 regulates inflammatory signals in adipose tissue M2-type macrophages. *PloS One*, 12(7), e0179696.

Namour, F., Galien, R., Van Kaem, T., Van der Aa, A., Vanhoutte, F., Beetens, J. and Van't Klooster, G. (2016) Safety, pharmacokinetics and pharmacodynamics of GLPG0974, a potent and selective FFA2 antagonist, in healthy male subjects. *British Journal of Clinical Pharmacology,* 82(1), 139-148.

Naylor, J., Suckow, A.T., Seth, A., Baker, D.J., Sermadiras, I., Ravn, P., Howes, R., Li, J., Snaith, M.R., Coghlan, M.P. and Hornigold, D.C. (2016) Use of CRISPR/Cas9-engineered INS-1 pancreatic beta cells to define the pharmacology of dual GIPR/GLP-1R agonists. *The Biochemical Journal*, 473(18), 2881-2891.

Ning, S.L., Zheng, W.S., Su, J., Liang, N., Li, H., Zhang, D.L., Liu, C.H., Dong, J.H., Zhang, Z.K., Cui, M., Hu, Q.X., Chen, C.C., Liu, C.H., Wang, C., Pang, Q., Chen, Y.X., Yu, X. and Sun, J.P. (2015) Different downstream signalling of CCK1 receptors regulates distinct functions of CCK in pancreatic beta cells. *British Journal of Pharmacology,* 172(21), 5050-5067.

Niswender, C.M. and Conn, P.J. (2010) Metabotropic glutamate receptors: physiology, pharmacology, and disease. *Annual Review of Pharmacology and Toxicology*, 50, 295-322.

Nordmann, T.M., Dror, E., Schulze, F., Traub, S., Berishvili, E., Barbieux, C., Boni-Schnetzler, M. and Donath, M.Y. (2017) The Role of Inflammation in beta-cell Dedifferentiation. *Scientific Reports*, 7(1), 6285-017-06731-w.

Nordstrom, K.J., Lagerstrom, M.C., Waller, L.M., Fredriksson, R. and Schioth, H.B. (2009) The Secretin GPCRs descended from the family of Adhesion GPCRs. *Molecular Biology and Evolution,* 26(1), 71-84.

O'Dowd, B.F., Nguyen, T., Marchese, A., Cheng, R., Lynch, K.R., Heng, H.H., Kolakowski, L.F.,Jr and George, S.R. (1998) Discovery of three novel G-protein-coupled receptor genes. *Genomics,* 47(2), 310-313.

Oh, D.Y., Talukdar, S., Bae, E.J., Imamura, T., Morinaga, H., Fan, W., Li, P., Lu, W.J., Watkins, S.M. and Olefsky, J.M. (2010) GPR120 is an omega-3 fatty acid receptor mediating potent anti-inflammatory and insulin-sensitizing effects. *Cell,* 142(5), 687-698.

Oh, D.Y., Walenta, E., Akiyama, T.E., Lagakos, W.S., Lackey, D., Pessentheiner, A.R., Sasik, R., Hah, N., Chi, T.J., Cox, J.M., Powels, M.A., Di Salvo, J., Sinz, C., Watkins, S.M., Armando, A.M., Chung, H., Evans, R.M., Quehenberger, O., McNelis, J., Bogner-Strauss, J.G. and Olefsky, J.M. (2014) A Gpr120-selective agonist improves insulin resistance and chronic inflammation in obese mice. *Nature Medicine,* 20(8), 942-947.

Otero, Y.F., Stafford, J.M. and McGuinness, O.P. (2014) Pathway-selective insulin resistance and metabolic disease: the importance of nutrient flux. *The Journal of Biological Chemistry,* 289(30), 20462-20469.

Otieno, M.A., Snoeys, J., Lam, W., Ghosh, A., Player, M.R., Pocai, A., Salter, R., Simic, D., Skaggs, H., Singh, B. and Lim, H.K. (2018) Fasiglifam (TAK-875): Mechanistic Investigation and Retrospective Identification of Hazards for Drug Induced Liver Injury. *Toxicological Sciences: An Official Journal of the Society of Toxicology,* 163(2), 374-384.

Pacher, P. and Kunos, G. (2013) Modulating the endocannabinoid system in human health and disease--successes and failures. *The FEBS Journal*, 280(9), 1918-1943.

Palczewski, K. (2006) G protein-coupled receptor rhodopsin. *Annual Review of Biochemistry,* 75, 743-767.

Palumbo, P.J. (1998) Metformin: effects on cardiovascular risk factors in patients with non-insulin-dependent diabetes mellitus. *Journal of Diabetes and its Complications*, 12(2), 110-119.

Paschou, S.A., Papadopoulou-Marketou, N., Chrousos, G.P. and Kanaka-Gantenbein, C. (2018) On type 1 diabetes mellitus pathogenesis. *Endocrine Connections,* 7(1), R38-R46.

Pathak, N.M., Pathak, V., Lynch, A.M., Irwin, N., Gault, V.A. and Flatt, P.R. (2015) Stable oxyntomodulin analogues exert positive effects on hippocampal neurogenesis and gene expression as well as improving glucose homeostasis in high fat fed mice. *Molecular and Cellular Endocrinology,* 412, 95-103.

Paulsen, S.J., Larsen, L.K., Hansen, G., Chelur, S., Larsen, P.J. and Vrang, N. (2014) Expression of the fatty acid receptor GPR120 in the gut of diet-induced-obese rats and its role in GLP-1 secretion. *PloS One,* 9(2), e88227.

Peng, X.V., Marcinak, J.F., Raanan, M.G. and Cao, C. (2017) Combining the G-protein-coupled receptor 40 agonist fasiglifam with sitagliptin improves glycaemic control in patients with type 2 diabetes with or without metformin: A randomized, 12-week trial. *Diabetes, Obesity & Metabolism,* 19(8), 1127-1134.

Pocai, A. (2013) Action and therapeutic potential of oxyntomodulin. *Molecular Metabolism,* 3(3), 241-251.

Polli, J.W., Hussey, E., Bush, M., Generaux, G., Smith, G., Collins, D., McMullen, S., Turner, N. and Nunez, D.J. (2013) Evaluation of drug interactions of GSK1292263 (a GPR119 agonist) with statins: from in vitro data to clinical study design. *Xenobiotica; the Fate of Foreign Compounds in Biological Systems*, 43(6), 498-508.

Portela-Gomes, G.M., Grimelius, L., Westermark, P. and Stridsberg, M. (2010) Somatostatin receptor subtypes in human type 2 diabetic islets. *Pancreas,* 39(6), 836-842.

Putney, J.W. and Tomita, T. (2012) Phospholipase C signaling and calcium influx. *Advances in Biological Regulation,* 52(1), 152-164.

Quinn, C.E., Hamilton, P.K., Lockhart, C.J. and McVeigh, G.E. (2008) Thiazolidinediones: effects on insulin resistance and the cardiovascular system. *British Journal of Pharmacology,* 153(4), 636-645.

Ran, F.A., Hsu, P.D., Wright, J., Agarwala, V., Scott, D.A. and Zhang, F. (2013) Genome engineering using the CRISPR-Cas9 system. *Nature Protocols,* 8(11), 2281-2308.

Rani, P.R. and Begum, J. (2016) Screening and Diagnosis of Gestational Diabetes Mellitus, Where Do We Stand. *Journal of Clinical and Diagnostic Research : JCDR,* 10(4), QE01-4.

Rao, D.D., Vorhies, J.S., Senzer, N. and Nemunaitis, J. (2009) siRNA vs. shRNA: similarities and differences. *Advanced Drug Delivery Reviews,* 61(9), 746-759.

Reggio, P.H. (2010) Endocannabinoid binding to the cannabinoid receptors: what is known and what remains unknown. *Current Medicinal Chemistry,* 17(14), 1468-1486.

Rehfeld, J.F. (2014) Gastrointestinal hormones and their targets. *Advances in Experimental Medicine and Biology,* 817, 157-175.

Rehfeld, J.F. (2017) Cholecystokinin-From Local Gut Hormone to Ubiquitous Messenger. *Frontiers in Endocrinology,* 8, 47.

Rehfeld, J.F., Friis-Hansen, L., Goetze, J.P. and Hansen, T.V. (2007) The biology of cholecystokinin and gastrin peptides. *Current Topics in Medicinal Chemistry,* 7(12), 1154-1165.

Reimann, F. and Gribble, F.M. (2016) G protein-coupled receptors as new therapeutic targets for type 2 diabetes. *Diabetologia,* 59(2), 229-233.

Reinehr, T., Enriori, P.J., Harz, K., Cowley, M.A. and Roth, C.L. (2006) Pancreatic polypeptide in obese children before and after weight loss. *International Journal of Obesity (2005),* 30(10), 1476-1481.

Ren, J. and Chung, S.H. (2007) Anti-inflammatory effect of alpha-linolenic acid and its mode of action through the inhibition of nitric oxide production and inducible nitric oxide synthase gene expression via NF-kappaB and mitogen-activated protein kinase pathways. *Journal of Agricultural and Food Chemistry,* 55(13), 5073-5080.

Rendell, M. (2004) The role of sulphonylureas in the management of type 2 diabetes mellitus. *Drugs,* 64(12), 1339-1358.

Ribes, G., Gross, R., Chenon, D., Puech, R. and Loubatieres-Mariani, M.M. (1987) In vivo study of glucose-induced somatostatin secretion: comparison in normal and alloxan-diabetic dogs. *Pancreas,* 2(6), 638-644.

Ritter, K., Buning, C., Halland, N., Poverlein, C. and Schwink, L. (2016) G Protein-Coupled Receptor 119 (GPR119) Agonists for the Treatment of Diabetes: Recent Progress and Prevailing Challenges. *Journal of Medicinal Chemistry,* 59(8), 3579-3592.

Robertson, R.P. and Harmon, J.S. (2007) Pancreatic islet beta-cell and oxidative stress: the importance of glutathione peroxidase. *FEBS Letters,* 581(19), 3743-3748.

Roder, P.V., Wu, B., Liu, Y. and Han, W. (2016) Pancreatic regulation of glucose homeostasis. *Experimental & Molecular Medicine,* 48, e219.

Rojas, L.B. and Gomes, M.B. (2013) Metformin: an old but still the best treatment for type 2 diabetes. *Diabetology & Metabolic Syndrome,* 5(1), 6-5996-5-6.

Rorsman, P. and Renstrom, E. (2003) Insulin granule dynamics in pancreatic beta cells. *Diabetologia,* 46(8), 1029-1045.

Rosenbaum, D.M., Rasmussen, S.G. and Kobilka, B.K. (2009) The structure and function of G-protein-coupled receptors. *Nature,* 459(7245), 356-363.

Rozenfeld, R. and Devi, L.A. (2011) Exploring a role for heteromerization in GPCR signalling specificity. *The Biochemical Journal,* 433(1), 11-18.

Rutter, G.A. (2001) Nutrient-secretion coupling in the pancreatic islet beta-cell: recent advances. *Molecular Aspects of Medicine,* 22(6), 247-284.

Ruz-Maldonado, I., Pingitore, A., Liu, B., Atanes, P., Huang, G.C., Baker, D., Alonso, F.J., Bermudez-Silva, F.J. and Persaud, S.J. (2018) LH-21 and abnormal cannabidiol improve beta-cell function in isolated human and mouse islets through GPR55-dependent and -independent signalling. *Diabetes, Obesity & Metabolism,* 20(4), 930-942.

Ryberg, E., Larsson, N., Sjogren, S., Hjorth, S., Hermansson, N.O., Leonova, J., Elebring, T., Nilsson, K., Drmota, T. and Greasley, P.J. (2007) The orphan receptor GPR55 is a novel cannabinoid receptor. *British Journal of Pharmacology,* 152(7), 1092-1101.

Sabir, S., Saleem, A., Akhtar, M.F., Saleem, M. and Raza, M. (2018) Increasing beta cell mass to treat diabetes mellitus. *Advances in Clinical and Experimental Medicine: Official Organ Wroclaw Medical University,* 27(9), 1309-1315.

Sam, A.H., Salem, V. and Ghatei, M.A. (2011) Rimonabant: From RIO to Ban. *Journal of Obesity,* 2011, e432607.

Sanchez-Fernandez, G., Cabezudo, S., Garcia-Hoz, C., Beninca, C., Aragay, A.M., Mayor, F.,Jr and Ribas, C. (2014) Galphaq signalling: the new and the old. *Cellular Signalling*, 26(5), 833-848.

Sanchez-Reyes, O.B., Romero-Avila, M.T., Castillo-Badillo, J.A., Takei, Y., Hirasawa, A., Tsujimoto, G., Villalobos-Molina, R. and Garcia-Sainz, J.A. (2014) Free fatty acids and protein kinase C activation induce GPR120 (free fatty acid receptor 4) phosphorylation. *European Journal of Pharmacology*, 723, 368-374.

Sandoval, D.A. and D'Alessio, D.A. (2015) Physiology of proglucagon peptides: role of glucagon and GLP-1 in health and disease. *Physiological Reviews*, 95(2), 513-548.

Sankoda, A., Harada, N., Iwasaki, K., Yamane, S., Murata, Y., Shibue, K., Thewjitcharoen, Y., Suzuki, K., Harada, T., Kanemaru, Y., Shimazu-Kuwahara, S., Hirasawa, A. and Inagaki, N. (2017) Long-Chain Free Fatty Acid Receptor GPR120 Mediates Oil-Induced GIP Secretion Through CCK in Male Mice. *Endocrinology*, 158(5), 1172-1180.

Sano, H., Kane, S., Sano, E., Miinea, C.P., Asara, J.M., Lane, W.S., Garner, C.W. and Lienhard, G.E. (2003) Insulin-stimulated phosphorylation of a Rab GTPase-activating protein regulates GLUT4 translocation. *The Journal of Biological Chemistry*, 278(17), 14599-14602.

Sawzdargo, M., Nguyen, T., Lee, D.K., Lynch, K.R., Cheng, R., Heng, H.H., George, S.R. and O'Dowd, B.F. (1999) Identification and cloning of three novel human G protein-coupled receptor genes GPR52, PsiGPR53 and GPR55: GPR55 is extensively expressed in human brain. *Brain Research.Molecular Brain Research*, 64(2), 193-198.

Schicho, R., Bashashati, M., Bawa, M., McHugh, D., Saur, D., Hu, H.M., Zimmer, A., Lutz, B., Mackie, K., Bradshaw, H.B., McCafferty, D.M., Sharkey, K.A. and Storr, M. (2011) The atypical cannabinoid O-1602 protects against experimental colitis and inhibits neutrophil recruitment. *Inflammatory Bowel Diseases*, 17(8), 1651-1664.

Schicho, R. and Storr, M. (2012) A potential role for GPR55 in gastrointestinal functions. *Current Opinion in Pharmacology*, 12(6), 653-658.

Schmidt, P.T., Naslund, E., Gryback, P., Jacobsson, H., Holst, J.J., Hilsted, L. and Hellstrom, P.M. (2005) A role for pancreatic polypeptide in the regulation of gastric emptying and short-term metabolic control. *The Journal of Clinical Endocrinology and Metabolism,* 90(9), 5241-5246.

Schommers, P., Thurau, A., Bultmann-Mellin, I., Guschlbauer, M., Klatt, A.R., Rozman, J., Klingenspor, M., de Angelis, M.H., Alber, J., Grundemann, D., Sterner-Kock, A. and Wiesner, R.J. (2017) Metformin causes a futile intestinal-hepatic cycle which increases energy expenditure and slows down development of a type 2 diabetes-like state. *Molecular Metabolism,* 6(7), 737-747.

Senechal, M., Slaght, J., Bharti, N. and Bouchard, D.R. (2014) Independent and combined effect of diet and exercise in adults with prediabetes. *Diabetes, Metabolic Syndrome and Obesity: Targets and Therapy,* 7, 521-529.

Sharir, H. and Abood, M.E. (2010) Pharmacological characterization of GPR55, a putative cannabinoid receptor. *Pharmacology & Therapeutics,* 126(3), 301-313.

Shi, H., Chen, H., Gu, Z., Zhang, H., Chen, W. and Chen, Y.Q. (2016) Application of a delta-6 desaturase with alpha-linolenic acid preference on eicosapentaenoic acid production in Mortierella alpina. *Microbial Cell Factories,* 15(1), 117-016-0516-5.

Shi, Q.X., Yang, L.K., Shi, W.L., Wang, L., Zhou, S.M., Guan, S.Y., Zhao, M.G. and Yang, Q. (2017) The novel cannabinoid receptor GPR55 mediates anxiolytic-like effects in the medial orbital cortex of mice with acute stress. *Molecular Brain,* 10(1), 38-017-0318-7.

Shimpukade, B., Hudson, B.D., Hovgaard, C.K., Milligan, G. and Ulven, T. (2012) Discovery of a potent and selective GPR120 agonist. *Journal of Medicinal Chemistry,* 55(9), 4511-4515.

Shore, D.M. and Reggio, P.H. (2015) The therapeutic potential of orphan GPCRs, GPR35 and GPR55. *Frontiers in Pharmacology,* 6, 69-69.

Siddiqui, N.I. (2009) Incretin mimetics and DPP-4 inhibitors: new approach to treatment of type 2 diabetes mellitus. *Mymensingh Medical Journal: MMJ,* 18(1), 113-124.

Siehler, S. (2009) Regulation of RhoGEF proteins by G12/13-coupled receptors. *British Journal of Pharmacology*, 158(1), 41-49.

Simcocks, A.C., O'Keefe, L., Jenkin, K.A., Mathai, M.L., Hryciw, D.H. and McAinch, A.J. (2014) A potential role for GPR55 in the regulation of energy homeostasis. *Drug Discovery Today*, 19(8), 1145-1151.

Singh, M. and Kumar, A. (2018) Risks Associated with SGLT2 Inhibitors: An Overview. *Current Drug Safety*, 13(2), 84-91.

Sola, D., Rossi, L., Schianca, G.P., Maffioli, P., Bigliocca, M., Mella, R., Corliano, F., Fra, G.P., Bartoli, E. and Derosa, G. (2015) Sulfonylureas and their use in clinical practice. *Archives of Medical Science: AMS*, 11(4), 840-848.

Song, T., Yang, Y., Zhou, Y., Wei, H. and Peng, J. (2017) GPR120: a critical role in adipogenesis, inflammation, and energy metabolism in adipose tissue. *Cellular and Molecular Life Sciences: CMLS*, 74(15), 2723-2733.

Sparks, S.M., Chen, G., Collins, J.L., Danger, D., Dock, S.T., Jayawickreme, C., Jenkinson, S., Laudeman, C., Leesnitzer, M.A., Liang, X., Maloney, P., McCoy, D.C., Moncol, D., Rash, V., Rimele, T., Vulimiri, P., Way, J.M. and Ross, S. (2014) Identification of diarylsulfonamides as agonists of the free fatty acid receptor 4 (FFA4/GPR120). *Bioorganic & Medicinal Chemistry Letters*, 24(14), 3100-3103.

Sriram, K. and Insel, P.A. (2018) G Protein-Coupled Receptors as Targets for Approved Drugs: How Many Targets and How Many Drugs? *Molecular Pharmacology*, 93(4), 251-258.

Stancic, A., Jandl, K., Hasenohrl, C., Reichmann, F., Marsche, G., Schuligoi, R., Heinemann, A., Storr, M. and Schicho, R. (2015) The GPR55 antagonist CID16020046 protects against intestinal inflammation. *Neurogastroenterology and Motility: The Official Journal of the European Gastrointestinal Motility Society*, 27(10), 1432-1445.

Starback, P., Wraith, A., Eriksson, H. and Larhammar, D. (2000) Neuropeptide Y receptor gene y6: multiple deaths or resurrections? *Biochemical and Biophysical Research Communications*, 277(1), 264-269.

Stein, S.A., Lamos, E.M. and Davis, S.N. (2013) A review of the efficacy and safety of oral antidiabetic drugs. *Expert Opinion on Drug Safety*, 12(2), 153-175.

Steiner, D.J., Kim, A., Miller, K. and Hara, M. (2010) Pancreatic islet plasticity: interspecies comparison of islet architecture and composition. *Islets,* 2(3), 135-145.

Steneberg, P., Rubins, N., Bartoov-Shifman, R., Walker, M.D. and Edlund, H. (2005) The FFA receptor GPR40 links hyperinsulinemia, hepatic steatosis, and impaired glucose homeostasis in mouse. *Cell Metabolism,* 1(4), 245-258.

Stewart, A.F., Hussain, M.A., Garcia-Ocana, A., Vasavada, R.C., Bhushan, A., Bernal-Mizrachi, E. and Kulkarni, R.N. (2015) Human beta-cell proliferation and intracellular signaling: part 3. *Diabetes,* 64(6), 1872-1885.

Stewart, G., Hira, T., Higgins, A., Smith, C.P. and McLaughlin, J.T. (2006) Mouse GPR40 heterologously expressed in Xenopus oocytes is activated by short-, medium-, and long-chain fatty acids. *American Journal of Physiology.Cell Physiology*, 290(3), C785-C792.

Stoddart, L.A., Smith, N.J. and Milligan, G. (2008) International Union of Pharmacology. LXXI. Free fatty acid receptors FFA1, -2, and -3: pharmacology and pathophysiological functions. *Pharmacological Reviews,* 60(4), 405-417.

Stone, V.M., Dhayal, S., Brocklehurst, K.J., Lenaghan, C., Sorhede Winzell, M., Hammar, M., Xu, X., Smith, D.M. and Morgan, N.G. (2014) GPR120 (FFAR4) is preferentially expressed in pancreatic delta cells and regulates somatostatin secretion from murine islets of Langerhans. *Diabetologia,* 57(6), 1182-1191.

Strowski, M.Z., Parmar, R.M., Blake, A.D. and Schaeffer, J.M. (2000) Somatostatin inhibits insulin and glucagon secretion via two receptors subtypes: an in vitro study of pancreatic islets from somatostatin receptor 2 knockout mice. *Endocrinology,* 141(1), 111-117.

Su, J.Y. and Vo, A.C. (2007) 2-Arachidonylglyceryl ether and abnormal cannabidiol-induced vascular smooth muscle relaxation in rabbit pulmonary arteries via receptor-pertussis toxin sensitive G proteins-ERK1/2 signaling. *European Journal of Pharmacology,* 559(2-3), 189-195.

Suckow, A.T., Polidori, D., Yan, W., Chon, S., Ma, J.Y., Leonard, J. and Briscoe, C.P. (2014) Alteration of the glucagon axis in GPR120 (FFAR4) knockout mice: a role for GPR120 in glucagon secretion. *The Journal of Biological Chemistry*, 289(22), 15751-15763.

Sun, E.W., de Fontgalland, D., Rabbitt, P., Hollington, P., Sposato, L., Due, S.L., Wattchow, D.A., Rayner, C.K., Deane, A.M., Young, R.L. and Keating, D.J. (2017) Mechanisms Controlling Glucose-Induced GLP-1 Secretion in Human Small Intestine. *Diabetes*, 66(8), 2144-2149.

Svizenska, I., Dubovy, P. and Sulcova, A. (2008) Cannabinoid receptors 1 and 2 (CB1 and CB2), their distribution, ligands and functional involvement in nervous system structures--a short review. *Pharmacology, Biochemistry, and Behavior*, 90(4), 501-511.

Swaminath, G. (2008) Fatty acid binding receptors and their physiological role in type 2 diabetes. *Archiv Der Pharmazie*, 341(12), 753-761.

Swinnen, S.G., Hoekstra, J.B. and DeVries, J.H. (2009) Insulin therapy for type 2 diabetes. *Diabetes Care*, 32 Suppl 2, S253-9.

Syrovatkina, V., Alegre, K.O., Dey, R. and Huang, X.Y. (2016) Regulation, Signaling, and Physiological Functions of G-Proteins. *Journal of Molecular Biology*, 428(19), 3850-3868.

Takeda, S., Kadowaki, S., Haga, T., Takaesu, H. and Mitaku, S. (2002) Identification of G protein-coupled receptor genes from the human genome sequence. *FEBS Letters*, 520(1-3), 97-101.

Tanaka, H., Yoshida, S., Minoura, H., Negoro, K., Shimaya, A., Shimokawa, T. and Shibasaki, M. (2014) Novel GPR40 agonist AS2575959 exhibits glucose metabolism improvement and synergistic effect with sitagliptin on insulin and incretin secretion. *Life Sciences*, 94(2), 115-121.

Tanaka, T., Yano, T., Adachi, T., Koshimizu, T.A., Hirasawa, A. and Tsujimoto, G. (2008) Cloning and characterization of the rat free fatty acid receptor GPR120: in vivo effect of the natural ligand on GLP-1 secretion and proliferation of pancreatic beta cells. *Naunyn-Schmiedeberg's Archives of Pharmacology*, 377(4-6), 515-522.

Tarantola, E., Bertone, V., Milanesi, G., Capelli, E., Ferrigno, A., Neri, D., Vairetti, M., Barni, S. and Freitas, I. (2012) Dipeptidylpeptidase--IV, a key enzyme for the degradation of incretins and neuropeptides: activity and expression in the liver of lean and obese rats. *European Journal of Histochemistry: EJH*, 56(4), e41.

Todoric, J., Loffler, M., Huber, J., Bilban, M., Reimers, M., Kadl, A., Zeyda, M., Waldhausl, W. and Stulnig, T.M. (2006) Adipose tissue inflammation induced by high-fat diet in obese diabetic mice is prevented by n-3 polyunsaturated fatty acids. *Diabetologia*, 49(9), 2109-2119.

Trudeau, L. and Gilbert, J. (2018) Diabetes and Hypertension: The Low and High Points. *Canadian Journal of Diabetes*, 42(2), 113-114.

Tuduri, E., Imbernon, M., Hernandez-Bautista, R.J., Tojo, M., Ferno, J., Dieguez, C. and Nogueiras, R. (2017) GPR55: a new promising target for metabolism? *Journal of Molecular Endocrinology*, 58(3), R191-R202.

Turner, R.C., Cull, C.A., Frighi, V. and Holman, R.R. (1999) Glycemic control with diet, sulfonylurea, metformin, or insulin in patients with type 2 diabetes mellitus: progressive requirement for multiple therapies (UKPDS 49). UK Prospective Diabetes Study (UKPDS) Group. *Jama*, 281(21), 2005-2012.

Ugleholdt, R., Poulsen, M.L., Holst, P.J., Irminger, J.C., Orskov, C., Pedersen, J., Rosenkilde, M.M., Zhu, X., Steiner, D.F. and Holst, J.J. (2006) Prohormone convertase 1/3 is essential for processing of the glucose-dependent insulinotropic polypeptide precursor. *The Journal of Biological Chemistry*, 281(16), 11050-11057.

Vallee Marcotte, B., Cormier, H., Rudkowska, I., Lemieux, S., Couture, P. and Vohl, M.C. (2017) Polymorphisms in FFAR4 (GPR120) Gene Modulate Insulin Levels and Sensitivity after Fish Oil Supplementation. *Journal of Personalized Medicine*, 7(4), 10.3390/jpm7040015.

Vanderheiden, A., Harrison, L.B., Warshauer, J.T., Adams-Huet, B., Li, X., Yuan, Q., Hulsey, K., Dimitrov, I., Yokoo, T., Jaster, A.W., Pinho, D.F., Pedrosa, I., Lenkinski, R.E., Pop, L.M. and Lingvay, I. (2016) Mechanisms of Action of Liraglutide in Patients With Type 2 Diabetes Treated With High-Dose Insulin. *The Journal of Clinical Endocrinology and Metabolism*, 101(4), 1798-1806.

Vangaveti, V., Shashidhar, V., Jarrod, G., Baune, B.T. and Kennedy, R.L. (2010) Free fatty acid receptors: emerging targets for treatment of diabetes and its complications. *Therapeutic Advances in Endocrinology and Metabolism*, 1(4), 165-175.

Vargas, E. and Carrillo Sepulveda, M.A. (2018) Biochemistry, Insulin, Metabolic Effects. *In:* Anon.*StatPearls*. Treasure Island (FL): StatPearls Publishing LLC,

Vasu, S., McClenaghan, N.H., McCluskey, J.T. and Flatt, P.R. (2013) Cellular responses of novel human pancreatic beta-cell line, 1.1B4 to hyperglycemia. *Islets*, 5(4), 170-177.

Vasu, S., Moffett, R.C., Thorens, B. and Flatt, P.R. (2014) Role of endogenous GLP-1 and GIP in beta cell compensatory responses to insulin resistance and cellular stress. *PloS One*, 9(6), e101005.

Vasudevan, S., Goswami, P., Sonika, U., Thakur, B., Sreenivas, V. and Saraya, A. (2018) Comparison of Various Scoring Systems and Biochemical Markers in Predicting the Outcome in Acute Pancreatitis. *Pancreas*, 47(1), 65-71.

Vilsboll, T. (2009) The effects of glucagon-like peptide-1 on the beta cell. *Diabetes, Obesity & Metabolism*, 11 Suppl 3, 11-18.

Viollet, B., Guigas, B., Sanz Garcia, N., Leclerc, J., Foretz, M. and Andreelli, F. (2012) Cellular and molecular mechanisms of metformin: an overview. *Clinical Science (London, England: 1979)*, 122(6), 253-270.

Wang, D.Q., Liu, X.L., Rong, Q.F., Han, L. and Zhao, N.Q. (2013) Alpha-linolenic acid improves insulin sensitivity in obese patients. *Zhonghua Yi Xue Za Zhi*, 93(2), 132-134.

Wank, S.A., Pisegna, J.R. and de Weerth, A. (1992) Brain and gastrointestinal cholecystokinin receptor family: structure and functional expression. *Proceedings of the National Academy of Sciences of the United States of America*, 89(18), 8691-8695.

Watson, S.J., Brown, A.J. and Holliday, N.D. (2012) Differential signaling by splice variants of the human free fatty acid receptor GPR120. *Molecular Pharmacology*, 81(5), 631-642.

Wettschureck, N. and Offermanns, S. (2005) Mammalian G proteins and their cell type specific functions. *Physiological Reviews*, 85(4), 1159-1204.

Wewer Albrechtsen, N.J., Kuhre, R.E., Pedersen, J., Knop, F.K. and Holst, J.J. (2016) The biology of glucagon and the consequences of hyperglucagonemia. *Biomarkers in Medicine*, 10(11), 1141-1151.

Whalley, N.M., Pritchard, L.E., Smith, D.M. and White, A. (2011) Processing of proglucagon to GLP-1 in pancreatic alpha-cells: is this a paracrine mechanism enabling GLP-1 to act on beta-cells? *The Journal of Endocrinology*, 211(1), 99-106.

Wiley, J.L., Burston, J.J., Leggett, D.C., Alekseeva, O.O., Razdan, R.K., Mahadevan, A. and Martin, B.R. (2005) CB1 cannabinoid receptor-mediated modulation of food intake in mice. *British Journal of Pharmacology*, 145(3), 293-300.

Wu, H., Wang, C., Gregory, K.J., Han, G.W., Cho, H.P., Xia, Y., Niswender, C.M., Katritch, V., Meiler, J., Cherezov, V., Conn, P.J. and Stevens, R.C. (2014) Structure of a class C GPCR metabotropic glutamate receptor 1 bound to an allosteric modulator. *Science (New York, N.Y.)*, 344(6179), 58-64.

Wu, J., Xie, N., Zhao, X., Nice, E.C. and Huang, C. (2012) Dissection of aberrant GPCR signaling in tumorigenesis--a systems biology approach. *Cancer Genomics & Proteomics*, 9(1), 37-50.

Yen, H.Y., Hopper, J.T.S., Liko, I., Allison, T.M., Zhu, Y., Wang, D., Stegmann, M., Mohammed, S., Wu, B. and Robinson, C.V. (2017) Ligand binding to a G protein-coupled receptor captured in a mass spectrometer. *Science Advances*, 3(6), e1701016.

Yi, J., Warunek, D. and Craft, D. (2015) Degradation and Stabilization of Peptide Hormones in Human Blood Specimens. *PloS One*, 10(7), e0134427.

Yonezawa, T., Kurata, R., Yoshida, K., Murayama, M.A., Cui, X. and Hasegawa, A. (2013) Free fatty acids-sensing G protein-coupled receptors in drug targeting and therapeutics. *Current Medicinal Chemistry*, 20(31), 3855-3871.

Yu, O.M. and Brown, J.H. (2015) G Protein-Coupled Receptor and RhoA-Stimulated Transcriptional Responses: Links to Inflammation, Differentiation, and Cell Proliferation. *Molecular Pharmacology*, 88(1), 171-180.

Yulyaningsih, E., Loh, K., Lin, S., Lau, J., Zhang, L., Shi, Y., Berning, B.A., Enriquez, R., Driessler, F., Macia, L., Khor, E.C., Qi, Y., Baldock, P., Sainsbury, A. and Herzog,

H. (2014) Pancreatic polypeptide controls energy homeostasis via Npy6r signaling in the suprachiasmatic nucleus in mice. *Cell Metabolism,* 19(1), 58-72.

Zhang, D., Zhao, Q. and Wu, B. (2015) Structural Studies of G Protein-Coupled Receptors. *Molecules and Cells,* 38(10), 836-842.

Zhang, L. and Shi, G. (2016) Gq-Coupled Receptors in Autoimmunity. *Journal of Immunology Research,* 2016, e3969023.

Zheng, Y., Ley, S.H. and Hu, F.B. (2018) Global aetiology and epidemiology of type 2 diabetes mellitus and its complications. *Nature Reviews.Endocrinology,* 14(2), 88-98.

Zhou, L., Cai, X., Han, X. and Ji, L. (2014) P38 plays an important role in glucolipotoxicity-induced apoptosis in INS-1 cells. *Journal of Diabetes Research,* 2014, e834528.

Zipf, W.B., O'Dorisio, T.M., Cataland, S. and Sotos, J. (1981) Blunted pancreatic polypeptide responses in children with obesity of Prader-Willi syndrome. *The Journal of Clinical Endocrinology and Metabolism,* 52(6), 1264-1266.